Published by Empress Catherine II
Saint Petersburg Mining University

SINCE 1907

E-ISSN 2541-9404
ISSN 2411-3336

JOURNAL OF MINING INSTITUTE

ZAPISKI GORNOGO INSTITUTA

SCIENTIFIC JOURNAL

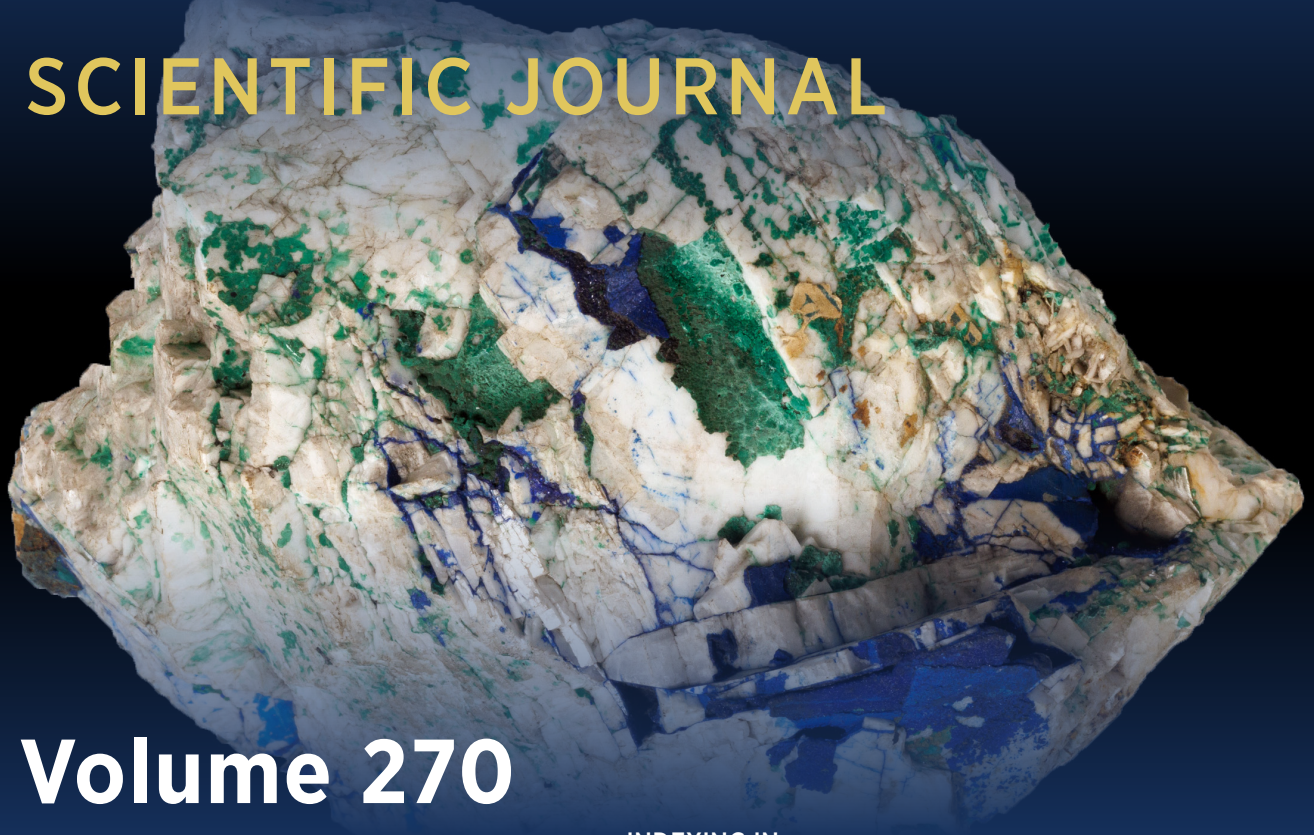

Volume 270

№ 6 • 2024

INDEXING IN
SCOPUS (Q1)
WEB OF SCIENCE (ESCI)

WWW.PMI.SPMI.RU

Journal of Mining Institute

Empress Catherine II Saint Petersburg Mining University

The International Competence Center for Mining Engineering Education under the auspices of UNESCO

The scientific periodical “Journal of Mining Institute” is published since 1907 by Empress Catherine II Saint Petersburg Mining University – the first higher technical educational institution in Russia, founded in 1773 by the decree of Catherine II as the embodiment of the ideas of Peter I and M.V. Lomonosov on the training of engineers for the development of mining business.

The International Competence Center for Mining Engineering Education under the auspices of UNESCO operates on the basis of Empress Catherine II Saint Petersburg Mining University and contributes to active interaction of the Journal with the international scientific community.

The purpose of the Journal is to create an information space in which Russian and foreign scientists can present results of their theoretical and empirical research on the problems of the mining sector.

Published articles cover the issues of geology, geotechnical engineering and engineering geology, mining and petroleum engineering, mineral processing, energy, geoecology and life safety, economics of raw materials industries.

The Journal is indexed by Scopus (Q1), Web of Science Core Collection (ESCI), DOAJ Seal, RSCI, GeoRef, Google Scholar, RSCI. It is included in the White list of the Ministry of Education and Science of the Russian Federation.

The Journal is published six times a year. The average first decision time is one month.

Articles are published free of charge. Translation is provided by the author.

The cover shows an exhibit of the Mining Museum – barite in shell-like aggregates with dolomite. The name of the mineral is translated from the Greek “barys” – heavy. Barite has a high density, is a raw material for the production of barium and is used for weighting of drilling fluids.

The Mining Museum is the world’s third largest natural-science exposition, it contains more than 230 thousand exhibits, including precious metals and stones, unique collections of minerals, ores, rocks, paleontological remains, meteorites, a collection of models and prototypes of mining equipment, pieces of stone-cutting and jewelry art.

JOURNAL OF MINING INSTITUTE

ZAPISKI GORNOGO INSTITUTA

PEER-REVIEWED SCIENTIFIC JOURNAL

Published since 1907

ISSN 2411-3336
e-ISSN 2541-9404

Volume 270

ST. PETERSBURG • 2024

Journal founder: Empress Catherine II Saint Petersburg Mining University

CHIEF EDITOR
V.S.Litvinenko, Doctor of Engineering Sciences, Professor, Member of the International Academy of Higher Education, RANS, RAHS, MANEB, Rector (Empress Catherine II Saint Petersburg Mining University, Saint Petersburg, Russia)

DEPUTY CHIEF EDITOR
S.G.Skublov, Doctor of Geological and Mineralogical Sciences, Professor, Member of the Russian Mineralogical Society, Expert of the RSF and RAS (Empress Catherine II Saint Petersburg Mining University, Saint Petersburg, Russia)

EXECUTIVE SECRETARY
S.V.Sinyavina, Candidate of Engineering Sciences, Director of the Publishing House (Empress Catherine II Saint Petersburg Mining University, Saint Petersburg, Russia)

EDITORIAL TEAM

O.Ye.Aksyutin, Doctor of Engineering Sciences, Corresponding Member of the RAS, Board Member, Head of Department (PAO Gazprom, Moscow, Russia)
A.A.Baryakh, Doctor of Engineering Sciences, Professor, Member of the RAS, Director (Perm Federal Research Center Ural Branch RAS, Perm, Russia)
V.N.Brichkin, Doctor of Engineering Sciences, Professor, Vice Rector for Scientific Personnel Training (Empress Catherine II Saint Petersburg Mining University, Saint Petersburg, Russia)
S.G.Gendler, Doctor of Engineering Sciences, Professor, Member of the RANS, Head of Department of Occupational Safety (Empress Catherine II Saint Petersburg Mining University, Saint Petersburg, Russia)
O.M.Ermilov, Doctor of Engineering Sciences, Professor, Member of the RAS, RAHS, Deputy Engineer-in-Chief of Science Programmes (OOO Gazprom Development Nadym, Nadym, Russia)
V.P.Zubov, Doctor of Engineering Sciences, Professor, Head of Department of Underground Mining (Empress Catherine II Saint Petersburg Mining University, Saint Petersburg, Russia)
G.B.Kleiner, Doctor of Economics, Professor, Corresponding Member of the RAS, Deputy Director (Central Research Institute of Economics and Mathematics of the RAS, Moscow, Russia)
A.V.Kozlov, Doctor of Geological and Mineralogical Sciences, Member of the Russian Mineralogical Society, Head of Department of Geology and Exploration of Mineral Deposits (Empress Catherine II Saint Petersburg Mining University, Saint Petersburg, Russia)
Yu.B.Marin, Doctor of Geological and Mineralogical Sciences, Professor, Corresponding Member of the RAS, Honorary President (Russian Mineralogical Society, Saint Petersburg, Russia)
V.A.Morenov, Candidate of Engineering Sciences, Associate Professor (Empress Catherine II Saint Petersburg Mining University, Saint Petersburg, Russia)
M.A.Pashkevich, Doctor of Engineering Sciences, Professor, Head of Department of Geoecology (Empress Catherine II Saint Petersburg Mining University, Saint Petersburg, Russia)
T.V.Ponomarenko, Doctor of Economics, Professor (Empress Catherine II Saint Petersburg Mining University, Saint Petersburg, Russia)
O.M.Prishchepa, Doctor of Geological and Mineralogical Sciences, Member of the RANS, Head of Department of Geology of Oil and Gas (Empress Catherine II Saint Petersburg Mining University, Saint Petersburg, Russia)
A.G.Protosenya, Doctor of Engineering Sciences, Professor, Head of Department of Construction of Mining Enterprises and Underground Structures (Empress Catherine II Saint Petersburg Mining University, Saint Petersburg, Russia)
V.E.Somov, Doctor of Economics, Candidate of Engineering Sciences, Member of the RANS, Director (OOO Kinef, Kirishi, Russia)
A.A.Tronin, Doctor of Geological and Mineralogical Sciences, Director (Saint Petersburg Scientific-Research Centre for Ecological Safety RAS, Saint Petersburg, Russia)
V.L.Trushko, Doctor of Engineering Sciences, Professor, Member of the International Higher Education Academy of Sciences, RANS, RAHS, MANEB, Head of Department of Mechanics (Empress Catherine II Saint Petersburg Mining University, Saint Petersburg, Russia)
P.S.Tsvetkov, Candidate of Economics, Associate Professor (Empress Catherine II Saint Petersburg Mining University, Saint Petersburg, Russia)
A.E.Cherepovitsyn, Doctor of Economics, Professor, Head of Department of Economics, Organization and Management (Empress Catherine II Saint Petersburg Mining University, Saint Petersburg, Russia)
Ya.E.Shklyarskii, Doctor of Engineering Sciences, Professor, Head of the Department of General Electric Engineering (Empress Catherine II Saint Petersburg Mining University, Saint Petersburg, Russia)
Oleg Antzutkin, Professor (University of Technology, Luleo, Sweden)
Gabriel Weiss, Doctor of Sciences, Professor, Pro-Rector for Science and Research (Technical University, Kosice, Slovakia)
Hal Gurgenci, Professor (School of Mining Machine-Building in University of Queensland, Brisbane, Australia)
Edwin Kroke, Doctor of Sciences, Professor (Institute of Inorganic Chemistry in Freiberg Mining Academy, Freiberg, Germany)
Zhou Fubao, Doctor of Sciences, Professor, Vice President (China University of Mining and Technology, Beijing, PR China)
Zhao Yuemin, Doctor of Sciences, Professor, Director of Academic Committee (China University of Mining and Technology, Beijing, PR China)

Sections

• Geology • Geotechnical Engineering and Engineering Geology • Economic Geology • Energy

Registration Certificate PI N FS77-70453 dated 20.07.2017

PH License N 06517 dated 09.01.02

Editorial staff: Head of the Editorial Center V.L.Lebedev; Editors: E.S.Dribinskaya, M.G.Khachirova, L.V.Nabieva
Computer Design: N.N.Sedykh, V.I.Kashirina, E.A.Golovinskaya

© Empress Catherine II Saint Petersburg Mining University, 2024

Passed for printing 25.12.2024. Format 60 × 84/8. Academic Publishing Division 49.
Circulation: 300 copies. Order 720. Printed by RIC of Empress Catherine II Saint Petersburg Mining University. Free sale price.

Mailing address of the Journal Founder and the Editorial Board
21st Linia V.O., N 2, St. Petersburg, Russia, 199106
Phone: +7 (812) 328-8416; Fax +7 (812) 327-7359;
E-mail: pmi@spmi.ru Journal website: pmi.spmi.ru

CONTENTS

Geology

Geotechnical Engineering and Engineering Geology

Economic Geology

Energy

ISSN 2411-3336; e-ISSN 2541-9404

JOURNAL OF MINING INSTITUTE

Zapiski Gornogo instituta

Journal homepage: pmi.spmi.ru

Research article

Peculiarities of formation, isomorphism and geochemistry of trace elements of sphalerite and wurtzite unusual varieties from the Goniatite occurrence (Pai-Khoi Ridge, Nenets Autonomous District)

Aleksandr B. Makeyev✉, Ilya V. Vikentyev, Elena V. Kovalchuk, Vera D. Abramova, Vsevolod Yu. Prokofyev

Institute of Geology of Ore Deposits, Petrography, Mineralogy and Geochemistry, RAS, Moscow, Russia

***How to cite this article*:** Makeyev A.B.,Vikentyev I.V., Kovalchuk E.V., Abramova V.D., Prokofyev V.Yu. Peculiarities of formation, isomorphism and geochemistry of trace elements of sphalerite and wurtzite unusual varieties from the Goniatite occurrence (Pai-Khoi Ridge, Nenets Autonomous District). Journal of Mining Institute. 2024. Vol. 270, p. 861-876.

Abstract

A unique Mn-, Cd-bearing sphalerite from quartz-calcite veins in the coal-bearing series (Visean C_1v) marine sediments in a 50 km segment of the middle course of the Silova-Yakha River in the Arctic zone of the European part of Russia (Pai-Khoi Ridge) has been studied. The veins have a conformable and cross-cutting occurrence in two types of rocks: gray limestones and black siliceous-carbonaceous shales, the area is known as the Goniatite occurrence. The sulfide content in vein samples ranges from 0.1 to 2 vol.%. The chemical composition of 27 monomineral samples of Mn-, Cd-bearing sphalerites was studied, 82 points were analyzed. Correlations between typomorphic elements-impurities were revealed and correlation matrix was constructed. Cu, V, Ga, In, Sn, As, Sb, Bi, Pb, Tl, Se, Ag, Au, Ni are positively correlated with each other; Cd, Mn and Ge are negatively correlated with each other. The hydrothermal fluid involved in crystallization of sphalerite is characterized by low temperature (164-211 °C) and average salinity of 5-6 wt.% eq. NaCl. An updated "portrait" of typomorphic features (composition and properties) of sphalerite of the Pai-Khoi province was obtained. The features allowing to determine the type of impurity entering the sphalerite structure – in the form of isomorphic impurity or in the form of microinclusions of paragenetic association minerals – have been established. Submicron inclusions of sulvanite and colusite, invisible by other methods, were detected in sphalerite (by LA-ICP-MS method).The cathodoluminescence data of sphalerite from the Pai-Khoi province were typified. In contrast to other provinces, ZnS crystals here are characterized by almost complete absence of isomorphic iron. This allowed us to study pure isomorphism schemes of ZnS↔MnS, ZnS↔CdS, namely cathodoluminescence and other types of luminescence. The presence of a rare wurtzite-4H polytype in assemblage with sphalerite was revealed. High contents of strategic metals Cd, Ga, In, Ge in the ZnS matrix, as well as sulvanite (V, Cu) in a single paragenesis were found. A serious reassessment of the potential for industrial use of this mineralization will be required.

Keywords

sphalerite; wurtzite; Pai-Khoi; LA-ICP-MS; trace elements; fluid; cathodoluminescence

Funding

The work was carried out within the framework of the state task of IGEM RAS N FMMN-2021-0005, the studies by LA-ICP-MS method were performed under the RNF grant N 23-17-00266.

Received: 21.06.2023 ***Accepted: 27.12.2023*** ***Online: 04.04.2024*** ***Published: 25.12.2024***

Introduction.

Natural zinc sulfides – cubic sphalerite and hexagonal wurtzite – are widespread minerals [1, 2] and informative indicators of conditions of mineral formation [3-5]. Due to simplicity of the crystal structure and diversity of formation mechanisms in a large number of rock types, many trace elements (Ag, Au, As, Bi, Cd, Co, Cu, Fe, Ga, Ge, Ge, Hg, In, Mn, Ni, Pb, Sb, Se, Te, Sn, Tl, V) can be accumulated in ZnS. In some cases, these impurities are extracted mainly from ores containing sphalerite and wurtzite (e.g., Cd, Ga, Ge, Tl). These chemical elements can exist in different chemical states: (*A*) enter the structure of sphalerite in "invisible" form as isomorphic impurity (Fe, Mn, Cd, Hg, Tl) or as nanoparticles (Ag, Au, Cu); (*B*) become part of microinclusions of some

This is an open access article under the CC BY 4.0 license

minerals (e.g., chalcopyrite, tennantite-tetrahedrite, petzite, sulvanite) in the matrix of zinc sulfides (e.g. As, Bi, Sb, Te, V). Sometimes these heterogeneous microinclusions cannot be identified in the host mineral even by the EPMA or LA-ICP-MS methods. The structural and chemical forms of some impurity elements can vary (e.g. Au, Ag, Cu, Pb, Ga, Ge) depending on the type of deposit. There are also additional difficulties associated with the occurrence of minerals characterized by the same type of structure (e.g. chalcopyrite, sulvanite, colusite) in a similar mineral paragenesis. In sphalerite and wurtzite intergrowths and sprouting zones and sectors in which some impurities accumulate in sphalerite and others in the zones composed of wurtzite are observed [6]. Understanding of physicochemical properties and oxidation degree of impurity elements in zinc sulfides helps to improve the recovery of valuable metals at mining and processing plants, which is also important from ecological point of view. In recent years, the extraction of a number of rare "critical" metals (In, Ga, Ge) has become particularly relevant, as their consumption in the world is growing dramatically. Impurities of rare and rare-earth elements, as well as spectroscopy of minerals are widely used in the assessment of geochemical environments, which allows us to study the conditions of formation of minerals of different genesis, such as diamond [7, 8], zircon [9, 10], garnet [11], beryl [12, 13] and many others.

The concentrations of the main isomorphic impurity elements in the samples of Pai-Khoi sphalerite Mn, Cd, Fe [14], as well as partially Cu and Ga were determined earlier by wet chemistry and microprobe analysis. In the present study, the list of elements determined by LA-ICP-MS was extended to 18 elements: Ag, Au, As, Bi, Cd, Cu, Fe, Ga, Ge, In, Mn, Ni, Pb, Sb, Se, Sn, Tl, V. Cobalt was analyzed but was not detected in any sample. Mercury was not quantitatively analyzed.

The objectives of this study are as follows: determination of isomorphic capacity of Pai-Khoi zinc sulfide with respect to a wide range of impurity elements, which previously were impossible to quantify; establishment of correlation relations between them and analysis of the type of occurrence (isomorphic impurity or in the form of microinclusions); identification of the dependence of impurity concentration on the composition of the host rocks; study of conditions of mineral formation and parameters of hydrothermal fluid, as well as features of cathodoluminescence of sphalerite.

Geological position and characteristics of the object of study.

The Pai-Khoi celestine-barite-fluorite-sphalerite-sulvanite formation is represented by an almost continuous series of small zinc ore occurrences and mineralization points confined to the linear zone of hydrothermal alteration of Lower Carboniferous C_1v-s limestones and systems of spearheading fractures in black clay shales stretching along the north-eastern part of the Pai-Khoi anticlinorium (Arkhangelsk region, Nenets Autonomous District). Numerous rocky outcrops of marine sedimentary calcareous-siliceous rocks are exposed in a narrow strip (several tens of meters wide) in the valleys of the Silova-Yakha, Kara, and Sopcha rivers. The rest of the sites are sodden and covered with tundra vegetation. The visible part of sulfide mineralization is confined only to these outcrops [1, 14]. Sphalerite is found in hydrothermal-metasomatic quartz-calcite veins 1-20 cm thick and 1-5 m long. It forms individual grains or aggregates (0.5-4 cm) of irregular shape or is represented by small crystals of regular shape (0.5-3 mm). Characteristic simple crystallographic forms of sphalerite are: tetrahedron {111}, pseudo-octahedron {111, 1$\bar{1}$1}, trigontritetrahedron {112}. Polysynthetic spinel law twins [111] of unusual wurtzite-like habitus are widespread [15]. In some cases, sphalerite aggregates are surrounded by thin rims of columnar calcite.

Rare crystals of wurtzite in paragenesis with sphalerite are formed by several simple crystallographic forms: hexagonal prism {1120}, pyramid {1121}, pinacoid {0001}. The same crystallographic forms are characteristic of sphalerite twins. X-ray diagrams and strokes on faces of prism and pyramid allow to identify crystals of sphalerite twins. Wurtzite is characterized by the presence of 2H

This is an open access article under the CC BY 4.0 license

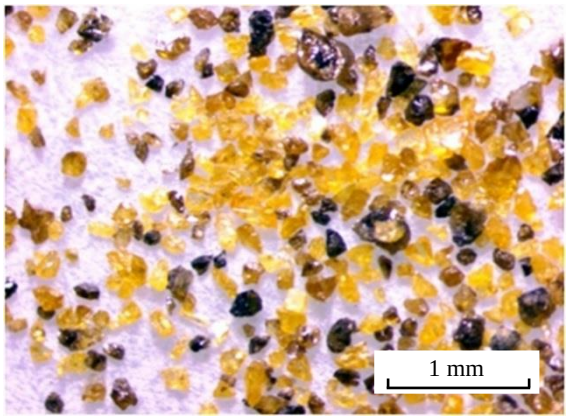

Fig.1. Monomineral fraction (sample M-454) of Cd-, Mn-sphalerite grains isolated from a quartz-calcite vein

Fig.2. Crystals of polysynthetic sphalerite twins (3C/3C'), sample B-1003 [15]

and 4H polytypes that form accretions with polysynthetic sphalerite microtwins (3C/3C′). The features of polytypy and twinning of these crystals were described in [15].

Sphalerite of the Goniatite occurrence has colours varying from light yellow to dark orange, red, brown, brownish-red and brown (Fig.1, 2). Regular brightening of sphalerite colour is observed up the section of the Visean-Serpukhov (C_1v-s) calcareous-slate strata saturated with sphalerite-bearing quartz-calcite veins. The sulfide content in the veins varies from 0.1 to 2 vol.%. Some of sphalerite crystals and grains are zonal: the inner part is dark orange and the outer part is orange-yellow. Zoning is indistinguishable in reflected light, but it is clearly visible in the dark field of the ore optical microscope, on images in the backscattered electron (BSE) mode [14]. Numerous but small in homogeneities arising from the polycrystalline structure of grains, increased content of manganese, cadmium and other impurities are clearly visible only in the cathodoluminescence mode.

Cadmium sphalerite in association with yushkinite $V_{1-x}S{\cdot}n[(Mg, Al)(OH)_2]$, fluorite and sulvanite [16, 17] often contains solid mineral and gas-liquid inclusions. Visible solid inclusions are represented by sulvanite and vein nonmetallic minerals. The size of fluid inclusions varies from 0.003 to 0.05 mm. The value of the filling factor varies within narrow limits – 0.90-0.95. The shape of gas-fluid inclusions is isometric (rounded) or in the form of well-defined negative crystals: in sphalerite the shape of negative crystals is tetrahedral or cubo-tetrahedral. Crushing of quartz-calcite veins causes a distinct hydrogen sulfide odour. The presence of nugget sulfur and hydrogen sulfide is confirmed by N.V.Sokerina, the temperature of formation of mineral association Cd-sphalerite is estimated at 120-150 °C [18].

The chemical composition of the studied sphalerite samples has noticeable features – it is dominated by varieties with an abnormally high content of manganese (up to 14.53 mol.% MnS) and cadmium (up to 3.83 mol.% CdS) and with a very low iron content – 0.01- 0.30 mol.% [14]. Crystals with high Mn and Cd content are usually represented by syntactic intergrowths of 2H and 4H wurtzite polytypes with polysynthetic sphalerite twins. Unusual impurities of V and Ni, as well as relatively high contents of Cu, Ga, Tl, Sb and Sn make this type of sphalerite an excellent object for research. The maximum concentration of impurities is noted in dark brown crystals. The high V content may be due to microinclusions of sulvanite Cu_3VS_4 or similar minerals.

The chemical composition of the studied samples is closely related to the type of host rocks [14]. Manganese-containing sphalerite is associated with black siliceous-carbonaceous-clayey shales, and cadmium-bearing sphalerite is associated with limestones. Obviously, this reflects the connection between mineral formation and the pH environment: Mn-containing sphalerite crystallized under moderately acidic conditions; on the contrary, Cd-sphalerite – under moderately alkaline conditions.

This is an open access article under the CC BY 4.0 license

Lavender-yellow Cd-sphalerite, containing up to 7.83 wt.% Cd (6.83 mol.% CdS), occurs in the northeastern part of the western flank of the Pai-Khoi anticlinorium in quartz-calcite veins among Serpukhov (C_1s) limestones of similar age and siliceous shales [16].

We attribute the Mn-, Cd-containing sphalerite with sulvanite of the Goniatite occurrence to the first (I) mineral assemblage. Limestones of different ages contain quartz-calcite veins with Cd-sphalerite, which is a member of three mineral assemblages: (II) sphalerite-sulvanite-yushkinite-fluorite (Fluorite stream, Yushkinite gorge in the upper reaches of the Silova-Yakha river basin, limestones of the Serpukhov stage C_1s, lavender-yellow sphalerite); (III) sphalerite-(sulvanite)-fahlore-V-As-germanite – (middle reaches of the Silova-Yakha River, C_2, lavender-yellow sphalerite); (IV) fluorite-galena-sphalerite (Buredan fluorite deposit, Serpukhov C_1s limestones with brown-red sphalerite) [1, 16, 19].

Cadmium-bearing sphalerite occurs in the form of transparent brownish-red or lavender-yellow isometric grains, and also exists in crystals of hexagonal habitus, which are polysynthetic twins or 6H polytypes. Characteristic features of its composition are the absence of iron and low manganese content [16]. Thus, we can observe a mechanism of direct substitution of Zn↔Cd. The variations and impurity concentrations are generally similar to Mn-bearing zinc sulfides; however, the absence of Sb and the presence of As and Ge are important indicators of this type of sphalerite. High concentrations of arsenic and germanium are very probably related to microinclusions of V-As-germanite [19].

The specific composition of the studied sphalerite affects its physical properties. The studied Cd-sphalerite exhibits photoluminescence with maximum luminescence peaks at 485-495 and 580-590 nm, which is due to the presence of copper and manganese centres. The intensity of luminescence decreases with increasing cadmium and manganese content, which is in good agreement with studies of similar materials. A prolonged phosphorescence was also observed for these samples. A less intense photoluminescence peak at 590 nm was noted for manganese sphalerite [14]. This luminescence goes out with increasing Mn concentration.

The thermoluminescence of Cd-bearing sphalerite is also specific. The maximum thermoluminescence levels are noted at 70 °C, another peak with lower intensity at 200 °C. The Cu ion replacing Zn is responsible for the appearance of electron capture centres, forbidden zone energy $E_j(70°)$ = = 0.37 eV. Analyses of thermoluminescence spectra show that this energy is transferred to the emission centres Cu (530 nm) and Mn (590 nm) Thermoluminescent properties of Mn-sphalerite are different: maximum thermoluminescence is observed at 200-210 °C and 280-320 °C, with the intensity of the second peak 3-6 times lower compared to the first peak; they are associated with the emitting Mn-centres. The total thermoluminescence level for Cd-sphalerite is 10-100 times higher than for Mn-sphalerite [14]. Any types of luminescence are not characteristic for iron-bearing zinc sulfides.

Clear correlations between chemical composition and cell parameter of the studied crystals have been established. Cd and Mn impurities lead to an increase in the cell parameter of ZnS (Mn-sphalerite: a_0 = 5.416-5.449, average 5.429 Å; Cd-sphalerite: a_0 = 5.413-5.437, average 5.420 Å), the following regression equation was calculated for ZnS with Cd, Mn, Fe impurities:

$$a_0 = 5.4083 + 0.000456X + 0.00210Y + 0.00424Z, \quad (1)$$

where X, Y, Z are the concentrations of FeS, MnS, CdS in mol.%, respectively [14].

This relationship closely corresponds to the known Skinner equation [20] for synthetic sphalerite crystals.

The influence of chemical composition on sphalerite density (D) was revealed earlier for both Mn- and Fe-bearing sphalerites. The density of Mn-ZnS (3.981-4.075 g/cm^3, average 4.040 g/cm^3) and Fe-bearing sphalerites (3.972-4.094, average 4.071 g/cm^3) is lower than the theoretical density of pure sphalerite (4.089 g/cm^3). On the contrary, the density of Cd-ZnS is higher (4.088-4.129, average 4.101 g/cm^3) [14]. The following regression equation was calculated:

$$D = 4.081 - 0.00498X - 0.00817Y + 0.00741Z, \quad (2)$$

where X, Y, Z are FeS, MnS, CdS mol.%, respectively [14].

This is an open access article under the CC BY 4.0 license

Mn- and Fe-bearing sphalerite is paramagnetic, while Cd-bearing sphalerite is diamagnetic. Therefore, the magnetic susceptibility χ of crystals from a collection of Fe- and Mn-containing sphalerite was studied [14]. The following equation relating the concentrations of these impurities and the magnetic susceptibility was proposed:

$$\chi = -0.30 + 1.10X + 1.68Y \cdot 10^{-6} \text{ cm}^3/\text{g}, \quad (3)$$

where X and Y are the concentration of Fe and Mn, %.

Thus, the chemical composition of sphalerite containing Mn, Cd and Fe can be fairly confidently calculated from its physical properties. To achieve this goal, it is necessary to solve the system of three equations (1)-(3) with three known crystallochemical and physical parameters [14].

The ZnS-MnS system was studied in hydrothermal conditions at temperatures of 300-550 °C and pressure of 500-1500 atm [14], and the ZnS-CuS system was similarly studied [21]. Based on the obtained results and literature data, isobaric (1000 atm) cross sections of the subsolidus part of the phase diagram of these systems were constructed. A single-crystal X-ray study of artificial crystals representing a mixture of sphalerite and wurtzite-2H was carried out. It was found that isomorphous admixture of manganese and copper in zinc sulfide significantly reduces the temperature of the phase transition between sphalerite and wurtzite.

Methods.

Chemical analyses of the Pai-Khoi sphalerite collection were carried out by the EPMA (JEOL JXA-8200 microanalyser equipped with five wave dispersive spectrometers) and LA-ICP-MS (Thermo XSeries 2 quadrupole mass spectrometer with New Wave UP213 laser sampling system) methods according to the standard methodology at the IGEM-Analytics collaborative centre in IGEM RAS. Microthermometric study was carried out at IGEM RAS using a measuring complex consisting of a Linkam THMSG 600 camera (England) mounted on an Olympus BX51 microscope (Japan), combined with a video camera and a control computer. The chemical composition of the fluid in the inclusions was estimated from measurements of phase transitions and transformations that occurred during heating and cooling of the polished plate. The accuracy of the temperature measurement was 0.2 °C in the temperature range from –20 to +20 °C; it decreases at higher and lower temperatures.

The composition of salts prevailing in the aqueous solutions of fluid inclusions was estimated by measuring the melting point of the eutectic [22]. The total concentration of salts in two-phase fluid inclusions was calculated from the ice melting temperature based on experimental data for the NaCl-H_2O system [23]. Salt concentrations and liquid densities were estimated using FLINCOR software [24].

Studies by the colour cathodoluminescence (CCL) method of sphalerite were carried out in the LAMV laboratory of IGEM RAS (O.M.Zhilicheva) on the X-ray microanalyser MS-46 of the "Cameca" company. The optical system of the device was upgraded and adapted to a high-resolution CCD-digital camera of "Videoscan" (Russia) model 285/C/P-USB (SONY ICX285AQ, colour, TE-cooled). Control software "Videoscan Viewer". Unlike commercially produced types of CL detectors, the proposed scheme developed in Glaukon OOO (Russia) allows to obtain images of cathodoluminescence in real colours and subject them to further mathematical processing. Luminescence excitation in the samples was carried out by electron beam irradiation in vacuum at room temperature. CCL registration was carried out in the screen mode at an accelerating voltage of 20 kV and a current of 25 nA. The exposure time of one frame in the scanning mode was 240 s. Due to the constructive limitation of the imaging area and to achieve stability of the probe characteristics, it is possible to register either individual small grains or a consecutive series of frames of larger extractions with a window of 300 × 350 μm. The preparations were sputtered with a thin layer of carbon.

The advantage of the cathodoluminescence facility at IGEM RAS is the possibility of using two wave spectrometers for phase identification in the (BSE) mode and direct visualization of the CCL colour at the point of electron probe incidence.

Cathodoluminescence. One of the features of Mn- and Cd-bearing sphalerites is intense cathodoluminescence. This characteristic and well-known property of manganese-cadmium sphalerites is never

This is an open access article under the CC BY 4.0 license

observed in iron-rich varieties. In grains of manganese-cadmium sphalerite cathodoluminescence in orange and orange-brown luminescence is intensely manifested over the entire surface, and bright orange only in some parts of the crystal. The intensity of cathodoluminescence decreases with increasing Mn content.

The cathodoluminescence of sphalerite crystals from quartz-calcite veins in four mineral associations of the Pai-Khoi province was studied in order to typify sphalerite by colour and reveal its internal structure: (I) Orange, yellow, brown colouredsphalerite from Mn-, Cd-bearing sphalerite-wurtzite-sulvanite-quartz-calcite association in limestones and schists of Visean age (C_1v) – Goniatite occurrence; (II) Lavender-yellow sphalerite of Cd-sphalerite-sulvanite-yushkinite-fluorite-quartz-calcite association in limestones of Serpukhov (C_1s) age [16, 17]; (III) lavender-yellow sphaleritefrom Cd-sphalerite-(sulvanite)-fahlore-V, As-germanite-quartz-calcite association in limestones of Middle Carboniferous (C_2) age; (IV) red sphalerite from Cd-sphalerite-chouleite-galenite-fluorite-quartz-calcite association in limestones of Buredan occurrence of Serpukhov age (C_1s). The chemical composition of polished preparations of sphalerite (Table 1) was analyzed by the microprobe.

Table 1

Normalized chemical composition (EPMA) of a representative sample of sphalerite and wurtzite of the Pai-Khoi anticlinorium (for the study by CCL method), wt.%

Samples	Association	Zn	Mn	Cd	Fe	S	Sum
M-443	I	62.91	2.26	2.06	0.01	32.76	100.0
M-446	– " –	59.66	5.50	1.82	0.02	33.00	100.0
M-457a	– " –	58.83	6.11	2.05	0.01	33.00	100.0
M-462g	– " –	62.50	2.24	2.57	0.02	32.67	100.0
M-464	– " –	61.53	3.70	1.84	0.07	32.86	100.0
M-410	II	63.38	0.21	4.03	0.02	32.36	100.0
M-431	III	64.64	0.33	2.43	0.01	32.59	100.0
M-415	IV	66.44	0.07	0.64	0.03	32.82	100.0

We obtained 160 CCL and 150 BSE images of grains and crystals of 14 sphalerite samples, including two samples of high-iron sphalerite (with 6.7-7.2 wt.% Fe), in which no CCL was shown. Manganese-cadmium sphalerites of the first (I) mineral association of the Goniatite occurrence (Fig.3) possess bright orange-brown CL luminescence caused by isomorphic manganese centres. The internal structure of crystals is expressed by: sectorial structure, growth zones with different concentration of impurities, twinning bands and zones composed of 2H, 4H wurtzite polytypes, as well as inclusions of vein minerals (quartz and calcite). Calcite has its own red-orange luminescence and often forms thin rims (up to 10-30 μm) of columnar-fibrous structure around sphalerite grains. Quartz does not glow and appears in the obtained images as a black structureless field.

Crystals and grains of cadmium sphalerite of all three other mineral associations have homogeneous composition and do not possess noticeable features of internal structure, and the intensity of colouring of CCL is conditioned only by the thickness of preparations. However, they luminesce differently in the three colours. Cd-sphalerite (II) of the mineral association has a very bright blue luminescence (Fig.4), and sphalerite (III) of the mineral association has a bright green luminescence (Fig.5 *a*, *b*), which may be due to the corresponding impurities (centres) entering the crystal structure in accordance with the following heterovalent isomorphism schemes: $Cu^{+} + Ga^{3+} \rightarrow 2Zn^{2+}$ or $Ag^{+} + Ga^{3+} \rightarrow 2Zn^{2+}$ [14].

Cd-sphalerite crystallites (Fig.5 *c*, *d*) from the Buredan sphalerite-galenite-fluorite occurrence (IV association) have brown CCL (with Mn^{2+} and Ge^{4+} luminescence centres). The peculiarity of sphalerite of this occurrence is the presence of thin rims of chouleite around all sphalerite grains 5-10 μm thick with a green CCL.

This is an open access article under the CC BY 4.0 license

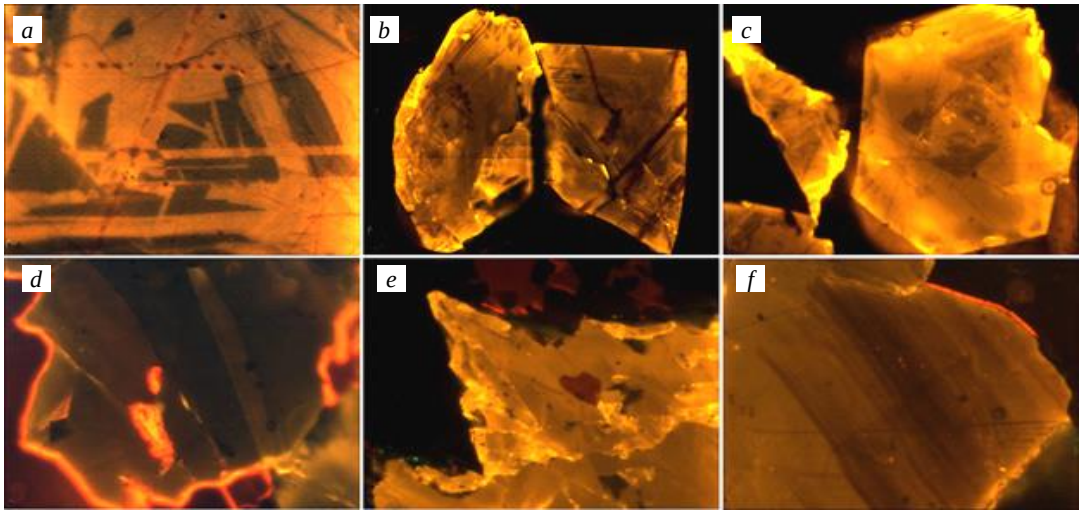

Fig.3. Orange-brown cathodoluminescence of Mn-, Cd-bearing sphalerite (*a, b, d-f*) and wurtzite (*c*) of the Goniatite occurrence. Samples: *a* – M-443, *b, c* – M-446, *d* – M-457a, *e* – M-462g, *f* – M-464. The width of all images is 350 μm

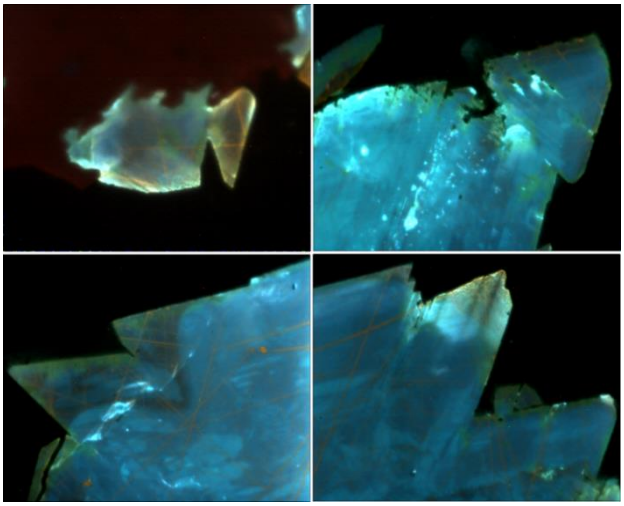

Fig.4. Blue cathodoluminescence of cadmium sphalerite from (II) mineral association, sample M-410. Image width 350 μm

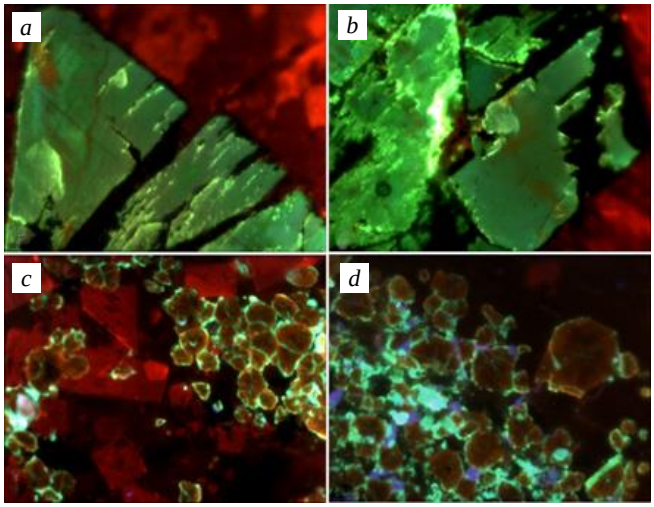

Fig.5. Green cathodoluminescence of cadmium sphalerite (*a, b*) from mineral association III, sample M-431. Brown cathodoluminescence of cadmium sphalerite (*c, d*) from mineral association IV, sample M-415. Calcite glows red, fluorite – violet, chouleite (CdS) – green, quartz (black) has no luminescence

Trace elements in sphalerite and wurtzite. Twenty-seven samples (82 analysis points) were studied by the LA-ICP-MS method. The analyses were performed both in point (in the centre, in the middle and along the outer edge of grains) and linear (profile ablation) modes (Fig.6). The profile ablation mode was used to study the distribution of minor trace elements in grains. The distribution of all studied elements in different grains of the same sample is homogeneous. At the same time, significant variations were noted in the compositions of several grains of a number of samples. The results of studies of chemical composition of sphalerite of Goniatite occurrence and their statistical processing are presented in Tables 2-5. In Tables 2 and 3 the results of chemical analyses are given only partially (in Table 2 – 14 samples, 42 points of analyses; in Table 3 – 9 samples, 27 points of analyses). Due to the large amount of information, only the most representative samples were selected for publication on the grounds of diversity and breadth of sampling variation. The statistical sampling (Tables 4, 5) includes all analyzed samples: Mn, Cd-ZnS – 13 samples, 43 analyses (from shales); Cd, Mn-ZnS – 14 samples, 39 analyses (from limestones). In addition, we expected to find monomineral zones and crystal sections composed only of sphalerite and only of wurtzite, with

This is an open access article under the CC BY 4.0 license

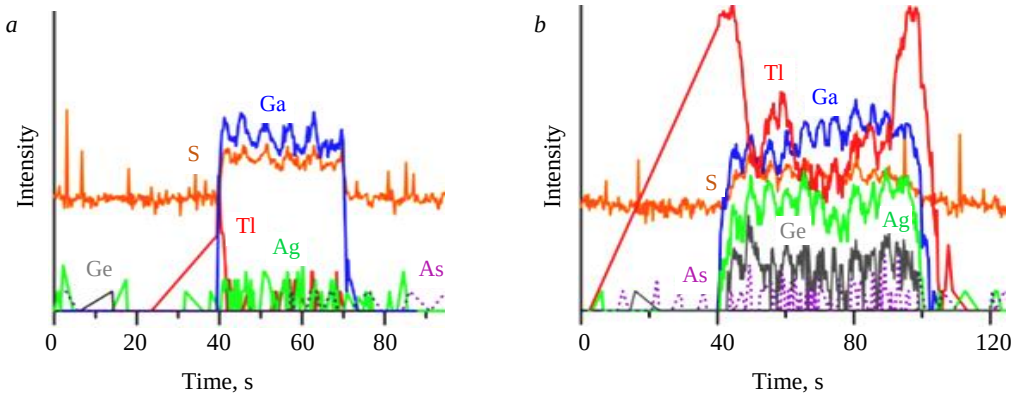

Fig.6. Typical LA-ICP-MS spectra of composition distribution of Pai-Khoi Mn-, Cd-sphalerites along the grain profile: *a* – yellow sphalerite (M-454) without impurities of paragenetic minerals; *b* – brown sphalerite (M-455) with visually invisible sulvanite (colusite?) ingrowth. Fluctuations of S and impurity elements (Tl, Ga, Ge, As, Ag) contents were revealed. The size of the zone of increased isomorphic contents of S, Ga, Ag is 30 μm, inclusion is 50 μm

different capacities with respect to impurity elements. However, without the involvement of local X-ray diffraction studies, it has not yet been possible to do so. Manganese sphalerite has relatively higher isomorphic capacity with respect to many elements: Fe, In, Ga, Se, Au, Ni, As. Cadmium sphalerite has relatively higher isomorphic capacity with respect to Ge, Tl, Sb, Sn, V.

Table 2

EPMA analyses of zinc sulfide of the Goniatite occurrence, wt.%

Sample number	Average composition (2σ)					Colour of sphalerite grains Intervening rock
	Zn	Mn	Cd	S	Sum	
M-453	64.43 0.17	1.60 0.07	1.16 0.02	32.84 0.11	100.03	Brown limestone
M-454	63.27 0.29	1.41 0.05	2.71 0.14	32.62 0.17	100.01	Yellow and brown limestone
M-455	63.37 0.30	1.28 0.05	2.76 0.05	32.6 0.09	100.01	Brown limestone
M-456	62.72 0.18	2.49 0.85	2.02 0.28	32.78 0.04	100.01	Brown limestone
M-458a	62.29 0.20	1.83 0.02	3.26 0.19	32.56 0.15	99.94	Brown limestone
M-459a	63.66 0.26	1.25 0.03	2.40 0.12	32.65 0.13	99.96	Yellow limestone
M-459-2	63.71 0.28	1.25 0.03	2.32 0.17	32.66 0.17	99.94	Yellow limestone
M-463	61.55 0.25	3.67 0.16	1.83 0.09	32.88 0.27	99.93	Red-orange black slates
M-709	63.84 0.24	1.22 0.16	2.29 0.18	32.66 0.11	100.01	Brown limestone
M-713	62.33 0.16	2.47 0.13	2.46 0.11	32.72 0.16	99.98	Yellow and brown limestone
M-719	60.26 0.34	4.98 0.21	1.80 0.11	32.97 0.21	100.01	Brown black slates
M-720	62.66 0.23	1.86 0.12	2.83 0.08	32.63 0.12	99.98	Brown limestone
M-732	63.73 0.15	1.02 0.05	2.67 0.08	32.6 0.14	100.02	Brown limestone
M-734	61.38 0.26	3.71 0.20	2.02 0.16	32.86 0.21	99.97	Orange and brown black shale

This is an open access article under the CC BY 4.0 license

Table 3

Chemical composition of Pai-Khoi sphalerite samples (Goniatite occurrence) according to LA-ICP-MS data (27 analysis points), g/t

Sample number	Content of impurity elements in sphalerite (mean±2σ), minimum-maximum values								
	Mn (1)	Cd (3)	Fe (3)	In (0.1)	Ga (0.1)	Ge (0.4)	Tl (0.02)	Ag (0.3)	Se (4)
M-453	16100±3300 14000-17700	14900±500 14600-15000	56±22 43-68	8.2±3.9 5.4-10.1	238±37 218-255	1.4±0.7 Bdl-1.7	0.84±0.73 Bdl -1.51	1.5±1.2 0.2-2.8	60±22 76-533
M-454	14700±150 14600-14900	34500±4800 27400-38000	150±42 123-174	13.6±1.3 12.1-14.8	457±39 404-486	1.3±0.7 Bdl-2.0	0.97±0.73 0.09-1.75	1.7±0.9 1.12-2.1	308±81 256-343
M-455	13100±2800 11800-14600	24300±700 23700-25000	197±64 169-232	17.0±3.7 14.9-18.2	717±363 508-835	16.6±3.0 14.7-18.7	56.04±38.67 16.30-91.70	64.5±21.6 52.2-72.3	218±154 51-348
M-456	41400±6200 39600-43200	15000±4000 13700-17300	122±89 79-168	7.2±2.7 6.1-8.7	277±55 250-313	5.1±0.1 5.0-5.2	2.92±1.34 1.85-4.11	5.16±2.15 4.47-6.4	32±22 20-42
M-709	11300±1200 11000-12000	19000±2600 17800-20400	58±30 43-73	8.4±2.8 7.0-9.8	599±107 493-737	2.1±0.9 1.0-3.3	3.27±0.79 2.52-4.10	4.4±2.8 1.4-7.2	61±11 55-66
M-719	46400±10500 43200-52400	10700±3000 9100-12100	181±82 134-207	9.6±5.6 7.12-8.6	479±81 398-571	10.1±6.8 2.4-17.7	2.69±1.07 1.72-3.86	4.8±4.1 Bdl-8.6	475±244 226-690
M-721	15200±3700 13800-17300	16800±1500 16000-17500	120±21 109-130	10.7±3.7 8.8-12.4	500±152 338-652	9.2±6.5 1.3-16.5	2.17±0.73 1.81-2.54	25.1±19.0 3.0-44.4	113±37 93-130
M-732	10400±800 10000-10800	21200±3700 17500-24800	166±45 147-191	9.1±1.8 8.2-10.0	321±191 226-417	1.8±1.7 Bdl-3.6	8.20±5.14 2.11-13.70	2.4+1.4 0.7-4.0	335±75 292-361
M-734	40100±7600 35900-44700	14400±2300 13300-15500	153±75 110-178	22.1±12.4 16.5-29.8	632±308 371-917	1.6±1.3 0.7-3.0	2.11±0.72 1.60-2.45	8.3±5.8 Bdl-15.1	74±6 69-81

Sample number	Content of impurity elements in sphalerite, minimum-maximum values								
	Cu (8)	Au (0.04)	Ni (0.6)	As (1.8)	Sb (0.06)	Bi (0.02)	Pb (0.04)	Sn (0.2)	V (0.1)
M-453	243-572	Bdl-0.21	Bdl	Bdl	Bdl-0.47	Bdl-0.53	1.09-2.27	0.5-26.6	Bdl-22.6
M-454	467-511	Bdl-0.53	1.0-2.1	Bdl	0.23-0.52	0.03-1.00	1.22-1.97	1.2-11.6	Bdl-5.0
M-455	2290-2780	0.02-0.49	1.0-2.9	8.3-12.9	52.90-82.90	0.16-0.41	1.41-2.89	281-427	174.0-235.0
M-456	455-749	Bdl-0.65	0.4-2.1	2.2-8.7	5.63-17.40	0.08-0.56	0.95-1.73	33.5-74.5	22-51.3
M-709	635-1073	Bdl	Bdl-1.1	Bdl-3.3	2.90-18.90	0.07-0.28	0.86-1.22	8.7-54.8	9.4-51.5
M-719	700-1074	Bdl-0.21	Bdl-1.1	Bdl-3.1	3.30-8.50	0.28-1.22	0.83-1.49	18.5-125	12.9-89.0
M-721	504-2013	0.34-0.63	Bdl-1.1	1.5-6.2	5.22-50.80	0.12-0.63	0.73-1.06	30.7-323	16.7-199.0
M-732	289-641	0.12-1.20	1.0-1.5	1.9-3.4	0.32-5.52	0.23-0.82	1.03-2.33	2.4-28.9	1.2-21.4
M-734	408-1020	0.05-2.50	Bdl-10.8	Bdl-3.0	0.99-6.08	0.22-0.59	0.97-2.51	13.0-61.7	Bdl-37.1

Note. The chemical element symbol is followed by the detection limit. Samples M-455 and M-721 contain thin emulsion phenocrysts of sulvanite (Cu_3VS_4); samples M-453, M-454, M-455, M-456, M-709, M-721, M-732 – from veins in limestone; samples M-719 and M-734 – from veins in shale. Bdl – below detection limit.

This is an open access article under the CC BY 4.0 license

Journal of Mining Institute. 2024. Vol. 270. P. 861-876

©Aleksandr B. Makeyev, Ilya V. Vikentyev, Elena V. Kovalchuk, Vera D. Abramova, Vsevolod Yu. Prokofyev, 2024

This is an open access article under the CC BY 4.0 license

Journal of Mining Institute. 2024. Vol. 270. P. 861-876

©Aleksandr B. Makeyev, Ilya V. Vikentyev, Elena V. Kovalchuk, Vera D. Abramova, Vsevolod Yu. Prokofyev, 2024

Table 4

Correlation matrix of Pai-Khoi sphalerite composition (82 points of analyses)

Elements	Mn	Cd	Fe	In	Ga	Ge	Tl	Ag	Se	Cu	Au	Ni	As	Sb	Bi	Pb	Sn	V
Mn	1	–0.531	0.137	0.331	–0.022	–0.170	–0.220	–0.136	0.408	–0.179	0.204	0.045	0.496	–0.280	0.113	0.066	–0.272	–0.188
Cd	–0.531	1	–0.063	–0.089	0.132	0.089	0.166	0.119	–0.040	0.205	–0.211	–0.102	–0.188	0.254	–0.208	0.011	0.268	0.148
Fe	0.137	–0.063	1	–0.007	–0.069	0.020	0.024	–0.009	0.050	–0.017	0.059	0.057	0.008	–0.025	–0.016	0.013	–0.011	–0.017
In	0.331	–0.089	–0.007	1	0.665	0.018	0.079	0.012	–0.090	0.302	0.391	–0.110	0.134	0.131	0.045	0.151	0.133	0.051
Ga	–0.022	0.132	–0.069	0.665	1	0.067	0.326	0.327	–0.236	0.701	0.060	–0.097	0.031	0.499	–0.112	–0.116	0.555	0.395
Ge	–0.170	0.089	0.020	0.048	0.067	1	0.056	0.037	0.011	0.100	–0.015	–0.036	–0.068	0.094	–0.040	–0.090	0.100	0.079
Tl	–0.220	0.166	0.024	0.079	0.326	0.056	1	0.233	0.072	0.463	–0.061	–0.045	0.056	0.579	–0.062	–0.017	0.497	0.353
Ag	–0.136	0.119	–0.009	0.012	0.327	0.037	0.233	1	–0.059	0.518	0.035	0.301	0.253	0.503	–0.057	0.012	0.553	0.451
Se	0.408	–0.040	0.050	–0.090	–0.236	0.011	0.072	–0.059	1	–0.059	0.065	0.021	0.368	–0.106	0.107	0.114	–0.127	0.071
Cu	–0.179	0.205	–0.017	0.302	0.701	0.100	0.463	0.518	–0.059	1	–0.007	–0.086	0.234	0.854	–0.103	–0.035	0.929	0.895
Au	0.204	–0.211	0.059	0.391	0.060	–0.015	–0.061	0.035	0.065	–0.007	1	0.144	0.265	–0.042	0.490	0.439	–0.083	–0.112
Ni	0.045	–0.102	0.057	–0.110	–0.097	–0.036	–0.045	0.301	0.021	–0.086	0.144	1	0.172	–0.067	0.130	0.113	–0.070	–0.075
As	0.496	–0.188	0.008	0.134	0.031	–0.068	0.056	0.253	0.368	0.234	0.265	0.172	1	0.276	0.292	0.367	0.194	0.248
Sb	–0.280	0.254	–0.016	0.131	0.499	0.094	0.579	0.503	–0.106	0.854	–0.042	–0.067	0.276	1	–0.095	–0.019	0.925	0.732
Bi	0.113	–0.208	0.113	0.045	–0.112	–0.040	–0.062	–0.057	0.107	–0.103	0.490	0.13	0.292	–0.095	1	0.436	–0.112	–0.123
Pb	0.066	0.011	0.113	0.151	–0.116	–0.090	–0.017	0.012	0.114	–0.035	0.439	0.113	0.367	–0.119	0.436	1	–0.012	–0.080
Sn	–0.272	0.268	–0.011	0.133	0.555	0.100	0.497	0.553	–0.127	0.929	–0.083	–0.070	0.194	0.925	–0.112	–0.012	1	0.812
V	–0.188	0.148	–0.017	0.051	0.395	0.079	0.353	0.451	0.071	0.895	–0.112	–0.075	0.248	0.732	–0.123	–0.080	0.812	1

Note. The intensity of the colouring of the cells shows an increase in the degree of correlations.

Table 5

Statistical parameters of composition of Pai-Khoi sphalerites, g/t

Indicator	*T*, °C	Components (min & max)																	
		Mn	Cd	Fe	In	Ga	Ge	Tl	Ag	Se	Cu	Au	Ni	As	Sb	Bi	Pb	Sn	V
Number of points	48	82	82	82	82	82	82	82	82	82	82	82	82	82	82	82	82	82	82
Sample $n = 27$	min	9550	9060	27	2.68	144.5	0.14	0.05	0.17	46	185	0.01	0.28	1.18	0.07	0.02	0.73	0.33	0.05
	max	62800	38000	1680	53	952	362	91.7	254	690	3060	34.3	210	17.9	82.9	52	7.13	436	390
Average indicators	157.2	31267	17632	154.3	12.16	402.2	7.70	3.44	12.87	263.0	724.0	1.44	6.74	6.40	7.84	2.11	2.17	49.5	38.9
Mn, Cd-ZnS	167.4	45724	14658	180.4	14.89	415.0	2.76	0.93	12.62	308.7	669.5	2.21	10.91	8.04	4.81	2.25	2.19	29.1	32.8
Cd, Mn-ZnS	147.7	16105	20752	127.0	9.29	388.8	12.88	6.07	13.14	215.0	781.2	0.64	2.37	4.69	11.01	1.95	2.15	70.9	45.3

Note. Orange-red Mn, Cd-ZnS sphalerite is confined to shales, and yellow-brown Cd, Mn-ZnS is confined to limestones. Manganese sphalerite has relatively large isomorphic capacity with respect to Fe, In, Ga, Se, Au, Ni, As. Cadmium sphalerite has a relatively large isomorphic capacity with respect to Ge, Tl, Sb, Sn, and V. Temperature calculated from geothermometer [6]. Samples with very high vanadium content showed unrealistic values, so data from only 48 samples are considered.

Table 4 presents the results of correlation analysis of the total sample for all (n = 82) observation points. Threshold value r = 0.14, with 95% confidence interval. The following elements are positively correlated with each other: Cu, V, Ga, In, Sn, As, Sb, Bi, Pb, Tl, Se, Ag, Au, Ni; negatively to them – Cd, Mn and Ge. For a part of elements pair correlation is not established. The first set of impurity elements tends both isomorphous incorporation into zinc sulfide and formation of microinclusions of various chalcogenides: sulvanite, colusite, renierite, stannite, fahlore and others. The second combines isomorphic elements-impurities.

All studied samples were characterized by low Fe content, varying from 43 to 293 g/t. This is characteristic of low-temperature varieties of zinc sulfide and corresponds to the light colour of its crystals, Au content is below 2.5 g/t, Ni usually does not exceed 10 g/t, but often below their detection limits.

The most important feature of zinc sulfides of the Pai-Khoi anticlinorium is the presence of V in their chemical composition. It should be reminded that sulvanite is a paragenetic mineral in the described mineral association. The ratio of sulvanite : sphalerite ≈ 1 : 10. Grains and cubic crystals of sulvanite 0.5-2 mm in size are present in each sample. To a visually controlled monomineral quality, these two minerals are fairly "cleanly" separated in the concentrate by magnetic separation (as sulvanite is diamagnetic). Sample M-455 shows maximum V content (up to 235 g/t). It also attracts attention with slightly higher concentrations (g/t) compared to the other samples: Ge 14.7-18.7; In 8.2-14.9; Cu 2290-2780; Ag 52-72.3; As 8.3-12.9; Sb 52.9-82.9; Tl 16.3-91.7. In addition, it is less homogeneous compared to other samples. This fact can be explained by the presence of tiny submicron inclusions of sulvanite – Cu_3VS_4 and colusite group minerals – $Cu_{26}V_2(As, Sn, Sb)_6S_{32}$ in the sphalerite matrix (Fig.6). These inclusions are invisible even with scanning electron microscopy. Sulvanite and colusite have a close structure, consisting of the same elements, which could be incorporated into the sphalerite structure, forming the same type of inclusions in it. The only difference is the value of the unit cell parameter. Moreover, both sulvanite and colusite are marked in ore occurrences of the province by their own mineral phases [19]. The same regularities can be found in other samples, except for yellow-coloured samples of sphalerite M-453 and M-454. Concentrations of all impurities in these samples are 10 times lower in comparison with sulvanite- and colusite-bearing ZnS grains. Thus, samples with numbers M-453 and M-454 represent "pure" monomineral zinc sulfide without solid microinclusions.

Some elements prefer to accumulate in sphalerite and wurtzite as inclusions of separate minerals. The ratio of antimony and arsenic contents (Sb > As) is the same in all samples. The maximum value of C_{Sb} antimony concentration is 82.9 g/t. In some cases, $C_{Sb} > C_{As}$ by a factor of 5-10, see, for example, sample M-721 (Table 3), in which C_{As} ranges from 1.5 to 6.2 g/t and C_{Sb} ranges from 5.2 to 50.8 g/t. Compared to other semi-metal elements. Bi content in the samples is minimal. Bismuth was not detected in light coloured ZnS grains (C_{Bi} does not exceed 1 g/t), although its concentration for dark grains is only slightly higher (up to 1.22 g/t).

In dark-coloured samples, Ge content ranges from 1 to 18.70 g/t, Ga from 277 to 917 g/t, Tl from 1.72 to 91.70 g/t, and Ag from "not detected" to 52.2 g/t. Recall that earlier [14] very high local concentrations of gallium in brown wurtzite-4H of the same province were determined using microprobe. In pure yellow-coloured sphalerite these concentrations are much lower (g/t): Ge content varied from "not detected" to 1.97, Ga from 218 to 487, Tl from "not detected" to 1.75, Ag from 0.21 to 2.75.

Fluid inclusions. Fluid inclusions were studied in preparations (polished plates of sample B-1003) made from a quartz vein with prismatic orange-red crystals (see Fig.2), composed of polysynthetic twins of manganese sphalerite from a rocky outcrop in the valley of the river Putyu, southeastern slope of the Pai-Khoi anticlinorium [15].

According to known criteria [25], primary, secondary, and mixed primary-secondary fluid inclusions were identified among fluid inclusions in quartz (Fig.7). Fluid inclusions that are uniformly

This is an open access article under the CC BY 4.0 license

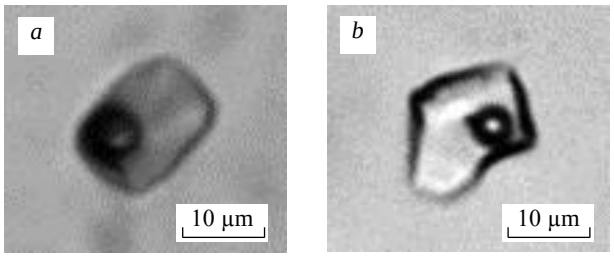

Fig.7. Primary (*a*) and primary-secondary (*b*) two-phase fluid inclusions in quartz in accretion with sphalerite (ZnS-Mn)

distributed throughout the host mineral or related to growth zones are primary. Inclusions confined to cracks cutting the host mineral are considered secondary. Primary-secondary fluid inclusions are confined to cracks that do not reach the outer boundaries of crystals and grains. Their composition in terms of phase filling is close to primary inclusions. In sphalerite crystals, a few analogous fluid inclusions of a similar phase composition were found – two-phase gas-liquid inclusions of water-salt solutions. Due to the intense color of sphalerite, it turned out to be impossible to conduct thermo-cryometric studies, so the same primary inclusions in paragenetic quartz were chosen for the study. They are evenly distributed throughout the volume of the quartz grain. The parameters of phase transitions were obtained from primary-secondary inclusions. Secondary inclusions were not studied. The close paragenesis of these two minerals (ZnS and quartz) is proven by the presence of induction surfaces of joint growth.

Table 6 shows the results of thermo- and cryometric studies of individual fluid inclusions in quartz intergrown with sphalerite. The ore-forming fluid contained predominantly sodium chloride (NaCl). This is evidenced by the eutectic temperatures of inclusion solutions (from –22 to –21 °C). Two-phase gas-liquid inclusions in quartz (Fig.7) homogenize into liquid at temperatures from 164 to 211 °C. Salt concentration varies from 5.2 to 6.1 wt.% eq. NaCl. The density of the liquid is 0.90-0.95 g/cm^3.

Table 6

Results of thermo- and cryometric studies of fluid two-phase gas-liquid inclusions in quartz in paragenesis with sphalerite

Inclusion type	*n*	Temperature homogenization, °C	Temperature eutectic,°C	Temperature melting, °C	Concentration, wt.% eq. NaCl	Density, g/sm^3
Primary	3	211	–21	–3.8	6.1	0.90
Primary	3	196	–21	–3.9	6.2	0.92
Primary-secondary	3	182	–22	–3.2	5.2	0.93
Primary-secondary	4	164	–22	–3.8	6.1	0.95

Thus, the hydrothermal fluid from which sphalerite crystallized was characterized by a relatively low temperature (164-211 °C) and average salinity.

Discussion of results.

One of the objectives of the study was to determine the degree of monomineralisation of zinc sulfide crystals and to establish the nature and type of distribution of impurity elements in them. The greatest amount of microimpurities is characteristic of dark-coloured varieties of sphalerite (brown, dark red), and the areas with inclusions of wurtzite polytypes 2H and 4H are also confined to them [15]. Perhaps, a reliable enough way to distinguish the samples with microinclusions of sulvanite from monomineral “pure” ZnS is the presence of intercorrelating impurities of Cu, V, As, and As was not detected in samples M-453 and M-454, although “traces” of V were found in them, but only up to 22.6 g/t. Probably chalcophilic behavior of vanadium should be connected with low level of oxygen fugacity and with participation of bituminous materials in the studied mineral-forming hydrothermal system [1]. Due to the absence of As admixture it is possible to distinguish Mn-, Cd-sphalerite samples, conditionally “pure” – in contrast to ZnS grains with inclusions of other micron-sized minerals (with noticeable As admixture).

The statistical analysis of the samples (see Table 3) shows that C_{Pb} concentration is clearly not related to mineral microinclusions. Lead correlates only with Au, As and Bi. It is known that high concentrations of Pb and Sb are noted in sphalerite from Bosnia and Herzegovina [26]; researchers assume their probable isomorphic incorporation into the structure of sphalerite. Although it is also known that Pb is an isomorphous impurity in stibiocolusite [27]. The hypothesis about the presence

This is an open access article under the CC BY 4.0 license

of microinclusions of tin minerals in sphalerite is indirectly confirmed by wide variations of Sn in all samples. The maximum amount of Sn is contained in brown grains of zinc sulfide of sample M-455 (281-427 g/t), but it is also observed in yellow ZnS. There are known reports about isomorphic form of tin occurrence in sphalerite [28, 29].

The discussion of the forms of incorporation of Ge, Ga, Tl. and Ag in ZnS is a more difficult task. High concentrations of these elements can be explained both by substitution mechanisms and by the presence of individual minerals as microinclusions [30-32]. It is believed that Ag, Ga, Ge and Tl are characteristic elements for low-temperature environments of mineral formation [31-33]. However, these same elements are found in colusite group minerals: germanite and renierite with wide variations of compositions. In addition, germanite $(Cu, Ag, Tl)_{26}Fe_2(As, Sn, Ge, Sb, Bi, Ga)_6S_{32}$ often contains V [34, 35], and renierite $(Cu, Zn)_{11}Fe_4(Ge, As, Ga, Sb, Bi)_2S_{16}$ often contains Pb.

A significant isomorphic capacity of sphalerite with respect to indium and gold has been experimentally proven [36]. A more significant isomorphic incorporation of Au into sphalerite is promoted by trivalent iron and indium in heterovalent substitution mechanism.

Variations in the concentrations of Ga, In, Tl, on the one hand, and Ag, Au, Cu, on the other hand, are interconnected, and they probably enter sphalerite according to the heterovalent scheme of isomorphism $(Ga^{3+}, Tl^{3+}, In^{3+}) + (Cu^{+}, Ag^{+}, Au^{+}) \leftrightarrow 2Zn^{2+}$ [33, 36, 37]. At the same time, the same elements can be directly incorporated into colusite, sulvanite, and renierite. These circumstances do not allow us to unambiguously determine the nature of these impurities.

The concentration of In is also very informative [31, 38, 39]. Indium varies insignificantly in the composition of all samples studied by us, because usually In is not clearly included in the structure of sulvanite, colusite, germanite, renierite, stannite and other minerals, but, most likely [40], is in isomorphous form. Ga, Ge and Tl were considered as typical isomorphic impurity elements in the structure of zinc sulfides [29, 31, 32].

It is interesting to note that the existence of chemically bound form of Au in sphalerite is associated with its insignificant concentration in the "invisible" form in pyrite, arsenic pyrite and sphalerite: from 120 to 300 g/t in the Iranian deposit Zarshuran [41, 42].

Rare reports of arsenic in sphalerite [43], for example, in the Alcoran mine (Chile) and selenium [44] – in the Baccu Locci deposit (Sardinia), confirm our assumptions about the possible isomorphic form of their incorporation into sphalerite.

According to the study [18], the crystallization temperature of cadmium sphalerite from the same quartz-calcite Pai-Khoi veins in association with yushkinite is somewhat lower – 120-150 °C. The results of calculation of probable crystallization temperatures of manganese-cadmium sphalerites using the Frenzel geothermometer [45], presented in Table 5, are in good agreement with these experimental data. According to these data, high-manganese sphalerite from quartz-calcite veins localized in black shales crystallized from the fluid at a higher temperature (167 °C on average) than cadmium-manganese sphalerite, which is present in veins localized in grey limestones, where it crystallized at a lower temperature (147 °C on average).

Conclusion.

We have characterized typomorphic features (composition and properties) of low-temperature zinc sulfide of the Pai-Khoi province. Impurity elements in Pai-Khoi sphalerite – Mn, Cd, Fe, Ga, Ge, Ge, Tl, Au, In, Ni, Au, Te, Se – enter the structure of ZnS mainly isomorphically. However, our data show that many impurities (Ag, Cu, Pb, V, As, Sb, Bi, Sn, Ge) can be found in sphalerite and wurtzite grains in the form of submicroscopic (which are sometimes even invisible when using the EPMA method) inclusions of sulvanite, colusite group minerals and others. Apparently, a distinctive feature of sulvanite- and colusite-bearing ZnS is a higher content of Cu, V, and As in grains. Thus, As was not detected in the "pure" samples of Mn, Cd-ZnS (M-453 and M-454), but minimal values of V (up to 22.6 g/t) were noted in the yellow varieties, which may indicate insignificant isomorphic entry of vanadium into the sphalerite composition. Thus, the noticeable As content is an important criterion for dividing ZnS samples into "pure", on the one hand, and those containing sulvanite and colusite as inclusions, on the other hand.

This is an open access article under the CC BY 4.0 license

The list of minerals forming accretions with sphalerite can be significantly expanded due to improved analytical techniques and methods of analysis. Further studies by the EBSD method will be aimed at revealing zones in crystals composed of hexagonal ZnS-wurtzite to compare them with sphalerite sites; analysis of the chemical composition of these zones will allow to additionally characterizing the "capacity" of these minerals concerning impurity elements.

The conducted studies allowed us to typify sphalerite occurrences of four mineral associations of the Pai-Khoi anticlinorium based on the colour of cathodoluminescence and the internal structure of crystals. Crystals of Mn-, Cd-sphalerite have a characteristic internal structure (sectoriality, zonality, twinning, polytypism) and orange-brown CCL. Crystals of Cd-sphalerite of other three associations have no peculiarities of internal structure, but possess typomorphic colour of the CCL: blue, green and brown.

High contents of strategic metals Cd, Ga, Ge, In in ZnS matrix, as well as in sulvanite (V, Cu) in a single paragenesis with sphalerite were established. This sulfide mineralization in quartz-calcite veins belongs to the ores easily enriched by gravity and magnetic separation. The Goniatite occurrence is likely to require a major reassessment of the potential for commercial exploitation of this mineralization.

The authors thank O.M.Zhilicheva for assistance in cathodoluminescence studies of sphalerite and wurtzite crystals. The research used the equipment of IGEM RAS (*Center for Collective Use* "*IGEM-Analitika*").

REFERENCES

1. Yushkin N.P., Eremin N.I., Makeyev A.B., Petrov T.G. Sphalerite of the Paikhoi-Yuzhnonovozemelskaya province – topominerology and typomorphism. *Trudy Institutag eologii Komi filial Akademii nauk SSSR. Problemy regionalnoi mineralogii*. 1978. Iss. 24, p. 23-52. (in Russian).

2. Cook N.J., Ciobanu C.L., Pring A. et al. Trace and minor elements in sphalerite. *Geochimica et Cosmochimica Acta*. 2009. Vol. 73. Iss. 16, p. 4761-4791. DOI: 10.1016/j.gca.2009.05.045

3. Cugerone A., Cenki-Tok B., Chauvet A. et al. Relationships between the occurrence of accessory Ge-minerals and sphalerite in Variscan Pb-Zn deposits of the Bossost anticlinorium. French Pyrenean Axial Zone: Chemistry, microstructures and ore-deposit setting. *Ore Geology Reviews*. 2018. Vol. 95, p. 1-19. DOI: 10.1016/j.oregeorev.2018.02.016

4. Frenzel M., Hirsch T., Gutzmer J. Gallium, germanium, indium, and other trace and minor elements in sphalerite as a function of deposit type – A meta-analysis. *Ore Geology Reviews*. 2016. Vol. 76, p. 52-78. DOI: 10.1016/j.oregeorev.2015.12.017

5. Lockington J.A., Cook N.J., Ciobanu C.L. Trace and minor elements in sphalerite from metamorphosed sulphide deposits. *Mineralogy and Petrology*. 2014. Vol. 108. Iss. 6, p. 873-890. DOI: 10.1007/s00710-014-0346-2

6. Pring A., Wade B., McFadden A. et al. Coupled Substitutions of Minor and Trace Elements in Co-Existing Sphalerite and Wurtzite. *Minerals*. 2020. Vol. 10. Iss. 2. N 147. DOI: 10.3390/min10020147

7. Vasilev E.A. Defects of diamond crystal structure as an indicator of crystallogenesis. *Journal of Mining Institute*. 2021. Vol. 250, p. 481-491. DOI:10.31897/PMI.2021.4.1

8. Vasilev E.A., Kriulina G.Yu., Garanin V.K. Thermal history of diamond from Arkhangelskaya and Karpinsky-I kimberlite pipes. *Journal of Mining Institute*, 2022. Vol. 255, p. 327-336. DOI: 10.31897/PMI.2022.57

9. Skublov S.G., Rumyantseva N.A., Li Q. et al. Zircon Xenocrysts from the Shaka Ridge Record Ancient Continental Crust: New U-Pb Geochronological and Oxygen Isotopic Data. *Journal of Earth Science*. 2022. Vol. 33. Iss. 1, p. 5-16. DOI: 10.1007/s12583-021-1422-2

10. Levashova E.V., Mamykina M.E., Skublov S.G. et al. Geochemistry (TE, REE, Oxygen) of Zircon from Leucogranitesof the Belokurikhinsky massif, Gorny Altai, as Indicator of Formation Conditions. *Geochemistry International*. 2023. Vol. 61. Iss. 13, p. 1323-1339. DOI: 10.1134/S001670292311006X

11. Stativko V.S., Skublov S.G., Smolenskiy V.V., Kuznetsov A.B. Trace and rare-earth elements in garnets from silicate-carbonate formations of the Kusa-Kopan complex (Southern Urals). *Lithosphere*. 2023. Vol. 23. N 2, p. 225-246 (in Russian). DOI: 10.24930/1681-9004-2023-23-2-225-246

12. Gavrilchik A.K., Skublov S.G., Kotova E.L. Trace Element Composition of Beryl from the Sherlovaya Gora Deposit. South-Eastern Transbaikalia, Russia. *Zapiski Rossiiskogo mineralogicheskogo obshchestva*. 2021. Vol. 150. N 2, p. 69-82 (in Russian). DOI: 10.31857/S0869605521020052

13. Skublov S.G., Gavrilchik A.K., Berezin A.V. Geochemistry of beryl varieties: comparative analysis and visualization of analytical data by principal component analysis (PCA) and t-distributed stochastic neighbor embedding (t-SNE). *Journal of Mining Institute*. 2022. Vol. 255, p. 455-469. DOI:10.31897/PMI.2022.40

14. Makeyev A.B. Isomorphism manganese and cadmium in sphalerite. Leningrad: Nauka, 1985, p. 128 (in Russian).

15. Makeyev A.B., Tauson V.L. On the possible genesis of some ZnS polytypes (according to a study of Pai-Khoi sphalerites). Kristallokhimiya i strukturnaya mineralogiya. Leningrad: Nauka, 1979, p. 18-25 (in Russian).

This is an open access article under the CC BY 4.0 license

16. Makeyev A.B., Pavlov L.V. A new cadmium variety of sphalerite. *Doklady Akademii nauk SSSR*. 1977. Vol. 236. N 1, p. 208-211 (in Russian).

17. Makeyev A.B., Evstigneeva T.L., Troneva N.V. et al. Yushkinit, $V_{1-x}S{\cdot}n[(Mg,Al)(OH)_2]$ – a new hybrid mineral. *Mineralogicheskii zhurnal*. 1984. Vol. 6. N 5, p. 91-98 (in Russian).

18. Sokerina N.V., Kovalchuk N.S., Isaenko S.I., Sokerin M.Y. Conditions of the Formation of Unique Mineralization with Yushkinite$V_{1-x}S{\cdot}n[(Mg,Al)(OH)_2]$ in Quartz–Calcite Veins, Pai-Khoi Ridge: Evidence from Study of Fluid Inclusions. *Doklady Earth Sciences*. 2020. Vol. 492. Iss. 2, p. 411-414. DOI: 10.1134/S1028334X20060197

19. Yushkin N.P., Makeyev A.B. Arsenic minerals of the Paikhoi-Yuzhnonovozemelskaja province. *Trudy Instituta geologii Komi filial Akademii nauk SSSR. Geologiya i poleznye iskopaemye Severo-Vostoka SSSR*. 1978. Iss. 27, p. 79-84 (in Russian).

20. Skinner B.J. Unit-cell edges of natural and synthetic sphalerites. *American Mineralogist*. 1961. Vol. 46. N 11-12, p. 1399-1411.

21. Tauson V.L., Makeyev A.B., Akimov V.V., Paradina L.F. Distribution of copper in zinc sulfide minerals. *Geokhimiya*. 1988. N 4, p. 492-505 (in Russian).

22. Borisenko A.S. Cryometric technique applied to studies of the saline composition of solution in gaseos fluid inclusions in minerals. *Russian Geology and Geophysics*. 1977. N 8, p. 16-27.

23. Bodnar R.J., Vityk M.O. Interpretation of microthermometric data for H_2O-NaCl fluid inclusions. Fluid Inclusions in Minerals: Methods and Applications. Blacksburg: Virginia Tech, 1994, p. 117-130.

24. Brown P.E. FLINCOR: a microcomputer program for the reduction and investigation of fluid-inclusion data. *American Mineralogist*. 1989. Vol. 74. N 11-12, p. 1390-1393.

25. Redder E. Fluid inclusions in mineral. Vol. 1. The nature of inclusions and methods for their study. Moscow: Mir, 1987. p. 557 (in Russian).

26. Radosavljević S.A., Stojanović J.N., Radosavljević-Mihajlović A.S., Vuković N.S. (Pb–Sb)-bearing sphalerite from the Čumavići polymetallic ore deposit. Podrinje Metallogenic District, East Bosnia and Herzegovina. *Ore Geology Reviews*. 2016. Vol. 72. Part 1, p. 253-268. DOI: 10.1016/j.oregeorev.2015.07.008

27. Spiridonov E.M., Badalov A.S., Kovachev V.V. Stibiocolusitis $Cu_{26}V_2(Sb,Sn,As)_6S_{32}$: a new mineral. *Doklady Akademii nauk SSSR*. 1992. Vol. 324. N 2, p. 411-414 (in Russian).

28. Evrard C., Fouquet Y., Moëlo Y. et al. Tin concentration in hydrothermal sulphides related to ultramafic rocks along the Mid-Atlantic Ridge: a mineralogical study. *European Journal of Mineralogy*. 2015. Vol. 27. N 5, p. 627-638. DOI: 10.1127/ejm/2015/0027-2472

29. Voudouris P., Repstock A., Spry P.G. et al. Physicochemical constraints on indium-, tin-, germanium-, gallium-, gold-, and tellurium-bearing mineralizations in the Pefka and St Philippos polymetallic vein- and breccia-type deposits, Greece. *Ore Geology Reviews*. 2021. Vol. 140. N 104348. DOI: 10.1016/j.oregeorev.2021.104348

30. Rambaldi E.R., Rajan R.S., Housley R.M., Wang D. Gallium-bearing sphalerite in a metal-sulfide nodule of the Qingzhen (EH3) chondrite. *Meteoritics & Planetary Science*. 1986. Vol. 21. Iss. 1, p. 23-31. DOI: 10.1111/j.1945-5100.1986.tb01223.x

31. Paradis S. Indium. germanium and gallium in volcanic- and sediment-hosted base-metal sulphide deposits. Symposium on Critical and Strategic Materials Proceedings, 13-14 November 2015, Victoria, British Columbia. British Columbia Geological Survey Paper 2015-3, p. 23-29.

32. Xiong Y. Hydrothermal thallium mineralization up to 300 °C: A thermodynamic approach. *Ore Geology Reviews*. 2007. Vol. 32. Iss. 1-2, p. 291-313. DOI: 10.1016/j.oregeorev.2006.10.003

33. Paiement J.-P., Beaudoin G., Paradis S., Ullrich T. Geochemistry and Metallogeny of Ag-Pb-Zn Veins in the Purcell Basin, British Columbia. *Economic Geology*, 2012. Vol. 107. N 6, p. 1303-1320. DOI: 10.2113/econgeo.107.6.1303

34. Spiridonov E.M., Kachalovskaya V.M., Badalov A.S. Varieties of colusite, about vanadium and vanadium-arsenic "germanite". *Vestnik Moskovskogo universiteta. Seriya 4. Geologiya*. 1986. Iss. 3, p. 60-69 (in Russian).

35. Spiridonov E.M. On the composition of germanite. *Doklady Akademii nauk SSSR*. 1987. VOL. 295. N 2, P. 477-481 (IN RUSSIAN).

36. Tonkacheev D.E., Chareev D.A., Abramova V.D. et al. The substitution mechanism of Au in In-, Fe- and In-Fe-bearing synthetic crystals of sphalerite, based on the data from EPMA and LA-ICP-MS study. *Lithosphere*. 2019. Vol. 19. N 1, p. 148-161 (in Russian). DOI: 10.24930/1681-9004-2019-19-1-148-161

37. Huston D.L., Sie S.H., Suter G.F. et al. Trace elements in sulfide minerals from eastern Australian volcanic-hosted massive sulfide deposits; Part I. Proton microprobe analyses of pyrite, chalcopyrite, and sphalerite, and Part II. Selenium levels in pyrite; comparison with $\delta^{34}S$ values and implications for the source of sulfur in volcanogenic hydrothermal systems. *Economic Geology*. 1995. Vol. 90. N 5, p. 1167-1196. DOI: 10.2113/gsecongeo.90.5.1167

38. Ishihara S., Hoshino K., Murakami H., Endo Y. Resource Evaluation and Some Genetic Aspects of Indium in the Japanese Ore Deposits. *Resource Geology*. 2006. Vol. 56. Iss. 3, p. 347-364. DOI: 10.1111/j.1751-3928.2006.tb00288.x

39. Johan Z. Indium and germanium in the structure of sphalerite: an example of coupled substitution with Copper. *Mineralogy and Petrology*. 1988. Vol. 39. Iss. 3-4, p. 211-229. DOI: 10.1007/BF01163036

40. Filimonova O.N., Trigub A.L., Tonkacheev D.E. et al. Substitution mechanisms in In-, Au-, and Cu-bearing sphalerites studied by X-ray absorption spectroscopy of synthetic compounds and natural minerals. *Mineralogical Magazine*. 2019. Vol. 83. Iss. 3, p. 435-451. DOI: 10.1180/mgm.2019.10

41. Asadi H.H., Voncken J.H.L., Hale M. Invisible gold at Zarshuran. Iran. *Economic Geology*. 1999. Vol. 94. N 8, p. 1367-1374. DOI: 10.2113/gsecongeo.94.8.1367

42. Filippov V.A., Ryabinin V.F., Syzoeva Z.Z. The Gagarka gold deposit in the central Urals. Russia. *Geology of Ore Deposits*. 2013. Vol. 55. N 1, p. 27-40. DOI 10.1134/S1075701513010030

43. Clark A.H. Arsenian sphalerite from Mina Alcarán, Pampa Larga, Copiapó, Chile. *American Mineralogist*. 1970. Vol. 55. N 9-10, p. 1794-1797.

This is an open access article under the CC BY 4.0 license

44. Pirri I.V. On the occurrence of selenium in sulfides of the ore deposits of Baccu Locci (Gerrei, SE Sardinia). *Neues Jahrbuchfür Mineralogie*. 2002. Vol. 5, p. 207-224. DOI: 10.1127/0028-3649/2002/2002-0207

45. Frenzel M., Voudouris P., Cook N.J. et al. Evolution of a hydrothermal ore-forming system recorded by sulfide mineral chemistry: a case study from the Plaka Pb–Zn–Ag Deposit, Lavrion, Greece. *Mineralium Deposita*. 2022. Vol. 57. Iss. 3, p. 417-438. DOI: 10.1007/s00126-021-01067-y

***Authors*: Aleksandr B. Makeyev,** *Doctor of Geological and Mineralogical Sciences, Leading Researcher, abmakeev@mail.ru. https://orcid.org/0000-0001-8815-0959* (*Institute of Geology of Ore Deposits, Petrography, Mineralogy and Geochemistry, RAS, Moscow, Russia*). **Ilya V. Vikentyev,** *Doctor of Geological and Mineralogical Sciences, Chief Researcher, https://orcid.org/0000-0001-9133-7562* (*Institute of Geology of Ore Deposits, Petrography, Mineralogy and Geochemistry, RAS, Moscow, Russia*). **Elena V. Kovalchuk,** *Junior Researcher, https://orcid.org/0000-0002-6522-8212* (*Institute of Geology of Ore Deposits, Petrography, Mineralogy and Geochemistry, RAS, Moscow, Russia*), **Vera D. Abramova,** *Junior Researcher, https://orcid.org/0000-0002-7021-5272* (*Institute of Geology of Ore Deposits, Petrography, Mineralogy and Geochemistry, RAS, Moscow, Russia*). **Vsevolod Yu. Prokofyev,** *Doctor of Geological and Mineralogical Sciences, Head of Laboratory, https://orcid.org/0000-0001-7134-2655* (*Institute of Geology of Ore Deposits, Petrography, Mineralogy and Geochemistry, RAS, Moscow, Russia*).

The authors declare no conflict of interests.

This is an open access article under the CC BY 4.0 license

ISSN 2411-3336; e-ISSN 2541-9404

JOURNAL OF MINING INSTITUTE

Zapiski Gornogo instituta

Journal homepage: pmi.spmi.ru

Research article

Trace element composition of silicate minerals from Kunashak Meteorite (L6)

Kristina G. Sukhanova✉, Olga L. Galankina

Institute of Precambrian Geology and Geochronology RAS, Saint Petersburg, Russia

***How to cite this article*:** Sukhanova K.G, Galankina O.L. Trace element composition of silicate minerals from Kunashak Meteorite (L6). Journal of Mining Institute. 2024. Vol. 270, p. 877-892.

Abstract

Major (EPMA) and trace (SIMS) element geochemistry in the silicate minerals (olivine, pyroxene and plagioclase) of Kunashak equilibrated ordinary chondrite (L6) is described. No variations in the major element concentrations of the silicate minerals have been found, which is characteristic of equilibrated chondrites of petrological type VI. Low-Ca pyroxene and plagioclase from the radiated olivine-pyroxene chondrule of Kunashak Meteorite contain an abundance of trace elements (Yb, Cr, Nb and Ti – pyroxene; Sr, Y, Ti and Zr – plagioclase), which is not characteristic of minerals from the porphyritic olivine and olivine-pyroxene chondrules of the meteorite. The porphyritic olivine-pyroxene chondrule of the Kunashak Meteorite has high trace element concentrations in olivine, in particular, the highest Yb concentration (0.12 ppm on the average) relative to porphyritic and radiated olivine-pyroxene chondrules (0.02 ppm). High trace element concentrations indicate rapid crystallization of a radiated chondrule in a nebula and show no traces of trace element homogenization upon thermal metamorphism. The trace element composition of silicate minerals from Kunashak Meteorite has retained the individual melting pattern of the chondrules and remained unaffected by thermal metamorphism on the parent bodies of the chondrules. Similar results, obtained in the study of Bushkhov Meteorite (L6), indicate that trace elements in olivine and low-Ca pyroxene are resistant to thermal metamorphism. The persistence of the individual pattern of the chondrules enables us to use equilibrated ordinary chondrites for the study of processes at early stages in the formation of the Solar System and to better understand chondrule and planet formation mechanisms.

Keywords

Ordinary chondrites; trace elements; olivine; pyroxene; plagioclase; ion probe

Funding

The study was carried out within the framework of the research topic of the IPGG RAS (N FMUW-2022-0005).

Received: 08.11.2023 ***Accepted: 02.05.2024*** ***Online: 26.07.2024*** ***Published: 25.12.2024***

Introduction.

Kunashak stone meteorite rain fell on June 11th, 1949, at 8:14 a.m. local time, in the Kunashak District, Chelyabinsk Region. The falling of the bolide was accompanied by bright light in the sky, 350 km from the falling site. The workers of the Chelyabinsk Teachers' Training Institute, the Mining and Geological Institute at the Uralian Branch of the USSR Academy of Sciences and representatives of the Committee for Meteorites, USSR Academy of Sciences, together with local residents, collected and described 13 fragments of the meteorite totaling about 200 kg in weight and calculated the falling trajectory of the meteorite and the dispersion ellipse of the fragments [1].

It was shown in early descriptions that the meteorite is divided by a sharp boundary into black and light-grey sectors, that it has neither melting crust nor regmaglypts and that it has abundant solidified jets and drops of plessite and silicates [1]. In 1951, local residents found two 250 and 700 g fragments [2]. Another fragment weighing 2.5 kg was found in the summer of 2014 [3]. In 1960, the frontal portion of the dispersion ellipse of Kunashak Rain was shown to contain meteorite dust particles [4]. The details of the falling [5] and the meteorite's orbit parameters [6] were determined later. The meteorite was studied thoroughly by Russian and foreign researchers and was used for comparison of methods employed for analyzing the composition of small bodies in the Solar System [7].

Kunashak Meteorite is of a group of olivine-hypersthene low-iron equilibrated ordinary chondrites (L6). Equilibrated ordinary chondrites (EOC) are the most common group of meteorites known

This is an open access article under the CC BY 4.0 license

on earth, making up 90 % of the entire meteoritic matter. Chondrites consist of silicate spherules (chondrules), less than 1 mm in size, composed of olivine, low-Ca pyroxene and mesostasis. The chondrules, occurring as drops of melt solidified at zero gravity in a nebula, are the oldest objects in the Solar system [8, 9]. Chondrules vary in structure and are divided into two groups: porphyritic and nonporphyritic (radiated, barred, granular, cryptocrystalline, etc.). The diversity of the structural types of chondrules indicates variations in their conditions of formation in a nebula.

Experiments on the reproduction of chondrule structure have shown the heating temperature of the precursor mineral, the number of crystallization and chondrule solidification rate. Precursor minerals in porphyritic chondrules are typically heated below the liquidus temperature of the melt (1,400-1,700 °C), an abundance of seeds is retained and solidification is slow (1-500 °C/h). Barred chondrules are crystallized when heated slightly above the liquidus temperature, when a small number of seeds remain unchanged and when cooling is rapid (500-3,000 °C/h). The chondrules of nonporphyritic (radiated and cryptocrystalline) structures require temperatures much higher than the liquidus temperature, the destruction of all seeds and instant cooling (1000-3000 °C/h) [10, 11].

The porphyritic chondrules of unequilibrated ordinary chondrites (UOC) sometimes contain isolated refractory olivine grains that are considerably enriched in MgO and differ in the isotopic composition of oxygen from the olivine of a chondrule [12, 13] and the higher-Mg nuclei of olivine grains overgrown with lower-Mg forsterite rims [14]. The presence of relict olivine grains in porphyritic chondrules suggests that they were formed by the melting of precursor minerals. Refractory inclusions (CAI and AOA) [15], the fine-grained material of chondrite matrix, as well as the chondrules and fragments of chondrules of previous generations, may behave as precursor material. Other examples are fragments of planetesimals [16], H_2O ice [17, 18], "relict" olivine [19] and clusters of dust [20].

Most ordinary chondrites known on earth show traces of thermal metamorphism. As a result, FeO and MgO concentrations in olivine and low-Ca pyroxene were homogenized on parent chondrite bodies, mesostasis was recrystallized into plagioclase and apatite and chromite were formed. Ordinary chondrites seldom display traces of dissolution and high porosity [21], indicating the involvement of solutions upon thermal metamorphism on the parent bodies of chondrites. Ordinary chondrites are divided into petrological types, based on the presence of well-defined traces of thermal metamorphism and FeO and MgO homogenization. Non-equilibrated ordinary chondrites with no traces of metamorphism are understood as type III. Equilibrated ordinary chondrites are assessed as petrological types IV-VI, based on their thermal metamorphic grade. Equilibrated ordinary chondrites are common, but they are poorly understood, because it was believed that traces of chondrule and planet formation were obliterated by thermal metamorphism [22].

Trace and rare-earth elements are widely used for assessment of the geochemical settings and conditions of formation of genetically different minerals, e.g. zircon [23-25], garnet [26, 27], beryl [28, 29], etc. In addition, the migration of trace elements in olivine and low-Ca pyroxene is poorly affected by thermal and/or impact [30] metamorphism on the parent bodies of chondrites [31, 32]. Therefore, they can be used for the study of early stages in the formation of the Solar System [33] and the study of minerals from equilibrated ordinary chondrites (EOC).

Earlier studies showed that trace elements in EOC minerals remain unequilibrated in meteorites of petrological type V and partly type VI [34]. Trace element distribution in chondrule minerals was not found to depend on the chemical group and petrological type of the meteorite [35].

In our study, we assessed the effect of thermal metamorphism on the mobility of trace elements in the silicate minerals of the porphyritic and radiated chondrules of equilibrated ordinary Kunashak chondrite (L6).

This is an open access article under the CC BY 4.0 license

Analytical methods.

The Kunashak chondrite sample analyzed (L6) was made available by the Mining Museum of Saint Petersburg Mining University.

The major element chemical composition of minerals was determined using the EPMA method at IGGD RAS on a Jeol JXA-8230 microprobe analyzer with five wave spectrometers. The meteorite substance was placed in a standard epoxy resin mould sprayed with carbon after polishing. Point measurements of mineral compositions were carried out at an accelerating voltage of 20 kV and a current of 20 nA for olivine and pyroxene and at 10 nA for mesostasis. The focused beam was 3 μm in diameter. Natural minerals, pure oxides and metals were used as standards. ZAF algorithm was used for correcting the matrix effect. Kα1 lines were measured for all elements.

Trace and rare-earth element (REE) concentrations in minerals were identified using the secondary ion mass spectrometry (SIMS) method on a Cameca IMS-4f ion microprobe at the Valiev IPT, RAS, Yaroslavl Branch using, the technique described in [36, 37]. The preparation was sprayed with gold prior to measurements. Survey on a Cameca IMS-4f ion microprobe was done under the following conditions: a primary ion beam was $16O_2$, beam diameter was ~ 20 μm; ion current was 5-7 nA; and the accele-rating voltage of the primary beam was 15 keV. The measurement error was no more than 10 % for impurities with concentrations over 1 ppm and 20 % for concentrations of less than 1 ppm. The trace element composition of rock-forming minerals was analyzed as close as possible to the analytical points of major elements using the EPMA method. REE distribution spectra in minerals were CI chondrite-normalized [38].

Results.

The Kunashak Meteorite sample contains porphyritic-, barred-, radiated- and granular-structured chondrules varying in size from 1 to 0.5 mm. Chondrule-matrix boundaries are always well-defined, and no metallic rims are present. The matrix consists of coarse olivine and low-Ca pyroxene (clinoenstatite) grains. High-Ca pyroxene (augite-diopside), plagioclase of oligoclase composition, apatite, chromite, kamacite-taenite and troilite. The matrix has melting pockets and fractures filled with ore minerals. The matrix and chondrules of the meteorite are highly porous. No minerals produced by earth weathering have been found.

When studying the trace element composition of chondrule minerals, we analyzed porphyritic olivine 8PO-1 and olivine-pyroxenitic 8POP-3 chondrules, as well as radiated olivine-pyroxenitic chondrule 8ROP-2 (Fig.1). Chondrules 8PO-1 and

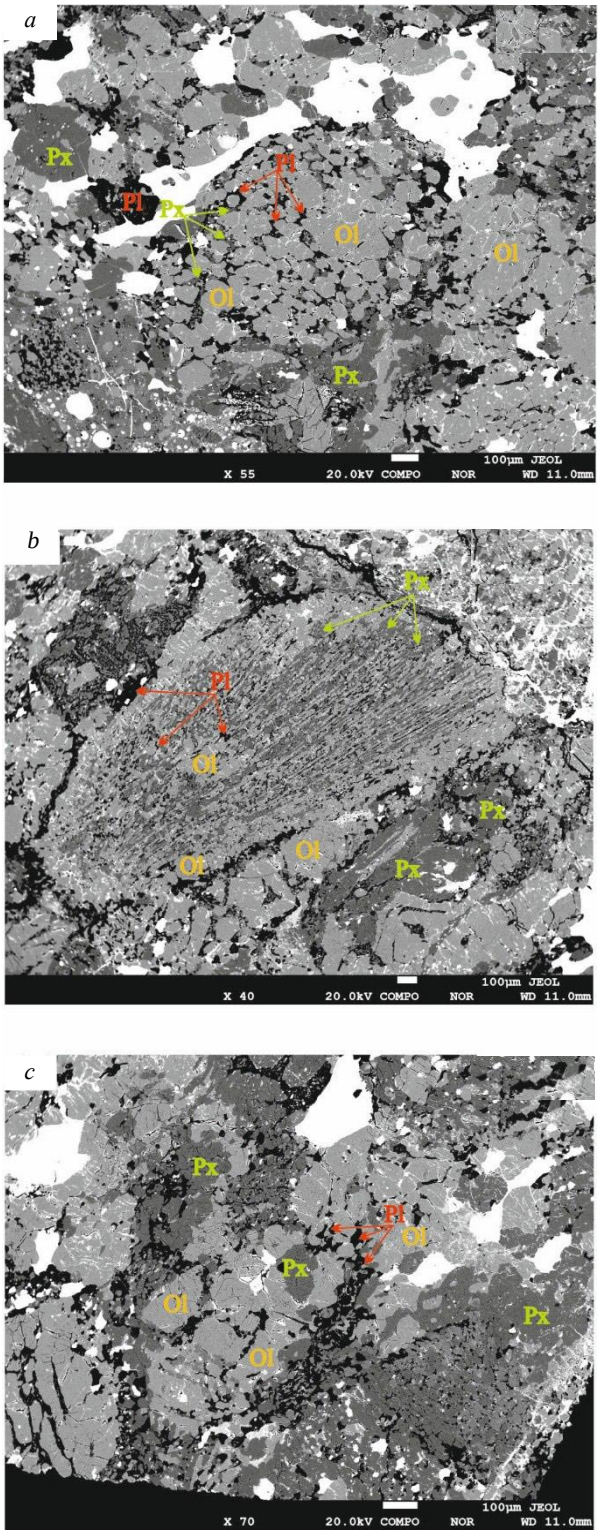

Fig.1. BSE images of chondrules of the Kunashak Meteorite:
a – 8PO-1; *b* – 8ROP-2; *c* – 8POP-3;
Ol – olivine, Px – low-Ca pyroxene, Pl – plagioclase

This is an open access article under the CC BY 4.0 license

8ROP-2 are about 1 mm in size and show well-defined chondrule-matrix boundaries. Chondrule 8POP-3 is smaller (0.5 mm) and shows indistinct boundaries. The chondrules have no metallic rims, but 8ROP-2 has an olivine rim along the perimeter.

Chondrule 8PO-1 consists of small (100 μm on the average) isometric olivine grains, scarce small (less than 50 μm) xenomorphic low-Ca pyroxene and plagioclase grains (Fig.1, *a*). Coarse (300-500 μm) olivine, pyroxene and plagioclase grains are present in the matrix, near the chondrule. Ore mineral streaks are scarce.

Olivine in porphyritic chondrule 8PO-1 was recognized as forsterite (Fo 75). It is present as a coarse grain in the centre of the chondrule and small grains throughout the chondrule. Idiomorphic olivine grains do not contact each other within the chondrule. No well-defined fractures and pores in the grains were found. The composition of major elements in olivine is homogeneous. There are no differences between olivine in the centre and olivine on the margin of the chondrule, as well as olivine in the meteorite matrix, near the chondrule (Table 1).

Table 1

Major (wt.%) and trace (ppm) element composition of silicate minerals from 8PO-1 chondrule of the Kunashak Meteorite

Element	Olivine			Pyroxene			Plagioclase		
	Centre	Rim	Matrix	Centre	Rim	Matrix	Centre	Rim	Matrix
SiO_2	38.73	38.63	38.89	55.39	55.91	55.07	65.53	65.21	65.61
Al_2O_3	0.01	0.01	b.d.l.	0.29	0.15	0.31	21.07	21.20	21.19
MgO	38.74	38.70	39.31	28.12	28.22	28.04	0.06	0.17	0.04
TiO_2	0.04	0.01	0.03	0.33	0.21	0.41	0.01	0.02	0.02
CaO	0.02	0.03	0.02	0.82	0.76	1.04	2.19	2.40	2.24
FeO	22.72	22.89	22.37	14.08	13.90	13.77	0.66	0.64	0.32
MnO	0.44	0.43	0.42	0.48	0.46	0.45	–	–	–
Cr_2O_3	b.d.l.	0.08	0.01	0.16	0.09	0.26	–	–	–
NiO	b.d.l.	0.03	0.02	0.01	b.d.l.	b.d.l.	–	–	–
Na_2O	–	–	–	0.04	b.d.l.	b.d.l.	10.36	9.95	10.02
K_2O	–	–	–	b.d.l.	b.d.l.	b.d.l.	0.75	0.99	0.93
Total	100.69	100.80	101.07	99.72	99.71	99.34	100.63	100.59	100.35
Zr	1.29	2.39	0.75	61.2	4.29	1.91	2.32	1.15	7.00
Hf	0.05	0.05	0.06	1.61	0.12	0.08	0.13	0.04	0.16
Ca	4,531	4,665	4,715	7,266	6,018	6,373	–	–	–
Y	0.06	0.12	0.07	0.48	0.41	0.32	0.11	0.15	1.11
Al	39.5	172	61.6	283	536	585	–	–	–
Ti	241	136	99.2	186	986	1,306	226	250	1,101
Nb	2.27	0.46	0.17	0.69	0.45	0.11	0.42	0.17	0.68
La	0.05	0.14	0.08	1.93	0.12	0.04	0.09	0.08	0.77
Ce	0.11	0.12	0.09	8.00	0.25	0.19	0.12	0.14	1.16
Pr	0.01	0.04	0.02	0.40	0.02	0.02	0.02	0.02	0.23
Nd	0.07	0.11	0.06	2.16	0.05	0.08	0.13	0.04	0.64
Sm	0.02	0.02	b.d.l.	0.31	0.12	b.d.l.	b.d.l.	b.d.l.	0.12
Eu	0.01	b.d.l.	0.01	0.06	0.03	0.01	0.27	0.38	0.23
Gd	0.02	0.05	0.03	1.31	0.10	b.d.l.	0.01	0.02	0.26
Dy	b.d.l.	0.03	0.02	0.05	0.05	0.05	b.d.l.	0.02	0.19
Er	0.02	0.03	b.d.l.	0.06	0.07	0.07	b.d.l.	0.14	0.14
Yb	0.03	0.02	0.03	0.08	0.10	0.11	0.04	0.04	0.16
Lu	b.d.l.	0.01	0.01	0.03	0.01	0.02	0.01	0.01	0.03
Sr	0.18	0.40	0.16	1.06	0.55	0.25	51.2	71.7	35.5
Ba	0.18	0.51	0.23	5.09	0.51	0.38	26.5	36.9	7.05

This is an open access article under the CC BY 4.0 license

End of Table 1

Element	Olivine			Pyroxene			Plagioclase		
	Centre	Rim	Matrix		Centre	Rim	Matrix		Centre
V	18.2	18.5	18.8	33.7	41.0	50.4	28.4	13.5	53.7
Ni	40.0	94.6	35.0	193	298	104	–	–	–
Cr	520	503	436	1,180	809	991	792	35.2	1,176
Rb	1.39	1.59	1.76	2.46	1.44	0.84	7.21	9.22	2.91
REE	0.36	0.57	0.35	14.4	0.93	0.60	0.69	0.88	3.92
LREE	0.29	0.44	0.26	12.9	0.60	0.35	0.63	0.65	3.15
HREE	0.07	0.13	0.09	1.53	0.33	0.26	0.06	0.22	0.77

Note. Empty cell – no element detected; b.d.l. – element content is below the detection limit.

The composition of trace elements in the olivine of chondrule 8PO-1 is also homogeneous. Nb concentration decreases from the centre of the chondrule (2.26 ppm) to the margin (0.46 ppm) and matrix (0.17 ppm) of the meteorite. Trace element concentrations are below chondrite values. The trace element distribution spectrum is subhorizontal (Fig.2, *a*).

Refractory trace element concentrations in the olivine of chondrule 8 PO-1 exceeds unequilibrated chondrite concentrations in olivine [39], except for Al, and fully coincides with respect to volatile elements (Sr, Ba and Ni).

The low-Ca pyroxene of chondrule 8PO-1 seldom occurs in the chondrule. It does not form its own grains and usually grows on olivine grains. Pyroxene is present as small (50 μm) xenomorphic aggregates and has much in common with plagioclase. Low-Ca pyroxene is present as clinoenstatite (En 76, Wo 1-2). It shows no significant variations in major element composition. However, low-Ca pyroxene in the matrix contains more TiO_2, CaO and Cr_2O_3 than pyroxene in the centre and on the margin of the chondrule (Table 1).

Trace element concentrations in low-Ca pyroxene from chondrule 8PO-1 decreases from the centre to the margin of the chondrule and the matrix of the meteorite. Pyroxene in the centre of the chondrule is richer in all refractory elements (Zr, Hf, Nb, LREE), as well as in Sr and Ba, than pyroxene on the margin and in the matrix of the meteorite. Pyroxene on the chondrule margin shows intermediate concentrations of the above elements in comparison with the centre of the chondrule centre and the matrix of the meteorite, while pyroxene in the matrix is impoverished in them.

The trace element composition of low-Ca pyroxene is consistent with chondrite values, so that trace element composition in unequilibrated ordinary chondrites is exceeded. The rare earth element distribution spectrum is poorly differentiated, but it shows the prevalence of LREE over HREE, especially in pyroxene from the centre of the chondrule (Fig.2, *b*).

Plagioclase in chondrule 8PO-1 is scarce. It commonly occurs as small xenomorphic aggregates filling interstices between olivine and pyroxene. Plagioclase in the chondrule is present as oligoclase (An 10-11, Or 5-4). Major element composition remains unchanged (Table 1).

Trace element concentrations in plagioclase are highly heterogeneous. Plagioclase in the matrix is richer in trace elements and REE than plagioclase in the chondrule. Plagioclase on the chondrule margin is poor in Zr, Hf and Nb. Plagioclase in the centre of the chondrule occupies an intermediate position.

The trace element distribution spectrum shows trace element concentrations consistent with chondrite values (Fig.2, *c*). Plagioclase in the matrix mainly coincides with the spectrum of plagioclase for Vigarano Meteorite, although it is slightly impoverished in HREE. The spidergram for plagioclase in the chondrule is similar to the diagram of plagioclase for Renazzo Meteorite.

Radiated chondrule 8ROP-2 consists of fine elongated skeletal olivine and low-Ca pyroxene crystals extending from a common centre. The ~1 mm chondrule is oval in shape and has a

This is an open access article under the CC BY 4.0 license

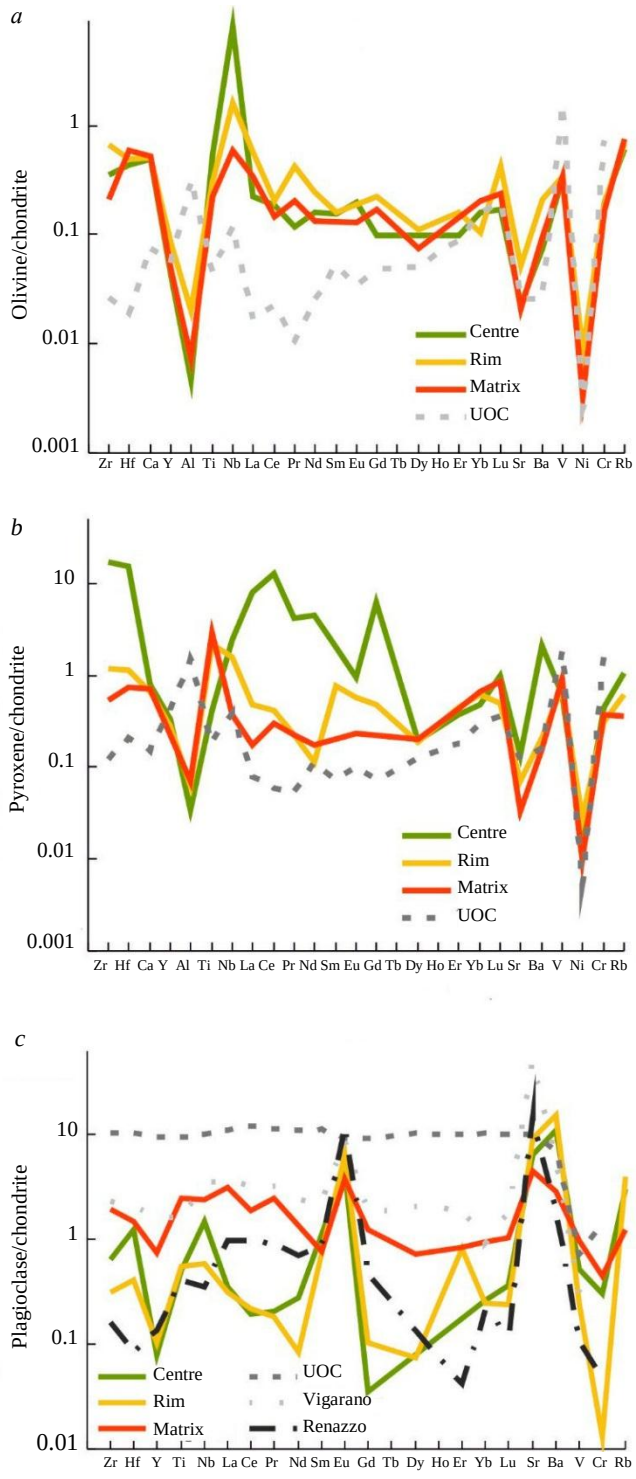

Fig.2. Spider diagrams for trace elements normalized to CI chondrite. Chondrule 8PO-1: olivine (*a*); low-Ca pyroxene (*b*) and mesostasis (*c*). Data on the composition of UOC, Vigarano and Renazzo minerals are given according [38, 40]

well-defined boundary with matrix and an olivine along the perimeter. On the wide side, it is bounded by a fracture and a melting pocket with abundant ore streaks (see Fig.1, *b*).

Olivine in chondrule 8ROP-2 forms thin (up to 100 μm in width) elongated beams extending from one chondrule margin to the other from a common centre. The olivine grains are homogeneous, have no fractures and are often overgrown with ore minerals. Olivine in the chondrule is present as forsterite (Fo 75). The major element composition is homogeneous (Table 2).

The trace element composition of olivine in chondrule 8ROP-2 varies with the position of the analytical point. Olivine in the centre of the chondrule is poorer in HREE than olivine on the chondrule margin and in the meteorite matrix. Olivine in the meteorite matrix has minimum Al concentration (54.5 ppm).

The trace element distribution spectrum for olivine in chondrule 8ROP-2 is poorly differentiated. HREE does not prevail over LREE (Fig.3, *a*). Trace element concentrations in the olivine of the chondrule are below chondrite values, but exceed refractory element concentrations in the porphyritic chondrules of unequilibrated ordinary chondrites.

Low-Ca pyroxene in chondrule 8ROP-2 is present as clinoenstatite (En 76, Wo 1). Its major element concentrations are constant, although pyroxene in the matrix is poor in impurity elements (Al_2O_3, TiO_2, CaO, Cr_2O_3) (Table 2). Low-Ca pyroxene seldom occurs in chondrules. It commonly overgrows skeletal olivine crystals. It often occurs as fine (up to 50 μm) xenomorphic aggregates.

Low-Ca pyroxene in the centre of chondrule 8ROP-2 contains higher trace element concentrations than pyroxene on the chondrule margin and in the matrix of the meteorite. Pyroxene on the chondrule margin and in the matrix of the meteorite has similar trace element concentrations, but pyroxene on the chondrule margin has minimum moderately volatile Sr and Ba concentrations.

The trace element distribution spectrum for low-Ca pyroxene in chondrule 8ROP-2 displays chondrite values, slightly exceeding trace element concentrations in pyroxene from the chondrules of unequilibrated ordinary chondrites (Fig.3, *c*). Low-Ca pyroxene in chondrule 8ROP-2 contains more Ti than UOC. The rare-earth distribution spectrum shows that HREE clearly dominates over LREE in the low-Ca pyroxene of chondrule ROP-2.

Plagioclase in chondrule 8ROP-2 is present as oligoclase (An 10-12, Or 4). Albite grains (An 9, Or 5) occur in the matrix (Table 2). In the chondrule, plagioclase fills small (~10 μm)

This is an open access article under the CC BY 4.0 license

interstices between olivine and pyroxene and, therefore, cannot be studied. Major element composition in plagioclase is permanent, although minor variations in impurity element (Mg, Fe) concentrations take place.

Table 2

Major (wt.%) and trace (ppm) element composition of silicate minerals from 8ROP-2 chondrule of the Kunashak Meteorite

Element	Olivine			Pyroxene			Plagioclase		
	Centre	Rim	Matrix	Centre	Rim	Matrix	Centre	Matrix	Matrix
SiO_2	38.75	38.30	38.22	55.22	55.07	55.91	65.63	65.70	65.18
Al_2O_3	0.01	0.02	b.d.l.	0.40	0.37	0.15	21.13	21.21	21.01
MgO	38.81	39.27	39.21	28.28	28.07	28.53	0.13	0.09	0.10
TiO_2	0.02	0.01	0.00	0.46	0.39	0.20	0.03	0.02	0.03
CaO	0.02	0.02	0.02	0.84	0.87	0.63	2.66	2.32	2.07
FeO	22.85	22.22	22.77	13.70	14.65	14.05	0.72	0.40	0.52
MnO	0.48	0.50	0.46	0.45	0.48	0.48	–	–	–
Cr_2O_3	0.02	0.02	0.01	0.22	0.24	0.09	–	–	–
NiO	b.d.l.	0.01	b.d.l.	0.02	0.09	0.02	–	–	–
Na_2O	–	–	–	0.02	b.d.l.	0.01	9.47	10.28	10.20
K_2O	–	–	–	b.d.l.	0.02	b.d.l.	0.71	0.88	0.99
Total	100.96	100.37	100.68	99.61	100.23	100.07	100.49	100.89	100.09
Zr	0.67	0.81	0.57	19.6	3.13	1.16	44.1	4.43	6.96
Hf	b.d.l.	0.06	b.d.l.	0.49	0.10	0.04	0.95	0.24	0.16
Ca	5,658	5,122	5,208	27,607	6,545	6,374	–	–	–
Y	0.03	0.09	0.08	2.21	0.50	0.29	0.30	0.34	1.10
Al	236	1,055	54.6	8,825	1,395	613	–	–	–
Ti	88.6	113	55.1	1,240	2,555	1,245	422	624	1,094
Nb	0.37	0.36	0.06	1.47	0.32	0.13	0.59	0.77	0.68
La	0.03	0.02	0.05	0.14	0.06	0.02	1.63	0.13	0.77
Ce	0.07	0.09	0.08	0.44	0.10	0.20	1.60	0.25	1.15
Pr	0.01	0,01	0.02	0.05	0.01	0.01	0.38	0.04	0.23
Nd	0.06	0.05	0.06	0.32	0.05	0.05	1.23	0.11	0.64
Sm	b.d.l.	0.05	b.d.l.	0.10	0.03	0.03	0.13	b.d.l.	0.12
Eu	0.00	0.01	0.01	0.04	0.02	0.01	0.63	0.05	0.22
Gd	0.03	0.09	0.06	0.15	0.06	0.05	0.19	0.05	0.26
Dy	0.01	0.04	0.04	0.32	0.05	0.04	0.03	0.05	0.19
Er	b.d.l.	0.03	0.04	0.33	0.03	0.04	0.06	0.09	0.14
Yb	0.01	0.04	0.09	0.34	0.22	0.13	0.07	0.07	0.16
Lu	0.01	0.01	0.01	0.04	0.02	0.01	0.02	0.04	0.03
Sr	0.44	1.14	0.19	10.8	0.17	1.32	109	6.76	35.3
Ba	0.42	0.66	0.29	4.11	0.13	0.22	27.3	2.47	7.00
V	23.2	20.5	18.2	117	82.9	49.7	18.5	38.5	53.3
Ni	45.3	49.9	44.0	110	370	286	–	–	–
Cr	889	520	472	1,672	1,582	884	168	587	1,168
Rb	2.06	2.58	1.46	3.18	1.01	0.59	13.1	8.81	2.89
REE	0.24	0.45	0.45	2.27	0.65	0.60	5.98	0.88	3.90
LREE	0.17	0.24	0.22	1.09	0.27	0.33	5.61	0.58	3.13
HREE	0.07	0.21	0.24	1.19	0.39	0.27	0.37	0.30	0.77

This is an open access article under the CC BY 4.0 license

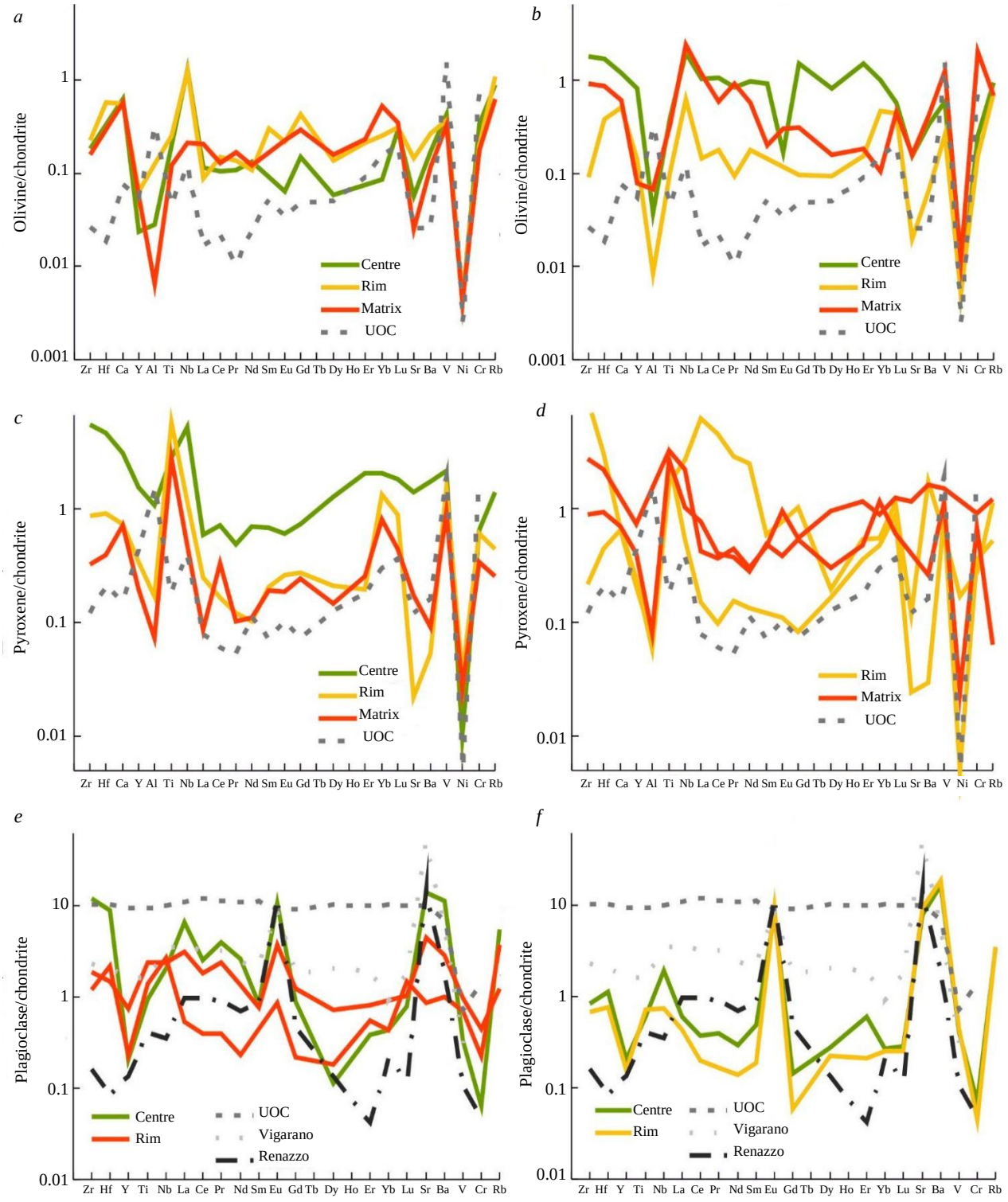

Fig.3. Spider diagrams for trace elements normalized to CI chondrite.
Chondrule 8ROP-2: olivine (*a*); low-Ca pyroxene (*c*) and mesostasis (*e*);
chondrule 8POP-3: olivine (*b*); low-Ca pyroxene (*d*) and mesostasis (*f*).
Data on the composition of UOC, Vigarano and Renazzo minerals are given according [38, 40]

Trace element concentrations in plagioclase from chondrule 8ROP-2 are heterogeneous. In the centre of the chondrule, plagioclase is richer in trace elements than plagioclase in the matrix, except for HREE. In the matrix, plagioclase grains contain various trace element concentrations, although the trace element distribution spectra resemble each other (Fig.3, *e*). Trace element concentrations in the plagioclase of chondrule 8ROP-2 and in the matrix are above chondrite values.

This is an open access article under the CC BY 4.0 license

The trace element distribution spectra in chondrule 8ROP-2 are more similar to plagioclase in Renazzo coaly chondrite [38, 40], but refractory and rare-earth element concentrations are higher. The distribution spectra are poorly differentiated, a well-defined europium anomaly is present and LREE prevails over HREE in plagioclase from the centre of the chondrule.

Porphyritic olivine-pyroxene chondrule 8POP-3 (see Fig.1, *c*), 0.5 mm in size, contains coarse olivine and plagioclase grains and has an obliterated boundary with the matrix. Occurring near the chondrule is a plagioclase-olivine aggregate showing the integrated xenomorphic manifestation of plagioclase, which contains fine (up to 50 μm by elongation) elongated olivine grains.

In chondrule 8POP-3, olivine is present as forsterite (Fo 75). Its major element composition is stable (Table 3). Olivine makes up the bulk of chondrule POP-3, occurring as coarse (200-300 μm) idiomorphic grains. It looks homogeneous and slightly fractured on BSE-images.

The trace element composition of olivine is heterogeneous. In the centre of the chondrule, olivine is richer in refractory elements than olivine on the margin and in the matrix of the meteorite. Olivine on the chondrule margin contains the lowest trace element concentrations. Olivine in the matrix occupies an intermediate position.

Trace element concentrations are consistent with chondrite values. They exceed refractory and rare-earth element concentrations in porphyritic chondrule olivine from unequilibrated ordinary chondrite (Fig.3, *b*). The trace element distribution in the olivine of chondrule 8POP-3 is poorly differentiated. LREE prevails over HREE in olivine from the matrix.

Low-Ca pyroxene in chondrule 8POP-3 is less common than olivine, making up no more than 10 % of the chondrule. Pyroxene is present as fine (up to 200 μm) xenomorphic grains occasionally growing on fine olivine grains. In back-scattered electrons, it looks homogeneous and has no fractures. Low-Ca pyroxene is present as clinoenstatite (En 76-77, Wo 1-2). Its major element composition is homogeneous, but impurity element (Ti, Cr) concentrations vary slightly (Table 3).

Table 3

Major (wt.%) and trace (ppm) element composition of silicate minerals from 8POP-3 chondrule of the Kunashak Meteorite

Element	Olivine			Pyroxene				Plagioclase	
	Centre	Rim	Matrix	Rim	Rim	Matrix	Matrix	Centre	Rim
SiO_2	38.32	38.05	38.73	56.38	56.32	56.17	55.49	63.63	65.44
Al_2O_3	b.d.l.	0.02	b.d.l.	0.16	0.12	0.16	0.17	20.25	20.96
MgO	38.75	38.60	38.64	28.56	28.68	28.44	28.27	0.99	0.18
TiO_2	b.d.l.	b.d.l.	0.04	0.20	0.13	0.19	0.20	b.d.l.	0.04
CaO	0.05	0.05	0.05	0.86	0.86	0.75	1.05	3.66	2.43
FeO	22.87	22.37	22.44	13.83	13.52	13.97	13.87	1.57	0.43
MnO	0.49	0.50	0.42	0.46	0.48	0.49	0.42	–	–
Cr_2O_3	b.d.l.	0.02	0.03	0.12	0.11	0.14	0.15	–	–
NiO	0.01	b.d.l.	b.d.l.	b.d.l.	b.d.l.	0.01	b.d.l.	–	–
Na_2O	–	–	–	0.03	b.d.l.	0.04	0.02	9.60	10.10
K_2O	–	–	–	0.00	0.01	0.01	0.01	0.87	0.78
Total	100.49	99.60	100.35	100.58	100.23	100.35	99.65	100.57	100.36
Zr	6.55	0.32	3.35	0.78	32.7	9.89	3.22	3.06	2.48
Hf	0.18	0.04	0.09	0.05	0.32	0.23	0.10	0.12	0.08
Ca	11,012	4,690	5,527	5,877	6,012	–	6,332	–	–
Y	1.20	0.21	0.12	0.30	0.35	1.06	0.57	0.31	0.23
Al	314	71.4	565	591	489	–	670	–	–
Ti	175	46.2	147	1,214	730	1,426	1,177	276	327

This is an open access article under the CC BY 4.0 license

End of Table 3

Element	Olivine			Pyroxene				Plagioclase	
	Centre	Rim	Matrix	Rim	Rim	Matrix	Matrix	Centre	Rim
Nb	0.56	0.18	0.68	0.15	0.76	0.61	0.29	0.56	0.21
La	0.25	0.04	0.28	0.04	1.46	0.10	0.18	0.15	0.11
Ce	0.66	0.11	0.36	0.06	2.79	0.23	0.25	0.23	0.12
Pr	0.08	0.01	0.09	0.01	0.26	0.04	0.03	0.04	0.02
Nd	0.46	0.08	0.27	0.06	1.18	0.14	0.13	0.14	0.07
Sm	0.14	b.d.l.	0.03	b.d.l.	0.09	0.07	0.07	0.08	0.03
Eu	0.01	b.d.l.	0.02	0.01	0.04	0.06	0.02	0.47	0.56
Gd	0.31	0.02	0.06	0.02	0.21	0.11	0.11	0.03	0.01
Dy	0.21	0.02	0.04	0.04	0.05	0.24	0.08	0.07	0.06
Er	0.25	0.03	0.03	0.06	0.09	0.19	0.08	0.10	0.04
Yb	0.17	0.08	0.02	0.08	0.09	0.15	0.19	0.05	0.04
Lu	0.01	0.01	0.01	0.02	0.03	0.03	0.01	0.01	0.01
Sr	1.20	0.15	1.23	0.19	0.92	8.84	3.13	63.0	73.7
Ba	0.82	0.16	1.05	0.07	4.17	3.87	0.62	40.7	46.6
V	32.4	14.2	68.8	45.8	33.0	81.0	60.4	22.6	24.6
Ni	56.1	55.7	127	53.6	1,813	–	260	–	–
Cr	665	407	5,290	922	717	2,328	1,786	185	117
Rb	2.21	1.67	1.59	1.20	2.59	2.79	0.15	7.92	8.21
REE	2.56	0.40	1.22	0.40	6.30	1.35	1.17	1.36	1.06
LREE	1.60	0.24	1.05	0.18	5.83	0.64	0.69	1.11	0.90
HREE	0.96	0.16	0.16	0.22	0.47	0.72	0.47	0.25	0.16

Trace element concentrations are fairly heterogeneous in low-Ca pyroxene from chondrule 8POP-3. Grains with very high and very low LREE concentrations, relative to those in the pyroxene of the matrix, occur in the pyroxene of the chondrule margin. Pyroxene in the matrix is richer in Y, Sr and Ba than pyroxene in the chondrule. It occupies an intermediate position with respect to REE concentration.

The trace element distribution spectrum in low-Ca pyroxene from chondrule 8POP-3 is highly differentiated and is consistent with chondrite values (Fig.3, *d*). Trace element concentrations in low-Ca pyroxene from chondrule 8POP-3 are higher than those in the pyroxene of porphyritic chondrules in unequilibrated ordinary chondrites.

Plagioclase in chondrule 8POP-3 is present as oligoclase (An 10-16, Or 4) with high variable impurity element (CaO, MgO, FeO) composition (Table 3). Plagioclase in chondrule 8POP-3 occurs in interstices between olivine and pyroxene. It is not abundant in the chondrule, forming aggregates no more than 50 μm in size.

Trace element concentrations in the plagioclase of chondrule 8POP-3 are homogeneous. Trace element concentrations in plagioclase are consistent with chondrite values, coinciding with plagioclase in Renazzo coaly chondrite (Fig.3, *f*). The distribution spectra are poorly differentiated. They display a well-defined europium anomaly and show no prevalence of LREE over HREE.

Discussion.

The silicate minerals of porphyritic (8PO-1, 8POP-3) and radiated (8ROP-2) chondrules do not differ in major element concentrations but differ in the trace element composition of these minerals.

The trace element distribution spectrum for olvine in chondrules is poorly differentiated, but some grains of porphyritic chondrule 8POP-3 are enriched in incompatible LREE, Sr and Ba (Fig.4, *a*). Olivine in this chondrule is more abundant than olivine in other chondrules, presumably indicating a relationship between grain size and trace element concentration. No considerable differences in the trace element composition of mineral grains occurring inside the chondrule or in the meteorite matrix were found (Fig.4, *b*).

This is an open access article under the CC BY 4.0 license

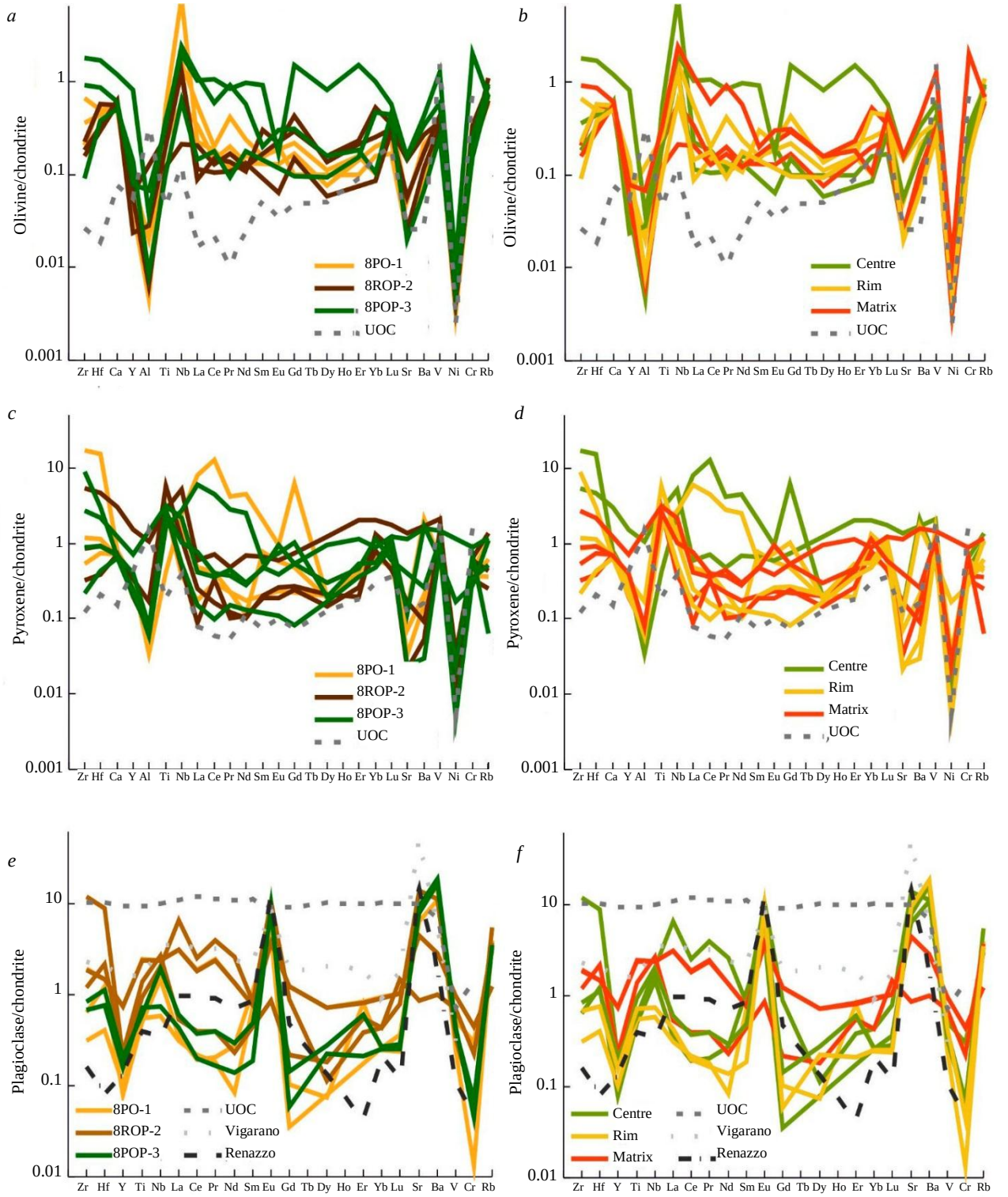

Fig.4. Spider diagrams for trace elements normalized to CI chondrite in olivine, low-Ca pyroxene and plagioclase from the Kunashak Meteorite: relative to different chondrules (*a*, *c*, *e*) and the location of grains inside/outside the chondrule (*b*, *d*, *f*). Data on the composition of UOC, Vigarano and Renazzo minerals are given according to [38, 40]

Differences between olivine in the chondrules in diagrams showing Rb-Yb (Fig.5, *a*) and Zr-Ti relationships (Fig.5, *b*) are better defined than those in trace element distribution spectra. For instance, Rb-Yb relationship shows that olivine in chondrule 8ROP-2 is enriched in moderately volatile and incompatible Rb, while olivine in porphyritic olivine-pyroxene chondrule 8POP-3 is enriched in refractory Yb. Olivine in chondrule 8PO-1 is poor in these elements.

This is an open access article under the CC BY 4.0 license

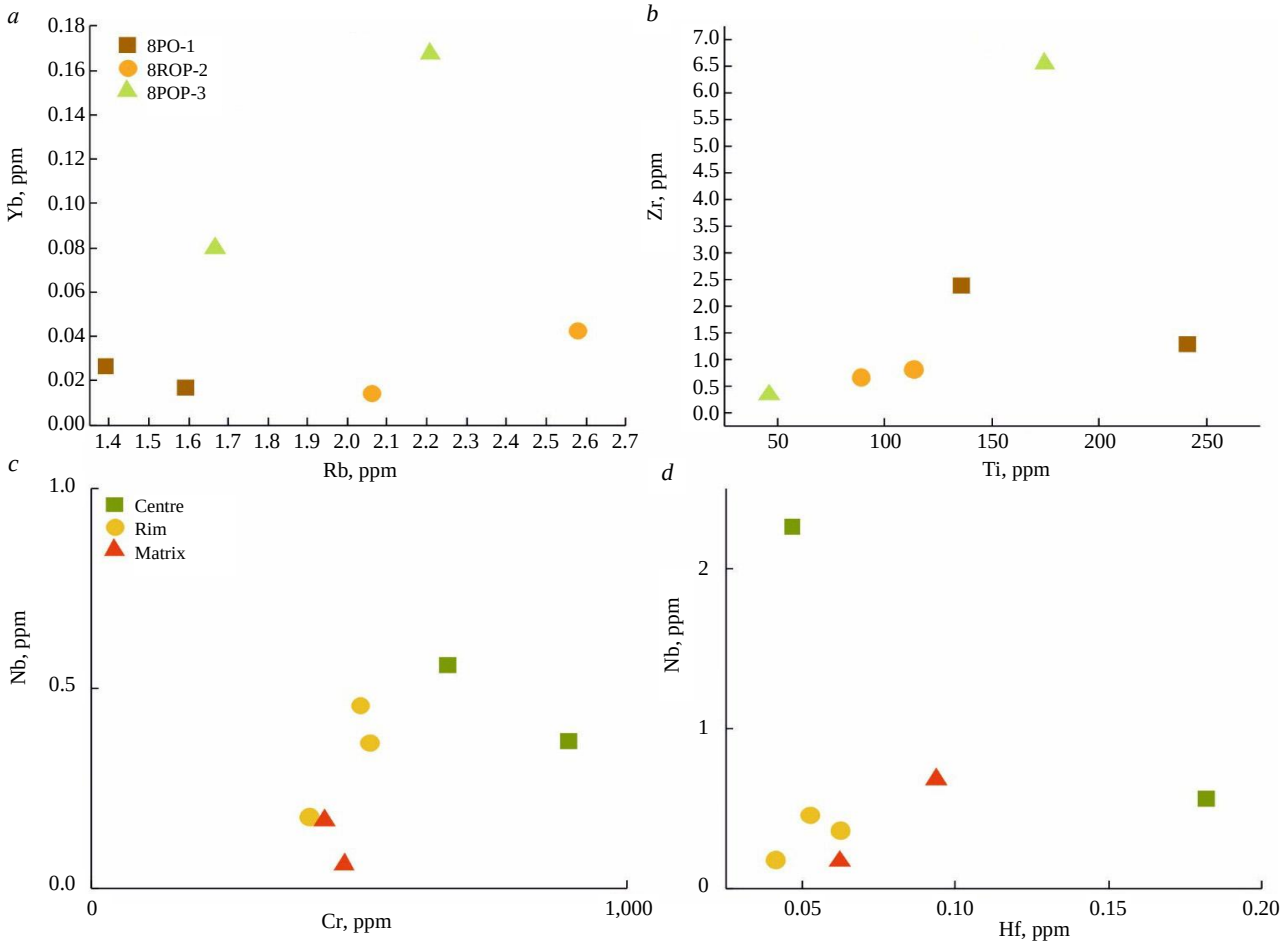

Fig.5. The Yb/Rb (*a*), Zr/Ti (b), Nb/Cr (*c*) and Nb/Hf (*d*) in olivine from Kunashak Meteorite

The diagram for refractory Zr-Ti relationship, conversely, shows that olivine in porphyritic olivine chondrule 8PO-1 is enriched in these elements, while olivine in the radiated chondrule is impoverished in them, and olivine in porphyritic chondrule 8POP-3 may show different values.

The diagram for Cr-Nb relationship (Fig.5, *в*) shows a difference between olivine in the centre of the chondrules enriched in these elements and olivine on the chondrule margin and in the matrix of the meteorite, which is usually impoverished in them.

The relationship of refractory Hf and Nb (Fig.5, *d*) also indicates elevated concentrations of the above elements in olivine in the centre of the chondrule and minimum concentrations in olivine on the chondrule margin and in the matrix of the meteorite.

Trace element distribution spectra in low-Ca pyroxene are more differentiated than spectra for olivine, indicating elevated trace element concentrations in pyroxene from porphyritic chondrules (8PO-1, 8POP-3) (see Fig.4, *c*). No considerable differences between low-Ca pyroxene in the centre and on the margin of the chondrule, as well as the meteorite matrix, were revealed, but pyroxene grains in the centre of the chondrule tend to be enriched in trace elements (see Fig.4, *d*).

Low-Ca pyroxene in radiated chondrule 8ROP-2 is clearly different, as shown by diagrams for Zr/Cr, Hf/Yb and Nb/Ti relationships (Fig.6, *a*, *c*, *e*). For instance, pyroxene in the radiated chondrule has higher Cr, Yb, Nb and Ti concentrations than pyroxenes in porphyritic chondrules, which display no differences.

The diagrams showing Nb-Hf, HREE-Rb and Zr-Yb relationships (Fig.6, *b*, *d*, *f*) indicate the enrichment of low-Ca pyroxene in the central zones of the chondrule relative to low-Ca pyroxene on the chondrule margin and in the meteorite matrix. The diagram for Nb and Hf shows that these elements are directly correlated in pyroxene from the chondrule margin and the meteorite matrix, which is not traced in pyroxene from the centre of the chondrule. HREE-Rb relationship indicates that its value tends to increase upon transition from pyroxene in the meteorite matrix to pyroxene on the chondrule margin. Low-Ca pyroxene in the centre of the chondrule has the highest HREE and Rb concentrations.

This is an open access article under the CC BY 4.0 license

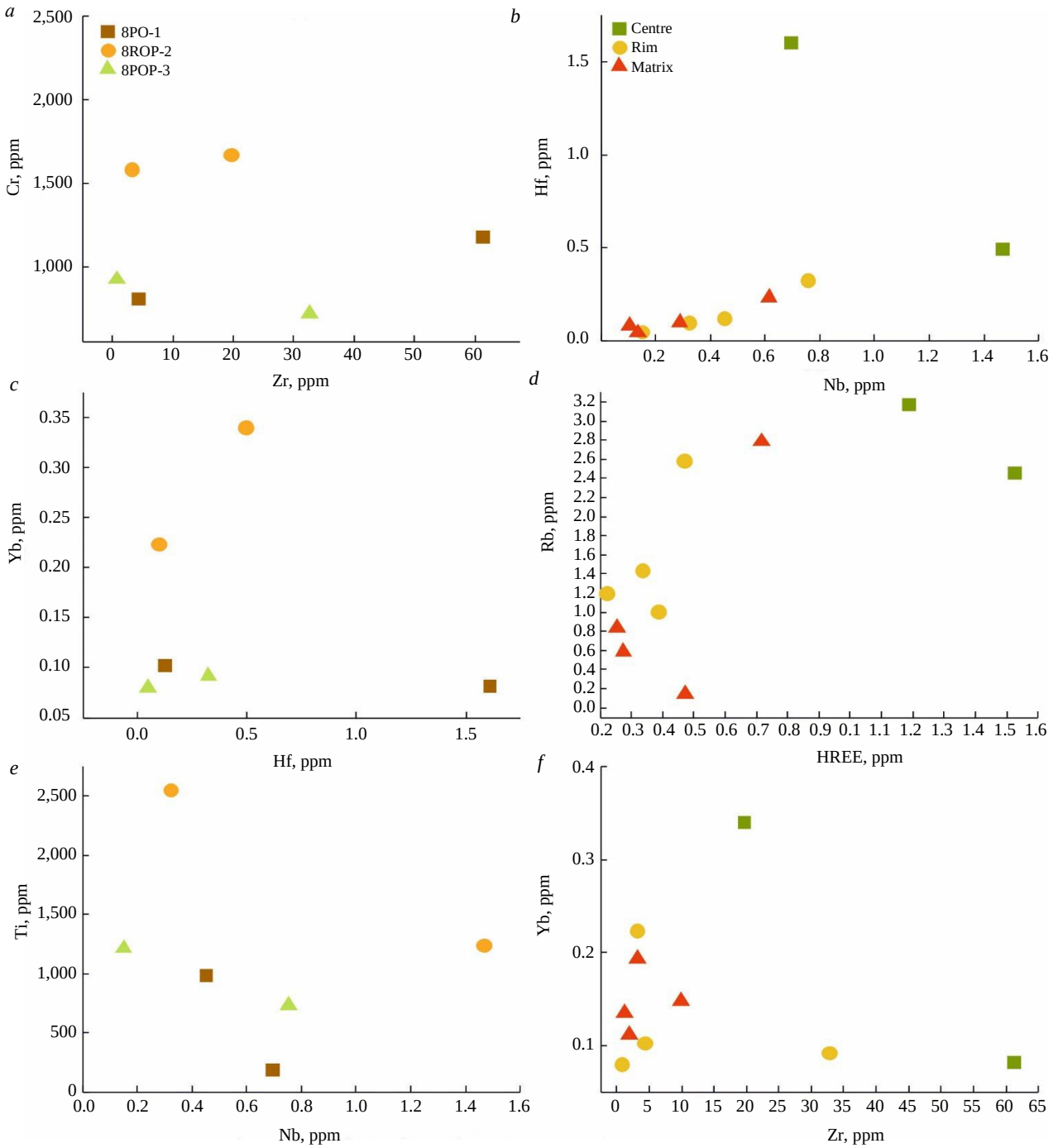

Fig.6. The Cr/Zr (*a*), Hf/Nb (*b*), Yb/Hf (*c*), Rb/HREE (*d*), Ti/Nb (*e*), Yb/Zr (*f*) ratios in low-Ca pyroxene from Kunashak Meteorite

Plagioclase displays the greatest differentiation of trace element distribution spectra in comparison with olivine and low-Ca pyroxene in Kunashak Meteorite (see Fig.4, *e*). Plagioclase from the chondrules analyzed is similar in trace element distribution spectra to plagioclase from Renazzo coaly chondrite. A similar spectrum was obtained for plagioclase from the most heavily metamorphosed ordinary chondrites. This evidence is supported by petrological type VI of Kunashak Meteorite.

Plagioclase in radiated chondrule 8ROP-2 is remarkable for its spectrum, which is most similar to plagioclase from Vigarano coaly chondrite and differs in elevated refractory and REE concentrations from other plagioclases in Kunashak Meteorite.

No significant differences between trace element distribution spectra in plagioclase from the centre, margin or matrix of the meteorite have been found, although plagioclase from the chondrule

This is an open access article under the CC BY 4.0 license

margin tends to be impoverished in trace elements, as compared with plagioclase from the central zone of the chondrule and the matrix of the meteorite (see Fig.4, *f*).

Differences between plagioclase in chondrules 8PO-1, 8POP-3 and 8ROP-2 are shown on diagrams for Sr-Ba, Ti-Y and Zr-Y relationships (Fig.7, *a*, *c*, *e*). The correlation of moderately volatile compatible Sr and Ba indicates that plagioclase from porphyritic chondrules is enriched in Ba and is poor in Sr, while plagioclase from the radiated chondrule displays a reverse distribution with high Sr and low Ba concentrations.

The graph of the Y and Ti ratio shows a direct correlation, in which the plagioclase of the porphyritic olivine chondrule is depleted in these elements, the plagioclase of the radial chondrule is enriched in them, and the plagioclase of the porphyritic olivine-pyroxene chondrule occupies an intermediate position.

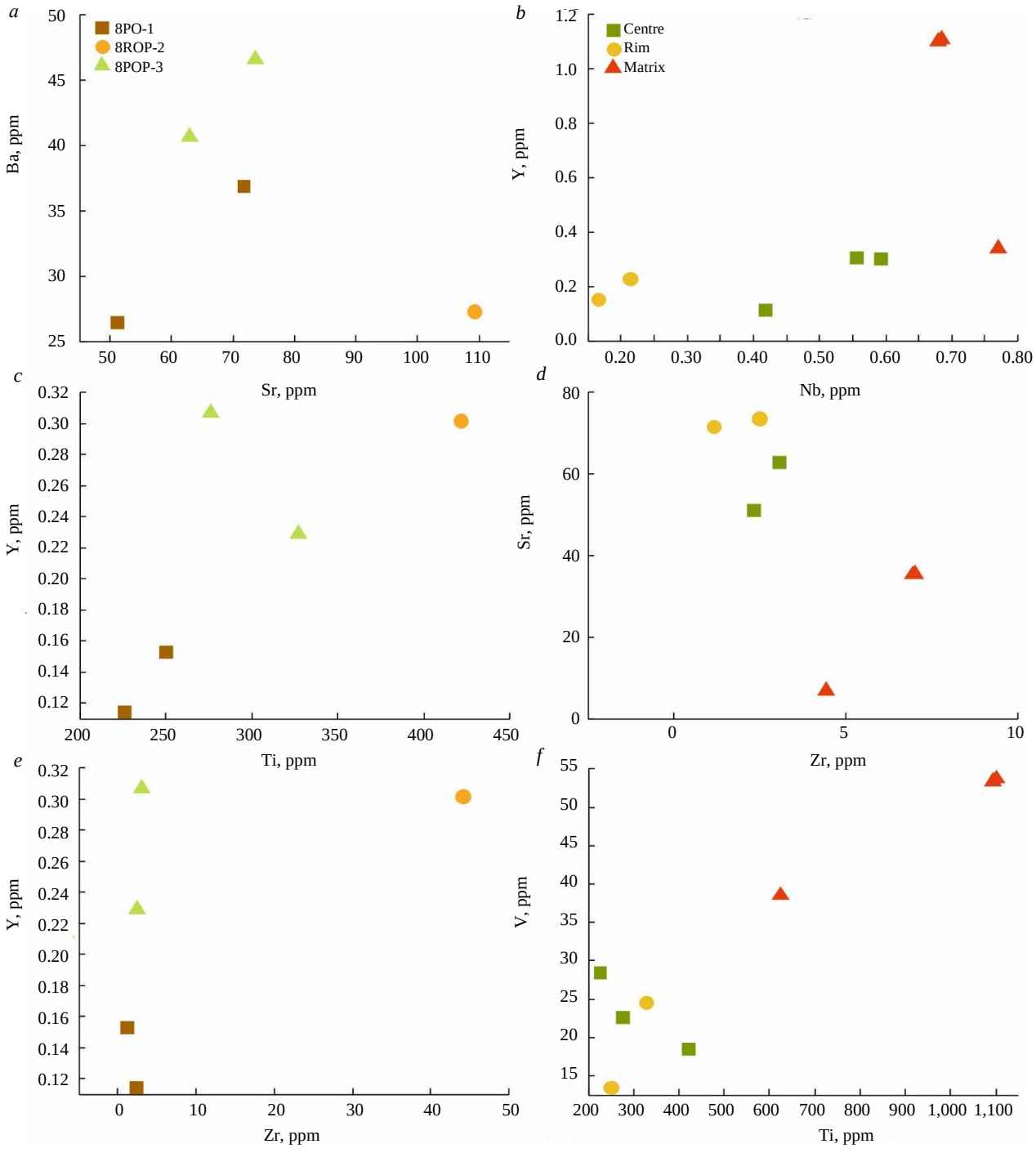

Fig.7. The Ba/Sr (*a*), Y/Nb (*b*), Y/Ti (*c*), Sr/Zr (*d*), Y/Zr (*e*), V/Ti (*f*) ratios in plagioclase from Kunashak Meteorite

This is an open access article under the CC BY 4.0 license

The Zr and Y ratio reflects the enrichment of the plagioclase of the porphyritic olivine-pyroxene chondrule in Y, high concentrations of Zr in the plagioclase of the radial chondrule and a low content of both elements in the plagioclase of the porphyritic olivine chondrule. The ratio of Nb/Y, Zr/Sr and Ti/V allows us to identify the characteristic features of the trace element composition of the plagioclase of the center, the rim of the chondrule and the matrix of the meteorite (Fig.7, *b*, *d*, *e*). The chondrules typically display low Sr and Ba concentrations. Plagioclase from the centre of the chondrules occupies an intermediate position with respect to Nb concentration.

The diagram for Zr and Sr shows a gradual decline in moderately volatile Sr concentration and a rise in Zr concentration from the margin to the centre of the chondrule and then to the meteorite matrix.

Also, plagioclase from the meteorite matrix has high refractory Ti and moderately volatile V concentrations, although plagioclase from the chondrules is typically poor in Ti and V.

Conclusion.

Porphyritic olivine-pyroxene chondrule 8POP-3 contains elevated trace element concentrations in olivine and especially the highest Yb concentrations (~0.12 ppm) in comparison with chondrules 8PO-1 and 8ROP-2 (0.02 ppm).

Radiated chondrule 8ROP-2 contains low-Ca pyroxene and plagioclase with high trace element concentrations. Low-Ca pyroxee typically has elevated Yb, Cr, Nb and Ti concentrations. Pyroxene from porphyritic chondrules contains minimum concentrations of the above elements. Plagioclase from the radiated chondrule is rich in Sr, Y, Ti, and Zr. Elevated trace element concentrations in low-Ca pyroxene and plagioclase from the radiated chondrule are indicative of rapid chondrule crystallization (over 1,000 °C/h). The incompatible LREE and Ba distribution coefficient in olivine and low-Ca pyroxene was found to increase 100-fold when cooling rate increases, but it becomes only twice as high for compatible Yb and Lu [41].

Thus, the trace element composition of silicate minerals from Kunashak Meteorite has retained the individual distinctive features of chondrule melting, and was not affected by thermal metamorphism on parent chondrite bodies. Similar results were obtained by studying Bushkhov Meteorite (L6) [34]. We are sure that trace elements in olivine and low-Ca pyroxene are resistant to thermal metamorphism.

The persistence of the distinctive features of chondrules enables us to use equilibrated ordinary chondrites for study of processes that took place at early stages in the formation of the Solar System and for a better understanding of chondrule and planet formation mechanisms.

The authors are grateful to S.G.Simakin and E.V.Potapov (Valiev IPT, RAS, Yaroslavl Branch) for analytical work.

REFERENCES

1. Krinov E.L. Kunashak stone meteor shower. *Meteoritika*. 1950. N 8, p. 66-77 (in Russian).
2. Yudin I.A. New data on the Kunashak meteorite shower. *Meteoritika*. 1951. N 9, p. 122-123 (in Russian).
3. Erokhin Y.V., Koroteev V.A., Khiller V.V. et al. Kunashak meteorite: new data on mineralogy. *Doklady Earth Sciences.* 2015. Vol. 464. N 2, p. 1058-1061. DOI: 10.1134/S1028334X15100128
4. Yudin I.A. On the presence of meteoric dust in the area of the fall of the Kunashak meteorite shower. *Meteoritika*. 1960. N 18, p. 113-118 (in Russian).
5. Zotkin I.T., Krinov E.L. Study of the conditions of the fall of the Kunashak meteorite shower. *Meteoritika*. 1958. N 15, p. 51-81 (in Russian).
6. Tsvetkov V. On meteorite orbits. *Earth, Moon, and Planets*. 1987. Vol. 37. Iss. 2, p. 133-140. DOI: 10.1007/BF00130888
7. Lindsay S.S., Dunn T.L., Emery J.P., Bowles N.E. The Red Edge Problem in asteroid band parameter analysis. *Meteoritics & Planetary Science*. 2016. Vol. 51. Iss. 4, p. 806-817. DOI: 10.1111/maps.12611
8. Pape J., Mezger K., Bouvier A.-S., Baumgartner L.P. Time and duration of chondrule formation: Constraints from ^{26}Al-^{26}Mg ages of individual chondrules. *Geochimica et Cosmochimica Acta*. 2019. Vol. 244, p. 416-436. DOI: 10.1016/j.gca.2018.10.017
9. Piralla M., Villeneuve J., Batanova V. et al. Conditions of chondrule formation in ordinary chondrites. *Geochimica et Cosmochimica Acta*. 2021. Vol. 313, p. 295-312. DOI: 10.1016/j.gca.2021.08.007
10. Hewins R.H., Connolly H.C., Lofgren Jr. G.E., Libourel G. Experimental Constraints on Chondrule Formation. Chondrites and the protoplanetary disk: Proceedings of a workshop held at the Radisson Kaua'i Beach Resort, 8-11 November 2004, Kaua'i, Hawai'i. San Francisco: Astronomical Society of the Pacific, 2005. Vol. 341, p. 286-316.
11. Russell S.S., Connolly Jr. H.C., Krot A.N. Chondrules. Records of Protoplanetary Disk Processes. Cambridge University Press, 2018, p. 56. DOI: 10.1017/9781108284073
12. Jacquet E., Piralla M., Kersaho P., Marrocchi Y. Origin of isolated olivine grains in carbonaceous chondrites. *Meteoritics & Planetary Science*. 2021. Vol. 56. Iss. 1, p. 13-33. DOI: 10.1111/maps.13583

This is an open access article under the CC BY 4.0 license

13. Marrocchi Y., Euverte R., Villeneuve J. et al. Formation of CV chondrules by recycling of amoeboid olivine aggregate-like precursors. *Geochimica et Cosmochimica Acta*. 2019. Vol. 247, p. 121-141. DOI: 10.1016/j.gca.2018.12.038
14. Nardi L., Palomba E., Longobardo A. et al. Mapping olivine abundance on asteroid (25143) Itokawa from Hayabusa/NIRS data. *Icarus*. 2019. Vol. 321, p. 14-28. DOI: 10.1016/j.icarus.2018.10.035
15. Jacquet E., Marrocchi Y. Chondrule heritage and thermal histories from trace element and oxygen isotope analyses of chondrules and amoeboid olivine aggregates. *Meteoritics & Planetary Science*. 2017. Vol. 52. Iss. 12, p. 2672-2694. DOI: 10.1111/maps.12985
16. Libourel G., Krot A.N. Evidence for the presence of planetesimal material among the precursors of magnesian chondrules of nebular origin. *Earth and Planetary Science Letters*. 2007. Vol. 254. Iss. 1-2, p. 1-8. DOI: 10.1016/j.epsl.2006.11.013
17. Tenner T.J., Nakashima D., Ushikubo T. et al. Oxygen isotope ratios of FeO-poor chondrules in CR3 chondrites: Influence of dust enrichment and H_2O during chondrule formation. *Geochimica et Cosmochimica Acta*. 2015. Vol. 148, p. 228-250. DOI: 10.1016/j.gca.2014.09.025
18. Varela M.E., Zinner E. Unraveling the role of liquids during chondrule formation processes. *Geochimica et Cosmochimica Acta*. 2018. Vol. 221, p. 358-378. DOI: 10.1016/j.gca.2017.03.038
19. Ruzicka A.M., Greenwood R.C., Armstrong K. et al. Petrology and oxygen isotopic composition of large igneous inclusions in ordinary chondrites: Early solar system igneous processes and oxygen reservoirs. *Geochimica et Cosmochimica Acta*. 2019. Vol. 266, p. 497-528. DOI: 10.1016/j.gca.2019.01.017
20. Bischoff A., Schleiting M., Wieler R., Patzek M. Brecciation among 2280 ordinary chondrites – Constraints on the evolution of their parent bodies. *Geochimica et Cosmochimica Acta*. 2018. Vol. 238, p. 516-541. DOI: 10.1016/j.gca.2018.07.020
21. Lewis J.A., Jones R.H., Garcea S.C. Chondrule porosity in the L4 chondrite Saratov: Dissolution, chemical transport, and fluid flow. *Geochimica et Cosmochimica Acta*. 2018. Vol. 240, p. 293-313. DOI: 10.1016/j.gca.2018.08.002
22. Varela M.E. Bulk trace elements of Mg-rich cryptocrystalline and ferrous radiating pyroxene chondrules from Acfer 182: Their evolution paths. *Geochimica et Cosmochimica Acta*. 2019. Vol. 257, p. 1-15. DOI: 10.1016/j.gca.2019.04.025
23. Levashova E.V., Mamykina M.E., Skublov S.G. et al. Geochemistry (TE, REE, Oxygen) of Zircon from Leucogranites of the Belokurikhinsky Massif, Gorny Altai, as Indicator of Formation Conditions. *Geochemistry International*. 2023. Vol. 61. Iss. 13, p. 1323-1339. DOI: 10.1134/S001670292311006X
24. Skublov S.G., Rumyantseva N.A., Vanshtein B.G. et al. Zircon Xenocrysts from the Shaka Ridge Record Ancient Continental Crust: New U-Pb Geochronological and Oxygen Isotopic Data. *Journal of Earth Science*. 2022. Vol. 33. Iss. 1, p. 5-16. DOI: 10.1007/s12583-021-1422-2
25. Skublov S.G., Levashova E.V., Mamykina M.E. et al. The polyphase Belokurikhinsky granite massif, Gorny Altai: isotope-geochemical study of zircon. *Journal of Mining Institute*. 2024, p. 24 (Online first).
26. Salimgaraeva L.I., Berezin A.V. Garnetites from Marun-Keu eclogite complex (Polar Urals): geochemistry and the problem of genesis. *Journal of Mining Institute*. 2023. Vol. 262, p. 509-525.
27. Stativko V.S., Skublov S.G., Smolenskiy V.V., Kuznetsov A.B. Trace and rare-earth elements in garnets from silicate-carbonate formations of the Kusa-Kopan complex (Southern Urals). *Lithosphere*. 2023. Vol. 23. N 2, p. 225-246 (in Russian). DOI: 10.24930/1681-9004-2023-23-2-225-246
28. Skublov S.G., Gavrilchik A.K., Berezin A.V. Geochemistry of beryl varieties: comparative analysis and visualization of analytical data by principal component analysis (PCA) and t-distributed stochastic neighbor embedding (t-SNE). *Journal of Mining Institute*. Vol. 255, p. 455-469. DOI: 10.31897/PMI.2022.40
29. Gavrilchik A.K., Skublov S.G., Kotova E.L. Trace Element Composition of Beryl from the Sherlovaya Gora Deposit, Southea-stern Transbaikal Region, Russia. *Geology of Ore Deposits*. 2022. Vol. 64. N 7, p. 442-451. DOI: 10.1134/s1075701522070054
30. Lichtenberg T., Golabek G.J., Dullemond C.P. et al. Impact splash chondrule formation during planetesimal recycling. *Icarus*. 2018. Vol. 302, p. 27-43. DOI: 10.1016/j.icarus.2017.11.004
31. Chakraborty S. Diffusion Coefficients in Olivine, Wadsleyite and Ringwoodite. *Reviews in Mineralogy and Geochemistry*. 2010. Vol. 72. N 1, p. 603-639. DOI: 10.2138/rmg.2010.72.13
32. Cherniak D.J. REE diffusion in olivine. *American Mineralogist*. 2010. Vol. 95. Iss. 2-3, p. 362-368. DOI: 10.2138/am.2010.3345
33. Marrocchi Y., Villeneuve J., Batanova V. et al. Oxygen isotopic diversity of chondrule precursors and the nebular origin of chondrules. *Earth and Planetary Science Letters*. 2018. Vol. 496, p. 132-141. DOI: 10.1016/j.epsl.2018.05.042
34. Sukhanova K.G., Skublov S.G., Galankina O.L. et al. Trace Element Composition of Silicate Minerals in the Chondrules and Matrix of the Buschhof Meteorite. *Geochemistry International*. 2020. Vol. 58. N 12, p. 1321-1330. DOI: 10.1134/S001670292012006X
35. Sukhanova K.G. Composition of silicate minerals as a reflection of the evolution of equilibrium ordinary chondrites: Avtoref. dis. … kand. geol.-mineral. nauk. Moscow: Moskovskii gosudarstvennyi universitet imeni M.V.Lomonosova, 2022, p. 21.
36. Batanova V.G., Suhr G., Sobolev A.V. Origin of Geochemical Heterogeneity in the Mantle Peridotites from the Bay of Islands Ophiolite, Newfoundland, Canada: Ion Probe Study of Clinopyroxenes. *Geochimica et Cosmochimica Acta*. 1998. Vol. 62. Iss. 5, p. 853-866. DOI: 10.1016/S0016-7037(97)00384-0
37. Portnyagin M., Almeev R., Matveev S., Holtz F. Experimental evidence for rapid water exchange between melt inclusions in olivine and host magma. *Earth and Planetary Science Letters*. 2008. Vol. 272. Iss. 3-4, p. 541-552. DOI: 10.1016/j.epsl.2008.05.020
38. Palme H., Lodders K., Jones A. 2.2 – Solar System Abundances of the Elements. Treatise on Geochemistry. Elsevier, 2014. Vol. 2: Planets, Asteriods, Comets and The Solar System, p. 15-36. DOI: 10.1016/b978-0-08-095975-7.00118-2
39. Jacquet E., Alard O., Gounelle M. Trace element geochemistry of ordinary chondrite chondrules: The type I/type II chondrule dichotomy. *Geochimica et Cosmochimica Acta*. 2015. Vol. 155, p. 47-67. DOI: 10.1016/j.gca.2015.02.005
40. Jacquet E., Alard O., Gounelle M. Chondrule trace element geochemistry at the mineral scale. *Meteoritics and Planetary Science*. 2012. Vol. 47. Iss. 11, p. 1695-1714. DOI: 10.1111/maps.12005
41. Kennedy A.K., Lofgren G.E., Wasserburg G.J. An experimental study of trace element partitioning between olivine, orthopyroxene and melt in chondrules: equilibrium values and kinetic effects. *Earth and Planetary Science Letters*. 1993. Vol. 115. Iss. 1-4, p. 177-195. DOI: 10.1016/0012-821X(93)90221-T

Authors: **Kristina G. Sukhanova,** *Candidate of Geological and Mineralogical Sciences, Junior Researcher, cris.suhanova92@yandex.ru, https://orcid.org/0000-0001-5695-0767* (*Institute of Precambrian Geology and Geochronology RAS, Saint Petersburg, Russia*), **Olga L. Galankina,** *Candidate of Geological and Mineralogical Sciences, Senior Researcher, https://orcid.org/0000-0003-2761-2835* (*Institute of Precambrian Geology and Geochronology RAS, Saint Petersburg, Russia*).

The authors declare no conflict of interests.

This is an open access article under the CC BY 4.0 license

ISSN 2411-3336; e-ISSN 2541-9404

JOURNAL OF MINING INSTITUTE

Zapiski Gornogo instituta

Journal homepage: pmi.spmi.ru

Research article

A new insight into recording the mineral composition of carbonate reservoirs at well killing: experimental studies

Vasilii I. Chernykh[1], **Dmitrii A. Martyushev**[2]✉, **Inna N. Ponomareva**[2]

[1] *Branch of OOO "LUKOIL-Engineering" "PermNIPIneft" in Perm, Perm, Russia*

[2] *Perm National Research Polytechnic University, Perm, Russia*

***How to cite this article*:** Chernykh V.I., Martyushev D.A., Ponomareva I.N. A new insight into recording the mineral composition of carbonate reservoirs at well killing: experimental studies. Journal of Mining Institute. 2024. Vol. 270, p. 893-903.

Abstract

Well killing operation remains an important technological stage before well workover or servicing, during which filtrate penetrates the bottomhole area of the formation. The impact of process fluids and their filtrate on rock has a significant influence on permeability and porosity of carbonate reservoirs, which decrease due to fines migration. There are few known scientific studies of the interaction of killing fluid filtrate with carbonate rock and fines migration. In our experiments, an aqueous phase was used which is the basis for well killing in pure form, for the preparation of blocking agents and is used in reservoir pressure maintenance system. Core samples taken from the pay of the reservoir were used to simulate the well killing process with generation of reservoir thermobaric conditions. Killing fluid filtrate was kept for seven days, which characterizes the average workover time at flowing wells in the fields of the Perm Territory. Using micro-X-ray tomography and scanning electron microscope, images were obtained before and after the experiment, which allowed confirming a decrease in total number of voids due to fines migration and, as a consequence, a decreasing permeability of samples. Measurement of pH and fines concentration in the aqueous phase was performed before and after the experiment and pointed to mineral reactions occurring as a result of rock dissolution. The results of experiments made it possible to record a decrease in permeability of carbonate samples by an average of 50 % due to clogging of void space and migration of fines (clayey and non-clayey).

Keywords

fines; dissolution; micro-X-ray tomography; scanning electron microscope; permeability; clay minerals; low mineralized water

Funding

The research was conducted with support of the Ministry of Science and Higher Education of the Russian Federation (project N FSNM-2024-0005).

Received: 07.07.2023 ***Accepted: 27.12.2023*** ***Online: 11.04.2024*** ***Published: 25.12.2024***

Introduction.

Killing fluids are used in well workover to prevent the formation fluids from penetrating into the well-bore [1, 2]. As a rule, in this case, the killing fluid filtrate penetrates the bot-tomhole area of the formation, which can lead to deterioration of reservoir properties or "damage of the formation" [3-5]. The influence of process fluid filtrate on rock properties is more significant in reservoirs characterized by a high permeability and a network of cracks and cavities [6, 7]. The main mechanisms causing formation damage include incompatibility of filtrate with formation fluid, rock and filtrate, penetration and deposition of solid particles in the void space of rock, chemical adsorption, swelling of clay minerals, migration of fines and biological activity [8]. Well capacity after workover will largely depend on the interaction degree between the filtrate of process fluids and

This is an open access article under the CC BY 4.0 license

rock in the bottomhole area [9, 10]. The main and urgent task when working with the pay is to minimize the negative impact of filtrate of process fluids, including those used for well killing, on reservoir properties.

The technologies using aqueous solutions of inorganic salts or blocking agents in aqueous phase are applied to kill wells in oil fields of the Perm Territory. Back pressure on the formation is created, due to which the killing fluid (or its filtrate) penetrates the reservoir. Interaction of killing fluid filtrate with rock-forming minerals and formation fluids leads to a deterioration in reservoir properties of the formation in the penetration zone. As a consequence, the process of bringing the well to stable production becomes more complicated, and well capacity decreases [11].

Specific features of interaction of drilling fluid filtrate and killing fluids with terrigenous and shale rocks are well studied [12-14]. The investigations showed that the content of aqueous phase and its chemical composition had a major impact on petrophysical properties of rock. The content of aqueous phase can influence the structure and the integrity of rock as well as the swelling of clay minerals, which leads to a change in the void space [15]. For example, the authors of [16] studied the effect of duration of interaction between process fluid filtrate and the rock, and found that after five days of exposure, the porosity of the Berea Buff field reservoir decreased by 41 %, which is associated with serious changes in rock pore structure.

However, for carbonate reservoirs there are few similar studies related to the assessment of changes in their properties under the influence of process fluids including killing fluids. Carbonate rocks, like sandstones, can have a complex mineralogical composition [17]. Silicate minerals have a significant impact on physical and chemical properties of carbonate rock due to their small particle size, large surface area and cation-exchange capacity [18]. In study [19], the authors investigated the effect of injected "smart" water on clay minerals in carbonate rocks. To evaluate the swelling and migration of clays, they used microfluidic tests with the presence of kaolinite and montmorillonite clays. As a result of the study, it was ascertained that the injected water with salt concentration below critical led to swelling and migration of clay minerals and, as a consequence, a decrease in the number of voids and rock permeability.

Analysis of scientific literature shows that the influence of mineralogy or the initial internal struc-ture of rock on the specific features of well killing is considered in few studies. In papers [20, 21] it was concluded that a heterogeneous pore size or pore shape distribution will affect the dissolution mechanisms and lead to different dissolution patterns within the rock. Other studies [22, 23] determined new dissolution patterns related to the internal structure of rock. On a large scale, major structural heterogeneities, such as cracks, affect the rate and form of rock dissolution [24].

This study is aimed at investigating the influence of killing fluid filtrate on reservoir properties of carbonate formations. The study makes a new contribution to analysing the interactions between the filtrate of process fluids (fluid for well killing) and carbonate sediments in two fields in the Perm Territory (Sukharev and Vinnikovskoe), a detailed geological description of which is presented in [17]. Chemical composition of fluid filtrate, mineralogical composition of carbonate rocks, formation pressure and temperature, and extent of the "filtrate – rock" contact are considered in this work as the key factors influencing the reservoir properties.

Methodology.

To study the impact of process fluids on carbonate reservoirs (Tournaisian-Famennian), 10 samples were prepared from the pay of reservoir in the Sukharev and Vinnikovskoe fields. The choice of these formations was due to different structure of the void space and mineral composition of inclusions and new growths, which were assessed using X-ray phase and X-ray fluo-rescence analyses, scanning electron microscopy and micro-X-ray tomography [17]. Microscopic studies of core samples with diagnostics of minerals based on microprobe analysis and the description of specific features

This is an open access article under the CC BY 4.0 license

of microstructure and microtexture as well as the construction of 3D models of the structure of core samples with histograms of void distribution by size were con-ducted before and after the filtration experiments on assessment of the impact of killing fluid filtrate on rock.

Then, core samples were prepared for filtration experiments, while residual water saturation was produced using formation water specially taken from the well in the reservoir. Filtration tests were conducted on core testing unit UIK-5VG and AFS-300 under thermobaric formation conditions: pore pressure 18 MPa, hydraulic compression pressure 30 MPa, temperature 30±1 °C. Reservoir oil with viscosity of 4.9 mPa·s was used in experiments. Holding time of killing fluid filtrate is seven days, it characterizes average duration of flowing wells workover in the fields under consideration. Filtration experiments were accomplished according to the following scheme [25]:

- a sample saturated with kerosene is placed in a filtration unit;
- thermodynamic conditions are created;
- kerosene is filtered through the sample in a direction simulating the "formation – well" operation, permeability to kerosene is determined;
- kerosene in the sample is replaced by oil through its filtration in the amount of at least three pore volumes;
- oil flow from the formation into the well is simulated by filtering oil through the sample in the corresponding direction; permeability of sample to oil is determined (K_{o1});
- well killing is simulated with penetration of process water into formation, for which it is pumped through the sample in the "well – formation" direction and maintained under specified thermodynamic conditions for seven days (average workover duration);
- well completion after workover is simulated, oil is filtered through the sample in the "formation-well" direction, permeability to oil (K_{o2}) and porosity of samples to helium are determined.

Thus, a series of experiments allowed determining the porosity and permeability of core samples to oil before and after well killing simulation with process water. In the course of experiments, the quantitative chemical analysis of the aqueous phase (filtrate) of well killing fluid was performed.

Results.

Assessment of chemical analysis of killing fluid filtrate is presented below: pH value – 6.99; permanganate oxidability – 3.3 mg/dm^3; hydrocarbonate ion – 131.15 mg/dm^3; chloride ion – 76.33 mg/dm^3; sulphate ion – 68.33 mg/dm^3; nitrite nitrogen – 0.0 mg/dm^3; nitrate ion – 0.34 mg/dm^3; carbonate ion – 0.0 mg/dm^3; calcium – 60.14 mg/dm^3; total hardness – 3.64 °dH; total iron – 0.14 mg/dm^3; iron (3+) – 0.0 mg/dm^3; ammonium ion – 0.0 mg/dm^3; free carbon dioxide – 17.60 mg/dm^3; dry residue – 313 mg/dm^3; magnesium (calculation) – 7.7 mg/dm^3; total mass concentration of sodium and potassium ions (calculation) – 50.12 mg/dm^3.

Based on results of chemical analysis, it was ascertained that the aqueous phase corresponded to the first category according to SanPin 2.1.4.1074-01 and was characterized as low-mineralized.

The results of filtration experiments on simulation of well killing operation are given in Table 1 and Fig.1. Table 1 also presents the results of assessing the open porosity of core samples before and after filtration experiments. Table 1 shows the most informative results of filtration studies.

Table 1

Determination of core samples permeability to oil and porosity before and after well killing simulation [25]

Field (sample number)	Permeability, 10^{-3} μm^2 / Porosity, %	
	Before filtrate injection K_{o1}	After filtrate injection K_{o2}
Sukharev field (1)	78.10/8.28	37.83/8.04
Sukharev field (2)	41.70/5.80	11.8/5.25
Sukharev field (3)	1.62/8.07	0.76/8.04
Sukharev field (4)	4.70/6.72	2.65/6.57
Vinnikovskoe field (5)	7.51/14.20	6.53/14.19

This is an open access article under the CC BY 4.0 license

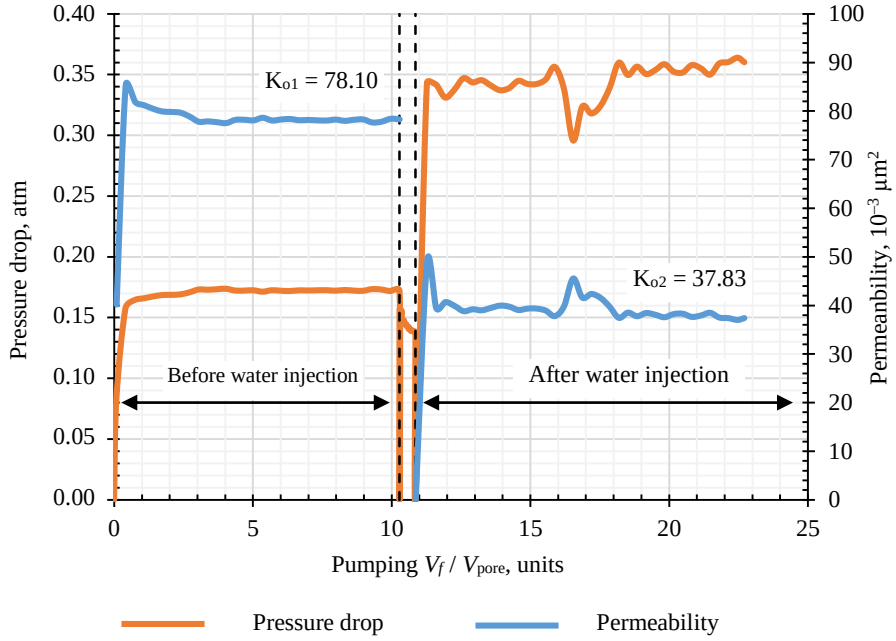

Fig.1. Dynamics of performance indicators for filtration experiments on well killing simulation on core sample N 1 from Sukharev field

Fig.2 shows the results of X-ray tomographic studies of core sample N 1 before and after well killing simulation. In Fig.2, *a*, colour shows the accumulated pore opening in accordance with the scale for the sample depth: brown and yellow hues are high values, blue and purple hues are low ones.

It was ascertained that as a result of the impact of killing fluid filtrate on rock, total number of voids decreased by 32.4 % (mainly due to voids in the range of 46-69 μm), and the volume of voids by 13.1 %.

The results of scanning electron microscopy before well killing simulation made it possible to determine that the main part of the void space was represented by microcavities and intergranular pores. They have different shapes and sizes, are filled with newly formed calcite crystals, between which there are intergranular pores, usually communicating. An extensive distribution of cracks of considerable extent is especially worth noting; crack opening reaches 0.2 mm. Based on relative orientation in rock, two systems of cracks can be distinguished approximately perpendicular to each other. Both the rock matrix and the newly formed substance have a calcite composition with microimpurities of silica, alumina and alkali metals, which can be associated with appearance of clayey matter (Table 2 and Fig.3).

Table 2

Chemical composition of limestone components, wt.%

Oxide	Before simulation		After simulation	
	Matrix	Inclusions in cavities and cracks	Matrix	Inclusions in cavities and cracks
CaO	56.32	54.59	55.08	53.53
MgO	0.21	0.31	0.20	0.39
FeO	0.14	0.07	0.08	0.73
SiO_2	0.15	0.51	0.09	0.45
TiO_2		0.07		0.01
Al_2O_3		0.10		0.14
K_2O		0.04		0.02
Na_2O		0.25		0.46

This is an open access article under the CC BY 4.0 license

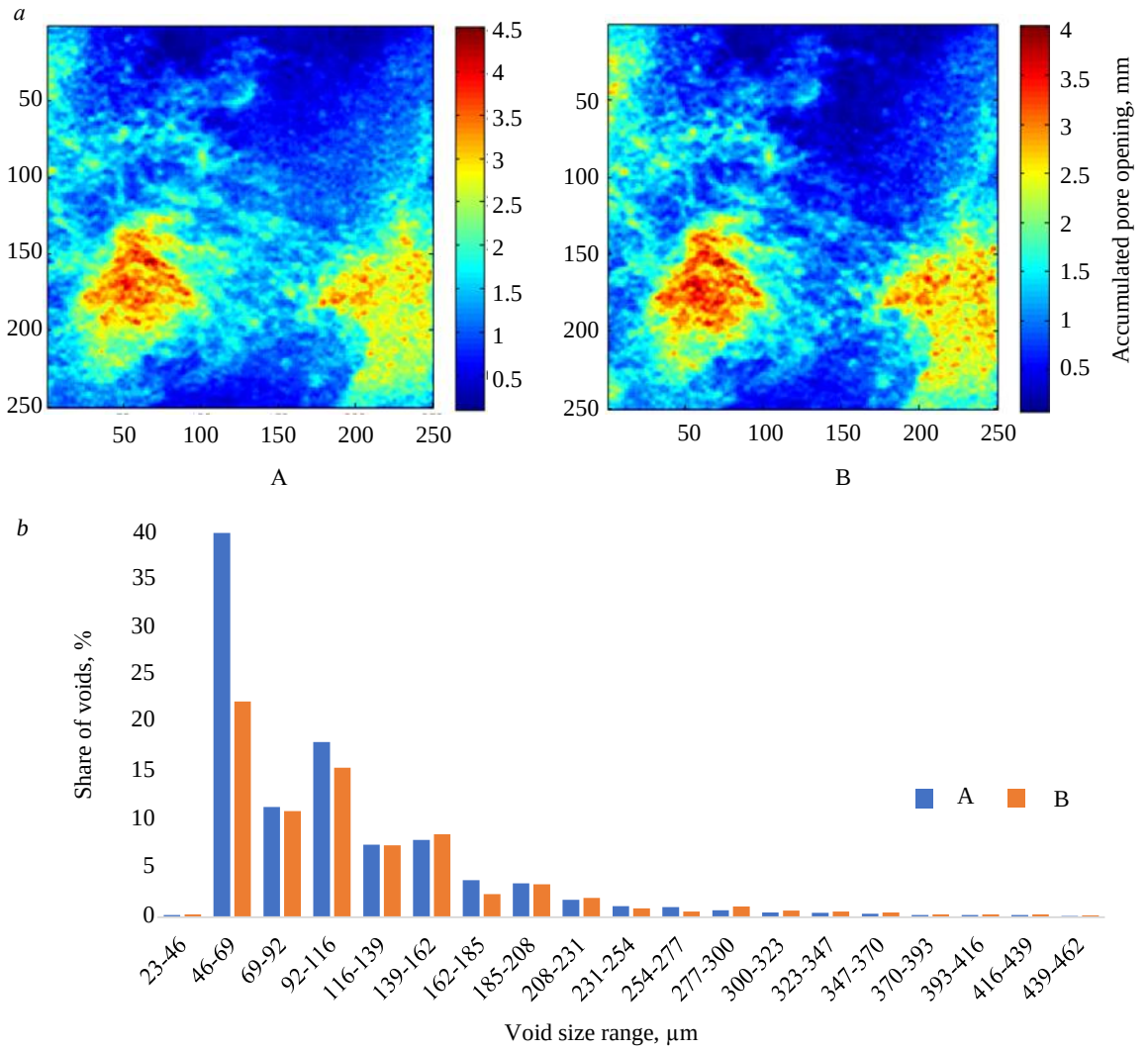

Fig.2. Results of X-ray tomographic studies of core sample N 1 before (A) and after (B) well killing simulation: *a* – void map; *b* – histogram of void size distribution

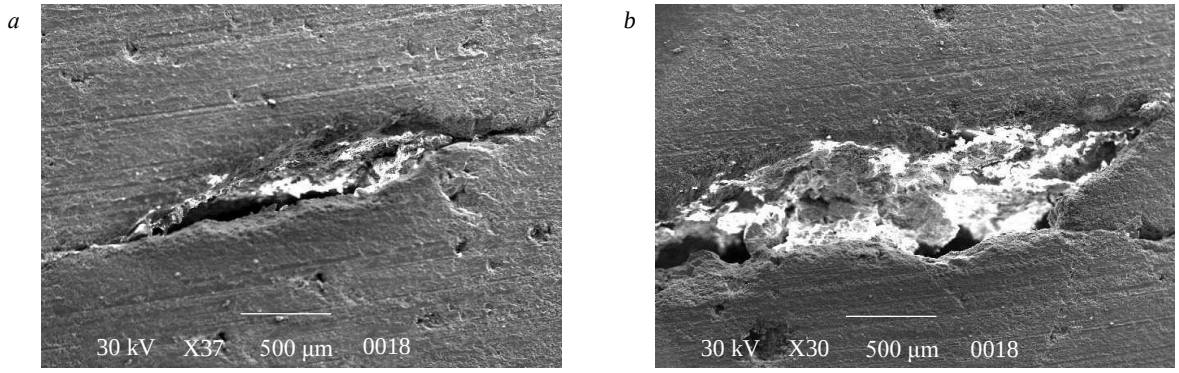

Fig.3. Scanning electron microscopy results before (*a*) and after (*b*) well killing simulation [25]

Scanning electron microscopy studies after filtration experiments showed that the void space was partly filled with fines. There are two types: clayey (montmorillonite and illite) and non-clayey (quartz, feldspar and carbonates). Newly formed calcite crystals to 0.1 mm in size also occur, especially in microcavities (Fig.4, *a*). The formation of amoeba-shaped films and aggregates recorded in certain areas of the sample should be noted (Fig.4, *b*).

This is an open access article under the CC BY 4.0 license

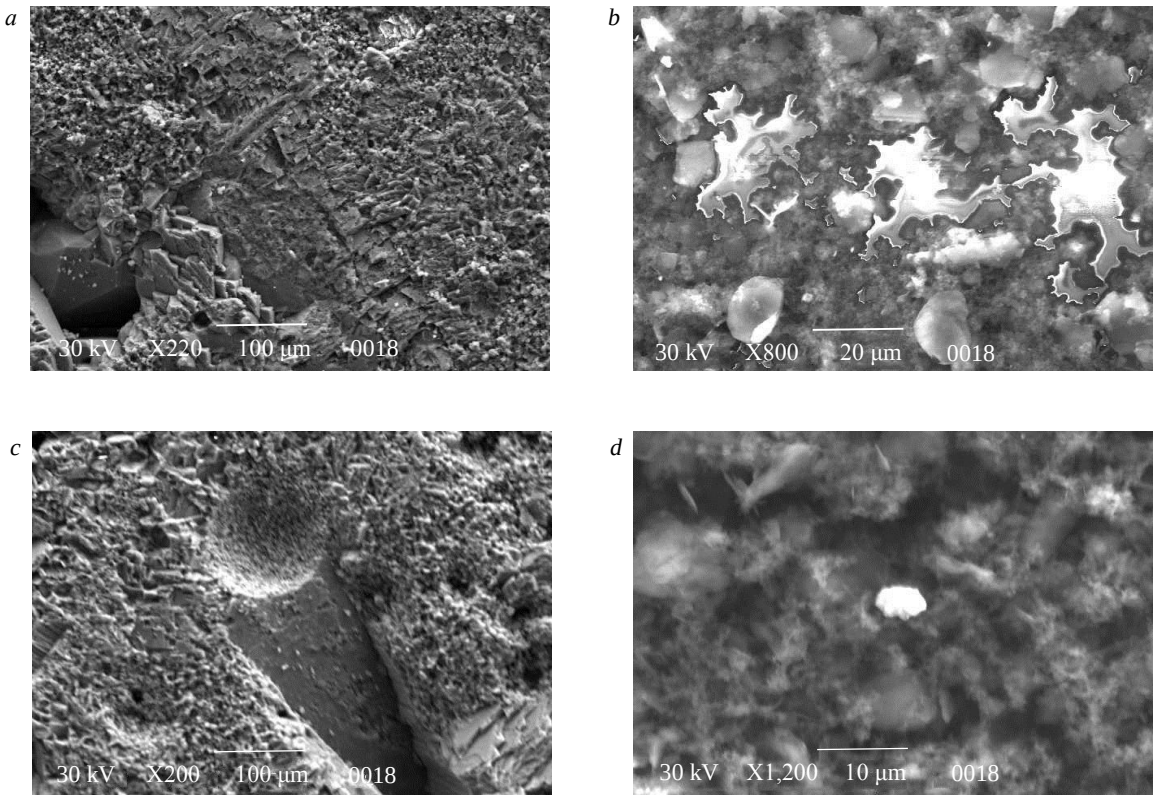

Fig.4. Scanning electron microscopy results before and after well killing simulation: *a* – newly formed calcite crystals in microcavities; *b* – amoeba-like carbonate secretions; *c* – pseudomorph after spicule; *d* – inclusions of ferruginous minerals

Recrystallization phenomena with formation of larger calcite precipitates were recorded. These new formations often do not have a clear crystallographic faceting and are often round. During recrystallization fossils are replaced by calcite (Fig.4, *c*), ferrugination occurs showing up in the formation of films on the carbonate matrix surface and the appearance of newly formed calcite crystals (Fig.4, *d*).

Features of microstructure illustrated in Fig.4 were not recorded in the course of similar studies before the filtration experiments, which points to their technogenic nature. Scanning electron microscopy images show the expansion of voids caused by dissolution and their blockage due to fines migration, grain redistribution, and mineral precipitation. Mineral reactions dissolve the surface of grains and intergranular cement releasing rock grains, which leads to a decrease in permeability and corresponds to the conclusions given in [26]. The results presented in [23] also showed that the presence of oil in rock voids significantly slowed down rock creep under pressure. Oil covers calcite crystals and inhibits this process preventing the contact between the rock and aqueous phase, which is necessary for dissolution, transfer and precipitation of calcite [27, 28]. However, sticking of hydrocarbons to the surface of calcite can change its wetting properties and, thus, prevent diagenetic reactions (generation of secondary porosity). In relation to the described experiments, the formation of secondary voids is not recorded in the scanning electron microscope images. Interaction of killing fluid filtrate and clay minerals leads to swelling and migration and, further, to a decrease in permeability [29, 30].

Thus, comprehensive tomography and scanning electron microscopy results show that the penetration of killing fluid filtrate into rock disturbs the geochemical equilibrium between the formation fluids and rock minerals, thereby causing dissolution of carbonate minerals.

This is an open access article under the CC BY 4.0 license

© Vasilii I. Chernykh, Dmitrii A. Martyushev, Inna N. Ponomareva, 2024

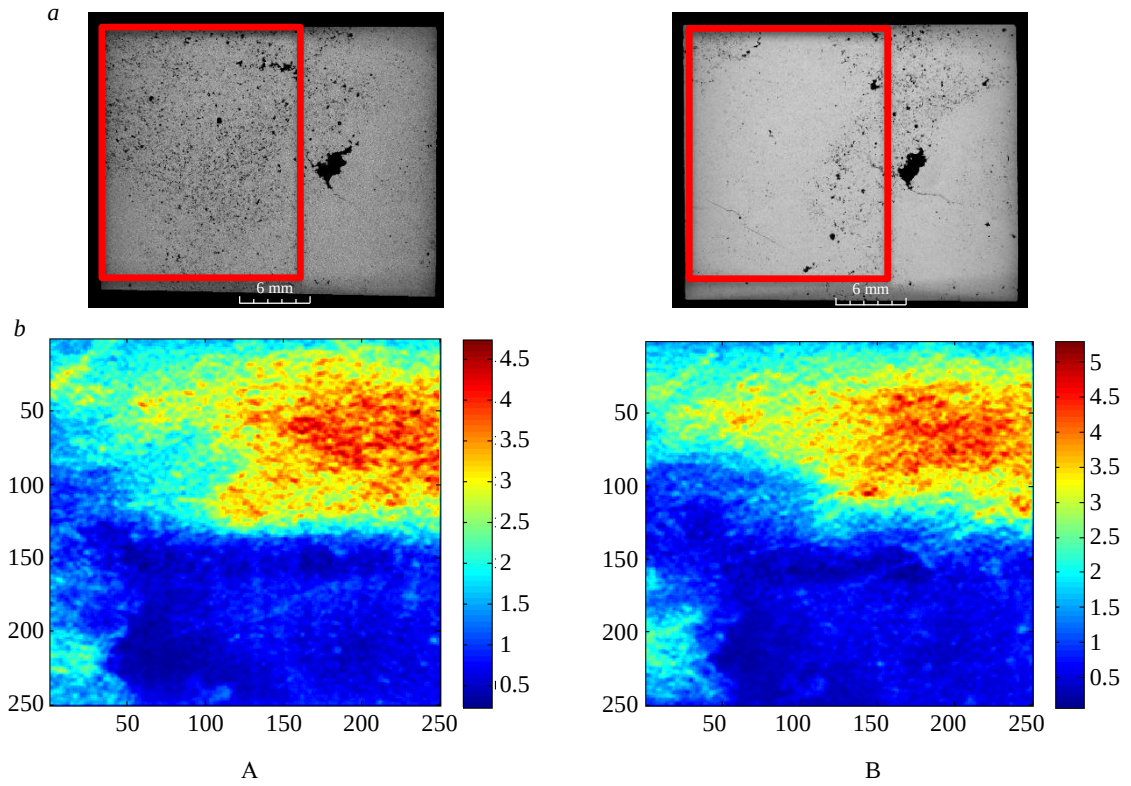

Fig.5. Results of X-ray tomographic studies of core sample N 2 before (A) and after (B) well killing simulation:
a – section of tomogram of samples, density is shown as a grey gradient; *b* – void map

Fig.5 shows the results of X-ray tomographic studies of core sample N 2 before and after well killing simulation, which confirm the previously described decrease in reservoir properties (Table 1).

Comparison of tomography results before and after well killing simulation shows that there were changes in the structure of the void space of rock. This conclusion is confirmed by the quantitative distribution of voids – before the impact, the proportion of voids less than 100 μm in size in the sample was about 60 %, and after it, only about 40 %.

Contrasting results were obtained at well killing simulation on core samples from the Vinnikovskoe field. When comparing the results of tomographic studies and scanning electron microscopy, no major changes in the structure of the void space were recorded. This conclusion is clearly illustrated by the histogram of void distribution (Fig.6), from which it follows that the number of voids decreased by only 2 %.

The analysis of pH assessment of killing fluid filtrate indicates its change as well as an increase in chemical elements in the sample when simulating on core samples from the Sukharev field, which points to mineral reactions [31-33] occurring as a result of rock dissolution. A change in pH after well killing simulation was 6.99 before holding at the Sukharev and Vinnikovskoe fields, and after holding 7.27 at the Sukharev field and 7.01 at the Vinnikovskoe field.

Discussion.

Currently, there are virtually no publications presenting the results of detailed studies on the impact of low-mineralized water on carbonate rocks, in contrast to terrigenous rocks. This area of research was not touched upon by scientists, since it is commonly presumed that carbonate reservoirs do not contain clay minerals that can, upon contact with low-mineralized water, change the wettability and, as a consequence, the permeability of rock [34].

At the same time, dissolution of carbonates is one of the main mineral reactions that can cause fines to break off and thereby change the rock permeability. In the course of the described experiments,

This is an open access article under the CC BY 4.0 license

when killing fluid filtrate was injected into carbonate rock, an increase in injection pressure was recorded (see Fig.1), which is, probably, due to fines migration, clogging of voids and is confirmed by the results of research [35, 36]. Due to dissolution of carbonates, clay minerals are also separated and can partly clog the void space, which is confirmed by scanning electron microscopy (see Fig.3).

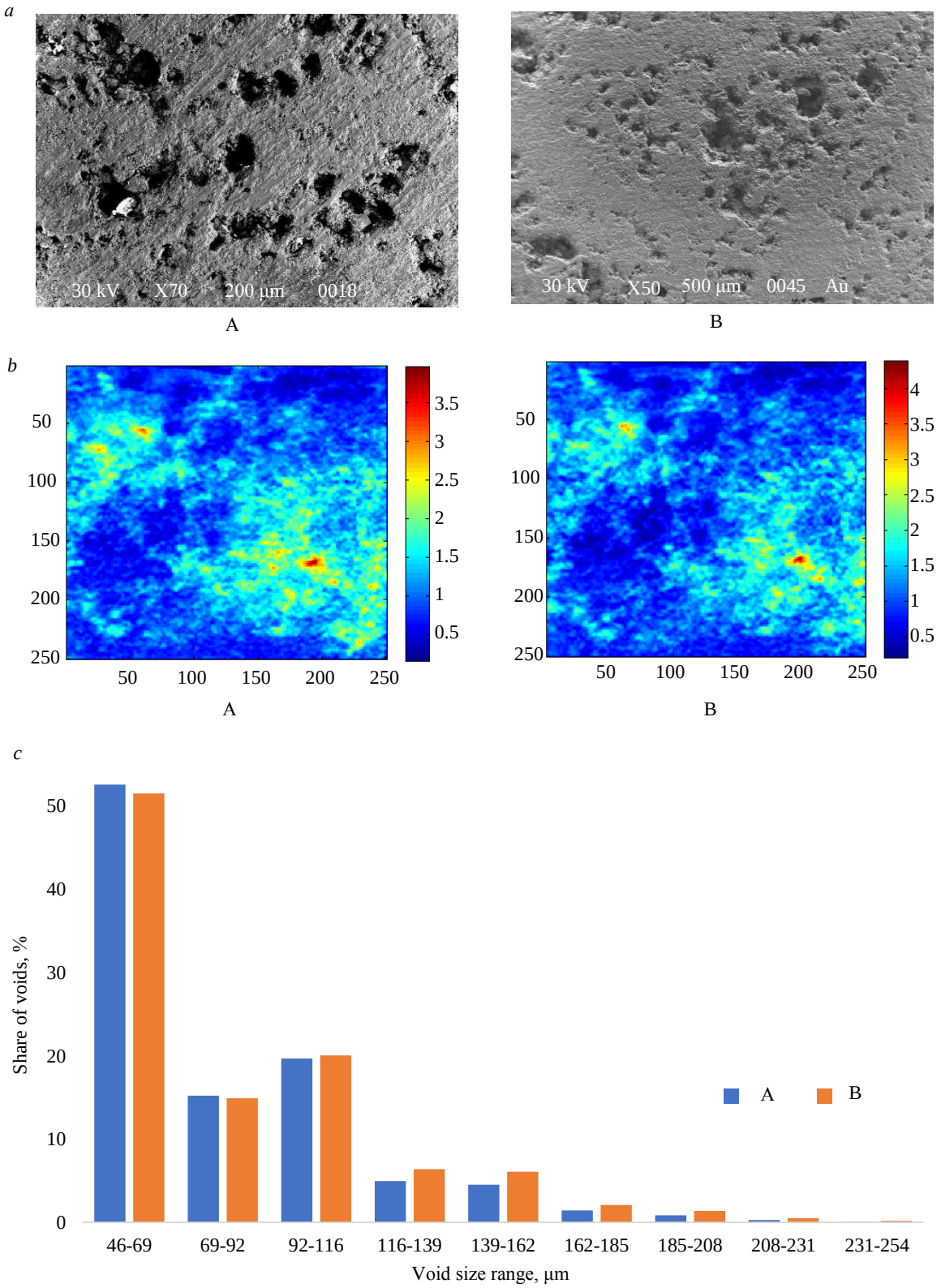

Fig.6. Results of X-ray tomographic studies of core sample from Vinnikovskoe field before (A) and after (B) well killing simulation: *a* – results of scanning electron microscopy; *b* – void map; *c* – histogram of void size distribution

This is an open access article under the CC BY 4.0 license

There are scientific publications describing the processes of interaction of water with different salinity with carbonate rocks, but mostly in relation to waterflooding processes in order to increase the recovery of hydrocarbon reserves. We present several results that show the effect of injecting water of different salinity on the properties of carbonate reservoirs. It is known that a decrease in water salinity causes swelling of dispersed clay due to osmotic pressure and cation exchange depending on minerals and their crystal structure [37, 38]. It was shown in [39] that when mineralized water comes into contact with clay minerals, and the surface charge of cations is greater than that of salt ions, water will migrate into the space between clay layers and, therefore, cause their swelling. Montmorillonite clay has a higher swelling ability due to its very high cation exchange capacity compared to kaolinite. Article [40] states that montmorillonite clay became swollen from ~3.9 to 5.1 μm in diameter (~30 %) after brine salinity (NaCl) decreased from 5,000 mg/l to 0 (fresh water). The authors of [41] found that after replacing the injected fluid from formation water (9,662.9 mg/l) with fresh water, the permeability of core samples decreased by an average of 38 %. Thus, clay swelling can lead to a major decrease in reservoir properties of the formation since the exfoliated clays increase in size and are suspended until they re-precipitate in voids. The initial size of clay particles is the main factor determining their behaviour at break-off. Articles [27, 36] show that salinity decrease of injected water below the critical concentration causes swelling and migration of clay minerals and a subsequent decrease in permeability. When studying clay migration in the presence and absence of oil, it was found in [42] that at salinity below 4,000 ppm, clay migration occurs in both cases.

It is possible that the mechanisms of the investigated processes (waterflooding and well killing operations) are in many ways similar, however, the duration of interaction of the "water – rock" system and the dynamics of the process proper are different, which will determine the degree of reservoir clogging. Therefore, it can be concluded that our study presents a new insight into the interaction processes of water-based killing fluids with carbonate rocks. The published works indicated that the migration of fines is possible only in sandy rocks due to a higher concentration of potentially transported material. The research presented in this article points to manifestation of the described effect in carbonates also, which leads to a significant decrease in reservoir properties to be taken into account when using the aqueous phase as various types of process fluids.

A number of articles [43-45] indicate that a conventional acid attack rather efficiently eliminates clogging of voids with fines and increases rock permeability, however, planning of acid treatment requires a separate study.

Conclusion.

This article focuses on the influence of killing fluid filtrate on reservoir properties of carbonate formations in oil fields in the Perm Territory. Using core samples from the Sukharev and Vinnikovskoe oil fields, the experimental studies with simulation of actual conditions of well killing operations were conducted. The use of micro-X-ray tomography and a scanning electron microscope before and after the simulation experiments allowed recording a decrease in total number of voids caused by migration and clogging by fines and, as a consequence, a decrease in permeability of core samples. Thus, the use of low-salinity water as a base for killing fluids or an agent for the formation pressure maintenance system for the carbonate reservoir at the Sukharev field will involve a high risk of void space clogging due to dissolution and precipitation of carbonate rock minerals. Promising trends are: changing water salinity or the use of nanoparticles to maintain the geochemical equilibrium and reduce mineral dissolution of rocks.

This is an open access article under the CC BY 4.0 license

Studies of core samples were conducted at the Centre for Collective Use of Unique Scientific Equipment at the Perm National Research Polytechnic University.

REFERENCES

1. Mardashov D.V. Development of blocking compositions with a bridging agent for oil well killing in conditions of abnormally low formation pressure and carbonate reservoir rocks. *Journal of Mining Institute*. 2021. Vol. 251, p. 667-677. DOI:10.31897/PMI.2021.5.6
2. Zhi Zhang, Baojiang Sun, Zhiyuan Wang et al. Intelligent well killing control method driven by coupling multiphase flow simulation and real-time data. *Journal of Petroleum Science and Engineering*. 2022. Vol. 213. N 110337. DOI: 10.1016/j.petrol.2022.110337
3. Ebrahimi M.A., Sanati A. On the potential of alyssum as an herbal fiber to improve the filtration and rheological characteristics of water-based drilling muds. *Petroleum*. 2022. Vol. 8. Iss. 4, p. 509-515. DOI: 10.1016/j.petlm.2021.04.005
4. Mardashov D.V. Improving the efficiency of oil well killing at the fields of the Volga-Ural oil and gas province with abnormally low reservoir pressure. *Bulletin of the Tomsk Polytechnic University. Geo Assets Engineering*. 2022. Vol. 333. N 7, p. 185-194 (in Russian). DOI: 10.18799/24131830/2022/7/3707
5. Mardashov D.V., Bondarenko A.V., Raupov I.R. Technique for calculating technological parameters of non-Newtonian liquids injection into oil well during workover. *Journal of Mining Institute*. 2022. Vol. 258, p. 881-894. DOI: 10.31897/PMI.2022.16
6. Krishna S., Ridha S., Vasant P. et al. Conventional and intelligent models for detection and prediction of fluid loss events during drilling operations: A comprehensive review. *Journal of Petroleum Science and Engineering*. 2020. Vol. 195. N 107818. DOI: 10.1016/j.petrol.2020.107818
7. Dokhani V., Ma Y., Geng T. et al. Transient analysis of mud loss in fractured formations. *Journal of Petroleum Science and Engineering*. 2020. Vol. 195. N 107722. DOI: 10.1016/j.petrol.2020.107722
8. de Azevedo Novaes A.M., de Faria R.M.B., da Silva M.A.P., Peçanha R.P. Evaluation of rock-fluid interaction in a carbonate reservoir: Backflow test and reactive transport simulations. *Geoenergy Science and Engineering*. 2023. Vol. 230. N 212158. DOI: 10.1016/j.geoen.2023.212158
9. Jia H., Wu X. Killing fluid loss mechanism and productivity recovery in a gas condensate reservoir considering the phase behavior change. *Petroleum Exploration and Development*. 2017. Vol. 44. Iss. 4, p. 659-666. DOI: 10.1016/S1876-3804(17)30075-7
10. Civan F. Chapter 1 – Overview of formation damage. Reservoir Formation Damage (Fourth Edition). *Fundamentals, Modeling, Assessment, and Mitigation*. 2023, p. 1-12. DOI: 10.1016/B978-0-323-90228-1.00023-6
11. Martyushev D.A., Govindarajan S.K. Development and study of a Visco-Elastic Gel with controlled destruction times for killing oil wells. *Journal of King University – Engineering Sciences*. 2022. Vol. 34. Iss. 7, p. 408-415. DOI: 10.1016/j.jksues.2021.06.007
12. Zhang Lufeng, Zhou Fujian, Zhang Shicheng et al. Evaluation of permeability damage caused by drilling and fracturing fluids in tight low permeability sandstone reservoirs. *Journal of Petroleum Science and Engineering*. 2019. Vol. 175, p. 1122-1135. DOI: 10.1016/j.petrol.2019.01.031
13. Klungtvedt K.R., Saasen A. A method for assessing drilling fluid induced formation damage in permeable formations using ceramic discs. *Journal of Petroleum Science and Engineering*. 2022. Vol. 213. N 110324. DOI: 10.1016/j.petrol.2022.110324
14. Chukwuemeka A.O., Amede G., Alfazazi U. A review of wellbore instability during well construction: Types, causes, prevention and control. *Petroleum and Coal*. 2017. Vol. 59. Iss. 5, p. 590-610.
15. Han Cao, Zheng Zhang, Ting Bao et al. Experimental Investigation of the Effects of Drilling Fluid Activity on the Hydration Behavior of Shale Reservoirs in Northwestern Hunan, China. *Energies*. 2019. Vol. 12. Iss. 16. N 3151. DOI: 10.3390/en12163151
16. Gamal H., Elkatatny S., Adebayo A., Bageri B. Effect of exposure time on the compressive strength and formation damage of sandstone while drilling horizontal wells. *Journal of Petroleum Science and Engineering*. 2020. Vol. 195. N 107590. DOI: 10.1016/j.petrol.2020.107590
17. Martyushev D.A., Ponomareva I.N., Chukhlov A.S. et al. Study of void space structure and its influence on carbonate reservoir properties: X-ray microtomography, electron microscopy, and well testing. *Marine and Petroleum Geology*. 2023. Vol. 151. N 106192. DOI: 10.1016/j.marpetgeo.2023.106192
18. Almutairi A., Wang Y., Le-Hussain F. Effect of type of ion and temperature on fines migration induced by mineral reactions during water injection into carbonate rocks. *Journal of Environmental Management*. 2023. Vol. 342. N 118193. DOI: 10.1016/j.jenvman.2023.118193
19. Karami M., Sedaee B., Nakhaee A. Effect of different injection fluids scenarios on swelling and migration of common clays in case of permeability variations: a micromodel study. *Journal of Petroleum Exploration and Production Technology*. 2023. Vol. 13. Iss. 8, p. 1761-1787. DOI: 10.1007/s13202-023-01628-z
20. Sentemov A.A., Dorfman M.B. Percolation approach in reservoir simulation of well treatment methods. *Bulletin of the Tomsk Polytechnic University. Geo Assets Engineering*. 2022. Vol. 333. N 7, p. 157-165 (in Russian). DOI: 10.18799/24131830/2022/7/3612
21. Dianshi Xiao, Shu Jiang, David Thul et al. Impacts of clay on pore structure, storage and percolation of tight sandstones from the Songliao Basin, China: Implications for genetic classification of tight sandstone reservoirs. *Fuel*. 2018. Vol. 211, p. 390-404. DOI: 10.1016/j.fuel.2017.09.084
22. Qian Li, Jing Li, Baolong Zhu. Experimental investigation of the influence of sequential water-rock reactions on the mineral alterations and porosity evolution of shale. *Construction and Building Materials*. 2022. Vol. 317. N 125859. DOI: 10.1016/j.conbuildmat.2021.125859
23. Neveux L., Grgic D., Carpentier C. et al. Influence of hydrocarbon injection on the compaction by pressure-solution of a carbonate rock: An experimental study under triaxial stresses. *Marine and Petroleum Geology*. 2014. Vol. 55, p. 282-294. DOI: 10.1016/j.marpetgeo.2014.01.012
24. Leger M., Luquot L., Roubinet D. Role of mineralogical, structural and hydrodynamic rock properties in conduits formation in three distinct carbonate rock types. *Chemical Geology*. 2022. Vol. 607. N 121008. DOI: 10.1016/j.chemgeo.2022.121008

This is an open access article under the CC BY 4.0 license

25. Chernykh V.I. Experimental simulation of process liquids impact on complexly composed carbonate reservoirs. *Oilfield engineering*. 2023. N 8 (656), p. 30-34 (in Russian). DOI: 10.33285/0207-2351-2023-8(656)-30-34
26. Wang Y., Almutairi A.L.Z., Bedrikovetsky P. et al. In-situ fines migration and grains redistribution induced by mineral reactions – Implications for clogging during water injection in carbonate aquifers. *Journal of Hydrology*. 2022. Vol. 614. Part A. N 128533. DOI: 10.1016/j.jhydrol.2022.128533
27. Barnaji M.J., Pourafshary P., Rasaie M.R. Visual investigation of the effects of clay minerals on enhancement of oil recovery by low salinity water flooding. *Fuel*. 2016. Vol. 184, p. 826-835. DOI: 10.1016/j.fuel.2016.07.076
28. Qiqiang Ren, Qiang Jin, Jianwei Feng et al. Mineral filling mechanism in complex carbonate reservoir fracture system: Enlightenment from numerical simulation of water-rock interaction. *Journal of Petroleum Science and Engineering*. 2020. Vol. 195. N 107769. DOI: 10.1016/j.petrol.2020.107769
29. Khabibullin M.Y. Research of a reservoir bottom zone destruction by filtering flow of the formation liquid and prevention of call formation in the well. *Bulletin of the Tomsk Polytechnic University. Geo Assets Engineering*. 2021. Vol. 332. N 10, p. 86-94 (in Russian). DOI: 10.18799/24131830/2021/10/3397
30. Ghasemi M., Shafiei A. Influence of brine compositions on wetting preference of montmorillonite in rock/brine/oil system: An in silico study. *Applied Surface Science*. 2022. Vol. 606. N 154882. DOI: 10.1016/j.apsusc.2022.154882
31. Zhichao Yu, Zhizhang Wang, Caspar Daniel Adenutsi. Genesis of authigenic clay minerals and their impacts on reservoir quality in tight conglomerate reservoirs of the Triassic Baikouquan formation in the Mahu Sag, Junggar Basin, Western China. *Marine and Petroleum Geology*. 2023. Vol. 148. N 106041. DOI: 10.1016/j.marpetgeo.2022.106041
32. Malki M.L., Saberi M.R., Kolawole O. et al. Underlying mechanisms and controlling factors of carbonate reservoir characterization from rock physics perspective: A comprehensive review. *Geoenergy Science and Engineering*. 2023. N 211793. DOI: 10.1016/j.geoen.2023.211793
33. Hao J., Mohammadkhani S., Shahverdi H. et al. Mechanisms of smart waterflooding in carbonate oil reservoirs – A review. *Journal of Petroleum Science and Engineering*. 2019. Vol. 179, p. 276-291. DOI: 10.1016/j.petrol.2019.04.049
34. Al Shalabi E.W., Sepehrnoori K., Delshad M. Mechanisms behind low salinity water injection in carbonate reservoirs. *Fuel*. 2014. Vol. 121, p. 11-19. DOI: 10.1016/j.fuel.2013.12.045
35. Feyzulaev H.A., Agalarova S.V. Forecasting of the Technological Parameters of the Oil Displacement with the Various Mineral Content Water in the Clay Storage Collector. *SOCAR Proceedings*. 2020. N 3, p. 135-141 (in Russian). DOI: 10.5510/OGP20200300454
36. Song W., Kovscek A.R. Direct visualization of pore-scale fines migration and formation damage during low-salinity waterflooding. *Journal of Natural Gas Science and Engineering*. 2016. Vol. 34, p. 1276-1283. DOI: 10.1016/j.jngse.2016.07.055
37. Ghasemi M., Shafiei A. Atomistic insights into role of low salinity water on montmorillonite-brine interface: Implications for EOR from clay-bearing sandstone reservoirs. *Journal of Molecular Liquids*. 2022. Vol. 353. N 118803. DOI: 10.1016/j.molliq.2022.118803
38. Yang Y., Jaber M., Michot L.J. et al. Analysis of the microstructure and morphology of disordered kaolinite based on the particle size distribution. *Applied Clay Science*. 2023. Vol. 232. N 106801. DOI: 10.1016/j.clay.2022.106801
39. Roshan H., Masoumi H., Zhang Y. et al. Microstructural effects on mechanical properties of shaly sandstone. *Journal of Geotechnical and Geoenvironmental Engineering*. 2018. Vol. 144. Iss. 2. N 06017019. DOI: 10.1061/(ASCE)GT.1943-5606.0001831
40. Yan Zhuang, Xiangjun Liu, Hanqiao Xiong, Lixi Liang. Microscopic Mechanism of Clay Minerals on Reservoir Damage during Steam Injection in Unconsolidated Sandstone. *Energy & Fuels*. 2018. Vol. 32. Iss. 4, p. 4671-4681. DOI: 10.1021/acs.energyfuels.7b03686
41. Wenchao Fang, Hanqiao Jiang, Jie Li et al. Investigation of salt and alkali sensitivity damage mechanisms in clay-containing reservoirs using nuclear magnetic resonance. *Particulate Science and Technology*. 2017. Vol. 35. Iss. 5, p. 533-540. DOI: 10.1080/02726351.2016.1170082
42. Molnár Z., Pekker P., Dódony I., Pósfai M. Clay minerals affect calcium (magnesium) carbonate precipitation and aging. *Earth and Planetary Science Letters*. 2021. Vol. 567. N 116971. DOI: 10.1016/j.epsl.2021.116971
43. Karimi M., Ayatollahi S. A new wormhole mechanistic model for radial acid flow geometry using novel 3D flow correlations. *Geoenergy Science and Engineering*. 2023. Vol. 230. N 212176. DOI: 10.1016/j.geoen.2023.212176
44. Martyushev D.A., Govindarajan S.K., Li Y., Yang Y. Experimental study of the influence of the content of calcite and dolomite in the rock on the efficiency of acid treatment. *Journal of Petroleum Science and Engineering*. 2022. Vol. 208. Part E. N 109770. DOI: 10.1016/j.petrol.2021.109770
45. Al-Shargabi M., Davoodi S., Wood D.A. et al. A critical review of self-diverting acid treatments applied to carbonate oil and gas reservoirs. *Petroleum Science*. 2023. Vol. 20. Iss. 2, p. 922-950. DOI: 10.1016/j.petsci.2022.10.005

Authors: **Vasilii I. Chernykh,** *Leading Engineer, https://orcid.org/0000-0001-8152-0048 (Branch of OOO "LUKOIL-Engineering" "PermNIPIneft" in Perm, Perm, Russia),* **Dmitrii A. Martyushev,** *Doctor of Engineering Sciences, Associate Professor, martyushevd@inbox.ru, https://orcid.org/0000-0002-5745-4375 (Perm National Research Polytechnic University, Perm, Russia),* **Inna N. Ponomareva,** *Doctor of Engineering Sciences, Professor, https://orcid.org/0000-0003-0546-2506 (Perm National Research Polytechnic University, Perm, Russia).*

The authors declare no conflict of interests.

This is an open access article under the CC BY 4.0 license

ISSN 2411-3336; e-ISSN 2541-9404

JOURNAL OF MINING INSTITUTE

Zapiski Gornogo instituta

Journal homepage: pmi.spmi.ru

Research article

Modelling of compositional gradient for reservoir fluid in a gas condensate deposit with account for scattered liquid hydrocarbons

Ekaterina V. Kusochkova[1], **Ilya M. Indrupskii**[1]✉, **Dmitrii V. Surnachev**[1], **Yuliya V. Alekseeva**[1], **Aleksandr N. Drozdov**[2,3]

[1] *Oil and Gas Research Institute of RAS, Moscow, Russia*

[2] *Peoples's Friendship University of Russia named after Patrice Lumumba, Moscow, Russia*

[3] *Sergo Ordzhonikidze Russian State University for Geological Prospecting, Moscow, Russia*

How to cite this article: Kusochkova E.V., Indrupskii I.M., Surnachev D.V., Alekseeva Yu.V., Drozdov A.N. Modelling of compositional gradient for reservoir fluid in a gas condensate deposit with account for scattered liquid hydrocarbons. Journal of Mining Institute. 2024. Vol. 270, p. 904-918.

Abstract

In oil and gas reservoirs with significant hydrocarbon columns the dependency of the initial hydrocarbon composition on depth – the compositional gradient – is an important factor in assessing the initial amounts of components in place, the position of the gas-oil contact, and variations of fluid properties throughout the reservoir volume. Known models of the compositional gradient are based on thermodynamic relations assuming a quasi-equilibrium state of a multi-component hydrodynamically connected hydrocarbon system in the gravity field, taking into account the influence of the natural geothermal gradient. The corresponding algorithms allow for calculation of changes in pressure and hydrocarbon fluid composition with depth, including determination of the gas-oil contact (GOC) position. Above and below the GOC, the fluid state is considered single-phase. Many oil-gas-condensate reservoirs typically have a small initial fraction of the liquid hydrocarbon phase (LHC) – scattered oil – within the gas-saturated part of the reservoir. To account for this phenomenon, a special modification of the thermodynamic model has been proposed, and an algorithm for calculating the compositional gradient in a gas condensate reservoir with the presence of LHC has been implemented. Simulation cases modelling the characteristic compositions and conditions of three real oil-gas-condensate fields are considered. The results of the calculations using the proposed algorithm show peculiarities of variations of the LHC content and its impact on the distribution of gas condensate mixture composition with depth. The presence of LHC leads to an increase in the level and possible change in the type of the fluid contact. The character of the LHC fraction dependency on depth can be different and is governed by the dissolution of light components in the saturated liquid phase. The composition of the LHC in the gas condensate part of the reservoir changes with depth differently than in the oil zone, where the liquid phase is undersaturated with light hydrocarbons. The results of the study are significant for assessing initial amounts of hydrocarbon components and potential efficiency of their recovery in gas condensate and oil-gas-condensate reservoirs with large hydrocarbon columns.

Keywords

gas condensate reservoir; initial fluid composition; variation of composition with depth; compositional gradient; liquid hydrocarbons; scattered oil; phase equilibrium; mathematical modelling; numerical algorithm; Newton's method

Acknowledgments

The study was fulfilled in the framework of OGRI RAS state assignment, topics 122022800272-4 "Improving the methods of modelling, laboratory and field studies for creation of new technologies for efficient environmentally friendly hydrocarbon recovery in complex mining and geological conditions" and 122022800274-8 "Creation of scientific foundations for a new system methodology for forecasting, prospecting and development of hydrocarbon reservoirs, including matrix oil deposits in gas-saturated carbonate deposits of oil-gas-condensate fields".

Received: 14.08.2023 ***Accepted: 27.12.2023*** ***Online: 26.03.2024*** ***Published: 25.12.2024***

Introduction.

Assessing the distribution of the initial component composition of reservoir fluid within the productive formation is one of the key tasks in the comprehensive reservoir study, evaluation of hydrocarbons in place, and development planning. Actual data for analyzing the spatial variation in composition and properties of hydrocarbons are provided by studies of reservoir flui samples [1, 2],

This is an open access article under the CC BY 4.0 license

measurements of flow characteristics by formation testers [3, 4], well tests and gas condensate studies [5, 6], and optical methods [7]. Geochemical studies [8, 9], biomarkers [10, 11], hydrocarbon group and isotopic analysis [12, 13], combined with statistical analysis and clustering methods [14], and thorough analysis of reservoir pressure dynamics for developed objects [15] allow identifying various sources of hydrocarbon fluid influx into the reservoir, while well test studies, interference testing, tracer tests, and analysis of fluid contacts reveal the presence of hydrodynamically disconnected zones within the formation [16-18].

In many reservoirs, a regular change in fluid composition with depth is observed. Most often it manifests as an increase in density and a decrease in solution gas-oil ratio and saturation pressure for oil, or an increase in condensate content and saturation (dew point) pressure for gas condensate system [1, 2, 19]. This phenomenon is referred to as the compositional gradient. Theoretical models of the compositional gradient, calibrated against actual data, are used to calculate the initial content of hydrocarbons in the formation, refine the position of gas-oil contacts, obtain initial data for designing the reservoir development and initializing mathematical models of the formation [1, 20, 21]. Information on variations in composition and phase state of the fluid helps to optimize well operation regimes and production equipment, assess alternative recovery methods and injection agents, considering the dependency of fluid properties and miscibility conditions on depth. Ultimately, these factors can significantly influence the field development strategy from the economic perspective [22, 23].

In the case of oil-gas-condensate reservoirs, existing models of the compositional gradient allow calculating changes in composition and pressure within the gas-saturated and oil-saturated intervals, as well as assessing the position of the gas-oil contact (GOC). However, they do not account for the possible presence of what is known as scattered oil (liquid hydrocarbons – LHC) in the gas condensate part of the reservoir from the beginning of development, confirmed for a number of large oil-gas-condensate fields.

This article presents a modification of the method and algorithm for calculating the compositional gradient, taking into account the presence of LHC in the gas condensate part of the reservoir. It studies the peculiarities of variations in the initial fluid composition and LHC fraction in the gas-saturated interval based on three cases modeling the conditions of real oil-gas-condensate reservoirs.

Methods.

Theoretical models of compositional gradient. Compositional gradient models can be categorized into isothermal and those considering the natural temperature (geothermal) gradient.

The relation for calculating the change in fluid composition under the effect of gravity in an isothermal system was first derived by Gibbs [24]. He demonstrated that for a multi-component isothermal system in equilibrium conditions in the gravity field, a balance holds between the change in chemical and gravitational potential with depth. The equilibrium condition is expressed as

$$\frac{d\mu_i}{dh} = M_i g, \quad i = 1, \ldots, N, \tag{1}$$

where μ_i is the chemical potential of component i at depth h; M_i is the molar mass of component i; g is the gravity constant (acceleration of gravity); N is the number of components in the system.

By integrating (1) and expressing chemical potentials via fugacities using the equation of state, the relationship can be transformed into a system of algebraic equations for sequential determination of pressure values and component concentrations at different depths with a step Δh [1]. Thus, moving upwards and downwards from a reference point with given fluid composition and pressure allows for calculation of the vertical distributions for pressure and component concentrations. The described procedure is applicable to a single-phase state of the reservoir hydrocarbon system. Features related to determining the position of the GOC are discussed below.

This is an open access article under the CC BY 4.0 license

© Ekaterina V. Kusochkova, Ilya M. Indrupskii, Dmitrii V. Surnachev, Yuliya V. Alekseeva, Aleksandr N. Drozdov, 2024

Equation (1) assumes that the system as a whole is at a constant temperature ($dT/dh = 0$). The isothermal model is applicable to real reservoirs with small depth ranges (hydrocarbon columns) and temperature gradients. In other cases, it is recommended to consider the influence of the geothermal gradient.

In the natural geothermal field, the vertical temperature gradient causes the thermodiffusion effect – an additional "thermal force" that influences the distribution of component concentrations with depth. To quantitatively assess the influence of thermodiffusion, models that consider both gravitational and thermal factors are used. The quasi-equilibrium distribution of composition with depth formed by these factors obeys the following general balance equation [20]

$$\sum_{k=1}^{N-1}\left[\left(\frac{\partial \mu_i}{\partial z_k}\right)_{p,T,z_{i\neq k}}\left(\frac{dz_k}{dh}\right)\right] = F_i^g - F_i^T\frac{1}{T}\left(\frac{dT}{dh}\right),\ i=1,\ldots,N,$$

where z_i is the component molar fraction; h is the depth; F_i^g and F_i^T are the gravity segregation force and the thermal force for component i, respectively.

The main factor controlling the change in composition with depth is usually the gravitational force. Thermodiffusion typically acts against gravity and weakens its influence on the manifestation of the compositional gradient. In most reservoirs, the impact of the thermal force is less than that of the gravity force [20, 25].

One of the most theoretically justified and practically convenient models for the thermal force was proposed by Haase [26, 27]. In this model, the thermal force can be obtained via the limiting values of thermodiffusion coefficients at temperature gradient approaching zero and takes the form:

$$F_i^T = \frac{M_i}{M}H - \tilde{H}_i,$$

where M_i and $\tilde{H}_i$ are the molecular mass and partial molar enthalpy of component i; M and H are the molecular mass and molar enthalpy of the mixture.

Based on the Haase model, Pedersen and Lindelof derived the following relationship for calculating the compositional gradient [19, 21, 28]:

$$\ln f_i\left(p,\bar{z}\right)|_{h_2} - \ln f_i\left(p,\bar{z}\right)|_{h_1} = \frac{1}{RT_1}\left[M_i g\left(h_2-h_1\right) - M_i\left(\frac{H}{M}-\frac{\tilde{H}_i}{M_i}\right)\frac{T_2-T_1}{T_1}\right],\quad i=1,\ldots,N, \qquad (2)$$

where p is the pressure; $\bar{z}$ is the vector of molar component concentrations in the mixture (molar composition of the mixture); T_1 and T_2, h_1 and h_2 are the values of temperature and depth for the first and second points considered, respectively; R is the universal gas constant; f_i is the fugacity of component i.

The dependence of fugacities on pressure and mixture composition is determined by solving the cubic equation of state, for example, the Peng – Robinson equation. The system of equations (2) is solved for pressure and fluid composition at point h_2 at each step in depth, given the known values at point h_1. Details of the enthalpy calculations are presented in [19, 29].

Practical implementation of the compositional gradient model. In this study, a conservative finite difference scheme [30] is used to implement the compositional gradient model (the problem of compositional grading). To solve the obtained system of nonlinear algebraic equations, Newton's method is applied providing an efficient solution to the compositional grading problems when using the solution from the previous step as the initial approximation [1, 2]. Sequential search for the values of the basic unknowns is performed at each iteration by solving the system of linear equations $AY = b$ using the Gauss elimination method, the choice of which is determined by the dense structure of the matrix and the typical dimensionality of several tens of equations:

This is an open access article under the CC BY 4.0 license

© Ekaterina V. Kusochkova, Ilya M. Indrupskii, Dmitrii V. Surnachev, Yuliya V. Alekseeva, Aleksandr N. Drozdov, 2024

$$A=\begin{bmatrix} \frac{\partial \ln f_1}{\partial z_1} & \frac{\partial \ln f_1}{\partial z_2} & \dots & \frac{\partial \ln f_1}{\partial z_N} & \frac{\partial \ln f_1}{\partial p} \\ \dots & \dots & \dots & \dots & \dots \\ \frac{\partial \ln f_N}{\partial z_1} & \frac{\partial \ln f_N}{\partial z_2} & \dots & \frac{\partial \ln f_N}{\partial z_N} & \frac{\partial \ln f_N}{\partial p} \\ 1 & 1 & \dots & 1 & 0 \end{bmatrix}, \quad b=\begin{bmatrix} \psi_1 \\ \psi_2 \\ \dots \\ \psi_N \\ 0 \end{bmatrix}, \quad Y=\begin{bmatrix} z_1^m - z_1^{m-1} \\ z_2^m - z_2^{m-1} \\ \dots \\ z_N^m - z_N^{m-1} \\ p^m - p^{m-1} \end{bmatrix}=\begin{bmatrix} \Delta z_1^m \\ \Delta z_2^m \\ \dots \\ \Delta z_N^m \\ \Delta p^m \end{bmatrix},$$

where superscript m corresponds to the current, and $m-1$ – to the previous iteration; ψ_i is the misfit of equation (2) for component i at the previous iteration (with opposite sign); Δ is the change in the basic unknown at the current iteration. As the initial approximation at the first iteration, the values at depth h_1 are used.

Thus, if the composition and pressure are known at the reference depth, they can be sequentially determined for any other specified depth using the system (2). The temperature values at each depth are considered known according to the specified geothermal gradient. The input data of the model are the parameters of the equation of state and specific enthalpies of the components. For pure substances, these are reference data, while for pseudocomponents and fractions they are determined by using correlations presented in the literature and solving identification problems with actual measurements from the studies of formation fluid samples.

The described model is applicable for a single-phase state of the system. The classical calculation of the compositional gradient assumes that the mixture reaches the saturation point and transitions to the two-phase state at the depth of GOC. To check the phase state of the mixture, a special iterative procedure is used – the Michelsen stability test [31]. Stability obtained in this test indicates the single-phase state of the mixture, while instability indicates the two-phase state corresponding to crossing the GOC. Thus, to search for the GOC, the stability of the mixture is checked for the obtained pressure and composition at each depth. If the mixture becomes unstable at the successive step, a bisection algorithm is implemented within the corresponding depth interval to determine the precise GOC position [32].

At the depth of the GOC, the pressure equals the saturation (dew point) pressure of the gas phase (when approaching from above) and the saturation pressure of the liquid phase (when approaching from below). Therefore, an alternative method for finding the GOC involves calculating the pressure of mixture transition to the two-phase state at each step in depth [33]. Once the GOC position is found, a transition is necessary from the gas phase composition to the equilibrium liquid phase composition, or vice versa. For this, the phase equilibrium problem is solved [1, 2].

These features are valid for the classical (saturated) GOC. In deep formations with high pressures and temperatures, the transition from gas to liquid phase may be supercritical. In this case, a two-phase state within the reservoir does not occur, but the single-phase fluid changes its type from gaseous to liquid at the GOC. At the GOC, the mixture saturation pressure reaches its maximum, which is lower than the pressure at the GOC.

It is important to note the differences between the thermodynamic calculations of the compositional gradient and the principles used in the equilibrium initialization of the flow simulation models for oil and gas reservoirs. In flow simulations, the effects of thermodiffusion are not considered, whereas classical calculations of the compositional gradient do not account for the presence of the gas – oil capillary transition zone. The coexistence of gaseous and liquid hydrocarbon phases is assumed at the GOC only.

The gas – oil transition zone is usually limited to few, rarer first tens of meters, which is due to greater difference in phase densities and lower values of surface tension than for the oil – water system. Whereas the effect of the compositional gradient manifests itself over larger depth ranges, measured by hundreds of meters. At the same time, the influence of capillary pressure on the gas – oil phase equilibria is not significant even in tight reservoirs [1, 22], and has a noticeable effect only in

This is an open access article under the CC BY 4.0 license

© Ekaterina V. Kusochkova, Ilya M. Indrupskii, Dmitrii V. Surnachev, Yuliya V. Alekseeva, Aleksandr N. Drozdov, 2024

shale reservoirs. Thus, it is assumed that neglecting the influence of capillary pressure and the presence of the two-phase gas – oil transition zone does not significantly affect the calculation of the initial hydrocarbon composition distribution with depth. In this study, the authors also follow this approach and do not account for the presence of the gas – oil capillary transition zone. The possibility to overcome this limitation is discussed in the conclusions.

Compositional gradient in the presence of scattered liquid hydrocarbon phase. In gas condensate reservoirs, the presence in the pores of a small volume of immobile LHC is often reported, referred to as scattered, relict, residual, or matrix oil [1, 34]. In this case, the described classical calculation of quasi-equilibrium initial fluid distribution is not applicable, as it assumes the coexistence of two phases at the GOC only [22].

The presence of such fluid type in the gas condensate part of the reservoir was first identified for the Orenburg oil-gas-condensate field (OGCF) both by core data and phase behavior characteristics of the fluid [1, 35]. The presence of LHC in gas-saturated intervals has been confirmed for the main reservoir of the Vuktyl OGCF [34] and is probably characteristic for other OGCFs [22]. Unlike condensate, LHC is present in the gas-saturated zone of the formation from the beginning of development and is distinguished by heavier composition, including resins and asphaltenes. The presence of LHC is noted throughout the depth interval of the gas-saturated zone, not just in the relatively small capillary transition zone near the GOC. The saturation for scattered LHC is usually estimated at 5-15 %.

Studies [34, 35] offered the following explanation for this phenomenon. The terms “matrix oil” and “LHC” in this context correspond to the paradigm of oil-gas source properties of hydrocarbon bearing carbonate deposits that form gas condensate and oil-gas-condensate fields, in particular, the Vuktyl and Orenburg fields. The presence of inherent (matrix) oil, transformed into liquid hydrocarbons of the oil sequence (LHC), in the pore space of the carbonate rocks of the gas part of these fields has been demonstrated as a result of previous studies. The established oil-gas source properties and early stages of oil generation in hydrocarbon bearing deposits allow for the assertion that even before the start of development LHC are present in their gas part in thermodynamic equilibrium with gas, but at saturations below the critical values (flow threshold). These are the LHC considered in this study.

To account for LHC in the gas condensate part of the reservoir, a modified algorithm for the compositional gradient was proposed in [36]. It assumes that the gas phase is continuously connected through depth and its composition corresponds to the quasi-equilibrium conditions (2). The liquid phase is immobile and not connected between depths, so the quasi-equilibrium conditions for the liquid phase are not satisfied. However, at each depth, the liquid phase is in equilibrium with the corresponding composition of the gas phase.

As in the classical calculation, the initial data for the modified algorithm include the fluid composition at the reference depth, pressure, temperature, and the geothermal gradient. Due to the presence of LHC, the overall composition of the fluid at the reference depth must correspond to a two-phase state with a fraction of the liquid hydrocarbon phase estimated from well logging and core analysis. For this purpose, the composition of the gas condensate fluid obtained from samples is preliminarily saturated to the corresponding molar fraction of LHC L_0 [22].

This saturation procedure is necessary for the following reason. Due to the presence of LHC in the gas condensate part of the reservoir, any change in reservoir pressure near the well converts the system into the two-phase state associated not only with condensate dropout but also with gas liberation from the saturated oil (LHC). This leads to some distortion of the fluid composition during standard procedures of gas condensate tests. As a result, the fluid sample may become undersaturated, which prevents using its composition as that of the reservoir gas condensate mixture in the presence of LHC. For example, in the case of the Vuktyl OGCF, the difference between the reservoir pressure and the saturation pressure by samples ranges from 20 to 40 bar and increases with depth [34].

This is an open access article under the CC BY 4.0 license

Thus, unlike the classical compositional gradient, the input composition in the algorithm with LHC at the reference depth is set to be unstable. This is controlled by the Michelsen stability test [31]. The next step is to determine the corresponding equilibrium compositions of the gas (vapor) and liquid phases, as well as the calculated fraction of LHC by solving the phase equilibrium problem [2]. The calculated LHC fraction must match the value L_0. The obtained gas phase composition $\bar{y}_0$ is saturated and is further used as the input mixture composition $\bar{z}_0$ for calculating the compositional gradient upwards and downwards from the reference point.

When moving downwards, the composition of the gas condensate mixture becomes heavier (richer). The gas phase, saturated at the previous step, becomes oversaturated at the new point, i.e., transforms into a two-phase mixture $\bar{z}_1$. For this mixture, at the pressure and temperature of the new depth, the equilibrium compositions of the gas phase $\bar{y}_1$ and liquid phase $\bar{x}_1$, and their fractions $V_h = 1 - L_h$ and L_h are determined. The resulting gas phase $\bar{y}_1$ again becomes saturated.

When moving upwards, the composition of the gas condensate mixture $\bar{z}_1$ becomes lighter (leaner), so the mixture becomes undersaturated. A pseudoequilibrium liquid phase composition $\bar{x}_1$ can be calculated for the mixture using the Negative Flash procedure proposed by Whitson and Michelsen [37].

The Negative Flash extends the standard phase equilibrium algorithm beyond the two-phase region to enable calculations when the fluid is single-phase. The value of the gas phase molar fraction $0 < V_h < 1$, both in the standard phase equilibrium calculation and in the Negative Flash, implies that V_h moles of gas of the calculated composition $\bar{y}_1$ need to be added to $1 - V_h$ moles of liquid of the calculated composition $\bar{x}_1$ to restore the original mixture composition $\bar{z}_1$. Similarly, $V_h > 1$ (undersaturated gas) in the Negative Flash procedure is interpreted as the $V_h - 1$ moles of liquid with composition $\bar{x}_1$ need to be removed from V_h moles of gas of composition $\bar{y}_1$ to restore one mole of the original mixture $\bar{z}_1$.

Thus, in the both cases (steps upwards and downwards), the saturated gas phase composition $\bar{y}_1$ obtained as a result of the Negative Flash procedure is taken as the final composition of the gas condensate mixture at the new depth, and the composition of the liquid phase $\bar{x}_1$ is considered the equilibrium LHC composition at that depth. The LHC fraction is adjusted compared to the value at the previous depth, taking into account additional condensation from the gas condensate mixture upon oversaturation (step downwards) or, conversely, evaporation upon undersaturation (step upwards):

$$L_1 = L_0 + (1 - L_0) L_h,$$

where L_1 is the final LHC fraction at the new depth; L_h is the LHC fraction obtained from the Negative Flash procedure.

During the movement downwards in the algorithm with LHC, reaching the GOC is controlled with $L_1 = 1$ (transition to the single-phase liquid state). When moving upwards, the possible transition to the single-phase gas state ($L_1 = 0$) is controlled. In both the cases, further steps are carried out using the classical (single-phase) calculation of the compositional gradient.

The overall flowchart of the algorithm considering LHC is presented in Fig.1.

Discussion of results.

Evaluation of the impact of LHC on the composition distribution in gas condensate reservoirs. The described algorithms for compositional grading were used for computational assessment of the impact of LHC on the distribution of pressure and composition in gas condensate reservoirs. The parameters of multi-component fluid models, reservoir conditions, and initial data at reference depth were taken close to characteristics of three different gas condensate reservoirs: one of the Achimov reservoirs of the Urengoy OGCF, the main reservoir of the Orenburg OGCF, and the main reservoir of the Vuktyl OGCF.

This is an open access article under the CC BY 4.0 license

© Ekaterina V. Kusochkova, Ilya M. Indrupskii, Dmitrii V. Surnachev, Yuliya V. Alekseeva, Aleksandr N. Drozdov, 2024

According to core data, the hydrocarbon bearing carbonate oil-gas source rocks of large OGCFs (Vuktyl and Orenburg) before the start of the development are difobic [35], i.e., they express phobicity to water and to a lesser extent to liquid hydrocarbons, with the contact angle of 110-120°. Considering the significant hydrocarbon columns of the studied reservoirs, this becomes an additional factor to consider the size of the transition zone and the influence of capillary forces to be insignificant for this study.

The calculations performed do not account for the entire specificity of the chosen reservoirs and investigate the features of the LHC influence only within the assumptions of the model. For instance, direct studies for the Orenburg OGCF showed the presence of a significant fraction of heavy bitumoids (heavy resins and asphaltenes) in the formation [35]. In the problem formulation con-

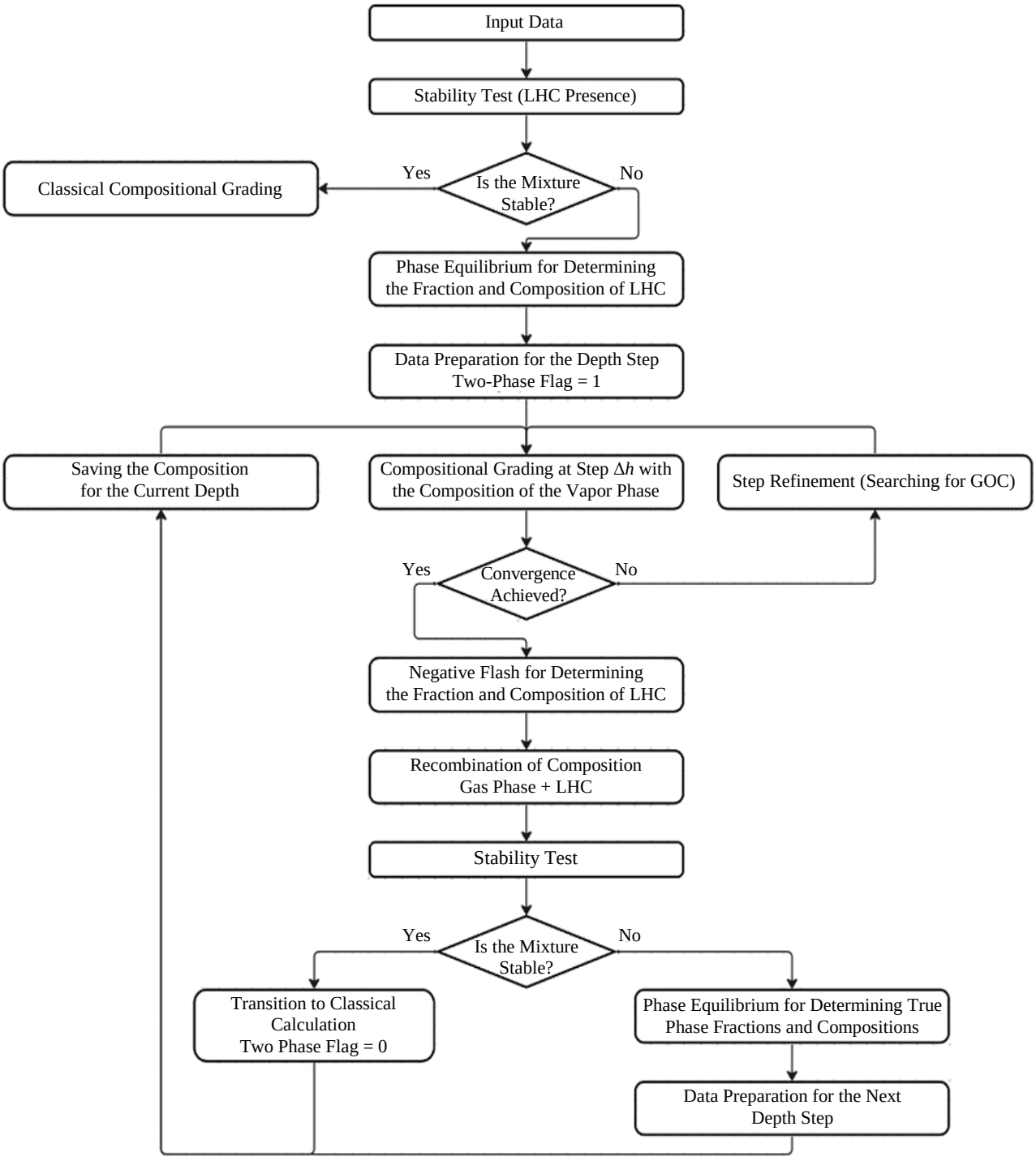

Fig.1. Flowchart of the compositional grading algorithm considering LHC

This is an open access article under the CC BY 4.0 license

sidered, their presence and interaction with the modeled reservoir fluid is not accounted for, despite their high adsorption capacity towards light hydrocarbon components. Furthermore, the increased concentrations of heavy bitumoids due to the oil-source properties of the carbonate rocks of the Orenburg OGCF are generally associated with low-permeability hydrophilic intervals with high gas-water capillary pressures, which can have a peculiar "block" effect for the gas phase. The assessment of the influence of these and other additional factors extends beyond the scope of the current stage of the research.

Composition 1 closely resembles the conditions of one of the Achimov reservoirs of the Urengoy OGCF with a unique condensate content of the reservoir gas. The reservoir fluid is modeled by a mixture of 24 components (Table 1). The reference depth is h = 3754.6 m, pressure at the reference depth is p = 633 bar, temperature is T = 107.85 °C, and the geothermal gradient is dT = = 0.029 °C/m. The composition corresponds to a sample of gas condensate fluid at this depth. The calculation was performed in the depth range of 3614 to 4050 m with the 1 m step.

Table 1

Input data for composition 1

Components	Molar fraction z, %	Molar mass M, g/mol	Critical temperature T_c, °C	Critical pressure p_c, bar	Acentric factor ω	Molar enthalpy $^*H_{ref}$, J	Coefficients of cubic approximation for ideal gas heat capacity **[38]			
							A	*B*	*C*	*D*
N_2	0.247	28.013	–146.95	33.9439	0.04	8330.789	31.1488	-0.0136	0.0	0.0
CO_2	0.631	44.01	31.55	73.8659	0.225	19459.1011	19.7946	0.0734	–0.0001	0.0
C_1	75.2122	16.043	–82.55	46.0421	0.013	2.6425	19.2503	0.0521	0.0	0.0
C_2	7.2009	30.07	32.28	48.8387	0.0986	9761.1347	5.4092	0.1781	–0.0001	0.0
C_3	4.394	44.097	96.65	42.4552	0.1524	19519.6224	–4.2244	0.3063	–0.0002	0.0
iC_4	0.953	58.124	134.95	36.477	0.1848	29278.1232	–1.39	0.3847	–0.0002	0.0
nC_4	1.514	58.124	152.05	37.9665	0.201	29278.1212	9.487	0.3313	–0.0001	0.0
iC_5	0.537	72.151	187.25	33.8932	0.227	39036.6099	–9.5247	0.5066	–0.0003	0.0
nC_5	0.565	72.151	196.45	33.7007	0.251	39036.6099	–3.6257	0.4873	–0.0003	0.0
C_6	0.772	78.93	245.97	34.7	0.243	48795.1026	–4.4128	0.5819	–0.0003	0.0
C_7	1.16	91.8	265.95	32.5	0.292	52706.294	–5.7687	0.5393	–0.0002	0.0
C_8	1.33	103.35	295.077	29.928	0.34	60741.5508	–4.0418	0.5889	–0.0002	0.0
C_9	0.801	119.17	322.415	27.987	0.388	71747.4235	–3.2364	0.6745	–0.0003	0.0
C_{10}	0.698	133.0	346.673	26.238	0.435	81368.8653	–0.7145	0.7468	–0.0003	0.0
C_{11+}	0.853	153.1083	377.537	24.1149	0.4991	63652.7132	27.5423	0.9068	–0.0004	0.0
C_{13+}	0.659	180.4253	415.592	21.9509	0.5828	75009.3798	32.4562	1.0686	–0.0004	0.0
C_{15+}	0.542	206.7519	447.928	20.3132	0.6605	85954.3171	37.1921	1.2246	–0.0005	0.0
C_{17+}	0.544	237.3727	479.571	18.6716	0.7466	98684.4935	42.7004	1.4059	–0.0005	0.0
C_{20+}	0.386	273.544	511.485	17.0456	0.8454	113722.2268	49.2071	1.6202	–0.0006	0.0
C_{22+}	0.278	308.9098	539.266	15.7848	0.9382	128425.0729	55.569	1.8296	–0.0007	0.0
C_{25+}	0.206	341.7057	561.92	14.7838	1.0222	142059.533	61.4685	2.0239	–0.0008	0.0
C_{27+}	0.152	373.5677	581.777	13.9428	1.1019	155305.7262	67.2001	2.2126	–0.0009	0.0
C_{30+}	0.137	408.5766	601.806	13.1577	1.1878	169860.2063	73.4978	2.42	–0.0009	0.0
C_{36+}	0.228	650.0	630.02	12.2	1.5	270228.725	116.9268	3.8499	–0.0015	0.0

* Partial molar enthalpy in the ideal gas state at 273.15 K, J.
** Coefficients *A*, *B*, *C*, and *D* are used in enthalpy calculations.

Figure 2 presents the results of the classical algorithm (not considering LHC). PC_{5+} denotes the potential content of the C_{5+} component group in the reservoir gas condensate mixture characterizing the amount of dissolved hydrocarbons that exist in liquid state (condensate) in normal conditions [1].

Figure 2 shows that pressure and PC_{5+} increase with depth (Fig.2, *a*, *b*), while the concentration decreases for light components (Fig.2, *c*) and increases for heavy ones (Fig.2, *d*, *e*).

The considered gas condensate reservoir is characterized by near-critical reservoir conditions. Therefore, in Fig.2, *a* the pressure and saturation pressure at its peak point (GOC) do not match, and a continuous supercritical transition from the gas phase to the liquid phase is seen on the PC_{5+} curve (Fig.2, *b*).

This is an open access article under the CC BY 4.0 license

Journal of Mining Institute. 2024. Vol. 270. P. 904-918
© Ekaterina V. Kusochkova, Ilya M. Indrupskii, Dmitrii V. Surnachev, Yuliya V. Alekseeva, Aleksandr N. Drozdov, 2024

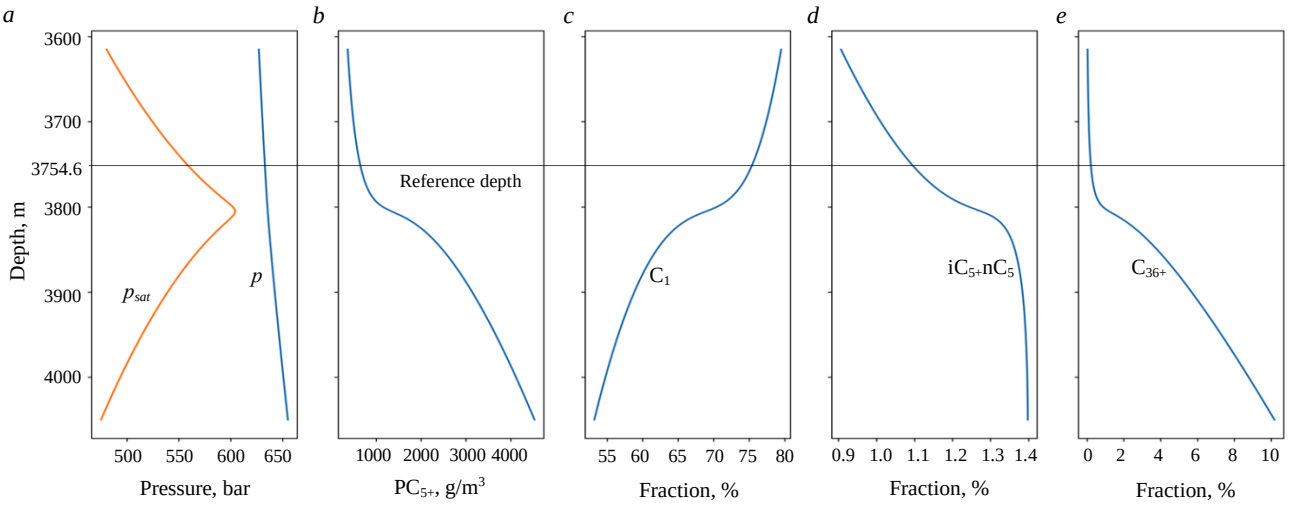

Fig.2. Results of the classical algorithm for composition 1

Calculated dependencies on depth for: *a* – pressure *p* and saturation pressure p_{sat}, bar; *b* – PC_{5+}, g/m^3; *c* – molar fraction of methane, %; *d* – molar fraction of pentanes, %; *e* – molar fraction of the C_{36+} group, %

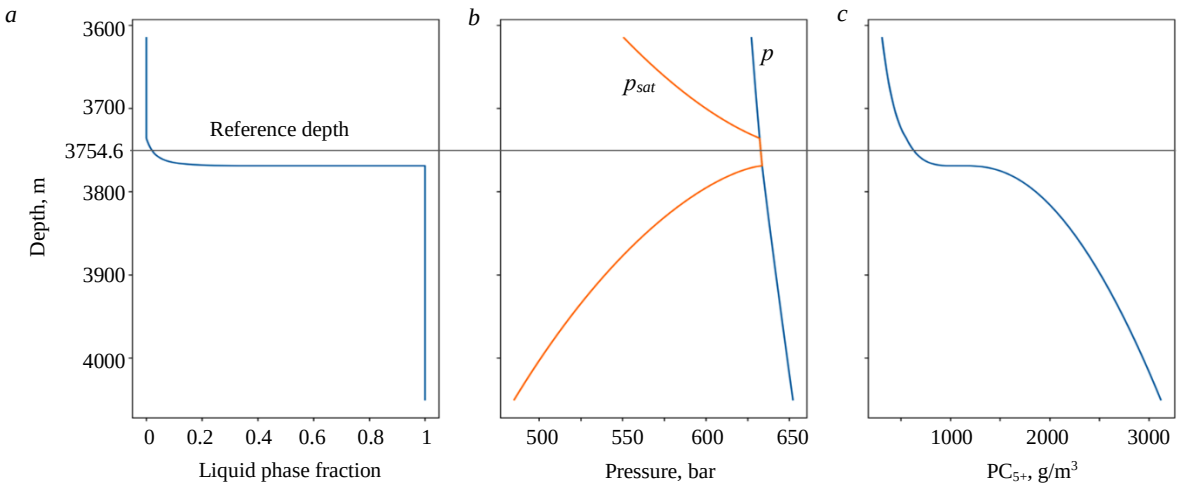

Fig.3. Results of the modified algorithm for composition 1

Calculated dependencies on depth for: *a* – molar fraction of the liquid phase; *b* – pressure *p* and saturation pressure p_{sat}, bar; *c* – PC_{5+}, g/m^3

To demonstrate the impact of LHC on the component distribution, the mixture composition at the reference point is modified. Pseudo-equilibrium liquid phase with the composition obtained from the Negative Flash procedure is added to the original composition from Table 1, until achieving the LHC molar fraction of 3 % (L_0 = 0.03). The results of the calculations using the modified compositional grading algorithm (considering LHC) are shown in Fig.3.

From Fig.3, *a* it is evident that when moving upwards from the reference depth of 3754.6 m, the LHC fraction expectedly decreases, while it increases when moving downwards. The change in the LHC fraction from 0 to 1 occurs in the depth interval from 3736 to 3769 m. Within this interval, the reservoir pressure and the saturation (dew point) pressure are equal (Fig.3, *b*), indicating the two-phase state: the gas phase is saturated, and the liquid phase is present. Above and below this interval, the plots in Fig.3, *b* do not match, indicating a transition to the single-phase region. Above the 3736 m level, the gas condensate mixture becomes undersaturated, with no LHC present. At the 3769 m level, the GOC is observed, and the LHC fraction reaches 100 %. When comparing Fig.2 and 3, it is apparent that considering LHC leads to the replacement of the supercritical gas-oil contact with the classical one and increase in PC_{5+} values (Fig.3, *c*), i.e., to higher condensate content in the reservoir gas.

This is an open access article under the CC BY 4.0 license

© Ekaterina V. Kusochkova, Ilya M. Indrupskii, Dmitrii V. Surnachev, Yuliya V. Alekseeva, Aleksandr N. Drozdov, 2024

Main parameters of the Composition 2 are close to the conditions of the main reservoir of the Orenburg OGCF. The reservoir fluid is modeled with a mixture of 23 components, including 15 pseudo-fractions (Table 2). The reference depth is h = 1250 m, pressure at the reference depth is p = = 195 bar, temperature is T = 29.34 °C, and the geothermal gradient is dT = 0.009 °C/m. At the reference point, the composition is saturated to the LHC molar fraction of 8% (L_0 = 0.08).

The results of the modified algorithm are shown in Fig.4.

Table 2

Input data for composition 2

Components	Molar fraction z, %	Molar mass M, g/mol	Critical temperature T_c, °C	Critical pressure p_c, bar	Acentric factor ω	Molar enthalpy H_{ref}, J	Coefficients of cubic approximation for ideal gas heat capacity [38]			
							A	*B*	*C*	*D*
N_2	5.4704	28.013	–146.95	33.944	0.04	8330.789	31.1488	-0.0136	0.0	0.0
CO_2	0.6595	44.01	31.55	73.866	0.225	19459.1011	19.7946	0.0734	–0.0001	0.0
H_2S	1.7432	34.076	100.45	89.369	0.1	12550.8657	31.9401	0.0014	0.0	0.0
C_1	83.2209	16.043	–82.55	46.042	0.013	2.6425	19.2503	0.0521	0.0	0.0
C_2	4.0362	30.07	32.28	48.839	0.0986	9761.1347	5.4092	0.1781	–0.0001	0.0
C_3	1.7471	44.097	96.65	42.455	0.1524	19519.6224	–4.2244	0.3063	–0.0002	0.0
IC_4	0.3152	58.124	134.95	36.477	0.1848	29278.1212	–1.39	0.3847	–0.0002	0.0
C_4	0.6338	58.124	146.35	37.47	0.1956	29278.1212	9.487	0.3313	–0.0001	0.0
F_1	0.9559	84.0	226.5	30.7	0.2706	34921.866	15.1105	0.4975	–0.0002	0.0
F_2	0.436	94.0	264.5	30.92	0.324	39079.231	16.9094	0.5568	–0.0002	0.0
F_3	0.2809	110.0	301.1	29.07	0.3566	45731.015	19.7876	0.6515	–0.0003	0.0
F_4	0.1706	126.0	333.7	27.04	0.4078	52382.799	22.6658	0.7463	–0.0003	0.0
F_5	0.1005	141.0	364.0	25.37	0.4764	58618.8465	25.3641	0.8351	–0.0003	0.0
F_6	0.051	156.0	395.2	24.28	0.5427	64854.894	28.0624	0.924	–0.0004	0.0
F_7	0.0378	173.0	424.8	23.03	0.6141	71922.4145	31.1205	1.0247	–0.0004	0.0
F_8	0.0383	203.0	456.2	20.93	0.6437	84394.5095	36.5171	1.2024	–0.0005	0.0
F_9	0.0292	220.0	487.7	20.58	0.7118	91462.03	39.5752	1.303	–0.0005	0.0
F_{10}	0.025	273.0	514.4	17.3	0.728	113496.0645	49.1093	1.617	–0.0006	0.0
F_{11}	0.0115	296.0	539.1	16.46	0.8339	123058.004	53.2467	1.7532	–0.0007	0.0
F_{12}	0.0104	310.0	562.9	16.13	0.976	128878.315	55.7651	1.8361	–0.0007	0.0
F_{13}	0.0074	356.0	588.9	14.64	1.0396	148002.194	64.0399	2.1086	–0.0008	0.0
F_{14}	0.0019	372.0	605.0	14.29	1.1295	154653.978	66.9181	2.2033	–0.0009	0.0
F_{15}	0.0173	565.0	668.8	10.58	1.1534	234891.1225	101.6364	3.3464	–0.0013	0.0

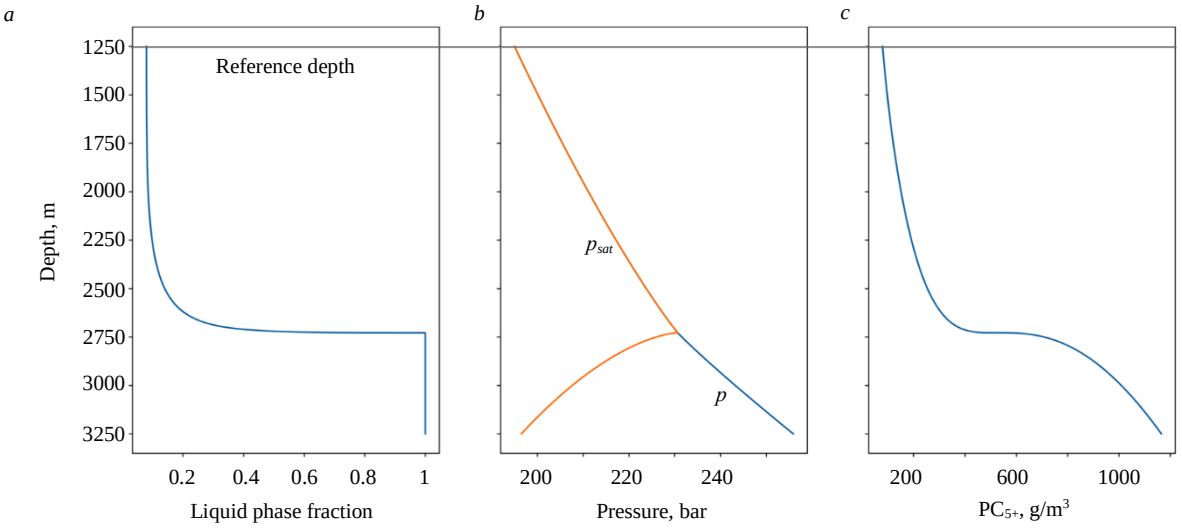

Fig.4. Results of the modified algorithm for composition 2

Calculated dependencies on depth for: *a* – molar fraction of the liquid phase; *b* – pressure p and saturation pressure p_{sat}, bar; *c* – PC_{5+}, g/m^3

This is an open access article under the CC BY 4.0 license

Journal of Mining Institute. 2024. Vol. 270. P. 904-918
© Ekaterina V. Kusochkova, Ilya M. Indrupskii, Dmitrii V. Surnachev, Yuliya V. Alekseeva, Aleksandr N. Drozdov, 2024

Up to the depth of 2728 m, the saturation (dew point) pressure and the reservoir pressure are equal (Fig.4, *b*), indicating the presence of the saturated gas condensate mixture and LHC. The LHC fraction increases with depth, reaching 100 % at the 2728 m level, showing a classical GOC (Fig.4, *a*). Below the GOC, the reservoir pressure and saturation pressure no longer match (Fig.4, *b*), corresponding to the single-phase region with undersaturated oil – the oil rim. PC_{5+} values increase with depth quite uniformly in the gas condensate region and more intensively below the GOC (Fig.4, *c*), reflecting the specifics of increase in the content of heavy components.

Composition 3 models the conditions similar to the main reservoir of the Vuktyl OGCF. The fluid is represented by a mixture of 19 components (Table 3). The reference depth is h = 3025 m, pressure at the reference depth is p = 362.9 bar, temperature is T = 61.4 °C, and the geothermal gradient is dT = 0.0175 °C/m. At the reference point, the composition is saturated to the LHC molar fraction of 14% (L_0 = 0.14).

The results of the modified algorithm are presented in Fig.5.

Table 3

Input data for composition 3

Components	Molar fraction z, %	Molar mass M, g/mol	Critical temperature T_c, °C	Critical pressure p_c, bar	Acentric factor ω	Molar enthalpy H_{ef}, J	Coefficients of cubic approximation for ideal gas heat capacity [38]			
							A	*B*	*C*	*D*
N_2	4.8184	28.013	–146.8889	33.9912	0.045	8330.789	31.1488	–0.0136	0.0	0.0
CO_2	0.0408	44.01	31.0556	73.8153	0.231	19459.1011	19.7946	0.0734	–0.0001	0.0
C_1	72.8929	16.043	–82.5722	46.0432	0.0115	2.6425	19.2503	0.0521	0.0	0.0
C_2	8.7255	30.07	32.2722	48.8011	0.0908	9761.1347	5.4092	0.1781	–0.0001	0.0
C_3	3.5793	44.097	96.6722	42.4924	0.1454	19519.6224	–4.2244	0.3063	–0.0002	0.0
IC_4	0.4663	58.124	134.9889	36.4802	0.1756	29278.1212	–1.39	0.3847	–0.0002	0.0
C_4	0.8435	58.124	152.0278	37.9694	0.1928	29278.1212	9.487	0.3313	–0.0001	0.0
IC_5	0.1743	72.151	187.2778	33.8119	0.2273	39036.6099	–9.5247	0.5066	–0.0003	0.0
C_5	0.1409	72.151	196.5	33.6878	0.251	39036.6099	–3.6257	0.4873	–0.0003	0.0
C_6P_1	2.018	85.0188	250.9278	26.6887	0.1208	35345.4179	7.9027	0.5004	–0.0002	0.0
C_6P_2	3.138	110.457	318.9667	24.7149	0.2351	45921.0074	6.0966	0.6562	–0.0002	0.0
C_6P_3	1.815	157.953	398.0444	20.7256	0.3625	65666.8306	11.8058	0.9287	–0.0004	0.0
C_6P_4	0.5837	231.218	488.5167	16.8437	0.5589	96125.7653	22.824	1.3619	–0.0005	0.0
C_6P_5	0.299	338.184	586.3389	13.5525	0.7602	140595.426	42.4439	1.9968	–0.0008	0.0
C_6P_6	0.1931	500.0	679.6444	10.5933	1.0268	207868.25	75.7996	2.9481	–0.0011	0.0
C_6P_7	0.1216	598.0	674.6278	7.5153	1.3	248610.427	25.5721	3.407	–0.0014	0.0
C_6P_8	0.0778	794.1	737.6278	5.9157	1.481	330136.3547	33.1361	4.5271	–0.0018	0.0
C_6P_9	0.0475	1004.1	790.0722	4.8401	1.627	417441.0197	40.9978	5.7255	–0.0023	0.0
C_6P_{10}	0.0242	1284.2	845.0722	3.916	1.781	533888.7808	50.3553	7.3196	–0.0029	0.0

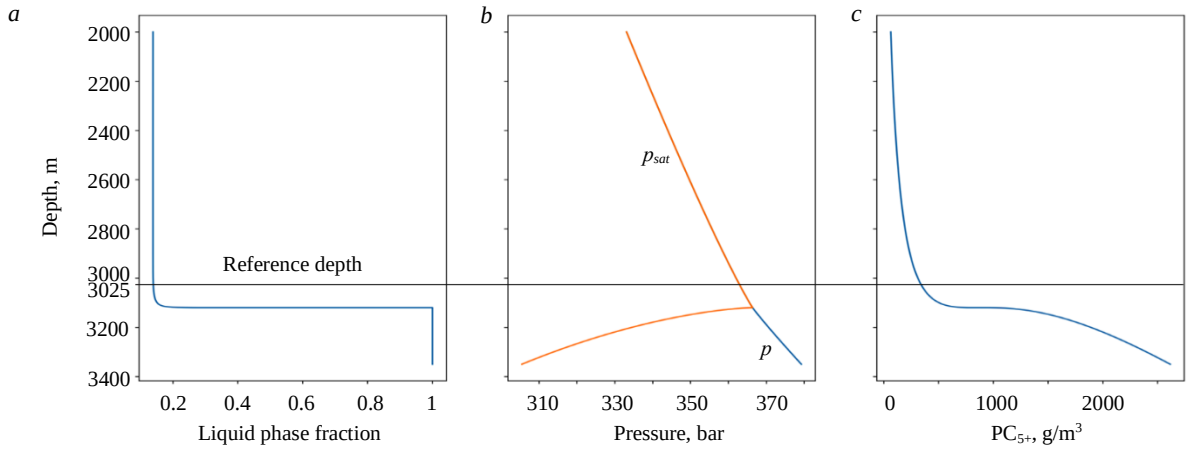

Fig.5. Results of the modified algorithm for composition 3
Calculated dependencies on depth for: *a* – molar fraction of the liquid phase; *b* – pressure p and saturation pressure p_{sat}, bar; *c* – PC_{5+}, g/m^3

This is an open access article under the CC BY 4.0 license

© Ekaterina V. Kusochkova, Ilya M. Indrupskii, Dmitrii V. Surnachev, Yuliya V. Alekseeva, Aleksandr N. Drozdov, 2024

For Composition 3, the change in the LHC fraction occurs up to the depth of 3120 m, where the LHC fraction reaches 100 %, and a classical GOC is observed (Fig.5, *a*). Below, the reservoir pressure and saturation pressure no longer match (Fig.5, *b*), corresponding to the single-phase undersaturated liquid state. The behavior of the PC_{5+} curve is similar to the Composition 2, but with more intensive increase below the GOC (Fig.5, *c*).

It is interesting to compare the results for Compositions 2 and 3 (Fig.6). Here the depth axis is relative, with the zero point set at the GOC level for each reservoir. The PC_{5+} plots for Compositions 2 and 3 are similar across almost the entire depth interval of the gas condensate region, excluding the interval near the GOC. Here, for Composition 3, the increase in the PC_{5+} is more gradual than for Composition 2 (Fig.6, *b*). However, the dependencies of the LHC fraction on depth differ significantly (Fig.6, *a*). For Composition 2, the LHC fraction smoothly increases throughout the depth interval down to the GOC. For Composition 3, a significant change in the LHC fraction is noted only when approaching the GOC level.

To analyze these differences, consider the depth variation of individual component fractions in the liquid phase obtained by the Negative Flash calculation. Plots of the component fractions from the top boundary of the calculation depths to the GOC are shown in Fig.7 for Compositions 2 and 3. It is noteworthy that the component C_1 – methane – contributes most to the change in the LHC fraction (Fig.7, *a*, *f*). It can be observed that for Composition 2, the change in the methane fraction in the liquid phase is quite uniform throughout the entire calculated depth interval, while for Composition 3 significant changes begin near the GOC. A similar behavior is observed in the plot for the LHC fraction (Fig.7, *e*, *j*).

Thus, the character of the LHC fraction dependence on depth is determined by the swelling effect due to the dissolution of light components, particularly methane, which has the highest concentration in the liquid phase. It is important to note that the composition of the LHC in the gas condensate region of the reservoir changes with depth differently than in the oil region. The pressure and the fraction of intermediate components increase with depth in the gas phase, and consequently – in the liquid phase equilibrated with it. With an increased concentration of C_3-C_4 in the saturated liquid phase, the solubility of methane increases. This trend is opposite to the heaving of the liquid phase, characteristic for the undersaturated state below the GOC. It is worth noting that the noticeable sharp decrease in the content of intermediate and some heavy components near the GOC, as seen in Fig.7, is associated with the increase in methane content and normalization of concentrations.

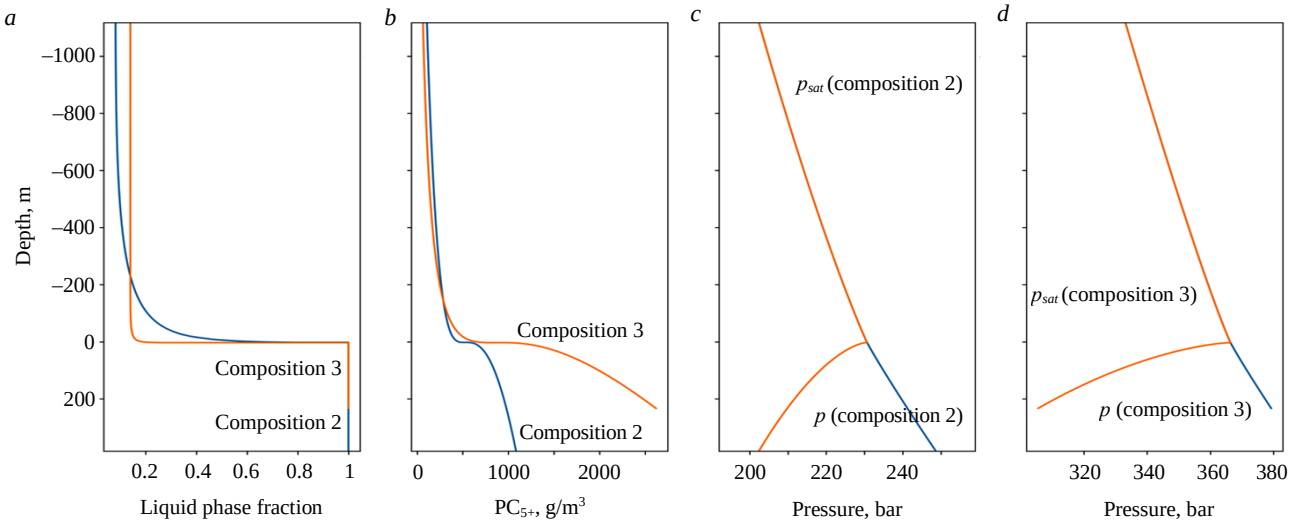

Fig.6. Comparison of the modified algorithm results for compositions 2 and 3

Calculated dependencies on depth for: *a* – molar fraction of the liquid phase, compositions 2 and 3; *b* – PC_{5+}, g/m^3, compositions 2 and 3; *c* – pressure *p* and saturation pressure p_{sat}, bar, composition 2; *d* – pressure *p* and saturation pressure p_{sat}, bar, composition 3

This is an open access article under the CC BY 4.0 license

© Ekaterina V. Kusochkova, Ilya M. Indrupskii, Dmitrii V. Surnachev, Yuliya V. Alekseeva, Aleksandr N. Drozdov, 2024

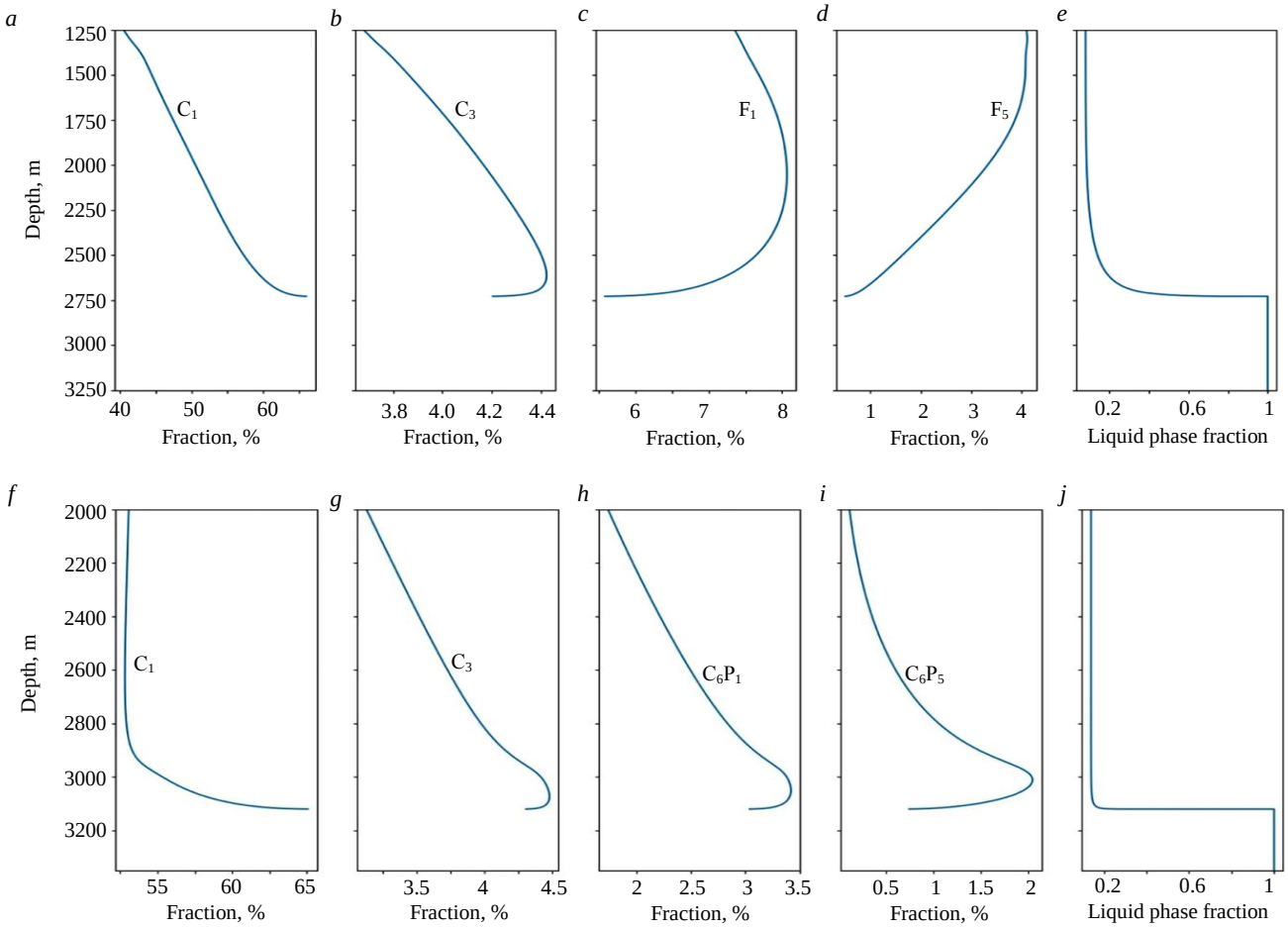

Fig.7. Plots of the molar component concentrations in the liquid phase for compositions 2 and 3

Calculated dependencies on depth for: *a* – molar fraction of methane, %; *b* – molar fraction of propane, %; *c* – molar fraction of group F_1, %; *d* – molar fraction of group F_5, %; *e* – molar fraction of the liquid phase (composition 2); *f* – molar fraction of methane, %; *g* – molar fraction of propane, %; *h* – molar fraction of group C_6P_1, %; *i* – molar fraction of group C_6P_5, %; *j* – molar fraction of the liquid phase (composition 3)

Conclusion.

The presence of a small fraction of scattered LHC in many gas condensate reservoirs necessitates changes in approaches to calculating the initial composition distribution with depth. In this case, classical methods of compositional grading are not applicable.

The modified algorithm for compositional grading discussed and implemented in this study makes it possible not to completely abandon the concept of quasi-equilibrium initial state of the hydrocarbon system, but to supplement it with necessary assumptions and calculation procedures for consistent consideration of the scattered LHC.

Calculation cases presented for different gas condensate mixtures, close by composition and conditions to real oil-gas-condensate reservoirs with significant hydrocarbon columns, demonstrate several characteristic features of the LHC impact on the compositional gradient: elevation and possible change of type for the fluid contact, as well as for the PC_{5+} dependency on depth. In regions with the LHC, the reservoir gas condensate fluid is saturated, and the saturation (dew point) pressure matches the reservoir pressure.

It is shown that the character of the LHC fraction change with depth can be different. Light components, particularly methane, contribute most, which is explained by the swelling effect of the saturated liquid phase. The change in the LHC composition with depth in the gas condensate part of the reservoir also shows significantly different trends than in the oil zone, where the liquid phase is undersaturated with light hydrocarbons.

This is an open access article under the CC BY 4.0 license

The proposed approach to considering LHC, as well as the concept of quasi-equilibrium compositional gradient, allow calculating in a thermodynamically consistent way the initial state of oil-gas-condensate reservoirs with the presence of scattered LHC, estimating the GOC position and distribution of volumes in place for gas, liquid hydrocarbons, and individual components. The results of compositional grading considering LHC define the initial conditions when modeling field development and justifying technological solutions for efficient hydrocarbon recovery.

The presented method relies on assumptions of pseudo-equilibrium distribution of the gas phase with depth and local thermodynamic equilibrium between the gas condensate fluid and the scattered LHC. Their applicability to the conditions of specific oil-gas-condensate reservoirs requires further examination considering the formation specifics and accumulated actual data.

When analyzing the accuracy of the compositional gradient calculations, it is recommended to include a check of calculated concentrations of the C_{5+} group components at control points in depth. Typically, they are expected to satisfy the two-parameter gamma distribution [2]. For some reservoirs, it has been noted that the actual change in the concentrations of C_{5+} components with depth is predominantly linear [34].

Future refinements of the presented method could include accounting for capillary pressure and the gas-oil transition zone, for example, analogously to the work [39]. The current version of the method also predicts formation of a transition zone with the LHC saturation increasing to 100 % at the GOC (see Fig.3, *a*, 4, *a*, 5, *a*), but based on thermodynamics rather than on capillary effects.

REFERENCES

1. Brusilovskii A.I. Phase transitions in oil and gas field development. Moscow: Graal, 2002, p. 575 (in Russian).
2. Whitson C.H., Brulé M.R. Phase behavior. Richardson: Society of Petroleum Engineers, 2000. Vol. 20, p. 240. DOI: 10.2118/9781555630874
3. Novikov S., Weinheber P., Charupa M. et al. Tight Gas Achimov Formation Evaluation and Sampling with Wireline Logging Tools: Advanced Approaches and Technologies. SPE Russian Petroleum Technology Conference, 26-28 October 2015, Moscow, Russia. OnePetro, 2015. N SPE-176591-MS. DOI: 10.2118/176591-MS
4. Gusev S., Garaev A., Zeybek M. et al. Reservoir Connectivity and Compartmentalization Detection with Down Hole Fluid Analysis Compositional Grading. SPE Russian Petroleum Technology Conference, 26-29 October 2020. OnePetro, 2020. N SPE-201895-MS. DOI: 10.2118/201895-MS
5. Fundamentals of formation testing. Ed. by A.G.Zagurenko. Moscow, Izhevsk: Institut kompyuternykh issledovanii, 2012, p. 432 (in Russian).
6. Aliev Z.S., Ismagilov R.N. Gas-hydrodynamic fundamentals of gas-condensate well testing. Moscow: Nedra, 2012, p. 214 (in Russian).
7. Raupov I., Burkhanov R., Lutfullin A. et al. Experience in the Application of Hydrocarbon Optical Studies in Oil Field Development. *Energies*. 2022. Vol. 15. Iss. 10. N 3626. DOI: 10.3390/en15103626
8. Asemani M., Rabbani A.R., Sarafdokht H. Implementation of an Integrated Geochemical Approach Using Polar and Non-polar Components of Crude Oil for Reservoir-Continuity Assessment: Verification with Reservoir-Engineering Evidences. *SPE Journal*. 2021. Vol. 26. Iss. 5, p. 3237-3254. N SPE-205388-PA. DOI: 10.2118/205388-PA
9. Kuklinsky A.Ya., Shtun S.Yu., Moroshkin A.N. Applying reservoir geochemistry methods to determine performance of each of jointly operated formations with different oil molecular composition. *Geology, geophysics and development of oil and gas fi elds.* 2021. N 1 (349), p. 39-43 (in Russian). DOI: 10.33285/2413-5011-2021-1(349)-39-43
10. Dantsova K.I., Iskaziyev K.O., Khafizov S.F. Geochemical characteristics of the organic matter of the Jurassic sediments of the southern regions of Western Siberia. *Oil Industry.* 2021. N 5, p. 50-53 (in Russian). DOI: 10.24887/0028-2448-2021-5-50-53
11. Chen Q., Kristensen M., Johansen Y.B. et al. Analysis of Lateral Fluid Gradients from DFA Measurements and Simulation of Reservoir Fluid Mixing Processes over Geologic Time. *Petrophysics*. 2021. Vol. 62. Iss. 1, p. 16-30. N SPWLA-2021-v62n1a1. DOI: 10.30632/PJV62N1-2021a1
12. Reitblat E.A., Zanochuev S.A., Goncharov I.V. et al. Study of gas composition and properties differentiation of Ach_{3-4} formation at the Novy Urengoy license area. *Gas Industry Journal.* 2021. N 12 (628), p. 46-52 (in Russian).
13. Goncharov I.V., Veklich M.A., Oblasov N.V. et al. Nature of Hydrocarbon Fluids at the Fields in the North of Western Siberia: the Geochemical Aspect. *Geochemistry International.* 2023. Vol. 61. Iss. 2, p. 103-126. DOI: 10.1134/S0016702923020040
14. Mukhametshin V.Sh., Khakimzyanov I.N. Features of grouping low-producing oil deposits in carbonate reservoirs for the rational use of resources within the Ural-Volga region. *Journal of Mining Institute.* 2021. Vol. 252, p. 896-907. DOI: 10.31897/PMI.2021.6.11
15. Galkin S.V., Krivoshchekov S.N., Kozyrev N.D. et al. Accounting of geomechanical layer properties in multi-layer oil field development. *Journal of Mining Institute.* 2020. Vol. 244, p. 408-417. DOI: 10.31897/PMI.2020.4.3

This is an open access article under the CC BY 4.0 license

16. Ali Al-Amani Hj Azlan, Muda W.M.W., Mubaraki A.H et al. New Approach of Synergizing Advanced Well Test Deconvolution, Rate Transient Analysis and Dynamic Modeling in Evaluating Reservoir Compartmentalization Uncertainty at K Field in Sarawak Basin; A Case Study. SPE Middle East Oil and Gas Show and Conference, 18-21 March 2019, Manama, Bahrain. OnePetro, 2019. N SPE-195038-MS. DOI: 10.2118/195038-MS

17. Pylev Ye.A., Churikov Yu.M., Polyakov Ye.Ye et al. Assessment of fault conductivity by well pressure interference tests: case of Chayanda oil-gas-condensate field. *Vesti Gazovoy Nauki*. 2021. Vol. 3 (48), p. 192-202 (in Russian).

18. Plyusnin A.V., Gyokche M.I., Shavarov R.D., Nikulin E.V. Geodynamic and tectonic factors of the formation and destruction of carbonate Vendian-Cambrian hydrocarbon deposits in the south of the Nepa-Botuoba anteclise. *Geosphere Research*. 2023. N 1, p. 20-35 (in Russian).

19. Pedersen K.S., Christensen P.L., Skaikh J.A. Phase behavior of petroleum reservoir fluids. Boca Raton: CRC Press, 2014, p. 465. DOI: 10.1201/b17887

20. Høier L., Whitson C.H. Compositional Grading – Theory and Practice. *SPE Reservoir Evaluation & Engineering*. 2001. Vol. 4. Iss. 6, p. 525-535. N SPE-74714-PA. DOI: 10.2118/74714-PA

21. Pedersen K.S., Hjermstad H.P. Modeling of Compositional Variation with Depth for Five North Sea Reservoirs. SPE Annual Technical Conference and Exhibition, 28-30 September 2015, Houston, TX, USA. OnePetro, 2015. N SPE-175085-MS. DOI: 10.2118/175085-MS

22. Yazkov A.V., Gorobets V.E., Surkov E.V. et al. Complex Phase Behavior Study of a Near-Critical Gas Condensate Fluid in a Tight HPHT Reservoir. SPE Russian Petroleum Technology Conference, 26-29 October, 2020. OnePetro, 2020. N SPE-201997-MS. DOI: 10.2118/201997-MS

23. Sajjad F.M., Chandra S., Ivan P. et al. The Effect of Compositional Gradient in Field Development. SPE/IATMI Asia Pacific Oil & Gas Conference and Exhibition, 12-14 October 2021. OnePetro, 2021. N SPE-205801-MS. DOI: 10.2118/205801-MS

24. Gibbs J.W. The Collected Works of J. Willard Gibbs. Yale University Press, 1948. In 2 vol.

25. Montel F., Gouel P.L. Prediction of Compositional Grading in a Reservoir Fluid Column. SPE Annual Technical Conference and Exhibition, 22-26 September 1985, Las Vegas, NV, USA. OnePetro, 1985. N SPE-14410-MS. DOI: 10.2118/14410-MS

26. Haase R., Borgmann H.-W., Dücker K.-H., Lee W.-P. Thermodiffusion im kritischen Verdampfungsgebiet binärer Systeme. *Zeitschrift für Naturforschung A*. 1971. Vol. 26. Iss. 7, p. 1224-1227. DOI: 10.1515/zna-1971-0722

27. *Haase R.* Thermodynamik der Irreversiblen Prozesse. Darmstadt: Dr. Dietrich Steinkopff Verlag, 1963, p. 554. DOI: 10.1007/978-3-642-88485-6

28. Pedersen K.S., Lindeloff N. Simulations of Compositional Gradients in Hydrocarbon Reservoirs under the Influence of a Temperature Gradient. SPE Annual Technical Conference and Exhibition, 5-8 October 2003, Denver, Colorado. OnePetro, 2003. N SPE-84364-MS. DOI: 10.2118/84364-MS

29. Pedersen K.S., Fredenslund A., Thomassen P. Properties of oils and natural gases. Houston: Gulf Publishing Company, 1989, p. 252.

30. Popov S.B. Compositional grading by depth in gas and oil fields with temperature gradient. *Keldysh Institute PREPRINTS*. N 38, p. 32 (in Russian). DOI: 10.20948/prepr-2018-38

31. Michelsen M.L. The isothermal flash problem. Part I. Stability. *Fluid Phase Equilibria*. 1982. Vol. 9. Iss. 1, p. 1-19. DOI: 10.1016/0378-3812(82)85001-2

32. Popov S.B. Compositional grading with a depth in gas-oil reservoirs. *Keldysh Institute PREPRINTS*. N 61, p. 30 (in Russian). DOI: 10.20948/prepr-2017-61

33. Whitson C.H., Belery P. Compositional Gradients in Petroleum Reservoirs. University of Tulsa Centennial Petroleum Engineering Symposium, 29-31 August 1994, Tulsa, OK, USA. OnePetro, 1994. N SPE-28000-MS. DOI: 10.2118/28000-MS

34. Surnachev D.V., Skibitskaya N.A., Indrupskiy I.M., Bolshakov M.N. Assessment of the content and composition of liquid hydrocarbons of matrix oil in the gas-saturated part of productive deposits of oil and gas condensate fields: the case of the Vuktyl oil and gas condensate field. *Actual Problems of Oil and Gas*. 2022. Iss. 1 (36), p. 42-65 (in Russian). DOI: 10.29222/ipng.2078-5712.2022-36.art3

35. Skibitskaya N., Bolshakov M., Burkhanova I. et al. Tight Oil in Oil-And-Gas Source Carbonate Deposits' Gas Saturation Zones of Gas-Condensate and Oil-Gas Condensate Fields. SPE Russian Petroleum Technology Conference and Exhibition, 24-26 October 2016, Moscow, Russia. OnePetro, 2016. N SPE-182076-MS. DOI: 10.2118/182076-MS

36. Kusochkova E.V., Indrupskiy I.M., Kuryakov V.N. Distribution of the Initial Fluid Composition in an Oil-Gas-Condensate Reservoir with Incomplete Gravity Segregation. IOP Conference Series: Earth and Environmental Science. 2021. Vol. 931. N 012012. DOI: 10.1088/1755-1315/931/1/012012

37. Whitson C.H., Michelsen M.L. The negative flash. *Fluid Phase Equilibria*. 1989. Vol. 53, p. 51-71. DOI: 10.1016/0378-3812(89)80072-X

38. Reid R.C., Prausnitz J.M., Poling B.E. The Properties of Gases and Liquids. McGraw-Hill, 1987, p. 741.

39. Wheaton R.J. Treatment of Variations of Composition with Depth in Gas-Condensate Reservoirs. *SPE Reservoir Engineering*. 1991. Vol. 6. Iss. 2, p. 239-244. N SPE-18267-PA. DOI: 10.2118/18267-PA

***Authors*: Ekaterina V. Kusochkova,** *Junior Researcher, https://orcid.org/0009-0000-3537-5521 (Oil and Gas Research Institute of RAS, Moscow, Russia)*, **Ilya M. Indrupskii,** *Doctor of Engineering Sciences, Deputy Director for Research, Chief Researcher, i-ind@ipng.ru, https://orcid.org/0000-0002-0038-6279 (Oil and Gas Research Institute of RAS, Moscow, Russia)*, **Dmitrii V. Surnachev,** *Candidate of Physics and Mathematics, Senior Researcher, https://orcid.org/0009-0001-8257-4272 (Oil and Gas Research Institute of RAS, Moscow, Russia)*, **Yuliya V. Alekseeva,** *Junior Researcher, https://orcid.org/0000-0001-5108-5874 (Oil and Gas Research Institute of RAS, Moscow, Russia)*, **Aleksandr N. Drozdov,** *Doctor of Engineering Sciences, Professor, https://orcid.org/0000-0001-9509-203X (Peoples's Friendship University of Russia named after Patrice Lumumba, Moscow, Russia; Sergo Ordzhonikidze Russian State University for Geological Prospecting, Moscow, Russia)*.

The authors declare no conflict of interests.

This is an open access article under the CC BY 4.0 license

ISSN 2411-3336; e-ISSN 2541-9404

JOURNAL OF MINING INSTITUTE

Zapiski Gornogo instituta

Journal homepage: pmi.spmi.ru

Research article

Complete extraction of conditioned ores from complex-structured blocks due to partial admixture of substandard ores

Bayan R. Rakishev

Kazakh National Research Technical University named after K.I.Satpayev (Satbayev University), Almaty, Republic of Kazakhstan

***How to cite this article*:** Rakishev B.R. Complete extraction of conditioned ores from complex-structured blocks due to partial admixture of substandard ores. Journal of Mining Institute. 2024. Vol. 270, p. 919-930.

Abstract

The paper presents mining-technological substantiation of complete extraction of conditioned ores from complex-structured blocks of benches by mixing a layer of substandard ores of certain sizes. The relevance of the work consists in the development of innovative methods of establishing the parameters of the substandard layer of ores to be added to the conditioned ores. The main problem is to ensure complete extraction of useful components into concentrate from shipped ore with acceptable deviations from the required ones. A new typification of complex-structured ore blocks of the bench has been carried out. Analytical dependences of mining and geological characteristics of complex-structured ore blocks were obtained. Theoretical dependences for determining the main indicators of mineral processing are derived. Analytical dependences for determination of the content of useful component in shipped ore α' – mixture of conditioned ore with the content of useful component α and admixed layer of substandard ore with the content of useful component α'' are offered. For the first time in mining science, a new approach of complete extraction of conditioned ores from complex-structured blocks of benches by grabbing a certain part of substandard ores during excavation, increasing the volume of extracted ore and expanding the extraction of useful components in the concentrate has been substantiated. The increment of useful components can reach 10-15 % of the total volume of extraction, which allows predicting a significant increase in the completeness of mineral extraction from the Earth's interior.

Keywords

complex blocks of benches; types of blocks; mining and geological characteristics; content of useful components; admixed layers of substandard ores; complete extraction of conditioned ores

Funding

The article was prepared as part of a project funded by the Ministry of Science and Higher Education of the Republic of Kazakhstan 2023/AP19676591 “Development of innovative technologies for the complete extraction of scattered conditioned ores from complex-structured blocks of benches”.

Received: 05.07.2023 ***Accepted: 03.06.2024*** ***Online: 03.10.2024*** ***Published: 25.12.2024***

Introduction.

Complete extraction of minerals from the subsurface, including conditioned ores, reduction of their losses and dilution during the exploitation of various deposits is one of the most acute and urgent tasks of mining science and industry [1-3]. The problem becomes especially important in the development of complex-structured ore deposits [4-6], which are usually represented by a diverse combination of ore bodies and host rocks (substandard ores) of complex configuration, different sizes and physical, technical and geological characteristics. Contacts between conditioned and substandard ores are visually indistinguishable and are probabilistic in nature. The share of complex-structured blocks at non-ferrous metallurgy enterprises of CIS countries is 60-90 %, and operational losses of ore during their development can reach 20-35 % [7-9].

The main reasons for the high level of losses and dilution during open pit mining of complex-structured minerals are insufficient study of the geological and morphological structure of complex-structured blocks of benches; inconsistency of the applied technologies of excavation and loading operations with the real mining and geological conditions of occurrence of complex-structured minerals in the massif and in the blasted state; use of private methods of determining and rationing

This is an open access article under the CC BY 4.0 license

of losses and dilution, focused on mining and geological objects with clear geological boundaries – veins, lenses, layers and stratification of deposits. Quantitative and qualitative losses of minerals in them are usually established for the contour areas of ore blocks.

The majority of non-ferrous, noble and rare metal ore deposits in Kazakhstan are complex-structured. Ore areas have complex geological and morphological structure, irregular mineralization, visually indistinguishable boundaries with host rocks. They are characterized by different shape, size of ore bodies, placement in the considered space, mineralization and physical and mechanical properties of rocks [10-12]. The totality of these features determines the degree of complexity of the geological and morphological structure of complex mineral sites. The development of innovative methods for assessing the complexity of such areas and their use to significantly reduce losses and dilution during the development of complex-structured minerals is an urgent and priority task of mining science and industry.

The purpose of the research is mining and technological justification of complete extraction of conditioned ores from complex-structured blocks of benches by means of mixing a layer of substandard ores of set sizes. In this case the extraction of useful components into concentrate with acceptable deviations from the required ones is provided.

Methods.

To assess the geological and morphological structure of complex-structured ore blocks (CSOB) of the bench and its use in the effective development of these blocks, their mining and geological models are created. The mining and geological model contains data of interval sampling of exploration well cores for the content of useful components and harmful impurities, information on well depths and geometric parameters of disparate ore bodies. On the basis of these data, taking into account the requirements presented by the customer to the commercial ore, the boundaries between conditioned and substandard ores are established, ore bodies in the ore block of the bench are delineated, and the CSOB of the bench is typified.

Analysis of literature sources on modeling [13-15] and typification [16-18] of complex-structured blocks [19-21], their theoretical understanding [22-24] show that complex-structured blocks of benches can be divided into only two types by the nature of ore bodies location and their geometric parameters [10]. At the same time, the spatial arrangement of fixed ore bodies in the ore block of the bench and their fragmentation (separation of ore bodies in the block by the host rocks – unconfined ores) are considered as determining features [25-27].

Ore bodies are defined as volumes of conditioned ore reserves established by analyzing blast hole samples and other geophysical methods. They do not always coincide with the balance sheet ore reserves, as they are identified as a result of additional exploration. In addition, the host rocks in contact with the ore bodies represent substandard ores.

The first type of CSOB benches includes blocks composed of scattered continuous ore bodies of various shapes and sizes with rectilinear contacts with rock interlayers (Fig.1).

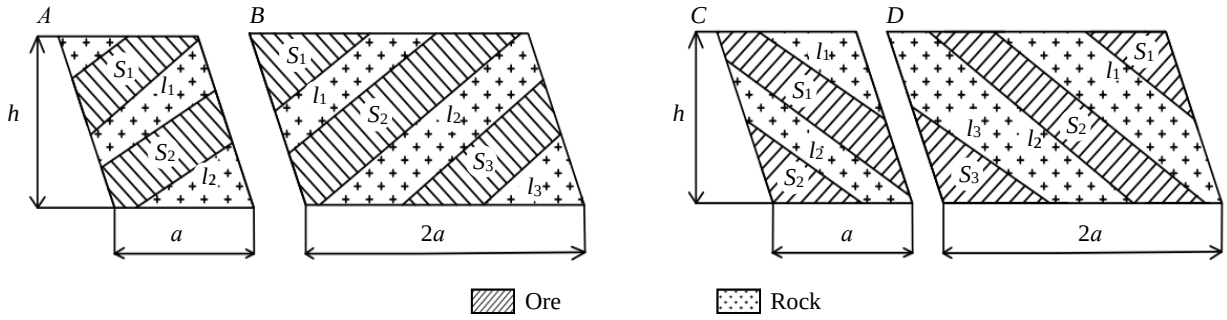

Fig.1. Types of complex-structured bench blocks composed of discontinuous continuous ore bodies:
A, *B* – angle of bodies dip from 0 to π/2; *C*, *D* – angle of bodies dip from π/2 to π
h – block height; *a*, 2*a* – block width; S_i – cross-sectional area of the *i*-th ore body; l_i – length of contact lines of the *i*-th ore body with host rocks

This is an open access article under the CC BY 4.0 license

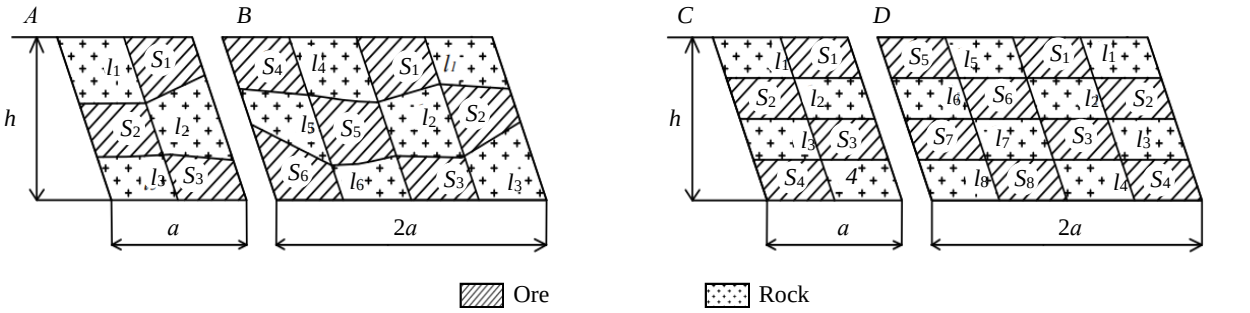

Fig.2. Types of complex-structured blocks composed of dispersed ore bodies:
A, B – trapezoidal bodies; *C, D* – parallelogram bodies

Datamine, Surpac, Micromine, etc. software products provide only straight-line contacts in block model. They extend from one block boundary (mining unit) to another and form angles varying from 0 to π with the horizon.

The first type of CSOB benches may be represented by horizontal, inclined or vertical bedded ore bodies of relatively mature thickness (contact lines are parallel) or lens-shaped inclusions of variable thickness, between which interlayers of host rocks (unconfined ores) are placed.

The second type of CSOB benches is represented by blocks composed of dispersed ore bodies in the form of geometric figures of various shapes and sizes, such as polygons with rectilinear contacts with the host rocks (Fig. 2). The contact lines are located inside the block (mining unit). This type of complex blocks may consist of nested ore bodies of various shapes and sizes, etc.

The given types of CSOB (Fig.1, 2) serve as a basis for determining their technological characteristics, analytically interconnecting all the identified geometric parameters of the geological and morphological structure of the blocks. Only in this case they will objectively reflect the natural state of the studied object and contribute to a more complete extraction of minerals from the subsurface through the appointment of the most effective technologies of drilling and blasting and excavation-loading operations in the conditions of complex-structured blocks.

Discussion of results.

Mining and geological characteristics of complex-structured ore blocks of the bench. The most common and relatively easy to measure values – the ore saturation coefficient of the block and the index of complexity of the geological structure of the block – can be considered as the sought mining and geological characteristics.

The given schemes of ore bodies placement of complex-structured blocks (Fig.1, 2) are characterized by the level of their mineral saturation. This property for the considered section of the block can be estimated by the ore saturation coefficient of the block

$$k_{\text{os}} = \sum_{i=1}^{n} S_i \Big/ S_{\text{b}},$$

where S_{b} is the area of the considered cross-section of the complex-structured block, m^2; n is the number of ore bodies.

The average ore saturation factor for the whole complex-structured block is determined by the following dependence:

$$k_{\text{os}}^{\text{av}} = \frac{1}{m} \sum_{j=1}^{m} \left(\sum_{i=1}^{n} S_i \Big/ S_{\text{b}} \right),$$

where m is the number of cuts; j is the index of the current block cut.

The number of sections depends on the extent of the complex block. Each section covers a zone with an extent equal, as a rule, to the distance between wells in a row.

When determining the numerical values of k_{os} it is necessary to take into account that in open-pit mining with the use of modern mobile mining and loading equipment the height of a complex-structured mining bench usually does not exceed 10 m, and the smallest width of the drift along

This is an open access article under the CC BY 4.0 license

the pillar is 8-10 m. In case of explosive crushing of such blocks, excavation of the mineral layer with thickness below 2.5 m is economically unprofitable and sometimes technically impossible. Therefore, the lower value of the considered indicator can be taken as 0.25, and the upper one – 0.75. This means that in most cases the ore saturation coefficient of a complex-structured block lies within the range of 0.25-0.75.

Complex-structured blocks are subdivided by the degree of ore-saturation into more ore-saturated (k_{os} = 0.75-0.6); moderately ore-saturated (k_{os} = 0.6-0.4); less ore-saturated (k_{os} = 0.4-0.25).

The less ore saturated a block is, the more difficult it is to mine it without small quantitative and qualitative losses. However, as the experience of mining enterprises shows, at the same value of the ore saturation index, different final results of mineral recovery from various complex-structured blocks are achieved. The determining parameters of the block in this case are the size of the area of individual ore bodies and the lines of their contacts with the host rocks (substandard ores) in the volume under consideration, the ratio of which characterizes the degree of complexity of the structure of the CSOB and is calculated using the complexity factor of the geological and morphological structure of the block

$$k_{cf} = \sum_{i=1}^{n} l_i t' \Big/ \sum_{i=1}^{n} S_i , \quad (1)$$

where t' is the thickness of the layer of host rocks (or ores) falling into the ore mass (or into the shipped rock) during excavation, m.

When excluding the sum signs from dependence (1), the complexity factor of the structure of the i-th ore body in the block is determined.

The block complexity index k_{cf} expresses the ratio of the total surface area of the adjacent layer of admixed rock or lost ore to the total surface area of ore bodies in a given section. In other words, equation (1) defines the level of quantitative and qualitative losses of ore during its extraction from the CSOB of the bench in fractions of one unit. Depending on the content of the numerator, this indicator represents losses, dilution, or both. The smaller the sum of the areas of ore bodies, the greater the complexity factor of the geological and morphological structure of the block, and vice versa. This circumstance reflects quite fully the real state of affairs at mining enterprises.

If the thickness of the near-contact layer of admixed rock or lost ore for all ore bodies of the CSOB is a constant value, it can be taken beyond the sign of the sum. Then quantitative and qualitative losses will be proportional to the ratio of the sums of contact line lengths to the total area of ore bodies in a given block section:

$$k_{cf} = \mu\left(\sum_{i=1}^{n} l_i \Big/ \sum_{i=1}^{n} S_i \right),$$

where μ is some proportionality factor, $\mu = t'$ (m).

As can be seen from equation (1), the index of complexity of the geological structure of ore blocks depends on the thickness of the admixed layer of rock or ore. Calculations show that for complex-structured deposits the considered criterion at the value of t', equal to 0.25 m (a tenth of the smallest thickness of the ore layer), varies within 0.1-0.3. And the greater k_{cf} , the more complex the block structure and the greater the source of losses. Based on this position complex ore blocks of benches, according to the nature of geological and morphological structure, can be divided into complex-structured (k_{cf} = 0.1-0.2) and more complex-structured (k_{cf} = 0.2-0.3). If the value exceeds 0.3, selective extraction of minerals from the CSOB for economic reasons becomes very problematic, as the current costs of extraction reach irrecoverable amounts.

Analysis of mining and geological characteristics of the CSOB. The results of using the developed method of determining the mining and geological characteristics of the CSOB are presented in Table 1 by numerical values. The height of blocks was taken equal to the height of the bench,

This is an open access article under the CC BY 4.0 license

i.e. h = 10 m, width of blocks a = 9, $2a$ = 18 m. Areas of ore bodies S_i and lengths of contact lines of ore bodies with host rocks (or substandard ores) l_i were assumed to be close to those in open pits of non-ferrous metallurgy of CIS countries.

Table 1

Mining and geological characteristics of CSOBs composed of discontinuous continuous ore bodies

A	*B*	*C*	*D*
$S_1(l_1)$ = 21.12 (13.25) $S_2(l_2)$ = 26.93 (15.94)	$S_1(l_1)$ = 17.69 (7.64) $S_2(l_2)$ = 50.09 (28.23) $S_3(l_3)$ = 29.35 (18.17)	$S_1(l_1)$ = 34.43 (23.89) $S_2(l_2)$ = 13.89 (8.92)	$S_1(l_1)$ = 13.23 (8.69) $S_2(l_2)$ = 44.29 (33.48) $S_3(l_3)$ = 19.34 (10.54)
$\Sigma S_i(\Sigma l_i)$ = 48.05 (29.19)	$\Sigma S_i(\Sigma l_i)$ = 97.13 (54.04)	$\Sigma S_i(\Sigma l_i)$ = 48.32 (32.81)	$\Sigma S_i(\Sigma l_i)$ = 76.86 (52.71)
k_{cf} = 0.157; k_{cf} = 0.148	k_{cf} = 0.108; k_{cf} = 0.141; k_{cf} = 0.155	k_{cf} = 0.173; k_{cf} = 0.160	k_{cf} = 0.164; k_{cf} = 0.189; k_{cf} = 0.136
k_{os} = 0.534; k_{cf} = 0.152	k_{os} = 0.539; k_{cf} = 0.139	k_{os} = 0.536; k_{cf} = 0.169	k_{os} = 0.427; k_{cf} = 0.171

Table 2

Mining and geological characteristics of CSOBs composed of dispersed ore bodies

A	*B*	*C*	*D*
$S_1(l_1)$ = 14.59 (8.58)	$S_1(l_1)$ = 15.52 (11.5) $S_2(l_2)$ = 14.50 (13.58)	$S_1(l_1)$ = 11.25 (7.16)	$S_1(l_1)$ = 11.25 (9.82) $S_2(l_2)$ = 11.25 (11.66)
$S_2(l_2)$ = 14.41 (12.20)	$S_3(l_3)$ = 12.01 (10.3) $S_4(l_4)$ = 14.95 (8.39)	$S_2(l_2)$ = 11.25 (11.66)	$S_3(l_3)$ = 11.25 (14.32) $S_4(l_4)$ = 11.25(7.16)
$S_3(l_3)$ = 12.08 (7.64)	$S_5(l_5)$ = 17.25 (16.95) $S_6(l_6)$ = 15.10 (8.19)	$S_3(l_3)$ = 11.25 (11.66)	$S_5(l_5)$ = 11.25 (7.16) $S_6(l_6)$ = 11.25 (14.32)
		$S_4(l_4)$ = 11.25 (7.16)	$S_7(l_7)$ = 11.25 (11.66) $S_8(l_8)$ = 11.25 (9.82)
$\Sigma S_i(\Sigma l_i)$ = 41.08 (28.42)	$\Sigma S_i(\Sigma l_i)$ = 89.33 (68.91)	$\Sigma S_i(\Sigma l_i)$ = 45 (37.64)	$\Sigma S_i(\Sigma l_i)$ = 90 (85.92)
k_{cf} = 0.147; k_{cf} = 0.212 k_{cf} = 0.158	k_{cf} = 0.185; k_{cf} = 0.235 k_{cf} = 0.215; k_{cf} = 0.14 k_{cf} = 0.245; k_{cf} = 0.135	k_{cf} = 0.159; k_{cf} = 0.260 k_{cf} = 0.260; k_{cf} = 0.159	k_{cf} = 0.218; k_{cf} = 0.259 k_{cf} = 0.318; k_{cf} = 0.159 k_{cf} = 0.159; k_{cf} = 0.318 k_{cf} = 0.259; k_{cf} = 0.218
k_{os} = 0.456; k_{cf} = 0.173	k_{os} = 0.496; k_{cf} = 0.193	k_{os} = 0.500; k_{cf} = 0.209	k_{os} = 0.500; k_{cf} = 0.238

The values of complexity coefficients of structure of separate ore bodies and blocks are presented for variants *A, B, C, D,* containing ore bodies of different configurations, sizes and various mutual arrangement (Fig.1, 2).

Analysis of the data in Tables 1, 2 shows that both ore blocks are moderately ore-saturated (k_{os} = 0.427-0.539) and complex-structured (k_{cf} = 0.139-0.193). The exception is the CSOBs composed of dispersed ore bodies (*C*, *D*), for which k_{cf} = 0.209-0.238. Consequently, these blocks are more complex. Blocks of the second type have a relatively higher value (k_{cf} = 0.173-0.238) than blocks of the first type (k_{cf} = 0.139-0.171). This predetermines a higher level of quantitative and qualitative mineral losses in blocks of the second type, which is quite natural.

The highest value of k_{cf} has ore bodies S_2, S_3 (k_{cf} = 0.260) of block *B* and ore bodies S_3, S_6 (k_{cf} = 0.318) of block *D* of the second type of CSOB, i.e. at extraction of these ore bodies quantitative and qualitative losses make 26.0 and 31.8 % respectively.

Analytical definition of the main indicators of mineral processing. For mining and technological justification of complete extraction of ores from complex blocks without losses and dilution, it is necessary to consider the main indicators of the ore dressing process. The content of useful component in concentrate β is the ratio of the mass of useful component M_{uc} to the mass of concentrate M_c, and the content of useful component in tailings δ is the ratio of the mass of useful component in tailings M_{ut} to the mass of tailings M_t :

$$\beta = M_{uc}/M_c\ ;\ \delta = M_{ut}/M_t .$$

This is an open access article under the CC BY 4.0 license

The numerical values of β and δ are established by chemical analysis.

Concentrate yield γ_c is calculated as the ratio of concentrate mass M_c to feedstock mass M_f, and tailings yield γ_t is the ratio of their mass M_t to feedstock mass M_f:

$$\gamma_c = M_c/M_f;\ \ \gamma_t = M_t/M_f.$$

The recovery of useful component to concentrate ε_c and the recovery of useful component to tailings ε_t are calculated as follows:

$$\varepsilon_c = M_{uc}/M_f\,\alpha = M_c\beta/M_f\,\alpha;\ \ \varepsilon_t = M_{ut}/M_f\,\alpha = M_c\delta/M_f\,\alpha.$$

These enrichment parameters are usually established by direct measurements and calculations [9, 28, 29]. To determine them theoretically, it is necessary to make an equation of the balance of the mass of ore entering the plant and enrichment products, as well as an equation of the balance of useful components in ore, concentrate, and tailings:

$$M_f = M_c + M_t;\ \ M_f\alpha = M_{uc} + M_{ut} = M_c\beta + M_t\delta. \tag{2}$$

By solving equations (2) together, the following relations can be obtained:

• for concentrate yield

$$\gamma_c = \frac{M_c}{M_f} = \frac{\alpha-\delta}{\beta-\delta}; \tag{3}$$

• tailings outlet

$$\gamma_t = \frac{M_t}{M_f} = \frac{\beta-\alpha}{\beta-\delta}; \tag{4}$$

• to extract the useful component into a concentrate

$$\varepsilon_c = \frac{M_c\beta}{M_f\alpha} = \frac{\alpha-\delta}{\beta-\delta}\frac{\beta}{\alpha}; \tag{5}$$

• for recovery of a useful component in tailings

$$\varepsilon_t = \frac{M_t\delta}{M_f\alpha} = \frac{\beta-\alpha}{\beta-\delta}\frac{\delta}{\alpha}; \tag{6}$$

As can be seen, with known values α, β, δ by the formulas (3)-(6) the main indicators that characterize the process of mineral processing are easily calculated.

Since the masses of ore, concentrate and tailings can be measured, the recovery and yields of the beneficiation products can also be assumed to be known, as they are calculated using formulas (3)-(6).

The extraction of a useful component into the enrichment products and its yields are mutually linked by the following relationships:

$$\varepsilon_c = \gamma_c\frac{\beta}{\alpha};\ \ \varepsilon_t = \gamma_t\frac{\delta}{\alpha}.$$

From formulas (3)-(6) it follows that

$$\gamma_c + \gamma_t = 1;\ \ \varepsilon_c + \varepsilon_t = 1.$$

These results are quite natural and confirm the validity of expressions (3)-(6). Analytical dependences (3)-(6) for determining the main enrichment parameters differ slightly in form from the known ones [30-32]. However, they are obtained by joint solution of the equations of the mass balance of ore raw materials and the balance of useful components during their processing, as well as

This is an open access article under the CC BY 4.0 license

clearly argued, which eliminates the roughness inherent in the known formulas. It follows from the dependencies that in the ideal technology of mineral raw materials beneficiation useful components in the tailings should be absent, so $\varepsilon_c = 1$, and the yield of concentrate (3) is equal to the ratio of the content of a useful component in the feedstock to the same in the concentrate. The more metal in the concentrate, the lower the concentrate yield, these conclusions are confirmed by the practice of mining and processing enterprises.

Conclusions are also confirmed by the enrichment indicators of the most common copper, lead and zinc ores with the content of useful component in the raw material α_{Cu} = 0.40-1.0, α_{Pb} = 0.8-3.0, α_{Zn} = 1.0-5.5 %; in the concentrate β_{Cu} = 20.0, β_{Pb} = 45.0, β_{Zn} = 40.0 %, in the tailings δ_{Cu} = 0.06, δ_{Pb} = 0.07, δ_{Zn} = 0.08 %. The results of calculations are shown in Table 3 and Fig. 3. With the increase in the content of useful component in the ore, the performance of their enrichment improves, which is the case in real life. Using equations (3)-(6), it is possible to predict the mineral beneficiation indicators of interest at different values of α, β and δ.

Table 3

Ore beneficiation rates at different grades of the useful component in the ore

Copper ore, %					Lead ore, %					Zinc ore, %				
α	ε_c	γ_c	ε_t	γ_t	α	ε_c	γ_c	ε_t	γ_t	α	ε_c	γ_c	ε_t	γ_t
0.40	85.26	1.71	14.74	98.29	0.80	91.39	1.62	8.61	98.38	1.00	92.18	2.30	7.82	97.70
0.45	86.93	1.96	13.07	98.04	1.00	93.14	2.07	6.86	97.93	1.40	94.47	3.31	5.53	96.69
0.50	88.26	2.21	11.74	97.79	1.20	94.31	2.52	5.69	97.48	1.80	95.75	4.31	4.25	95.69
0.55	89.36	2.46	10.64	97.54	1.40	95.15	2.96	4.85	97.04	2.20	96.56	5.31	3.44	94.69
0.60	90.27	2.71	9.73	97.29	1.60	95.77	3.41	4.23	96.59	2.60	97.12	6.31	2.88	93.69
0.65	91.04	2.96	8.96	97.04	1.80	96.26	3.85	3.74	96.15	3.00	97.53	7.31	2.47	92.69
0.70	91.70	3.21	8.30	96.79	2.00	96.65	4.30	3.35	95.70	3.40	97.84	8.32	2.16	91.68
0.75	92.28	3.46	7.72	96.54	2.20	96.97	4.74	3.03	95.26	3.80	98.09	9.32	1.91	90.68
0.80	92.78	3.71	7.22	96.29	2.40	97.23	5.19	2.77	94.81	4.20	98.29	10.32	1.71	89.68
0.85	93.22	3.96	6.78	96.04	2.60	97.46	5.63	2.54	94.37	4.60	98.46	11.32	1.54	88.68
0.90	93.61	4.21	6.39	95.79	2.80	97.65	6.08	2.35	93.92	5.00	98.60	12.32	1.40	87.68
0.95	93.97	4.46	6.03	95.54	3.00	97.82	6.52	2.18	93.48	5.40	98.72	13.33	1.28	86.67
1.00	94.28	4.71	5.72	95.29						5.50	98.74	13.58	1.26	86.42

Justification of complete extraction of ores from complex blocks of benches. To solve the task at hand, it is necessary to pay attention to the principles of delineation of conditioned ores, which is carried out on the basis of the maximum permissible minimum value of useful components in the ore α, adopted for technological and economic reasons.

Ore volumes with the content of useful component below the specified level (< α) are considered substandard and are included in the host rocks. At the same time, from the geology of deposits, in particular ores of non-ferrous, noble and rare metals [33-35], it is known that the decrease in the content of the useful component with distance from the center of the ore body occurs gradually. This means that the content of the useful component of substandard ores directly in contact with the conditioned ores is insignificantly different from the normative. However, as the specified volume increases, the grade of the useful component in the total shipped ore decreases. The content of useful component in such ore mass in 3D is determined by the formula:

$$\alpha' = \frac{V_{co} + \lambda V_{so}}{V_{co} + V_{so}} \alpha, \qquad (7)$$

where V_{co} – volume of conditioned ore, m^3; V_{so} – volume of the added layer of substandard ore, m^3; λ – relative content of the useful component in the added volume of substandard ore, at the distance from the contour of the ore body equal to 0.25; 0.4; 0.5 m; λ is 0.75; 0.6; 0.5, respectively.

This is an open access article under the CC BY 4.0 license

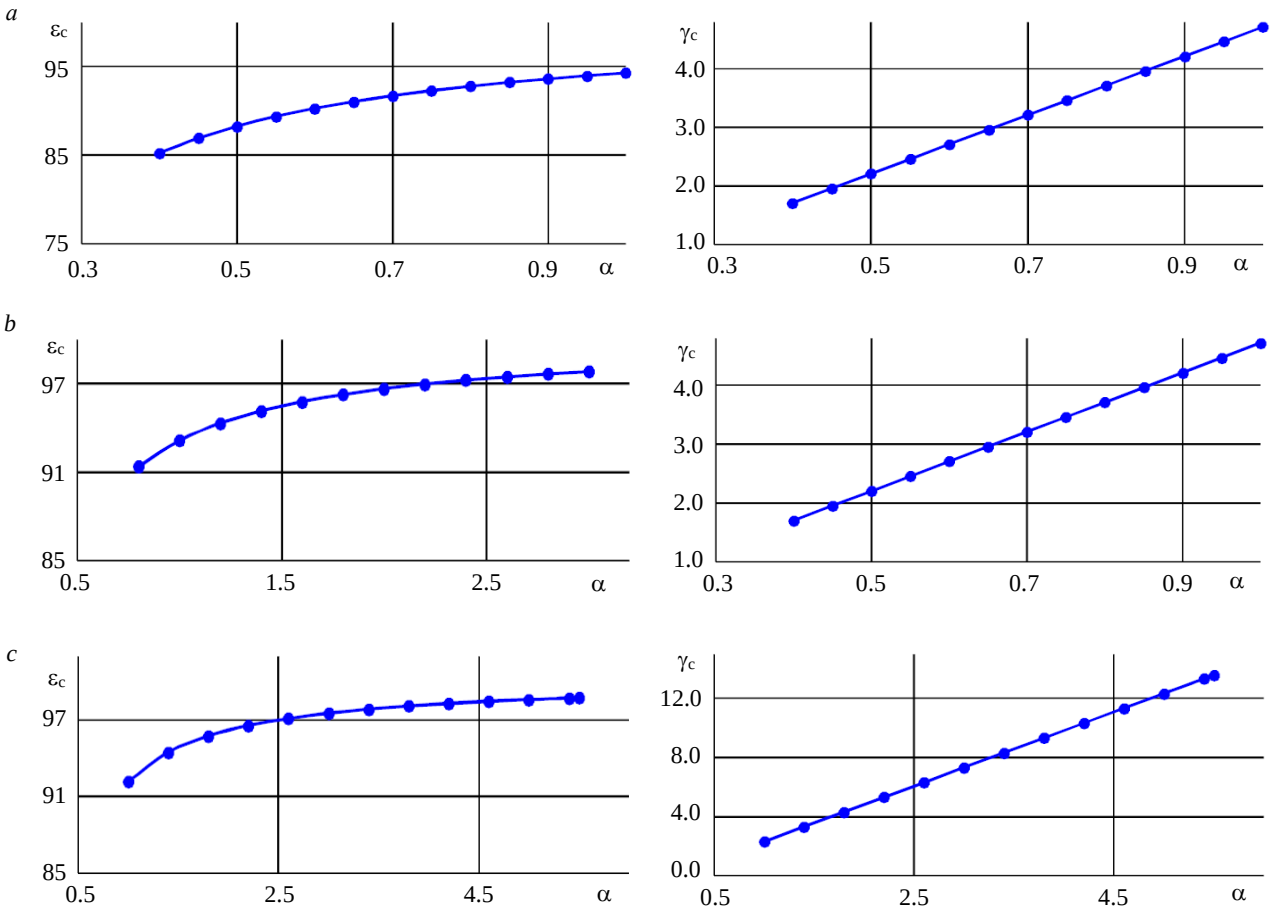

Fig.3. Graphs of change of enrichment indicators (ε_c, γ_c) of copper (*a*), lead (*b*) and zinc (*c*) ores depending on the content of useful component in ore

At given values of areas of ore bodies, lengths of their contact lines with substandard ores (see Fig.1, 2) the content of useful component in shipped ore in 2D-format is calculated according to the following dependence:

$$\alpha' = \frac{S_i + \lambda l_i t'}{S_i + l_i}\alpha, \tag{8}$$

where t' is the thickness of admixed layers of substandard ores.

Usually, the minimum thickness t of the ore layer of complex-structured blocks at the open pits of non-ferrous metallurgy of the CIS countries is 2.5 m (Fig.4). The area of the extracted ore body per unit thickness of the ore block at this cross-section is tl, the area of admixed layers of substandard ore is $2t'l$, and the area of all shipped ore is $(t + 2t')l$. The grade of the useful component in the shipped ore in a linear format is determined using the expression

$$\alpha' = \frac{t + 2\lambda t'}{t + 2t'}\alpha. \tag{9}$$

As can be seen from equations (7)-(9), the content of the useful component in the shipped ore from complex-structured blocks is very dependent on the patterns of decreasing content of the useful component in the ore as it moves away from the center of the ore body and the size of the zones of substandard ore. Taking into account the combination of these parameters, it is possible to establish their most favorable values for the full development of established mineral reserves without losses and dilution.

This is an open access article under the CC BY 4.0 license

In general, the volumes of conditioned and mixed substandard ores at a given cross-section of complex-structured blocks (see Fig.1, 2) are determined by the following formulas:

$$V_{co} = \sum_{i=1}^{n} S_i z_i;\ V_{so} = \sum_{i=1}^{n} l_i t_i z_i,$$

where z_i – depth of excavation of conditioned and substandard ores by excavation and loading equipment, m; t_i – thickness of admixed substandard ores, m.

Acceptable (rational) is the volume of substandard ore that provides the required content of useful component in the shipped ore in accordance with expressions (7)-(9).

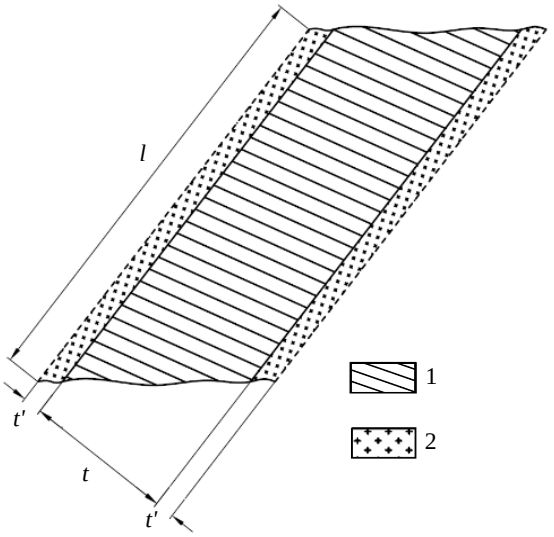

Fig.4. Scheme to determine the content of useful component in the shipped ore

1 – conditioned ore; 2 – substandard ore

Testing of the methodology for determining the copper grade in shipped ore from complex blocks was carried out in the conditions of Aktogay copper ore deposit, mined by 10-meter high benches. The minimum thickness of the mined ore layer is 2.5 m. The open pit ore production capacity is 24.3 million t per annum, the current copper grade is 0.56 %, the established cut-off grade is 0.45 %, the copper grade in concentrate is 20 %, in tailings is 0.06 %, and the recovery in concentrate is 86 %.

Three variants of complete extraction of conditioned mineral reserves together with some part of substandard ores of complex-structured blocks at the minimum thickness of the ore body of 2.5 m are considered. Other values of variables: variant 1 t' = 0.25 m, λ = 0.75; variant 2 t' = 0.4, λ = 0.6; variant 3 t' = 0.5, λ = 0.5. The content of useful components in the shipped ore and their recovery into concentrate for copper, lead and zinc ores are given in Table 4.

Table 4

Mineral content in the shipped ore and their recovery into concentrate at different sizes of admixed layers of substandard ores, %

Metal	Options							
	Initial		1		2		3	
	α	ε_c	α	ε_c	α	ε_c	α	ε_c
Copper	0.45	86.93	0.43	86.35	0.41	85.49	0.39	84.70
	0.60	90.27	0.58	89.83	0.54	89.19	0.51	88.60
	0.75	92.28	0.72	91.93	0.68	91.42	0.64	90.94
	0.95	93.97	0.91	93.69	0.86	93.29	0.81	92.91
Lead	1.00	93.14	0.96	92.84	0.90	92.39	0.86	91.98
	1.60	95.77	1.53	95.58	1.44	95.30	1.37	95.04
	2.20	96.97	2.11	96.83	1.99	96.63	1.89	96.44
	2.80	97.65	2.68	97.54	2.53	97.38	2.40	97.23
Zinc	1.40	94.47	1.34	94.23	1.26	93.86	1.20	93.52
	2.60	97.12	2.49	96.98	2.35	96.79	2.23	96.60
	4.20	98.29	4.03	98.21	3.79	98.09	3.60	97.97
	5.40	98.72	5.18	98.65	4.88	98.56	4.63	98.47

The content of the useful component in the shipped copper ore increases with its content in the conditioned ore in all variants and decreases with distance from the contour of the ore body (Table 4). The similar tendency is characteristic for copper recovery in concentrate. However,

This is an open access article under the CC BY 4.0 license

these changes are insignificant. To assess their impact on the final result – recovery of useful component in concentrate – it is necessary to consider the deviations of indicators in the cases under consideration.

Absolute and relative deviations of these indicators are presented in Table 5. Relative deviation of useful component content in shipped ore depending on its content in conditioned ore in all variants remains at the same level – 4.17; 9.7; 14.29 %. Relative deviation of extraction of useful component in concentrate in the first variant varies from 0.67 to 0.29 %, in the second – from 1.65 to 0.72 %, in the third – from 2.56 to 1.1 %. These indicators with the change of parameters of admixed layers of substandard ores depending on the content of useful component in the conditioned ore indicate that the relative deviation of extraction of useful component in the concentrate from the required is insignificant and lies within acceptable limits. This means that at complete extraction of conditioned ores from complex blocks of benches by mixing a layer of substandard ores of certain sizes the required quality of shipped ore mass and increase of its volume are ensured.

Thus, under the new approach to the development of complex blocks, the expected diluting part of substandard ores is transferred to the category of recoverable reserves. As a result, both the volume of recoverable ore and the enhanced recovery of useful components in the concentrate increase. Such an increase of useful components may reach 10-15 % of the total volume of extraction.

Table 5

Deviations of investigated parameters from the conditioned ones at different sizes of admixed layers of substandard ores, %

Metal	Options					
	1		2		3	
	$\Delta\alpha'$	$\Delta\varepsilon_c$	$\Delta\alpha'$	$\Delta\varepsilon_c$	$\Delta\alpha'$	$\Delta\varepsilon_c$
Copper	0.02 4.17	0.58 0.67	0.04 9.70	1.44 1.65	0.06 14.29	2.23 2.56
	0.03 4.17	0.44 0.48	0.06 9.70	1.08 1.19	0.09 14.29	1.67 1.85
	0.03 4.17	0.35 0.38	0.07 9.70	0.86 0.93	0.11 14.29	1.34 1.45
	0.04 4.17	0.28 0.29	0.09 9.70	0.68 0.72	0.14 14.29	1.06 1.12
Lead	0.04 4.17	0.30 0.33	0.10 9.70	0.75 0.81	0.14 14.29	1.17 1.25
	0.07 4.17	0.19 0.20	0.16 9.70	0.47 0.49	0.23 14.29	0.73 0.76
	0.09 4.17	0.14 0.14	0.21 9.70	0.34 0.35	0.31 14.29	0.53 0.55
	0.12 4.17	0.11 0.11	0.27 9.70	0.27 0.28	0.40 14.29	0.42 0.43
Zinc	0.06 4.17	0.25 0.26	0.14 9.70	0.61 0.65	0.20 14.29	0.95 1.01
	0.11 4.17	0.13 0.14	0.25 9.70	0.33 0.34	0.37 14.29	0.51 0.53
	0.18 4.17	0.08 0.08	0.41 9.70	0.20 0.21	0.60 14.29	0.32 0.32
	0.23 4.17	0.06 0.07	0.52 9.70	0.16 0.16	0.77 14.29	0.25 0.25

Note. Absolute deviations are given in the numerator and relative deviations in the denominator.

If the annual capacity of copper ore mine is 10 million t, and the reduction of operational losses is only 5 %, the increment of recovered ore will reach 500 thousand t. At a copper content of 0.45 % ore at a cost of 6,500 dollars/t, the economic effect will be 14,625 thousand dollars.

This is an open access article under the CC BY 4.0 license

Conclusion.

As a result of the studies carried out, a new typification of complex-structured ore blocks of the bench was carried out. The first type includes blocks composed of scattered continuous ore bodies of various shapes and sizes with rectilinear contacts with rock interlayers. The second type of benches is represented by blocks composed of scattered ore bodies in the form of polygons with rectilinear contacts with host rocks.

The ore saturation coefficient of the block and the index of complexity of the geological structure of the block are considered as the desired mining and geological characteristics of complex-structured ore blocks, analytical dependencies of these characteristics are presented.

Analysis of the numerical values of the characteristics showed that both ore blocks are moderately ore-saturated (k_{os} = 0.427-0.539) and complex-structured (k_{cf} = 0.139-0.193). The exceptions are variants *B* and *D* of complex-structured blocks composed of dispersed ore bodies. They are more complex-structured.

Theoretical dependencies for determining the main indicators of mineral processing are derived. They are obtained by solving the equations of the mass balance of ore raw materials and the balance of useful components during their processing.

To justify the complete extraction of ores from complex-structured blocks of benches, analytical dependences for determining the content of useful component in the shipped ore α', which is a mixture of conditioned ore with the content of useful component α and the admixed layer of substandard ore with the content of useful component α'' are proposed.

According to the values of the content of useful component in the shipped ore, the relative deviations of its extraction into concentrate were determined at different variants of changing the parameters of the admixed layer of substandard ores depending on the content of useful component in the conditioned ore. They are insignificant and lie within acceptable limits.

With the new approach to the development of complex blocks, the estimated diluting portion of substandard ore is transferred to the category of recoverable reserves. Both the volume of recoverable ore and the enhanced recovery of useful components into concentrate are increased. The increment of useful components can reach 10-15 % of the total production volume, thus creating prerequisites for a significant increase in the completeness of mineral extraction from the subsurface.

REFERENCES

1. Shabarov A.N., Kuranov A.D. Basic development trends in mining sector in complicating geotechnical conditions. *Gornyi zhurnal*. 2023. N 5, p. 5-10 (in Russian). DOI: 10.17580/gzh.2023.05.01

2. Trubetskoi K.N., Peshkov A.A., Matsko N.A. Determination of the application area of methods of steeply falling deposits development with the use of preformed open pit mining space. *Gornyi zhurnal*. 1994. N 1, p. 51-59 (in Russian).

3. Trushko V.L., Protosenya A.G. Prospects of Geomechanics Development in the Context of New Technological Paradigm. *Journal of Mining Institute.* 2019. Vol. 236, p. 162-166. DOI: 10.31897/PMI.2019.2.162

4. Yakovlev V.L. Innovative basis of the strategy of integrated development of mineral resources. Ekaterinburg: Uralskoe otdelenie RAN, 2018, p. 360 (in Russian).

5. Kantemirov V.D., Iakovlev A.M., Titov R.S. Applying geoinformation technologies of block modelling to improve the methods of assessing quality indicators of minerals. *News of the Higher Institutions. Mining Journal.* 2021. N 1, p. 63-73 (in Russian). DOI: 10.21440/0536-1028-2021-1-63-73

6. Cheban A., Sekisov G. Complex structural ore blocks and their systematization. *Transbaikal State University Journal.* 2020. Vol. 26. N 6, p. 43-53 (in Russian). DOI: 10.21209/2227-9245-2020-26-6-43-53

7. Lobyntsev A.K., Fomin S.I. Assessment of the influence of mining factors degree on the standard of prepared reserves when designing open-pit mining of complex structured ore deposits. *Mineral Mining & Concervation.* 2021. N 5, p. 40-43 (in Russian). DOI: 10.26121/RON.2021.52.15.004

8. Kushnarev P.I. Hidden losses and dilution. *Zoloto i tekhnologii*. 2017. N 3 (37), p. 82-87 (in Russian).

9. Rakishev B.R. Technological resources for improving the quality and completeness of use of the mineral raw materials. *News of the National Academy of Sciences of the Republic of Kazakhstan. Series of Geology and Technical Sciences.* 2017. Vol. 2. N 422, p. 116-124.

10. Rakishev B.R. Development of the Bozshakol and Aktogay copper ore deposits in Kazakhstan. *Gornyi zhurnal*. 2019. N 1, p. 89-93 (in Russian). DOI: 10.17580/gzh.2019.01.18

11. Tolovkhan B., Demin V., Amanzholov Zh. et al. Substantiating the rock mass control parameters based on the geomechanical model of the Severny Katpar deposit, Kazakhstan. *Mining of Mineral Deposits*. 2022. Vol. 16. Iss. 3, p. 123-133. DOI: 10.33271/mining16.03.123

This is an open access article under the CC BY 4.0 license

12. Suiekpayev Y.S., Sapargaliyev Y.M., Dolgopolova A.V. et al. Mineralogy, geochemistry and U-Pb zircon age of the Karaotkel Ti-Zr placer deposit, Eastern Kazakhstan and its genetic link to the Karaotkel-Preobrazhenka intrusion. *Ore Geology Reviews*. 2021. Vol. 131. N 104015. DOI: 10.1016/j.oregeorev.2021.104015

13. Wellmann F., Caumon G. Chapter One – 3-D Structural geological models: Concepts, methods, and uncertainties. *Advances in Geophysics. Elsevier*. 2018. Vol. 59, p. 1-121. DOI: 10.1016/bs.agph.2018.09.001

14. Dagasan Y., Renard P., Straubhaar J. et al. Pilot Point Optimization of Mining Boundaries for Lateritic Metal Deposits: Finding the Trade-off Between Dilution and Ore Loss. *Natural Resources Research*. 2019. Vol. 28. Iss. 1, p. 153-171. DOI: 10.1007/s11053-018-9380-9

15. Masoumi I., Kamali G., Asghari O., Emery X. Assessing the Impact of Geologic Contact Dilution in Ore/Waste Classification in the Gol-Gohar Iron Ore Mine, Southeastern Iran. *Minerals*. 2020. Vol. 10. Iss. 4. N 336. DOI: 10.3390/min10040336

16. Vasiukhina D. 3D geological modeling for mineral resource assessment of the Galeshchynske iron ore deposit, Ukraine. Geoinformatics: Theoretical and Applied Aspects 2020, 11-14 May 2020, Kyiv, Ukraine. European Association of Geoscientists & Engineers, 2020. Vol. 2020, p. 5. DOI: 10.3997/2214-4609.2020geo067

17. Remezova O.O., Khrushchov D.P., Vasylenko S.P., Yaremenko O.V. Innovative approaches to information modeling of placer deposits. Geoinformatics, 11-14 May 2021. European Association of Geoscientists & Engineers, 2021. Vol. 2021, p. 6. DOI: 10.3997/2214-4609.20215521100

18. Bala G., Kurylo M., Virshylo I. Modeling and Estimation of Iron Ore Reserves in the Leapfrog on the Example of the Azovsky Block Deposit. 16th International Conference Monitoring of Geological Processes and Ecological Condition of the Environment, 15-18 November 2022, Kyiv, Ukraine. European Association of Geoscientists & Engineers, 2022. Vol. 2022, p.5. DOI: 10.3997/2214-4609.2022580256

19. Zeqiri R. Nickel discretization and quality review in Gllavica mine, Kosovo. *Mining of Mineral Deposits*. 2021. Vol. 15. Iss. 1, p. 35-41. DOI: 10.33271/mining15.01.035

20. Morales N., Seguel S., Cáceres A. et al. Incorporation of Geometallurgical Attributes and Geological Uncertainty into Long-Term Open-Pit Mine Planning. *Minerals*. 2019. Vol. 9. Iss. 2. N 108. DOI: 10.3390/min9020108

21. Osterholt V., Dimitrakopoulos R. Simulation of Orebody Geology with Multiple-Point Geostatistics – Application at Yandi Channel Iron Ore Deposit, WA, and Implications for Resource Uncertainty. Advances in Applied Strategic Mine Planning. Cham: Springer, 2018, p. 335-352. DOI: 10.1007/978-3-319-69320-0_22

22. Cowan E.J. Deposit-scale structural architecture of the Sigma-Lamaque gold deposit, Canada – insights from a newly proposed 3D method for assessing structural controls from drill hole data. *Mineralium Deposita*. 2020. Vol. 55. Iss. 2, p. 217-240. DOI: 10.1007/s00126-019-00949-6

23. Xing Jin, Gongwen Wang, Ping Tang et al. 3D geological modelling and uncertainty analysis for 3D targeting in Shanggong gold deposit (China). *Journal of Geochemical Exploration*. 2020. Vol. 210. N 106442. DOI: 10.1016/j.gexplo.2019.106442

24. Renguang Zuo, Kreuzer O.P., Jian Wang et al. Uncertainties in GIS-Based Mineral Prospectivity Mapping: Key Types, Potential Impacts and Possible Solutions. *Natural Resources Research*. 2021. Vol. 30. Iss. 5, p. 3059-3079. DOI: 10.1007/s11053-021-09871-z

25. Dowd P.A., Dare-Bryan P.C. Planning, Planning, Designing and Optimising Production Using Geostatistical Simulation. Advances in Applied Strategic Mine Planning. Cham: Springer, 2018, p. 421-449. DOI: 10.1007/978-3-319-69320-0_26

26. Rakishev B., Rakisheva Z., Auezova A., Orynbay A. Automated determination of rock crushing zones in the collapse. *Mining of Mineral Deposits*. 2022. Vol. 16. Iss. 3, p. 109-114. DOI: 10.33271/mining16.03.109

27. Lukichev S.V., Nagovitsyn O.V., Shishkin A.S. Break line and shotpile surfaces modeling in design of large-scale blasts. Mining goes Digital: Proceedings of the 39th International Symposium "Application of Computers and Operations Research in the Mineral Industry", 4-6 June 2019, Wroclaw, Poland. London: CRC Press, 2019, p. 279-285. DOI: 10.1201/9780429320774

28. Pelikh V.V., Salov V.M., Burdonov A.E., Lukyanov N.D. Model of baddeleyite recovery from dump products of an apatite-baddeleyite processing plant using a CVD6 concentrator. *Journal of Mining Institute*. 2021. Vol. 248, p. 281-289. DOI: 10.31897/PMI.2021.2.12

29. Mutalova M., Khakimova D. Investigation of the recovery of useful components from slags by the flotation method. *International Journal of Advanced Technology and Natural Sciences.* 2020. Vol. 1. N 2, p. 26-30 (in Russian). DOI: 10.24412/2181-144X-2020-2-26-30

30. Opalev A.S., Alekseeva S.A. Methodological substantiation of the choice for optimal modes of equipment operation during the stage-wise concentrate removal in iron ores beneficiation. *Journal of Mining Institute.* 2022. Vol. 256, p. 593-602. DOI: 10.31897/PMI.2022.80

31. Pelevin A.E. Using the results of the phase composition of magnetit ore for prediction of the concentrate yield. *Mining Informational and Analytical Bulletin.* 2022. N 5-1, p. 131-144 (in Russian). DOI: 10.25018/0236_1493_2022_51_0_131

32. Golik V.I., Razorenov Y.I., Brigida V.S., Burdzieva O.G. Mechanochemical technology of metal mining from enriching tails. *Bulletin of the Tomsk Polytechnic University. Geo Assets Engineering.* 2020. Vol. 331. N 6, p. 175-183 (in Russian). DOI: 10.18799/24131830/2020/6/2687

33. Ovseychuk V. Classification of ore formations of Streltsovsky type uranium deposits. *Transbaikal State University Journal.* 2021. Vol. 27. N 8, p. 35-47 (in Russian). DOI: 10.21209/2227-9245-2021-27-8-35-47

34. Turtygina N.A., Okhrimenko A.V. Quantitative assessment of natural variation in quality of copper ore in roof of intrusion. *Mining Informational and Analytical Bulletin.* 2019. N 8, p. 146-156 (in Russian). DOI: 10.25018/0236-1493-2019-08-0-146-156

35. Zaskind E.S., Konkina O.M. Sulfide Cu-Ni and PGM deposit typification for forecasting and prospecting. *National Geology.* 2019. N 2, p. 3-15 (in Russian). DOI: 10.24411/0869-7175-2019-10010

***Author* Bayan R. Rakishev,** *Doctor of Technical Sciences, Academician of the National Academy of Sciences of Republic of Kazakhstan, Professor, b.rakishev@satbayev.university, https://orcid.org/0000-0001-5445-070X* (*Kazakh National Research Technical University named after K.I.Satpayev (Satbayev University), Almaty, Republic of Kazakhstan*).

The author declare no conflict of interests.

This is an open access article under the CC BY 4.0 license

ISSN 2411-3336; e-ISSN 2541-9404

JOURNAL OF MINING INSTITUTE

Zapiski Gornogo instituta

Journal homepage: pmi.spmi.ru

Research article

Analysis of the assessment of the prospects for the burial of CO_2 in unexplored aquifer complexes on the example of a facility in the Perm Region

Riazi Masoud[1], **Pavel Yu. Ilyushin**[2], **Tatyana R. Baldina**[3], **Nadezhda S. Sannikova**[2], **Anton V. Kozlov**[4]✉, **Kirill A. Ravelev**[5]

[1] *Nazarbayev University, Astana, Kazakhstan*
[2] *Perm National Research Polytechnic University, Perm, Russia*
[3] *LLC SIE "PrognozRNM", Perm, Russia*
[4] *Perm World-class Scientific and Educational Center "Rational Subsoil Use", Perm, Russia*
[5] *Gazprom Neft Company Group, Saint Petersburg, Russia*

***How to cite this article*:** Riazi Masoud, Ilyushin P.Yu., Baldina T.R., Sannikova N.S., Kozlov A.V., Ravelev K.A. Analysis of the assessment of the prospects for the burial of CO_2 in unexplored aquifer complexes on the example of a facility in the Perm Region. Journal of Mining Institute. 2024. Vol. 270, p. 931-940.

Abstract

One of the most important problems of our time is the annual increase in greenhouse gas emissions into the atmosphere. It is possible to combat this phenomenon by reducing emissions or developing and applying technologies for capturing, storing, using and disposing of CO_2. In this work, an assessment of the expediency and possibility of carbon dioxide burial in deep aquifers is considered, the study of which is carried out to a small extent and due to the lack of useful material in them. The parameters and results of CO_2 injection into the aquifer of one of the oil fields of the Perm Region, the geological properties and characteristics of which are determined in this work, are studied. The criteria of applicability, methods of estimating the volume of the reservoir and laboratory studies to determine the properties of CO_2 and the features of its interaction with the model of the reservoir fluid are considered. The injection object and reservoir volume were determined, PVT studies of the target gas were performed, and its solubility in reservoir water was determined. The duration of filling the full volume of the trap when capturing 400 thousand tons of CO_2 per year from the target industrial facility is calculated to be 202 years. This conclusion signals the prospects for the burial of carbon dioxide in the underground deposits of an undeveloped aquifer complex in the Perm Region, which reflects the importance of studying such geological CO_2 burial sites in order to achieve global carbon neutrality goals.

Keywords

carbon dioxide; aquifer; burial; laboratory studies; carbon footprint

Funding

The research was carried out with the financial support of the Strategic Academic Leadership Program "Priority 2030".

Received: 21.09.2022 ***Accepted: 03.06.2024*** ***Online: 23.10.2024*** ***Published: 25.12.2024***

Introduction.

An important problem that has received significant publicity in the last decade is the increase in the average temperature on the planet* due to the emission of greenhouse gases into the atmosphere [1]. At the same time, carbon dioxide is the main greenhouse gas (more than 70 % of global emissions)**. Currently, there are no signs of a reduction in greenhouse gas emissions [2, 3]. At the same time, the potential growth of industrial production in developing countries, the slow transition to renewable sources and energy crises suggest an increase in these emissions in the coming years [4]. There are two ways to combat global warming – minimizing the number of sources of emissions or developing

* The Production Gap: 2020 Report. URL: https://productiongap.org/2020report/ (accessed 21.09.2022).

** Global Greenhouse Gas Emissions. URL: https://www.epa.gov/ghgemissions/global-greenhouse-gas-emissions-data (accessed 21.09.2022).

This is an open access article under the CC BY 4.0 license

© Riazi Masoud, Pavel Yu. Ilyushin, Tatyana R. Baldina, Nadezhda S. Sannikova, Anton V. Kozlov, Kirill A. Ravelev, 2024

CO_2 capture technologies. The use of CO_2 capture and storage methods can play a crucial role in preventing global warming [5]. A detailed analysis of existing technologies is carried out in [6, 7].

Carbon emission reduction technologies can be divided into four categories – capture, storage, application, and disposal. CO_2 capture technologies are quite advanced and are represented by chemical absorption or various membrane technologies [8-10]. CO_2 transport technologies are also developed and used in industry, with more than 6,500 km of pipelines worldwide [11, 12]. CO_2 storage technologies are known all over the world, currently there are a large number of existing projects for the disposal of carbon dioxide. According to the works [13, 14], the utilization of this gas is also actively used in various industries. In particular, these technologies can be found in the food, construction, and chemical industries [15, 16]. CO_2 also finds useful applications [17, 18] as a component in the composition of a product. Scientific publications [19, 20] report on the use of CO_2 in industry, for example, in the production of various materials, chemicals and as an agent for increasing oil recovery (IOR). Due to the global trend towards reducing CO_2 emissions, new projects involving the burial of gas in various aggregate states and in different facilities are being prepared. In this paper, an evolving method of CO_2 disposal is considered – disposal into depleted mining facilities, salt formations, coal deposits or aquifers [21-23].

The disadvantages of CO_2 burial in coal seams are the low efficiency of methane storage, insufficient knowledge of the interaction of methane and CO_2 under the conditions under consideration, and imperfection of the technology [24-26]. Injection into saline and saline aquifers is the most preferable, since it can be used in industrial, agricultural and other applications [27]. These horizons have the greatest ability to sequester CO_2 [28, 29]. A brief analysis of the world experience in CO_2 burial, given in [30-32], is presented to determine the most optimal characteristics of reservoir formations. Basically, this experience is presented in foreign markets, since foreign countries addressed the issue of carbon dioxide utilization much earlier [33-35]. Based on the results of the performed assessment and on the basis of the work [36], it was concluded that the cost of implementing CO_2 storage technologies in depleted oil deposits and in deep salt formations is similar, while storage in gas deposits can cost much more. Injection into oil fields for IOR and increased extraction of coal methane CO_2 has a positive effect and can make burial more economically attractive, however, in this case, many factors must be taken into account (technology efficiency, oil/methane prices, etc.). At the same time, the main costs in the implementation of most technologies, with the exception of burial in coal reservoirs, are capital expenditures for injection equipment [37].

A comprehensive work is presented to substantiate the choice of an object for CO_2 injection, the properties of the collector are determined, laboratory studies are performed to determine the pressure-volume-temperature (PVT) properties of the target gas, as well as its dissolution coefficient in the reservoir fluid and to determine the volume of injection of the target gas into the studied deposit.

Methods.

Geological requirements for reservoirs for efficient CO_2 disposal. A review of global CO_2 storage projects shows that the rock must have high porosity, be permeable to carbon dioxide; the reservoir must be covered with impermeable rocks, located at a depth at which the gas is under pressure corresponding to liquid or supercritical conditions, and be composed of rocks that do not react with CO_2 in the presence of water (sandstone, mudstone, siltstone, etc.). The availability of infrastructure and communications in the region is also an indispensable criterion. Criteria for selecting an object:

• collector horizons should have caps stacked with impermeable plastic or hard rocks above them;

• the cap above the selected object must be sustained in the area of distribution, its capacity must be at least 2-6 m at a depth of up to 600 m and 4-5 m at a depth of more than 600 m;

• the depth of the collector must ensure that CO_2 is in supercritical or liquid states;

This is an open access article under the CC BY 4.0 license

• in order to ensure the long-term operation of storage facilities, additional interlayers with sealing ability must be identified in the section;

• there should be no tectonic disturbances within the design contour of the future CO_2 storage, causing a decrease in the tightness of the main and backup caps;

• the permeability of the cap to carbon dioxide should not exceed 7-10 μm^2.

The results of the research have shown that for CO_2 storage facilities at elevated pressure, the depth of its deposition is of great importance. To prevent gas leaks through cracks, the hydrostatic pressure of groundwater along the storage contour must exceed the internal gas pressure. Large granitoid massifs are recognized as the best in terms of stability of underground structures. In the practice of selecting locations for underground gas storage facilities, great importance is attached to the search for monolithic structural blocks in geological formations.

In [38], the properties of CO_2 were studied under various conditions and it was determined that the depth of the reservoir for its injection should be more than 1000 m, since at this mark the injected CO_2 will be in a supercritical state.

Selection of the research object and quantitative assessment of the reservoir volume. Based on certain criteria and analysis of oil field development facilities, an aquifer complex of one of the oil fields in the south of the Perm Region, in particular, the Famensk deposits, was selected for CO_2 storage.

An expert assessment of the volume of the reservoir, which theoretically can accommodate the injected carbon dioxide, was carried out on the basis of the formula for calculating reserves by the volumetric method, excluding variables responsible for saturation:

$$V_{res} = Sh_{eff}k_p, \quad (1)$$

where S – collector distribution area, m^2; h_{eff} – effective thickness of the reservoir, m; k_p – porosity coefficient, fraction units.

To calculate the area of the formation under consideration, a structural map of the roof of its surface was created, based on a map based on the reflecting horizon II_k (roof of Visean terrigenous deposits) using the convergence method in the Surfer and CorelDraw software product. Using well breakdowns, the thickness values from the known surface along the roof of the Tula terrigenous horizon to the roof of the Famensk deposits were determined. The Isochore map is based on these data. Combining the structural map according to II_k with the isochore map, when they intersect, it is possible to determine the absolute mark of the required surface – the roof of the Famen deposits at many points on the map, the calculation is performed according to the rules of algebraic summation. As a result, a structural map of the roof of the Famen deposits was obtained.

The area is calculated within the last closed isohypse lying inside the boundaries of the license area. A closed stratoisogypse with an absolute mark of 1,420 m was selected. Within this isohypse, the area is calculated using the GetCurve macro in the CorelDraw software. As a result, the area of the selected site is 102.2 km^2. Famensk oil deposits are distributed in the south of the Perm Region and are confined to the southeastern side of the Kamsko-Kinel system of deflections. The effective thickness and porosity were determined based on the analysis of the field experience of exploitation of these Famen deposits. The data set for thickness was 107 values, and for porosity – 3,991. Based on the obtained values, histograms are constructed, the boundaries of the values are determined and a statistical analysis is carried out. For the best prediction of the determined indicator, the built-in analysis packages in the Excel software product are used. Using the TRIANG_INV function, where limits are set in the form of minimum, maximum, and modal values, 10 thousand random variables (for representativeness) are modeled according to the porosity coefficient and effective thickness, the reservoir propagation area remains unchanged. According to the formula for estimating the reservoir volume, 10 thousand values were obtained.

This is an open access article under the CC BY 4.0 license

© Riazi Masoud, Pavel Yu. Ilyushin, Tatyana R. Baldina, Nadezhda S. Sannikova,
Anton V. Kozlov, Kirill A. Ravelev, 2024

Physico-chemical properties of the studied sample of water and carbon dioxide. To implement PVT research, a model of gas coming from the short-cycle adsorption unit (SCA) of one of the industrial facilities of the Perm Region has been artificially created. This gas is a mixture of two gases – carbon dioxide (93 %) and methane (7 %). The density of the studied water under normal conditions is 1,180 kg/m^3, viscosity is 1.55 mPa·s, mineralization is 256.6 g/l. Since sampling from an undeveloped object is not possible, the sample was taken from an overlying object. According to the project document for the development of the field in question, the properties of reservoir water at these facilities differ slightly and do not make any changes to the results of laboratory experiments.

Laboratory tests on a PVT installation. The following equipment was used in the research: AMCore AMR-F 1004.01 thermodynamic research unit, AMCore AMR-T 1000.15 sample recombination unit, AMCore AMR-F 1002 automatic gasometer, Anton Paar GmbH liquid density analyzer, AMCore AMR-AMP200 automatic measuring press, AERUS 210/24 air piston coaxial compressor, low-temperature liquid thermostat KRIO-VT-12-1 series MASTER of LLC "TERMEX".

The main stages of research:

• estimation of the phase state of the target gas under various pressure conditions;

• analysis of the density of the target gas under various pressure conditions;

• determination of the compressibility coefficient of the target gas under various pressure conditions;

• estimation of the dissolution coefficient of the target gas in reservoir water under various pressure conditions.

The analysis of the phase state of the target gas consisted in obtaining the *P*-*V* dependence for the test sample with the release of a critical pressure corresponding to the transition of the gas from a liquid state to a mixed one (liquid + gas). In other words, at a given pressure, the first bubble of gas is released from the liquid. The temperature of the performed studies in all cases is 28 °C, which corresponds to the thermal conditions of the studied formation. The density of the mixture was also determined to represent its physical properties in reservoir conditions. Taking into account these values of gas density under various pressure conditions, the compressibility coefficients of the studied mixture are calculated:

$$Z = \frac{P\rho_0 T_0}{P_0 \rho T}, \tag{2}$$

where ρ – the density of the target gas at pressure *P* (MPa) and temperature *T* (K) modeled in a PVT cell, kg/m^3; ρ_0 – the density of the target gas under standard conditions (P_0 = 0.101325 MPa, T_0 = 293.15 K), assumed to be 1.983 kg/m^3.

The estimation of the gas dissolution coefficient in reservoir water plays an important role in determining the possible volume of CO_2 burial in connection with the known fact of gas dissolution in reservoir waters, as a result of which it is necessary to estimate the volume of the studied gas capable of dissolving in water that saturates the target formation. To do this, a series of studies was carried out on a PVT installation, into which a certain amount of a gas mixture and a 4.6 ml water sample were pumped using auxiliary laboratory equipment.

Assessment of the possible volume of injection of the target gas into the studied deposit. Based on the calculations of the volume of the deposit and the properties of the target gas, it was necessary to calculate the volume of gas that the deposit in question can accommodate. To do this, it was necessary to determine the maximum pressure that can be created in the reservoir, based on an estimate of the hydraulic fracturing pressure and the maximum pressure limited by the technological equipment. The injection volume is defined as the ratio of CO_2 emissions to the calculated reservoir volume.

Determination of the maximum pressure in the target deposit. According to the analysis of the technical characteristics of the existing technological equipment, the maximum pressure

This is an open access article under the CC BY 4.0 license

is about 35 MPa. When estimating hydraulic fracturing pressure, a calculation scheme using the Hubbert – Willis formula was used:

$$P_{frac} = 1/3(P_{rock} - P_{res}) + P_{res}, \quad (3)$$

where P_{rock} – rock pressure, $P_{rock} = \rho_{rock} g H_{res}$, MPa; ρ_{rock} – rock density, kg/m^3; g – acceleration of free fall, g = 9,81 m/s^2; H_{res} – reservoir depth, m; P_{res} – reservoir pressure, $P_{res} = \rho_w g H_{res}$, MPa; ρ_w – water density, kg/m^3.

Discussion of the results.

The estimation of the reservoir volume was performed according to the described method. As a result of statistical analysis using percentiles, the following results were obtained:

• The 10th percentile means that only 10 % of the sample collector volume takes values less than or equal to 103,177.6 thousand m^3;

• The 50th percentile – it is equally likely that the volume of the collector can take values both less and more than 269,216.9 thousand m^3;

• The 90th percentile – only 10 % of the sample collector volume takes values greater than and equal to 591,583.8 thousand m^3.

The authors of the work for further research adopted the volume according to the worst case scenario, i.e. 10 percentile – 103,177.6 thousand m^3.

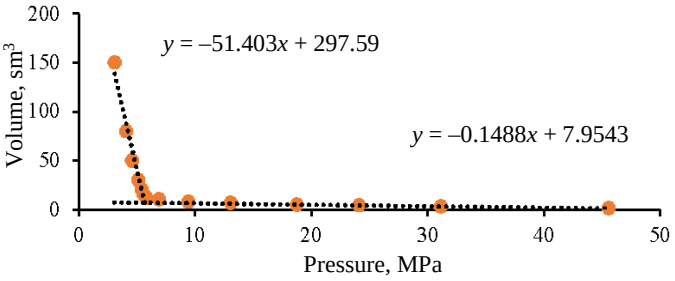

Fig.1. *P-V* dependence of the target gas

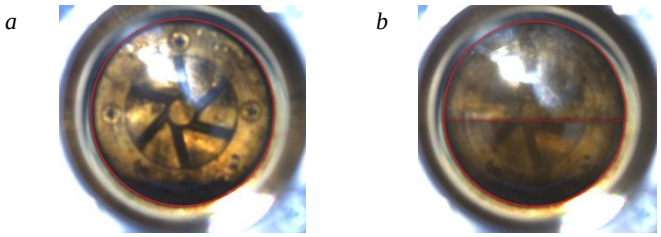

Fig.2. Cells filled with the target gas at different pressures: P = 45.51 MPa (*a*); P = 5.12 MPa (*b*)

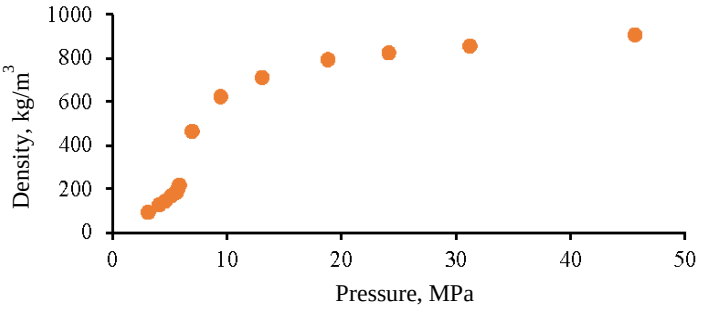

Fig.3. Dependence of the target gas density on the pressure created in the PVT unit cell

Studies of PVT properties of the target gas. Based on the results of the interpretation of the *P-V* dependence of the target gas (Fig.1), it was determined that the critical pressure of the transition from a liquid state to a mixed one corresponds to a value of 5.59 MPa. Images of a cell filled with a target gas are presented. At a pressure of 45.51 MPa, the target gas is completely in the liquid phase (Fig.2, *a*) and a phase boundary is observed at 5.12 MPa (Fig.2, *b*). The obtained critical pressure is confirmed by visual analysis.

The result of the measurement of the density of the mixture performed in this study is shown in Fig.3. Based on the results of the density assessment, the values of the compressibility coefficient are calculated according to the formula (2). When the pressure increases to a critical value, the compressibility coefficient decreases from 0.64 to 0.51, after which it decreases to 0.28 at a pressure of 6.9 MPa. With a further increase in pressure, this parameter increases to 0.29 at a pressure of 9.4 MPa, 0.35 at 13.0 MPa, 0.56 at 24.1 MPa and 0.96 at 45.51 MPa. The value of the results obtained lies in the possibility of increasing the accuracy of estimating the numerical values of gas injection volumes from the SCA block to the target object.

The results of the study of the dissolution coefficient of the target gas in reservoir water are shown in Fig.4. The interface between the phases of the target gas and water is clearly visible in the image of a PVT cell filled with a mixture of the target gas and reservoir water at a pressure of 39.12 MPa (Fig.5).

This is an open access article under the CC BY 4.0 license

Journal of Mining Institute. 2024. Vol. 270. P. 931-940
© Riazi Masoud, Pavel Yu. Ilyushin, Tatyana R. Baldina, Nadezhda S. Sannikova, Anton V. Kozlov, Kirill A. Ravelev, 2024

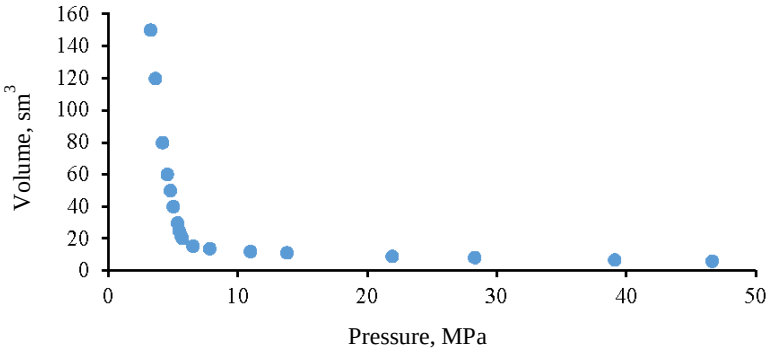

Fig.4. *P-V* dependence of the mixture of the target gas and water

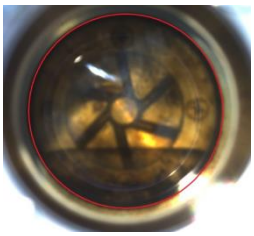

Fig.5. A cell filled with a mixture of target gas and reservoir water at P = 39.12 MPa

To estimate the coefficient of dissolution of the target gas in reservoir water, a combined graph of *P-V* dependencies was constructed, and a graph of the *P-V* dependence of the mixture of target gas and reservoir water minus the volume of this water was added, which allows, when analyzing graphs, to estimate the dissolved volume of gas in water under various baric conditions (Fig.6). The superimposition of red (a mixture of gases) and green (a mixture of gases and water (minus the volume of water) lines indicates that the process of dissolving the target gas in reservoir water is absent in the entire range of considered baric conditions at reservoir temperature, therefore, when estimating the volume of gas injection from the SCA block into the Famensk deposits, it must be taken into account that the entire volume of injected gas will be in a free state under reservoir conditions

The experience of CO_2 burial [31, 34, 35] also indicates the low solubility of this gas in reservoir water. In [39-41], laboratory studies of the effect of various factors on the solubility of CO_2 in water were carried out, which showed a decrease in solubility with an increase in water mineralization. Moreover, the solubility of CO_2 increases significantly with an increase in the temperature of the study. Based on this analysis, it can be concluded that the research is correct.

Determination of the volume of injection of the target gas into the studied deposit. It is assumed that the entire volume of the Famensk deposit will be occupied by this gas, and the reservoir water is displaced beyond the established volume of the trap within the license area. This assumption is justified by the laws of gravitational phase separation due to the lower density of the target gas in the considered pressure range.

The analysis of hydraulic fracturing pressures at the Famensk deposits of the Perm Region, as well as according to equation (2), showed that the hydraulic fracturing pressure corresponds to a value of 23 MPa, which is less than the maximum allowable pressure of the technological equipment used. As a result, when estimating the volume of injection of the target gas into the deposit under consideration, it is necessary to limit the pressure of hydraulic fracturing with a margin of 20 %, i.e. the calculation of the volumes of the target gas was carried out at a critical pressure of 18.4 MPa. To determine the mass of the injected volume of the target gas into the reservoir, an extrapolation of the graph of the dependence of the density of the target gas on pressure was performed (see Fig.3). It was determined that at an approved critical pressure of 18.4 MPa, the density of the gas mixture under study will be 784.6 kg/m^3, while the gas must be in a liquid state.

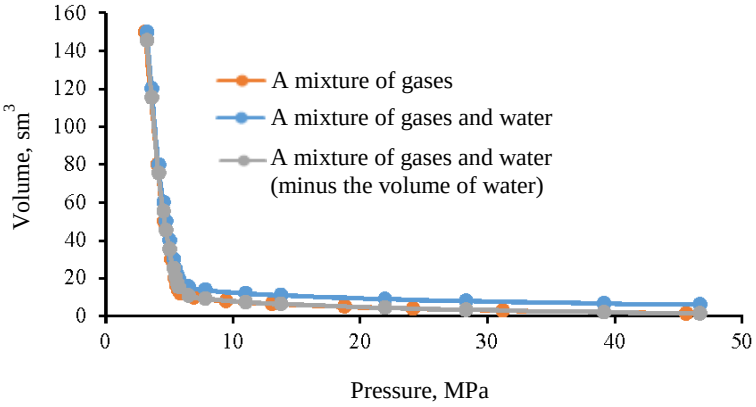

Fig.6. *P-V* dependencies of the target gas, a mixture of the target gas and reservoir water

This is an open access article under the CC BY 4.0 license

Taking into account the volume of the Famensk deposit, the mass of the target gas has been determined, which is able to fit into this deposit according to the results of the implemented studies – gas injection from the SCA block can last for 202 years (assuming a gas consumption of 400 thousand tons per year) and will eventually amount to 80.95 million t.

Economic assessment of the project. The economic model of the proposed project involves assistance from the state in the form of subsidies. This is due to the high cost at which the accumulated discounted net cash flow (CDCF) is negative at the end of the estimated period. The model contains all the costs of capital investments (construction of a carbon dioxide pipeline, well construction, necessary equipment) and operating costs to ensure the operation of the system. One of the important items of expenditure is the necessary complex of works on the additional study of deposits and fluids for the final justification of the possibility and expediency of the project. Large fines for carbon dioxide emissions into the atmosphere are included in the profit column.

Economic calculations, according to which the payback period of the project was adopted, equal to 15 years, showed that with a state subsidy of 24.6 rub. per ton of recycled gas, the project reaches a positive CDCF. According to the authors, this model reflects a realistic version of the project. With an increase in the accepted payback period, subsidies decrease.

Assessment of risks and environmental impacts in the implementation of CO_2 *disposal technology.* Mechanisms contributing to the re-release of carbon dioxide to the surface [42, 43]:

• migration of gas in separate parts through disturbed and permeable rocks, as well as through injection wells (corrosion, wear);

• molecular diffusion and dissolution of carbon dioxide through the covering rocks;

• movement of CO_2 along with moving aquifers;

• man-made land disturbance, mining dumps, tailings ponds, contributing to the disturbance of the underground geological space and an increase in CO_2 leaks.

It is noted in [44] that pumping large volumes of carbon dioxide into underground storage facilities can lead to earthquakes, collapse of the storage facility and subsequent emissions into the atmosphere. The risks associated with leakage as a result of CO_2 storage in geological reservoirs are divided into global and local. Risks at the global level are associated with CO_2 emissions, which can significantly contribute to climate change if a certain proportion of gas leaks into the atmosphere [45]. Local-level risks can be classified as risks to health, safety and the environment – leakage of CO_2 into the atmosphere or shallow Earth layers, intensification of chemical processes due to the ingress of dissolved CO_2 into the subsurface and effects arising from the displacement of liquids by injected CO_2 [46, 47]. The classic ways to reduce the danger associated with these types of leaks are careful design and selection of a storage system location, as well as the use of early leak detection methods (preferably long before CO_2 reaches the earth's surface) [48-50].

Conclusion.

The development and practical application of CO_2 disposal technologies is one of the most important areas in the fight against global warming. The proposed technology for using carbon dioxide can become the main one in solving the problem of CO_2 emissions both at the considered enterprise and in Russia as a whole.

The criteria for selecting an object for the implementation of carbon dioxide burial technology in geological reservoirs are determined. Taking into account the geological structure, the optimal target object was determined on the territory of the Perm Region, the volume of the deposit was estimated, which with a probability of 90 % will be at least 103177.6 thousand m^3.

Laboratory studies were performed, according to the results of which the PVT properties of the target gas, its density and compressibility coefficient under various barometric conditions, as well as

This is an open access article under the CC BY 4.0 license

solubility in reservoir water were determined. The results obtained show that the entire volume of the injected gas will be in a free state under reservoir conditions, and not partially dissolved.

The assessment of the injection parameters and calculations showed that when 400 thousand t of CO_2 are captured from an industrial facility per year, injection until the reservoir volume is fully filled can last for 202 years, and will amount to 80.95 million t of this gas.

The creation of an economic model allows us to approve the payback of the proposed project over a fifteen-year period with the support of the state (for the disposal of CO_2 emissions into the Earth's atmosphere) in the amount of 24.6 rub./t.

The significant environmental effect of carbon dioxide burials in the underground sediments of an undeveloped aquifer complex indicates the need to draw attention to these objects, which are currently little or not studied at all due to the lack of industrial significance.

As recommendations for further study of the host structure (determining the boundaries of the deposit, its structure and characteristics), as well as the processes occurring in the reservoir, it is proposed to conduct field and geophysical studies of existing wells and drilling new ones; laboratory studies, including PVT studies and filtration.

REFERENCES

1. Ilinova A.A., Romasheva N.V., Stroykov G.A. Prospects and social effects of carbon dioxide sequestration and utilization projects. *Journal of Mining Institute.* 2020. Vol. 244, p. 493-502. DOI: 10.31897/PMI.2020.4.12

2. Le Quéré C., Korsbakken J.I., Wilson C. et al. Drivers of declining CO_2 emissions in 18 developed economies. *Nature Climate Change*. 2019. Vol. 9, p. 213-217. DOI: 10.1038/s41558-019-0419-7

3. Fawad M., Mondol N.H. Monitoring geological storage of CO_2: a new approach. *Scientific Reports*. 2021. Vol. 11. N 5942. DOI: 10.1038/s41598-021-85346-8

4. Quarton C.J., Samsatli S. The value of hydrogen and carbon capture, storage and utilisation in decarbonising energy: Insights from integrated value chain optimisation. *Applied Energy*. 2020. Vol. 257. N 113936. DOI: 10.1016/j.apenergy.2019.113936

5. Rosa L., Sanchez D.L., Realmonte G. et al. The water footprint of carbon capture and storage technologies. *Renewable and Sustainable Energy Reviews*. 2021. Vol. 138. N 110511. DOI: 10.1016/j.rser.2020.110511

6. Bui M., Adjiman C.S., Bardow A. et al. Carbon capture and storage (CCS): the way forward. *Energy & Environmental Science*. 2018. Vol. 11. Iss. 5, p. 1062-1176. DOI: 10.1039/C7EE02342A

7. Gür T.M. Carbon Dioxide Emissions, Capture, Storage and Utilization: Review of Materials, Processes and Technologies. *Progress in Energy and Combustion Science*. 2022. Vol. 89. N 100965. DOI: 10.1016/j.pecs.2021.100965

8. Fedoseev S.V., Tcvetkov P.S. Key Factors of Public Perception of Carbon Dioxide Capture and Storage Projects. *Journal of Mining Institute.* 2019. Vol. 237, p. 361-368. DOI: 10.31897/PMI.2019.3.361

9. Shirinkina E.S., Sliusar N.N., Korotaev V.N. CO_2 Capturing from Stationary Sources with Following Use for Enhanced Oil Recovery: A Review Of Recent Technologies. *Ecology and Industry of Russia.* 2021. Vol. 25. N 10, p. 64-71 (in Russian). DOI: 10.18412/1816-0395-2021-10-64-71

10. Chunfeng Song, Qingling Liu, Na Ji et al. Alternative pathways for efficient CO_2 capture by hybrid processes – A review. *Renewable and Sustainable Energy Reviews*. 2018. Vol. 82. Part 1, p. 215-231. DOI: 10.1016/j.rser.2017.09.040

11. Al Baroudi H., Awoyomi A., Patchigolla K. et al. A review of large-scale CO_2 shipping and marine emissions management for carbon capture, utilisation and storage. *Applied Energy*. 2021. Vol. 287. N 116510. DOI: 10.1016/j.apenergy.2021.116510

12. Wei Lu, Hao Hu, Guansheng Qi. Effect of Pipe Diameter and Inlet Parameters on Liquid CO_2 Flow in Transportation by Pipeline with Large Height Difference. *Processes*. 2019. Vol. 7. Iss. 10. N 756. DOI: 10.3390/pr7100756

13. Ravikumar D., Duo Zhang, Keoleian G. et al. Carbon dioxide utilization in concrete curing or mixing might not produce a net climate benefit. *Nature Communications*. 2021. Vol. 12. N 855. DOI: 10.1038/s41467-021-21148-w

14. Qian Zhu. Developments on CO_2-utilization technologies. *Clean Energy*. 2019. Vol. 3. N 2, p. 85-100. DOI: 10.1093/ce/zkz008

15. Alper E., Orhan O.Y. CO_2 utilization: Developments in conversion processes. *Petroleum*. 2017. Vol. 3. Iss. 1, p. 109-126. DOI: 10.1016/j.petlm.2016.11.003

16. Medrano-García J.D., Javaloyes-Antón J., Vázquez D. et al. Alternative carbon dioxide utilization in dimethyl carbonate synthesis and comparison with current technologies. *Journal of CO_2 Utilization*. 2021. Vol. 45. N 101436. DOI: 10.1016/j.jcou.2021.101436

17. Beheshti E., Riahi S., Riazi M. Impacts of oil components on the stability of aqueous bulk CO_2 foams: An experimental study. *Colloids and Surfaces A: Physicochemical and Engineering Aspects*. 2022. Vol. 648. N 129328. DOI: 10.1016/j.colsurfa.2022.129328

18. Farajzadeh R., Eftekhari A.A., Dafnomilis G. et al. On the sustainability of CO_2 storage through CO_2 – Enhanced oil recovery. *Applied Energy*. 2020. Vol. 261. N 114467. DOI: 10.1016/j.apenergy.2019.114467

This is an open access article under the CC BY 4.0 license

19. Bommareddy R.R., Yanming Wang, Pearcy N. et al. A Sustainable Chemicals Manufacturing Paradigm Using CO_2 and Renewable H_2. *iScience*. 2020. Vol. 23. Iss. 6. N 101218. DOI: 10.1016/j.isci.2020.101218

20. Von Witzendorff P., Pohl L., Suttmann O. et al. Additive manufacturing of glass: CO_2-Laser glass deposition printing. *Procedia CIRP*. 2018. Vol. 74, p. 272-275. DOI: 10.1016/j.procir.2018.08.109

21. Ajayi T., Gomes J.S., Bera A. A review of CO_2 storage in geological formations emphasizing modeling, monitoring and capacity estimation approaches. *Petroleum Science*. 2019. Vol. 16. Iss. 5, p. 1028-1063. DOI: 10.1007/s12182-019-0340-8

22. Kelemen P., Benson S.M., Pilorgé H. et al. An Overview of the Status and Challenges of CO_2 Storage in Minerals and Geological Formations. *Frontiers in Climate*. 2019. Vol. 1. N 9. DOI: 10.3389/fclim.2019.00009

23. Dorokhin V.G. The method of using carbon dioxide in various aggregate states in underground storage of gas: Avtoref. dis. … kand. tekhn. nauk. Moscow: Nauchno-issledovatelskii institut prirodnykh gazov i gazovykh tekhnologii, 2017, p. 26 (in Russian).

24. Liangliang Jiang, Zhangxin Chen, Farouq Ali S.M. Feasibility of carbon dioxide storage in post-burn underground coal gasification cavities. *Applied Energy*. 2019. Vol. 252. N 113479. DOI: 10.1016/j.apenergy.2019.113479

25. Kai Wang, Jienan Pan, Enying Wang et al. Potential impact of CO_2 injection into coal matrix in molecular terms. *Chemical Engineering Journal*. 2020. Vol. 401. N 126071. DOI: 10.1016/j.cej.2020.126071

26. Yang Bai, Hai-Fei Lin, Shu-Gang Li et al. Molecular simulation of N_2 and CO_2 injection into a coal model containing adsorbed methane at different temperatures. *Energy*. 2021. Vol. 219. N 119686. DOI: 10.1016/j.energy.2020.119686

27. Aydin G., Karakurt I., Aydiner K. Evaluation of geologic storage options of CO_2: Applicability, cost, storage capacity and safety. *Energy Policy*. 2010. Vol. 38. Iss. 9, p. 5072-5080. DOI: 10.1016/j.enpol.2010.04.035

28. Babarinde O., Schwartz B., Jingyao Meng et al. An overview of geological carbon sequestration and its geomechanical aspects. *Geological Society, London, Special Publications*. 2023. Vol. 528, p. 61-72. DOI: 10.1144/SP528-2022-51

29. Khan S.A. The analysis of world projects on catching and a burial place of carbonic gas. *Georesources.* 2010. N 4 (36), p. 55-62 (in Russian).

30. Estublier A., Fornel A., Brosse É. et al. Simulation of a Potential CO_2 Storage in the West Paris Basin: Site Characterization and Assessment of the Long-Term Hydrodynamical and Geochemical Impacts Induced by the CO_2 Injection. *Oil & Gas Science and Technology – Revue d'IFP Energies nouvelles*. 2017. Vol. 72. Iss. 4. T 22. DOI: 10.2516/ogst/2017021

31. Bonto M., Welch M.J., Lüthje M. et al. Challenges and enablers for large-scale CO_2 storage in chalk formations. *Earth-Science Reviews*. 2021. Vol. 222. N 103826. DOI: 10.1016/j.earscirev.2021.103826

32. Tasianas A., Koukouzas N. CO_2 Storage Capacity Estimate in the Lithology of the Mesohellenic Trough, Greece. *Energy Procedia*. 2016. Vol. 86, p. 334-341. DOI: 10.1016/j.egypro.2016.01.034

33. Shogenov K., Shogenova A., Gei D., Forlin E. Synergy of CO_2 Storage and Oil Recovery in Different Geological Formations: Case Study in the Baltic Sea. *Energy Procedia*. 2017. Vol. 114, p. 7047-7054. DOI: 10.1016/j.egypro.2017.03.1846

34. Sliaupa S., Shogenova A., Shogenov K. et al. Industrial carbon dioxide emissions and potential geological sinks in the Baltic states. *Oil Shale*. 2008. Vol. 25. N 4, p. 465-484. DOI: 10.3176/oil.2008.4.06

35. Verdon J.P., Stork A.L., Bissell R.C. et al. Simulation of seismic events induced by CO_2 injection at In Salah, Algeria. *Earth and Planetary Science Letters*. 2015. Vol. 426, p. 118-129. DOI: 10.1016/j.epsl.2015.06.029

36. Toth F.L., Miketa A. The Costs of the Geological Disposal of Carbon Dioxide and Radioactive Waste. Geological Disposal of Carbon Dioxide and Radioactive Waste: A Comparative Assessment. Dordrecht: Springer, 2011, p. 215-262. DOI: 10.1007/978-90-481-8712-6_8

37. Heddle G., Herzog H., Klett M. The Economics of CO_2 Storage. Cambridge: Massachusetts Institute of Technology, Laboratory for Energy and the Environment, 2003, p. 115.

38. Khan S.A., Dorokhin V.G., Bondarenko N.P. How carbon dioxide aggregate state aspects serve to partially replace gas storage buffer volume. *Gazovaya promyshlennost*. 2016. N. 4, p. 50-54 (in Russian).

39. Esene C., Rezaei N., Aborig A., Zendehboudi S. Comprehensive review of carbonated water injection for enhanced oil recovery. *Fuel*. 2019. Vol. 237, p. 1086-1107. DOI: 10.1016/j.fuel.2018.08.106

40. Thomas C., Dehaeck S., De Wit A. Convective dissolution of CO_2 in water and salt solutions. *International Journal of Greenhouse Gas Control*. 2018. Vol. 72, p. 105-116. DOI: 10.1016/j.ijggc.2018.01.019

41. Guodong Cui, Yi Wang, Zhenhua Rui et al. Assessing the combined influence of fluid-rock interactions on reservoir properties and injectivity during CO_2 storage in saline aquifers. *Energy*. 2018. Vol. 155, p. 281-296. DOI: 10.1016/j.energy.2018.05.024

42. Hang Deng, Bielicki J.M., Oppenheimer M. et al. Leakage risks of geologic CO_2 storage and the impacts on the global energy system and climate change mitigation. *Climatic Change*. 2017. Vol. 144. Iss. 2, p. 151-163. DOI: 10.1007/s10584-017-2035-8

43. Pla C., Cuezva S., Martinez-Martinez J. et al. Role of soil pore structure in water infiltration and CO_2 exchange between the atmosphere and underground air in the vadose zone: A combined laboratory and field approach. *Catena*. 2017. Vol. 149. Part 1, p. 402-416. DOI: 10.1016/j.catena.2016.10.018

44. Lan-Cui Liu, Qi Li, Jiu-Tian Zhang, Dong Cao. Toward a framework of environmental risk management for CO_2 geological storage in china: gaps and suggestions for future regulations. *Mitigation and Adaptation Strategies for Global Change*. 2016. Vol. 21. Iss. 2, p. 191-207. DOI: 10.1007/s11027-014-9589-9

45. Pawar R.J., Bromhal G.S., Carey J.W. et al. Recent advances in risk assessment and risk management of geologic CO_2 storage. *International Journal of Greenhouse Gas Control*. 2015. Vol. 40, p. 292-311. DOI: 10.1016/j.ijggc.2015.06.014

46. Qi Li, Guizhen Liu. Risk Assessment of the Geological Storage of CO_2: A Review. Geologic Carbon Sequestration. Cham: Springer, 2016, p. 249-284. DOI: 10.1007/978-3-319-27019-7_13

47. Arora V., Saran R.K., Kumar R., Yadav S. Separation and sequestration of CO_2 in geological formations. *Materials Science for Energy Technologies*. 2019. Vol. 2. Iss. 3, p. 647-656. DOI: 10.1016/j.mset.2019.08.006

This is an open access article under the CC BY 4.0 license

48. Hladik V., Prochac R., Opletal V. et al. CO_2-SPICER – Czech-Norwegian Project to prepare a CO_2 storage pilot in a carbonate reservoir. TCCS-11 – Trondheim Conference on CO_2 Capture, Transport and Storage, 21-23 June 2021, Trondheim, Norway. SINTEF Academic Press, 2021, p. 318-322.

49. Fawad M., Mondol N.H. Monitoring geological storage of CO_2: a new approach. *Scientific Reports*. 2021. Vol. 11. N 5942. DOI: 10.1038/s41598-021-85346-8

50. Flohr A., Schaap A., Achterberg E.P. et al. Towards improved monitoring of offshore carbon storage: A real-world field experiment detecting a controlled sub-seafloor CO_2 release. *International Journal of Greenhouse Gas Control*. 2021. Vol. 106. N 103237. DOI: 10.1016/j.ijggc.2020.103237

Authors: **Riazi Masoud**, *Candidate of Engineering Sciences, Associate Professor,* https://orcid.org/0000-0002-6843-621X (*Nazarbayev University, Astana, Kazakhstan*), **Pavel Yu. Ilyushin**, *Candidate of Engineering Sciences, Director of the Scientific and Educational Center,* https://orcid.org/0000-0003-4463-0883 (*Perm National Research Polytechnic University, Perm, Russia*), **Tatyana R. Baldina**, *First Deputy Director,* https://orcid.org/0000-0001-8217-4167 (*LLC SIE "PrognozRNM", Perm, Russia*), **Nadezhda S. Sannikova**, *Leading Engineer,* https://orcid.org/0000-0003-0002-4187 (*Perm National Research Polytechnic University, Perm, Russia*), **Anton V. Kozlov**, *Project Manager, anton.kozlov@perm-science.ru,* https://orcid.org/0000-0003-2350-2153 (*Perm World-class Scientific and Educational Center "Rational Subsoil Use", Perm, Russia*), **Kirill A. Ravelev**, *Chief Specialist,* https://orcid.org/0000-0002-7402-2830 (*Gazprom Neft Company Group, Saint Petersburg, Russia*).

The authors declare no conflict of interests.

This is an open access article under the CC BY 4.0 license

ISSN 2411-3336; e-ISSN 2541-9404

JOURNAL OF MINING INSTITUTE

Zapiski Gornogo instituta

Journal homepage: pmi.spmi.ru

Research article

Evaluation of the effectiveness of water dust-suppressing emulsions based on acrylic and alkyd polymers

Valeria V. Strokova, Anastasiya Yu. Ryazanova✉, Irina Yu. Markova, Margarita A. Stepanenko, Eduard M. Ishmukhametov

Belgorod State Technological University named after V.G.Shukhov, Belgorod, Russia

***How to cite this article*:** Strokova V.V., Ryazanova A.Yu., Markova I.Yu., Stepanenko M.A., Ishmukhametov E.M. Evaluation of the effectiveness of water dust-suppressing emulsions based on acrylic and alkyd polymers. Journal of Mining Institute. 2024. Vol. 270, p. 941-949.

Abstract

Currently, the use of special dust-suppressing reagents is promising to reduce the level of dust in the vicinity and on the territories of pits, mining and processing plants and other facilities with a high content of fine dust. The analysis of ways to reduce the dust-forming ability of inorganic dispersions with a high degree of dusting is carried out. Due to the lack of regulatory and technical documentation devoted to the standardization of quality control methods for dust-suppressing compounds, it becomes necessary to analyze existing parameters and methods for their determination in order to develop mandatory methods for controlling the properties of dust-suppressing compounds, films formed by them and consolidated systems. The study is devoted to substantiating the necessary methods for assessing the dust-forming ability of inorganic dispersions after treatment with various dust suppressants and evaluating their effectiveness. The parameters are considered and methods for quantifying the determination of the quality of the consolidated layer of dust samples using different dust-suppressing compositions are described. As a result of the analysis of the set of parameter values, it was found that the most resistant to the effects of negative factors due to the formation of a denser and more durable polymer matrix mesh are dusting surface samples treated with an emulsion of alkyd glypthalic resin on a water basis with a high agglomerating effect on particles of inorganic dispersion and the formation of a consolidated layer with a wetting angle of 92.5° and a compressive strength 0.56 MPa.

Keywords

dust suppression; water-based emulsion; spraying; dust; alkyd resin

Funding

The research was carried out at the expense of a grant from the Russian Science Foundation N 23-19-00796.

Received: 31.01.2024 ***Accepted: 02.05.2024*** ***Online: 19.06.2024*** ***Published: 25.12.2024***

Introduction.

Dust formation at industrial facilities during the warehouse, storage and transportation of bulk materials is one of the main sources of air pollution, causing irreparable harm to not only human health [1] and causing breakdowns of special equipment.

Dust at industrial facilities (mining sites, pit or industrial roads [2], dumps [3, 4], tailings dumps [5], landfills [6], agricultural lands, etc. [7, 8]) differs in chemical composition and dispersion. Weather and natural phenomena causing wind erosion, as well as man-made processes (formation of dust clouds during blasting, arable and construction works) are considered to be decisive factors [9, 10]. The main principle of solving the problem of preventing the formation of a dust cloud is the consolidation of dust particles (their adhesion) under the action of dust-suppressing compounds (DC), which leads to the enlargement and weighting of particles of inorganic aerosol dispersion (dust-forming dispersion) [11-13]. This reduces the level of dusting, as heavy particles are less susceptible to erosion.

Despite the importance of controlling the dust-suppressing ability of a particular composition, an analysis of the scientific literature summarized in the article [14] showed that Russian and foreign researchers pay insufficient attention to methods for evaluating the properties of both the dust-

This is an open access article under the CC BY 4.0 license

suppressing composition itself and the dust-forming dispersion (DD) – dust-suppressing compound. The reasons for the difficulties and, as a result, the low coverage of the topic in scientific papers can be considered the lack of regulatory, technical and other normative documents on the standardization of quality control methods for dust suppression compounds. There is an urgent need to analyze existing parameters and methods for their determination in order to develop a mandatory list of methods for controlling the properties of dust-suppressing compounds, films formed by them and consolidated systems.

Currently, there are regulatory documents that reflect methods for determining properties, methods of application, transportation, storage and other characteristics of reagents (emulsions, fluids, foams) that are used to assess the quality of dust-suppressing compounds: GOST 33290-2015, GOST R 58952.1-2020, GOST R 51037-97, GOST R 52056-2003, GOST 30491-2012. It is also possible to use existing regulatory documentation designed for the quality of paints, adhesives or primers. However, it is important to keep in mind that all the proposed methods require adaptation to the needed control sample. For emulsions, researchers identify the following main controlled characteristics: specific consumption of the emulsion; thickness of the film coating; surface tension at the boundary "film of dust-suppressing emulsion – liquid"; wetting angle on the surface of the film of dust-suppressing emulsion [14]. In each of the studied works, the authors propose to investigate the following additional parameters that affect the dust-suppressing characteristics of polymer solutions, foams and water-based emulsions: wetting ability [15-17]; depth of penetration of the composition into the dusting surface [18]; viscosity [19]; dust residue after surface treatment of dust-forming dispersion [20-22]; morphological features of molecules (bubbles) of composition [23] and films formed after their drying [24]; dust suppression time depending on the concentration of dust particles [25, 26]; resistance to erosion with temperature changes [27, 28]; moisture retention [29]; swelling of the tread rubber of motor vehicles [30]; physical and mechanical characteristics of the film [31]; the rate of spraying of the composition onto the dust-forming dispersion [32]; IR spectra of the dust-forming dispersion before and after treatment with the composition [33].

The parameters are considered and methods for determining the quality of dust samples with a consolidated layer (CL) are described when using different dust-suppressing compounds, taking into account the operating conditions of industrial roads: the ability to agglomerate dust particles; visual assessment of the stability of dust samples treated with dust-suppressing compounds in an aqueous medium; compressive strength of samples with a consolidated layer at temperatures of 20 and 50 °C; the wetting angle of the consolidated layer of the sample; structural features of the consolidated layer of the treated dusting surface.

Methods.

The analysis of the effectiveness of dust suppression and the qualitative characteristics of the polymer films formed was carried out using tap water (a common method of dedusting in industrial areas) and two samples of aqueous polymer emulsion systems: an industrial-grade emulsion – Concentrate Polymer acrylic emulsion (chosen because of the greatest similarity both in composition and in the intended area of its use – as a DC) and a synthesized emulsion of alkyd glypthalic resin. The processing of samples (cylinder sample size 3 × 3 cm was obtained by pressing at 7.5 kN pressure) of the model dispersion with dust-suppressing compounds was carried out by a single and uniform spray application over the entire surface of the cylinder with a flow rate of 0.75 l/m^2.

The composition of the emulsion developed by the authors [34, 35] includes (in terms of 100 % by weight) the following components: the dispersed phase of the emulsion is alkyd glypthalic resin 56.1 %; the dispersion medium is water 37.5 %; emulsifier – AMP-95 (2-amino-2-methyl-1-propanol) – 0.3 %; phase boundary modifiers are ethylene glycol 6 % and a mixture of cobalt and zirconium siccatives 0.034 and 0.066 %, respectively. Main characteristics: the dynamic viscosity of the emulsion is up to 50.7 MPa·s; the life of the emulsion is up to 87 days; the size of the emulsion droplets is up to 3 microns; the drying time of the emulsion is 19 hours; the hardness of the film formed after complete drying of the emulsion is 0.32 c.u.; the edge angle of the film is 97.5°; free energy the surface area is

This is an open access article under the CC BY 4.0 license

36.7 mN/m [35]. The environmental friendliness of the substances was considered at the stage of choosing the raw materials of the emulsion, it is recommended to apply the composition to the dust-forming dispersion by spraying – a protective layer is formed with a minimum thickness, which minimizes the negative impact on the ecosphere. At the same time, the content of organic substances in the developed emulsion does not exceed the content in traditionally used DC.

To evaluate the effectiveness of the emulsions under consideration, a model dispersion was used as samples of dust-forming dispersion in the form of a mixture of pulverized quartz grade B (manufacturer of OOO "OPT6") and kaolin clay from the Latnenskoe deposit (in dry form, clay has a dusty structure) in a ratio of 3:1. The component composition of the dust selected as an aerosol-type inorganic dispersion sample is explained by the ubiquity of rock-forming minerals (quartz and kaolinite) in the composition of the vast majority of rocks and soils of the earth's crust, as well as due to the characteristics of the components (minimum porosity of quartz and the possibility of water absorption of kaolinite).

The degree of agglomeration of dust particles is determined by sieving the treated dispersion through sieves with a cell size of 0.1-10 mm and determining the partial residue on each sieve after processing the dust-forming dispersion with dust-suppressing compounds.

A visual assessment of the stability of samples with a treated surface in an aqueous medium is not a normalized parameter and was carried out to determine the possibility of further assessment of the waterproofness and swelling of the samples. The preparation of samples from a clay-sand mixture was carried out according to the standard methodology corresponding to GOST 9128-2013 "Mixtures of asphalt concrete, polymerasfalt concrete, asphalt concrete, polymerasfalt concrete for highways and airfields. Technical conditions". The sample cylinder is treated with a dust-suppressing compound superficially by uniform spraying from a spray gun.

The study of the strength characteristics of the consolidated layer on the surface of the dust sample formed after drying of the alkyd resin emulsion was carried out according to the GOST 30491-2012 method "Organomineral mixtures and soils reinforced with organic binders for road and airfield construction" at temperatures of 20 and 50 °C with determination of the compressive strength of the cylinder samples. The sample cylinder is treated with a dust-suppressing compound superficially by uniform spraying from a spray gun. This technique is an indirect assessment of dust-suppressing properties [14], however, the method is informative from the point of view of evaluating the binding properties of the emulsion.

The edge angle was determined using a Kruss DSA 30 contact wetting angle measuring device using ADVANCED software by the recumbent drop method. Distilled water was used as the test liquid. The ADVANCED program automatically outputs the average value based on all measurements of the contact angle. The samples were prepared by pressing a mixture of dust-forming dispersion at a pressure of 7.5 kN.

The structural features of the consolidated layer of dust-forming dispersion were studied by scanning electron microscopy using a Tescan MIRA 3 LMU scanning electron microscope.

The characteristics of the dust-forming dispersion were carried out according to the methods of GOST R 51037-97 "Polymer protective insulating coatings, localizing dust-suppressing and deactivating. General technical requirements". The study was carried out using the equipment of the High Technology Center at the BSTU named after V.G.Shukhov.

Applied concepts and their definitions:

Dust-forming dispersion (*inorganic dispersion of aerosol type*) is a mixture of inorganic dust particles corresponding to a number of dust classifications by dispersion – 4th and 3rd; stickiness (characteristic indicator – breaking strength of the dust layer according to E.I.Andrianov) – non-sticking; wettability – well wetted.

A dust-suppressing composition is a reagent with high dust-suppressing characteristics, the aggregate state (liquid or dry) and morphological structure (solution, foam, emulsion) of which are able to reduce the degree of dust formation of inorganic dispersions.

This is an open access article under the CC BY 4.0 license

Journal of Mining Institute. 2024. Vol. 270. P. 941-949
© Valeria V. Strokova, Anastasiya Yu. Ryazanova, Irina Yu. Markova, Margarita A. Stepanenko, Eduard M. Ishmukhametov, 2024

The consolidated layer is a temporary protective coating formed on the surface of the dust-forming dispersion after complete drying of the dust-suppressing composition.

Discussion of the results.

Taking into account the intended field of application of the developed alkyd emulsion for dedusting (dusty objects of the construction and mining industries), it was necessary to quantify the complex of indicators of the consolidated layer formed after the distribution of the dust-suppressing composition. Since the developed alkyd emulsion includes products of the paint and varnish industry, and its main functional purpose is the localization of dust and the formation of a protective coating, when evaluating the dust-suppressing effectiveness from the point of view of a protective polymer coating, it is advisable to follow the requirements of GOST R 51037-97. Based on the specified regulatory document, the indicators were selected to establish the compliance of the dust-suppressing protective polymer coating formed by the developed emulsion with the regulated requirements (Table 1). The analysis of the obtained values of the normalized characteristics of the consolidated layer showed that the developed alkyd emulsion makes it possible to obtain a dust-suppressing protective coating that meets the requirements of GOST R 51037-97 in all respects.

Table 1

Characteristics of dust-forming dispersion according to GOST R 51037-97

The indicator name	Technical requirements	The actual value
Preliminary surface preparation (temperature 5-30 °C, humidity up to 95 %)	None	None
Degree of pelletizing, %	> 80	93
Application surface temperature, °C	–10 … +50	+5 … +25
Holding time before the start of operation, h	< 24	19
Resistance to water, day	> 180	198
Temperature resistance, °C	5-30	79
Service life, day	> 180	180

However, the use of methods for determining the normalized indicators does not allow to fully study the interaction of the dust-suppressing composition with the dust-forming dispersion. This is due to the use of regulatory techniques for evaluating a polymer coating on a hard surface (glass or metal plate). The analysis of the indicators obtained on monolithic static surfaces is necessary, but insufficient to assess the effectiveness of formulations applied to highly dispersed, conditionally mobile materials.

Due to the lack of uniform control standards fixed in regulatory documents, as well as uniform requirements for dust suppression compounds, it is very difficult to conduct a comparative assessment of the effectiveness of certain types of reagents and their compositions. Based on the analysis of the methods used by various scientific groups and the controlled parameters, a number of indicators were selected that are recommended as the most informative for proving the dust-suppressing ability of alkyd emulsions.

The main processes providing dust suppression during surface treatment with a polymer-based compound are enlargement (gluing) and film formation. The more adhesive the polymer component of the dust-suppressing composition is, the better the particle agglomeration will be. The result of assessing the degree of agglomeration of DD particles was to obtain a partial residue after sieving (the mass of the substance on each sieve). The processed model dispersion is characterized by the absence of fractions with particles less than 0.25 mm (Fig.1). The right part of the graph is of the greatest interest for evaluating the ability to agglomerate particles of the model dispersion after DC processing. Thus, agglomeration of particles with water showed the worst result – the formation of agglomerates is in the range of 1-5 mm. The partial residues on the sieves are presented in Table 2.

This is an open access article under the CC BY 4.0 license

© Valeria V. Strokova, Anastasiya Yu. Ryazanova, Irina Yu. Markova, Margarita A. Stepanenko, Eduard M. Ishmukhametov, 2024

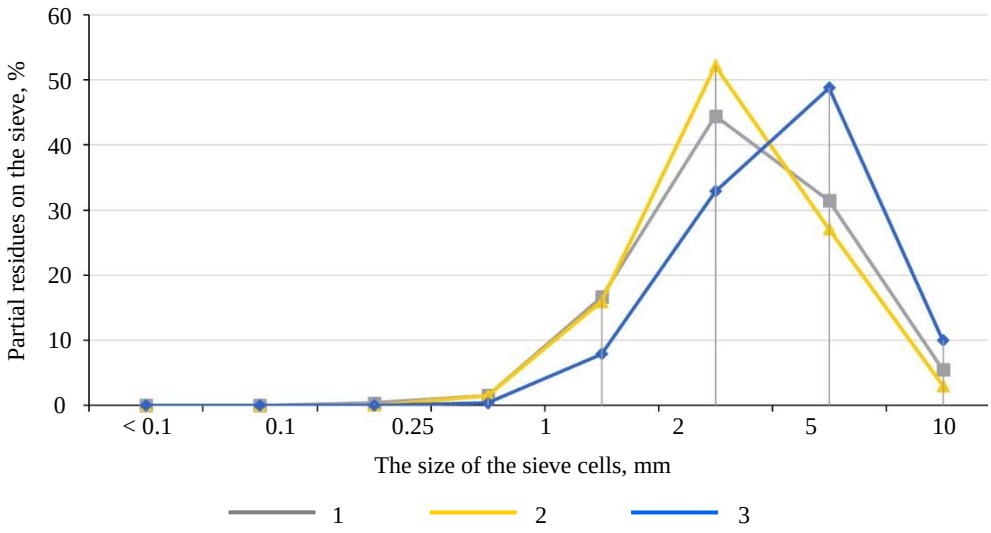

Fig.1. Granulometric composition of the model dust-forming dispersion 1 – tap water; 2 – acrylic emulsion; 3 – alkyd emulsion

Table 2

The partial residues on the sieves, %

Type of processing	The size of the sieve cells, mm			
	1	2	5	10
Water	16.7	44.4	31.5	7.4
Acrylic emulsion	15.9	52.2	27.1	4.8
Alkyd emulsion	7.9	32.9	48.8	10.4

The analysis of the obtained data on the granulometric composition of the treated dispersion with various dust-suppressing compositions determined by the sieve analysis method allows to judge the best ability to agglomerate the inorganic dispersion when using the developed emulsion. This is evidenced by the maximum mass of large aggregates on a sieve with a cell size of 5 mm, whereas when using water, the maximum mass of aggregates is noted on a sieve with cells of 2 mm. Its effectiveness in agglomeration of dusty particles can be explained by the best film-forming ability (stickiness) of the polymer component of the emulsion – alkyd resin, which indicates the best dust-suppressing effect.

When visually evaluating a sample of clay-sand particles treated with an acrylic emulsion (Fig.2), rapid absorption of the product into the sample surface was observed, which remains unchanged upon drying. However, when treated with a synthesized emulsion, a film is formed on the surface (before immersion in water). Then the processed samples were immersed in a container with water for a while. The assessment was performed based on the destruction of the sample in an aqueous medium with time fixation.

Three samples were taken for analysis: sample 1 – model dispersion without DC treatment; sample 2 – dispersion treated with acrylic emulsion; sample 3 – dispersion treated with synthesized emulsion.

The observation continued until the complete destruction of the samples in the water. Sample 1 showed the worst result with complete destruction after 30 min. Sample 2 showed partial destruction of the cylinder surface after 30 min and complete destruction after an hour. Sample 3 showed the best result after 30 min in the water – a flat surface without visible destruction. After an hour, the destruction of the walls in sample 3 is noted with the internal preservation of the shape. Thus, a visual

This is an open access article under the CC BY 4.0 license

Journal of Mining Institute. *2024. Vol. 270. P. 941-949*
© Valeria V. Strokova, Anastasiya Yu. Ryazanova, Irina Yu. Markova, Margarita A. Stepanenko, Eduard M. Ishmukhametov, 2024

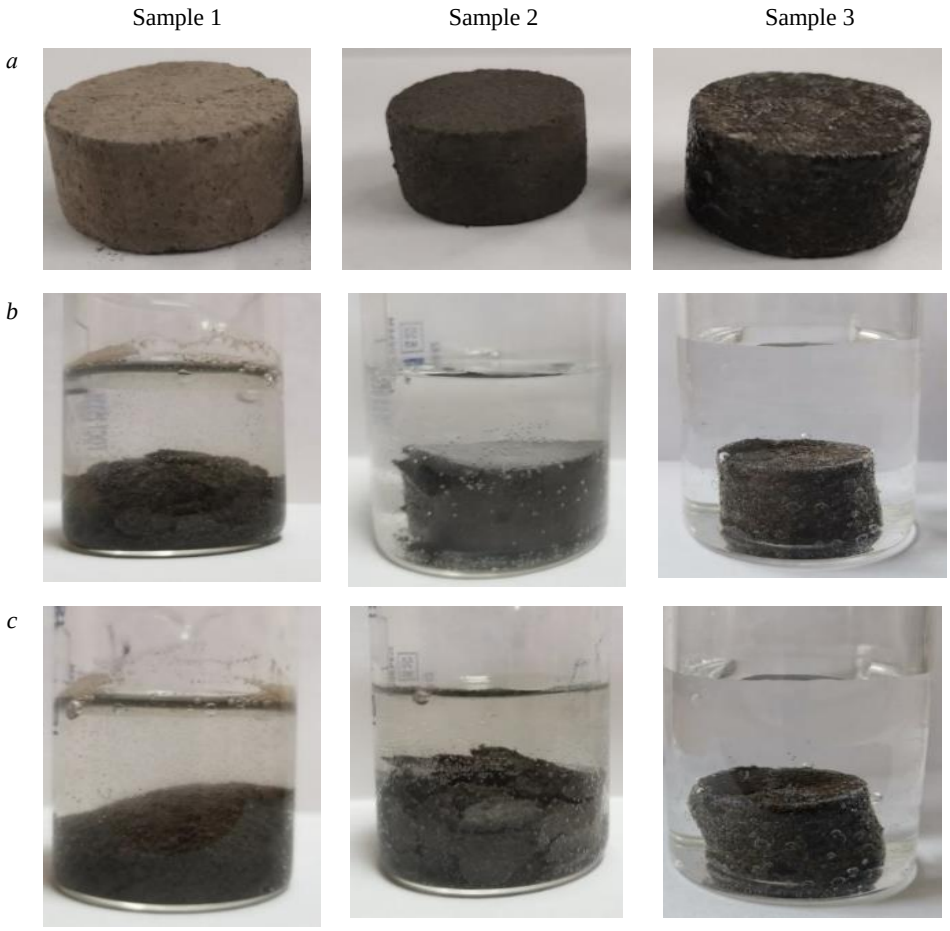

Fig.2. Destruction of samples from a mixture of dusty particles treated with dust-suppressing compounds before immersion in water (*a*); after 30 min (*b*); after 60 min (*c*)

assessment of the treated samples from a model clay-quartz mixture of dust particles showed that the consolidated layer formed by the synthesized emulsion has the best exposure in water due to the formation of a more durable polymer film on the surface of the compressed dispersion.

Analysis of the compressive strength of cylinders treated with surface dust-suppressing compounds showed that the strength of samples treated with polymer emulsions at 20 °C is higher than that treated at 50 °C (Table 3). However, when comparing samples treated with emulsions, the highest strength values are observed in samples whose consolidated layer was formed after complete drying of the alkyd resin emulsion at both 20 °C and 50 °C; compared with samples treated with acrylic emulsion, it is 32 % higher at 20 °C and 35 % – at 50 °C. An increase in the strength of the sample, the surface of which was treated with an emulsion of alkyd glypthalic resin, indicates the formation of a more durable polymer matrix, which is probably due to the high adhesion (stickiness) of the resin to dust particles.

Table 3

Soil strength indicators

Type of sample	Compressive strength at various temperatures, MPa	
	20 °C	50 °C
Treated with an acrylic emulsion “Concentrate Polymer”	0.38	0.13
Treated with an emulsion of alkyd glypthalic resin	0.56	0.2

This is an open access article under the CC BY 4.0 license

© Valeria V. Strokova, Anastasiya Yu. Ryazanova, Irina Yu. Markova, Margarita A. Stepanenko, Eduard M. Ishmukhametov, 2024

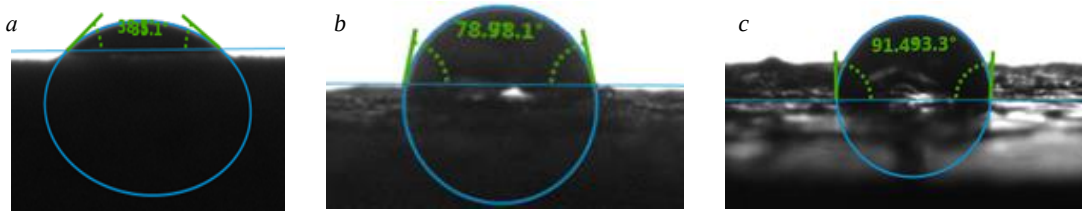

Fig.3. Values of the wetting angle of samples from a mixture of dusty particles treated with dust-suppressing compounds in a test liquid (water): *a* – without treatment (38.5°); *b* – a sample treated with an acrylic emulsion "Concentrate Polymer" (78.9°); *c* – a sample treated with an emulsion of alkyd glypthalic resin (92.5°)

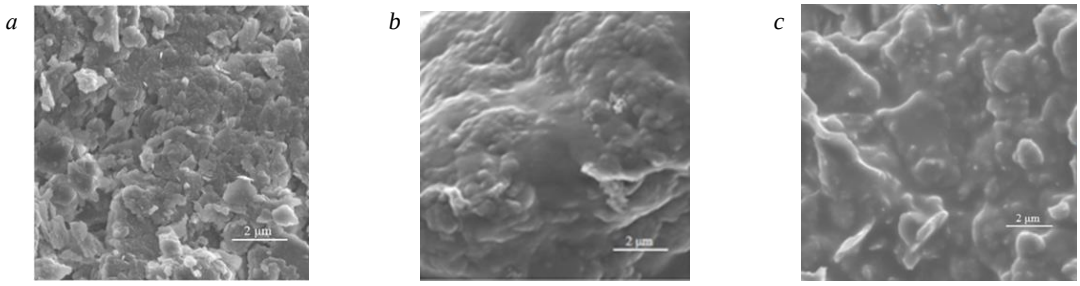

Fig.4. Characteristics of the surface of the inorganic dispersion after treatment with dust-suppressing compounds: *a* – sample without treatment (control); *b* – sample treated with acrylic emulsion "Concentrate Polymer"; *c* – sample treated with alkyd emulsion

To study the effectiveness of dust-suppressing films formed on the treated surface and their insulating ability, a change in the wetting edge angle was investigated. The higher the value of the wetting angle, the higher the insulating ability of the film obtained during the consolidation of dusty particles, expressed in the hydrophobic ability.

The analysis of the obtained values (Fig.3) showed the highest efficiency of the alkyd-based dust suppression compound. Thus, the values of the wetting edge angle of the consolidated layer formed when using an alkyd emulsion are one and a half times higher than when using an acrylic emulsion, and three times higher than that of the original (untreated) composition. The values of the limiting wetting angle of the sample surface when using a synthesized emulsion of more than 90° indicate hydrophobicity.

The final stage of the study was to identify the features of the structure formation of alkyd oligomer films on a substrate of dusty particles. The analysis of the polymer film structure formation was carried out after the emulsion was cured (Fig.4). Despite the fact that polymer emulsions were used in both cases, the structure of the sample of dusty particles treated with acrylic emulsion (Fig.4, *b*) does not visually differ from the original sample without treatment. Probably, the presence of a polymer matrix is not fixed due to the low polymer content or low viscosity of the emulsion, which requires two or three surface treatments. This also explains the worst indicators of the parameters considered.

A comparative assessment of the microstructure shows (Fig.4, c) the effectiveness of the synthesized emulsion as a means of dust suppression in terms of the ability to form a protective film on the surface of the dusting model system. The light areas are well distinguished in the structure, evenly distributed over the surface of the sample from a mixture of dusty particles. In addition, it is noted that when using a dust-suppressing synthesized composition, the surface of the sample changes from a loose granular to a smoother monolithic one. This is due to the high adhesion (good stickiness of the resin droplet to the particle of the model dispersion) of the selected polymer component of

This is an open access article under the CC BY 4.0 license

the resulting emulsion, as well as its high viscosity (compared to the acrylic emulsion "Concentrate Polymer") due to the excess resin in the composition.

Conclusion.

The analysis of the parameters determined in the framework of the study made it possible to qualitatively and quantitatively determine the physico-mechanical, colloidal-chemical properties and structural features of the consolidated layer of dust-forming dispersion formed on the surface of an inorganic aerosol-type dispersion after drying of the polymer composition.

The analysis of the granulometric composition of dust treated with various reagents by the sieve analysis method showed a better ability to agglomerate dust when using an alkyd emulsion. This is evidenced by the maximum mass of large aggregates on a sieve with a mesh size of 5 mm, whereas when using water, the maximum mass of aggregates is 2 mm. The high agglomerating ability is explained by the best film-forming ability (stickiness) of the alkyd resin.

An analysis of the assessment of water resistance of dust samples treated with two types of formulations showed that the consolidated layer formed by an alkyd emulsion has the best exposure in water. This is explained by the formation of a more durable polymer film on the surface of the samples, which is confirmed by the results of an assessment of the structural features of the protective coating and a high value of the wetting angle (92.5°). The compressive strength of the samples when using both emulsions at 50 °C is reduced by half, which indicates a negative effect of temperature on the strength characteristics of the protective polymer layer and a limited temperature range of the composition used during its operation in industrial areas, but not a deterioration in the dust-suppressing effectiveness of the alkyd resin emulsion.

REFERENCES

1. Vishnevsky A. The use of industrial wastes for dust control of roads. *Transbaikal State University Journal.* 2017. Vol. 23. N 11, p. 12-18 (in Russian). DOI: 10.21209/2227-9245-2017-23-11-12-18

2. Buryanov I.A., Logachev K.I., Uvarov V.A. Determination of the main properties of dust particles in the grinding area. *Bulletin of Belgorod State Technological University named after V.G.Shukhov.* 2020. Vol. 5. N 10, p. 23-32 (in Russian). DOI: 10.34031/2071-7318-2020-5-10-23-32

3. Shuvalov Yu.V., Veselov A.P., Bulbashev A.P. et al. Dust control in mining enterprises using long- and short-lived foams of increased multiplicity. *Gornyi informatsionno-analiticheskii byulleten.* 2007. N S12, p. 171-179. (in Russian).

4. Kireeva E.V., Kondrasheva N.K., Zyryanova O.V. et al. Aqueous film-forming dispersions for dust collecting compounds. *Lakokrasochnye materialy i ikh primenenie.* 2018. N 7-8, p. 42-45 (in Russian).

5. Ospanova Zh.B., Toktagul S., Tasmagambetova A., Asadov M. Preparation of foaming agents for dust suppression of coal particles. *Chemical Bulletin of Kazakh National University.* 2019. Vol. 94. N 3, p. 12-18 (in Russian). DOI: 10.15328/cb1071

6. Shegolkov Y.S., Kolosov A.A., Pasechnaya V.Y. Effect of dispersion of industrial dust on the occupational morbidity of workers. Fundamentalnye i prikladnye nauchnye issledovaniya: aktualnye voprosy, dostizheniya i innovatsii: sbornik statei VIII Mezhdunarodnoi nauchno-prakticheskoi konferentsii, 15 oktyabrya 2017, Penza, Rossiya: v 4 chastyakh. Penza: Nauka i prosveshchenie, 2017. Part 1, p. 175-177 (in Russian).

7. Wu Mingyue, Hu Xiangming, Zhang Qian et al. Study on preparation and properties of environmentally-friendly dust suppressant with semi-interpenetrating network structure. *Journal of Cleaner Production*. 2020. Vol. 259. N 120870. DOI: 10.1016/j.jclepro.2020.120870

8. Wenjin Niu, Wen Nie, Mingyue Yuan et al. Study of the microscopic mechanism of lauryl glucoside wetting coal dust: Environmental pollution prevention and control. *Journal of Hazardous Materials*. 2021. Vol. 412. N 125223. DOI: 10.1016/j.jhazmat.2021.125223

9. Romanchenko S.B., Naganovckiy Yu.K., Kornev A.V. Innovative ways to control dust and explosion safety of mine workings. *Journal of Mining Institute.* 2021. Vol. 252, p. 927-936. DOI: 10.31897/PMI.2021.6.14

10. Strokova V.V., Ishmukhametov E.M., Esina A.Yu. et al. Water-based dust suppressing compositions: analysis of the state and prospects of development. *Bulletin of the Technological University.* 2021. Vol. 24. N 12, p. 5-38 (in Russian).

11. Lyashenko V.I., Gurin A.A. Justification of environmental protection technologies and means for dust suppression at tailings ponds of hydrometallurgy. *Mining Informational and Analytical Bulletin.* 2018. N 9, p. 58-72 (in Russian). DOI: 10.25018/0236-1493-2018-9-0-58-72

12. Dabizha O.N., Bespolitov D.V., Konovalova N.A. et al. Application of the Stabilizing Polymer Additives for Protection of Dump Overflow from Wind Erosion. *Problems of Contemporary Science and Practice. Vernadsky University.* 2021. N 1 (79), p. 26-39 (in Russian). DOI: 10.17277/voprosy.2021.01.pp.026-039

13. Jianwei Cheng, Xinrui Zheng, Yadong Lei et al. A compound binder of coal dust wetting and suppression for coal pile. *Process Safety and Environmental Protection*. 2021. Vol. 147, p. 92-102. DOI: 10.1016/j.psep.2020.08.031

14. Jiayi Yan, Wen Nie, Haihan Zhang et al. Synthesis and performance measurement of a modified polymer dust suppressant. *Advanced Powder Technology*. 2020. Vol. 31. Iss. 2, p. 792-803. DOI: 10.1016/j.apt.2019.11.033

This is an open access article under the CC BY 4.0 license

15. Kai Wang, Yuchen Zhang, Weiyao Cai et al. Study on the microscopic mechanism and optimization of dust suppression by compounding biological surfactants. *Colloids and Surfaces A: Physicochemical and Engineering Aspects*. 2021. Vol. 625. N 126850. DOI: 10.1016/j.colsurfa.2021.126850

16. Strokova V.V., Ishmukhametov E.M., Esina A.Yu. Evaluation of emulsifier effect on the properties of water-based alkyd emulsion. *Chemical Bulletin.* 2022. Vol. 5. N 3, p. 39-48 (in Russian).

17. Strokova V.V., Ishmukhametov E.M., Esina A.Yu. Analysis of methods for obtaining water based alkyd emulsion. *Bulletin of the Technological University.* 2022. Vol. 25. N 7, p. 43-48 (in Russian). DOI: 10.55421/1998-7072_2022_25_7_43

18. Sachkova O.S., Samoilov V.V., Elin A.M. Estimate researches on efficiency and safety of a biological dust suppression preparation. *Science and Technology in Transport.* 2021. N 2, p. 101-107 (in Russian).

19. Akimov A.M., Kotelnikova S.A. Investigation of dust-retaining solutions during transportation of rock masses. *Power Plants and Technologies.* Vol. 7. N 2, p. 148-151 (in Russian).

20. Qiu Bao, Wen Nie, Changqi Liu et al. The preparation of a novel hydrogel based on crosslinked polymers for suppressing coal dusts. *Journal of Cleaner Production*. 2020. Vol. 249. N 119343. DOI: 10.1016/j.jclepro.2019.119343

21. Evtushenko A.I., Evtushenko I.I., Nor-Arevyan S.L., Belskaya Y.B. On the question of research ways to improve the effectiveness of dust control irrigation. *Engineering Journal of Don.* 2016. N 3 (42), p. 9 (in Russian).

22. Ivanov A.V., Smirnov Yu. D., Chupin S.A. Development of the concept of an innovative laboratory installation for the study of dust-forming surfaces. *Journal of Mining Institute.* 2021. Vol. 251, p. 757-766. DOI: 10.31897/PMI.2021.5.15

23. Xiaobin Wei, Hetang Wang, Ying Xie, Yunhe Du. An experimental investigation on the effect of carboxymethyl cellulose on morphological characteristics of dust-suppression foam and its mechanism exploration. *Process Safety and Environmental Protection*. 2020. Vol. 135, p. 126-134. DOI: 10.1016/j.psep.2019.12.009

24. Alosmanov M.S., Ataev M.Sh., Sultanzade S.S. et al. A means for dust control. *Herald of Science and Education.* Vol. 1. N 2 (38), p. 17-21 (in Russian). DOI: 10.20861/2312-8089-2018-38-003

25. Qing Guo, Wanxing Ren, Jingtai Shi. Foam for coal dust suppression during underground coal mine tunneling. *Tunnelling and Underground Space Technology*. Vol. 89. 2019, p. 170-178. DOI: 10.1016/j.tust.2019.04.009

26. Zongqi Liu, Gang Zhou, Jinjie Duan et al. Preparation of composite high-efficiency dust suppressant and relevant molecular dynamics simulation for wetting coal surface. *Fuel*. 2021. Vol. 296. N 120579. DOI: 10.1016/j.fuel.2021.120579

27. Podobrazhin S.N. Prevention of dust emissions to the mine atmosphere during wind erosion. *Occupational Safety in Industry.* 2011. N 6, p. 16-22 (in Russian).

28. Ping Chang, Zidong Zhao, Guang Xu et al. Evaluation of the coal dust suppression efficiency of different surfactants: A factorial experiment. *Colloids and Surfaces A: Physicochemical and Engineering Aspects*. 2020. Vol. 595. N 124686. DOI: 10.1016/j.colsurfa.2020.124686

29. Nguyen V.G. Patent № US 8052890 B2. Compositions for dust suppression and methods. Publ. 22.12.2005.

30. Rulin Liu, Gang Zhou, Kaili Wang et al. Experimental investigation on highly efficient collection and cleaning for fine coal dust particles by dry-wet mixed chemical method. *Journal of Environmental Chemical Engineering*. 2021. Vol. 9. Iss. 5. N 105861. DOI: 10.1016/j.jece.2021.105861

31. Anagnostopoulos C.A., Kandiliotis P., Lola M., Karavatos S. Improving Properties of Sand Using Epoxy Resin and Electrokinetics. *Geotechnical and Geological Engineering*. 2014. Vol. 32. Iss. 4, p. 859-872. DOI: 10.1007/s10706-014-9763-6

32. Hetang Wang, Yunhe Du, Xiaobin Wei, Xinxin He. An experimental comparison of the spray performance of typical water-based dust reduction media. *Powder Technology*. 2019. Vol. 345, p. 580-588. DOI: 10.1016/j.powtec.2019.01.032

33. Guo-Qing Shi, Cong Han, Yan-ming Wang, He-Tang Wang. Experimental study on synergistic wetting of a coal dust with dust suppressant compounded with noncationic surfactants and its mechanism analysis. *Powder Technology*. 2019. Vol. 356, p. 1077-1086. DOI: 10.1016/j.powtec.2019.09.040

34. Kirwin R.C. Patent № EP 0197714 A2. Method for the control of dust. Publ. 15.10.1986.

35. Hetang Wang, Xiaobin Wei, Yunhe Du, Deming Wang. Effect of water-soluble polymers on the performance of dust-suppression foams: Wettability, surface viscosity and stability. *Colloids and Surfaces A: Physicochemical and Engineering Aspects*. 2019. Vol. 568, p. 92-98. DOI: 10.1016/j.colsurfa.2019.01.062

***Authors*: Valeria V. Strokova,** *Doctor of Engineering Sciences, Head of the Department, https://orcid.org/0000-0001-6895-4511* (*Belgorod State Technological University named after V.G.Shukhov, Belgorod, Russia*), **Anastasiya Yu. Ryazanova,** *Postgraduate Student, yanastasia.24@yandex.ru, https://orcid.org/0000-0002-8247-7755* (*Belgorod State Technological University named after V.G.Shukhov, Belgorod, Russia*), **Irina Yu. Markova,** *Candidate of Engineering Sciences, Associate Professor, https://orcid.org/0000-0002-7569-1825* (*Belgorod State Technological University named after V.G.Shukhov, Belgorod, Russia*), **Margarita A. Stepanenko,** *Postgraduate Student, https://orcid.org/0000-0002-4130-5703* (*Belgorod State Technological University named after V.G.Shukhov, Belgorod, Russia*), **Eduard M. Ishmukhametov,** *Researcher, https://orcid.org/0000-0002-1782-823X* (*Belgorod State Technological University named after V.G.Shukhov, Belgorod, Russia*).

The authors declare no conflict of interests.

This is an open access article under the CC BY 4.0 license

ISSN 2411-3336; e-ISSN 2541-9404

JOURNAL OF MINING INSTITUTE

Zapiski Gornogo instituta

Journal homepage: pmi.spmi.ru

Research article

Study of the possibility of using high mineralization water for hydraulic fracturing

Shamil K. Sultanov[1], **Vyacheslav Sh. Mukhametshin**[2]✉, **Alexandras P. Stabinskas**[3], **Elchin F. Veliev**[4], **Artem V. Churakov**[3]

[1] *Ufa State Petroleum Technological University, Ufa, Republic of Bashkortostan, Russia*

[2] *Institute of Oil and Gas of the Federal State Budgetary Educational Institution of Higher Education "Ufa State Petroleum Technological University" in the City of Oktyabrsky, Oktyabrsky, Republic of Bashkortostan, Russia*

[3] *LLC "Gazpromneft S&TC", Saint Petersburg, Russia*

[4] *NIPI "Neftegaz", SOCAR, Baku, Republic of Azerbaijan*

How to cite this article: Sultanov S.K., Mukhametshin V.Sh., Stabinskas A.P., Veliev E.F., Churakov A.V. Study of the possibility of using high mineralization water for hydraulic fracturing. Journal of Mining Institute. 2024. Vol. 270, p. 950-962.

Abstract

The results of laboratory studies aimed at developing hydraulic fracturing fluid based on alternative sources of high mineralization water are presented. It is shown that Cenomanian sources have the most stable mineralization parameters, while bottom water and mixed waters collected from pressure maintenance systems differ significantly in their properties, with iron content varying several times, and hardness and mineralization undergoing substantial changes. The quality of the examined hydraulic fracturing fluids based on alternative water sources is confirmed by their impact on residual permeability, as well as residual proppant pack conductivity and permeability. The experimental results show similar values for these parameters. The comprehensive laboratory studies confirm the potential for industrial use of high mineralization water in hydraulic fracturing operations.

Keywords

well; hydraulic fracturing; hydraulic fracturing fluid; bottom water; Cenomanian water; mixed water; permeability; high mineralization waters; guar fluid

Funding

The research was funded by the Ministry of Science and Higher Education of the Russian Federation under agreement N 075-15-2020-900 as part of the development program of the World-Class Research Center.

Received: 01.03.2022 ***Accepted: 03.06.2024*** ***Online: 08.11.2024*** ***Published: 25.12.2024***

Introduction.

The increasing consumption of natural resources by humanity, alongside with the increase of production capacities through active engagement in the development of with hard-to-recover deposits [1-3] poses a significant challenge reducing negative environmental impacts. There is a growing interest in solutions that enable optimization of industrial technologies aimed at lowering production costs, while considering both geological and physical properties of reservoirs [4-6] and minimizing environmental impact. Companies focused on technological development strive to offer innovations that meet new environmental requirements in the oil and gas sector.

One direction for optimizing and reducing current costs associated with hydraulic fracturing operations is the use of alternative sources for preparing hydraulic fracturing fluids, such as Cenomanian, mixed, or bottom waters. This solution allows for the optimization of the speed and quality of work performed without wasting resources or time [7-9]. The main objective of this study is to conduct research to determine the most stable guar-based hydraulic fracturing fluid system that allows for hydraulic fracturing operations using water with a high mineralization degree. To achieve this goal, it is necessary to address tasks related to evaluating the viscosity characteristics of fluids

This is an open access article under the CC BY 4.0 license

depending on various shear rates; assessing residual permeability and conductivity of the proppant pack; and determining the influence of hydraulic fracturing fluid (HF) on rock permeability under reservoir conditions. The aim is to determine hydraulic fracturing fluids with an optimal composition, including stabilizing additives, and to establish criteria for their applicability to real geological and reservoir conditions of fields, taking into account the features of modern hydraulic fracturing equipment. Additionally, methods and criteria for the applicability of stabilizing components will be developed to enable operations using bottom, mixed, or Cenomanian waters. The results obtained will allow for the "regulation" of hydraulic fracturing fluids during field operations to be carried out promptly based on the actual mineralogical composition in a stationary field laboratory, without the need for specialized equipment or costly studies.

Subject and relevance of the research.

Hydraulic fracturing is one of the most effective technologies for intensifying production and injection wells operation [10-12]. This geological engineering activity (GEA) is a widely used technology that requires significant technical and material resources, considering the technological solutions conditioned by the particular geological facility [13-15]. It is noteworthy that due to the necessity of involving into development increasingly complex geological facilities [16-18], the hydraulic fracturing technology is evolving [19-21]. This evolution influences the increasing volumes of freshwater used for preparing fracturing fluids, chemical reagents, and technological equipment.

Given the global trend towards reducing production costs [22-24] and minimizing negative environmental impacts*, the prospects for using high-mineralization waters for fracturing fluids are being considered. Such an approach can reduce environmental impact factors and lower the cost of extracted hydrocarbons [25-27]. One solution to this issue is the use of alternative (mineralized) water sources for preparing hydraulic fracturing fluids without special preliminary treatment. These sources include bottom waters, mixed waters (a combination of bottom and freshwater), and Cenomanian waters, which are typically utilized in pressure maintenance systems (PMS) of injection well fields [28].

A significant problem in using alternative water sources in hydraulic fracturing fluid systems is their aggressive chemical composition compared to traditional freshwater and, for the most part, surface water sources. This, in turn, necessitates the development of complex stabilizing and auxiliary additives that reduce the negative impact of high mineralization at all stages of preparing the hydraulic fracturing fluid, taking into account the actual composition of the specific source [29-31], and additionally, these additives should not impair the reservoir properties and should feature a simplified preparation technology.

According to the results of previously conducted studies on the influence of the technological fluid injected during hydraulic fracturing on the reservoir filtration-capacity properties (FCP), dependencies have been confirmed that indicate that with an increase in the volume of injected working fluid by 1 m of productive layer, there is a deterioration in FCP due to the clogging caused by the gelling agent present in the fluid system [32]. The development of a complex of auxiliary additives addresses the challenge of conducting HF operations using traditional concentrations of guar gelling agents. This approach allows for the proppant transportation with minimal reservoir and fractures contamination, which is one of the most relevant directions in the technological development of hydraulic fracturing [33]. The choice of working fluid system is always significant, as it affects the geometry of the fracture created, the proppant transportation quality and its placement in the reservoir, as well as the conductivity of the channels created during the operation. Thus, the characteristics of HF fluids

* UN General Assembly Resolution N A/RES/70/1 dated 25.09.2015 "Transforming our world: The 2030 Agenda for Sustainable Development", p. 44. URL: https://documents.un.org/doc/undoc/gen/n15/291/92/pdf/n1529192.pdf (accessed 27.06.2024).

This is an open access article under the CC BY 4.0 license

are important parameters that require detailed study to achieve stable, predictable, and high-yielding well operations [34, 35].

The physicochemical properties of associated produced water depend on numerous factors, such as the geological structure of the deposit, mineral composition, chemical processes occurring during sediment accumulation, type of hydrocarbons, the activity and species of microorganisms, as well as reservoir temperature and pressure. Associated produced water contains suspended particles and various water-soluble components, representing a mixture of organic and inorganic compounds, some of which are present in formation water. Others emerge during the development and implementation of various geological and technological methods [36-38].

The assessment of water suitability for the preparation of hydraulic fracturing fluids is conducted based on a six-component water analysis, which allows for the rapid determination of the of key critical components content in the water. However, to understand the individual components influence on the properties of the fracturing fluid and to develop a high-quality, stable system, a more in-depth investigation of the source composition is required, utilizing a more comprehensive elemental analysis. The formulations of guar-based fluids are highly sensitive to the quality of the water used, particularly to the content of iron, calcium, and magnesium ions. Therefore, the use of unconditioned mineralized water without prior and costly treatment is not feasible. Previously proposed solutions for the potential use of bottom and Cenomanian waters have provided isolated approaches that do not sufficiently account for these critical factors. To improve the properties of guar-based HF fluids with borate crosslinkers, water-soluble amino alcohols were introduced into their composition, and chelating additives were applied to combat excessive hardness [39]. Most of these solutions are characterized by limitations on the compositions of "suitable" waters; some of them are associated with high costs due to the use of modified gelling agents [15, 40, 41] and/or crosslinkers [42-44].

Methodology.

Based on the results of a series of tests, a methodology for the application of additives has been proposed, which allows for the rapid selection of the necessary components for the HF fluids preparation using alternative source waters, without requiring modifications to the primary functional components of the system – guar gelling agents and borate crosslinkers. To implement this task, the following laboratory investigations were conducted:

• Rheological properties investigation. Viscosity characteristics were evaluated depending on various shear rates at room temperature and atmospheric pressure, as well as under conditions approximating reservoir conditions. Such experiments adhere to international industry standards. The properties of the fluids were assessed using an atmospheric rotational viscometer with a coaxial cylinder system and a rotor-bob-spring geometry R1-B1-F1 (ISO 13503-1:2011), as well as high-pressure and high-temperature viscometers with a rotor-bob-spring geometry R1-B5-F1 (ISO 13503-1:2011).

• Assessing residual permeability and conductivity of proppant packs. The pack, contaminated with HF fluids, was studied using specialized equipment in accordance with ISO 13503-5 standards. Observations were made on sandstone core material. The proppant used for all tests was ceramic proppant with a 16/20 mesh size. The testing temperature was set at 90 °C, and readings were taken over a pressure range of 5000-9000 psi in 100 psi increments.

• Filtration studies to determine the HF fluids impact on rock permeability under reservoir-simulating conditions. The rocks were placed in a core holder, and reservoir conditions (pore pressure, temperature) were modeled, followed by oil circulation until stabilization of parameters, and then left to sit for 12 h. Subsequently, oil was pumped through the core column in the direction of reservoir-to-well, determining the working volumetric flow rate, corresponding to a linear flow rate of 3-5 m/day at 3-5 different flow

This is an open access article under the CC BY 4.0 license

rates, subsequently calculating the initial (base) permeability through oil. In the direction of well-to-reservoir, while maintaining constant repression, a broken gel solution was injected for the time required for HF operations. The system was held in static conditions for 12 h. Measurements of the amount of influent solution/filtrate into the core were taken. Following this, five pore volumes were injected into the core in the reservoir-to-well direction until stabilization pressure drop occurred, and filtration was performed using 3-5 different modes. Afterwards, permeability through oil was recalculated, with intermediate values fixed along the column.

Materials of the experiments. The subjects of the tests were real mineralized waters – Cenomanian, bottom, and mixed waters from the deposits of LLC "Gazpromneft-Khantos." In total, more than 50 water samples were analyzed from over 15 sampling points (sources) and hydraulic fracturing fluids prepared based on them. Table 1 presents the average values of the main parameters for the three types of investigated waters. According to the test results, it is evident that the examined waters possess high salinity, and the content of the main elements depends on the type of water. The Cenomanian waters exhibit the most stable parameters, whereas the bottom and mixed waters sampled from the main formation-pressure maintenance system pipelines show significant differences in properties, with iron concentration varying considerably, and hardness and total mineralization also undergoing substantial changes. The primary reason for such behavior of the indicated water systems in the formation-pressure maintenance system is the unstable operating modes of the injection well stock, where the flow rates of bottom and fresh waters differ. Thus, the considered bottom, mixed, and Cenomanian waters have high mineralization, with the greatest contribution coming from chloride ions, sodium, calcium ions, and bicarbonates.

Table 1

Avarage individual parameter values depending on the water type

Parameter	Water type		
	Bottom	Bottom + fresh (mixed)	Cenomanian
pH	7.9	7.9	7.8
Density at 20 °C, g/cm^3	1.005	1.003	1.010
Specific conductivity at 20 °C, μS/cm	207	161	496
Suspended solids, mg/dm^3	90	68	81
Total Fe, mg/dm^3	2.5	3.0	6.5
Oil products, mg/dm^3	4.0	3.3	0.2
Cl^-, mg/dm^3	3450	2463	9600
K^+, mg/dm^3	41	28	43
Na^+, mg/dm^3	3410	2175	5550
Ca^{2+}, mg/dm^3	263	198	360
Mg^{2+}, mg/dm^3	15	16	95
Sr^{2+}, mg/dm^3	7	5	29
Hardness, °dH (degrees of hardness)	14.4	11.2	26.2
HCO_3^-, mg/dm^3	1238	970	195
B^+, mg/dm^3	7.5	6.1	9.9
Total mineralization, mg/dm^3	8449	5876	15900

Rheological studies of the fracturing fluids were conducted on water samples from the sources of LLC "Gazpromneft-Khantos" (sewage pumping stations for bottom and mixed water, separate wells for Senomanian.) To model the effect of the developed fracturing fluids on the rock permeability, and to evaluate the dynamic transport of the proppant agent, model compositions were prepared from pure salts that simulate bottom and Senoman water (Table 2). Table 3 presents the formulations of the fracturing gels used in complex tests on model mineralized waters. The compositions include auxiliary (stabilizing) additives – a pH buffer (linear gel stabilizer) and a crosslinking stabilizer.

This is an open access article under the CC BY 4.0 license

Journal of Mining Institute. 2024. Vol. 270. P. 950-962
© Shamil K. Sultanov, Vyacheslav Sh. Mukhametshin, Alexandras P. Stabinskas,
Elchin F. Veliev, Artem V. Churakov, 2024

Table 2

Model mineralized waters composition, g/l

Bottom water		Cenomanian water	
Component	Content	Component	Content
$NaHCO_3$	1.7048	$NaHCO_3$	0.2688
NaCl	4.7699	NaCl	13.9291
KCl	0.0789	KCl	0.0820
$MgCl_2$	0.0610	$MgCl_2$	0.3768
$CaCl_2$	0.7309	$CaCl_2$	0.9990
$FeCl_3$	0.0073	$FeCl_3$	0.0189
H_3BO_3	0.0423	H_3BO_3	0.0558
Mineralization	7.4	Mineralization	15.73

Table 3

Guaro-borat formulation for water modelling

Bottom water		Cenomanian water	
Component	Concentration	Component	Concentration
Gelling agent, kg/m^3	3.6	Gelling agent, kg/m^3	3.6
Crosslinker, l/m^3	2.8	Crosslinker, l/m^3	2.8
Demulsifier, l/m^3	1.0	Demulsifier, l/m^3	1.0
Biocide, kg/m^3	0.02	Biocide, kg/m^3	0.02
pH buffer, kg/m^3	1.4	pH buffer, kg/m^3	–
Crosslinking stabilizer, l/m^3	1.0	Crosslinking stabilizer, l/m^3	1.0
Destructor, l/m^3	0.5	Destructor, l/m^3	0.5

Discussion.

Rheological testing and methodology for selecting the design of fracturing fluids from alternative sources. To assess the impact of water from alternative sources composition, a series of rheological tests was conducted to evaluate the stability of a classical guar system with a gelling agent concentration of 3.6 kg/m^3 and a borate crosslinker concentration of 3.0 l/m^3 at a temperature of 90 °C. The established requirement for the stability time of the system (viscosity above 400 mPa·s), which guided the system development, is set at 100 (±20) min. The test results and the graph of this system using distilled water are presented in Fig.1. According to the provided graphs, the characteristic behavior of the fracturing fluid prepared with mineralized sources without auxiliary additives under the specified conditions can be considered as follows: the absence of crosslinking of the linear gel (Fig.1, *a*), the initial drop in viscosity (prolonged crosslinking) of the system (Fig.1, *b*), and insufficient high-temperature stability of the system (Fig.1, *c*). A combination of these negative manifestations cannot be ruled out. It is important to note the problems associated with the hydration of the guar polymer in mineralized water, as in some cases there is a lack of viscosity build-up of the linear gel, low hydration rates, and viscosity drop. Additionally, with significant concentrations of crosslinking elements in the water, the linear gel may achieve abnormally high viscosity.

To eliminate the aforementioned negative manifestations, targeted or complex actions are necessary to neutralize the negatively influencing components of water from alternative sources. The main elements or parameters of water that need to be neutralized are: increased water hardness (above 500 mg/l – 10 °dH); increased alkalinity (bicarbonate ion concentration above 500 mg/l); elevated iron content (above 8 mg/l); high mineralization (above 1000 mg/l); and the presence of crosslinking ions in the water.

The high content of bicarbonate ions (increased alkalinity) and the presence of divalent and trivalent metal ions negatively affect the hydration parameters of guar. In such cases, a stabilizer for the linear gel is used, which consists of a water-soluble organic acid. The addition of this agent is made to the water before the hydration of the polymer begins.

This is an open access article under the CC BY 4.0 license

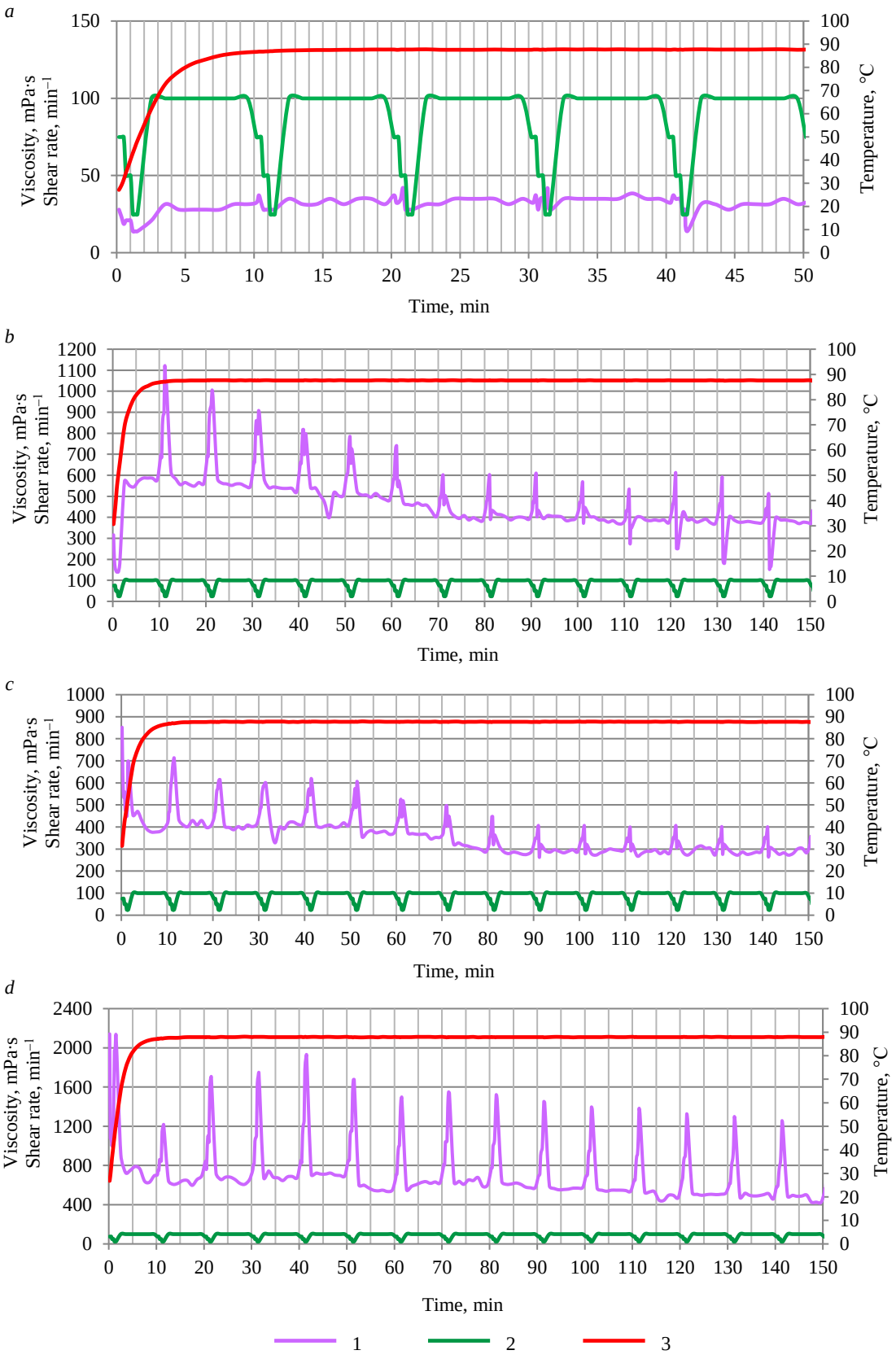

Fig.1. Classical guar system on water from alternative sources behavior:
a – bottom water: mineralization 7700 mg/l, hardness 20 °dH, alkalinity 1200 mg/l;
b – bottom water: mineralization 6800 mg/l, hardness 4 °dH, alkalinity 1400 mg/l; *c* – mixed water:
mineralization 3300 mg/l, hardness 11 °dH, alkalinity 770 mg/l; *d* – fresh (distilled) water
1 – viscosity; 2 – shear rate; 3 – temperature

This is an open access article under the CC BY 4.0 license

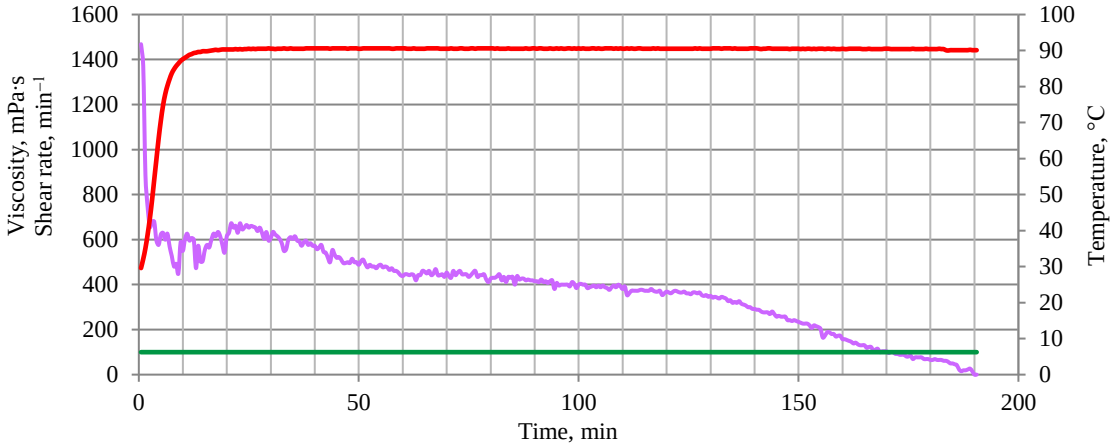

Fig.2. The change in the hydraulic fracturing fluid effective viscosity on the bottom water from the temperature and characteristics of the gels (at a constant value of the shear rate of 100 m/min). See the legend in Fig.1

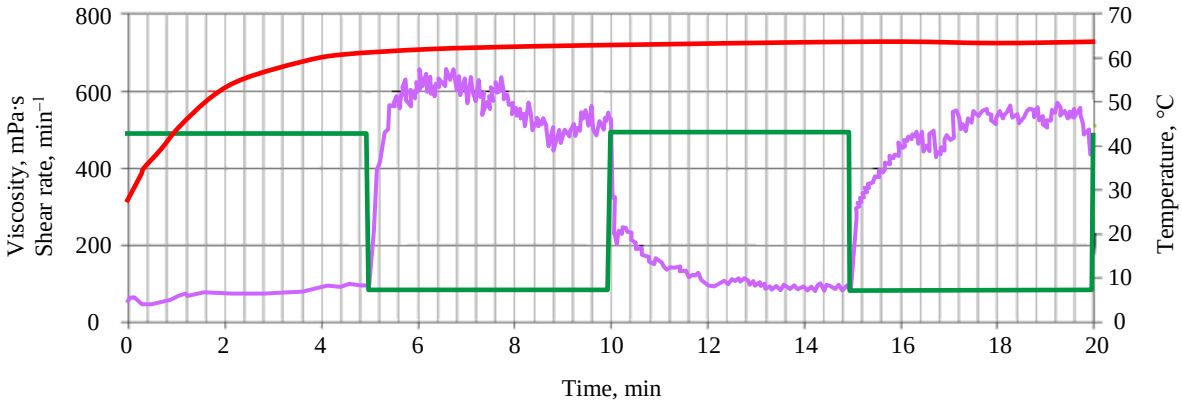

Fig.3. A test to determine the sensitivity of hydraulic fracturing fluid on bottom water to a change in shear load. See the legend in Fig.1

Increased water hardness is another negative parameter limiting the use of alternative sources for standard guar systems. Two directions have been proposed to solve this problem: the use of a chelating additive based on organic salt and the use of a combined crosslinking stabilizer based on amino alcohols. The results of a comprehensive study of the rheological properties of the developed systems in some real waters using the above stabilizers are presented.

• Bottom water – mineralization is 4700 mg/l, hardness is 2.4 °dH, alkalinity is 880 mg/l. Without specialized additives, the cross-linked system shows insufficient stability (about 50 min), which does not meet the criteria given earlier: bactericide is 0.02 l/m^3, gel breaker is 2.0 l/m^3, gelling agent is 3.6 kg/m^3, destructor is 0.4 l/m^3, delayed action cross-linker is 3.2 l/m^3, crosslinking stabilizer is 1.0 l/m^3.

The change in the effective viscosity of the liquid with hydraulic fracturing gels parameters from temperature is shown in Fig.2. The liquid stability at the specified component content is optimal for 100 min, which corresponds to the criteria set in the study: linear gel – viscosity is 26.0 mPa·s, closing temperature is 40 °C, pH value is 8.2; crosslinked gel – closing time of the funnel is 30 s, full cross-linking time is 45 s, pH value is 9.0.

Figure 3 shows the result of testing the sensitivity of the fracturing fluid closed on the bottom water to a change in the shear rate. The restoration of the system to the effective viscosity values after applied shear loads occurs in less than 30 s, which is an acceptable indicator for hydraulic fracturing operations. Static tests for the transportation of a proppant material, a ceramic proppant of fraction 16/20 with a concentration of 400 kg/m^3, were carried out at a formation temperature. The results

This is an open access article under the CC BY 4.0 license

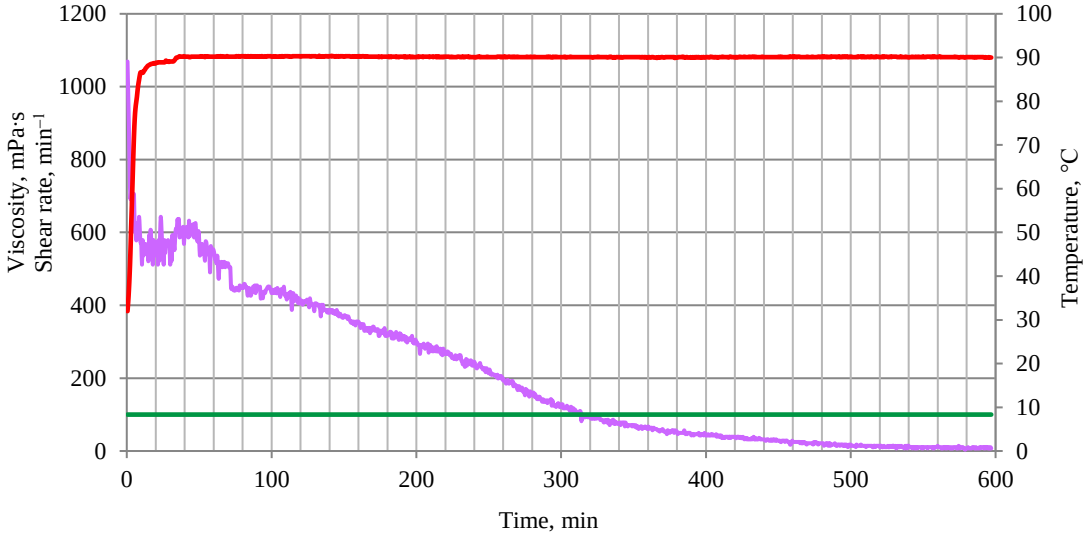

Fig.4. The change in the effective viscosity of the hydraulic fracturing fluid in mixed water from the temperature and gels characteristics (at a constant shear rate value of 100 m/min). See the legend in Fig.1

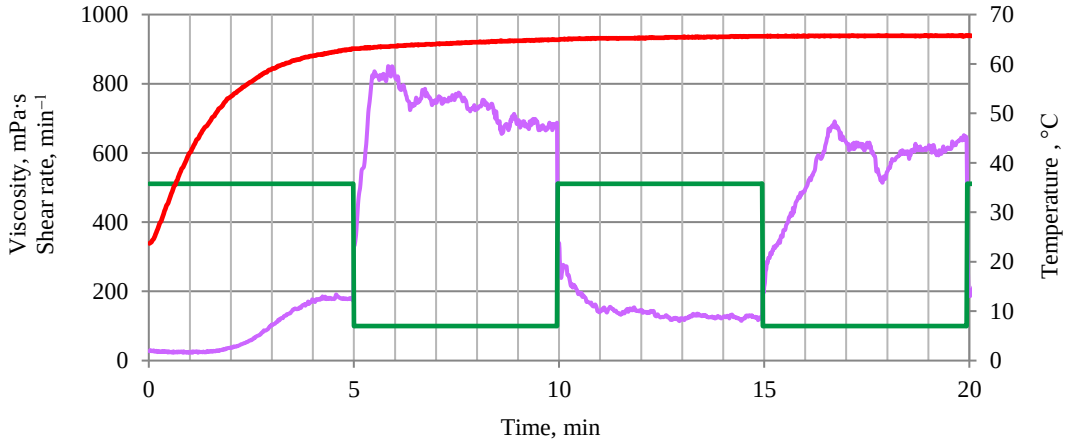

Fig.5. Test to determine the sensitivity of hydraulic fracturing fluid on mixed water to shear load. See the legend in Fig.1

obtained under the same conditions on distilled water (without special additives) were compared. Both tests showed satisfactory results in comparison with freshwater systems. At the end of the hydraulic fracturing fluid rheological tests, a test for complete and rapid destruction was carried out. The viscosity of the destroyed gel was less than 5 mPa·s.

• Mixed water – mineralization is 5400 mg/l, hardness is 12 °dH, alkalinity is 710 mg/l. During the evaluation test, the additive-free system showed no crosslinking. The reason for the lack of crosslinking and the deterioration of the rheological properties of the system is the increased water mineralization, as well as high hardness, which determine the use of a crosslinking stabilizer and a chelating agent for this water. The formulation of the guar system for operation on mixed water is given: bactericide is 0.02 l/m^3, demulsifier is 2.0 l/m^3, linear gel stabilizer is 1.4 kg/m^3, chelating agent is 0.25 kg/m^3, gelling agent is 3.6 kg/m^3, destructor is 0.5 l/m^3, delayed action crosslinker is 2.8 l/m^3, stabilizer crosslinking is 0.5 l/m^3. The change in effective viscosity from temperature indicates acceptable stability of the system (Fig.4): linear gel – viscosity is 22.0 mPa·s, closing temperature is 40 °C, pH value is 5.6; crosslinked gel – closing time of the funnel is 60 s, full crosslinking time is 65 s, pH value is 8.6. Figure 5 shows the result of testing hydraulic fracturing fluid on mixed water for its sensitivity to shear rate changes.

This is an open access article under the CC BY 4.0 license

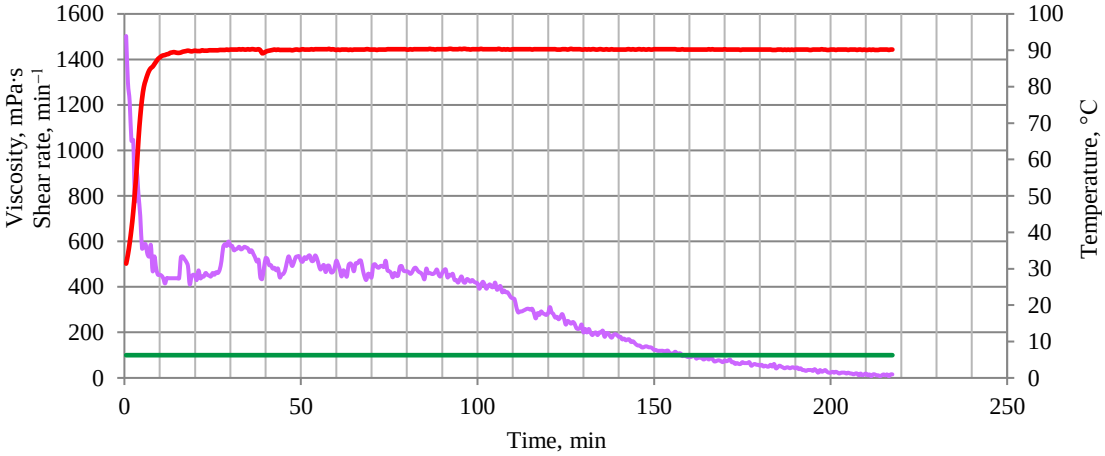

Fig.6. The change in the effective viscosity of the hydraulic fracturing fluid in Cenomanian water from the temperature and gels characteristics (at a constant shear rate of 100 m/min). See the legend in Fig.1

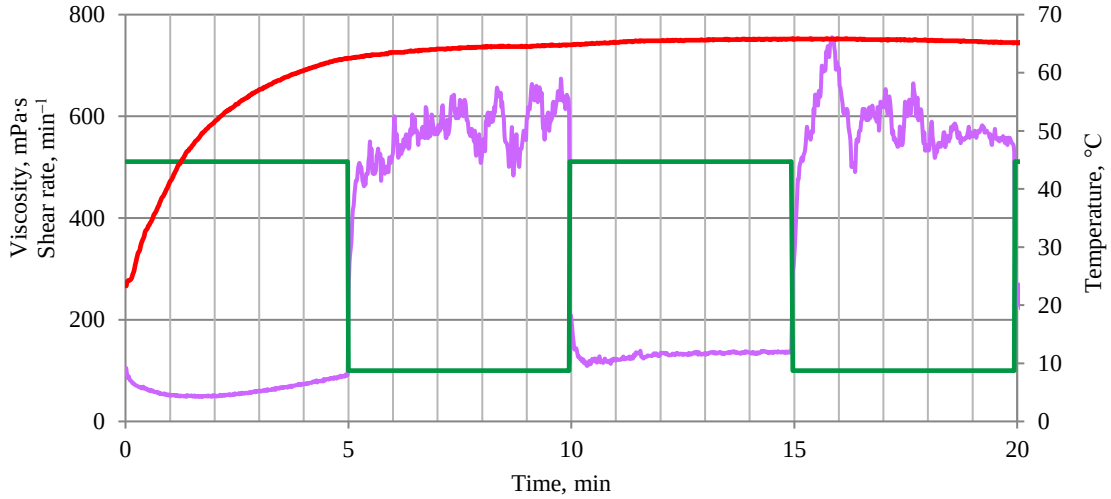

Fig.7. Test to determine the sensitivity of hydraulic fracturing fluid to changes in shear load at the Cenomanian source. See the legend in Fig.1

• Cenomanian – mineralization is 17300 mg/l, hardness is 30 °dH, alkalinity is 190 mg/l. A feature of the behavior of the system at most Cenomanian sources in the case of using no stabilizers is high temperature destruction. To obtain the required properties, the main emphasis is placed on suppressing increased mineralization and hardness in comparison with bottom and mixed sources. The use of a linear gel stabilizer in such cases is either not required at all, or is limited to low dosages. The high water hardness is neutralized by the chelating agent and/or a crosslinking stabilizer introduction into the classical guar system. The results of the work on the fracturing fluid system design selection at the Cenomanian source: bactericide is 0.02 l/m^3, demulsifier is 2.0 l/m^3, gelling agent is 3.6 kg/m^3, destructor is 0.5 l/m^3, delayed action crosslinker is 3.0 l/m^3, crosslinking stabilizer is 2.0 l/m^3. Figure 6 shows the change in the hydraulic fracturing fluid effective viscosity from the temperature with gel parameters: linear gel viscosity is 26.0 mPa·s, closing temperature is 40 °C, pH value is 7.6; crosslinked gel – funnel closing time is 30 s, full crosslinking time is 45 s, pH value is 9.0. Liquid stability at the specified content of the components is the optimal 100 min. Figure 7 shows the system under consideration behavior under shear loads. Of the listed negatively affecting components, it is also necessary to consider the increased iron content and crosslinking ions

This is an open access article under the CC BY 4.0 license

contained in water. From the practice of hydraulic fracturing operations, compositions of stabilizers are known, for example, based on sugars, which effectively suppress the action of this element. The stabilizing additives noted in rheological tests are also able to effectively affect the excess iron in the waters of alternative sources. The issue of boron ion suppression is solved, as a rule, by introducing crosslinking retarders based on highly soluble sugars into the system.

Core tests. One of the key factors determining the fluid work efficiency after the fracturing operation is its effect on the rock reservoir properties. As part of a comprehensive study, tests of the developed hydraulic fracturing fluid designs that have successfully passed rheological tests were carried out to assess the impact on the rock properties. The compositions of hydraulic fracturing fluids (Table 3) on mineralized waters (see Table 2) tested on the core material of the Priobsky and Yuzhno-Priobsky deposits (target formation AC12.3-5), which investigated the effect of compositions on the rock permeability under conditions simulating formation conditions. Lithologically, the samples are represented by sandstones and siltstones. The open water porosity, determined from 40 samples, varies from 13.8 to 18.7 % (the average value is 16.4 %). The open porosity of helium, determined from 104 samples, varies from 2.3 to 18.4 % (the average value is 14.3 %). After that, tests were carried out to assess the effect of hydraulic fracturing fluids on rock permeability (Table 4).

Table 4

Generalized results of determining the hydraulic fracturing fluids effect on reservoir rock permeability

Type of hydraulic fracturing fluid	Laboratory number of the sample	Open porosity by water, %	Absolute gas permeability K_{per}, $10^{-3}\mu M^2$	Residual water saturation K_w, %	The basic permeability of the oil sample, 10^{-3}mkm^2	Permeability recovery coefficient after exposure HF, %	Permeability recovery after depression coefficient, %	Water saturation after operation value, %	Change in water saturation, %
Gel 1 Bottom water/ guar system	28244-10	14.4	1.23	36.6	0.334	19.7	32.1	25.0	–11.5
	28229-10	16.4	1.08	44.1	0.240	23.6	45.7	35.5	–8.6
	23596-18	16.5	0.91	39.4	0.197	27.8	42.6	30.5	–8.9
	28159-10	16.6	0.75	41.9	0.120	43.5	60.6	35.2	–6.7
		15.9	**0.99**	**40.5**	**0.223**	**28.6**	**45.2**	**31.6**	**–8.9**
Gel 2 Cenomanian water/ guar system	28235-10	16.5	1.14	38.6	0.255	23.1	39.7	29.4	–9.2
	28242-10	15.3	1.04	37.2	0.186	21.9	43.3	29.5	–7.7
	28154-10	16.1	0.87	41.7	0.127	28.3	40.3	34.0	–7.7
	28237-10	15.7	0.69	42.5	0.102	29.8	38.3	33.7	–8.8
		15.9	**0.94**	**40.0**	**0.168**	**25.8**	**40.4**	**31.7**	**–8.4**
Gel 3 Distilled water/ guar system	23625-18	15.7	1.70	34.1	0.452	23.37	35.03	28.7	–5.4

According to the results obtained, systems based on alternative sources are not inferior to the guar system in terms of their effect on the residual permeability of the reservoir prepared with distilled water. This is evidenced by permeability recovery coefficients values, which indicate that the permeability during the period from the immediate hydraulic fracturing to the start of commissioning of the well is restored by 1.5 times due to the time of helium composition destruction.

Conclusions.

The bottom, mixed, and Cenomanian waters considered in this article have a high mineralization, the greatest contribution to which is made by chlorine ion, sodium ions, calcium and bicarbonates. The determining factor in liquid and stabilizing additive choosing is the composition and properties of water from a single source, which are subject to significant change and depend on many factors such as time and method of selection, temperature, interaction with the environment, etc.

This is an open access article under the CC BY 4.0 license

Cenomanian sources have the most stable mineralization parameters, while the bottom and mixed waters selected from the pressure maintenance system have significant differences in properties. For such sources, the amount of iron can vary significantly, and the hardness and overall mineralization also undergo significant changes.

The quality of the considered fracturing fluids based on alternative water sources is confirmed by their effect on the residual formation permeability, as well as the residual permeability and proppant pack permeability. The experimental results presented in this paper show similar values of these parameters. The results of studies on the determination of the remaining conductivity and permeability of the proppant pack at 6000 psi showed that for guar, Cenomanian and fresh waters, the residual conductivity was respectively 38; 37; 36 %, and the residual permeability was 38; 38; 36 %.

The considered hydraulic fracturing fluids based on alternative water sources are a promising direction for industrial use in the oil industry, as they contribute to reducing the produced hydrocarbons cost by minimizing the cost of their preparation and delivery, reducing the negative impact on the environment while maintaining the quality inherent in classical systems of liquid at fresh sources. For the best understanding of the key properties and features of the developed formulations, large-scale pilot tests are necessary, which will consolidate and improve the results achieved at the current stage.

REFERENCES

1. Kontorovich A.E., Burshtein L.M., Livshits V.R., Ryzhkova S.V. Main Directions of Development of the Oil Complex of Russia in the First Half of the Twenty-First Century. *Herald of the RAS.* 2019. Vol. 89. N 6, p. 558-566. DOI: 10.31857/S0869-587389111095-1104

2. Dmitrievsky A.N. Resource-innovative strategy for the development of the Russian economy. *Oil Industry Journal.* 2017. N 5, p. 6-7 (in Russian).

3. Muslimov R.Kh. A new strategy for the development of oil fields in modern Russia is to optimize production and maximize KIN (oil recovery factor). *Neft. Gaz. Novatsii*. 2016. N 4 (187), p. 8-17 (in Russian).

4. Mukhametshin V.Sh., Khakimzyanov I.N., Bakhtizin R.N., Kuleshova L.S. Differentiation and grouping of complex-structured oil reservoirs in carbonate reservoirs in development management problems solving. *SOCAR Proceedings.* 2021. Special Issue 1, p. 88-97 (in Russian). DOI: 10.5510/OGP2021SI100513

5. Mukhametshin V.V., Bakhtizin R.N., Kuleshova L.S. et al. Screening and assessing the conditions for effective oil recovery enhancing techniques application for hard to recover high-water cut reserves. *SOCAR Proceedings.* 2021. Special Issue 2, p. 48-56 (in Russian). DOI: 10.5510/OGP2021SI200588

6. Yang S., Siddhamshetty P., Kwon J. S.-I. Optimal pumping schedule design to achieve a uniform proppant concentration level in hydraulic fracturing. *Computers & Chemical Engineering*. 2017. Vol. 101, p. 138-147. DOI: 10.1016/j.compchemeng.2017.02.035

7. Grishchenko V.A., Rabaev R.U., Asylgareev I.N. et al. Methodological approach to optimal geological and technological characteristics determining when planning hydraulic fracturing at multilayer facilities. *SOCAR Proceedings.* 2021. Special Issue 2, p. 182-191 (in Russian). DOI: 10.5510/OGP2021SI200587

8. Grishchenko V.A., Pozdnyakova T.V., Mukhamadiyev B.M. et al. Improving the carbonate reservoirs development efficiency on the example of the Tournaisian stage deposits. *SOCAR Proceedings.* 2021. Special Issue 2, p. 238-247 (in Russian). DOI: 10.5510/OGP2021SI200603

9. Wijaya N., Sheng J.J. Comparative study of well soaking timing (pre vs. post flowback) for water blockage removal from matrix-fracture interface. *Petroleum*. 2020. Vol. 6. Iss. 3, p. 286-292. DOI: 10.1016/j.petlm.2019.11.001

10. Mukhametshin V.V. Eliminating uncertainties in solving bottom hole zone stimulation tasks. *Bulletin of the Tomsk Polytechnic University. Geo Assets Engineering.* 2017. Vol. 328. N 7, p. 40-50 (in Russian).

11. Khisamiev T.R., Bashirov I.R., Mukhametshin V.Sh. et al. Results of the development system optimization and increasing the efficiency of carbonate reserves extraction of the turney stage of the Chetyrmansky deposit. *SOCAR Proceedings.* 2021. Special Issue 2, p. 131-142 (in Russian). DOI: 10.5510/OGP2021SI200598

12. Jiaxiang Xu, Yunhong Ding, Lifeng Yang et al. Effect of proppant deformation and embedment on fracture conductivity after fracturing fluid loss. *Journal of Natural Gas Science and Engineering*. 2019. Vol. 71. N 102986. DOI: 10.1016/j.jngse.2019.102986

13. Galkin V.I., Koltyrin A.N. Investigation of probabilistic models for forecasting the efficiency of proppant hydraulic fracturing technology. *Journal of Mining Institute.* 2020. Vol. 246, p. 650-659. DOI: 10.31897/PMI.2020.6.7

14. Yakupov R.F., Mukhametshin V.Sh., Khakimzyanov I.N., Trofimov V.E. Optimization of reserve production from water oil zones of D3ps horizon of Shkapovsky oil field by means of horizontal wells. *Georesources.* 2019. Vol. 21. N 3, p. 55-61 (in Russian). DOI: 10.18599/grs.2019.3.55-61

15. Fokker P.A., Borello E.S., Verga F., Viberti D. Harmonic pulse testing for well performance monitoring. *Journal of Petroleum Science and Engineering*. 2018. Vol. 162, p. 446-459. DOI: 10.1016/j.petrol.2017.12.053

This is an open access article under the CC BY 4.0 license

16. Grishchenko V.A., Gareev R.R., Tsiklis I.M. et al. Expanding the amount of preferential royalty facilities with hard-to-recover oil reserves. *SOCAR Proceedings.* 2021. Special Issue 2, p. 8-17 (in Russian). DOI: 10.5510/OGP2021SI200575

17. *Cheng Jing, Xiaowei Dong, Wenhao Cui et al.* Artificial neural network-based time-domain interwell tracer testing for ultralow-permeability fractured reservoirs. *Journal of Petroleum Science and Engineering*. 2020. Vol. 195. N 107558. DOI: 10.1016/j.petrol.2020.107558

18. Yakupov R.F., Mukhametshin V.S., Tyncherov K.T. Filtration model of oil coning in a bottom water-drive reservoir. *Periódico Tchê Química*. 2018. Vol. 15. Iss. 30, p. 725-733. DOI: 10.52571/PTQ.v15.n30.2018.725_Periodico30_pgs_725_733.pdf

19. Fattakhov I.G., Kuleshova L.S., Bakhtizin R.N. et al. Complexing the hydraulic fracturing simulation results when hybrid acid-propant treatment performing and with the simultaneous hydraulic fracture initiation in separated intervals. *SOCAR Proceedings.* 2021. Special Issue 2, p. 103-111 (in Russian). DOI: 10.5510/OGP2021SI200577

20. Kuleshova L.S., Fattakhov I.G., Sultanov Sh.Kh. et al. Experience in conducting multi-zone hydraulic fracturing on the oilfield of PJSC "Tatneft". *SOCAR Proceedings.* 2021. Special Issue 1, p. 68-76 (in Russian). DOI: 10.5510/OGP2021SI100511

21. Keshavarz A., Yulong Yang, Badalyan A. et al. Laboratory-based mathematical modelling of graded proppant injection in CBM reservoirs. *International Journal of Coal Geology*. 2014. Vol. 136, p. 1-16. DOI: 10.1016/j.coal.2014.10.005

22. Grishchenko V.A., Asylgareev I.N., Bakhtizin R.N. et al. Methodological approach to the resource base efficiency monitoring in oil fields development. *SOCAR Proceedings.* 2021. Special Issue 2, p. 229-237 (in Russian). DOI: 10.5510/OGP2021SI200604

23. Mukhametshin V.V. Improving the Efficiency of Managing the Development of the West Siberian Oil and Gas Province Fields on the Basis of Differentiation and Grouping. *Russian Geology and Geophysics.* 2021. Vol. 62. N 12, p. 1373-1384. DOI: 10.15372/GiG2021102

24. Nurgaliev R.Z., Kozikhin R.A., Fattakhov I.G., Kuleshova L.S. Application prospects for new technologies in geological and technological risk assessment. *Gornyi zhurnal.* 2019. N 4, p. 36-40 (in Russian). DOI: 10.17580/gzh.2019.04.08

25. Temizel C., Canbaz C.H., Palabiyik Y. et al. A Review of Hydraulic Fracturing and Latest Developments in Unconventional Reservoirs. Offshore Technology Conference, 2-5 May 2022, Houston, TX, USA. OnePetro, 2022. N OTC-31942-MS. DOI: 10.4043/31942-MS

26. Linsong Cheng, Deqiang Wang, Renyi Cao, Rufeng Xia. The influence of hydraulic fractures on oil recovery by water flooding processes in tight oil reservoirs: An experimental and numerical approach. *Journal of Petroleum Science and Engineering*. 2020. Vol. 185. N 106572. . DOI: 10.1016/j.petrol.2019.106572

27. Khuzin R.R., Andreev V.E., Mukhametshin V.V. et al. Influence of hydraulic compression on porosity and permeability properties of reservoirs. *Journal of Mining Institute.* 2021. Vol. 251, p. 688-697. DOI: 10.31897/PMI.2021.5.8

28. Nesic S., Streletskaya V.V. An integrated approach for produced water treatment and injection. *Georesources.* 2018. Vol. 20. N 1, p. 25-31. DOI: 10.18599/grs.2018.1.25-31

29. Kontorovich A.E., Varlamov A.I., Efimov A.S. et al. Stratigraphic Scheme of Cambrian Deposits, South of the Cis-Yenisei Area of West Siberia. *Russian Geology and Geophysics.* 2021. Vol. 62. N 3, p. 357-376. DOI: 10.15372/GiG2020206

30. Stabinskas A.P., Sultanov Sh.Kh., Mukhametshin V.Sh. et al. Evolution of hydraulic fracturing fluid: from guar systems to synthetic gelling polymers. *SOCAR Proceedings.* 2021. Special Issue 2, p. 172-181 (in Russian). DOI: 10.5510/OGP2021SI200599

31. Sergeev V.V., Sharapov R.R., Kudymov A.Y. et al. Experimental research of the colloidal systems with nanoparticles influence on filtration characteristics of hydraulic fractures. *Nanotechnologies in Construction.* 2020. Vol. 12. N 2, p. 100-107. DOI: 10.15828/2075-8545-2020-12-2-100-107

32. Stabinskas A.P. Efficiency estimation of oil well after hydraulic fracturing treatment. *Problems of Gathering, Treatment and Transportation of Oil and Oil Products.* 2014. N 1 (95), p. 10-20 (in Russian).

33. Chenguang Zhang, Xiting Long, Xiangwei Tang et al. Implementation of water treatment processes to optimize the water saving in chemically enhanced oil recovery and hydraulic fracturing methods. *Energy Reports.* 2021. Vol. 7, p. 1720-1727. DOI: 10.1016/j.egyr.2021.03.027

34. Zakharov L.A., Martyushev D.A., Ponomareva I.N. Predicting dynamic formation pressure using artificial intelligence methods. *Journal of Mining Institute.* 2022. Vol. 253, p. 23-32. DOI: 10.31897/PMI.2022.11

35. Krivoshchekov S.N., Kochnev A.A., Ravelev K.A. Development of an algorithm for determining the technological parameters of acid composition injection during treatment of the near-bottomhole zone, taking into account economic efficiency. *Journal of Mining Institute.* 2021. Vol. 250, p. 587-595. DOI: 10.31897/PMI.2021.4.12

36. Khuzin R.R., Andreev V.E., Mukhametshin V.V. et al. Influence of hydraulic compression on porosity and permeability properties of reservoirs. *Journal of Mining Institute.* 2021. Vol. 251, p. 688-697. DOI: 10.31897/PMI.2021.5.8

37. Siddhamshetty P., Mao S., Wu K., Kwon J.S.-I. Multi-Size Proppant Pumping Schedule of Hydraulic Fracturing: Application to a MP-PIC Model of Unconventional Reservoir for Enhanced Gas Production. *Processes*. 2020. Vol. 8. Iss. 5. N 570. DOI: 10.3390/pr8050570

38. Veil J.A., Clark C. Produced Water Volume Estimates and Management Practices. *SPE Production & Operations*. 2011. Vol. 26. Iss. 3, p. 234-239. DOI: 10.2118/125999-PA

39. Sun Huning, Xie Xuan, Gao Guanghui et al. Patent N CN 10275778 B. Fracturing fluid capable of resisting high salinity water quality. Publ. 14.08.2012.

40. Rogachev M.K., Mukhametshin V.V., Kuleshova L.S. Improving the efficiency of using resource base of liquid hydrocarbons in Jurassic deposits of Western Siberia. *Journal of Mining Institute.* 2019. Vol. 240, p. 711-715. DOI: 10.31897/PMI.2019.6.711

This is an open access article under the CC BY 4.0 license

41. Shlyapkin A.S., Tatosov A.V. Formation of a hydraulic fracture by a high-viscous gel. *Geology, Geophysics and Development of Oil and Gas Fields.* 2020. N 9 (345), p. 109-112 (in Russian). DOI: 10.30713/2413-5011-2020-9(345)-109-112

42. Kakadjian S., Thompson J., Torres R. Fracturing Fluids from Produced Water. SPE Production and Operations Symposium, 1-5 March 2015, Oklahoma City, OK, USA. OnePetro, 2015. N SPE-173602-MS.

43. Wang Shi Ben, Guo Jian Chun, Lai Ji et al. Patent N CN 103497753 B. One is applicable to the of the fracturing fluid linking agent of concentrated water. Publ. 30.09.2013.

44. Siddhamshetty P., Seeyub Yang, Kwon J.S.-I. Modeling of hydraulic fracturing and designing of online pumping schedules to achieve uniform proppant concentration in conventional oil reservoirs. *Computers & Chemical Engineering*. 2018. Vol. 114, p. 306-317. DOI: 10.1016/j.compchemeng.2017.10.032

Authors: **Shamil K. Sultanov,** *Doctor of Engineering Sciences, Professor, https://orcid.org/0000-0003-3481-9519* (*Ufa State Petroleum Technological University, Ufa, Republic of Bashkortostan, Russia*), **Vyacheslav Sh. Mukhametshin**, *Doctor of Geological and Mineralogical Sciences, Director, vsh@of.ugntu.ru, https://orcid.org/0000-0002-3951-4936* (*Institute of Oil and Gas of the Federal State Budgetary Educational Institution of Higher Education "Ufa State Petroleum Technological University" in the City of Oktyabrsky, Oktyabrsky, Republic of Bashkortostan, Russia*), **Alexandras P. Stabinskas,** *Head of the Department, https://orcid.org/0000-0002-3833-8096* (*LLC "Gazpromneft S&TC", Saint Petersburg, Russia*), **Elchin F. Veliev,** *Candidate of Engineering Sciences, Deputy Head of the Laboratory, https://orcid.org/0000-0003-2803-4467* (*NIPI "Neftegaz", SOCAR, Baku, Republic of Azerbaijan*), **Artem V. Churakov**, *Head of the Center, https://orcid.org/0000-0001-6070-9255* (*LLC "Gazpromneft S&TC", Saint Petersburg, Russia*).

The authors declare no conflict of interests.

This is an open access article under the CC BY 4.0 license

ISSN 2411-3336; e-ISSN 2541-9404

JOURNAL OF MINING INSTITUTE

Zapiski Gornogo instituta

Journal homepage: pmi.spmi.ru

Research article

Normalized impulse response testing in underground constructions monitoring

Aleksei A. Churkin[1], **Vladimir V. Kapustin**[2], **Mikhail S. Pleshko**[3]✉

[1] *Gersevanov Research Institute of Bases and Underground Structures, Moscow, Russia*

[2] *Lomonosov Moscow State University, Moscow, Russia*

[3] *National University of Science and Technology "MISiS", Moscow, Russia*

How to cite this article: Churkin A.A., Kapustin V.V., Pleshko M.S. Normalized impulse response testing in underground constructions monitoring. Journal of Mining Institute. 2024. Vol. 270, p. 963-976.

Abstract

Impulse Response testing is a widespread geophysical technique of monolithic plate-like structures (foundation slabs, tunnel lining, and supports for vertical, inclined and horizontal mine shafts, retaining walls) contact state and grouting quality evaluation. Novel approach to data processing based on normalized response attributes analysis is presented. It is proposed to use the energy of the normalized signal calculated in the time domain and the normalized spectrum area and the average-weighted frequency calculated in the frequency domain as informative parameters of the signal. The proposed technique allows users a rapid and robust evaluation of underground structure's grouting or contact state quality. The advantage of this approach is the possibility of using geophysical equipment designed for low strain impact testing of piles length and integrity to collect data. Experimental study has been carried out on the application of the technique in examining a tunnel lining physical model with a known position of the loose contact area. As examples of the application of the methodology, the results of the several monolitic structures of operating municipal and transport infrastructure underground structures survey are presented. The applicability of the technique for examining the grouting of the tunnel lining and the control of injection under the foundation slabs is confirmed. For data interpretation the modified three-sigma criteria and the joint analysis of the attribute's behavior were successfully used. The features of the field work methodology, data collection and analysis are discussed in detail. Approaches to the techniques' development and its application in the framework of underground constructions monitoring are outlined. The issues arising during acoustic examination of reinforced concrete plate-like structures are outlined.

Keywords

nondestructive testing; technical geophysics; impulse response testing; underground constructions; soil-structure contact state; grouting quality; void detection; attribute analysis

Received: 27.07.2023 ***Accepted: 03.06.2024*** ***Online: 01.08.2024*** ***Published: 25.12.2024***

Introduction.

Reinforced concrete structures like tunnel lining, shaft support, foundation slabs, etc. (so-called plate-like structures) are widespread in underground construction. Many of them are operated in difficult conditions, characterized by great depths, high stress values, dynamic manifestations of rock pressure, intense water inflows, disturbance of the enclosing soils, etc. [1]. Those factors have a negative effect on the structures technical condition and lead to a significant growth of costs for their current maintenance and overhaul [2]. Another aspect of the urban underground construction is an excluding of the negative impact on the surrounding environment. In tunneling this is achieved by using modern shield systems with active face loading and the construction of lining immediately after the shield is moving [3, 4]. Grouting injection improves the distribution of the static loads, reduces material deformations, prevents the settlements, increases water tightness, and, as a result, increases the durability of construction [5-7].

This is an open access article under the CC BY 4.0 license

Quality control of soil-structure's contact state and performed grouting should be carried out systematically. To survey massive monolithic constructions of significant linear dimensions, geophysical techniques are often used due to their ability to indirectly assess the state of the structure and its interaction with soils [8-11]. To fulfil the task of underground structures state evaluation, a few non-destructive methods are mainly used:

• Ground-penetrating radar (GPR) profiling allows determining the reinforcement state and presence of defects in structure [12, 13], assessing the state of the lining-soil contact [14, 15] and even evaluation of grout layer thickness is possible [16].

• Ultrasonic tomography [17, 18] mainly used to assess the strength of concrete lining, the crack opening depth, presence of inner defects and the determination of the reinforcement step.

• Acoustic survey carried out by Impact-echo (IE) or Impulse Response (IR) techniques [19-21], makes it possible to evaluate the integral characteristics of the structure in different scales [22-24] and localize the zones of anomalous contact or grouting state [25, 26].

• Some techniques such as Infrared Thermometry profiling [27], Resistivity survey [28] or Surface Waves analysis [29-31], also used for examination of plate-like structures, but less often.

In this paper, we present a technique of normalized impulse response processing and analyzing (described in [26]), that allows to get rapid and robust assessment of the contact state or grouting quality for various types of underground structures. The advantage of this technique in comparison with the mobility response testing method, which is widely used in foreign practice, is that there is no need to use a calibrated signal source (a striker with a force sensor). The acoustic response is described by parameters whose behavior is determined by signal features that are stable to small changes in the impact force (the duration of the oscillation train and their distribution over a characteristic frequency range). In addition, the behavior of the response is sensitive to the presence of air-filled voids at the soil-structure interface, which allows the technique to be used in combination with GPR profiling (which makes it possible to successfully localize flooded zones, but does not allow air voids to be confidently identified) to increase the reliability of conclusions based on the results of a geophysical survey.

We use physical model of segmental liner with grout behind to make sure that proposed approach works. Based on the model results, some features of signal processing are described. Some examples of technique's application on surveying underground structures are given. Finally, we enlist some of leaks and gaps of our study and suggested directions for future investigations.

Methods.

In terms of acoustic survey, the grouted media may be described as multi-layered (structure-grout-soil) system. Thus, the tasks of grouting quality control and evaluation of soil-structure (two-layered system) contact conditions can be considered jointly. A complex wave field can be excited in that kind of media.

Impulse Response and Impact-echo techniques are based on the phenomenon of the occurrence of low-frequency and high-frequency resonant oscillations, respectively (Fig.1, *a*). Inducing free oscillations in a soil-structure system and analyzing of response in different frequency ranges therefore have different resolution capability. Selection of frequency ranges involves a "scale factor" – the higher frequencies are selected, the smaller the discontinuities affect the recorded data [22].

IE method is based on the "thickness resonance" phenomenon caused by the standing waves formation because of multiple reflections from the upper and lower surfaces of the structure. Data processing can be carried out both in the frequency and in the time domains (for thick slabs, when direct and reflected pulses are resolved in time). Spectral attributes analysis is actively used for data interpretation [20, 32-34]. IE testing allows detecting defects with size of tens of centimeters and therefore can be used for detailed inspection of a selected section of a structure.

This is an open access article under the CC BY 4.0 license

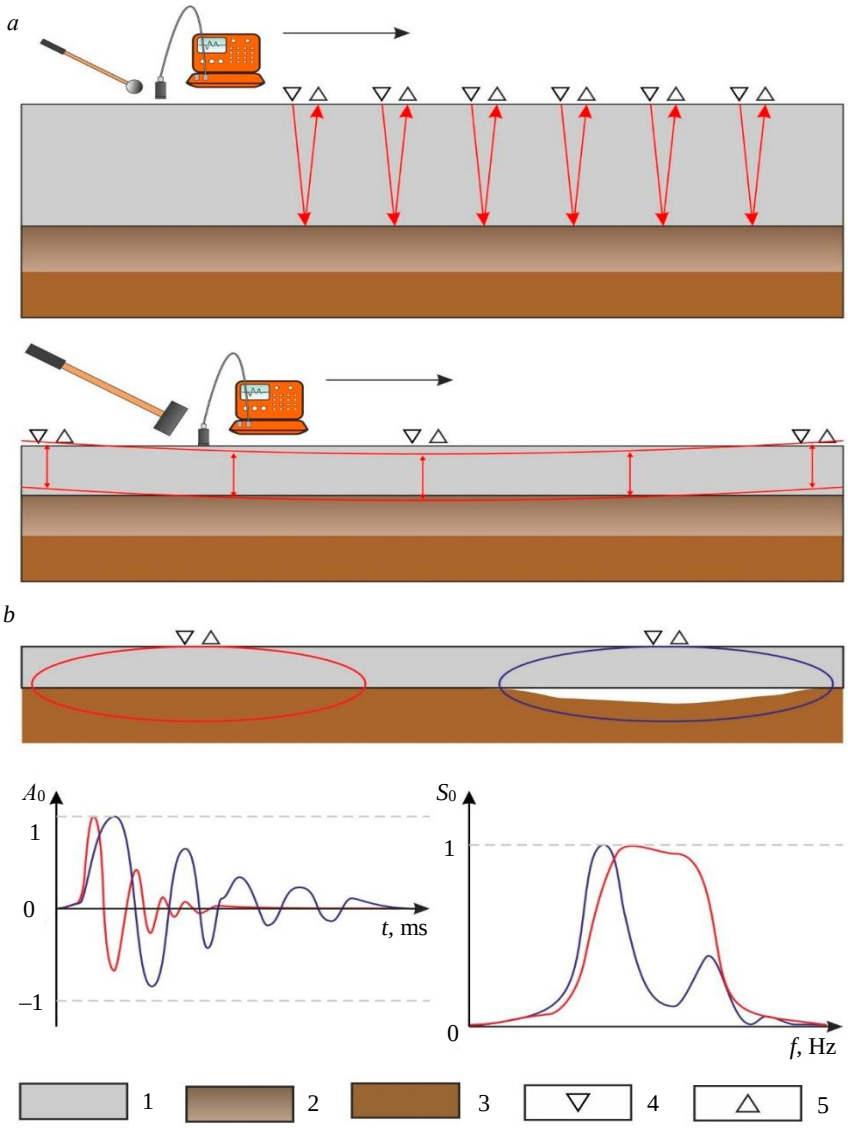

Fig.1. acoustic testing of plate-like structures
by impact-echo and impulse response (*a*) and the principle of a normalized impulse response formation (the volume of the medium involved in the oscillation and the idealized response in the time and frequency domains) (*b*)
1 – reinforced concrete; 2 – grouting; 3 – soil; 4 – source; 5 – receiver

IR method is based on the phenomenon of the low bending oscillations emergence of the medium volume between the defect (loose contact or grouting failure) and the free surface (plate-air interface). The idea of the technique itself is very similar to the "local defect resonance" concept in nonlinear ultrasonic testing [35]: bending oscillations in multi-layered structures cause harmonic resonance in zones of delamination. For linear-elastic body model wave-defect interaction manifests itself in amplitude and phase variations of the input signal. The technique has enough modifications, differing both in the type of oscillations induction (vibration or pulsed) and in the data processing [9, 26, 36, 37]. Low frequency IR testing is used to detect large contact state or grouting failures (from first meters in plan and more).

Bending oscillations of the massive plate-like structure lie in the low-frequency range of the Fourier spectrum. For a preliminary assessment of their frequency range, the hinged plate model may be used. The fundamental mode frequency of hinged plates oscillations may be determined by well-known analytical solutions for different shapes of plates:

$$\omega_1 \cong \pi^2 \left\{ \frac{a^2 + b^2}{a^2 b^2} \right\} \sqrt{\frac{Eh^2}{12\rho\left(1-\mu^2\right)}};$$

This is an open access article under the CC BY 4.0 license

$$\omega_1 \cong \frac{3.2h}{2r^2}\sqrt{\frac{E}{12\rho\left(1-\mu^2\right)}},$$

where a and b – length and width of rectangular plate respectively; r – radius of circular plate; h – plate thickness; E and μ – Young's modulus and Poisson's ratio of the plate; ρ – plate density.

There is a theoretically unsolved problem with a rigorous description of the occurrence of an anomalous response in zones of disturbed contact conditions [26, 36, 37]. For significant contact breaches (large areas of material removal under plate or zones of rock destruction behind the lining), the bending vibrations approach looks correct: the wavelength of the excited pulse is less than the linear dimensions of the structure section involved in the vibration. For small contact violations (local voids in rock massif or areas of weakened soils), the formation of an anomalous response occurs in a complex way, in the near zone of the impact source (and includes various nonlinear effects, dispersion of surface waves, etc.). However, the occurrence of an anomalous acoustic response can be clarified at the stage of geotechnical interpretation of the survey result.

Application of IR method makes it possible to obtain a qualitative assessment of the contact conditions of the plate-soil system. When free oscillations are induced in a layered structure, the efficiency of the grouting mortar or enclosing soils as a damper manifest itself in comparative response changes in the time and frequency domains. In case of contact failure (presence of delamination, void, cavity behind plate), there follows a noticeable increase in the duration and amplitude of the main oscillation train (Fig.1, *б*). The standard approaches of data interpreting are to analyze the response energy and the peak spectrum frequencies, calculate signal attributes such as *Q*-factor, use of numerical modeling and a priori information as supporting tools [38].

The principal questions, which are usually assigned to the qualification of a specialist, are data interpretation and final decision on contact state. This is, first of all, the choice of the criterion for the allocation of voids, i.e., set of parameters for quantitative classification of anomalous response areas.

The proposed approach to rapid data analysis were briefly described in [26] and provides an alternative view on data processing. It consists of analyzing the set of dynamic attributes of the normalized response. Technique allows avoiding the need to use a calibrated source with force sensor (which is required for the mobility analysis techniques [36]) by the analysis of the normalized response parameters that are more resistant to the signal excitation's conditions. Previously, the attributes were adapted for signal processing in vibration diagnostics of geotechnical structures, piles low strain integrity testing and parallel seismic survey [11, 39, 40].

Due to the approximation of concrete structure as the ideal linear elastic body under the low-amplitude dynamic impact, the response behavior in the time and frequency ranges does not depend on the applied force but depends on the working conditions and properties of the body itself. For real reinforced concrete structures, this property is fulfilled approximately, but this turns out to be sufficient for solving practical tasks. It was shown that signal reception conditions affect normalized response more than varying impact force in the usual field-testing range.

With this approach, the recorded acoustic trace $V(t)$ and its Fourier spectrum $S(j\omega)$ are represented a:

$$V(t) = A_{\max}V_0(t); \quad S(j\omega) = A_{\max}S_0(j\omega),$$

where $A_{\max}$ – maximum signal amplitude; $V_0(t)$ – signal value normalized to the maximum amplitude; $S_0(j\omega)$ – signal spectrum, normalized to the maximum spectral amplitude.

The attributes of the normalized signal energy E_n, the normalized spectrum area S_n and the average-weighted frequency f_s allows us to characterize the absorption nature of the oscillation energy, excited in the studied linear-elastic body, and are determined by the following formulas:

This is an open access article under the CC BY 4.0 license

$$E_n = \sum_0^T V_0(t) V_0(t);$$

$$S_n = \sum_i \left| S_0(i) \right| df;$$

$$f_s = \frac{\sum_i \left(S(i) f(i) \right)}{\sum_i S(i)},$$

where V_0 (t) – normalized signal's value, t = 0, … T, $df = \frac{\Delta f}{2(n-1)}$, Δf – sampling frequency; n – number of samples in the spectrum; i = 1, 2 … n; $S_0(i)$ – the value of the normalized spectrum at the i-th point; f (i) – frequency value at i-th point.

According to Parseval equality, the response energy can be determined as follows:

$$E = \int_0^T V(t)^2 dt = \int_0^\omega \left| S(j\omega) \right|^2 d\omega. \quad (1)$$

The signal energy, as can be seen from (1), is determined in the time domain by the signal amplitude $V(t)$ and the time interval (0; T), i.e., signal duration. In the frequency domain, the energy is determined by the spectral amplitude $|S(j\omega)|$ and frequency interval (0; ω). When using E_n attribute, its value is determined mainly by the duration of the signal T. When contact is broken, the duration of the acoustic response increases and, consequently, the attribute value increases. In accordance with the property of the Fourier transform, the response spectrum becomes narrower and the central frequency of the spectrum becomes lower. Therefore, S_n and f_s decrease with E_n growth (see Fig.1, *b*), and for good (*g*) and poor (*p*) contact state the following relationships can be written:

$$E_{ng} < E_{np};\ S_{ng} > S_{np};\ f_{sg} > f_{sp}. \quad (2)$$

General points regarding the relationship of the attributes of the normalized and unnormalized response with the characteristics of excited oscillations are given in Table 1. It should be noted that the S_n/f_s attribute allows to assess the nature of the oscillation energy attenuation, and has a similar physical meaning to the Q-factor. A decrease in this parameter is an indicator of a decrease in the quality factor of the "structure – soil" oscillatory system (energy is redistributed into pronounced low-frequency oscillations). However, unlike other methods of assessing the Q-factor, such an attribute is more resistant to small changes in the response spectrum (since its calculation is not tied to the shape of the main oscillation train) and is suitable for characterizing an oscillatory system with more than one pronounced oscillation frequency (a multi-layer system, which includes the "structure – plugging – soil" system).

Table 1

Connection of dynamic attributes of the normalized and unnormalized response with the properties of the oscillatory system

Attribute	Signal	Normalized signal
Energy E	Oscillation energy	Oscillation duration
Spectrum area S	Oscillation energy	Oscillation frequency bandwidth
Average-weighted frequency f_s	Dominant frequencies of the response spectrum	
S/f_s	Q-factor	

When choosing the impact source parameters, it is important to know the prevailing frequencies induced by the impact. Their range is related to the impact pulse duration τ, which, in turn, is related mostly to the parameters of the signal source (mass, material, radius of the contact surface and impact

This is an open access article under the CC BY 4.0 license

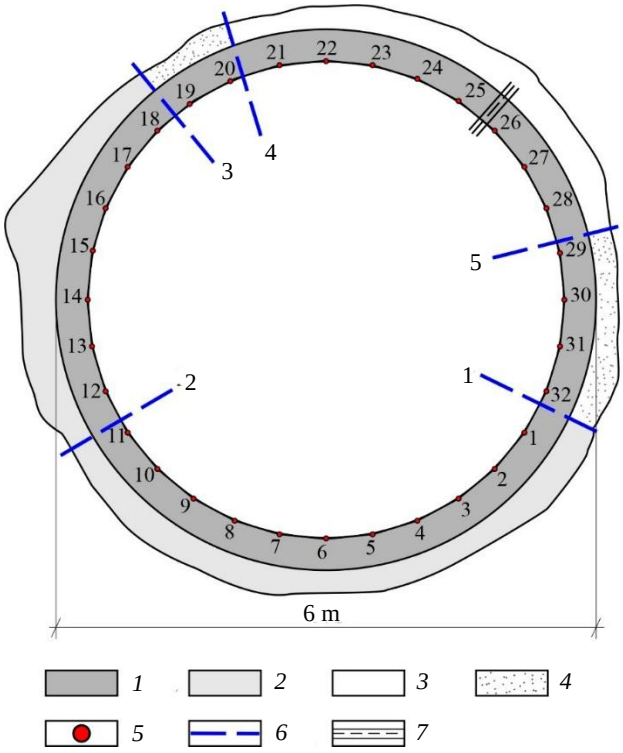

Fig.2. Tunnel liner physical model scheme
1 – reinforced concrete liner; *2* – grouting; *3* – cavity; *4* – loose soils; *5* – IR testing point; *6* – markers of different contact state zones; *7* – tunnel liner break

speed). The first three parameters are modulated by the choice of specific impactors, while the fourth is the most difficult to standardize. Although it varies within relatively small limits. The use of two impactors with "opposite" characteristics (compact metal hammer and a massive rubber mallet as example) has been anchored during the practice of carrying out the physical modeling experiment.

Experimental research was carried out on a model that simulates a tunnel lining. To test the proposed approach, physical modelling on a specially constructed laboratory bench was performed. The stand scheme and the observation points location are shown in Fig.2. A brief description of the experimental results for the energy attribute is given in [26].

Complete tunnel ring was assembled from standard concrete blocks 250 mm thick. The assembled ring was buried into the ground to a depth of the ring width. On the outer side of the ring, a gap between the liner and the soil was equipped with a width of at least 200 mm. For the greater half of the ring circumference (marks 1-2-3), the gap was filled with grouting mortar: the grout width was 20-30 cm for section between marks 1-2, 30-50 cm for section between marks 2-3. Sections 3-4 and 5-1 were filled with loose soil, section 4-5 was initially left unbacked to simulate a cavity/grouting fail behind liner and was backfilled with soil after the first measurement cycle.

The laboratory stand model was chosen to present in practice the main provisions of the technique – the connection between the attributes behavior of the normalized response and the presence of conditioned plugging between the structure and the surrounding soils, acting as a damper for the excited vibrations.

For field measurements, a two-channel seismic station IDS-1 (OOO Logicheskie sistemy) with omnidirectional velocity transducer GTSensor (OOO GEODEVICE) was used for response registration. The signal was induced using a rubber mallet (striker weight – 400 g) and a metal hammer (striker weight – 70 g). Signal processing for all the results presented in the article was carried out in the GeoTechControl software package (OOO GEODEVICE).

On the liner ring inner surface, 32 IR testing points were evenly distributed. Between observation points 25 and 26 (closer to point 26), there was a gap in the lining. For each point, a series of 4 impacts was performed with each of the impact sources. The impacts were applied within 10 cm from the sensor on four opposing sides to suppress the interference caused by the geometric factor when calculating the arithmetic mean and multiplicative spectra for each observation point. After completing a full cycle of observations, the cavity was covered with loose soil and repeated observations were made from point 18 to point 32.

Results and discussion.

Consider the signals behavior for two testing points representing opposite cases – good contact with the enclosing soil through the grouting layer (point 6) and poor contact with the enclosing soil without grouting (cavity, point 24). The calculation results of the attributes are shown in Table 2. The recorded signals, arithmetic mean and multiplicative spectra for both types of impact source are shown in Fig.3.

This is an open access article under the CC BY 4.0 license

Visual analysis confirms some of the considerations presented early. For both impact sources, the difference between good and poor contact state is expressed in the appearance of intense oscillations in the time domain ("ringing") and grown "irregularity" of the spectra in the frequency domain. The calculated attributes show a significant increase in the normalized signal energy and a noticeable decrease in the normalized spectrum area. The average-weighted frequency behavior differs from the expected – instead of a noticeable decrease, f_s slightly increases.

Table 2

Dynamic attributes of normalized response obtained for measurement points 6 (good contact) and 24 (poor contact)

Attribute	Point 6		Point 24	
	Metal	Rubber	Metal	Rubber
E_n, conv.un.	243	564	890	1,589
S_n, conv.un.	2,037	602	462	331
f_s, Hz	1,462	632	1,472	895
S_n/f_s, conv.un.	1.393	0.953	0.314	0.370

The observed phenomenon is associated with the limitations of the used single lining ring. When surveying real structures, their linear dimensions (the tunnel length or the slab dimensions in plan) significantly exceed the length of induced oscillations. In the case of the used physical model, the acoustic wave's reflections from the edges of the structure create an interfering signal. Therefore, upon induction of oscillation, not only modes of bending oscillation are recorded, but also various spatial resonance phenomena which associated peaks can be observed in the average and multiplicative spectra. In addition, a break in the tubing located near testing point 26 provides additional acoustic interference.

The calculation results of dynamic attributes for all observation points on the profile are presented in Fig.4. Normalized signal energy value E_n for a rubber mallet showed sensitivity to the grouting change to a cavity (the difference in values is 2.5-3 times, the points of anomalous observations correspond to the cement mortar change to the surrounding loose soil). E_n for a metal hammer showed less sensitivity to the cavity presence behind the liner. After filling the cavity with

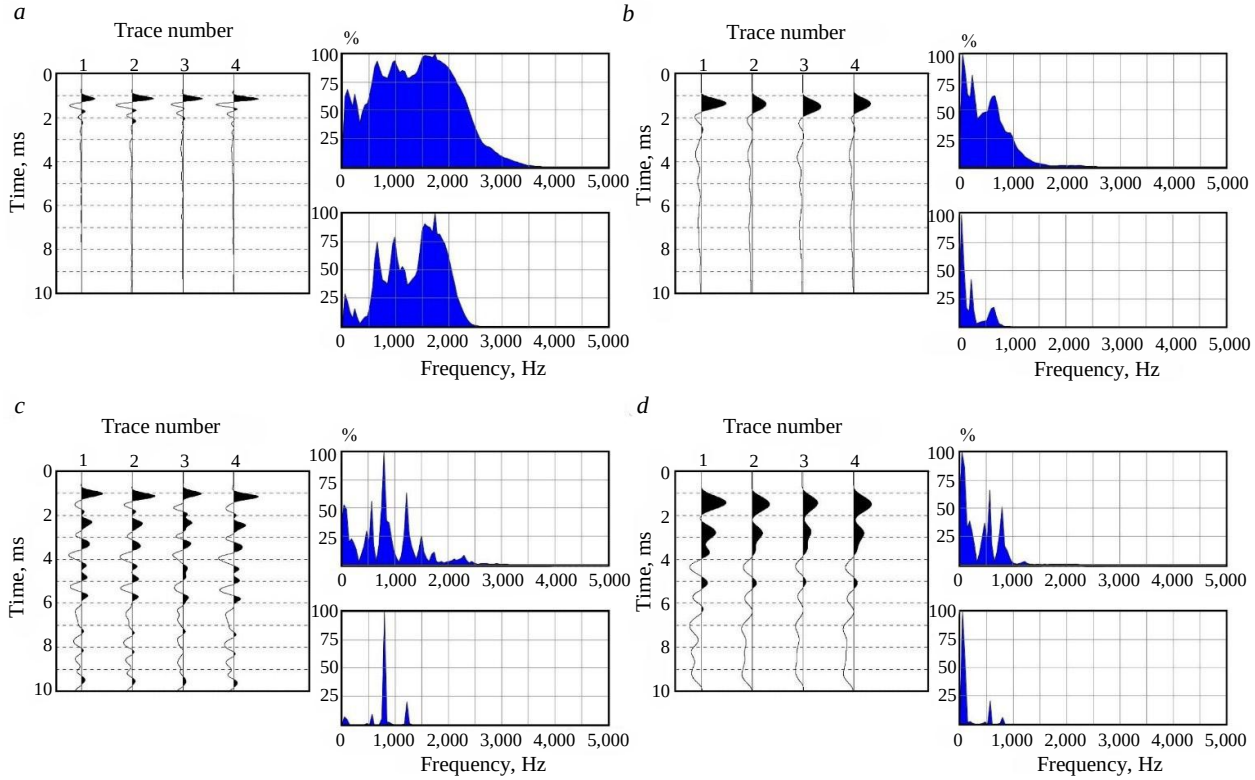

Fig.3. Response in time and frequency (arithmetic mean and multiplicative spectra) domains for points with (*a*, *b*) and without (*c*, *d*) grouting behind liner:
a – point 6, metal hammer; *b* – point 6, rubber mallet;
c – point 24, metal hammer; *d* – point 24, rubber mallet

This is an open access article under the CC BY 4.0 license

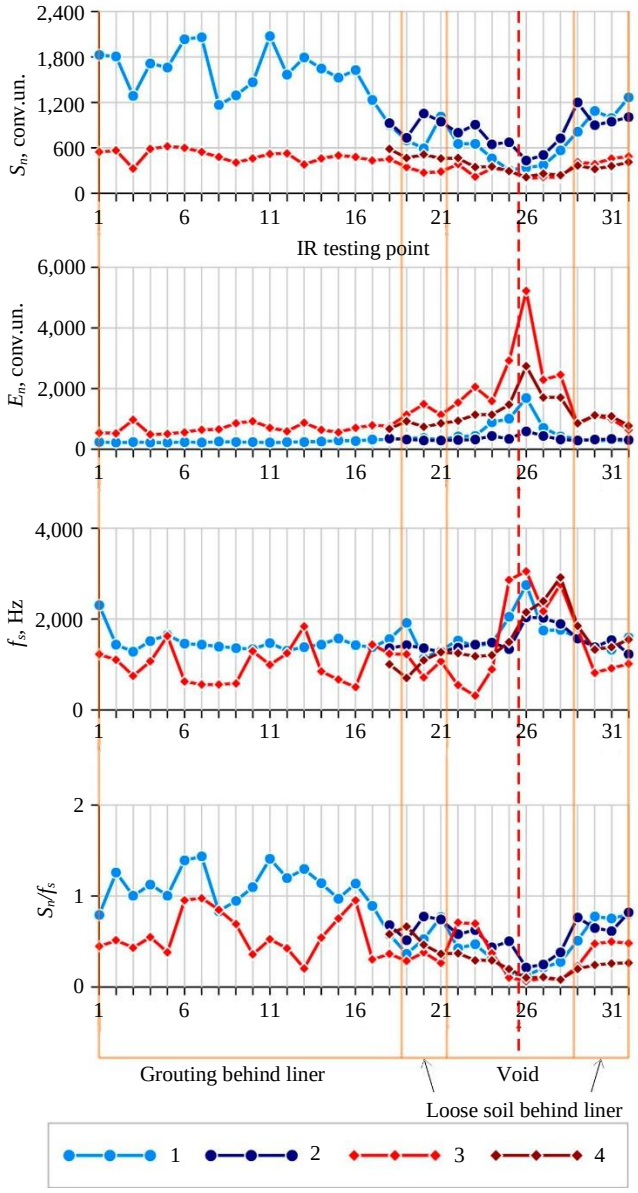

Fig.4. Attributes values obtained due physical modeling

1 – metal hammer, before cavity filling; 2 – after cavity filling; 3 – rubber mallet, before cavity filling; 4 – after cavity filling

loose soils, the anomaly intensity decreases. S_n for a metal hammer demonstrates greater sensitivity in comparison with rubber mallet – a decrease in the attribute values by 2 times coincides with the grout zone boundaries. The ring rupture near point 26 shows in intense anomalous values of the E_n and f_s.

Thus, the relationship between the state of the contact of the concrete-plugging-soil system and the behavior of the normalized response attributes is confirmed in practice. The next step is to clarify the methodology for performing field work, which can be substantiated by the results of a laboratory experiment.

The increased sensitivity of the attributes obtained with a low-frequency impact source (rubber mallet) to changes in the contact state allows selecting them for detailed analysis. Fig.5 shows the results of calculating the response attributes for the mallet, obtained before filling the cavity, with several significant changes made in the calculation.

To reduce the influence of interference of various origins on the attribute values, they were calculated separately for each recorded trace, after which the median value was taken as the attribute value for the research point. This allowed us to partially automate the procedure for rejec-ting broken signals. Manual rejection is difficult when accumulating a large array of data on a real object.

To increase the reliability of identifying points with an abnormal response, the experience of the specialists in mobility curve analysis was used. The mobility curve parameters are calculated for the frequency range (0, 1,000) Hz, since it was established that for this window the behavior of the mobility spectrum is most sensitive to the state of the "plate-like structure – soil" system [9, 21, 36]. In the case of normalized response analysis, the task is to localize the low-frequency "ringing" region for areas of contact failure or poor-quality plugging.

Attributes S_n and f_s were recalculated for (0, 1,000) Hz window. The results of the recalculation, presented in Fig.5, allow us to show the compliance of the behavior of the response attributes with the theoretical criterion (2) for the section with no plugging after making this change. A noticeable decrease of S_n (about 2 times) and f_s (about 25 %) corresponds the more than doubled E_n growth. The results of experiments on numerical modeling of the application of the technique for localizing voids (presented in [40]) also confirmed the correctness of these changes in the calculation method.

Addition of the set of selected attributes with recommendations for their calculation allows us to proceed to the interpretation of the acoustic survey of the structure. The application of the response analysis method allowed us to survey several operating underground structures. Examples of field work results allow us to demonstrate the specifics of analyzing the results using this method.

This is an open access article under the CC BY 4.0 license

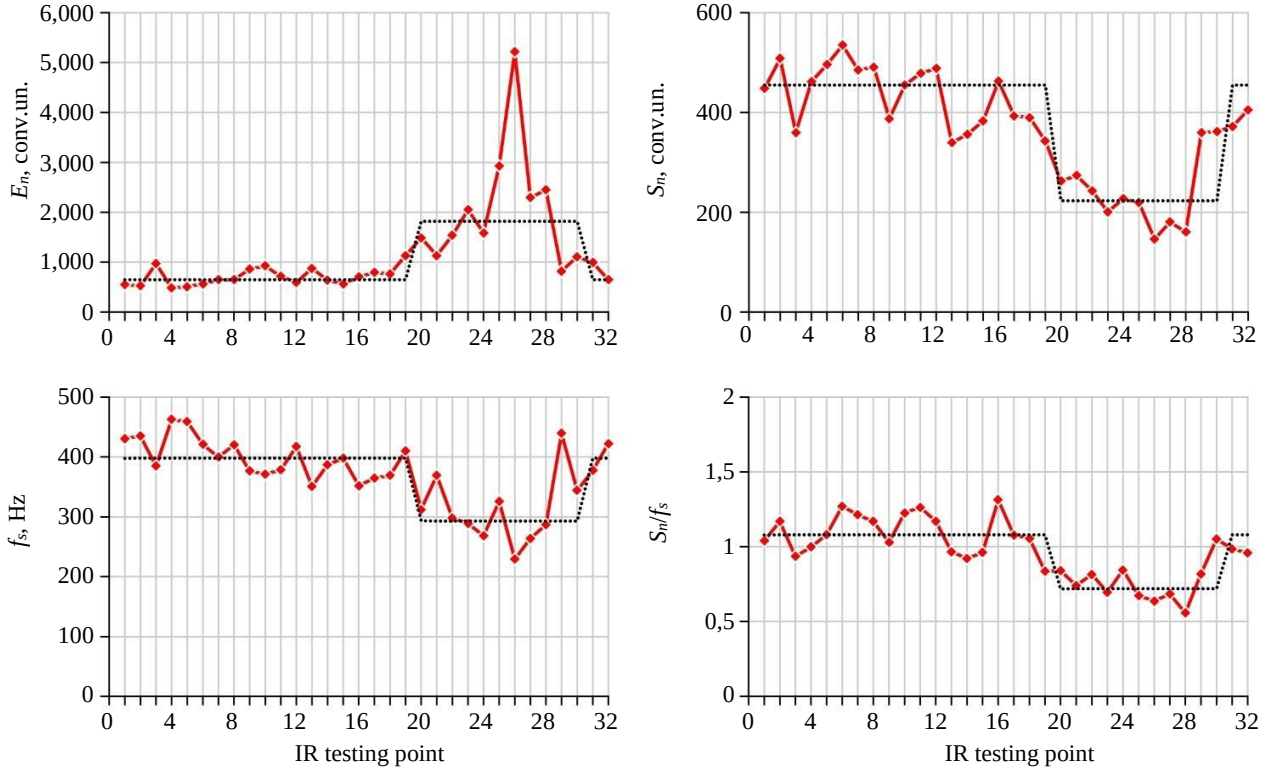

Fig.5. Attributes of the normalized response obtained from the rubber mallet,
after rejecting broken signals, calculating median values and recalculating for (0, 1,000) Hz window. The dashed black lines indicate the median values of attributes for areas of normal and abnormal state of the contact "lining – soil"

The first case study is the survey of 0.6 m thick foundation slabs of the object of construction in progress. This thickness value approximately corresponds to the upper limit for adequate survey results because excitation of bending oscillations for a thicker structure with a manual striker may be problematic [36]. An IDS-1 was used for response registration, a rubber mallet (350 g) was used as a source. For each measurement point, 5 signal accumulations were performed. Assigned task was to clarify the areas of contact failures between plates and the base soils with reference to the edges of structures. Previous visual investigations show some consequences of base soil decompaction.

The observation network was planned based on the task as follows – a dense measuring network (about 1 m between adjacent points) evenly covered the outer perimeter. The central parts of the structures were surveyed with less detailed longitudinal profiles (step between neighboring points about 5 m). An additional limitation for the observation network was the need to work outdoors in winter. The preparation of measurement points for the installation of sensors and the limited time for the survey did not allow for more detailed observations for the central parts of the slabs.

The results obtained make it possible to show options for data visualization. Attribute maps (values were interpolated between measuring points by kriging) are presented in Fig.6. Traditional way for the presentation of geophysical survey results is a visualization in the (min; max) color scale. More informative seems to be the use of a data visualization method that allows you to highlight areas of anomalous values in the plan using statistical criteria. The proposed approach to data visualization is in choosing color scale, where the color transitions are determined by the boundaries of the standard deviation σ of the attribute values. The modified 3σ criterion (three-sigma rule, empirical rule) gives a rough statistical estimation for the collected dataset. Its application makes it possible to identify significant deviations from the normal behavior of the studied parameters [26]. Figure 6, *a* shows a good match of the joint behavior of attributes to criterion (2).

This is an open access article under the CC BY 4.0 license

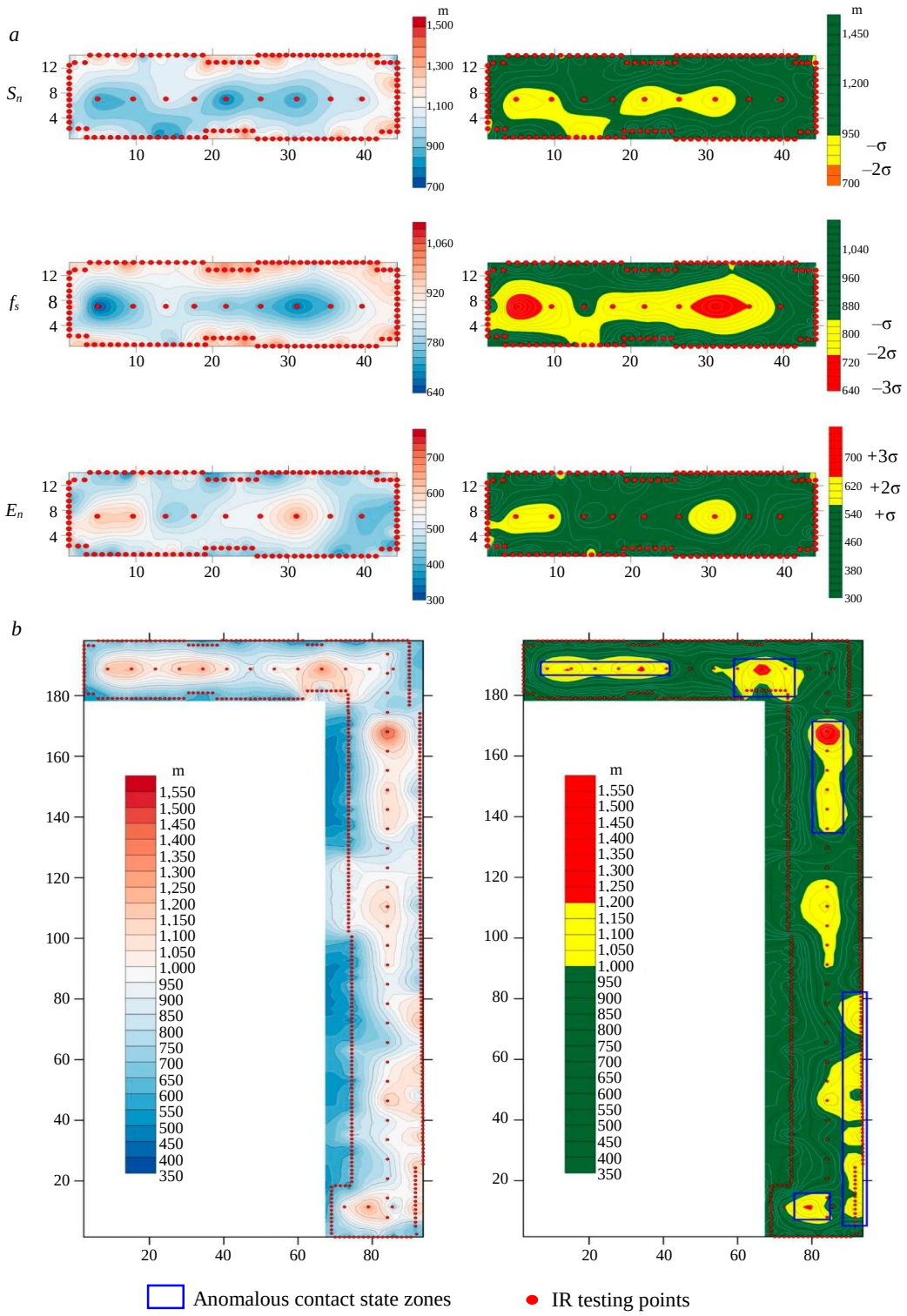

Fig.6. Attributes maps for first tested slab (*a*) and E_n map for second tested slab (*b*). The color scale on the left changes uniformly from minimum to maximum values; the color scale on the right is tied to the boundaries of the standard deviation

The second aspect of data analysis is the issue of incorrect use of statistical criteria for the selection of abnormal zones without considering their size and distribution within the tested area [11]. The relative spatial arrangement of the anomalous points allows us to separate random deviations (arising from instrumental or data collection errors) from zones of suspected contact failure traceable for several observation points. Fig.6, *b* shows an example of rejecting anomalous zones at the stage of results

This is an open access article under the CC BY 4.0 license

interpretation. The sections of the plate with an anomalous response traceable for several neighboring observation points were identified as "suspicious".

This allows us to conclude that the contact of the central part of the slabs with the base soil is relatively weakened. This can be explained by uneven soil settlements due to its incorrect compaction during preparation for the construction of structures. The results obtained from the survey were used in the planning of grout injection grids.

The second case study presents the results of a survey of the foundation slab at the base of the existing underground structure. Slab 32-35 mm thick was examined. In the process of strengthening the soil base of the structure, auxiliary soil-cement columns were manufactured, which led to uneven settlements of the floor slab. The complex of the IR testing and cement injections was used to localize areas of violation of the contact of the floor slab with the subgrade and the development of defects in the slab material.

For acoustic testing, IDS-2 (OOO Logicheskie sistemy, Russia) was used, a rubber mallet 450 g weight was used as an impact source. For each point, 10 signals were accumulated. Data collection was carried out from the surface of the examined structure. The blows with a mallet were applied from different directions from the registration point to increase signal to noise ratio.

The data were processed using the GeoTechControl software. The processing schedule included data sorting and collection, geometry assignment, and spatial filtering (to obtain an average response for each observation point). The attributes of the normalized response were then calculated and, after interpolation of the values (using kriging), maps were constructed (Fig.7). The 3σ criteria and the joint behavior of attributes were used to study the contact of the slab with the soil. Based on the results of the study, two anomalous zones were identified.

The anomalous area identified near observation point 67 was confirmed during hydraulic testing. The cement mortar pumped into the soil base from a depth of 1.5 m began to flow onto the surface of the slab through cracks and cavities in the construction material near the point 67. Decompression of the base soil in the area of points 17, 40, 55 was also eliminated when pumping with a solution.

Summing up the interim results, it is possible to bring up a number of issues for discussion. For the successful application of the proposed technique in underground structures monitoring, the following tasks should be solved:

• studying of the influence of acoustic interference waves and noises caused by the spatial and material characteristics of the structure on registered data;

• clarification of types of contact states due to acoustic response and the development of quantitative criteria for their separation;

• development of an instrumentation and hardware complex that allows quick collecting and processing of data when surveying a structure with non-trivial geometry and hindered access to the examination surface – old mine shafts, metro communications, elements of hydraulic structures.

The question of the influence of acoustic interference waves and noise on the recorded data regularly arises in classical analysis of the mobility curve [8, 9, 21, 22, 36]. The influence of edge effects can be taken into account at the planning stage (grid points are located at a distance from non-standard slab areas) or already during data analysis (zones of non-standard areas response changes are manually marked on the maps).

In Russian practice there are three traditionally distinguished "empirical" types of contact states: firm contact, weakened contact, breached contact [11, 26, 38]. The three-sigma rule can be adapted for this classification as shown above. However, due to the relativity of the criterion, it cannot serve as the only way to reject data and requires additional geophysical and geotechnical interpretation of the results. A number of authors are inclined to the point of view that it is possible to increase the reliability of the application of relative criteria by establishing a sufficient number of observations over the network (at least 200 in the case when quality control of the slab material is required) [36]. Similar guidelines can be developed for the normalized response analysis testing. Additional analysis tools include calculating the coefficient of variation of each attribute sample and constructing scatterplots to simplify the joint analysis of parameters.

This is an open access article under the CC BY 4.0 license

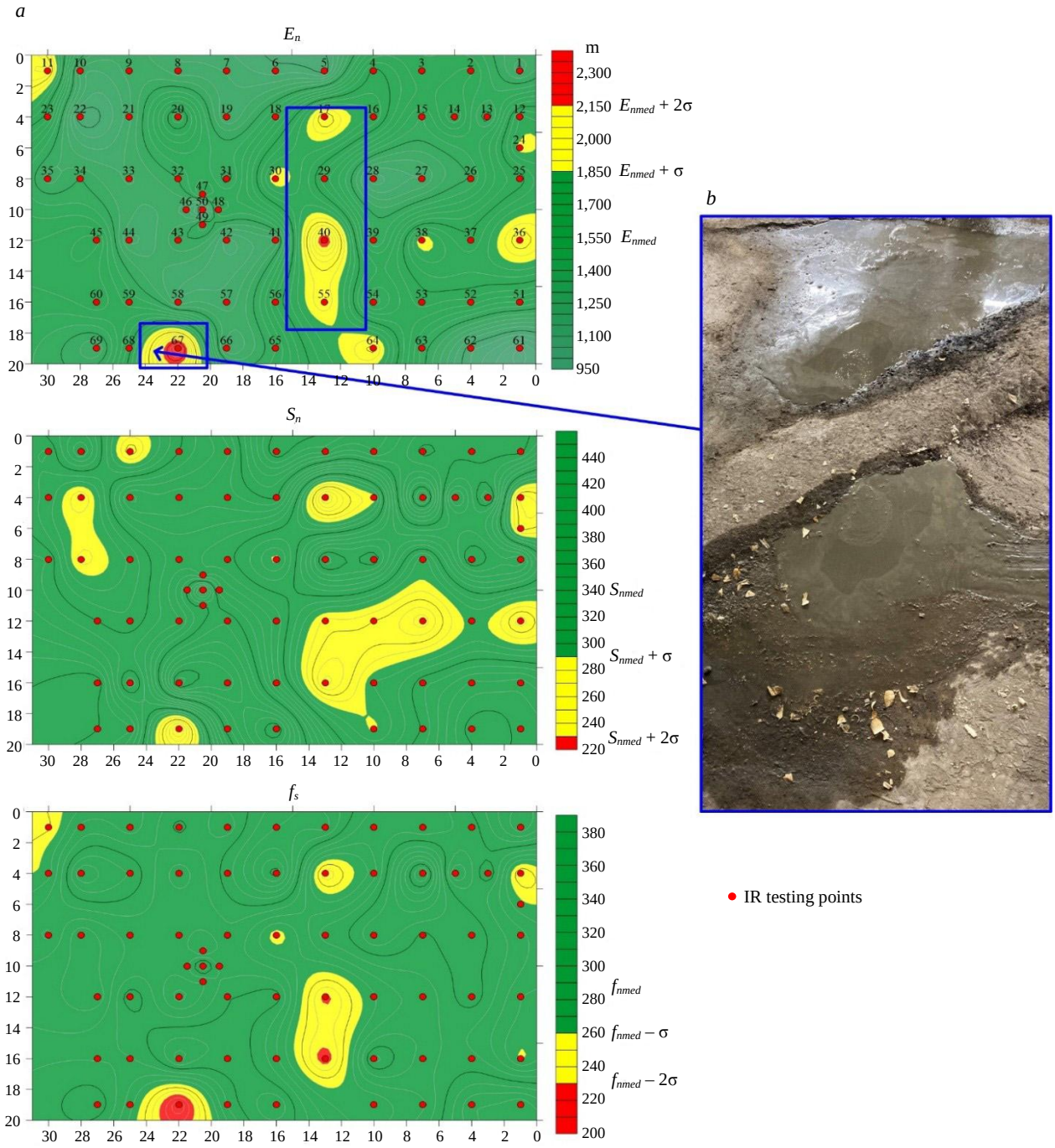

Fig.7. The results of the foundation slab survey at the base of the underground structure (*a*)
and confirmation of the defect in the body of the foundation slab near point 67 during the cement mortar injection (*b*).
The *nmed* index indicates the median value of the attribute

The development of new synthetic parameters characterizing the multilayer "concrete – grouting – soil" system may provide some perspectives. An interesting way of processing the data is to combine the attributes of the normalized response with the attributes of mobility curve, such as the void index or the slope of the mobility curve [21, 32, 37]. Thus, [40] presents the applicability of the void index from ASTM C1740 for the analysis of normalized response data. The use of spectral characteristics of the impact for response normalization can reduce errors associated with the conditions of signal excitation (despite the initial assumption that the impact force influence on the response is insignificant). An informative parameter can be extracted from a comparative analysis of nonlinear changes in the response. An interesting approach described in [41] still seems problematic for examining real structures, but also needs to be developed.

This is an open access article under the CC BY 4.0 license

Undoubtedly, as empirical material accumulates, the number of criteria may change. Of great interest is the emergence of quantitative assessments for the type of filling of cavities behind a structure [33, 38]. A necessary stage for the technique will be the machine learning algorithms (primarily cluster analysis) adaptation to identify anomalous points by analogy with the approach proposed in [42].

For the mobility analysis method, some manufacturers have developed hardware and software packages that completely solve the issue of conducting field tests in accordance with the requirements of ASTM C1740-16 [8-10, 36, 37]. Since normalized response analysis tests can be performed with equipment for pile integrity testing, the main issue is the development of a software package (for example, based on the applied GeoTechControl) and recommendations for equipment manufacturers on recording parameters (sampling frequency, recording length, dynamic range) for collecting good quality data.

Conclusion.

The proposed technique of normalized response attributes application makes it possible to implement a rapid and economical non-destructive technology for different plate-like structures evaluation. The calculation of the attributes is quite simple and does not take much time, which makes it possible to do semi-automatic data processing with a small participation of a data processing specialist. The technique can be used to assess the state of various underground structures during their construction, operation, and to assess the effectiveness of repair work using grout injection. A number of issues of the technique need to be developed and supplemented, which allows us to count on its elaboration in parallel with more widely used techniques for examining plate-like structures, such as the mobility analysis method or the impact echo method.

REFERENCES

1. Pleshko M.S., Pleshko M.V., Voynov I.V. Estimation of technical state of long-term service railway tunnels. *Mining Informational and Analytical Bulletin.* 2018. N 1, p. 34-40 (in Russian). DOI: 10.25018/0236-1493-2018-1-0-34-40

2. Prokopov A., Prokopova M., Rubtsova Y. The experience of strengthening subsidence of the soil under the existing building in the city of Rostov-on-Don. *MATEC Web of Conferences*. 2017. Vol. 106. N 02001. DOI: 10.1051/matecconf/201710602001

3. Wuzhou Zhai, David Chapman, Dongming Zhang, Hongwei Huang. Experimental study on the effectiveness of strengthening over-deformed segmental tunnel lining by steel plates. *Tunnelling and Underground Space Technology*. 2020. Vol. 104. N 103530. DOI: 10.1016/j.tust.2020.103530

4. Zhi-Feng Wang, Wen-Chieh Cheng, Ya-Qiong Wang. Quantitative Evaluation of Ground Movements Caused by Grouting during Shield Tunnelling in Clay. *Advances in Civil Engineering*. 2019. Vol. 2019. N 7498367. DOI: 10.1155/2019/7498367

5. James C. Ni, Wen-Chieh Cheng. Trial Grouting under Rigid Pavement: A Case History in Magong Airport, Penghu. *Journal of Testing and Evaluation*. 2012. Vol. 40. Iss. 1, p. 107-118. DOI: 10.1520/JTE103776

6. Qing Yu, Kexin Yin, Jinrong Ma, Hideki Shimada. Vertical Shaft Support Improvement Studies by Strata Grouting at Aquifer Zone. *Advances in Civil Engineering*. 2018. Vol. 2018. N 5365987. DOI: 10.1155/2018/5365987

7. João Ricardo Marques Conde Da Silva. Use of cement based grouts in the rehabilitation of concrete dams: a review. 5th International Conference on Smart Monitoring, Assessment and Rehabilitation of Civil Structures, 27-29 August 2019, Potsdam, Germany. e-Journal of Nondestructive Testing. 2020. Vol. 25 (1). 8 p.

8. Cardarelli E., Marrone C., Orlando L. Evaluation of tunnel stability using integrated geophysical methods. *Journal of Applied Geophysics*. 2003. Vol. 52. Iss. 2-3, p. 93-102. DOI: 10.1016/S0926-9851(02)00242-2

9. Davis A.G., Lim M.K., Petersen C.G. Rapid and economical evaluation of concrete tunnel linings with impulse response and impulse radar non-destructive methods. *NDT & E International*. 2005. Vol. 38, Iss. 3, p. 181-186. DOI: 10.1016/j.ndteint.2004.03.011

10. Hertlein B., Davis A. Nondestructive Testing of Deep Foundations. John Wiley & Sons, 2006, p. 296. DOI: 10.1002/0470034831

11. Kapustin V.V., Vladov M.L. Technical geophysics. Methods and tasks. *Geotechnics.* 2020. Vol. XII. N 4, p. 72-85 (in Russian). DOI: 10.25296/2221-5514-2020-12-4-72-85

12. Sheng Zhang, Wenchao He, Yongsuo Li, Yuchi Zou. Thickness Identification of Tunnel Lining Structure by Time–Energy Density Analysis Based on Wavelet Transform. *Journal of Engineering Science and Technology Review*. 2019. Vol. 12. Iss. 4, p. 28-37. DOI: 10.25103/jestr.124.04

13. Kravitz B., Mooney M., Karlovsek J. et al. Void detection in two-component annulus grout behind a pre-cast segmental tunnel liner using Ground Penetrating Radar. *Tunnelling and Underground Space Technology*. 2019. Vol. 83, p. 381-392. DOI: 10.1016/j.tust.2018.09.032

14. Ming Peng, Dengyi Wang, Liu Liu et al. Recent Advances in the GPR Detection of Grouting Defects behind Shield Tunnel Segments. *Remote Sensing*. 2021. Vol. 13. Iss. 22. N 4596. DOI: 10.3390/rs13224596

15. Nabatov V.V., Gaysin R.M. Handling of GPR data on voids in annular space. *Mining Informational and Analytical Bulletin.* 2018. N 1, p. 19-25 (in Russian). DOI: 10.25018/0236-1493-2018-1-0-19-25

16. Hui Qin, Yu Tang, Zhengzheng Wang et al. Shield tunnel grouting layer estimation using sliding window probabilistic inversion of GPR data. *Tunnelling and Underground Space Technology*. 2021. Vol. 112. N 103913. DOI: 10.1016/j.tust.2021.103913

This is an open access article under the CC BY 4.0 license

17. White J.B., Wieghaus K.T., Karthik M.M. et al. Nondestructive Testing Methods for Underwater Tunnel Linings: Practical Application at Chesapeake Channel Tunnel. *Journal of Infrastructure Systems*. 2017. Vol. 23. Iss. 3, p. 4. DOI: 10.1061/(ASCE)IS.1943-555X.0000350

18. Zatar W.A., Nguyen H.D., Nghiem H.M. Ultrasonic pitch and catch technique for non-destructive testing of reinforced concrete slabs. *Journal of Infrastructure Preservation and Resilience*. 2020. Vol. 1. N 12. DOI: 10.1186/s43065-020-00012-z

19. Chia-Chi Cheng, Chih-peng Yu, Jiunn-Hong Wu et al. Evaluating the integrity of the reinforced concrete structure repaired by epoxy injection using simulated transfer function of impact-echo response. 40th Annual Review of Progress in Quantitative Nondestructive Evaluation: Incorporating the 10th International Conference on Barkhausen Noise and Micromagnetic Testing, 21-26 July 2013, Baltimore, MD, USA. AIP Conference Proceedings, 2014. Vol. 1581. Iss. 1, p. 836-843. DOI: 10.1063/1.4864908

20. Bahati P.A., Le V.D., Lim Y. An impact echo method to detect cavities between railway track slabs and soil foundation. *Journal of Engineering and Applied Science*. 2021. Vol. 68. N 7. DOI: 10.1186/s44147-021-00008-w

21. Shokouhi P., Wöstmann J., Schneider G. et al. Nondestructive Detection of Delamination in Concrete Slabs: Multiple-Method Investigation. *Transportation Research Record: Journal of the Transportation Research Board*. 2011. Vol. 2251. Iss. 1, p. 103-113. DOI: 10.3141/2251-11

22. Sadowski Ł. Multi-Scale Evaluation of the Interphase Zone between the Overlay and Concrete Substrate: Methods and Descriptors. *Applied Sciences*. 2017. Vol. 7. Iss. 9. N 893. DOI: 10.3390/app7090893

23. Terzioglu T., Karthik M.M., Hurlebaus S. et al. Nondestructive evaluation of grout defects in internal tendons of post-tensioned girders. *NDT & E International*. 2018. Vol. 99, p. 23-35. DOI: 10.1016/j.ndteint.2018.05.013

24. Hai-xiang Tang, Shi-guo Long, Ting Li. Quantitative evaluation of tunnel lining voids by acoustic spectrum analysis. *Construction and Building Materials*. 2019. Vol. 228. N 116762. DOI: 10.1016/j.conbuildmat.2019.116762

25. Hendricks L.J., Baxter J.S., Chou Y. et al. High-Speed Acoustic Impact-Echo Sounding of Concrete Bridge Decks. *Journal of Nondestructive Evaluation*. 2020. Vol. 39. Iss. 3. N 58. DOI: 10.1007/s10921-020-00695-0

26. Churkin A.A., Khmelnitsky A.Y., Kapustin V.V. Evaluation of Soil-Structure Contact State by Normalized Acoustic Response Analysis. *Soil Mechanics and Foundation Engineering*. 2022. Vol. 59. N 5, p. 453-458. DOI: 10.1007/s11204-022-09836-1

27. Konishi S., Kawakami K., Taguchi M. Inspection Method with Infrared Thermometry for Detect Void in Subway Tunnel Lining. *Procedia Engineering*. 2016. Vol. 165, p. 474-483. DOI: 10.1016/j.proeng.2016.11.723

28. Jong-Ho Shin, Yong-Seok Shin, Jong-Ryeo Yoon, Ho-Jong Kim. A Study on leakage monitoring of tunnel linings using the electric resistivity survey. *Journal of Korean Tunnelling and Underground Space Association*. 2008. Vol. 10. N 3, p. 257-267.

29. Kumar J., Gohil R.R. Non-destructive testing of slab-like structures including pavements using Lamb and Rayleigh waves-based dispersion analysis. *International Journal of Pavement Engineering*. 2023. Vol. 24. Iss. 1. N 2180147. DOI: 10.1080/10298436.2023.2180147

30. Tremblay S.-P., Mhenni A., Karray M. et al. Non-intrusive Characterization of Shallow Soils and Utility Structures Below Pavements Using Rayleigh Waves. *Pure and Applied Geophysics*. 2020. Vol. 177. Iss. 2, p. 737-762. DOI: 10.1007/s00024-019-02333-x

31. Goel A. Applicability of SASW method for subsurface structural evaluation of layered asphalt pavements. NDE 2017 Conference & Exhibition of the society for NDT (ISNT), 14-16 December 2017, Chennai, T.N., India. e-Journal of Nondestructive Testing, 2018, p. 8.

32. Azari H., Yuan D., Nazarian S., Gucunski N. Sonic Methods to Detect Delamination in Concrete Bridge Decks: Impact of Testing Configuration and Data Analysis Approach. *Transportation Research Record: Journal of the Transportation Research Board*. 2012. Vol. 2292. Iss. 1, p. 113-124. DOI: 10.3141/2292-14

33. Cao R., Ma M., Liang R., Niu C. Detecting the Void behind the Tunnel Lining by Impact-Echo Methods with Different Signal Analysis Approaches. *Applied Sciences*. 2019. Vol. 9. Iss. 9. N 3280. DOI: 10.3390/app9163280

34. Chaudhary M.T.A. Effectiveness of Impact Echo testing in detecting flaws in prestressed concrete slabs. *Construction and Building Materials*. 2013. Vol. 47, p. 753-759. DOI: 10.1016/j.conbuildmat.2013.05.021

35. Solodov I., Bai J., Bekgulyan S., Busse G. A local defect resonance to enhance acoustic wave-defect interaction in ultrasonic nondestructive evaluation. *Applied Physics Letters*. 2011. Vol. 99. Iss. 21. N 211911. DOI: 10.1063/1.3663872

36. Sajid S., Chouinard L. Impulse response test for condition assessment of concrete: A review. *Construction and Building Materials*. 2019. Vol. 211, p. 317-328. DOI: 10.1016/j.conbuildmat.2019.03.174

37. Ottosen N.S., Ristinmaa M., Davis A.G. Theoretical Interpretation of Impulse Response Tests of Embedded Concrete Structures. *Journal of Engineering Mechanics*. 2004. Vol. 130. Iss. 9, p. 1062-1071. DOI: 10.1061/(ASCE)0733-9399(2004)130:9(1062)

38. Voznesenskii A.S., Nabatov V.V. Identification of filler type in cavities behind tunnel linings during a subway tunnel surveys using the impulse-response method. *Tunnelling and Underground Space Technology*. 2017. Vol. 70, p. 254-261. DOI: 10.1016/J.TUST.2017.07.010

39. Shmurak D.V., Churkin A.A., Lozovsky I.N., Zhostkov R.A. Spectral Analysis of Parallel Seismic Method Data for Surveying Underground Structures. *Bulletin of the Russian Academy of Sciences: Physics*. 2022. Vol. 86. N 1, p. 79-82. DOI: 10.3103/S1062873822010221

40. Churkin A.A., Lozovsky I.N., Volodin G.V., Zhostkov R.A. Evaluating the Integrity of Slab–Soil Contact with Impulse Response Testing: Insights from Numerical Simulations. *Soil Mechanics and Foundation Engineering*. 2024. Vol. 61. N 1, p. 62-67. DOI: 10.1007/s11204-024-09944-0

41. Hafiz A., Schumacher T., Raad A. A self-referencing non-destructive test method to detect damage in reinforced concrete bridge decks using nonlinear vibration response characteristics. *Construction and Building Materials*. 2022. Vol. 318. N 125924. DOI: 10.1016/j.conbuildmat.2021.125924

42. Sajid S., Chouinard L., Carino N. Condition assessment of concrete plates using impulse-response test with affinity propagation and homoscedasticity. *Mechanical Systems and Signal Processing*. 2022. Vol. 178. N 109289. DOI: 10.1016/j.ymssp.2022.109289

Authors: **Aleksei A. Churkin,** *Candidate of Engineering Sciences, Senior Researcher, https://orcid.org/0000-0002-4043-9590* (*Gersevanov Research Institute of Bases and Underground Structures, Moscow, Russia*), **Vladimir V. Kapustin,** *Candidate of Physics and Mathematics, Junior Researcher, https://orcid.org/0000-0001-9404-4407* (*Lomonosov Moscow State University, Moscow, Russia*), **Mikhail S. Pleshko,** *Doctor of Engineering Sciences, Professor, mixail-stepan@mail.ru, https://orcid.org/0000-0003-2412-3075* (*National University of Science and Technology "MISiS", Moscow, Russia*).

The authors declare no conflict of interests.

This is an open access article under the CC BY 4.0 license

ISSN 2411-3336; e-ISSN 2541-9404

JOURNAL OF MINING INSTITUTE

Zapiski Gornogo instituta

Journal homepage: pmi.spmi.ru

Review article

Modern approaches to barium ore benefication

Nataliya V. Yurkevich[1,2], **Tatyana V. Grosheva**[3], **Aleksei V. Edelev**[1], **Vadim N. Gureev**[1]✉, **Nikolai A. Mazov**[1]

[1] *Trofimuk Institute of Petroleum Geology and Geophysics SB RAS, Novosibirsk, Russia*

[2] *Scientific-Research Center "Ecology" SB RAS, Novosibirsk, Russia*

[3] *Tyumen Branch of SurgutNIPIneft, Surgutneftegas PJSC, Tyumen, Russia*

***How to cite this article*:** Yurkevich N.V., Grosheva T.V., Edelev A.V., Gureev V.N., Mazov N.A. Modern approaches to barium ore benefication. Journal of Mining Institute. 2024. Vol. 270, p. 977-993.

Abstract

Barite is one of the critically important minerals in several industries, including the fuel and energy, nuclear, and medical sectors. For decades, its extraction did not require any complex techniques; however, with the depletion of rich barite-bearing veins around the world, the circumstances have changed. While the demand for barite is growing widely, it is necessary to optimize and improve the existing methods for benefication of barite and barite-containing ores, and create new approaches to extracting this mineral, as well as develop technogenic barite deposits accumulated in large quantities during the previous ore production. Dumps and tailings often demonstrate high barite content, while new mining technologies make its extraction cost-efficient. Russian and foreign papers of the last 14 years provide data on the current state of primary and technogenic deposits, areas of barite use and the approaches employed for its benefication. Considering the expansion of the range of barite applications, the growing need for the mineral in the oil and gas industry and the difficulties in developing new barite deposits in Russia, the importance of new approaches to the enrichment of ore tailings in polymetallic deposits is revealed.

Keywords

barite; reclamation; tailing; flotation; gravity separation; magnetic separation

Funding

The study was performed under IPGG SB RAS projects (N FWZZ-2022-0029, FWZZ-2022-0028).

Received: 08.09.2023 ***Accepted: 03.06.2024*** ***Online: 06.09.2024*** ***Published: 25.12.2024***

Introduction.

Barite ores include natural mineral formations containing barite in concentrations that would be sufficient for its cost-efficient and technically feasible extraction. This mineral is found in nature in various conditions: carbonatite massifs, sea bottom sediments, stratiform and vein deposits, residual weathering crusts or sedimentary deposits [1, 2]. Barium feldspars, micas and aluminosilicates are usually developed in metamorphosed rocks, barite-polymetallic and barite-pyrite ores. The chemical composition of barite has more than two thousand variations. Barite can be found predominantly in the form of granular, lamellar, radiate and columnar fibrous aggregates. The mineral matrix often contains Sr, Ca, Mn, Mg, Fe, Pb, Zn, Cu, Ag, Au and Hg [3].

In China and the USA, barite is entered in the list of critical raw products with high significance for economic development, which is explained by its multi-purpose usage and unique properties: high specific gravity and density (4.3-4.7 g/cm^3), low hardness, weak chemical reactivity, whiteness, and ability to absorb ionizing radiation. Barite is actively used in the fuel and energy, nuclear, and medical industries.

When extracting barite, the final product is presented in lump (coarsely crushed), finely ground (powdered) and micronized forms or as a concentrate. Ground barite is used as a filler and weighting

This is an open access article under the CC BY 4.0 license

agent, lump barite is used as a raw material for the production of barium compounds. Barium concentrate is the most significant and expensive. Barite can be divided into two classes based on its granulometric composition. Class A, non-drilling barite has six subclasses (KB-1 through KB-6) and is used as a filler, barium-containing compound, or radioprotective material. Class B, drilling barite for drilling fluids is divided into KB-3, KB-5 and KB-6 and is used as a weighting agent. The highest consumption (60-80 %) accrues to class B barite.

World barite reserves currently amount to 1.5-2 billion tons, among which explored, preestimated and forecast reserves are distinguished. Explored sources account for 740 million tons[1], of which approximately half are proven. Based on an assessment of the length of the exploited wells, the construction of which is required for the vast majority of barite, the production and consumption of barite is significantly increasing throughout the world[1], although declines are sometimes observed in certain regions [4]. By the early 2020s, global barite consumption was 8.2 million tons per year[2].

Barite has been explored in 60 countries all over the world, with up to 60 % of the most significant deposits located in Asia. China, India and Morocco are currently the leaders in production; barite is mainly exported by China, India, Morocco, Turkey, and Kazakhstan, and imported by the USA, Saudi Arabia, Canada, Kuwait, Norway, Germany, and Italy [5]. Although Russia is among the top ten countries in both production and consumption of barite, its global share is rather small covering less than 2 % of barite production in 2022[1].

In Russia, only class B barite is extracted with the average annual production in the last decade of 150-210 thousand tons, tending to increase[1,3]. General requirements, however, exceed production and reach more than 300-500 thousand tons [6, 7], despite the fact that domestic production, at best, allows one to talk about the threshold of import dependence [5]. Class A barite is currently entirely imported [8], with almost half of all imports coming from Kazakhstan, followed by China and Turkey [5]. Russian barite is exported mainly to Belarus, and import to Russia is ten times higher than export [4]. By 2030, barite requirements in Russia may increase significantly by 2-4 times [4, 9]. The reserves of all known deposits may be exhausted: at the beginning of the 2020s they were estimated, according to various sources, at 12-22 million tons (of which more than 1.1 million tons are suitable for the extraction of class A barite [10]), then by 2030, with growing consumption, only a little over 2 million tons will remain [9]. By different estimates, the time for depletion of reserves varies from one year to 14 years. Therefore, it is reasonable to point out an acute shortage of this raw material, which makes important not only and not so much the exploration and discovery of new deposits as development of new promising methods for its extraction.

In recent decades, the general depletion of barite resources that do not require expensive and complex extraction [11], as well as a large number of dumps and tailings formed during the mining and processing of minerals, have led to the need to create new and improve previous approaches to barite extraction, including repeated processing of technogenic deposits. An analysis of the scientific literature shows a growing interest in modifying mineral extraction technologies by researchers and experts involved in the extraction and processing of barite. Consideration of tailings and dumps of mining and processing plants as promising sources of barite in the coming decades is consistent with the global trends in the extraction of minerals necessary for humans from technogenic deposits.

At the same time, the lack of papers summarizing Russian and international experience of recent years in the production of barite should be noted. Therefore, such a review becomes of particular importance, especially due to the constant expansion of barite applications and the high demand

[1] McRae M.E. Barite. Mineral Commodity Summaries 2023. U.S. Geological Survey, 2023, p. 38-39. URL: https://pubs.usgs.gov/ periodicals/mcs2023/mcs2023.pdf (accessed 19.04.2024).

[2] Schulz K.J., DeYoung J.H. Jr., Seal R.R. II, Bradley D.C. Critical mineral resources of the United States – Economic and environmental geology and prospects for future supply. Reston: U.S. Geological Survey, 2017. Professional Paper 1802, p. 797. DOI: 10.3133/pp1802. URL: https://pubs.usgs.gov/pp/1802/pp1802_entirebook.pdf (accessed 19.04.2024).

[3] Minerals Yearbook 2024. Vol. 1, Metals and Minerals. U.S. Geological Survey, 2024. URL: https://www.usgs.gov/centers/national-minerals-information-center/minerals-yearbook-metals-and-minerals (accessed 15.07.2024).

This is an open access article under the CC BY 4.0 license

for this mineral in the fuel and energy industry. The purpose of the paper is to analyze modern approaches to barite extraction, including those from dumps and ore processing tailings, in Russia and abroad. We also present the results of scientometric analysis of various technologies; outline trends in technological development in the coming years; consider modern areas of barite use, and describe the current state of Russian deposits. The review material can be useful both to young experts in the metallurgical and processing industries, as well as to researchers developing barite extraction techniques.

Range of barite application. *Class A barite* is actively used in various industries where its different properties are exploited.

Barite as a filler is useful in the following industries due to its chemical inertness and low reactivity:

• paper, where paste-like barite white pigments based on blanc fix (chemically precipitated barium sulfate – high-grade barite, of 96-98 % whiteness) is used for bleaching glossy and matte paper, including photographic paper;

• rubber and plastic, where barite serves as a white mineral filler, for example, to manufacture linoleum or rubber;

• paint and varnish, where barite is in use for production of fire- and acid-resistant paints. To produce enamels, lithopone is also used – a pigment based on a mixture of barium sulfate and zinc sulfide, which is cheap and environmentally friendly;

• ceramic, where lithopone is used in enamel production;

• construction, where barite is part of barite-concrete mixtures and special cements, completely or partially replacing quartz sand. Such mixtures are used both in the construction of load-bearing/protective structures and as finishing materials. Barite reduces the impact of aggressive environments, for example, in the foundations of heavy structures such as pipelines (including subwater), road surfaces with high requirements for their quality (for example, at airports where durable and flexible top layer is required). Despite the susceptibility to shrinkage deformations and poor resistance to the cyclic influence of temperatures, a careful selection of mixtures containing barite allows to achieve the strength properties of standard concrete compositions [12];

• automobile, where barite is added to the materials for brake pads, sparking plugs or soundinsulating composites of engines [13].

Barite as a barium-containing compound is the most expensive and demanding material in terms of quality, used primarily in the chemical industry for the following applications:

• medical, where chemical compounds of barium are used in the production of drugs, vitamins, hormones or blood coagulants;

• agricultural, where the toxic properties of barium salts (barium sulfate, barium carbonate, barium chloride, barium peroxide) from lump barite and barium concentrate are actively employed to prepare insecticides and exercise rodent control;

• glass, where barite is used for glass etching, in the production of electric vacuum and light bulb glass. Transparent variations of barite (optical barite) are used in the production of optical instruments including lenses and prisms;

• textile and leather, where barite is used as part of special impregnations – finishing agents;

• electrical engineering, where barite is used to prepare fire- and acid-resistant putties, as well as batteries;

• metallurgy;

• pyrotechnics.

Barite as a radio-, X-ray protective and environmentally friendly material is used in the following industries:

• nuclear, in the construction of nuclear reactors and waste storage facilities (final repositories), where mixtures and solutions that protect against γ- and neutron radiation are required [12, 14, 15]. In connection with the intensive advancement of the nuclear industry, the use of barite in the development of promising radio-protective construction materials is of increasing interest. Of note, barite is superior to many of those materials in terms of efficiency and low cost of production;

This is an open access article under the CC BY 4.0 license

© Nataliya V. Yurkevich, Tatyana V. Grosheva, Aleksei V. Edelev, Vadim N. Gureev, Nikolai A. Mazov, 2024

• medical, in the construction of special premises (tomography rooms, X-ray rooms), where special dry magnesium-barite mixtures are used, ensuring radiation safety with low-thickness finishing concrete or cement layer [16]. In addition to barite-based plaster, elastic self-adhesive materials are also used for radiation protection, successfully replacing lead sheets, known for their toxicity, and barite plaster [17]. Furthermore, barite is used as a radiopaque medium when examining the gastrointestinal tract for tumors.

Class B barite is produced by flotation (the most common in Russia) and gravity separation methods. It is used as a water-insoluble weighting agent for drilling and grouting fluids when drilling wells due to such properties as inertness, high density and low hardness (low abrasiveness and noneffect on the readings of electrical methods in comparison with ferrous weighting agents). Barite for drilling fluids accounts for 60 to 80 % of the total consumption of the mineral. This type of barite has been in active use since the late 1950s and is considered the most profitable [9]. In Russia, it is used extensively by such high-profile companies as Gazpromneft and Surgutneftegaz, and is represented in two industries, fuel and energy (oil and gas production) and geological exploration. In deep and ultra-deep drilling of oil and gas wells with abnormally high formation pressures, drilling fluids weighted with barite prevent solution aeration, collapses of the well walls and the influx of formation waters into the well by maintaining sufficient hydrostatic pressure of the liquid column [18-20]. The disadvantages of barite drilling fluids are associated primarily with the clogging ability of the barite filler when opening reservoirs with low filtration characteristics [21], as well as their sedimentation instability, which increases the likelihood of sticking of drilling tools [22].

It is important to note both the expanding scope of application of class A barite in various sectors of the national economy, and the increasing use of class B barite.

Geological types of barite deposits. Barite deposits can be divided into monomineral (9 %), where barite is the main and only useful element, and complex (91 %), where it is mined as a by-product. Based on mineral associations, barite and barite-containing types are distinguished. Barite type, where barite is the main ore-forming mineral, includes essentially barite, quartz-barite, calcite-barite and sand-clay-barite associations. The barite-containing type consists of barite-sulfide, barite-fluorite and barite-iron associations. By texture, barite ores can be divided into soft (coarse-grained and easily milled), and dense (fine-crystalline and difficult-to-mill).

The genesis of deposits has a strong influence on optimal geological exploration in terms of cost-reduction and the class of barite to be mined: with a content of over 80 %, class A barite is produced, with 80 % – class B barite. According to genesis, barite deposits are most often divided into the following types:

• Hydrothermal, the most abundant, when ore bodies are formed under the conditions of a hydrothermal process from medium- and low-temperature solutions. Additionally, they may contain other minerals and noble metals. Hydrothermal deposits may also include hydrothermal-metasomatic ones, formed either by the replacement of chemically active host rocks, or by recrystallization of ore, when the barite content in the ore increases [3].

• Sedimentary, stratiform sedimentary, stratiform volcanic-sedimentary, hydrothermal-sedimentary, are second most-widespread; but have the greatest industrial importance. Some researchers consider stratiform sedimentary and stratiform volcanogenic-sedimentary types as independent [5]. Historically, they are formed through sedimentation of ocean water components mixed with metal-bearing thermal waters of volcanic areas [3].

• Weathering, formed due to the destruction of barite-containing rocks and ores. Occurs mechanically or under the influence of chemical processes in weathering crusts, when the mechanical and mineralogical composition changes, the mass of rocks with barite is carried away by near-surface waters, and barite aggregates and grains are released from the minerals of the host rocks. As a result, up to 70 % of barite grade to a free state, i.e., the barite concentration increases significantly

This is an open access article under the CC BY 4.0 license

in comparison with the original rock [10, 23]. At the same time, the properties of barite are preserved during weathering processes. Such deposits are usually discovered incidentally, all Russian barite deposits of this type were discovered simultaneously during other geological explorations [10].

Geological and technological types of ores. According to geological and technological types, deposits are divided into the following:

• vein type, hydrothermal in genesis, they serve as the only raw material for the production of class A barite, since they demonstrate higher barium sulfate contents compared to other types. The width of ore veins, as a rule, is several meters; length is from tens to hundreds of meters; thickness is tens of centimeters. The downside of high quality vein barite is the difficulty of obtaining it due to the variable morphology of ore bodies. A significant part of deposits of this type is small. Barite from vein-type deposits is the only source for industries with high quality requirements;

• stratiform type, or strata, in siliceous-shale complexes, sedimentary in genesis, used for the production of class B barite. They extend up to two kilometers, with 3 to 15 m thickness. These deposits are the most widespread in the world and are cost-effective with relatively easy mining due to simple morphology of ore bodies;

• residual and alluvial (eluvial, deluvial and karst) type, formed akin to weathering; are considered as an alternative to vein-type deposits and can be used to extract class A barite. Despite the lower barite content in comparison with vein-type deposits, residual and alluvial deposits are cost-effective and easily extracted due to the simple morphology of ore bodies, surface bedding and the material composition of ores [7, 23]. These properties enable open mining and simple enrichment methods at relatively low costs.

In Russia, deposit development began in the 18th century [24]. Currently, more than 90 % of significant barite deposits are located in the south of Western Siberia (Khakassia, Tuva, Buryatia, the Altai Territory, the Kemerovo region) and in the Urals (the Chelyabinsk region, the Orenburg region, Komi, Bashkiria and the Yamal-Nenets Autonomous Okrug). In most of them it is possible to extract barite for drilling fluids. Class A barite is not mined, although deposits suitable for its extraction have been discovered in the Altai Mountains [8, 19] and Bashkiria [7, 23].

At the beginning of the 2020s, there were up to 20 deposits in Russia containing about 22 million tons of the mineral: 5 million tons of them were barite deposits (47 % of reserves) and 15 million tons were complex deposits (53 %). In most complex deposits, the quality of the ore is assessed as low or the size of the deposit is considered insignificant [4]. Seven deposits are of industrial importance: two barite-sulfide (1-2) and five barite-only deposits (3-7). Production is carried out at only two of them (6-7) in the Republic of Khakassia (where there are also other barite deposits of all three geological and industrial types [19]):

1. Quartzite Sopka (Salair, the Kemerovo region), mining had been carried out since the 1930s, in recent years by Salair Chemical Plant, and was discontinued in 2014. The length of ore bodies is 650-700 m, thickness is 35-130 m. This deposit is suitable for further development, and reserves are estimated at 5.3 million tons [5, 25].

2. Pervomaiskoe (Salair, the Kemerovo region), at the stage of preparation for opening. The length of the ore bodies is 16-180 m, thickness is 7-25 m, reserves – 300 thousand tons.

3. Khoilinskoe (Komi), production was carried out in 1998-2009 by Khoilinskii Mining and Processing Plant. The length of ore bodies is from 400 m to 1.5 km, thickness is 3.5-6.4 m. Reserves are estimated at 6.8 million tons, of which 2.1 million tons are ready for industrial development, while resources – 9.2 million tons [4, 26, 27].

4. Voishorskoe (the Yamal-Nenets Autonomous Okrug), at the stage of preparation for opening (AO Korporatsiya razvitiya). The length of the ore bodies is 50-320 m, thickness is 0.2-6.8 m. Reserves are estimated at 144-382 thousand tons, resources – 800 thousand tons [28, 29].

5. Medvedevskoe (the Chelyabinsk region) was discovered in the 19th century, but no mining was carried out. It is the largest Russian deposit of the weathering type. The length is 3.2 km; thickness is 0.2-16 m. Reserves are estimated at 6.6 million tons.

This is an open access article under the CC BY 4.0 license

6. Tolcheinskoe (Khakassia), mining has been carried out since 1995 by AO Barit, barite concentrate is produced at OOO Bogradskii Mining and Processing Plant. The deposit consists of the Main ore body of a lens-shaped shape and a northern deposit, 1 km length, 4.6-10 m thickness. Over the years of operation, 2,975 thousand tons of ore containing 1,243 thousand tons of barite have been mined, and the remaining reserves of 1.2 million tons should be enough for another 3-8 years [5, 19].

7. Kuten-Bulukskoe (Khakassia) has been developed since 2020 by OOO Khimtekh – Geologya. It produces 85 thousand tons of ore per year, containing 49 thousand tons of barite. The deposit consists of 11 accumulations with a length of 2 km and a thickness of 3.6 m. Forecast resources are estimated at 3.6 million tons, which should be enough for 11 years [5].

There are other promising deposits in Russia. Large forecast barite resources are located in the Far Eastern Federal District (the Magadan region, the Primorsk and Khabarovsk territories), the deposits of which can become an important raw material base for providing weighting material to drilling enterprises, taking into account the prospects for the development of the oil and gas industry in the Far East [9, 26]. Barite ores of the Murmansk region are considered an important source of barite for the development of Arctic hydrocarbon deposits (Sallanlatva) with ore reserves of 13 million tons of barite and resources of 160 million tons [20, 28]. Among the submarine hydrotherms, economically significant massive barite mineralization (Barite Hills) was discovered in the 1980s in the Deryugina depression of the Sea of Okhotsk near the northern tip of Sakhalin Island [30, 31]. Since the 1970s, barite concentrations have been known in the Sea of Japan [32]. Barite was also found in the deposits of the Middle and Southern Urals at the Safyanovskoe deposit [33]; in the Perm region, where barite is of minor significance and is included in celestine intergrowths [34]; in Tuva at the Karasug ore field [1]; and in Buryatia at the Khalyutinskoe and Gunduiskoe fields [1, 4].

Despite the abundance of barite deposits in Russia, its production is difficult for many regions, for example, due to harsh mining and geological conditions (in the North Caucasus), lack of production infrastructure (in Yakutia or the Krasnoyarsk Territory), insufficient geological descriptions of mineral deposits (in the Arctic zone of Russia), etc. [5, 28]. Thus, with the general depletion of highly profitable barite deposits both in Russia and abroad, accompanied with growing production needs for barite of both classes, it becomes increasingly more difficult and expensive to obtain high-quality barite concentrates. Therefore, processing technogenic deposits becomes important for the following reasons:

• many technogenic deposits are rich with barite content (15-30 %), which significantly expands the resource base of this mineral;

• barite-containing wastes do not require extraction from the subsoil and grinding, which significantly reduces the cost of obtaining a barite product;

• the important task of eliminating or reducing the area of tailings dumps, which negatively affect the environment and create risks for public health, is being solved, since barite-containing technogenic wastes are a source of soil, air and water pollution with heavy metals and barite dust [35, 36];

• in Russia, secondary development of tailings dumps in the short term appears to be extremely important in terms of import substitution and increasing the volume of domestic barite concentrate.

Extracting barite from tailings is becoming essential for increasing the ore mining efficiency and reducing the anthropogenic load on the environment. In Russia, promising objects of interest are, for example, dumps in Ursk, the Kemerovo region. The waste storage facility was formed in the 1930s after extracting gold by cyanidation from the oxidation zone of the Novo-Urskoe pyrite deposit, discovered in 1932 as part of the Urskoe ore field and comprised of the Novo-Urskoe, Beloklyuchevskoe, Samoilovskoe deposits, and several ore occurrences. Polymetallic deposits of the Ur group are confined to a complex of metamorphic formations, the primary composition of which is difficult to determine precisely [37]. Within the deposit, 11 ore bodies containing industrial ores were identified and explored [38]. Numerous researchers studied and described their structure, morphology, material composition, sequence of mineral formation, and mining history [39, 40]. In accordance with the soil survey report of the state geological map, the mining dumps of the Novo-

This is an open access article under the CC BY 4.0 license

Urskoye deposit are technogenic deposits of barite [41], the total reserves of technogenic raw materials are 700 thousand tons with a barite content of 15-30 wt.%. The predicted production volume of barite concentrate for the entire period of development of the tailing is about 180 thousand tons, the annual production level of barite concentrate is 20 thousand tons [42, 43].

The stored wastes from the enrichment of barite-polymetallic ores from the Salair ore field are also promising for the development [44]. Particularly, the barite content in the stored wastes of the Talmovskie sands tailings is estimated at 9 %, its horizons are represented by medium and small grains of 100-300 μm, as well as fine grains forming interlayers and cemented aggregates [45]. Technogenic barite deposits of interest also include the Zarechenskoe deposit in the Altai Territory [24]; the processing plants of the Kyzyl-Tashtyg deposit in the Republic of Tyva; the dumps of substandard barite ores from the Khoylinskii Mining and Processing Plant in the Komi Republic; technogenic wastes from the enrichment of the Uchalinskii mining and processing plant in the Chelyabinsk region [46], etc.

Much attention is paid to ore processing storage facilities in other countries that also observe depletion of natural deposits as well as high energy costs for barite extraction and the negative impact of tailings on the environment [47, 48].

Materials and methods.

Current approaches to obtaining barite are described, including those often used in the development of tailings ponds.

The review used the publications of Russian and foreign experts for 2010-2024, indexed in the following databases:

• VINITI abstract services: databases “Geography”, “Geology”, “Geophysics”, “Mining”, “Chemistry” and “Environmental Protection” (http://www.viniti.ru/products/abstract-journal);

• Scientific Electronic Library bibliographic database (https://www.elibrary.ru);

• American Chemical Society SciFinder-n database (https://scifinder-n.cas.org/);

• Scopus bibliographic database by Elsevier (https://www.scopus.com);

• Derwent Innovations Index patent database by Clarivate (https://clarivate.libguides.com/webofscienceplatform/dii).

Additionally, the reference lists of the papers selected for the review were analyzed. In total, more than 180 scientific articles and reviews were studied. The papers most relevant to the analyzed topic were included in this review.

Technologies for benefication of barite and barite-containing ores. Barite recovery methods depend on the type of deposit and, accordingly, its initial share in the ore. The processing of barite ores is the least costly, but such ores are steadily decreasing in the world. On the contrary, barite-polymetallic and technogenic deposits require more complex methods due to the low share of barite extraction into concentrate. The high cleavage of barite with other components has led to an abundance of various methods for the extraction, concentration and purification of barite and their permanent improvement based of the latest knowledge and technologies. The choice of one or other approach largely depends on the mineralogical composition and structure of the ore of polymetallic and technogenic deposits, the size of barite inclusions, the established requirements for the quality of the final product, etc.

When extracting barite and obtaining the most valuable barite concentrate the experts are mainly guided by GOST 4682-84 “Barite concentrate. Specifications”. In relation to barite for drilling liquids, many countries follow the regulatory requirements of the American Petroleum Institute (API)[4], ISO 13500:2008 “Petroleum and natural gas industries – Drilling fluid materials – Specifications and tests”. In Russia, GOST R 56946-2016 “Oil and Gas Industry. Drilling Mud Materials” applies. Due to the exhaustion of global reserves of easily mined barite, the criteria for its quality are periodically revised. In particular, lower-density barite-poor raw materials are involved in pro-

[4] API specification 13A. Drilling Fluids Materials. American Petroleum Institute, 2020, p. 124. URL: https://global.ihs.com/doc_detail.cfm? document_name=API%20SPEC%2013A&item_s_key=00010450 (accessed 19.04.2024).

This is an open access article under the CC BY 4.0 license

cessing, and preservation of the previous quality of the concentrate is compensated by increased requirements to its other characteristics, for example, to narrower fractionation of grain size composition [11], and extraction methods are complicated, improved and optimized.

Any barite production method begins with a washing step. Since barite is often mixed with clay and sand rocks, the properties of mechanical heterogeneity of components and water permeability of clays are exploited to disintegrate it. At the washing stages of disintegration (grinding to 25-100 mm), screening and classification, barite raw materials are separated from thin classes with working units of various machines (ball mills, etc.) that grind the rock under the influence of water and air. In rare cases, washing is sufficient to obtain barite of the desired quality.

Washing is used for coarse-grained ores, and when extracting barite from polymetallic and technogenic deposits, mechanical, chemical, and thermal benefication is used. Benefication is based on various barite properties, i.e., its flotation activity, high specific gravity, chemical inertness, weak magnetic ability, or reaction to heating. The two most common mechanical methods are flotation and gravity enrichment. More specific approaches include electromagnetic and radiometric separation, chemical bleaching, decripitation, and recovery in hydrocyclones.

Mechanical (physical) methods. *Flotation.* Flotation has been known since the 1930s, a detailed overview, stages of development of this approach and the equipment used are described in [49]. Often, barite flotation is only one of the stages of flotation benefication of polymetallic ores when extracting lead, copper, zinc, silver, etc. Therefore, it is used only in barite-polymetallic deposits, which account for up to a quarter of world barite production. It is mainly employed in the treatment of fine barite ores that cannot be separated by other methods. As a result of flotation, it is possible to obtain a high-quality barite concentrate suitable for the che-mical industry.

The flotation method is based on the difference in the surface properties of the components present in the ore or its processing tailings. Barite belongs to well-floated minerals and is easily separated from rocks or tailings. For the purpose, flotation reagents (collectors) can be added to it, which affect the surface of the barite particles. As a result, barite is trapped by air bubbles and rises to the surface as foam, while other components remain at the bottom.

An inverse scheme can also be used, when reagents (depressors) suppress the flotation properties of barite, as a result it precipitates, and other components of the material float [50]. Both procedures can be applied to increase the efficiency of flotation while collectors are added to some components of the initial material, and depressors to others.

Generalized process of barite flotation from tailings includes the following stages:

• Crushing of tailings obtained after extraction of barite from ore or after other stages of benefication, as a result of which a fraction suitable for flotation is created. For example, cone or jaw crushers are used in the crushing process. At this stage, an important task is to select the optimal size of crushing, since under some conditions a decrease in the size of the material leads to an increase in the concentration of barite [20], while after reaching a certain threshold, the content of barite in the crushed material, on the contrary, may decrease.

• Classification, when the resulting fine ore passes through screens that divide the material into different fractions depending on particle size. Barite is concentrated on the lower screen with small cells, and after sieving it enters the tray, from where it comes for grinding. The empty rock at the top of the screen is sent to the dump.

• Additional grinding in various types of mills including rod, ball, jet, drum or centrifugal. The initial material is ground into a fine fraction to facilitate subsequent processing. Dry and wet grinding are used.

• Preparation of barite ore pulp when ground tailings are mixed with water. At this stage, the mode of water treatment and pulp softening, and the establishment of the desired acidity (pH) of the pulp are important [51].

This is an open access article under the CC BY 4.0 license

• Addition of modifiers, foaming agents and barite collectors to the pulp. Modifiers include sodium sulfide or cyanide, zinc and copper sulfate, liquid glass (with the addition of sodium polyaluminosilicate to reduce the consumption of liquid glass). Collectors preferably represented by flotation reagents, which include the most commonly used oleic acid, citric acid, industrial (sulfate) soap, liquid glass, tall (mixed with kerosene) or pine oil, asidol, alkyl sulfates, alkyl sulfonates, soda ash, lime, baritol, ditalan, lauryl phosphate, VS-2 collectors, VS-4, DNS-VN, S-3, etc.

Dextrin, starch, chromic peak, permanganate, iodates, chloride, barium, sodium hexametaphosphate, gellan gum, etc. are used in reverse flotation with suppression of the flotation properties of barite leading to its precipitation.

In recent years, conceptually new approaches from biotechnology have been introduced. Microorganisms and their metabolic products are used to enrich ores that are poor in mineral content. Similar to traditional reagents, different properties of microorganisms (acidity, hydrophobicity, surface charge) are used to enhance foam formation, as collectors or agents for suppressing flotation properties, as well as modifiers [52, 53]. By microbial adsorption and redox reactions, microorganisms change the physicochemical properties of mineral surfaces, separating valuable minerals from waste rock.

In the past few years, microorganisms have been increasingly used in the flotation of various minerals and it often turns out to be a cheaper alternative to traditional reagents. The environmental friendliness of microorganism enrichment is higher due to a lower level of production waste and increased efficiency, and with microorganisms resistant to salt, acids and alkalis, prospects are outlined for the use of seawater and wastewater in the flotation process, which also makes production more environmentally friendly [54].

In barite flotation, microbial cells and their metabolites (proteins and polysaccharides) are used, which impact the mineral changing its surface properties like reagents, as a result of which the necessary characteristics for bioflotation or barite biodepression are achieved [55]. All these reagents, including biological reagents, are used both separately and in different combinations. Particular attention is paid to the optimal ratio of density of the collector/depressor sorption forms depending on the composition of the initial material and the specified parameters of the final product.

• Flotation which includes the mixing of material in various flotation chambers (for example, in a flotation column), when air or other gas is continuously supplied to the pulp, creating foam. Hydrophobic barite particles due to physically sorbed collector molecules adhere to foam bubbles and rise to the surface. Thus, barite is separated from the rest of the rocks and tailings. Often sulfide materials (for example, sphalerite or galena) undergo flotation, after which barite is simultaneously extracted from the tailings of sulfide flotation. Therefore, this step may involve several additional stripping steps after the main flotation and is completed by the control flotation.

The material can be preheated by microwave radiation, which increases the specific surface area of barite [56], to improve flotation properties. Ultrasound can also be used at this stage, which showed the following results in experiments:

– improved foaming, which enhances the selectivity effect (although the efficiency of flotation production of barite with and without ultrasound was significantly less pronounced in comparison with the other types of ores) [57];

– increased oil agglomeration of barite with an increased wetting angle, thus improved hydrophobicity of barite surface [58].

It is important to select the optimal ultrasound power.

• Cleaning, i.e., separation of concentrate from flotation reagents, for example, on a vibrating screen, its washing with appropriate solutions.

• Drying and calcination of barite is the final stage of flotation to improve the quality of barite concentrate and achieve the necessary characteristics.

This is an open access article under the CC BY 4.0 license

The technologies, the set of flotation reagents and the number of flotation steps may vary depending on the characteristics of the starting material, technical requirements and other conditions.

The disadvantages of flotation are primarily due to the use of the flotation reagents, which often are expensive, toxic (since many of them do not decompose [55]), and are also difficult to remove from the barite product obtained during flotation. The level of water-soluble salts and other fine fractions in the final product often exceeds acceptable values [20]. Although the removal of foreign impurities and reagent residues is inherent in the flotation scheme, in practice it turns out to be difficult and costly [59]. Residual flotation agents impair the wetting of barite in the mud and cause its foaming. In turn, increased air saturation (aeration) of the solution reduces the weighting capacity, increases viscosity and worsens washing of wells. Flotation benefication of barite is not always effective in the presence of components with similar flotation properties in the initial material: calcite, dolomite, quartz, and limestone.

Despite these disadvantages, the flotation method has a long history and a significant technological groundwork, the design of its technological scheme is being improved, first in the laboratory and then in the industry [48, 58]. New collectors and depressors are constantly being sought to improve flotation efficiency [60-62]. Much attention is paid to the search for affordable, highly efficient and selective reagents with low toxicity achieved by minimizing their use [48, 51, 63]. Therefore, in barite-polymetallic deposits, flotation remains one of the most common methods for extracting barite.

The flotation method continues to be actively employed in various countries in the development of both primary and technogenic deposits. In the last decade, the flotation mining method at technogenic deposits has been used, for example, at tailings dams in India for separation from quartz [59], at barite-polymetallic mines in Kazakhstan [64]; based on the results of laboratory studies its use at tailing dumps in Algeria are considered [65].

Gravity separation. The method of gravity separation, or gravitational benefication, for separating mineral complexes relies on the differences in contrast properties, in particular, the difference in density between barite and other minerals. The method is used for medium-grained ores, allowing to concentrate small fractions at a relatively low cost. As barite has high density, 1.5 times higher than the density of associated minerals, it can be separated by gravity when heavy barite particles move to the lower part of the device, while light minerals remain on the surface.

The main stages of gravity separation of barite include as follows:

• Crushing.

• Classification.

• Gravity separation based on differences in material densities. On gravitational equipment, the ore is subjected to gravitational forces separating barite from less dense components. The lifting power of water jet force large and heavy barite grains to accumulate in the tail of a table.

• Cleaning, which is an important step in washing the resulting concentrate, for example, from clay particles that impair rheological properties. The purpose of this step is to achieve the specified purity and quality of the concentrate.

• Drying, during which excess moisture is removed from the enriched barite.

Similar to the flotation method, it is important to optimally select the crushing time during gravity separation, as well as tune the gravity equipment adjusting vibration intensity (pulsation frequency) and amplitude, set the rate of stratification and transportation of particles, determine the required water flow rate, compressed air pressure, drum angle, etc. [20]. The concentration of barite content in the resulting product, as well as the scope of losses that escape to the tailings, largely depends on these criteria.

The disadvantages of gravity separation of barite include the difficulty of tuning the equipment and especially periodic reconfiguration for material with different initial content of barite,

This is an open access article under the CC BY 4.0 license

which often requires a complete shutdown. In addition, the final product may contain minerals with similar density, particularly, siderite, magnetite and sulfides, which prove difficult to separate by this method.

At the same time, gravity separation is devoid of the disadvantages of flotation. The barite weighting agent obtained through gravity separation does not have residual flotation reagents, water-soluble salts, and demonstrate an optimal particle size distribution; it is less consumed in the composition of drilling muds and provides higher density. It is also cheaper. The method is widely known in Russia [20] and abroad.

Hydrocyclones are technological cylindrical devices with a conical base, in which, under the influence of a rotating flow of liquids and centrifugal force, materials with different sizes and densities are separated. With regard to barite, the method undergoes experimental testing both at the level of microbarite [66] and separating barite from other components of tailings [67], as well as at extracting barite from spent drilling muds [68]. The barite recovery process with hydrocyclones typically involves the following steps:

• crushing;

• classification, where materials pass through hydrocyclones driven by piston pumps and are deposited centrifugally on the walls of the device;

• washing, where larger particles sent for repeated crushing and processing are removed, while small particles containing barite are collected in separate compartments;

• separating barite from water or other materials, for example, by filtration or centrifugation.

As with other barite processes, tuning is important in hydrocyclones. Thus, elevating the pressure in a hydrocyclone, optimizing the temperature regime, etc. can increase the efficiency of the procedure. Hydrocyclone advantages are easy operation and classification efficiency, including pellet size. Centrifuge enrichment is effective primarily for fine fractions of high-gravity minerals. With regard to relatively light and cheap barite, hydrocyclones can only slightly increase its yield. In addition, experts note extremely high-energy costs, which significantly reduces the economic feasibility of using hydrocyclones in the barite benefication.

Electromagnetic separation. Electromagnetic separation (magnetic separation, magnetic benefication) is widely used to enrich barite in the separation of minerals with magnetic susceptibility in tailings. Since barite does not possess magnetic properties, this method can be effective for its separation from other minerals from mixed ores, especially with a similar density, when gravity separation is useless. It is suitable for barite rocks containing quartz, iron impurities, and is effective for separating barite from hematite and magnetite.

The barite magnetic separation process includes the following steps:

• Crushing.

• Heating to 200-700 °C for ore pretreatment, creating the necessary differences in the conductivity of the components of the initial material. In some cases, various chemical reagents and powdered substances with a given conductivity are used that are adsorbed by the components of the material. In particular, oleic acid and graphite dust adsorbed by barite particles increase the conductivity of barite and facilitate its separation from quartz.

• Electromagnetic separation, when mixed material, passing through magnetic separators at a temperature of 93-240 °C, is exposed to magnetic fields. In this case, magnetic minerals are attracted and separated from non-magnetic particles containing barite. Separation of magnetic and non-magnetic fractions can take place in several stages.

• Classification, for example, on a sieve, pneumatic or magnetic separator, which may be required to further separate barite from the remaining minerals.

This is an open access article under the CC BY 4.0 license

As with other barite recovery methods, the efficiency of magnetic separation depends on the type of ore and its composition, the settings of the magnetic separators, for example, magnetic field strength, and other parameters.

The disadvantages of the method include high electricity consumption, especially at the stage of preliminary ore processing, which can entail significant economic costs. In addition, some other minerals, such as hematite or magnetite, can be separated along with barite. In such a case, it may be necessary to use additional technologies to further separate and obtain pure barite. The method is used in technogenic fields of Slovakia [69].

Chemical bleaching. This chemical method (also known as flocculation) is based on special chemical reagents used instead of mechanical opening of raw materials to agglomerate small barite particles into large globules, which simplifies their separation from the rest of the tailings. As a result, ground bleached barite is obtained. The technology should be considered as qualitative modification of the barite product rather than benefication. The method includes the following steps:

• In the crushing step, the barite ore is crushed to produce particles of the necessary size. This is required to increase the contact surface between the reagents and the ore.

• The ground ore is placed in large containers of water with added chemicals such as sulfuric, hydrochloric or nitric acids (15-20 % by weight of barite powder). Upon that, large aggregates of barite particles are formed, connected to each other as clumps larger and heavier than empty rock. Under the influence of gravity, they settle to the bottom of containers and can be separated from other minerals.

• Stages of multiple (up to 10 times) washing, dehydration and drying of the leached product, and subsequently the barite concentrate is separated from the remaining moisture and reagents, the presence of which is not allowed in the final product.

• From the obtained ground bleached barite, it is also possible to obtain an even higher quality product microbarite. It requires additional grinding in jet mills and acid treatment.

Thermal decripitation. Decripitation is a method of thermal benefication based on the heterogeneous thermal properties of the mineral and various consequences of thermal exposure to barite and empty rock. During decripitation, certain minerals are selectively destroyed under the influence of heating or the "heating – rapid cooling" cycle: the water contained in the minerals, when heated to 400-450 °C, leads to their cracking due to pressure. Minerals are destroyed along cleavage planes, or the links between minerals are significantly weakened. During decripitation, barite cracks and turns into a powder, while the accompanying minerals remain in their original state. The scheme is implemented in three stages:

• heating ore in a tube furnace;

• classification on a sieve, where the empty upper rock goes to the dump, and the lower goes to further processing;

• final sorting of barite on thin sieves.

Thermal decripitation has been known since the 1930s, it is used mainly for fine ores. Large process losses are frequent due to incomplete separation of thin material. Decripitation is effective in thermal dehydration of barite raw materials when it is processed into bleached microbarite, which should be considered modification rather than benefication. In Russia, it is not used in the industry.

Radiometric separation. The method implies large-scale separation for preliminary benefication and is based on the ability of minerals to emit, absorb or reflect various radiation [70], mainly X-ray radiometric separation is used[5,6]. The stages include crushing, screening, and washing of the class and the radiometric separation.

[5] Nuclear physical methods. Instruction N 97-YaF. Barium. Moscow: All-Union Scientific Research Institute of Mineral Raw Materials, 1970, 19 p. URL: https://meganorm.ru/Data2/1/4293753/4293753805.pdf (accessed: 19.04.2024).

[6] Methodological recommendations for the application of the Classification of deposit reserves and predicted resources of solid minerals. Barite ores. Moscow, 2007, 38 p. URL: https://www.geokniga.org/books/2465 (accessed: 19.04.2024).

This is an open access article under the CC BY 4.0 license

When considering the technological parameters of radiometric separation, the task of separating barite from silicate rocks is successfully solved. The ore varies in color from white to yellow and green to brown with a material size of –16 + 9 mm. Two-stage benefication is carried out with Sortex 621 M (a photometric belt-type separator with a vibrating feeder manufactured by Gunson's Sortex Ltd.). The intensity of reflected light is measured under free fall of mineral pieces. The sorting mechanism includes a pneumatic valve. For material with a size of 20 mm, the response frequency reaches 200-250 Hz, and for smaller material – 400-600 Hz. First, white barite concentrate ($BaSO_4$ content is 95.2 %) is released, then brown barite concentrate ($BaSO_4$ content is 91.1 %).

X-ray radiometric separation (based on measuring the energy of characteristic radiation from irradiating a substance with X-ray or γ-radiation) was used on barite ores of the Sobskoe deposit; the released BaO concentrate contained 93.1 % of the useful component.

It is possible to use the near-infrared method (determine the difference in the interaction of electromagnetic radiation in the near infrared range with molecules of the material surface) to separate barite and fluorite from calcite and dolomite [71].

In order to identify the demand for and prevalence of barite extraction approaches, a scientometric analysis was carried out on a full sample of reviewed papers, as well as patents from the Derwent Innovations Index database (see Figure). Flotation demonstrates the greatest interest at the global level. At the same time, it is important to note that flotation is applied mainly to polymetallic ores, where barit extraction is secondary and gives less than a quarter of the world mineral production. Gravity, electromagnetic separation and chemical bleaching are leading in barite and technogenic deposits; and patenting of the obtained results is noticeably prevailing in electromagnetic separation and chemical bleaching compared to research articles. This indicates the maturity of these technologies, when the volume of scientific research, reflected in journal articles, is declining and is replaced by registrable technological know-how published in patent documents. To a certain extent, the interest in the hydrocyclone method for barite production is increasing, although experts note its applicability mainly to fine fractions of the mineral, as well as high energy costs. The least interest in the last decade is observed in thermal decripitation and radiometric methods, for which there are no patents, and the number of research papers is low.

Most of the described methods are complementary and can be used jointly. Combined methods include magnetic flotation, roasting ore followed by magnetic separation, magnetic separation together with chemical bleaching, chemical bleaching with decripitation, etc. Also, some methods can be part of a technological chain of other approaches; it is especially characteristic of chemical methods that constitute an integral part of many other methods. In addition, in recent years, com-

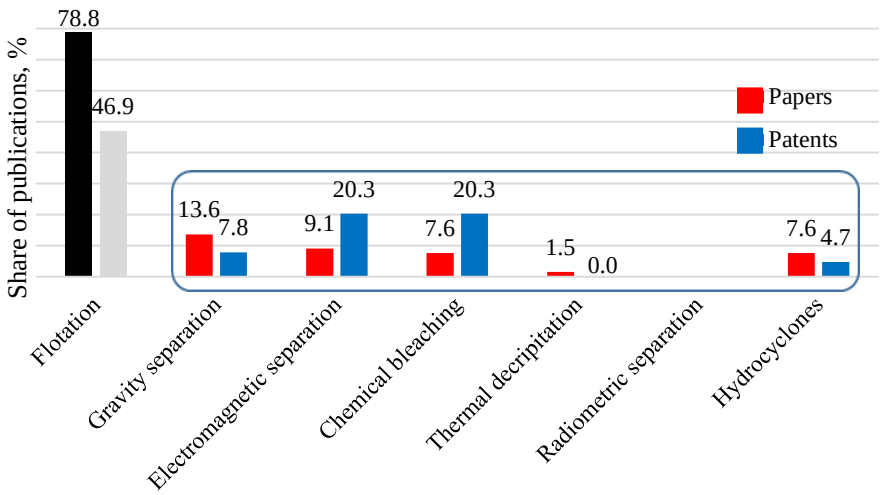

Distribution of the prevalence of barite benefication approaches in scientific papers and patents for 2010-2024. Some publications describe two or more approaches, so they are included simultaneously in several groups

This is an open access article under the CC BY 4.0 license

plex mathematical models have been increasingly used in each approach, including those based on neural networks that have become popular. They help determine the content of barite in the initial material, the degree of possible extraction of the mineral, calculate the optimal conditions in tuning the equipment [48], calculate the necessary benefication parameters for both barite and the products obtained with its participation, for example, concrete solutions [72].

The described methods of barite extraction are used to varying degrees in the regions of the world by companies for the extraction and production of class A and B barite (see Table).

The most productive countries, regions and companies in the barite industry

Country	Barite extraction regions	Barite Mining and Production Companies
India	Andhra Pradesh (Mangampet village) and Rajasthan	20 Microns (https://www.20microns.com); Chemi Enterprises (https://www.chemienterprises.in); Finokoats & Colours (https://finokoats.com); Gayatri Microns (http://www.gayatrimicrons.com); Girikandra Trading Company (https://www.girikandra.net); Golden Micro Chemicals (https://www.goldenmicrochemicals.in); Satya Laxmi Mud-Chem PVT (http://slmpl.com)
Kazakhstan	Zhambyl, Karaganda, Mangistau, Turkestan Regions	Dostau Litas (http://baritkz.kz); Global Chemicals Company (https://gcc.kz); Global Chemicals Industries / Karazhal Operating (http://gcind.kz)
China	Gansu, Guangzhou, Guizhou, Fujian, Hubei, Hunan, Shaanxi Provinces, Guangxi Zhuang Autonomous Region	Dalian Huanqiu Minerals (https://hq-minerals.com); GuiZhou Saboman (https://www.chinabarite.cc); Handan Tianmu Chemicals (https://tianmuchem.guidechem.com); Majiang JGL Barite Mine (https://yuensons.lookchem.com)
Morocco	Drâa-Tafilalet, Casablanca-Settat	Ado Barite Morocco (http://adomorocco.csglobal.com.tr); Bastion Industries (https://bastiongroup.net); Mounir Negoce (http://mounirnegoce.com); Terra Nova Minerals (https://terra-nova.ma)
Nigeria	Adamawa, Benue, Gombe States, Zamfara, Cross River, Nasarawa, Plateau, Taraba, Ebonai	Breitz Group (https://breitzgroup.co); Helicon Group (http://heli-ng.com); PolyGuard Investment Nigeria (https://polyguardinvestmentng.com)
Pakistan	Balochistan (Daddar districts, Las Bela) and Khyber Pakhtunkhwa (Hazara District)	Pakistan Mineral Development Corporation (https://pmdc.gov.pk); Pakistan Minerals Company (http://www.pakistanmineralscompany.com)
Turkey	Konya, Malatya, Sivas, Isparta	Barit Maden Turk (https://baritmaden.com); Baser Mining (https://basermining.com); Deep Drilling Chemicals (http://www.ddc-ltd.com); Efe Baryt Mining (https://www.efemaden.com.tr); Gulmer Madencilik (https://gulmercapricorn.com); Meta Global Madencilik (https://metaglobalchem.com)

Conclusion.

An analysis of the modern literature on barite ore benefication revealed significant and increasing importance of this mineral for a variety of industries. Despite the repeatedly announced transition to a green economy, the fuel and energy complex is still the paramount consumer of barite required for the annual drilling of all new wells. With the depletion of barite-rich deposits, wastes of mining and processing plants are of fundamental importance for barite production, as these technogenic deposits enable extraction of large amounts of barite.

Gravity and electromagnetic separation, as well as chemical bleaching are the most significant extraction approaches for the barite and technogenic deposits. At the same time, electromagnetic separation and chemical bleaching in the last decade are in the phase of active patenting of the relevant technologies, exceeding journal papers in the absolute as well as share numbers, which indicates the maturity of these methods.

This is an open access article under the CC BY 4.0 license

In the last decade, both the Russian and international research in the field of barite ore beneficiation cover the following interrelated areas:

• Making technologies and barite products increasingly environmentally friendly, which is achieved through decreased toxicity of current and emerging reagents used in separation of barite extraction. Conceptually new ways of benefication emerge relying on various microorganisms that do not harm nature. Due to an extensive variety of microorganisms, their rapid reproduction and a wide range of applications in benefication, bioflotation is considered as a solid basis for the industrial use of microorganisms in the coming years, as well as an effective solution for creating safe and environmentally friendly mineral production.

• Increasing the efficiency of methods where mathematical models come to the fore to optimize all technological processes, including neural networks.

• Reducing the total cost of benefication works, particularly decreasing energy and reagent consumption.

REFERENCES

1. Bolonin A.V., Nikiforov A.V. Intermediate Sulfates in Barite-Celestite Isomorphic Series: Composition and Mode of Occurrence. *Geology of Ore Deposits.* 2014. Vol. 56. N 4, p. 302-314. DOI: 10.1134/S1075701514040023

2. Lein A.Y., Kravchishina M.D. Barium Geochemical Cycle in the Ocean. *Lithology and Mineral Resources.* 2021. Vol. 56. N 4. P. 293-308. DOI: 10.1134/S0024490221040052

3. Egorova I.P., Akhmanov G.G., Bulatkina T.A. Typomorphic features of barite. *National Geology.* 2010. N 2, p. 3-8 (in Russia).

4. Kuznetsov D.S., Burtsev I.N., Kuznetsov S.K. Barite raw market and prospects for the development of deposits in the Republic of Komi. *The North and the Market: Forming the Economic Order*. 2022. Vol. 25. N 3, p. 171-185 (in Russian). DOI: 10.37614/2220-802X.3.2022.77.012

5. Boyarko G.Yu., Khatkov V.Yu. Current state of production and consumption of barite raw materials in Russia. *Bulletin of the Tomsk Polytechnic University. Geo Assets Engineering*. 2021. Vol. 332. N 10, p. 180-191 (in Russian). DOI: 10.18799/24131830/2021/10/3403

6. Akhmanov G.G., Egorova I.P., Bulatkina T.A. Method for determining the genesis barite field early exploration work. *Prospect and protection of mineral resources.* 2017. N 4, p. 11-15 (in Russian).

7. Akhmanov G.G., Bulatkina T.A., Egorova I.P. et al. Deposits of the residual type of the Republic of Bashkortostan – basis for the creation of raw material base of "non-drilling" barit. *Prospect and protection of mineral resources.* 2019. N 6, p. 14-18 (in Russian).

8. Senatorov P.P. Problems of the mineral resource base of the main types of non-metals used in the chemical complex of Russia. *Mineral Resources of Russia. Economics & Management.* 2019. N 1, p. 31-35 (in Russian).

9. Akhmanov G.G., Egorova I.P., Bulatkina T.A. Current status and development prospects of the barite mineral resources base. *Mineral Resources of Russia. Economics & Management.* 2017. N 6, p. 4-14 (in Russian)

10. Akhmanov G.G., Egorova I.P., Bulatkina T.A. Barite deposits weathering – a promising source of high-quality raw material. *National Geology.* 2016. N 2, p. 23-31 (in Russian).

11. Ryzhkov A.V., Koreshkov N.G. Current Status with Mineral Resource Base of Barite and New Requirements to Barite Weighting Agents in Drill Mud. *Neft. Gas. Novacii.* 2020. N 11 (239), p. 33-36 (in Russian).

12. Novikov N.V., Samchenko S.V., Okolnikova G.E. Barite-containing radiation protective building materials. *RUDN Journal of Engineering Research.* 2020. Vol. 21. N 1, p. 94-98 (in Russian). DOI: 10.22363/2312-8143-2020-21-1-94-98

13. Bhatti M.A., Kazmi K.R., Mehmood R. et al. Beneficiation Study on Barite Ore of Duddar Area, District Lasbela, Balochistan Province, Pakistan. *Pakistan Journal of Scientific and Industrial Research Series A: Physical Sciences*. 2017. Vol. 60. N 1, p. 9-21. DOI: 10.52763/PJSIR.PHYS.SCI.60.1.2017.9.22

14. Ahmad I., Shahzada K., Ahmad M.I. et al. Densification of Concrete using Barite as Fine Aggregate and its Effect on Concrete Mechanical and Radiation Shielding Properties. *Journal of Engineering Research*. 2019. Vol. 7. N 4, p. 81-95.

15. Samchenko S.V., Novikov N.V. Influence of a barite containing additive on the properties of cellular concrete. *Technique and Technology of Silicates.* 2022. Vol. 29. N 4, p. 335-341 (in Russian).

16. Chenhao Zeng, Qing Kang, Zhongshan Duan et al. Development of Polymer Composites in Radiation Shielding Applications: A Review. *Journal of Inorganic and Organometallic Polymers and Materials*. 2023. Vol. 33. Iss. 8, p. 2191-2239. DOI: 10.1007/s10904-023-02725-6

17. Cherkasov V.D., Yurkin Yu.V., Suntsov D.L. Technical and economic comparison of design solutions for radiation protection against X-ray radiation. *Engineering Journal of Don.* 2021. N 1, p. 230-243 (in Russian).

18. Ishbaev G., Dilmiev M., Khristenko A. et al. Development of more heavy thermally stable salt-saturated drilling mud by "BURINTECH" SPE" LLC. *Burenie & neft.* 2013. N 9, p. 47-48 (in Russian).

19. Akhmanov G.G., Egorova I.P., Bulatkina T.A. The state and prospects of development of the mineral resource base of barite of the Republic of Khakassia. *Prospect and protection of mineral resources.* 2022. N 7, p. 41-49 (in Russian). DOI: 10.53085/0034-026X_2022_07_41

20. Gershenkop A.Sh., Khokhulya M.S., Kontorina T.A. Development of the technology of gravity and magnetic separation of barite-siderite ores in Sallanlatva deposit. *Mining Informational and Analitical Bulletin*. 2007. N 10, p. 358-364.

This is an open access article under the CC BY 4.0 license

21. Leusheva E.L., Alikhanov N.T., Brovkina N.N. Study on the rheological properties of barite-free drilling mud with high density. *Journal of Mining Institute.* 2022. Vol. 258, p. 976-985. DOI: 10.31897/PMI.2022.38

22. Pereyma A.A., Dubov N.M., Cherkasova V.E. The mud on the basis of biopolymer for hole making in AHFP. *Construction of Oil and Gas Wells on Land and Sea.* 2010. N 4, p. 34-38 (in Russian).

23. Akhmanov G.G., Egorova I.P., Bulatkina T.A. The problem of providing the industry with high-quality barite raw materials, ways of its solution. *Prospect and protection of mineral resources.* 2021. N 8, p. 9-14 (in Russian).

24. Grinev O.M., Semiryakov A.S., Bestemyanova K.V., Grinev R.O. Morphostructure and stages of the formation of the Zmeinogorsk barite-polymetallic deposit (Rudny Altai). *Advances in current natural sciences.* 2022. N 8, p. 81-95 (in Russian). DOI: 10.17513/use.37872

25. Bortnikova S.B., Yurkevich N.V., Edelev A.V. et al. Hydrochemical and gaseous anomalies on sulfide tailings (Salair, Kemerovo region). *Izvestiya Tomskogo politekhnicheskogo universiteta. Inzhiniring georesursov*. 2021. Vol. 332. N 2, p. 26-35 (in Russian). DOI: 10.18799/24131830/2021/2/3040

26. Kalinin E.P. Barites of the Komi Republic: current state and development potential. *Vestnik of the Institute of Geology of the Komi Science Center of the Ural Branch of the Russian Academy of Sciences*. 2010. N 3, p. 2-5 (in Russian).

27. Kuznetsov S.K., Burtsev I.N., Tarbaev M.B. et al. Mineral resources of the Vorkuta region and the prospects of their development. *Proceedings of the Komi Science Centre of the Ural Division of the Russian Academy of Sciences.* 2021. N 3 (49), p. 65-74 (in Russian). DOI: 10.19110/1994-5655-2021-3-65-74

28. Senatorov P.P., Belyayev Y.V., Kuzmina I.A. Nonmetallic minerals in the Russian Arctic zone: resource potential and its utilization. *Mineral Resources of Russia. Economics & Management.* 2015. N 2, p. 9-21 (in Russian).

29. Vikentev I.V. Metallogenic studies in the Polar Urals and problems of developing its mineral resource potential. *Metallogeniya drevnikh i sovremennykh okeanov*. 2020. N 1, p. 36-40.

30. Akhmanov G.G., Egorova I.P., Michailik P.E. et al. To genesis of travertinopodobnye barites of Derugin basin (Okhotsk Sea). *National Geology.* 2015. N 1, p. 82-88 (in Russian).

31. Astakhov A.S., Ivin V.V., Karnaukh V.N. et al. Barite mineralization in the Deryugin Basin of the Okhotsk Sea: Active processes and formation conditions. *Russian Geology and Geophysics.* 2017. Vol. 58. N 2, p. 165-176. DOI: 10.1016/j.rgg.2017.01.002

32. Astakhova N.V. Barium in ferromanganese crusts from the Sea of Japan: peculiarities of allocation and interrelation with main ore phases. *Vestnik of the Institute of Geology of the Komi Science Center of the Ural Branch of the Russian Academy of Sciences.* 2019. N 3, p. 31-40 (in Russian). DOI: 10.19110/2221-1381-2019-03-31-40

33. Safina N.P., Melekestseva I.Yu., Ankusheva N.N. et al. Barite from ores of the Safyanovsky pyrite deposit (Middle Urals) and hydrothermal fields Semenov-1 and 3 (Mid-Atlantic Ridge): comparative analysis of formation conditions. *Metallogeniya drevnikh i sovremennykh okeanov*. 2015. N 1, p. 93-97.

34. Korotchenkova O.V. Celestine and barite of the Verkhnekamskoe salt deposit (Perm region). *Problemy mineralogii, petrografii i metallogenii. Nauchnye chteniya pamyati P.N.Chirvinskogo.* 2019. Vol. 22, p. 73-79.

35. Afolayan D.O., Eggleston C.M., Onwualu A.P. et al. Physicochemical Studies for Risk Identification, Assessment, and Characterization of Artisanal Barite Mining in Nigeria. *Sustainability*. 2021. Vol. 13. Iss. 23. N 12982. DOI: 10.3390/su132312982

36. Yurkevich N.V., Eltsov I.N., Gureev V.N. et al. Technogenic effect on the environment in the Russian arctic by the example of the Norilsk industrial area. *Bulletin of the Tomsk Polytechnic University. Geo Assets Engineering*. 2021. Vol. 332. N 12, p. 230-249 (in Russian). DOI: 10.18799/24131830/2021/12/3207

37. Bolgov G.P. Salair sulfides. Ur group of polymetallic deposits. *Izvestiya Tomskogo industrialnogo instituta*. 1937. Vol. 58. Iss. 1-3, p. 45-96.

38. Distanov E.G. Pyrite-polymetallic deposits of Siberia. Novosibirsk: Nauka. Sibirskoe otdelenie, 1977, p. 351.

39. Cherepnin V.K. Towadrs the composition and genesis of ores from the Ur deposits of Salair. *Izvestiya Tomskogo Ordena Trudovogo Krasnogo Znameni politekhnicheskogo instituta imeni S.M.Kirova*. 1958. Vol. 90, p. 56-68.

40. Olenchenko V.V., Kucher D.O., Bortnikova S.B. et al. Vertical and lateral spreading of highly mineralized acid drainage solutions (*Ur dump, Salair*): electrical resistivity tomography and hydrogeochemical data. *Russian Geology and Geophysics.* 2016. Vol. 57. N 4, p. 617-628. DOI: 10.1016/j.rgg.2015.05.014

41. Gosudarstvennaya geologicheskaya karta Rossiiskoi Federatsii masshtaba 1:200000. Izdanie vtoroe. Seriya Kuzbasskaya. List N-45XIV (Gur'evsk). Obyasnitelnaya zapiska. Saint Petersburg: Kartograficheskaya fabrika VSEGEI, 2002, p. 88.

42. Mishenin M.V., Yurkevich N.V. Experience in geological and economic assessment of technogenic deposits (using the example of barite). GeoEvraziya-2023. Geologorazvedochnye tekhnologii: nauka i biznes: Trudy VI Mezhdunarodnoi geologo-geofizicheskoi konferentsii, 27-29 March 2023, Moscow, Russia: v 3 tomakh. Tver: PoliPRESS, 2023. Vol. I (III), p. 44-47.

43. Khusainova A.Sh., Yurkevich N.V., Bortnikova Sv.B. Secondary barite from the Novo-Ursk dump. Geodynamics and Minerageny of Northern Eurasia: Materials of VI International scientific conference, 13-17 March 2023, Ulan-Ude, Russia. Ulan-Ude: Buryat State University Publishing Department, 2023, p. 567-570 (in Russian).

44. Khusainova A.Sh., Bortnikova S.B., Gaskova O.L. et al. Secondary minerals of Fe, Pb, Cu in sulfide-containing tailings: sequence of formation, electrochemical reactions and physicochemical model (Talmovskie Sands, Salaire, Russia). *Earth Sciences.* 2023. Vol. 23. N 1. N ES1006 (in Russian). DOI: 10.2205/2023ES000810

45. Yurkevich N.V., Khusainova A.Sh., Bortnikova S.B. Resources of barite, non-ferrous and precious metals in the Talmovskie peski tailing dump: mineralogical, geochemical and geophysical data. *Geology and mineral resources of Siberia.* 2023. N 3 (55), p. 105-114 (in Russia). DOI: 10.20403/2078-0575-2023-3-105-114

46. Leonteva E.V., Medyanik N.L., Kalugina N.L. Thermochemical chloro-ammonium processing of technogenic dump sulphide tailings. *Mining Informational and Analytical Bulletin.* 2017. N 1, p. 305-316 (in Russian).

47. Edelev A.V., Yurkevich N.V., Gureev V.N., Mazov N.A. Reclamation of Waste Storage Sites of the Mining Industry in the Russian Federation. *Journal of Mining Science.* 2022. Vol. 58. N 6, p. 1053-1068. DOI: 10.1134/S1062739122060205

48. Deniz V., Umucu Y., Deniz O.T. Estimation of grade and recovery in the concentration of barite tailings by the flotation using the MLR and ANN analyses. *Physicochemical Problems of Mineral Processing*. 2022. Vol. 58. Iss. 5. N 150646. DOI: 10.37190/ppmp/150646

49. Fuerstenau D.W., Pradip. A Century of Research Leading to Understanding the Scientific Basis of Selective Mineral Flotation and Design of Flotation Collectors. *Mining, Metallurgy & Exploration*. 2019. Vol. 36. Iss. 1, p. 3-20. DOI: 10.1007/s42461-018-0042-6

This is an open access article under the CC BY 4.0 license

50. Long Wang, Weijian Lyu, Lingyun Huang et al. Utilization of gellan gum as a novel eco-friendly depressant in the flotation separation of fluorite from barite. *Minerals Engineering*. 2022. Vol. 184. N 107640. DOI: 10.1016/j.mineng.2022.107640

51. Gudvill M.N., Bogidaev S.A. Study of collecting agent Fomol and mineral surface interaction in water recirculation environment. *Proceedings of the Siberian Department of the Section of Earth Sciences, Russian Academy of Natural Sciences. Geology, Prospecting and Exploration of Ore Deposits.* 2016. N 4 (57), p. 70-76 (in Russian). DOI: 10.21285/0130-108X-2016-57-4-70-76

52. Zhonghua Xue, Yali Feng, Haoran Li et al. A comprehensive review on progresses of coal and minerals bioflotation in presence of microorganisms. *Journal of Environmental Chemical Engineering*. 2023. Vol. 11. Iss. 6. N 111182. DOI: 10.1016/j.jece.2023.111182

53. Asgari K., Huang Q., Khoshdast H., Hassanzadeh A. A Review on Bioflotation of Coal and Minerals: Classification, Mechanisms, Challenges, and Future Perspectives. *Mineral Processing and Extractive Metallurgy Review*. 2024. Vol. 45. Iss. 1, p. 46-76. DOI: 10.1080/08827508.2022.2121919

54. San Martín F., Kracht W., Vargas T. Biodepression of pyrite using *Acidithiobacillus ferrooxidans* in seawater. *Minerals Engineering*. 2018. Vol. 117, p. 127-131. DOI: 10.1016/j.mineng.2017.11.005

55. Ashkavandi R.A., Azimi E., Hosseini M.R. *Bacillus licheniformis* a potential bio-collector for Barite-Quartz selective separation. *Minerals Engineering*. 2022. Vol. 175. N 107285. DOI: 10.1016/j.mineng.2021.107285

56. Jing Guo, Ming Wen, Jingxuan Wu. Mchanistic study on the flotation of barite with $C_{18}H_{33}NaO_2$ under microwave radiation based on UV-visible spectrophotometric analysis. *Physicochemical Problems of Mineral Processing*. 2022. Vol. 58. Iss. 6. N 156349. DOI: 10.37190/ppmp/156349

57. Cilek E.C., Ozgen S. Improvement of the Flotation Selectivity in a Mechanical Flotation Cell by Ultrasound. *Separation Science and Technology*. 2010. Vol. 45. Iss. 4, p. 572-579. DOI: 10.1080/01496390903484966

58. Esmeli K. The Effect of Ultrasound Treatment on Oil Agglomeration of Barite. *Mineral Processing and Extractive Metallurgy Review*. 2023. Vol. 44. Iss. 3, p. 189-200. DOI: 10.1080/08827508.2022.2155957

59. Raju G.B., Ratchambigai S., Rao M.A. et al. Beneficiation of Barite Dumps by Flotation Column; Lab-Scale Studies to Commercial Production. *Transactions of the Indian Institute of Metals*. 2016. Vol. 69. Iss. 1, p. 75-81. DOI: 10.1007/s12666-015-0700-z

60. Cheng Liu, Xinyue Zhang, Yunfei Zheng et al. Utilization of water glass as a dispersant to improve the separation performance of fluorite from barite slimes. *Colloids and Surfaces A: Physicochemical and Engineering Aspects*. 2022. Vol. 635. N 128036. DOI: 10.1016/j.colsurfa.2021.128036

61. Cheng Liu, Shaoxian Song, Hongqiang Li. Selective flotation of fluorite from barite using trisodium phosphate as a depressant. *Minerals Engineering*. 2019. Vol. 134, p. 390-393. DOI: 10.1016/j.mineng.2019.02.008

62. Ying Lu, Weiping Liu, Xuming Wang et al. Lauryl Phosphate Flotation Chemistry in Barite Flotation. *Minerals*. 2020. Vol. 10. Iss. 3. N 280. DOI: 10.3390/min10030280

63. Randin O.I., Gudvill M.N., Bogidaev S.A. Investigation of reagent "Phomol" interaction mechanism under barite ore flotation. *Proceedings of Irkutsk State Technical University*. 2012. N 6 (65), p. 119-123 (in Russian).

64. Turebekova K., Katkeeva G., Sultangaziev R. et al. Choice of Scheme and Reagents for Flotation of Technogenic Barite Raw Materials. *University Proceedings.* 2022. N 4 (89), p. 85-90 (in Russian). DOI: 10.52209/1609-1825_2022_4_85

65. Larachi N., Bali A., Ould Hamou M., Bensaadi S. Recovery of lead and barite from the abandoned Ichmoul mine wastes in Algeria. *Environmental Earth Sciences*. 2019. Vol. 78. Iss. 20. N 601. DOI: 10.1007/s12665-019-8593-5

66. Neesse Th., Dueck J., Schwemmer H., Farghaly M. Using a high pressure hydrocyclone for solids classification in the submicron range. *Minerals Engineering*. 2015. Vol. 71, p. 85-88. DOI: 10.1016/j.mineng.2014.10.017

67. Dueck J., Minkov L.L. On the Conditions of Clogging in a Hydrocyclone. *Theoretical Foundations of Chemical Engineering*. 2019. Vol. 53. N 4, p. 529-537. DOI: 10.1134/s0040579519040171

68. Wenjie Lv, Jinchao Zhao, Mingxun Hao et al. Enhancing classification and recovery of barite from waste drilling fluid by inlet particle arranging of hydrocyclone. *Journal of Water Process Engineering*. 2023. Vol. 56. N 104341. DOI: 10.1016/j.jwpe.2023.104341

69. Hredzák S., Dolinská S., Znamenáčková I. et al. Possibilities of Siderite and Barite Concentrates Preparation from Tailings of Settling Pit Nearby Markušovce Village (Eastern Slovakia). *Inżynieria Mineralna*. 2019. Vol. 1. N 1, p. 19-24. DOI: 10.29227/IM-2019-01-03

70. Boroznovskaya N.N., Zyryanova L.A., Pekov I.V. Luminescent Properties of Natural Barite: Evidence for Its Genesis. *Doklady Earth Sciences.* 2016. Vol. 471. Part 1, p. 1171-1173. DOI: 10.1134/s1028334x16110118

71. Kobzev A.S. Radiometric benefication of mineral raw materials. Moscow: Gornaya kniga, 2015, p. 25.

72. Tosee S.V.R., Faridmehr I. Mechanical properties prediction of heavyweight concrete using generalized regression neural network (GRNN). *Romanian Journal of Materials*. 2022. Vol. 52. N 3, p. 303-310.

Authors: **Nataliya V. Yurkevich,** *Candidate of Geological and Mineralogical Sciences, Head of Laboratory, https://orcid.org/0000-0001-8337-9148 (Trofimuk Institute of Petroleum Geology and Geophysics SB RAS, Novosibirsk, Russia; Scientific-Research Center "Ecology" SB RAS, Novosibirsk, Russia*), **Tatyana V. Grosheva,** *Candidate of Engineering Sciences, Head of Department, https://orcid.org/0009-0009-6452-0471 (Tyumen Branch of SurgutNIPIneft, Surgutneftegas PJSC, Tyumen, Russia*), **Aleksei V. Edelev,** *Candidate of Geological and Mineralogical Sciences, Senior Researcher, https://orcid.org/0000-0003-0045-999X (Trofimuk Institute of Petroleum Geology and Geophysics SB RAS, Novosibirsk, Russia*), **Vadim N. Gureev,** *Candidate of Pedagogical Sciences, Head of Center, GureyevVN@ipgg.sbras.ru, https://orcid.org/0000-0002-3460-0157 (Trofimuk Institute of Petroleum Geology and Geophysics SB RAS, Novosibirsk, Russia*), **Nikolai A. Mazov,** *Candidate of Engineering Sciences, Leading Researcher, https://orcid.org/0000-0003-4607-1122 (Trofimuk Institute of Petroleum Geology and Geophysics SB RAS, Novosibirsk, Russia*).

The authors declare no conflict of interests.

This is an open access article under the CC BY 4.0 license

ISSN 2411-3336; e-ISSN 2541-9404

JOURNAL OF MINING INSTITUTE

Zapiski Gornogo instituta

Journal homepage: pmi.spmi.ru

Research article

Improving the procedure for group expert assessment in the analysis of professional risks in fuel and energy companies

Ekaterina I. Karchina, Mariya V. Ivanova, Alla T. Volokhina, Elena V. Glebova, Aleksei E. Vikhrov✉
National University of Oil and Gas "Gubkin University", Moscow, Russia

***How to cite this article*:** Karchina E.I., Ivanova M.V., Volokhina A.T., Glebova E.V., Vikhrov A.E. Improving the procedure for group expert assessment in the analysis of professional risks in fuel and energy companies. Journal of Mining Institute. 2024. Vol. 270, p. 994-1003.

Abstract

The lack of a unified approach to the assessment of professional risks in fuel and energy companies (FEC) in the national regulatory environment and a high degree of subjectivity of the results of hazard identification and risk assessment makes mathematically sound recruitment of an expert group urgent and necessary. The article presents the results of a comprehensive study on hazard identification and risk assessment at 6,105 workplaces in 24 branches of a FEC company based on the application of the expert assessment method and a scientifically sound qualitative and quantitative selection of experts. The priority vectors of factors are determined, global priorities are calculated, the size of the expert group (15 persons) is determined and mathematically substantiated for carrying out hazard identification and risk assessment at workplaces with sufficient reliability of results. For the first time, a set of factors characterizing the FEC companies that influence the determination of professional competence of experts is proposed. The formed expert group presented more precise, objective and consistent results of risk assessment. Standards for free distribution of personal protective equipment (PPE) and wash-off agents to 7,234 company employees for implementation and trial use were developed. A fragment of the results obtained for a driller's workplace is presented. This approach allows a significant increase in objectivity and efficiency of the professional risk management system and provision of the PPE to employees in the concept of a risk-oriented approach helping to prevent industrial injuries and improve the level of occupational safety culture in fuel and energy companies taking into account global practice.

Keywords

risk-based approach; hazard identification; professional risk assessment; expert group; expert competence

Received*: 01.11.2023** ***Accepted: 02.05.2024 ***Online: 13.09.2024*** ***Published: 25.12.2024***

Introduction.

The paradigm of implementing a proactive risk-oriented approach is one of the fundamental conditions for a successful execution of the provisions of GOST R ISO 45001-2020 "Occupational safety and health management systems. Requirements and guidance for use" identical to the international standard ISO 45001:2018 [1]. In particular, the practice of foreign countries clearly confirms the efficiency of using a risk-oriented approach in providing employees with personal protective equipment (PPE) [2-4].

Currently, there are no regulated criteria for the mechanism for assessing the competence and recruiting an expert group to identify hazards and assess risks at workplaces in the fuel and energy companies (FEC). This necessitates improvement and experimental implementation. Given the specificity of the transformation of labour legislation[1] and the complexity of industry specificity, the

[1] Order of the Ministry of Labour of Russia dated October 29, 2021 N 767n "On approval of the Unified standards for the issuance of personal protective equipment and wash-off agents".

This is an open access article under the CC BY 4.0 license

discussion of practical aspects of implementing the risk-oriented approach in the FEC companies is particularly relevant [5, 6].

The expert assessment method chosen in this paper as a tool for improving the process of hazard identification and risk assessment at workplaces is widely used in various fields in cases where other methods for obtaining the necessary information are inapplicable or insufficiently efficient [7]. For example, in [8], the experts assessed the risks during construction of transportation infrastructure facilities. In article [9], the expert assessment method was used for the dynamic probabilistic analysis of accidents at construction sites. The involvement of experts in risk assessment and decision-making related to safety is considered in [10]. It is recommended to set up commissions or teams at the enterprise to assess the professional risks at workplaces [11]. The expert assessment method is used in expert examination of hazardous production facilities with prediction of the most optimal membership of the expert group [12] as well as in the analysis of hazard related to mothballed or abandoned oil and gas wells [13].

When applying the expert assessment method, the problem of selecting a team of competent experts whose objectivity and reliability of the assessment results would not be subject to doubt is of fundamental importance. Formation of such a team, both in terms of membership and size, is carried out exclusively using mathematically sound algorithms. Therefore, a wise solution of the problem of selecting experts directly affects the result of ensuring safe working conditions.

The objective of the study is mathematical substantiation of the qualitative and quantitative selection of an expert group for the practical implementation of a risk-oriented approach to providing the PPE to the fuel and energy sector employees.

The objective determines the formulation and solution of the main tasks:

• study of the practice of applying the expert assessment method in risk analysis;

• determination of criteria for the formation of an expert group for practical implementation of the risk-oriented approach to providing the employees with the PPE;

• formation of an expert group with a scientific rationale for identifying factors affecting the competence of experts;

• development of methodological principles for issuing the PPE to employees based on results of risk assessment at 6,105 workplaces.

Implementation of the proposed mechanism for improving the identification of hazards and risk assessment at workplaces in fuel and energy companies based on the use of the expert assessments method and scientifically grounded qualitative and quantitative selection of experts considerably increases the efficiency of the procedure for selecting the PPE with regard for the global trends and legislative requirements in the concept of the risk-oriented approach.

Methods.

The problem of high-quality and efficient risk management is a complex and urgent task. Risk assessment procedure is widely used in various industries. There are different risk assessment methods that are constantly being improved and kept up-to-date. Article [14] presents an impressive overview of numerous assessment methods applied using bibliometric analysis. Paper [15] gives an overview of scientific publications from 2000 to 2009 on the study, development and classification of the main methods of analysing and assessing the risks at workplaces. Article [16] analyses the works published from 2000 to 2019 and describing the evolution of risk level assessment methods. The publications on risk assessment methods adopted in mining industry were studied, and the need for the implementation of the latest reliable risk assessment methods in mining sector was specified [17, 18].

Identification of hazards and risk assessment at the enterprise under study was conducted by an expert group using the Fine – Kinney method [19][2]. This method of assessing professional risks is applied in both Russian [20-22], and foreign studies [23, 24]. To increase the degree of objectivity

[2] Kinney G.F., Wiruth A.D. Practical Risk Analysis for Safety Management. China Lake: Naval Weapons Center, 1976, p. 20.

This is an open access article under the CC BY 4.0 license

© Ekaterina I. Karchina, Mariya V. Ivanova, Alla T. Volokhina, Elena V. Glebova, Aleksei E. Vikhrov, 2024

of expert assessments regarding the problem under consideration, the opinions of several experts – competent specialists – should be taken into account. It is important to form an expert group in such a way that the results of expert assessment are consistent, high-quality and reliable.

Deputy chief engineers for labour protection, industrial and fire safety were selected as experts for identification of hazards at workplaces and risk assessment using the Fine – Kinney method. The selection of such specialists as potential experts was due to their production experience, core education and specific nature of the duties performed. Thus, 22 employees were involved in identification of hazards and risk assessment. However, the results of assessment showed a low degree of consistency (concordance coefficient less than 0.5), which became the basis for a scientifically grounded qualitative and quantitative selection of the expert group.

The procedure for selecting the experts can be divided into two main stages: drawing up a list of potential candidates n for conducting an expert examination of companies R and evaluating them in order to select the most competent professionals h, with $n > h$, who scored the maximum competence coefficients W [25].

To determine the professional competence of experts based on analysis of the available methods for forming expert groups and taking into account the sector-specific issues, the factors that affect the competence of experts in the matters under consideration were identified [25, 26]. These factors were presented to a group of independent experts with a proposal to select five that mostly affect the competence of experts in the field of hazard identification and risk assessment. Taking into account the responses of all experts, the following five factors were identified using mathematical processing:

1. Length of service. Total work experience of the expert is taken into account.

2. Length of service in the field of operational surveillance in a fuel and energy company. Work experience in the field of industrial safety, namely, operational surveillance in a fuel and energy company, is taken into account.

3. The degree of risk perception. This factor allows determining the expert's readiness for risk and understanding its necessity and advisability.

4. Analytical style of personality. The experts who are able to analyse a large volume of information and pay attention to details are identified. Such qualities will allow a more precise identification of hazards and risk assessment at workplaces.

5. The number of violations in the area of providing the PPE to fuel and energy company employees. Violations identified in 22 branches of the fuel and energy company where the experts were responsible for this area of activity for three years are taken into account.

The above set of factors, typical for fuel and energy companies, is proposed for the first time.

Table 1 presents these factors as well as weight coefficients for each factor determined depending on the answers of potential experts.

Table 1

Professional competence of experts

Factors	Value of weight coefficient		
1	1-5 years 0.2	5-10 years 0.3	> 10 years 0.5
2	– 0	1-5 years 0.4	> 5 years 0.6
3	> 20 points 0	< –30 points 0.4	From –10 to +10 points 0.6
4	3rd place 0.2	2nd place 0.3	1st place 0.5
5	> 10 violations 0.2	1-10 violations 0.3	– 0.5

This is an open access article under the CC BY 4.0 license

© Ekaterina I. Karchina, Mariya V. Ivanova, Alla T. Volokhina, Elena V. Glebova, Aleksei E. Vikhrov, 2024

To determine the level of risk perception, the potential experts were tested using the A.M.Schubert method. This 25-item survey is designed to determine the degree of risk readiness that could lead to adaptation in various life situations. The risk scoring system is used to analyse the questionnaire results. Overall test scoring is determined using a continuous scale reflecting deviations from the average value. Positive answers indicate risk readiness. Test scoring scale varies from –50 to +50 points.

It was ascertained that a score less than –30 points indicated excessive caution, from –10 to +10 – average risk readiness, and over +20 points – high risk readiness. High risk readiness is accompanied by a low motivation to prevent failures and is directly proportional to the number of mistakes made.

To analyse the analytical style of personality, an assessment of own personality style using the DISC typology was applied. This method is widely used in different companies. It is applied to determine personality styles for the purposes of leadership and communication management in the study [27], in paper [28] – to raise the company's productivity by increasing the efficiency of communications, in article [29] – when forming the company's employee pool. DISC is a methodology based on human behaviour which is formed by two axes in four sectors. One of the axes characterizes the level of activity, the other one, openness and control of interaction with the environment. Thus, four sectors are formed:

- High persuasiveness. Active.
- High responsiveness. More interested in people.
- Low persuasiveness. Reactive.
- Low responsiveness. Focused on solving the problem.

Four personality styles are formed: assertive, player, kind soul and analyst. In order to identify hazards and assess risks, it is important to have such qualities as attentiveness, meticulousness, concentration on details, and structuredness. A person with the analytical personality style has these qualities. The more this personality style prevails in an expert, the more qualitatively the expert examination will be carried out.

Algorithm for determining the professional competence of experts:

The sum of points scored by the *i*-th expert for all factors is calculated

$$\mathrm{SumX}_i = \sum_{j=1}^{m} a_{ij} ,$$

where m is the number of factors, $m = 5$; a_{ij} is the value of the weight coefficient scored by the i-th expert on the j-th factor.

The sum of factor points for all experts is determined:

$$\mathrm{SumF}_j = \sum_{i=1}^{n} a_{ij} ,$$

where n is the number of experts, $n = 22$.

The weight coefficient of experts for all factors is calculated:

$$W_i = \frac{\sum_{j=1}^{m} a_{ij}}{\sum_{i=1}^{n}\sum_{j=1}^{m} a_{ij}} ;$$

$$\sum_{i=1}^{n} W_i = 1 .$$

Table 2 shows the results of calculating weight coefficients for experts and factors.

This is an open access article under the CC BY 4.0 license

© Ekaterina I. Karchina, Mariya V. Ivanova, Alla T. Volokhina, Elena V. Glebova, Aleksei E. Vikhrov, 2024

Table 2

Weight coefficients of experts

Number of expert	Factors					SumX$_i$	W_i
	1	2	3	4	5		
1	0.5	0.6	0	0.2	0.3	1.6	0.039
2	0.5	0.6	0.6	0.5	0.5	2.7	0.066
3	0.3	0.4	0.6	0.5	0.3	2.1	0.051
4	0.2	0.4	0.6	0.3	0.3	1.8	0.044
5	0.3	0.6	0	0.2	0.5	1.6	0.039
…	…	…	…	…	…	…	…
21	0.3	0.6	0	0.3	0.3	1.5	0.036
22	0.3	0.4	0	0.5	0.3	1.5	0.036
SumF$_j$	7.7	11	7.4	7.5	7.6	41.2	1

For a more precise assessment of the expert's competence, weight coefficients were calculated based on the data from Table 2 for each factor. The calculation results are presented in Table 3. Then, the weight coefficients of experts for all $W2_i$ factors and the sum of the expert's weight coefficients for all factors SumE$_i$ are calculated. Taking into account the obtained weight coefficients, the potential experts were ranked according to their professional competence level.

Table 3

Weight coefficients of experts by factors

Number of expert	Factors					SumE$_i$	$W2_i$
	1	2	3	4	5		
1	0.065	0.055	0.000	0.027	0.039	0.186	0.037
2	0.065	0.055	0.081	0.067	0.066	0.333	0.067
3	0.039	0.036	0.081	0.067	0.039	0.263	0.053
4	0.026	0.036	0.081	0.040	0.039	0.223	0.045
5	0.039	0.055	0.000	0.027	0.066	0.186	0.037
…	…	…	…	…	…	…	…
21	0.039	0.055	0.000	0.040	0.039	0.173	0.035
22	0.039	0.036	0.000	0.067	0.039	0.181	0.036
Total points	1	1	1	1	1	5	1

Using the hierarchy analysis method proposed in [30-32], the vector of factor priorities was determined (Table 4). It represents a relative weight of factors. The higher the priority value, the more significant the corresponding factor. The hierarchy analysis method is applied to solve such problems, since it is based on expert assessments and allows taking into account an arbitrary number of factors [31, 32].

Table 4

Matrix of pairwise comparisons of factors

Factors	1	2	3	4	5	Geometric mean	Vector of priorities
1	1	0.5	0.333	1	0.5	0.608	0.108
2	2	1	2	3	2	1.888	0.334
3	3	0.5	1	3	2	1.552	0.275
4	1	0.333	0.333	1	0.333	0.517	0.092
5	2	0.5	0.5	3	1	1.084	0.192
Sum						5.650	

This is an open access article under the CC BY 4.0 license

To check the consistency of priorities, λ_{max}, the maximum eigenvalue of the matrix is first calculated by summing the products of columns by the priority vector. In this case, $\lambda_{max} = 5.187$. The closer λ_{max} to the matrix dimension, the more consistent the result [31]. The consistency index (CI) shows a deviation from consistency in the hierarchy analysis method,

$$CI = \frac{\lambda_{max} - m}{m - 1} = 0.047.$$

Next, the random consistency index (RCI) is determined. This is a calculated value for matrices of each order; the RCI for a matrix of order 5 is 1.12 [30]. The ratio of the CI to the RCI is called the consistency ratio (CR). The calculated CR value is 0.042. CR value less than or equal to 0.10 indicates the consistency of assessments in the matrix [31]. Table 4 shows that factors 2 (work experience in the field of operational surveillance in a fuel and energy company) and 3 (degree of risk perception) were identified by the expert group as most important for selecting the experts to be involved in hazard identification and risk assessment at workplaces.

Global priorities of the experts are identified taking into account the vector of factor priorities. In order to calculate global priorities (Table 5) for each expert it is necessary to determine the sum of weight coefficients of experts for each factor (see Table 3) multiplied by the corresponding vectors of priorities (Table 4). From Table 5 it is clear that the highest global priority is given to experts 12, 21, 15, 9, 18, 6, 3, 14, 5, 2, 17, 20. This means that such experts have advantages in forming groups for hazard identification and risk assessment at workplaces.

Table 5

Results of calculating global priorities of experts

Number of expert	Factors					Global priority
	1	2	3	4	5	
1	0.065	0.055	0.000	0.027	0.039	0.035
2	0.065	0.055	0.081	0.067	0.066	0.066
3	0.039	0.036	0.081	0.067	0.039	0.052
4	0.026	0.036	0.081	0.040	0.039	0.048
5	0.039	0.055	0.000	0.027	0.066	0.037
6	0.026	0.036	0.081	0.067	0.066	0.056
7	0.039	0.036	0.081	0.067	0.039	0.052
8	0.039	0.036	0.000	0.027	0.039	0.026
9	0.039	0.036	0.000	0.067	0.039	0.030
10	0.039	0.036	0.054	0.067	0.039	0.045
11	0.039	0.036	0.081	0.027	0.039	0.049
12	0.065	0.055	0.081	0.067	0.066	0.066
13	0.039	0.055	0.000	0.027	0.066	0.037
14	0.065	0.055	0.000	0.040	0.039	0.036
15	0.065	0.055	0.000	0.027	0.026	0.033
16	0.026	0.036	0.081	0.067	0.039	0.051
17	0.065	0.055	0.081	0.027	0.066	0.063
18	0.039	0.036	0.081	0.027	0.026	0.046
19	0.039	0.055	0.054	0.040	0.039	0.049
20	0.065	0.055	0.081	0.027	0.039	0.058
21	0.039	0.055	0.000	0.040	0.039	0.034
22	0.039	0.036	0.000	0.067	0.039	0.030

At the next stage, the size of the expert group is determined, i.e. the boundary is drawn that determines the required number of experts to perform hazard identification and risk assessment ensuring sufficient reliability of the results.

This is an open access article under the CC BY 4.0 license

The required number of experts from among the potential experts according to papers [25, 31] is calculated using the formula of non-repeated random sampling

$$h = \frac{t^2\sigma^2 n}{\Delta^2 n + t^2\sigma^2},$$

where t is confidence coefficient, $t = 3$ at a probability level $P = 0.997$ [25]; σ^2 is sample variance for data (see Table 3), $\sigma^2 = 0.024$; Δ is the maximum sampling error, $\Delta = 0.07$.

Thus, the required number of experts to carry out hazard identification and risk assessment at workplaces is $h = 15$ persons at a probability of 0.997 and a sampling error of no more than 7 %.

Discussion of results.

A selected expert group of 15 persons identified hazards and assessed risks using the Fine – Kinney method at all workplaces in the company to determine the list of the PPE and wash-off agents. As an example, a fragment of the results obtained for a driller's workplace is presented. The expert group drew up a register of hazards and determined the probability, susceptibility and consequences of each hazard for the employee. Table 6 presents the risk level and the need to issue the PPE, which were determined according to the classification of professional risk levels using the Fine – Kinney method. The professional risk index (PRI) was calculated applying the Fine – Kinney method:

$$PRI = Pr \cdot Susc \cdot Cons,$$

where Pr is probability; Susc, susceptibility; Cons, consequences of the event onset.

Table 6

Classification of professional risk levels using the Fine – Kinney method

PRI, points	Risk level	The need to take action
From 0 to 20	No risk or negligible risk	No action required
From 21 to 70	Low moderate risk	Action required, but enough time to plan it
From 71 to 200	Medium significant risk	Planning and implementation of actions in a short time frame required
From 201 to 400	High risk	Urgent action required
Over 400	Extremely high risk	Stopping activity required before taking action

PRI calculation data for individual hazards identified at the driller's workplace (slippery, icy, greasy, wet surfaces; rotating or moving equipment parts or tools; sharp edges and burrs; physical overload due to excessive efforts when lifting and moving objects and parts; increased noise levels and other unfavourable noise characteristics) are presented in Table 7. The PRI was determined similarly for all the identified hazards. PRI calculation results revealed hazards with a negligible risk (e.g. sharp edges and burrs). In accordance with the Rules[3], the employer has the right not to issue the PPE for hazards whose risk level will not result in harming the employee's health during work, the PPE for such hazards was not selected.

Hazards with a low moderate risk that require attention (e.g. slippery, icy, greasy, wet surfaces), medium significant (e.g. rotating or moving parts of equipment or tools) and high (e.g. physical overload with excessive physical effort when lifting and moving objects and parts) risk levels were identified that require planning and implementation of actions in a short time frame and urgent measures,

[3] Order of the Ministry of Labour of Russia dated October 29, 2021 N 766n "On approval of the Rules for providing employees with personal protective equipment and wash-off agents".

This is an open access article under the CC BY 4.0 license

respectively. For certain hazards, the PPE was selected from the list in Appendix N 2 to the Unified Standard Guidelines[4].

Based on the assessment of professional risks, the expert group selected a list of the PPE for each workplace. For example, for the driller's workplace, the characteristics of special footwear were expanded, the protective "anti-slip" characteristic was added, and a support belt for the abdomen and lower back was proposed taking into account the high risk of hazard "Physical overload due to excessive physical effort when lifting and moving objects and parts". These items were not previously provided for in the Consolidated list of free issuance of special clothing, special footwear and other personal protective equipment to employees of the considered fuel and energy company.

Table 7

Calculation of professional risk index

Hazard	Hazardous event	Probability		Susceptibility		Consequences		PRI
		Assessment	Points	Assessment	Points	Assessment	Points	
Slippery, icy, greasy, wet surfaces	Fall of an employee due to a loss of balance while slipping and moving	Highly probable	6	From time to time (weekly)	3	Minor accident (including group accident) with temporary disability	3	54
Rotating or moving parts of equipment or tools	Hitting an employee by a tool when used incorrectly, hitting by rotating or moving parts of equipment	Highly probable	6	From time to time (weekly)	3	A serious accident without serious consequences and disability	7	126
Sharp edges and burrs	Cutting of an employee's soft tissues by sharp edges and burrs	Non-typical, but possible	3	From time to time (weekly)	2	Minor accident (including group accident) with temporary disability	3	18
Physical overload due to excessive physical effort when lifting and moving objects and parts	Damage to the musculoskeletal system of an employee from physical overload due to excessive physical effort when lifting and moving objects and parts	Highly probable	6	Regularly (every working day, shift)	6	A serious accident without serious consequences or disability	7	252
Increased noise levels and other adverse noise characteristics	Impairment of auditory acuity, dullness of hearing, deafness due to exposure to elevated noise levels and other adverse noise characteristics	Highly probable	6	From time to time (weekly)	3	A serious accident (including a group accident) with loss of ability to work for a long period, occupational disease, disability	15	270

It should be noted that when assessing the risks, the initially formed group of 22 experts in this profession underestimated the probability of occurrence of the hazard "Slippery, icy, greasy, wet surfaces" and the risk level of hazard was determined as negligible, not requiring any action. However, statistical data on accidents that occurred in the company in the period from 2006 to 2020 indicate a high probability of the occurrence of this hazard. This example additionally confirms that the expert group formed using the method proposed in the study presented more precise, objective and consistent risk assessment results.

[4] Order of the Ministry of Labour of Russia dated October 29, 2021 N 767n "On approval of the Unified Standard Guidelines for the issuance of personal protective equipment and wash-off agents".

This is an open access article under the CC BY 4.0 license

Thus, the application of the proposed approach made it possible to identify hazards at each workplace and select an efficient set of the PPE as a result of assessing professional risks taking into account the expert assessment.

Conclusion.

The accomplished study, taking into account the global practice of implementing a risk-oriented approach, made it possible to substantiate and implement a mechanism for improving the process of hazard identification and risk assessment at workplaces in a fuel and energy company applying the competence-based selection of an expert group.

Vectors of factor priorities were determined using the hierarchy analysis method. With the help of such priority vectors, global priorities of experts were ascertained, i.e. the advantages of inclusion in the group for hazard identification and risk assessment at workplaces.

The number of experts in the group (15 persons) was calculated – a boundary was found that determines the required number of experts to identify hazards and assess risks at workplaces ensuring sufficient reliability of the results.

The formed expert group identified hazards and assessed risks using the Fine – Kinney method at 6,105 workplaces of 24 branches of the fuel and energy company to determine the list of the PPE and wash-off agents taking into account the risk-oriented approach.

REFERENCES

1. Glebova E.V., Volokhina A.T., Vikhrov A.E. Assessment of the efficiency of occupational safety culture management in fuel and energy companies. *Journal of Mining Institute.* 2023. Vol. 259, p. 68-78. DOI: 10.31897/PMI.2023.12

2. Bakhonina E.I., Matzos G.L., Karimova V.A. Features of providing PPE workers in the Russian Federation and foreign countries. *Life Safety.* 2022. N 6, p. 11-16 (in Russian).

3. Golubev I.G. Two by two? Foreign practice of providing workers with personal protective equipment. *Bezopasnost i okhrana truda.* 2017. N 1, p. 20-23 (in Russian).

4. Abikenova Sh.K., Dzhumagulova N.G., Abdrakhmanova N.B. Analysis of approaches to providing employees with personal protective equipment in the international aspect. *Bulletin of the Scientific Center of VostNII on Industrial and Environmental Safety.* 2022. N 3, p. 73-79 (in Russian). DOI: 10.25558/VOSTNII.2022.32.93.007

5. Karchina E.I., Ivanova M.V., Glebova E.V. Risk-Oriented Approach to Providing Employees with Personal Protective Equipment. *Occupational Safety in Industry.* 2022. N 9, p. 84-90 (in Russian). DOI: 10.24000/0409-2961-2022-9-84-91

6. Savicheva Yu.N., Mitrofanova N.S., Gabdrakhmanova R.R. Risk-based approach in workers providing with personal protective equipment. *Oil and Gas Business.* 2022. N 5, p. 67-83 (in Russian). DOI: 10.17122/ogbus-2022-5-67-83

7. Marycheva P.G. The method of assessment the competence of experts. *Vestnik of Samara State Technical University. Technical Sciences Series.* 2018. N 4 (60), p. 29-40 (in Russian).

8. Belanova N., Ershova N., Pyatkova N., Alpackaya I. Assessment of the risks of construction of transport infrastructure facilities. *Transportation Research Procedia*. 2022. Vol. 63, p. 1660-1667. DOI: 10.1016/j.trpro.2022.06.179

9. Rui Jin, Fan Wang, Donghai Liu. Dynamic probabilistic analysis of accidents in construction projects by combining precursor data and expert judgments. *Advanced Engineering Informatics*. 2020. Vol. 44. N 11062. DOI: 10.1016/j.aei.2020.101062

10. Rosqvist T. On the use of expert judgement in the qualification of risk assessment: Dissertation for the degree of Doctor of Technology: presented on the 11th of December, 2023. Espoo: VTT Publications 507, 2003, p. 48. URL: http://lib.tkk.fi/Diss/2003/isbn9513862445/isbn9513862445.pdf (accessed date 31.10.2023)

11. Ilin S.M., Samarskaya N.A., Simanovich S.V. et al. New Approaches to the Choice of Personal Protective Equipment against the Impact of Vibroacoustic Factors at the Workplace. *Occupational Safety in Industry.* 2022. N 10, p. 80-85 (in Russian). DOI: 10.24000/0409-2961-2022-10-80-85

12. Shamansurov S.S., Djurayev O.A., Suleymanov A.A., Abdurakhmanova A.D. Mathematical model of the estimated efficiency coefficient of the use of experts in the examination of hazardous production facilities. *Occupational Safety in Industry.* 2022. N 7, p. 65-71 (in Russian). DOI: 10.24000/0409-2961-2022-7-65-71

13. Rybalov E.A., Fomina E.E., Fomina E.E. Application of expert assessment methods in the analysis of the hazards of oil and gas wells in the state of conservation or liquidation. *Environmental protection in oil and gas complex.* 2022. N 2 (305), p. 49-55 (in Russian). DOI: 10.33285/2411-7013-2022-2(305)-49-55

14. Ran Liu, Hu-Chen Liu, Hua Shi, Xiuzhu Gu. Occupational health and safety risk assessment: A systematic literature review of models, methods, and applications. *Safety Science*. 2023. Vol. 160. N 106050. DOI: 10.1016/j.ssci.2022.106050

15. Marhavilas P.K., Koulouriotis D., Gemeni V. Risk analysis and assessment methodologies in the work sites: On a review, classification and comparative study of the scientific literature of the period 2000-2009. *Journal of Loss Prevention in the Process Industries*. 2011. Vol. 24. Iss. 5, p. 477-523. DOI: 10.1016/j.jlp.2011.03.004

16. George P.G., Renjith V.R. Evolution of Safety and Security Risk Assessment methodologies towards the use of Bayesian Networks in Process Industries. *Process Safety and Environmental Protection*. 2021. Vol. 149, p. 758-775. DOI: 10.1016/j.psep.2021.03.031

This is an open access article under the CC BY 4.0 license

17. Tubis A., Werbińska-Wojciechowska S., Wroblewski A. Risk Assessment Methods in Mining Industry – A Systematic Review. *Applied Sciences*. 2020. Vol. 10. Iss. 15. N 5172. DOI: 10.3390/app10155172

18. Verma S., Chaudhari S. Highlights from the literature on risk assessment techniques adopted in the mining industry: A review of past contributions, recent developments and future scope. *International Journal of Mining Science and Technology*. 2016. Vol. 26. Iss. 4, p. 691-702. DOI: 10.1016/j.ijmst.2016.05.023

19. Fine W.T. Mathematical Evaluations for Controlling Hazards. *Journal of Safety Research*. 1971. Vol. 3. N 4, p. 157-166.

20. Kuleshov V.V., Skuba P.Yu., Ignatovich I.A. Assessment of the Severity of the Last Accident Based on the Fine-Kinney Method. IOP Conference Series: Earth and Environmental Science. 2021. Vol. 720. N 012094. DOI: 10.1088/1755-1315/720/1/012094

21. Stepanov A.G., Strekalova T.A., Budnik E.V. Assessment of professional risks of construction workers. *Life Safety*. 2022. N 6, p. 24-28 (in Russian).

22. Bednarzhevsky S.S., Korol Zh.V. Application of Fine-Kinney method for professional risk assessment. *Science Prospects.* 2013. N 4 (43), p. 74-77 (in Russian).

23. Dogan B., Oturakci M., Dagsuyu C. Action selection in risk assessment with fuzzy Fine–Kinney-based AHP-TOPSIS approach: a case study in gas plant. *Environmental Science and Pollution Research*. 2022. Vol. 29. Iss. 44, p. 66222-66234. DOI: 10.1007/s11356-022-20498-2

24. Derse O. A New Approach to the Fine Kinney Method with AHP Based ELECTRE I and Math Model on Risk Assessment for Natural Disasters. *Journal of Geography*. 2021. Iss. 42, p. 155-164. DOI: 10.26650/JGEOG2021-875427

25. Petrichenko G.S., Petrichenko V.G. Methods of assessing the competence of experts. *Scientific Journal of KubSAU*. 2015. N 109 (05), p. 12 (in Russian).

26. Shkunova P.A., Volokhina A.T., Glebova E.V., Retinskaya I.V. Use of the cluster analysis for identification of professionally important qualities of oil and gas production operators. *Environmental protection in oil and gas complex.* 2018. N 6, p. 18-22 (in Russian). DOI: 10.30713/2411-7013-2018-6-18-22

27. Slowikowski M.K. Using the DISC Behavioral Instrument to Guide Leadership and Communication. *AORN Journal*. 2005. Vol. 82. Iss. 5, p. 835-843. DOI: 10.1016/s0001-2092(06)60276-7

28. Sugerman J. Using the DiSC® model to improve communication effectiveness. *Industrial and Commercial Training*. 2009. Vol. 41. Iss. 3, p. 151-154. DOI: 10.1108/00197850910950952

29. Kolesnikova Ju.S., Kamasheva A.V., Bury V.V. Use of DISC Technology in the Formation of the Personnel Reserve. *The Review of Economy, the Law and Sociology*. 2017. N 2, p. 23-26 (in Russian).

30. Petrichenko G.S., Grigoryan N.K., Medovshchikov M.I. Methodology for developing an expert system for a manager to take managerial decisions. *Nauchno-tekhnicheskie vedomosti Sankt-Peterburgskogo gosudarstvennogo politekhnicheskogo universiteta. Informatika. Telekommunikatsii. Upravlenie*. 2012. N 1 (140), p. 60-66 (in Russian).

31. Saati T. Decision making: Analytic hierarchy process. Moscow: Radio i svyaz, 1993, p. 314 (in Russian).

32. Seredenko N.N. Development of the analytic hierarchy process (AHP). *Otkrytoe obrazovanie*. 2011. N 2-1, p. 39-48 (in Russian).

Authors: **Ekaterina I. Karchina,** *Postgraduate Student, https://orcid.org/0009-0000-0616-2447* (*National University of Oil and Gas* "*Gubkin University*", *Moscow, Russia*), **Mariya V. Ivanova,** *Doctor of Engineering Sciences, Professor, https://orcid.org/0009-0006-1682-7055* (*National University of Oil and Gas* "*Gubkin University*", *Moscow, Russia*), **Alla T. Volokhina,** *Doctor of Engineering Sciences, Professor, https://orcid.org/0000-0002-3787-5391* (*National University of Oil and Gas* "*Gubkin University*", *Moscow, Russia*), **Elena V. Glebova,** *Doctor of Engineering Sciences, Professor, https://orcid.org/0000-0003-0190-1452* (*National University of Oil and Gas* "*Gubkin University*", *Moscow, Russia*), **Aleksei E. Vikhrov,** *Candidate of Engineering Sciences, Associate Professor, alexey.vikhrov.24@gmail.com, https://orcid.org/0000-0002-9884-2737* (*National University of Oil and Gas* "*Gubkin University*", *Moscow, Russia*).

The authors declare no conflict of interests.

This is an open access article under the CC BY 4.0 license

ISSN 2411-3336; e-ISSN 2541-9404

JOURNAL OF MINING INSTITUTE

Zapiski Gornogo instituta

Journal homepage: pmi.spmi.ru

Research article

Analysing the problems of reproducing the mineral resource base of scarce strategic minerals

Natalya V. Pashkevich, Vera S. Khloponina✉, Nikolai A. Pozdnyakov, Anastasiya A. Avericheva
Empress Catherine II Saint Petersburg Mining University, Saint Petersburg, Russia

***How to cite this article*:** Pashkevich N.V., Khloponina V.S., Pozdnyakov N.A., Avericheva A.A. Analysing the problems of reproducing the mineral resource base of scarce strategic minerals. Journal of Mining Institute. 2024. Vol. 270, p. 1004-1023.

Abstract
The results of studying the scarcity of strategic minerals in the Russian Federation are presented, domestic consumption of which is largely provided by forced imports and/or stored reserves. Relevance of the work is due to aggravation of the geopolitical situation and a growing necessity to meet the demand of national economy for raw materials from own sources. Analysis of the state of mineral resource base of scarce minerals in the Russian Federation was accomplished, problems were identified and prospects for its development were outlined taking into account the domestic demand for scarce minerals, their application areas and the main consumers. Reducing the deficit through the import of foreign raw materials and the development of foreign deposits does not ensure the reproduction of the domestic mineral resource base, independence of the country from imported raw materials as well as additional competitive advantages, economic stability and security. It was ascertained that a major factor holding back the development of the mineral resource base is insufficient implementation of new technological solutions for the use of low-quality ore. Improving the technologies in the industry is relevant for all types of scarce minerals to solve the problem of reproducing their resource base. Taking into account the prospects for the development of the resource base for the minerals under consideration (manganese, uranium, chromium, fluorspar, zirconium, titanium, graphite) requires a set of legal and economic measures aimed at increasing the investment attractiveness of geological exploration for subsoil users at their own expense without attracting public funding. The proposed measures, taking into account the analysis of positive experience of foreign countries, include the development of junior businesses with expansion of the "declarative" principle, the venture capital market, various tax incentives, preferential loans as well as conditions for the development of infrastructure in remote regions. The proposed solution to the problem of scarcity of strategic minerals will make it possible in future to present measures to eliminate the scarcity of certain types of strategic minerals taking into account their specificity.

Keywords
scarce minerals; strategic minerals; reproduction of mineral resource base; license; geological exploration; investments; financing of geological exploration; junior companies; venture capital; "declarative" principle

Received: 08.04.2024 ***Accepted: 13.06.2024*** ***Online: 26.07.2024*** ***Published: 25.12.2024***

Introduction.

The mineral resource base (MRB) of the Russian Federation is one of the largest in the world. In 2021, Russia held the leading position in reserves of many minerals (Table 1) possessing major mining and beneficiation capacities. Of 48 main types of mineral resources mined in the country, 22 are in the top ten. For comparison, 47 types of mineral raw materials are mined in China [1], 41 in the USA, 40 in Australia and Brazil, 36 in India, 35 in South Africa, and 34 in Canada[1].

[1] State report "On the state and use of mineral resources of the Russian Federation in 2021". Moscow, 2022, p. 626.

This is an open access article under the CC BY 4.0 license

Table 1

Mineral reserves in Russia

Mineral product	Reserves	Category of reserves	Place of the RF MRB in the world
Natural gas	44 trillion m^3	$A + B_1 + C_1$	1
Diamonds	1,018.9 million carats	$A + B + C_1 + C_2$	1
Gold	15,453.5 t	$A + B + C_1 + C_2$	1
Platinoids	16.03 Kt	$A + B + C_1 + C_2$	2
Iron ore	58.11 billion t	$A + B + C_1$	3
Coal	195.9 billion t	$A + B + C_1$	4
Liquid hydrocarbons	19.3 billion t	$A + B_1 + C_1$	5

Substantial reserves of mineral resources (MR) are the basis of national independence and sustainable development of the country, as they ensure the independence of national economy from foreign sources of raw materials and its competitiveness, guaranteeing a significant geopolitical advantage to the state [2-4]. Despite large reserves, Russia is forced to import some MR. According to the Order of the RF Government dated December 22, 2018, N 2914-r "On approval of the Strategy for development of the mineral resource base of the Russian Federation until 2035" (hereinafter, the Strategy), in-place reserves of the Russian mineral raw materials in terms of quantity and quality are divided into three groups.

The first group of MR has sufficient reserves to meet the needs of economy until 2035 under any scenario of its development[2].

Minerals of the second group at the achieved levels of their production are not sufficiently provided with reserves of developed deposits until 2035[2].

The third group consists of scarce minerals, the domestic consumption of which is largely ensured by forced imports and/or stored reserves. This group also includes types of MR whose MRB in Russia is characterized by predominantly low quality. The group consists of uranium, manganese, chromium, titanium, bauxites, molybdenum, tungsten, zirconium, beryllium, lithium, vanadium, niobium, tantalum, rare earth metals (except scandium and promethium), graphite, and fluorspar[2].

Order of the RF Government the dated August 30, 2022, N 2473-r "On approval of the list of the main types of strategic mineral raw materials" determined the list of strategic types of minerals. The main types of strategic mineral raw materials currently include oil, natural gas, helium, uranium, manganese, chromium, titanium, bauxites, copper, lead, antimony, tin, zinc, nickel, molybdenum, tungsten, cobalt, rare earth metals (lithium, rubidium, cesium, beryllium, scandium, rare earth metals (yttrium, lanthanum, cerium, praseodymium, neodymium, samarium, europium, gadolinium, terbium, dysprosium, holmium, erbium, thulium, ytterbium, lutetium), indium, gallium, germanium, zirconium, hafnium, vanadium, niobium, tantalum, rhenium), gold, silver, platinoids (ruthenium, rhodium, palladium, osmium, iridium, platinum), diamonds, graphite, phosphates (apatite ores), potassium salts , fluorspar, high pure quartz raw materials, and underground water[3].

The previous list of strategic mineral raw materials approved by Government Order N 50-r dated January 16, 1996, included only 29 items and remained in force for 26 years. Due to the fact that the list of strategic mineral raw materials is determined in accordance with the changing needs of national economy, a clause was added to Government Order N 2473-r on the necessity to update the list of types of strategic mineral raw materials at least once in three years[4].

[2] Order of the RF Government dated 16.04.2024, N 939-r "On approval of the List of scarce types of solid minerals and the List of products with a high share of added value manufactured using extracted scarce types of solid minerals".

[3] Order of the RF Government dated 30.08.2022, N 2473-r "On approval of the List of the main types of strategic mineral raw materials".

[4] Position 61 instead of 29: The Russian Government approved the list of the main types of strategic mineral raw materials. URL: https://www.mnr.gov.ru/press/news/61_pozitsiya_vmesto_29_pravitelstvo_rossii_utverdilo_perechen_osnovnykh_vidov_strategicheskogo_miner/ (accessed 08.04.2024).

This is an open access article under the CC BY 4.0 license

Journal of Mining Institute. 2024. Vol. 270. P. 1004-1023
© Natalya V. Pashkevich, Vera S. Khloponina, Nikolai A. Pozdnyakov, Anastasiya A. Avericheva, 2024

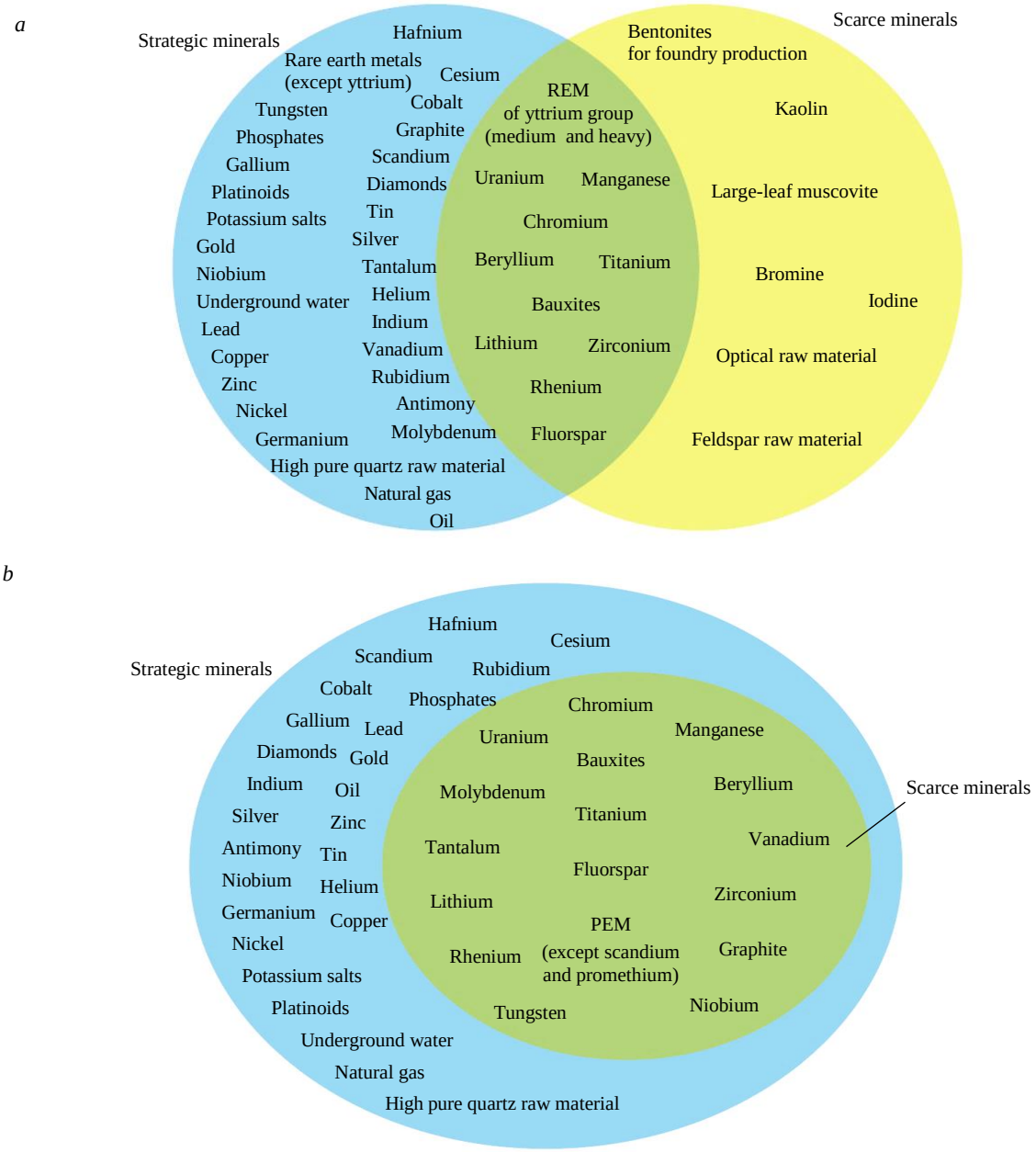

Fig.1. Strategic and scarce types of minerals before (*a*) and after (*b*) 26 April 2024[5]

Figure 1 shows groups of scarce minerals (yellow zone) in effect until April 26, 2024, and strategic types of minerals (blue zone). Scarce strategic mineral resources (SSMR) (green zone) included: chromium, uranium, manganese, molybdenum, titanium, beryllium, tantalum, vanadium, bauxites, lithium, zirconium, rhenium, graphite, tungsten, fluorspar, niobium, rare earth metals (except scandium and promethium). On April 26, 2024, a new Order came into force according to which the SSMR include: uranium, manganese, chromium, molybdenum, beryllium, tantalum, vanadium, lithium, bauxites, zirconium, rhenium, graphite, tungsten, titanium, niobium, fluorspar and rare earth metals (except scandium and promethium). Currently, all types of scarce minerals are included in the group of strategic minerals.

[5] Order of the RF Government dated 30.08.2022, N 2473-r "On approval of the List of the main types of strategic mineral raw materials".

This is an open access article under the CC BY 4.0 license

The relevance of the study lies in the fact that the reproduction of scarce strategic minerals is essential owing to their critical importance in combination with an acute scarcity of high-quality reserves. The problem of reproduction of the MRB in the RF from the legal, economic and financial points of view is discussed in the works of V.S.Litvinenko, N.V.Pashkevich, V.P.Orlov, O.V.Petrov, S.Ya.Kaganovich, D.B.Burdin, L.V.Oganesyan, A.P.Albertyan, G.Yu.Boyarko, V.N.Voitenko, A.A.Fedchenko, L.I.Iseeva, N.P.Grigorev, V.I.Nazarov, Z.M.Nazarova, O.S.Krasnov, and A.A.Gert.

The purpose of the work is to determine the ways to overcome the scarcity of certain strategic minerals based on a comprehensive analysis of the state of their MRB and the problems of reproducing the reserves.

The object of the study are the strategic minerals of the Russian Federation, domestic consumption of which is largely provided by forced imports and/or stored reserves.

The subject of research are the problems of reproducing scarce strategic types of minerals.

Methods.

The problem of reproducing the SSMR MRB is integrated and requires a systemic approach. Considering the needs of economy for the development of the MRB of a specific type of mineral, on the one hand, the reproduction of reserves implies intensification of geological exploration, which affects the licensing of subsoil users and their adequate financing from various sources (public and private); on the other hand, the supply of economy with raw materials depends on the development of technologies for extracting useful components from ores.

The research includes the following stages: analysis of the work on reproduction of the MRB in the RF in general and the SSMR MRB in particular; analysis of open data on the state of the SSMR MRB from reports taking into account the information on the current demand and needs of domestic economy for these types of raw materials; statistical processing of information using the method of grouping, tabulation, analysis, synthesis, and diagramming.

The research methodology is based on general scientific and special methods of obtaining knowledge: the use of results of industry expert assessments, analysis of domestic and foreign specialized literature, study of the Russian law on public management of mineral resources.

A significant part of the work is devoted to the study of global experience in operation of junior companies, the prospects for integrating this business practice into the Russian economy, taking into account industry-specific legal, financial, infrastructural, and natural climatic features.

Results.

Considering the criteria for classifying minerals into one of three groups, provision of the state with mineral raw materials of a particular type on a long-term basis is determined by production levels and the corresponding reserves characterized by quantitative and qualitative indicators. Production volumes are affected by demand for the products of the industry, technical resources of the industry, existing technologies, available financing sources, and other factors. The size and quality of reserves, in turn, depend on the results of geological exploration (GE), the purpose of which is to identify mineral deposits and prepare them for commercial development. GE is aimed at studying the emplacement conditions, occurrence patterns, mineral composition and structural features of deposits (main and accompanying components), variability of the morphology of deposits, composition and properties of minerals for forecasting, prospecting, exploration, geological and economic evaluation and preparation of deposits for exploitation.

The main result of geological exploration is getting information for subsoil users. Geological information plays the key role not only in the development of already known deposits (recommended mining conditions, content of useful components in ore, etc.), but also forms a basis for the long-term period, provides subsoil users with information about potential sites [5].

An integrated approach to investigating the problem of the SSMR in this study involves the comparison of dynamics of production and import of reserves for the corresponding types of MR,

This is an open access article under the CC BY 4.0 license

identifying problems that do not allow satisfying the internal needs of the Russian economy and in future exporting raw materials as well as identifying possible ways to eliminate the current scarcity of strategic MR. The amount of reserves is influenced by production levels and reserves growth.

A necessary condition for the expanded reproduction of the MRB is the rate of geological exploration that exceeds the level of deposits development. However, actual data show that such rates are currently unattainable. From 1991, when the critical lower limit of reproduction was reached, not exceeding 150-170 % of production, a decrease in the reproduction of the MRB was recorded. This indicator, although limiting the manoeuvrability in industrial development, allowed maintaining the achieved level of production, and from the viewpoint of economists and politicians of modern times was even regarded as excessive [6]. Simple reproduction with a 1:1 ratio (production volume to reserve growth) is considered sufficient, which is currently unattainable for some SSMR.

The strategy for development of the mineral resource base of the Russian Federation until 2035 provides for an indicator of efficiency of the MRB development in terms of economic and energy security of the country RMRB which is calculated from values taken over 10 years to level out fluctuations in indicators associated with discovery of new deposits. The RMRB value for one year can be calculated as the ratio of an increment in MR reserves to their production. An actual reduction in reserves will lead to negative RMRB indicators, which contradicts the principles of sustainable development implying the use of resources without unsettling the well-being of future generations [7].

Depending on the general state of indicators of the quantity and quality of the MRB of reserves of certain types of MR, the target and maximum permissible values of P_{MRB} are determined in accordance with the earlier discussed three groups and the maximum permissible value of P_{MRB} in accordance with three groups considered earlier (Table 2)[6].

Table 2

Maximum permissible and target values of P_{MRB}, %

Group of MR	Target value of P_{MRB}	Maximum permissible value of P_{MRB}
First	50	Unidentified
Second	100	75
Third	75	50

Some of the scarce MR in the Development Strategy belong to the first group (tungsten, tantalum, molybdenum and niobium), which currently contradicts the Order of the RF Government dated April 16, 2024, N 939-r, which came into force on April 26, 2024. The study did not evaluate the PMRB indicator for these types of SSMR. The elimination of contradictions in regulatory documents is expected with approval of the Development Strategy until 2050[7].

For comparability of the considered indicators, each graph in Fig.2 shows the dynamics of demand for each type of SSMR and the dynamics of their reserves. The demand indicator is introduced, which is the sum of production and import volumes. Levels of mineral raw materials extraction by the Russian companies demonstrate the part of the demand volume covered from own sources.

Comparison of volumes mined from the Russian ore deposits and of imported commercial ores and concentrates is a deliberate assumption to demonstrate the extent of dependence of domestic economy on imported mineral raw materials. For any other purpose, the combination of concentrates, imported commercial ores and raw materials mined in the territory of the RF is unacceptable due to different average concentrations of useful components in them.

[6] Order of the RF Government dated April 16, 2024, N 939-r "On approval of the List of scarce types of solid minerals and the List of products with a high share of added value manufactured using extracted scarce types of solid minerals".

[7] Emphasis on exploration and deep processing of scarce raw materials and two scenarios: the Ministry of Natural Resources prepared a Strategy for the development of the mineral resource base until 2050. URL: https://www.mnr.gov.ru/press/news/upor_na_razvedku_i_glubokuyu_rerabotku_defitsitnogo_syrya_i_dva_stsenariya_minprirody_podgotovilo_/ (accessed 08.04.2024).

This is an open access article under the CC BY 4.0 license

Calculation of the P_{MRB} parameter for the considered period showed that a reduction in reserves is not characteristic of all SSMR: bauxites – 116.79; uranium 148.79; manganese 22.08; chromium 2.04; titanium 297.93; zirconium 360.98; lithium 0; fluorspar 1.79 %. In Fig.2, the P_{MRB} values are given for comparison with actual trends in development of the SSMR MRB – the dynamics of reserves and changes in demand structure over time.

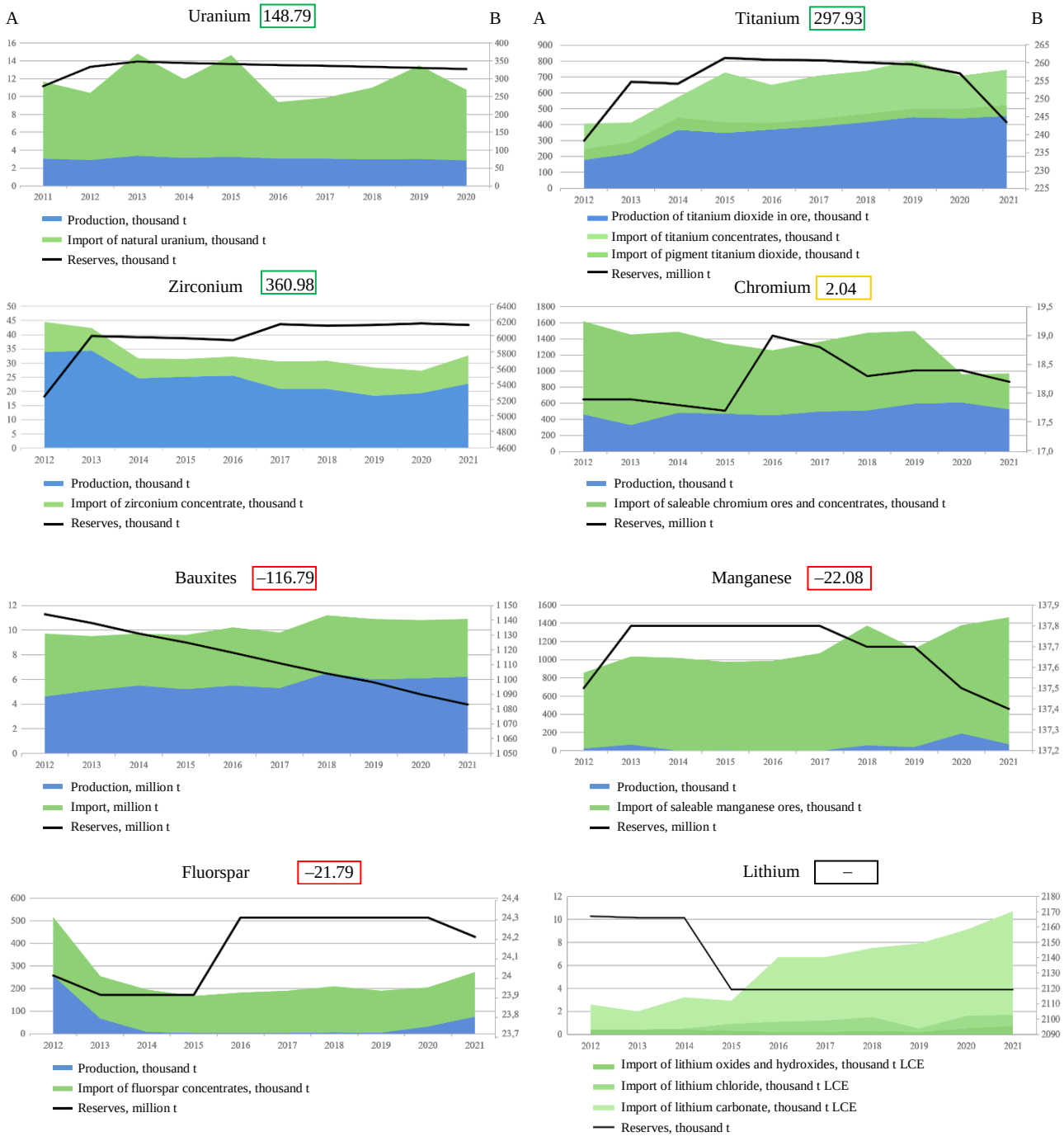

Fig.2. Reproduction and use indicators of MRB SSMR[8,9]
A – demand axis; B – reserves axis

[8] State report "On condition and use of mineral resources of the Russian Federation in 2021". Moscow, 2022, p. 626.
[9] State report "On condition and use of mineral resources of the Russian Federation in 2019". Moscow, 2020, p. 494.

This is an open access article under the CC BY 4.0 license

The obtained values for individual types of SSMR are extremely high, which is explained by the low base effect: a slight increment in the MRB is attributed to high production levels. For example, the indicator calculated for coal and gold is about 37 and 25 %, respectively.

High values of the P_{MRB} indicator do not specify that the problem of scarcity of the considered types of raw materials was overcome, which is a major disadvantage of the R_{MRB}. A comprehensive evaluation requires a detailed analysis of the qualitative structure of reserves increment and an assessment of the possibility of production in the near future.

The P_{MRB} indicator calculated for uranium, titanium and zirconium far exceeded the maximum permissible and target values amounting to 148.79, 297.93 and 360.98 %, respectively, which is explained by the low base effect (relevant for the SSMR MRB) and low production volumes of the considered MR.

Value of the P_{MRB} indicator for chromium was positive but was much lower than the limit values – 2.04 % with the marginal value 50 %. This is due to the fact that in 2012-2021 positive exploration and revaluation results did not compensate for the volumes of chromium ore production.

The indicators for bauxite, manganese and fluorspar are negative: –116.79, –22.08 and –21.79 %, respectively.

The most difficult situation is with lithium, since in the years under review its economic development was not carried out in Russia, therefore, the indicator cannot be calculated (denominator of the formula is zero).

Table 3 presents a characteristic of the state of the MRB of scarce strategic types of minerals, problems and prospects for its development.

The main factor hindering the development of the available SSMR MRB in the RF is the lack of industrial technologies that would allow the use of low-quality ores at an optimal level of profitability. New technological solutions could help significantly reduce the deficit without additional geological exploration, which is especially important for the SSMR types with no prospects for increasing the reserves.

Table 4 shows data on domestic demand for the SSMR taking into account the application areas and the list of the main consumers.

The dependence of Russian manufacturers on imports threatens the stability of development and the security of economy, since in modern geopolitical conditions of breakage of supply chains and refusal to cooperate can lead to downtime of production facilities and a major growth of production costs. Industrial enterprises should be uninterruptedly provided with the necessary materials, technologies, and components of appropriate quality despite changes in the industry caused by the sanctions pressure [8, 9].

Considering the current state of the SSMR MRB (see Table 3), solving the scarcity problem is possible by importing foreign raw materials, developing foreign deposits, conducting geological exploration in the Russian Federation (uranium, manganese, chromium, titanium, graphite), improving the technologies in the industry (all types of SSMR). Import of raw materials and development of foreign deposits do not ensure the strategic advantages at the geopolitical level, and do not offer a complete solution, since they do not resolve the problem of reproducing the domestic mineral resource base.

Solving the problem of the SSMR scarcity (especially for the SSMR with considerable increment prospects (Table 3) is primarily associated with active geological exploration. Since most of the SSMR consumers (Table 4) are subsoil users carrying out the full cycle: from geological exploration to the production of the final product shipped to the final buyer, the solution to the problem of reproducing the SSMR MRB can be associated with development of a set of measures to motivate businesses to prospecting and discovery of new deposits for increasing the available reserves (for example, tax incentives for the companies).

This is an open access article under the CC BY 4.0 license

© Natalya V. Pashkevich, Vera S. Khloponina, Nikolai A. Pozdnyakov, Anastasiya A. Avericheva, 2024

Table 3

Analysis of development prospects for the SSMR MRB[10]

Type of SSMR	Characteristic	Development prospects	Specific features
Uranium	Most of ores are of low quality, which hinders their mining; 29.8 % of in-place reserves are in the unallocated subsoil reserve fund; the development degree is relatively high	Significant increment prospects – C_{2cond} indicator is 30 % of the current in-place reserves. Increasing amount of reserves (P_{MRB} = 148.79 %) is accompanied by decreasing production volumes	Lack of cost-effective industrial technology for beneficiation of complex ores, uranium ores of the Elkon group deposits
Tungsten	A small number of profitable sites for ore mining, while Russia has one of the largest raw material bases for this MR. A major reduction in production over the last 10 years (–40 %) due to deterioration of the technological quality of processed raw materials accompanied by a decrease in its extraction into concentrates	A high share of deposits prepared for development and explored (64.2 %), the exploitation of which is expected to cover most of the need for raw materials	High production costs along with strong tax pressure on the industry; competition with Chinese producers and a growing sanctions pressure. The need for additional public support
Graphite	Low development degree of domestic raw material base: about 86 % of reserves are in the unallocated subsoil reserve fund; in development status – only 1.5 million t (1.5 % of reserves)	Prospects for a major increase in reserves of crystalline graphite: C_{2cond} indicator is comparable to in-place reserves. The prospect of a multiple increase in production due to development of the Topolikhinskii site of the Soyuznoe deposit in the Jewish Autonomous District	Logistics and infrastructure difficulties relevant for individual sites; low utilization degree of the available MRB
Molybdenum	High formal degree of development with a low actual level of reserves developed – actual share of developed reserves is about 4 %	C_{2cond} indicator is approximately 16 % of in-place reserves; at the same time, the quality of prognostic reserve fund ores is comparable to in-place reserves of similar deposits	High sensitivity to world prices for raw materials; low domestic demand for molybdenum products
Tantalum	Taken into account in ores of the Ulug-Tanzekskoe deposit, deposits of the Lovozerskii GOK and other deposits of complex ores	Due to the rarity of MR (valid for the whole world), the optimal development trend for the available MRB is the development and implementation of missing technologies, restoration of the chain "from ore to final products"	The need to organize tantalum powder production in Russia with subsequent introduction into domestic industry
Vanadium	Most of ores sufficient for industrial use are contained in the depths of iron ore mines. deposits of the Ural Federal District (Gusevogorskoe and Sobstvenno-Kachanarskoe); considered as the main component at the Srednyaya Padma deposit (Republic of Karelia)	Russia has a great potential for extracting vanadium from complex ores; at the same time, it is possible to develop zero-waste mining which involves vanadium production from oils and various types of industrial waste	Development of technologies of vanadium extraction from spent catalysts and other industrial waste containing vanadium
Niobium	Contained as an associated component in ores of the Afrikandovskoe deposit; in ores of the Ulug-Tanzekskoe deposit and the Zashikhinskoe deposit tantalum and niobium are the main components; found in commercial quantities in ores of the Lovozero deposit, etc.	The start of production at the prepared deposits will to a major extent satisfy the needs of economy	Search for additional investments for the development of potential sites

[10] State report "On the state and use of mineral resources of the Russian Federation in 2021". Moscow, 2022, p. 626.

This is an open access article under the CC BY 4.0 license

Table 3 continued

Type of SSMR	Characteristic	Development prospects	Specific features
Manganese	Manganese base as a whole does not meet the requirements of industry: low-quality ores with harmful impurities; low actual degree of development – about 0.5 % of reserves are developed; subsoil user, who had 93 % of allocated in-place reserves and part of allocated subsoil reserve fund, was declared bankrupt in January 2018	Prospects for a major increase: C_{2cond} indicator is about 50% of in-place reserves; reduction in the amount of reserves (P_{MRB} = –22.02 %) accompanied by resumption of production in the RF	Lack of infrastructure near major sites
Chromium	Low quality of raw materials (low-grade and lean ores); low degree of development: 11.3 % of reserves are developed; 7.9 % are at the stage of preparation for development and exploration; 80.7 % – unallocated subsoil reserve fund	Prospects for a major increment: C_{2cond} indicator is twice the value of in-place reserves; increasing reserves (P_{MRB} = 2.04 %) accompanied by growing production volumes	Ores that do not require beneficiation and are used in domestic industry make up only a quarter of reserves; mining engineering and infrastructure problems
Titanium	Low quality of ores and complicated occurrence environment limit the development of placer deposits; low degree of development – 2.9 % of reserves are involved in development; 28.2 % are prepared for development and explored, 68.9% remain in the unallocated subsoil reserve fund	Prospects for a major increment: C2cond indicator is approximately half of reserves; increasing of reserves (P_{MRB} = 297.93 %) accompanied by growing production volumes; obtaining of titanium concentrate from ores of the Khibiny deposits [10] as well as the technological mineralogy of titanium ores offer good prospects [11]	No possibility of using industrial technology for processing high-titanium titanomagnetite concentrates
Beryllium	Resumption of mining is associated with the Ermakovskoe deposit which was not developed since 1989; currently, OOO Ermakovskoe is working at this deposit planning to develop it by open pit mining	A potential trend could be the development of tailings dumps containing beryllium as one of components, which reduces the volume of mining waste and complies with the principles of a circular economy [12, 13]	The scientific community is actively discussing the need to organize full-cycle beryllium production – from ore to metal, which requires the appropriate technological solutions
Bauxites	Low quality of ores, mining engineering and infrastructural difficulties led to the situation when Russia uses only 43 % of bauxite reserves for alumina production. Average development of the raw material base: 53.1 % of reserves – unallocated subsoil reserve fund; 33.4 % involved in development and 13.5 % is being prepared for operation	Increment prospects are low: C_{2cond} indicator is less than 3 % of current in-place reserves; decreasing reserves (P_{MRB} = –116.79 %) are accompanied by growing volumes	The need to introduce into industrial production a more advanced technology for processing low-quality raw materials allowing work in modern economic conditions
Zirconium	Russian baddeleyite concentrate – a unique, high-quality zirconium raw material, is mainly exported. Low degree of the MRB development: 3.4 % reserves are involved in development; the share of deposits prepared for development and exploration is 28 %; 68.6 % remain in the unallocated subsoil reserve fund (according to 2022 data). Currently, the Tuganskii GOK largely satisfies the demands of domestic industry	Prospects for major increment: C_{2cond} indicator is comparable to the amount of in-place reserves. Increasing reserves (P_{MRB} = 360.98 %) accompanied by decreasing production volumes	Use of associated sources of zirconium raw materials: it is necessary to implement the industrial technology for beneficiation and extraction of zirconium from eudialyte ores. The use of complex, multi-stage processing technologies for ores from the Katuginskoe and Ulug-Tanzekskoe deposits is required

This is an open access article under the CC BY 4.0 license

End of Table 3

Type of SSMR	Characteristic	Development prospects	Specific features
Lithium	Most deposits, except those where lithium is an associated component are in the unallocated subsoil reserve fund. A complex composition of ores and their low dressability hinder the development of lithium deposits	There are no prospects for reserves increment: contingent reserves of category C_2 amount to 2.3 % of in-place reserves. Reduction in reserves as a result of revaluations is accompanied by absence of production in the RF. Potential lithium resources are associated with formation brines in areas of exploration and production of hydrocarbon raw materials	Lack of an efficient technology for beneficiation, extraction and processing is one of the reasons for non-involvement of existing sites of unallocated subsoil reserve fund into operation. Planned integrated projects based on the Kolmozerskoe (Rosatom and Norilsk Nickel) and Kovyktinskoe (Gazprom) deposits can cover the need of domestic economy for lithium
Fluorspar	Raw material base is extensive, but ore quality is low, so since 2014 the Russian consumers were dependent on imports. Low development degree of the raw material base: 38. 1% of reserves are involved in development; 7.8 % reserves are mined; 9.5 % – the share of deposits prepared for development and explored; 52.4 % of reserves remain in the unallocated subsoil reserve fund	The prospects for reserves increment are high: 28.9 million t in terms of contingent reserves of category C_2, which corresponds to the amount of in-place reserves. Reduction in reserves (P_{MRB} = –21.79 %) is accompanied by production renewal in the RF	To meet the needs of the Russian industry for fluorspar of chemical grades, it is necessary to improve the current technologies for beneficiation of fluorspar ores to increase fluorite content and reduce carbonate level
Rhenium	There are no active reserves, the reserves are associated with occurrence of rhenium in deposits of porphyry copper ores, molybdenum ores, tungsten-molybdenum ores, uranium ores in sandstones, fumarole gases of the Kudryavyi volcano [14]	Rhenium reserves in the RF are scarce, their replenishment has no prospects, therefore, it is necessary to search for new sources of raw materials and re-evaluate the deposits	It is planned to use borehole underground leaching technology with rhenium yield of 3.4 t per year by the end of 2024
Yttrium	Scarce reserves: deposit in the Revda Village, Murmansk Region, contains 1.3 % yttrium (of all mined REM). Reserves of medium and heavy REE – yttrium group – are taken into account along with all REE	The lack of demand from domestic producers does not allow using the associated raw materials in modern economic conditions	Poor infrastructure and harsh climatic conditions prevent the development of the Tomtorskoe deposit with yttrium trioxide content of about 0.5 %

Table 4

Areas of SSMR use[11,12,13]

Type of SSMR	Use	Main consumers
Uranium	The most significant volume of uranium raw materials in the RF is used to produce nuclear fuel for domestic and foreign nuclear power plants. Part of the needs in uranium are provided by supplies from Kazakhstan facilities of the "Rosatom" state corporation	Companies of AO TVEL (part of Rosatom) engaged in uranium conversion and enrichment: AO Angarsk Electrolyte Chemical Plant (AO AEKhK), AO PO Electrochemical Plant (AO PO EKhZ), AO Ural Electrochemical Plant (AO UEKhK), AO Siberian Chemical Plant (AO SKhK)
Tungsten	Use in heat-resistant and hard materials as an alloying additive in production of steels, special and acid-resistant alloys, in chemical industry and electronics. Main consumer industries: automotive industry, mining industry, tool industry, aerospace industry, power engineering, etc.	OAO Gidrometallurg, AO Kirovgrad Hard Alloy Plant, OOO Moliren

[11] State report "On the state and use of mineral resources of the Russian Federation in 2021". Moscow, 2022, p. 626.
[12] Official website of the Unified Information System in the field of procurement URL: https://zakupki.gov.ru/epz/main/public/home.html (accessed 08.04.2024).
[13] Market of manganese and products 2023. URL: https://www.metalresearch.ru/manganese_market.html (accessed 08.04.2024).

This is an open access article under the CC BY 4.0 license

Table 4 continued

Type of SSMR	Use	Main consumers
Graphite	High-tech areas (for example, production of high-capacity batteries); metallurgical industry (ferrous metallurgy, aluminium production, etc.); production of dyes, lubricants, graphite electrodes	ZAO Grafitservis, PAO Severstal, OAO NLMK, OAO MMK, OAO EVRAZ NTMK, OAO EVRAZ ZSMK, PAO Chelyabinsk Metallurgical Plant, PAO Magnezit Plant, OAO Dinur (refractory products manufacturers)
Molyb-denum	Production of ferroalloys and alloying elements, stainless steels; production of catalysts in chemical industry; use as an anti-friction lubricant, etc.	OOO SFMZ, OOO Moliren, OOO Nizhnevolzhskii Ferroalloy Plant, AO Ural Steel, PAO Severstal, OAO Oskol Electrometallurgical Plant
Tantalum	Use in modern electronics (production of high-quality capacitors), as a component in production of hard alloys, military industry, nuclear power engineering, etc.	Ekaterinburg Non-Ferrous Metals Processing Plant (OAO EZ OTsM), companies of Rosatom fuel division, electronics manufacturing companies
Vanadium	Battery production; ferrous metallurgy (increasing the strength of alloys, strength and wear resistance of steel); space, aviation, defense and other industries	AO PO Northern Machine-Building Company, PAO Ufaorgsintez, AO Votkinsk Plant, AO NPK Uralvagonzavod, research organizations
Niobium	Aerospace industry; electric power engineering; railway transport; electronics	AO NII NPO Luch, AO Research Institute of Machine Building, AO A.M.Isaev KBKhM, AO M.V.Khruchnev GKNPTs, AO Uranium ONE GROUP, PAO NPO Iskra, AO Votkinsk Plant, etc.
Manganese	Production of ferroalloys which are completely consumed by steel industry; use as an alloying metal; production of welding electrodes, water filters, fiberglass, ceramics and bricks (as a pigment); production of dry electric batteries; other areas of industry and medicine. Domestic consumption in 2021 accounted for 1.47 million t of manganese ores and concentrates. Consumption of manganese ferroalloys is for 74 % covered by domestic products, however, imported concentrates and ore are used for the production of ferroalloys	PAO Severstal, PAO Magnitogorsk Metallurgical Plant, PAO Novolipetsk Metallurgical Plant, PAO Kosogorsk Metallurgical Plant, PAO Nizhny Tagil Metallurgical Plant, AO Chelyabinsk Electrometallurgical Plant, Satka Iron Works, PAO Klyuchevsky Ferroalloy Plant, AO Chelyabinsk Zinc Plant
Chromium	Production of ferroalloys; production of metal chromium and chemical compounds; production of stainless steel; use as an alloying element; production of refractories, etc. Domestic consumption of chromium concentrates and commercial chromium ores is mainly provided by imports, on average in 2012-2019 domestic production covered about a third of all needs (from 24 to 45 %)	AO Chelyabinsk Electro-Metallurgical Plant, AO Novotroitsk Chromium Compounds Plant, AO Russian Chromium 1915, NSplav, PAO Klyuchevsky Ferroalloy Plant, AO Polema, OOO Tikhvin Ferroalloy Plant, OOO UK Industrial Metallurgical Holding (PMKh)
Titanium	Engine construction, shipbuilding, construction of drilling and production platforms, offshore equipment; power engineering; non-ferrous metallurgy; machine building and chemical industry; production of titanium metal; production of welding electrodes and welding wire; use by companies of paint and varnish industry and manufacturers of rubber products, photocatalysts, self-cleaning glasses, etc. All titanium raw materials used by the Russian companies is imported	PAO VSMPO-AVISMA Corporation, AO SMK, OOO “NPO Rusredmet, OOO Normin, OOO ZVM, etc.

This is an open access article under the CC BY 4.0 license

© Natalya V. Pashkevich, Vera S. Khloponina, Nikolai A. Pozdnyakov, Anastasiya A. Avericheva, 2024

End of Table 4

Type of SSMR	Use	Main consumers
Beryllium	Nuclear power engineering and renewable energy sources, defense and military industry, rocket and space industry (for example, use of beryllium oxide in production of rocket engines and as transparent protective coating on telescope mirrors); aircraft manufacturing; medical and industrial equipment; automotive industry; aircraft engineering, telecommunications equipment, etc.	PO Mayak, Rosatom (including AO D.V.Efremov NIIEFA, AO GNTs NIIAR, AO Uranium One Group), AO NII NPO Luch, AO NPK Systems of Precision Instrumentation Engineering
Bauxites	Production of alumina for aluminium smelting used in many industries; use as a flux in ferrous and non-ferrous metallurgy companies. Construction, aircraft, automotive and shipbuilding, packaging production, electrical items production, machine building and consumer goods, aluminium industry [15]. Only 35-40 % of needs of Russian aluminium smelters are covered by domestic products	Bogoslovskii and Ural alumina refineries
Zirconium	Production of ceramics, metal zirconium, refractories, abrasive products, non-stick coatings; aviation, rocket and space equipment and transport; foundry. Obtaining the world's only baddeleyite concentrate with a higher cost compared to zirconium concentrate. Russia's leadership in the world market in production of zirconium rolled products. Production of powders and ceramic products based on zirconium dioxide used by nuclear industry; chemical, oil and gas, medical, food industries. Apparent consumption of zirconium concentrates in Russia is 9.9-11.6 thousand t per year, more than 90 % of it is covered by imported zircon concentrates	OAO Dinur, AO Shcherbinsky Plant of Electrofused Refractories, AO Borovichi Refractories Plant, AO Podolskogneupor, AO NPO Yuzhuralinstrument, PAO Klyuchevsky Ferroalloy Plant, AO Chepetsky Mechanical Plant, AO Angarsk Electrolysis Chemical Plant, PAO Uralkhimplast, NPP Technology, NPP Ekon
lithium	Atomic industry; aluminium industry – in the composition of alloys containing magnesium; for production of batteries, fibres, special glasses, lithium ceramics. Russian consumers of lithium are mainly processing plants. Production of lithium items in the RF has a positive dynamics – in 2017-2020 it increased 1.5-fold (from 5,310 to 8,030 tons)	PAO Chemical Metallurgical Plant, PAO Novosibirsk Chemical Concentrates Plant (part of Rosatom and nuclear fuel producer AO TVEL), OOO TD Halmek
Fluorspar	Ferrous metallurgy is the main consumption; chemical and cement industry; non-ferrous metallurgy; production of electrodes, ceramics; building sector. Change in consumption from 2012 due to replacement of cryolite, the raw material of which is fluorspar, with aluminium fluoride in aluminium industry. In 2012-2021, domestic consumption of fluorspar concentrates varied from 160 to 390 thousand t, on average being about 210 thousand t. The maximum value was reached in 2012	PAO Novolipetsk Metallurgical Plant, PAO Magnitogorsk Metallurgical Plant, AO Oskol Electrometallurgical Plant, AO HaloPolymer Perm which produces fluoropolymer products, OOO Topkinskii Cement
Rhenium	Aviation; petrochemistry; non-ferrous metallurgy; metallurgical alloys; electrical engineering; nuclear industry (catalyst component); oil refining industry [16, 17]	OAO Stupino Metallurgical Company, VIAM GNTs RF ZAO Industrial Catalysts
Yttrium	Defense industry – production of high-temperature superconductors as well as guidance units for aviation; nuclear medicine – treatment of oncological diseases	OOO Bebig, manufacturers of REE products

This is an open access article under the CC BY 4.0 license

© Natalya V. Pashkevich, Vera S. Khloponina, Nikolai A. Pozdnyakov, Anastasiya A. Avericheva, 2024

An efficient mechanism for encouraging private companies to develop the SSMR deposit is interaction between the state and business. Thus, in 2022, the state corporation Rosatom and PAO "GMK "Norilsknickel" concluded an agreement on the implementation of a joint project for the development of the Kolmozerskoe deposit and further deep processing of lithium raw materials. Such an agreement makes exploration more accessible to business and also satisfies the needs of nuclear industry[14]. Sanctions pressure with limited access to innovation and software and tightening of environmental standards in connection with updating the climate agenda, etc., can be levelled out with support of the state corporations [8, 18, 19].

The current state of geological exploration for the SSMR in the RF is characterized by the following features.

Currently, geological exploration is carried out mainly at the expense of own funds of the companies. In 2022, the ratio of state and business participation in geological exploration in monetary terms was 13 : 10,000 for hydrocarbon raw materials and 2 : 25 for solid minerals (SM), while 10 years ago the ratio was 1 : 20 and 1 : 5, respectively. When assessing the financial investments in geological exploration, it is necessary to consider the long payback period and the demand for large investments [20].

According to the data in form N 7-gr "Information on geological exploration by exploration types and groups of minerals", there is a decrease in funding of geological exploration for the SSMR[15] (hereinafter, the SSMR do not include bauxites and fluorspar, since the information on these types of minerals is not outlined in form N 7-gr). Over the past three years, the extent of the SSMR funding decreased from 1,053 million roubles to 429 million roubles – by 59.3 % (Fig.3) [21].

Declining interest of subsoil users to geological exploration is also confirmed by results of analysing the dynamics of the SSMR financing for each type of mineral resource (Fig.4). The largest amount of financing for geological exploration is recorded for uranium and tungsten, while for zirconium there is neither public, nor private investments.

Funding of geological exploration for manganese from the federal budget was discontinued in the last three years; for chromium, in the last year; and for rare metals, in the last five years. Private investment adequately supports the reproduction of manganese and rare metals, and the exploration for chromium should receive public funding.

Geographic exploration that ensures the reproduction of uranium and chromium is financed primarily from the budget (41.6 and 49.3 % of total SSMR funding from the federal budget, respectively). Lack of funding for geological exploration of zirconium, both from the public and private investments, was recorded since 2017. In 2016, the share of funding from the federal budget for geological exploration of zirconium was 5.9 %, and in 2015 – 2.9 % at the expense of the companies' own funds. Manganese, chromium and graphite are characterized by low investment attractiveness which either increases or decreases over time.

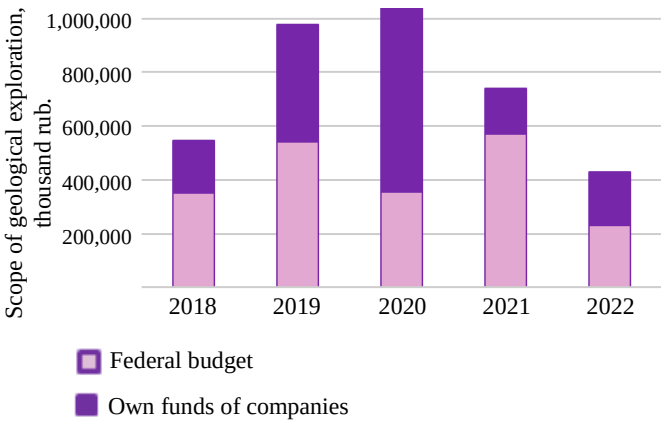

Fig.3. Dynamics of exploration financing for SSMR[16,17]

The MRB development strategy of the Russian Federation until 2035 represents as an internal challenge the reduction in budgetary funding for geological exploration of subsoil in

[14] State report "On the state and use of mineral resources of the Russian Federation in 2021". Moscow, 2022, p. 626.

[15] Form N 7-gr "Information on geological exploration by exploration types and groups of minerals". URL: https://www.rosnedra.gov.ru/article/13273.html (accessed 08.04.2024).

[16] Chromium market 2023. URL: https://www.metalresearch.ru/chromium_market.html (accessed 06.11.2024).

[17] Lithium and compounds market 2022. URL: https://www.metalresearch.ru/lithium_market.html (accessed 04.08.2024).

This is an open access article under the CC BY 4.0 license

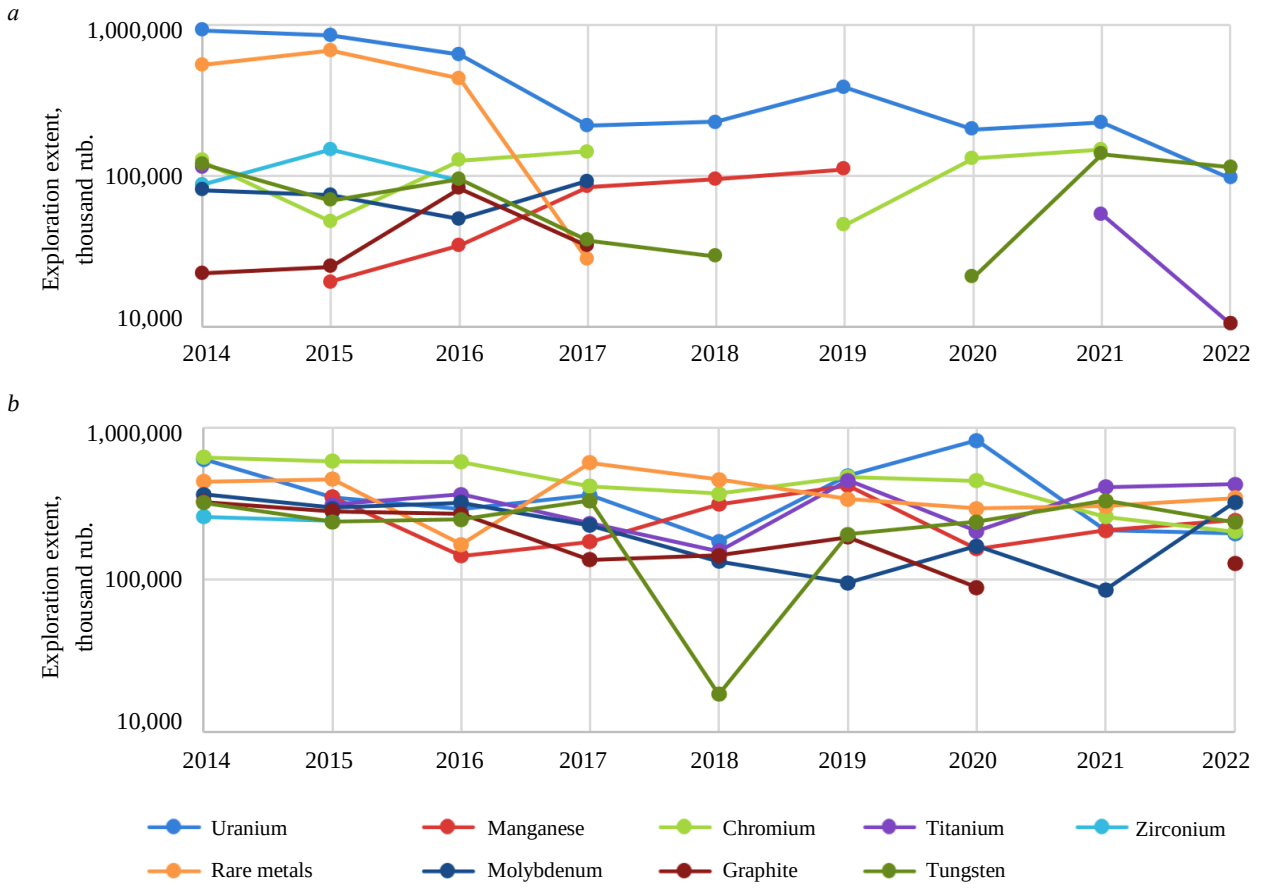

Fig.4. Dynamics of financing geological exploration for SSMR from the federal budget (*a*) and own funds of companies (*b*) for eight years[18]

the absence of a possibility of conducting regional research based on private investment. The federal budget does not finance geological exploration for manganese, chromium, and rare earth metals. Private investments adequately support the reproduction of manganese and rare earth metals, and exploration for chromium should receive public funding.

Financing of geological exploration at the expense of own funds of the companies is characterized by a positive dynamics, while funding from the federal budget is insufficient. However, subsoil users are not interested in geological exploration for zirconium and chromium, which is confirmed by results of analysis. According to para. 2 art. 23 of the Law of the RF "On Subsoil" dated February 21, 1992, N 2395-1, subsoil users are obliged to ensure the completeness of geological study and reasonable integrated use of subsoil.

Currently, the problem of intensifying geological exploration is relevant. The rate of additional exploration and putting the already discovered deposits into operation is much higher than the rate of exploration aimed at discovering new deposits in relatively poorly studied areas. Budgetary funding does not cover the expenses; there is a shortage of modern geological exploration, technological and analytical equipment. Production volumes are outstripping the exploration and development of deposits, and the prospecting reserves significantly decreased [22, 23].

The presence or lack of interest of subsoil users in geological exploration for the SSMR can also be assessed by the data on the activity of obtaining licenses of various categories (of primary interest are the exploration licenses of type P). Prospecting licenses allow their owners to conduct geological exploration including prospecting and evaluation of mineral deposits. Table 5 shows the statistics on the license for the SSMR type P valid as of 01.01.2022.

[18] Market of manganese and products in 2023. URL: https://www.metalresearch.ru/manganese_market.html (accessed 08.04.2024).

This is an open access article under the CC BY 4.0 license

Table 5

Analysis of SSMR licenses by type of use valid as of 01.01.2022[19]

Licenses	Uranium	Manganese	Chromium	Titanium	Bauxites	Lithium	Zirconium	Fluorspar	Rare earth metals
Licenses for geological study for prospecting and evaluation (issued on a declarative principle)	–	5	7	5	2	4	3	5	1
Licenses for geological study for prospecting and evaluation	1	5	9	7	2	4	5	6	3
For exploration and production (operation)	26	5	3	14	7	3	6	9	12
For geological study, exploration and production (combined)	2	5	9	7	11	–	2	3	2
Total number of licenses (2 + 3 + 4)	29	15	21	28	20	7	13	18	17

Most of valid licenses for geological study for prospecting and evaluation in the vast majority of cases (60-100 %, with the exception of uranium and rare earth metals) were obtained on a declarative principle, which points to the efficiency of the licensing mechanism introduced in 2014. Subsoil plots that could otherwise be ignored by subsoil users are now covered by prospecting and evaluation work [24, 25].

Total number of licenses in force in Russia shows that since 2020 about half of them were obtained on a declarative principle, although the funding attracted on its basis for geological exploration was much lower (for example, in 2021, 15.6 billion roubles, which is 26.9 % of total funds). This is explained by a small extent of activity of the companies receiving a license by a simplified mechanism; comparably higher risks when working in subsoil plots with no data available on the occurrence of solid minerals and/or predicted solid mineral resources of categories P_1 and/or P_2, if the plot is not considered to occur in the Arctic zone[20] or for other reasons.

Thus, the declarative mechanism can encourage subsoil users to engage in reproduction of the SSMR MRB through a simplified procedure for obtaining licenses, although in practice, in the vast majority of cases, the applications are submitted for placer gold (66 %) and ore gold (19 %) – 70 and 15 % of issued licenses for types of solid minerals, respectively[21]). Total number of valid licenses for geological studies for prospecting and evaluation issued on a declarative principle for the SSMR is 32 (Table 5), which is 0.66 % of total number of valid licenses received on a declarative principle in 2021.

These conclusions are confirmed by the Catalogue of accounting units of the State Register of Reserves, which makes it possible to analyse the activity of subsoil users on specific sites of the state in-place reserves (Table 6)[22].

The highest activity of subsoil users in exploration of deposits, both in absolute and relative values, is recorded for the following types of the SSMR: chromium (in 16 records of deposits the

[19] State report "On the state and use of mineral resources of the Russian Federation in 2021". Moscow, 2022, p. 626.

[20] Order of the Ministry of Natural Resources and Environment of the RF and the Federal Agency for Mineral Resources dated 28 October 2021, N 802/20 "On approval of the Procedure for granting the right to use subsoil plots for geological study of subsoil including prospecting and evaluation of mineral deposits, on a subsoil plot not included in the list of subsoil plots for geological study of subsoil, with the exception of subsoil in subsoil plots of federal significance and subsoil plots of local importance".

[21] Round table "Declarative principle" of licensing and other measures to stimulate geological study of subsoil in solid mineral deposits". URL: https://www.rosnedra.gov.ru/article/12909.html (accessed 04.08.2024).

[22] Catalogue of accounting units of the State Register of Reserves with data of consolidated state register of subsoil plots and licenses and gas condensate fields (including the Collection of consolidated materials on reserves of common mineral resources of the RF). URL: https://rfgf.ru/bal/a/ (accessed 08.04.2024).

This is an open access article under the CC BY 4.0 license

exploration is conducted, which is about 57 % of all records), manganese (exploration is underway at five sites out of nine) and uranium (11 records of deposits out of 30 were explored, which is 36.7 %).

Table 6

Extent of development of deposits with SSMR licenses as of May 22, 2024[23,24]

State	Uranium	Manganese	Chromium	Titanium	Bauxites	Zirconium	Beryllium	Lithium	Rhenium	Rare-earth metals	Fluorspar	Tungsten	Graphite	Vanadium	Niobium	Tantalum	Molybdenum
Number of records of deposits with a license	30	8	29	18	13	8	2	5	7	12	13	30	3	40	14	5	23
Development extent:																	
prepared for development	5	3	2	7	8	3	–	–	4	5	4	12	1	9	4	2	9
explored	11	5	16	4	1	4	1	1	2	–	1	10	–	5	–	–	4
developed	14	2	13	9	7	3	2	4	2	8	8	9	2	29	11	3	11
Not transferred for development (sites without a license)	31	21	11	19	43	15	–	13	1	8	30	66	9	9	27	27	12

Sites not transferred for development (without a license) (Table 6) are potential subsoil plots, due to which the SSMR MRB can be incremented, if they are transferred for development to subsoil users. It is impossible to interest subsoil users without solving the legal, technological and financial problems.

Creating favourable investment conditions, along with development of exchange-based financing instruments, help to attract private funds from investors both in mining industry in general [26], and in geological exploration in particular. Recommended measures: tax incentives for shareholders of exploration companies, development of venture capital market, partial subsidies for exploration, insurance of investments in geological exploration for the SSMR, tax preferences for exploration companies and subsoil users, preferential lending, public-private partnerships, interindustry agreements etc. The implementation of these measures also involves state monitoring of exploration projects for the SSMR for their classification according to the level of possible risks associated with both geological environment of geological exploration, as well as infrastructural, technological, economic and other factors.

In addition, the possibility of transferring rights to use subsoil to the third parties, bypassing the phase of active development as well as subsequent production, is a necessary condition for the development of minor geological exploration companies (juniors) specializing in prospecting deposits for subsequent sale to mining companies [27]. For example, one of the strongest and most competitive Canadian uranium junior companies, Denison Mines, was running several large projects since 1985 and increased their market share. Positive prospects for the existence of juniors: about 64 % of uranium juniors continue their activities, conduct exploration for another metal, engage in another business, and are also absorbed, the rest discontinue their activities or freeze the projects [28, 29].

International experience of functioning of junior business structures also presupposes access to exchange-traded instruments for financing their activities (there are about 2,000 junior issuers in

[23] Round table “Declarative principle” of licensing and other measures to stimulate geological study of subsoil in solid mineral deposits”. URL: https://www.rosnedra.gov.ru/article/12909.html (accessed 04.08.2024).

[24] Catalogue of accounting units of the State Register of Reserves with data of consolidated state register of subsoil plots and licenses and gas condensate fields (including the Collection of consolidated materials on reserves of common mineral resources of the RF). URL: https://rfgf.ru/bal/a/ (accessed 08.04.2024).

This is an open access article under the CC BY 4.0 license

total[25,26]). At the St. Petersburg Exchange, a separate segment "SPB Juniors" was set up, but currently not a single company went through the procedure of public offering of shares, though the issue of shares of PAO Almar was expected in 2023. The possibility of implementing a positive scenario for this segment is also supported by current trends in increasing number of expected IPOs of Russian companies, development of exchange financing practice in the country as a whole (according to Moscow Exchange estimates, 40 new IPOs could be held by 2025, which is a significant percentage of existing issuers in various sectors) [30, 31].

It is necessary to consider possible risks and difficulties associated with establishment of junior exploration companies. A detailed criticism of the proposed solution to the SSMR problem is discussed in [32]; paper [33] is devoted to possible risks of fraud on the part of new business structures. Since the practice of setting-up junior companies originated abroad, it is important to take global experience into account [34-36]. Key statistics demonstrating industry trends (including a major share of junior companies in discovery of new deposits around the world) are given in [37, 38]. Legal aspects of operation of such companies in other countries[27] are presented in [39], financial issues and evaluation of such companies are discussed in [40-42]. These scientific works, along with other studies devoted to junior companies, describe the accumulated experience in studying this trend of business, which is important for assessing its possible risks and prospects.

Conclusion.

In the current geopolitical conditions, the problem of scarcity of strategic mineral resources is a priority and requires relevant measures. Political events of recent years led to the breakage of many international relations, which once again showed the danger of national economy dependence on the import of key raw materials.

Analysis of the state of the SSMR MRB, demand for minerals, level of technology and equipment development showed that solving the problem of scarcity of considered minerals is associated with the following trends:

• the need for industrial implementation of new technologies for processing and beneficiation of raw materials;

• overcoming infrastructure difficulties (manganese, bauxites and yttrium);

• intensification of geological exploration for potential SSMR (manganese, uranium, chromium, fluorspar, zirconium, titanium).

Geological exploration for ensuring the development of the SSMR MRB involves resolving a set of legal and financial problems. After introduction of the declarative principle, not only the number of "prospecting" licenses for placer and ore gold increased enormously, but also this mechanism became a prerequisite for the development in the RF of junior business structures – minor geological exploration companies whose goal is to expand the MRB through the development of potential subsoil plots. International practice shows that in the last decade more than 65 % of all deposits were discovered by junior companies [37].

Economic and legal initiatives can further stimulate the development of the junior movement in Russia. For example, expanding the application of the declarative principle to a larger number of subsoil plots for individual mineral resources [43] (in particular the SSMR), considering the possibility of free trade in subsoil use rights between the Russian subsoil users, solving the problem of fines for discovering a deposit (the fine arises in the course of obtaining a license of R type by the discoverer who collected and registered the geological information at his own expense) [44].

[25] Kostina M. Role of juniors in geological exploration: global experience and prospects for the development of movement in Russia. URL: https://dprom.online/mtindustry/rol-yuniorov-v-geologorazvedke-mirovoj-opyt-i-perspektivy/ (accessed 08.04.2024).

[26] SPB Juniors. URL: https://spbexchange.ru/ru/listing/segments/spb_juniors/Default2.aspx (accessed 08.04.2024).

[27] Junior mining regulations need to be amended, says law firm. URL: https://www.miningweekly.com/article/junior-mining-regulations-need-to-be-amended-says-law-firm-2022-05-05 (accessed 08.04.2024).

This is an open access article under the CC BY 4.0 license

Lack of conditions for free sale of subsoil use rights does not allow minor exploration companies to operate for a long time accumulating practical experience and consolidating a larger number of fixed assets. After receiving positive results from work on a subsoil plot, a modern Russian junior will be absorbed by a major subsoil user, which is due to a possibility of transferring the license for subsoil use within one legal entity. A way for a geological exploration company to generate income that does not lead to absorption is the sale of geological information with a trade secret regime established for it (Article 27 of the RF Law "On Subsoil"). A major subsoil user acquiring information from a junior gains an advantage over the others, since the degree of uncertainty for a specific subsoil plot is reduced, and he can take a more weighted decision about the prospects of such a plot [45]. Creating conditions for freer trading of licenses can increase income opportunities for juniors and allow them to develop in the long term without moving into the mining stage.

Introduction of additional tax and other benefits (for example, provision of loans on preferential terms) for the companies engaged in prospecting and exploration (including for investors in junior projects) can help intensifying the discovery of new deposits and specifying the reserves for existing ones. Thus, the tax system of Canada, which is successfully developing at the expense of the mining business, uses the following methods of encouraging exploration: regulation of tax rates; granting "tax holidays"; a system of discounts and transfer of the tax burden to the field operation stage; tax benefits to investors financing exploration as well as to private sector with the right to transfer these benefits. The country has a flexible taxation system for subsoil use [46]. When drawing up the draft for such benefits, it is necessary to consider the potential benefits from geological exploration determined depending on the probability of success, which is controlled by the quality of the MRB of the RF for specific SSMR and the information available on them (see Table 3).

When analysing the main consumers of the SSMR, a potential measure to reduce the scarcity of the considered minerals was recognized – development of a set of tax incentives for large consumer companies for stimulating the exploration of subsoil by users at their own expense without attracting public funding. It is also advisable to extend tax benefits to activities related to the development of infrastructure in remote areas.

Thus, an integrated approach to solving the problem of scarcity of strategic minerals in the RF will provide favourable conditions for expanded reproduction of the SSMR MRB and reduce the level of dependence on foreign sources of raw materials.

REFERENCES

1. Semin A.N., Tretyakov A.P., Danilova K.A. On mining and reserves of mineral resources of the largest countries in the world: ranking analysis. *ETAP: Economic Theory, Analysis, and Practice.* 2022. N 1, p. 7-27 (in Russian). DOI: 10.24412/2071-6435-2022-1-7-27
2. Albertyan A.P. Development of the mineral resource complex as an increase in the geopolitical status of Russia. *World Politics.* 2022. № 1, p. 48-58 (in Russian). DOI: 10.25136/2409-8671.2022.1.37713
3. Pashkevich N.V., Tarabarinova T.A., Golovina E.I. Problems of reflecting information on subsoil assets in International Financial Reporting Standards. *Academy of Strategic Management Journal*. 2018. Vol. 17. N 3, p. 1-9.
4. Yurak V.V., Dushin A.V., Mochalova L.A. Vs sustainable development: scenarios for the future. *Journal of Mining Institute.* 2020. Vol. 242, p. 242-247. DOI: 10.31897/PMI.2020.2.242
5. Paveleva Yu., Fofanova E., Melnikova O. et al. Assessing the uncertainty and value of information as a tool for planning the exploration program. Rossiiskaya otraslevaya energeticheskaya konferentsiya: Sbornik materialov konferentsii, 3-5 oktyabrya 2023, Moskva, Rossiya. Moscow: Geomodel, 2023, p. 720-746 (in Russian).
6. Orlov V.P. On some achievements and challenges of national geological surveys over the past 50 years. *Mineral Resources of Russia. Economics & Management.* 2016. N 1-2, p. 11-17 (in Russian).
7. Ponomarenko T., Nevskaya M., Marinina O. An Assessment of the Applicability of Sustainability Measurement Tools to Resource-Based Economies of the Commonwealth of Independent States. *Sustainability*. 2020. Vol. 12. Iss. 14. N 5582. DOI: 10.3390/su12145582
8. Nevolin A.E., Cherepovitsyn A.E., Solovyova V.M. Methods for developing strategic alternatives for the mining and metals sector: A case study of Nornickel. *The North and the Market: Forming the Economic Order.* 2023. N 3, p. 44-60 (in Russian). DOI: 10.37614/2220-802X.3.2023.81.003

This is an open access article under the CC BY 4.0 license

9. Tcvetkov P. Small-scale LNG projects: Theoretical framework for interaction between stakeholders. *Energy Reports*. 2022. Vol. 8. S. 1, p. 928-933. DOI: 10.1016/j.egyr.2021.11.195

10. Mitrofanova G.V., Marchevskaya V.V., Taran A.E. Flotation separation of titanite concentrate from apatite-nepheline-titanite ores of anomalous zones of the Khibiny deposits. *Journal of Mining Institute.* 2022. Vol. 256, p. 560-566. DOI: 10.31897/PMI.2022.81

11. Kotova O.B., Ozhogina E.G., Ponaryadov A.V. Technological mineralogy: development of a comprehensive assessment of titanium ores (exemplified by the Pizhemskoye deposit). *Journal of Mining Institute.* 2022. Vol. 256, p. 632-641. DOI: 10.31897/PMI.2022.78

12. Ignatyeva M.N., Yurak V.V., Dushin A.V., Strovsky V.E. Technogenic mineral accumulations: problems of transition to circular economy. *Technogenic mineral accumulations: problems of transition to circular economy.* 2021. Vol. 6. N 2, p. 73-89 (in Russian). DOI: 10.17073/2500-0632-2021-2-73-89

13. Calvo G., Valero A. Strategic mineral resources: Availability and future estimations for the renewable energy sector. *Environmental Development*. 2022. Vol. 41. N 100640. DOI: 10.1016/j.envdev.2021.100640

14. Marinina O., Kirsanova N., Nevskaya M. Circular Economy Models in Industry: Developing a Conceptual Framework. *Energies*. 2022. Vol. 15. Iss. 24. N 9376. DOI: 10.3390/en15249376

15. Ilyushin Y.V., Kapostey E.I. Developing a Comprehensive Mathematical Model for Aluminium Production in a Soderberg Electrolyser. *Energies*. 2023. Vol. 16. Iss. 17. N 6313. DOI: 10.3390/en16176313

16. Chanturiya V.A. Scientific substantiation and development of innovative processes for the extraction of zirconium and rare earth elements in the deep and comprehensive treatment of eudialyte concentrate. *Journal of Mining Institute*. 2022. Vol. 256, p. 505-516. DOI: 10.31897/PMI.2022.31

17. Lutskiy D.S., Ignatovich A.S. Study on hydrometallurgical recovery of copper and rhenium in processing of substandard copper concentrates. *Journal of Mining Institute.* 2021. Vol. 251, p. 723-729. DOI: 10.31897/PMI.2021.5.11

18. Golovina E., Shchelkonogova O. Possibilities of Using the Unitization Model in the Development of Transboundary Groundwater Deposits. *Water*. 2023. Vol. 15. Iss. 2. N 298. DOI: 10.3390/w15020298

19. Blinova E., Ponomarenko T., Knysh V. Analyzing the Concept of Corporate Sustainability in the Context of Sustainable Business Development in the Mining Sector with Elements of Circular Economy. *Sustainability*. 2022. Vol. 14. Iss. 13. N 8163. DOI: 10.3390/su14138163

20. Litvinenko V.S., Petrov E.I., Vasilevskaya D.V. et al. Assessment of the role of the state in the management of mineral resources. *Journal of Mining Institute.* 2023. Vol. 259, p. 95-111. DOI: 10.31897/PMI.2022.100

21. Sarkarov R.A., Belan S.I., Huseynov N.M. Assessment of the current state and prospects mining of lithium and its compounds in Russia. *Industrial Economics.* 2022. N 2-1, p. 57-68 (in Russian). DOI: 10.47576/2712-7559_2022_2_1_57

22. Burdin D.B. Problematic issues of stimulating geological exploration. Prospects for a solution. *Nedropolzovanie XXI vek*. 2022. N 1 (93), p. 22-25 (in Russian).

23. Kuzina E.S. The problems of financing geological exploration in subsoil use. *Mineral Resources of Russia. Economics & Management.* 2020. N 6, p. 70-72 (in Russian).

24. Tretyakova E. Legal status of a subsoil user as a special participant in business activities. *Energy Policy.* 2023. N 3 (181), p. 76-88 (in Russian). DOI: 10.46920/2409-5516_2023_3181_76

25. Melgounov V.D., Kostareva A.N. On some problematic issues of legal regulation of relations involving the circulation of geological information and export of information about the subsoil. *Mineral Resources of Russia. Economics & Management.* 2023. N 3, p. 66-71 (in Russian).

26. Litvinenko V.S., Tsvetkov P.S., Molodtsov K.V. The social and market mechanism of sustainable development of public companies in the mineral resource sector. *Eurasian Mining*. 2020. N 1, p. 36-41. DOI: 10.17580/em.2020.01.07

27. Shcheglov E.V., Sotnikov M.S., Nugumanov E.K. Selecting a market value approach for greenfield projects. *Journal of Economics, Entrepreneurship and Law.* 2022. Vol. 12. N 12, p. 3345-3360 (in Russian). DOI: 10.18334/epp.12.12.116894

28. Dorokhova I. Uranium juniors – a rare species from the "Red Book". *Atomnyi ekspert*. 2021. Vol. 1-2, p. 216. URL: https://atomicexpert.com/uranium_juniors/ (accessed 15.10.2023) (in Russian).

29. Hodge R.A., Ericsson M., Löf O. et al. The global mining industry: corporate profile, complexity, and change. *Mineral Economics*. 2022. Vol. 35. Iss. 3-4, p. 587-606. DOI: 10.1007/s13563-022-00343-1

30. Pogudin S. Is it possible to make money from an IPO? *Finansovyi zhurnal*. 2024. URL: https://www.finam.ru/publications/item/ mozhno-li-zarabotat-na-ipo-20231026-1427/ (accessed 08.04.2024).

31. Bobylov Yu.A., Makiev S.S. Junior Exploration Companies for the Russian geological prospecting. *Bulletin of the Far Eastern Federal University. Economics and Management.* 2017. N 3 (83), p. 102-114 (in Russian). DOI: 10.24866/2311-2271/2017-3/102-114

32. Oganesian L.V. The state of exploration and the mineral resource base of Russia in the light of the formation of junior business structures. *Mineral Resources of Russia. Economics & Management.* 2023. N 2 (181), p. 4-18 (in Russian).

33. Shaklein S.V., Rogova T.B., Pisarenko M.V. Junior exploration companies at risk of criminalization. *Mineral Resources of Russia. Economics & Management.* 2023. N 3 (182), p. 42-52 (in Russian).

34. Nunez-Picado A., Martinus K., Sigler T. Globalisation strategies and roles among Australian junior mining firms in Latin America. *Geographical Research*. 2022. Vol. 60. Iss. 1, p. 179-195. DOI: 10.1111/1745-5871.12505

35. Nunez-Picado A., Martinus K., Sigler R. Junior Miner internationalisation in the globalising mining industry. *Resources Policy*. 2022. Vol. 79. N 103084. DOI: 10.1016/j.resourpol.2022.103084

36. Mulaba-Bafubiandi A.F., Singh N. Junior mining as innovation entrepreneurship in minerals industry in South Africa. Proceedings of the International Conference on Industrial Engineering and Operations Management Pretoria, 29 October – 1 November 2018, Johannesburg, South Africa. IEOM Society International, 2018, p. 1892-1898.

37. Kustra A., Kowal B., Ranosz R. Financing Sources of Exploration Works in the Light of Risk Related to their Activity. *Inżynieria Mineralna*. 2021. Vol. 1. N 1, p. 89-87. DOI: 10.29227/IM-2021-01-12

This is an open access article under the CC BY 4.0 license

38. Kneas D. Placing resources: Junior mining companies and the locus of mineral potential. *Geoforum*. 2020. Vol. 117, p. 268-278. DOI: 10.1016/j.geoforum.2020.05.007

39. Luning S. Liberalisation of the Gold Mining Sector in Burkina Faso. *Review of African Political Economy*. 2008. Vol. 35. Iss. 117, p. 387-401. DOI: 10.1080/03056240802411016

40. Leśniak T., Kustra A.J., Wilczyński G., Tobiasz R. Factors affecting the market value of junior mining companies listed on the Alternative Investment Market (AIM) London. *Gospodarka Surowcami Mineralnymi*. 2022. Vol. 38. Iss. 3, p. 151-172. DOI: 10.24425/gsm.2022.142786

41. Iddon C., Hettihewa S., Wright C.S. Value Relevance of Accounting and Other Variables in the Junior-Mining Sector. *Australasian Accounting, Business and Finance Journal*. Vol. 2015. Vol. 9. Iss. 1, p. 25-42. DOI: 10.14453/aabfj.v9i1.3

42. Klossek P., Klossek A. The Specific Value of Junior Mining Companies: Are Common Valuation Methods Appropriate? *Journal of Business Valuation and Economic Loss Analysis*. 2014. Vol. 9. Iss. 1, p. 105-144. DOI: 10.1515/jbvela-2013-0014

43. Shchirova E.O., Golovina E.I. The role of junior companies in the gold mining of the Russian Federation. Digital Transformation of Economic Systems: Problems and Prospects (ECOPROM-2022): Collection of works of the All-Russian scientific and practical conference with foreign participation, 11-12 November 2022, Saint Petersburg, Russia. Saint Petersburg: POLITEKh-PRESS, 2022, p. 436-439 (in Russian). DOI: 10.18720/IEP/2021.4/132

44. Burdin D.B. Analysis of the application and issues of improving the representation of the right to use the subsoil for the geological study of the subsoil according to the declarative principle in the Russian Federation. *Nedropolzovanie XXI vek.* 2022. N 3 (95), p. 24-29 (in Russian).

45. Litvinenko V.S. Digital Economy as a Factor in the Technological Development of the Mineral Sector. *Natural Resources Research*. 2020. Vol. 29. Iss. 3, p. 1521-1541. DOI: 10.1007/s11053-019-09568-4

46. Baimishev R.N. Effective International Approaches to Subsoil Public Administration. *Mining Science and Technology* (*Russia*). 2020. Vol. 5. N 2, p. 162-184 (in Russian). DOI: 10.17073/2500-0632-2020-2-162-184

***Authors*: Natalya V. Pashkevich,** *Doctor of Economics, First Vice-Rector, https://orcid.org/0009-0005-3629-9352* (*Empress Catherine II Saint Petersburg Mining University, Saint Petersburg, Russia*), **Vera S. Khloponina,** *Candidate of Economics, Chief Scientific Secretary, Khloponina_VS@pers.spmi.ru, https://orcid.org/0000-0001-9029-2788* (*Empress Catherine II Saint Petersburg Mining University, Saint Petersburg, Russia*), **Nikolai A. Pozdnyakov,** *Student, https://orcid.org/0009-0000-7934-0478* (*Empress Catherine II Saint Petersburg Mining University, Saint Petersburg, Russia*), **Anastasiya A. Avericheva,** *Student, https://orcid.org/0009-0000-2431-4387* (*Empress Catherine II Saint Petersburg Mining University, Saint Petersburg, Russia*).

The authors declare no conflict of interests.

This is an open access article under the CC BY 4.0 license

ISSN 2411-3336; e-ISSN 2541-9404

JOURNAL OF MINING INSTITUTE

Zapiski Gornogo instituta

Journal homepage: pmi.spmi.ru

Research article

Industrial clusters as an organizational model for the development of Russia petrochemical industry

Tatyana V. Ponomarenko, Ilya G. Gorbatyuk✉, Aleksei E. Cherepovitsyn
Empress Catherine II Saint Petersburg Mining University, Saint Petersburg, Russia

***How to cite this article*:** Ponomarenko T.V., Gorbatyuk I.G., Cherepovitsyn A.E. Industrial clusters as an organizational model for the development of Russia petrochemical industry. Journal of Mining Institute. 2024. Vol. 270, p. 1024-1037.

Abstract
The article explores the challenges facing Russia petrochemical industry over the past decade and examines the reasons behind its significant lag compared to other industrialized nations. It presents a review of academic research on clusters accompanied by a comparative analysis, generalization, and consolidation of factors influencing the development of the petrochemical industry in Russia. It is argued that advancing the petrochemical industry from production plants to integrated production complexes necessitates a shift towards clustering, which will improve resource utilization efficiency, bolster product competitiveness, and reduce production costs. The article examines and consolidates key cluster concepts, encompassing definitions, characteristics, composition, and constituent elements. It also examines strategic documents guiding the development of the petrochemical sector, assesses the progress made in forming petrochemical clusters in Russia, and draws upon European and Asian experiences and government support tools in the domain of petrochemical clusters. The successful development of petrochemical clusters in Russia is argued to be strongly dependent on state initiatives and support for infrastructure development. Additionally, the presence of research organizations within clusters is crucial for fostering high-tech product innovation and forming an efficient value chain that integrates research and development with specific assets. When establishing petrochemical clusters in Russia, it is essential to consider the unique characteristics of each cluster, including the types of raw materials and resources used, the necessary infrastructure, and the specific support measures and incentives provided by the state.

Keywords
petrochemicals; cluster organization; oil and gas industry; infrastructure; specific assets; public-private partnership

Received: 18.01.2024 ***Accepted: 02.05.2024*** ***Online: 22.05.2024*** ***Published: 25.12.2024***

Introduction.

In the coming decades, the petrochemical industry is going to be a promising area for oil utilization globally due to several reasons.

• Due to the green agenda, the energy transition to renewable energy sources, and the growing interest in environmental issues witnessed in both developed and developing countries, the global demand for crude oil will decrease[1] [1, 2]. Despite these trends, the prospect of transitioning to a low-carbon economy in Russia remains vague due to the influence of geopolitical, economic, and social factors, coupled with the fact that the country has major hydrocarbon reserves.

• The oil consumption mix is expected to change towards an increase in the share of petrochemicals. By 2040, the projected growth in petrochemical demand could lead to a 75 % rise in global oil demand, reaching approximately 17 million barrels per day, and the share of petrochemicals may increase from 12.8 % in 2019 to 16.3 % [3, 4].

[1] Global Energy and Climate Model. URL: https://www.iea.org/reports/global-energy-and-climate-model (accessed 09.04.2024).

This is an open access article under the CC BY 4.0 license

• The demand for petrochemical products is growing rapidly, particularly due to increased plastic consumption in the fast-developing Asia-Pacific region[2]. Global petrochemical capacity is forecasted to increase by 40 %, from 2,200 million tons per year in 2020 to 3,100 million tons per year in 2030, mainly in Asia (India and China) due to the rising demand in oil- and gas-producing regions including the CIS, the Middle East, and North Africa [5, 6].

• Petrochemical products yield substantially higher profit margins compared to oil refining, where the margin stands at about 10 %. Processing ethane into basic petrochemical products, for instance, quadruples the value of the product, while LPG processing increases its value by a factor of 1.7[3].

It should be noted that the share of petrochemicals in Russia (2 % of GDP) lags behind industrialized countries, where it can reach up to 10 % [7]. In 2022, petrochemicals accounted for only 1.13 % of Russia's GDP[4], compared to 4.9 % in China[5]. While Russia has a significant number of explored and developed hydrocarbon fields and an abundance of resources, changes in the structure of oil markets and technological factors limit the development of the petrochemical industry. The latter include the following: low quality of produced petrochemicals and low processing rates (71.5 % in Russia compared to 96 % in the USA and 85 % in Europe) [8, 9]; lack of processes focused on improving product quality [10]; lack of up-to-date equipment at oil refineries due to high depreciation rates [11]; lack of oil recycling equipment [12]; limited knowledge intensity in petrochemical production; a lack of resource efficiency technologies in the context of industrial digitalization[6] [13].

Organizational and economic factors also limit the effective development of the petrochemical industry. They include the following: poorly developed infrastructure of the sector; imperfect integration mechanisms among economic entities and the state; high capital intensity and complex organization of modern petrochemical projects [14]; the need for special mechanisms for attracting financial resources and sharing risks [15]; insufficient government management of business coordination and cooperation in the petrochemical sector [16].

Throughout the 20th century, the evolution of Russia's petrochemical chemistry went through a series of distinct organizational stages. The industrial stage of production (1930-1960) witnessed the establishment of so-called combines, or organizational structures facilitating the production of key petrochemical products through sequential technological processes. This stage was characterized by localized production, abundant raw materials, and a local market for products [17].

The subsequent stage saw the emergence of large petrochemical complexes (1960-1980) as forms of territorial and industrial complexes. During this period, the product range broadened, fostering production and technological interconnections among companies and facilities that could be separated by large distances. Collaboration became important, marking a departure from the model within which companies operated individually. Integration became the focal point; i.e. previous stages were supplemented to produce end products. Emphasis was placed on economies of scale as a determinant factor governing production capacities and product mixes [17].

[2] Petrochemical industry in Russia: Opportunities for growth. URL: https://www.csr.ru/upload/iblock/d88/9vy10zbpvss8f0h8z31616dij5zab3s6.pdf (accessed 09.04.2024).

[3] Khalbashkeev A. Petrochemistry: Results of 2021 and forecasts for the future. URL: https://nprom.online/market/neftehimiya-itogi-2021-g-i-prognozy/ (accessed 09.04.2024).

[4] Petrochemical industry in Russia 2023: Development prospects, consequences of sanctions, major players. URL: https://delprof.ru/press-center/open-analytics/neftekhimicheskaya-otrasl-v-rossii-2023-perspektivy-razvitiya-posledstviya-sanktsiy-krupneyshie-igro/ (accessed 09.04.2024).

[5] Wei Chen. China Issued Policy to Stimulate Petrochemical Industry. URL: https://www.lexology.com/library/detail.aspx?g=dd65fc5e-02dd-4083-a359-c1018dd94ebe#:~:text=In%202022%2C%20the%20gross%20production,approximately%204.9%25%20of%20China's%20GDP (accessed 09.04.2024).

[6] CO_2 as a new raw material – becoming a jack of all trades. URL: https://www.covestro.com/en/sustainability/lighthouse-projects/co2-dreams (accessed 09.04.2024).

This is an open access article under the CC BY 4.0 license

In the planned economy era, the construction of large plants and production complexes was actively pursued, aligning with the objectives of sectoral governance. However, in the contemporary market landscape, the utilization of traditional organizational models imposes constraints on progress in the petrochemical sector for several reasons. Firstly, the majority of industry products are characterized by innovation and, in some instances, specialization, and they are often produced in limited quantities. This necessitates intensive research and development (R&D), along with the formulation and implementation of state-led mechanisms to stimulate innovation. Additionally, fostering collaboration mechanisms and industry networking becomes important. Secondly, the high capital intensity of infrastructure, coupled with the imperative to assess infrastructure costs in determining the efficiency of petrochemical production, underscores the necessity of exploring financing sources, with due consideration given to state involvement. Thirdly, an array of risks, encompassing market dynamics among others, necessitates devising mechanisms for risk-sharing between the state and businesses in novel, flexible organizational frameworks.

The national economy's need for the development of the petrochemical sector underscores the state's role in strategic planning, investment, and interaction with private businesses. Therefore, transforming large-scale planned production into cluster forms of organization, which are widely used globally but underdeveloped in Russia, will foster the growth and effective development of the Russian petrochemical industry.

The main goal of this study is to substantiate the use of a cluster form of organization in Russia's petrochemical industry for its successful development. The primary objectives are: identifying the features of the cluster form of industrial organization, including its characteristics, composition, interpretation, and elements; clarifying the definition of an industrial cluster in Russia's petrochemical sector; and analyzing the processes of creating and operating petrochemical clusters in Russia, considering international experience.

Literature review.

Industrial clustering traces its roots back to the late 19th century, originating from the works of A.Marshall [18]. Marshall conceptualized clusters as groups of private businesses within a value system of buyers and suppliers, included companies in related technologies and shared factor or product markets. Over time, this model evolved to encompass institutions, such as universities, government agencies, and public-private organizations.

Our analysis showed that conceptual approaches to the definition and interpretation of the term "cluster", formed over more than 100 years, can be summarized as follows:

• American school, which includes concepts emphasizing the territorial forms of enhancing industry competitiveness (A.Marshall [18], M.Porter [19], and M.Enright [20]);

• British school, which includes concepts focusing on value chains and taking into account interconnections between local clusters (T.J.Dunning [21], J.Humphrey, and H.Schmitz [22]);

• Russian school, which includes concepts focusing on the formation of territorial and industrial complexes and the application of systems analysis methods (N.N.Kolosovsky [23] and B.S.Dondokov [24]);

• Scandinavian school, which includes concepts supporting new forms of production organization, integrating training organizations within industrial districts and regional clusters (B.Lundvall [25] and B.Johnson [26]);

• Different concepts based on the dominance of regional goals and ideas, such as regional specialization (A.Smith [27] and D.Riccardo [28]), regional development (W.Laundhart, M.Weber [29], and A.Lösch [30]), and urbanization (S.Rosenfeld [31] etc.).

An analysis of a number of works by Russian researchers[7] [32-34] has shown that there is no single approach to defining the term "cluster". However, common elements of a cluster can be identified, which, according to Russian authors, include a single territory (proximity of objects), government bodies, manufacturing companies, educational institutions, research centers, and

[7] Pomitov S.A. Clusters: Characteristics and models. URL: http://ekportal.ru/page-id-1805.html (accessed 09.04.2024).

This is an open access article under the CC BY 4.0 license

infrastructure. Cluster elements are not homogeneous. For example, the location of objects is currently not fundamentally important for the cluster, since the advantages of the cluster are not necessarily associated with locational rent. Also, cluster participants can combine business processes in a common business model of the cluster. Cluster infrastructure, which refers to the assets that ensure the functioning of the cluster and its business processes, includes assets classified as specific within the institutional approach. For petrochemical clusters, such assets are product pipelines.

In order to improve the conceptual toolkit in the field of petrochemical clusters, the definition of a cluster should be supplemented with specific attributes (or elements) and methods of their interaction (or connections between them).

A synthesis of studies [35-37] shows that researchers focus on several factors associated with the emergence of business clusters:

• spatial community (J.Humphrey and H.Schmitz [22]), which is discussed using concepts and tools such as new economic geography, business activity analysis, regional studies, and innovation at the regional level;

• formation conditions (E.Bergman and E.Feser [35]), such as externalities, innovative environment, competition, cooperation, and flexibility of technological development;

• cluster composition by attributes (T.Andersson [36]), among which are geographic concentration, specialization, participant functions, cooperative competition, cluster life cycle, innovative nature, and critical mass;

• the purpose and method of cluster formation (I.Gordon and P.McCann [37]), with a focus on models of agglomeration, industrial complexes, and network interaction.

Factors constituting the first group, which focuses on geography, have limited significance for petrochemical clusters in Russia due to several reasons. They include considerable distances between material assets (hydrocarbon fields) and production facilities (refineries, gas processing plants, etc.), the need to establish an extensive interregional transport infrastructure spanning hundreds of kilometers is imperative, and the necessity to collaborate at the industry level within the domain of research and development.

Some studies [35] are relevant for petrochemical clusters as they consider the influence of the petrochemical industry on related industries involved in the production, sale, and use of petrochemicals. They also consider the innovative development of technologies for producing specialized small-tonnage products[8] and the cooperation and coordination related to knowledge exchange within the cluster.

Some studies [36] center on the composition of clusters and their critical mass as key factors. Notably, petrochemical clusters focus on establishing an effective value-added chain alongside gas (ethane, LPG) and oil (naphtha, straight-run gasoline) industries. Large-tonnage petrochemicals serve as the foundation for small-tonnage products, characterized by diverse items serving various industries and market segments. While large companies may not be inclined to diversify their product offerings due to the associated innovation costs[9,10], small and medium-sized businesses often take on this role. They are typically more technologically agile but may lack the investment resources for R&D.

In another study [37], network interaction within industrial structures emerges as an important cluster feature, particularly in the realm of information, competencies, and knowledge exchange. The connectivity of organizations within a cluster can be categorized as internal (within cluster organizations) and external (between cluster organizations and external entities)[11]. Internal connectivity significantly influences the formation of the value chain, underscoring its critical role in cluster dynamics.

[8] Order of the Government of the Russian Federation N 2834-r "On the Action Plan (Road Map) for the Development of the Production of Small-Scale Chemicals in the Russian Federation until 2030" of December 15, 2017.

[9] Niyakovskaya N. A large role of small-tonnage chemicals: Innovative products and solving large-scale production problems. URL: https://belchemoil.by/news/tehnologii-i-trendy/bolshoj-ves-malotonnazhnoj-himii (accessed 09.04.2024).

[10] Nikishova I. Important small-tonnage products. *Element*[22]. 2020. N 4 (116), p. 8-10.

[11] Kutsenko E. Cluster policy regulations: Current situation and prospects for improvement. Clusters Opening Borders, May 12-13, 2016, St. Petersburg, Russia. 2016. URL: https://cluster.hse.ru/mirror/pubs/share/216093211 (accessed 09.04.2024).

This is an open access article under the CC BY 4.0 license

Many clusters are shaped by local factors and resources provided in the region[12]. Many clusters are shaped by local factors and resources provided in the region. Although clusters do not develop automatically, regional factors influence the likelihood of cluster formation. For example, when forming industrial clusters in China, the Chinese Government determined which Chinese regions could produce greater benefits under existing conditions[13].

Our analysis has shown that prerequisites for industrial cluster formation can be divided into several groups:

• Geographic concentration: Clusters include only organizations located in close proximity to one another. Geographic concentration leads to several positive effects, which diminish as the distance between organizations increases. This feature helps distinguish clusters from cluster-like phenomena, such as networks of firms that do not qualify as clusters.

• Natural and environmental factors: These factors include conditions that are specific to a particular geographical area due to its natural and climatic characteristics and environment. They include the availability of natural resources, natural geographical features, the quality of the environment, and other parameters.

• Economic prerequisites: These involve the potential for creating and utilizing a unified value chain, which includes a common scope of activity, availability of skilled labor, cooperation between companies, industrial infrastructure, specialized suppliers, demand levels, potential consumers, developed capital market, and other resource factors. A cluster assumes a high density of connections between organizations within a particular field and with other entities (e.g., buyers, suppliers, including small and medium-sized ones, as well as scientific and educational institutions).

• Political prerequisites: These reflect government regulation, including the active participation of regional or federal authorities in developing and applying incentives for cluster creation.

• Cultural prerequisites: These include the attitudes of local residents and organization employees towards cooperation, partnership, interaction, and adaptability to new developments.

We believe that these factors are of a general kind; they are necessary but not sufficient for cluster formation and do not facilitate its identification. Across diverse industry clusters, these factors serve as a general framework with varying degrees of importance. The importance of a specific factor is contingent upon the cluster's emphasis on earning particular types of economic rent. Analyzing these factors is imperative to evaluate the overall conditions for cluster formation, and it necessitates customization for each specific cluster.

In addition to these prerequisites, several sufficient conditions are crucial for cluster creation: a critical mass of participants, possession of specific assets, and active engagement in innovations demonstrated by cluster participants [17, 38, 39].

The presence of a critical mass depends on the concentration level of economic entities in a particular area. In Russia, the uneven distribution of oil and gas assets across regions is significant. Key hydrocarbon fields are concentrated in the Yamal Autonomous Okrug and the Khanty-Mansi Autonomous Okrug while refining capacities are located closer to sales markets and infrastructure elements such as ports and railway stations.

Asset specificity, as explained by O.Williamson in transaction cost theory [38], indicates that some assets or resources possess unique characteristics that make them less suitable or more expensive for use in other settings or with other partners. This specificity may stem from technological

[12] Brenner T. The Evolution of Localised Industrial Clusters: Identifying the Processes of Self-Organisation. *Papers on Economics & Evolution*. 2000. N 11.

[13] China's chemical industry in 2019: A review. URL: https://ect-center.com/blog/chemistry-inchina-2019 (accessed 09.04.2024).

This is an open access article under the CC BY 4.0 license

features, cost structure, or other factors limiting their alternative uses. Asset specificity influences organizational decisions regarding production, transactions, and business management. Depending on the degree of specificity of assets, organizations can choose various forms of internal integration or external market transactions. In the Russian oil and gas sector, specific assets include pipelines between oil producers and refineries, as well as between refineries and petrochemical production facilities.

The innovative activity of cluster participants involves companies actively seeking development through innovations such as new technologies, organizational changes, and marketing approaches. A high level of innovation activity often requires independence in research and development or collaboration with the scientific and educational community. Conducting R&D by individual cluster participants may be ineffective due to unpredictable demand and small production volumes of finished products[14] [32].

Among Russian researchers studying petrochemical clusters, noteworthy contributions have been made by V.A.Kryukov, A.Yu.Bannikov, E.S.Kutsenko, V.V.Shmat, N.V.Smorodinskaya, and others. They focus their studies on exploring cluster theory, the nuances of regional and innovation-driven clusters, regulatory frameworks in cluster policy, and comparative analyses of Russian and international experiences in clustering.

While general conceptual frameworks for cluster formation have been established, further research is needed concerning petrochemical clusters. Specifically, there is a need to focus on the prerequisites for their formation and their differences from similar forms of collaboration, to study the composition of subjects involved, and to examine the interaction between petrochemical clusters and academic institutions and research centers to foster innovative technologies. Additionally, optimizing logistics and transportation processes within clusters to cut costs and improve efficiency, as well as studying government support mechanisms and fostering collaboration among small and medium-sized enterprises within clusters to enhance their development and competitiveness, warrant further investigation.

Results.

Our analysis of the scientific literature reveals that there is no universally accepted definition of a "cluster" or a consensus on its characteristics. However, we can identify a set of essential elements for forming a cluster: geographic proximity of participants, involvement of production companies, participation of research and educational organizations, engagement of public authorities, involvement of auxiliary organizations, technological and organizational linkages among cluster participants, logistics infrastructure accounting for specific assets, a unified strategic direction for all participants, and innovation-driven (knowledge-intensive) activities within the cluster.

The establishment of a petrochemical cluster in Russia is shaped by both conventional prerequisites (geographic, natural and environmental, economic, political, etc.) and specific ones, namely: the presence of a critical mass of participants, specific assets and infrastructure, and state-supported innovative activities of participants [17].

The projected petrochemical clusters in Russia are significantly influenced by previously implemented projects grounded in the concept of forming industrial complexes [17] within a planned economy. Contemporary strategic planning documents emphasize the need for a top-down approach, initiated by the government, for the creation and effective operation of petrochemical clusters[15] [40]. Modern petrochemistry encompasses both large-scale production in developing nations and small-scale production in developed countries. Small-scale petrochemicals necessitate intensive research and development efforts, along with market assessment for specialized products. This entails additional risks, which must be shared between the state and businesses. Notably, small-scale petrochemical production constitutes a unique asset, yielding distinct products.

[14] Meeting on the strategic development of the petrochemical industry. URL: http://www.kremlin.ru/events/president/news/64529 (accessed 09.04.2024).

[15] Decree of the Government of the Russian Federation N 779 "On Industrial Clusters and Specialized Organizations of Industrial Clusters" of July 31, 2015 (revised 28.09.2023).

This is an open access article under the CC BY 4.0 license

Considering these factors, the definition of an industrial cluster in the Russian petrochemical industry can be formulated as follows: an industrial cluster is an association of entities engaged in joint activities within the framework of state-business interaction. This includes industrial production companies, research organizations, and educational institutions utilizing specific assets and a unified infrastructure. Government bodies initiate the organization of the cluster, which aims to produce high-tech, specialized products with high added value.

The formation of an industrial cluster in the petrochemical industry involves the combination of several key elements:

• Shared territory: A fundamental characteristic of a cluster is the geographic proximity of participating entities, which fosters communication and interaction among them. One key characteristic[16] of oil and gas cluster development is that, despite the speed of technological progress and the dynamics of innovation, significant cost reductions and competitive advantages can be achieved through the close integration of interdependent production units and substantial reductions in logistics costs[17]. While early clusters were strictly limited territorially, modern clusters can span multiple cities and even regions [17].

• Research and educational organizations: The presence of educational institutions and scientific centers engaged in petrochemical research, development, and training is vital [17].

• Government bodies: Government entities play a crucial role in creating a favorable investment and legal environment. Their involvement ensures coordination and support for the industry's development [17].

• Manufacturing companies: The participation of manufacturing companies promotes resource sharing, technological collaboration, and innovation exchange. These interactions enhance competitiveness and improve production efficiency [28].

• Interconnection of participants: Network connections and interactions between cluster participants are necessary for knowledge, experience, and resource exchange. These collaborations foster integration and cooperation within the cluster [41-43].

• Developed production infrastructure: A well-established production infrastructure, including transport networks, energy systems, and communication facilities, is essential. Additionally, specific assets necessary for petrochemical industry operations and development are integral components of the production infrastructure [17].

• General focus: Clusters are based on shared strategic goals developed collaboratively by cluster participants. These goals encompass a comprehensive, knowledge-intensive value chain, beginning with hydrocarbon production and ending with the sale of finished goods [17].

To create and effectively develop a petrochemical cluster, state initiation and support measures are required.

To create and effectively develop a petrochemical cluster, state initiation and support measures are required. The creation and activities of petrochemical clusters in Russia are regulated by various regulatory legal documents, including laws, regulations, orders, and other kinds of documents, which are outlined in Table 1.

An analysis of legal documents in Russia has revealed that initially, the primary objective of implementing cluster policy was to ensure rapid economic growth and diversification by enhancing the competitiveness of businesses. This encompassed suppliers of equipment, components, production and service providers, as well as research and educational organizations forming territorial production clusters[18]. The underlying assumption was that cluster policy would foster business competitiveness internationally through innovative technologies. However, later priorities shifted towards import substitution, stimulating domestic market demand for end products of the petrochemical industry, and increasing industry revenue contributions to the national budget.

[16] Center for Cluster Development and Project Management of the Republic of Tatarstan. URL: https://innokam.ru/ (accessed 09.04.2024).

[17] Caspian cluster. URL: https://minprom.astrobl.ru/napravleniya-deyatelnosti/kaspiiskii-klaster (accessed 09.04.2024).

[18] Methodological recommendations for the implementation of cluster policy in the constituent entities of the Russian Federation (approved by the Ministry of Economic Development of the Russian Federation on December 26, 2008, N 20615-ak/d19).

This is an open access article under the CC BY 4.0 license

Table 1

Key documents regulating the creation and activities of petrochemical clusters in Russia

Title	Essence
Federal Law N 488-FZ On Industrial Policy in the Russian Federation" of December 31, 2014[19]	A definition of an industrial cluster is given; measures to stimulate cluster formation are proposed; the connection with the Spatial Development Strategy of the Russian Federation dated February 13, 2019 N 207-r (Article 20)[20] is emphasized
Decree of the Government of the Russian Federation N 779 "On Industrial Clusters and Specialized Organizations of Industrial Clusters" of July 31, 2015	Requirements are established for industrial clusters and specialized organizations within industrial clusters in order to apply federal-level incentive measures in industry
Order of the Ministry of Energy of Russia N 939 "On Approval of Methodological Recommendations on the Structure and Mechanisms of the Functioning of Petrochemical Clusters" of December 9, 2015[21]	The document contains fundamental concepts and gives recommendations on the structure and mechanisms of a successful petrochemical cluster
Order N 651/172 "On Approval of the Development Strategy of the Chemical and Petrochemical Sector until 2030" of April 8, 2014 (as amended on January 14, 2016)	The document contains a plan with the goal of establishing six clusters with large pyrolysis capacities in Western Siberia, Volga, Caspian, Eastern Siberia, Northwestern, and Far Eastern regions
Order of the Government of the Russian Federation N 2834-r "On the Action Plan (Road Map) for the Development of the Production of Small-Scale Chemicals in the Russian Federation until 2030" of December 15, 2017	The document is a set of measures to improve the mechanisms of government regulation of small-tonnage petrochemical production in Russia, which include cuts in imports, fostering domestic production of small-tonnage and medium-tonnage petrochemical products, and creating the conditions necessary for the production of small-tonnage petrochemicals capable of competing in the domestic and global markets
Action Plan (Road Map) for the Development of the Russian Petrochemical Sector until 2025[22]	This document shows the key development objectives for the petrochemical industry until 2025, which include the creation of petrochemical clusters in Russia's Arctic and Far East, the development of transport and logistics infrastructure, and the training of highly qualified professionals for the industry

The existing regulatory documents on cluster policy are of a methodological and recommendatory nature. Therefore, further specification is required, owing to the individual nature of clusters and the necessity for a comprehensive project assessment in petrochemical clusters. This approach enables the differentiation of government support measures, considering the unique conditions and prerequisites for the formation and development strategy of each specific cluster.

We have conducted an assessment of the present state and key outcomes of developing petrochemical clusters in Russian conditions, as outlined in strategic planning documents (Table 2).

The data presented in Table 2 yields the following insights:

While the West Siberian cluster is referred to as a petrochemical cluster, it currently does not produce petrochemical products and primarily operates as an oil industry cluster. Some experts even argue that it functions akin to a combine [17]. The Caspian petrochemical cluster does not fulfill the criteria of a petrochemical cluster either. It lacks a general strategic direction and the necessary elements, such as research and educational organizations that contribute to the creation of knowledge-intensive finished products. Moreover, it lacks a fully developed value chain for the production of end products derived from petrochemicals, effectively making it function as a special economic zone (SEZ).

[19] Federal Law N 488-FZ On Industrial Policy in the Russian Federation" of December 31, 2014 (revised 12.12.2023).

[20] Decree of the Government of the Russian Federation N 207-r "On the Spatial Development Strategy of the Russian Federation until 2025" of February 13, 2019.

[21] Order of the Ministry of Energy of Russia N 939 "On Approval of Methodological Recommendations on the Structure and Mechanisms of the Functioning of Petrochemical Clusters" of December 9, 2015.

[22] Decree of the Government of the Russian Federation N 1241-r "On Approval of the Action Plan (Road Map) for the Development of the Russian Petrochemical Sector until 2025" of May 16, 2023.

This is an open access article under the CC BY 4.0 license

Table 2

Clustering in the petrochemical sector: An analysis of the results

Name	Plans	Results
West Siberian petrochemical cluster	Processing raw materials such as NGL, naphtha, ethane, and LPG sourced from associated gas from oil fields and unstable gas condensate from gas condensate fields in the Khanty-Mansiysk Okrug and the Yamalo-Nenets Autonomous Okrug. Production was scheduled to commence in 2013. The cluster's focus lies on goods suitable for long-distance transportation, catering to the demands of petrochemical production in Russia. Polymer production is the top priority	On March 15, 2021, an agreement to establish the Oil Industry Cluster was signed between the Government of the Tyumen Region and the Oil and Gas Cluster Association. This cluster comprises six large companies, including Gazpromneft-Zapolyarye, Gazpromneft-Yamal, Sibneftemash, GMS Neftemash, SibBurMash, and Teplolux-Tyumen. Additionally, it includes seven medium-sized and six small businesses, along with a higher education institution (Tyumen Industrial University). Organizational support and technological infrastructure are provided by the West Siberian Innovation Center and the Infra-structure Development Agency of the Tyumen Region. The Tyumen regional government provides support to the cluster. The Petrochemical Cluster of the Tyumen Region Association is responsible for supplier selection, contractor management, and general coordination. In 2024, five companies are providing services and manufacturing products (oil services, polystyrene foam, metal structures, electrical equipment, and rolled metal). Another eight companies are producing equipment and components in the field of metal structures and oilfield equipment. Five companies are involved in the production of final products (electronics, oil and gas production, oilfield equipment, drilling rigs, engineering support)
Volga Region cluster	Petrochemical production units in Tatarstan, Bashkiria, Nizhny Novgorod, and Samara. Expanding existing capacities and establishing new facilities. Utilizing raw materials such as naphtha from oil refineries in Tatarstan and Bashkiria, ethane derived from natural gas processing in the Republic of Kazakhstan, and LPG from gas processing plants in Western Siberia. Petrochemical production. RusVinyl and Tolyattikauchuk, part of SIBUR Holding, are prominent PVC producers, producing between 330 and 500 tons annually[23]	The cluster lacks official information, documents, or a representative website, making it challenging to conclusively affirm its successful operation
Caspian cluster	Stavrolen plant, a natural gas conversion facility in the Stavropol Krai with Lukoil as the project initiator. The facility was aimed at processing local raw materials. Ethane and LPG were anticipated to be sourced from a gas processing plant handling associated gas from oil fields on the Caspian shelf, owned by Lukoil	In accordance with the Government of the Russian Federation's Decree N 1792 dated November 7, 2020 ("On the Creation of a Special Economic Zone (SEZ) and the Caspian Cluster on the Territory of the Astrakhan Region"), the Caspian cluster was integrated with the LOTOS industrial production zone to serve as a node for the International North–South Transport Corridor. The primary activities within the LOTOS special economic zone include shipbuilding, production of components, manufacturing of oil and gas equipment and components, and high-tech industrial production. Within the LOTOS, there are 14 registered residents, but only two are focused on petrochemical production: LNG-Lotos, a project for the construction of an LNG plant, and Golden Industries Group, a project for an integrated natural gas conversion facility[24]

[23] Gordin M.V. Development of specialized industrial parks on the basis of large companies. Forum "Cluster Policy – the basis of innovative development of the national economy", September 11-12, 2014, Samara, Russia.

[24] Decree of the Government of the Russian Federation N 1792 "On the Creation of a Special Economic Zone (SEZ) and the Caspian Cluster on the Territory of the Astrakhan Region" of November 7, 2020.

This is an open access article under the CC BY 4.0 license

End of Table 2

Name	Plans	Results
East Siberian cluster	The concept of this cluster, situated in the south of the Krasnoyarsk Territory and Irkutsk, is based on utilizing local raw materials, whose processing is impossible without solving the issue of helium utilization, as this element is abundant in the local deposits, and building gas pipelines for the sale of dry gas	This cluster remains in project
Far Eastern cluster	Located in Primorye, this cluster is intended to be based on the use of raw materials in the south of Yakutia. Helium utilization and storage, the use of resources from fields in Eastern Siberia, and the use of the East Siberia-Pacific Ocean (ESPO) pipeline are the issues that need to be addressed. The final products are expected to be consumed both in the domestic market and internationally. New facilities were planned for commissioning between 2020-2025	This cluster remains in project
North-Western cluster	The cluster was planned to be established on the basis of petrochemical facilities in the Baltic (SIBUR Holding with a potential partner's involvement) and completed by 2017. The cluster was supposed to be located on the coast, which improved sales logistics and naturally oriented it towards exports to the European Union. The launch of production was planned for the period 2017-2020	Currently, a natural gas conversion plant is being designed on the basis of the previously planned cluster, focusing on methanol, ammonia, and urea production. Phased construction is scheduled from 2024 to 2030[25]

Of the six petrochemical clusters outlined in strategic planning documents, only two are fully operational. Notably, the Caspian cluster primarily focuses on shipbuilding and the production of oil and gas equipment and components, rather than petrochemical products.

The challenges encountered in establishing petrochemical clusters in Russia underscore the importance of analyzing international experiences in implementing clusters within the petrochemical domain. Specifically, we examined the Flanders cluster in Belgium[26], the Upper Austria cluster in Austria[27], and the Jurong cluster in Singapore[28]. These clusters were chosen due to their similarity to the Kama industrial cluster. Our analysis encompassed aspects such as cluster composition, model, structure, and necessary infrastructure.

Flanders serves as an industrial hub, hosting approximately 70 % of all Belgian industry, with its chemical cluster being one of the world's largest petrochemical clusters. Global chemical companies such as BASF, Dow Chemical, Exxon Mobil, SABIC, Dupont, Total, Bayer, Sumitomo Chemical, Akzo Nobel, Air Liquide, Evonik, Lindel Group and others are headquartered there.

[25] Baltic Methanol facility at the Ust-Luga seaport. URL: https://baltmethanol.ru/ (accessed 09.04.2024).
[26] Flanders Cluster Program – Cluster pacts. URL: https://www.interregeurope.eu/good-practices/flanders-cluster-program-cluster-pacts (accessed 09.04.2024).
[27] Cluster und Kooperationen. URL: https://www.biz-up.at/kooperation/unserecluster (accessed 09.04.2024).
[28] Jurong Island Vision Zero. URL: https://www.tal.sg/wshc/about-us/jurong-island-vision-zero (accessed 09.04.2024).

This is an open access article under the CC BY 4.0 license

Jurong accommodates about a hundred leading oil, petrochemical, and chemical corporations. Key investors include BASF, Exxon Mobil, Dupont, Mitsui Chemicals, Shell, Singapore Petroleum, Sumitomo Chemical, and other companies.

In Upper Austria, major international companies are involved, including Solvay Vienna, Ticona, Borealis, Eaton, Sony DADC, KTMchemicals, Philips, TCGUNITECH, PipeLife, Delphi, Siemens, ENGEL, PIOVAN, EREMA, ABB, HAIDLMAIR, HASCO, and Meusburger. Cluster participants specialize in raw material production and supply, polymer processing, and tool manufacturing. The share of large businesses in the total number of participants is 17 %, and the share of small and medium-sized companies is 83 %.

High-tech products are created by involving research centers and specialized universities. For example, the Jurong cluster includes business and industrial parks, the Institute of Chemical and Engineering Sciences, the National University of Singapore, and private research centers. The experience of Belgium shows successful collaborations with the largest research centers and universities, including the Universities of Ghent and Antwerp and research centers run by companies including Total Petrochemicals Feluy, Dow Corning, Procter&Gamble, Solvay, Recticel, Agfa-Gevaert, etc. Antwerp hosts technical competence centers of BASF, Evonik-Degussa, and Bayer. The Austrian cluster actively cooperates with the Johannes Kepler University and with institutes of applied sciences. Research centers not only produce new developments but are also responsible for quality control of finished products, i.e., both research and development and engineering functions are performed.

Our analysis has shown that in terms of their model and structure, petrochemical clusters amalgamate transnational corporations with major international investors alongside national small and medium-sized businesses along a cohesive value chain. For example, the state-owned Jurong Town Corporation (JTC Corporation) is the owner of the Jurong cluster's land and infrastructure and the developer and manager of Singapore's industrial complexes and related services. JTC reports to the Ministry of Trade and Industry of Singapore.

Logistics infrastructure and knowledge exchange are fundamental to cluster success, facilitated by well-developed pipeline systems, storage terminals, and distribution platforms. Moreover, an active exchange of experience and knowledge between cluster participants is necessary, including international assistance and consulting, i.e. in the development of networks of various types.

The government provides active research support and uses measures to attract external investors. They take various forms, including flexible taxation standards, R&D subsidies, close interaction with universities, support for technology start-ups, etc.

Cluster initiatives typically receive funding from various sources, which involve a combination of public and private financing. Public financing is provided in the form of subsidies provided by municipal, regional, national, and European authorities, usually in varying proportions. For instance, in the case of the ChemCoast cluster in Germany, infrastructure projects were supported by the governments of Lower Saxony and Schleswig-Holstein, alongside major chemical corporations such as Bayer Material Science and Sasol Germany [44].

In contrast, the effective formation and development of petrochemical clusters in Russia necessitate the creation of transport pipeline infrastructure through Public-Private Partnerships (PPP), accelerate the development and implementation of innovations, expedited innovation cycles, especially in small-scale petrochemicals, and application of tools for state support of petrochemical clusters.

Conclusions.

Our analysis of cluster concepts revealed a lack of consensus among Russian and international researchers regarding the definition of a cluster and its elements. Definitions vary based on geographic concentration, type of cluster members, organizational forms, coordination conditions, government

This is an open access article under the CC BY 4.0 license

participation, and infrastructure availability. This article has broadened the concept of an industrial cluster in the petrochemical sector and identified cluster elements and characteristics.

The study examined prerequisites for the formation of a petrochemical cluster, including innovative activity, specific assets, and logistics infrastructure. Our analysis of Russia's petrochemical clusters showed that out of six planned clusters, only two are operational. However, these two do not focus on petrochemicals but have different objectives. This situation can be attributed to imperfect regulations governing the creation and management of petrochemical clusters in Russia, a vague definition of what a cluster consists of, and a shift in national priorities regarding the economy.

Our study of successful petrochemical clusters around the world underscores the importance of research organizations contributing to high-tech product development, as well as the integration of participants to form an effective value chain, incorporating R&D and specialized infrastructure, and the development of government support tools. It is argued that successful clustering in the petrochemical industry relies on state initiatives and support for logistics infrastructure.

Progress in Russia's petrochemical sector can be facilitated through the adoption of a cluster-based organizational framework, distinguished from other territorial and vertically integrated structures by its strategic orientation, participant-government interaction dynamics, utilization of specific assets, and knowledge-intensive production and products. Initiating the formation of petrochemical clusters in Russia should be a state-driven endeavor, with essential economic support entailing the construction of pipeline infrastructure for both large-scale and small-scale petrochemical production, predominantly facilitated through concession agreements.

The insights garnered from this study hold practical implications. For instance, the identified characteristics and the refined definition of petrochemical clusters can be recommended for informing adjustments to regulatory frameworks, such as the Federal Law N 488-FZ of December 31, 2014 ("On Industrial Policy in the Russian Federation"), the Decree of the Government of the Russian Federation N 779 of July 31, 2015 ("On Industrial Clusters and Specialized Organizations of Industrial Clusters"), as well as updated development strategies and methodological documents on the establishment of petrochemical clusters.

The refined concepts proposed by the authors, the prerequisites for cluster formation, and elements of a cluster discussed in the study are specific to petrochemical clusters in the Russian context. This is due to the historical features of the development of the petrochemical industry in Russia and the relevant regulatory framework (in comparison with the experience of the leading countries in the industry, there is no clear focus typical for petrochemical clusters), and the structure of petrochemical production. It is essential to acknowledge the individuality and uniqueness of each cluster, taking into account factors such as raw materials, resources, necessary infrastructure, government support measures, and government incentives.

REFERENCES

1. Nevskaya M.A., Raikhlin S.M., Vinogradova V.V. et al. A Study of Factors Affecting National Energy Efficiency. *Energies*. 2023. Vol. 16. Iss. (13). N 5170. DOI: 10.3390/en16135170

2. Dmitrieva D., Solovyova V. Russian Arctic Mineral Resources Sustainable Development in the Context of Energy Transition, ESG Agenda and Geopolitical Tensions. *Energies*. 2023. Vol. 16. Iss. 13. N 5145. DOI: 10.3390/en16135145

3. Radoushinsky D., Radushinskaya A., Khaykin M. Improving the quality of implementation of the container transportation project along the NSR based on the environmental and energy transition agenda. *Polar Science*. 2023. Vol. 35. N 100923. DOI: 10.1016/j.polar.2022.100923

4. Zvorykina Yu.V., Pavlova O.A. Green modernization and prospects for petrochemicals. *Neftegaz.RU*. 2021. N 1 (109), p. 64-69 (in Russian).

5. Skovgaard J., Finkill G., Bauer F. et al. Finance for fossils – The role of public financing in expanding petrochemicals. *Global Environmental Change*. 2023. Vol. 80. N 102657. DOI: 10.1016/j.gloenvcha.2023.102657

This is an open access article under the CC BY 4.0 license

6. Ślusarczyk B. Industry 4.0 – Are we ready? *Polish Journal of Management Studies*. 2018. Vol. 17. N 1, p. 232-248. DOI: 10.17512/pjms.2018.17.1.19

7. Derushkin D., Khazova T., Gatunok A. Petrochemicals: realities and challenges. *Energy Policy*. 2020. N 11 (153), p. 40-55 (in Russian).

8. AL-Saadi T., Cherepovitsyn A., Semenova T. Iraq Oil Industry Infrastructure Development in the Conditions of the Global Economy Turbulence. *Energies*. 2022. Vol. 15. Iss. 17. N 6239. DOI: 10.3390/en15176239

9. Shinkevich M.V., Barsegyan N.V. The role of business initiatives in improving production management at petrochemical facilities. *Herald of the Belgorod University of Cooperation, Economics and Law*. 2019. N 2 (75), p. 358-369 (in Russian).

10. Kirsanova N., Nevskaya M., Raikhlin S. Sustainable Development of Mining Regions in the Arctic Zone of the Russian Federation. *Sustainability*. 2024. Vol. 16. Iss. 5. N 2060. DOI: 10.3390/su16052060

11. Filatova I., Nikolaichuk L., Zakaev D., Ilin I. Public-Private Partnership as a Tool of Sustainable Development in the Oil-Refining Sector: Russian Case. *Sustainability*. 2021. Vol. 13. Iss. 9. N 5153. DOI: 10.3390/su13095153

12. Litvinenko V.S., Petrov E.I., Vasilevskaya D.V. et al. Assessment of the role of the state in the management of mineral resources. *Journal of Mining Institute*. 2023. Vol. 259, p. 95-111. DOI: 10.31897/PMI.2022.100

13. Zakaev D., Nikolaichuk L., Filatova I. Problems of Oil Refining Industry Development in Russia. *International Journal of Engineering Research and Technology*. 2020. Vol. 13. N 2, p. 267-270. DOI: 10.37624/IJERT/13.2.2020.267-270

14. Romasheva N., Dmitrieva D. Energy Resources Exploitation in the Russian Arctic: Challenges and Prospects for the Sustainable Development of the Ecosystem. *Energies*. 2021. Vol. 14. Iss. 24. N 8300. DOI: 10.3390/en14248300

15. Tsiglianu P., Romasheva N., Nenko A. Conceptual Management Framework for Oil and Gas Engineering Project Implementation. *Resources*. 2023. Vol. 12. Iss. 6. № 64. DOI: 10.3390/resources12060064

16. Tsyglianu P.P., Romasheva N.V., Fadeeva M.L., Petrov I.V. Engineering projects in the Russian fuel and energy complex: actual problems, factors and recommendations for development. *Ugol'*. 2023. N 3, p. 45-51 (in Russian). DOI: 10.18796/0041-5790-2023-3-45-51

17. Kryukov V.A., Shmat V.V. Russian Petrochemical Industry in Space and Time. *Studies on Russian Economic Development*. 2020. Vol. 31. N 6, p. 629-635. DOI: 10.1134/S1075700720060088

18. Marshall A. Principles of Economics. London: Macmillan and Co., 1890. Vol. I, p. 754.

19. Porter M.E. On Competition. Moscow: Williams Publishing House, 2005, p. 608 (in Russian).

20. Enright M.J. The Globalization of Competition and the Localization of Competitive Advantage: Policies towards Regional Clustering. The Globalization of Multinational Enterprise Activity and Economic Development. London: Palgrave Macmillan, 2000, p. 303-331.

21. Dunning J.H. Multinationals, Technology and Competitiveness. London: Unwin Human, 1988, p. 280.

22. Humphrey J., Schmitz H. Governance and Upgrading: Linking Industrial Cluster and Global Value Chain Research. Brighton: Institute of Development Studies, 2000. IDS Working Paper 120, p. 37.

23. Kolosovskii N.N. The theory of economic zoning. Moscow: Mysl, 1969, p. 336 (in Russian).

24. Dondokov B.S. TIC and clusters: similarities and differences. *Mining Informational and Analytical Bulletin*. 2015. N 1, p. 381-385 (in Russian).

25. Lundvall B.-Å. The Social Dimension of the Learning Economy. Aalborg: Aalborg University, 1996. DRUID Working Paper 96-1, p. 29.

26. Lundvall B., Johnson B. The Learning Economy. *Journal of Industry Studies*. 1994. Vol. 1. Iss. 2, p. 23-42.

27. Smith A. An Inquiry into the Nature and Causes of the Wealth of Nations. Moscow: Sotsekzgiz, 1962, p. 684 (in Russian).

28. Rikkardo D. Works. In 5 volumes. Vol. 1. Moscow: Gospolitizdat, 1955, p. 360.

29. Veber A. Theory of the Location of Industries. Moscow: Kniga, 1926, p. 223 (in Russian).

30. Lesh A. The Economics of Location. Moscow: Izd-vo inostrannoi literatury, 1959, p. 455 (in Russian).

31. Rosenfeld S.A. Bringing business clusters into the mainstream of economic development. *European Planning Studies*. 1997. Vol. 5. Iss. 1, p. 3-23. DOI: 10.1080/09654319708720381

32. Islankina E.A. Cluster approach in economics: Conceptual foundations, history and modernity. Scientific discussion: Issues of economics and management. A collection of articles based on the materials of the XXIII International Science-to-Practice Conference. Moscow: International Center for Science and Education, 2014. Vol. 2 (23), p. 23-30.

33. Shechtman A.Y. Problems of formation and development of cluster educations. *Vestnik of Volzhsky University after V.N. Tatischev*. 2014. N 2 (31), p. 60-67 (in Russian).

34. Bergman E.M., Feser E.J. Industrial and Regional Clusters: Concepts and Comparative Applications. Morgantown: West Virginia University, 2020, p. 93.

35. Braginskii O. Current state and development trends of the national and global petrochemical industry. Open seminar "Energy Economics", November, 25, 2014, Moscow, Rassia. Moscow: Izd-vo Instituta narodnokhozyaistvennogo prognozirovaniya RAN, 2014, p. 85 (in Russian).

36. Andersson T., Schwaag-Serger S., Sörvik J., Emily Wise Hansson. The Cluster Policies Whitebook. Malmö: International Organisation for Knowledge Economy and Enterprise Development, 2004, p. 266.

37. Gordon I.R., McCann P. Industrial Clusters: Complexes, Agglomeration and/or Social Networks? *Urban Studies*. 2000. Vol. 37. Iss. 3, p. 513-532.

38. Williamson O.E. The Economic Institutions of Capitalism. Firms, Markets, Relational Contracting. New York: The Free Press, 1985, p. 450.

39. Vasilieva Z.A., Likhacheva T.P., Moskvina A.V., Yarichina G.F. Network forms of interorganizational interaction: efficiency assessment. *Journal of Creative Economy*. 2016. Vol. 10. N 11, p. 1273-1286 (in Russian). DOI: 10.18334/ce.10.11.37023

40. Buruk A.F., Kotelkin D.D., Markov L.S. Cluster project: concepts, typology and modeling approaches. *World of Economics and Management*. 2017. Vol. 17. N 3, p. 132-142 (in Russian).

This is an open access article under the CC BY 4.0 license

41. Ganchenko D.N. Network interaction in the economy: Types and forms. *Theory and Practice of Scientific Research: Psychology, Pedagogics, Economy and Management*. 2019. N 4 (8), p. 114-126 (in Russian).

42. Pronyaeva L.I., Pavlova A.V. Development of the interorganizational management system in clusters. *Research Result. Social studies and humanities series*. 2016. Vol. 2. N 1 (7), p. 19-26 (in Russian).

43. Stepnov I.M., Kovalchuk J.A., Gorchakova E.A. On Assessing the Efficiency of Intracluster Interaction for Industrial Enterprises. *Studies on Russian Economic Development*. 2019. Vol. 30. Iss. 3. P. 346-354. DOI: 10.1134/S107570071903016X

44. Bannikov A.Yu. Clusters as a new form of territorial organization of the chemical industry in Germany: A Candidate of Science dissertation thesis. Moscow: Moscow State University, 2015, p. 24.

Authors: **Tatyana V. Ponomarenko,** *Doctor of Economics, Professor,* *https://orcid.org/0000-0001-5047-2880* *(Empress Catherine II Saint Petersburg Mining University, Saint Petersburg, Russia),* **Ilya G. Gorbatyuk,** *Postgraduate Student, gorbatyukig@mail.ru,* *https://orcid.org/0000-0001-7784-2773* *(Empress Catherine II Saint Petersburg Mining University, Saint Petersburg, Russia),* **Aleksei E. Cherepovitsyn,** *Doctor of Economics, Professor,* *https://orcid.org/0000-0003-0472-026X* *(Empress Catherine II Saint Petersburg Mining University, Saint Petersburg, Russia).*

The authors declare no conflict of interests.

This is an open access article under the CC BY 4.0 license

ISSN 2411-3336; e-ISSN 2541-9404

JOURNAL OF MINING INSTITUTE

Zapiski Gornogo instituta

Journal homepage: pmi.spmi.ru

Research article

Development and validation of an approach to the environmental and economic assessment of decarbonization projects in the oil and gas sector

Nadezhda A. Sheveleva

Luzin Institute for Economic Studies of the Kola Science Centre of the RAS, Apatity, Russia

Gubkin Russian State University of Oil and Gas, Moscow, Russia

***How to cite this article*:** Sheveleva N.A. Development and validation of an approach to the environmental and economic assessment of decarbonization projects in the oil and gas sector. Journal of Mining Institute. 2024. Vol. 270, p. 1038-1055.

Abstract

This article addresses the problem of selecting a priority decarbonization project for an oil and gas company aiming to reduce greenhouse gas emissions. The wide range of decarbonization options and assessment methods prompted the development of a comprehensive ranking system for project selection. This system incorporates both internal and external factors of project implementation, a two-stage algorithm that filters out unsuitable projects taking into account sustainable development goals, and a quantitative evaluation approach using absolute and relative indicators. The proposed system evaluates decarbonization projects by considering not only the reduction of emissions in both absolute and relative terms, but also the broader environmental, social, and economic aspects relevant to the oil and gas company and the national economy. It includes a ranking mechanism for identifying priority projects and integrates carbon regulation incentives and green taxonomy tools into the economic assessment for more precise comparative analysis. The quantitative assessment in absolute terms involves a specialized net present value calculation, which accounts for revenue from both carbon credit sales and the potential sale of new low-carbon products, if applicable. The proposed assessment provides for targeted analysis of specific performance indicators, such as the cost per unit of emissions reduced, tax and social security contributions per unit of emissions reduced, energy efficiency improvements, and other indicators used for additional assessments of projects under otherwise equal conditions.

Keywords

oil and gas sector; carbon neutrality; carbon regulation; low-carbon development strategy; decarbonization projects; climate project; environmental and economic assessment; project ranking

Funding

This study was supported by a grant from the Russian Science Foundation (Project N 22-78-10181 “Decarbonization of the Russian Oil and Gas Sector: Concept, New Interfaces, Challenges, Technological, Organizational, and Managerial Transformations”).

Received: 15.11.2023 ***Accepted: 24.09.2024*** ***Online: 04.10.2024*** ***Published: 25.12.2024***

Introduction.

The sustainable development of oil and gas companies can be achieved through the adoption of low-carbon strategies that aim to minimize their impact on the climate and environment while maintaining economic and business operations. Many companies have set ambitious long-term goals, targeting reductions in specific greenhouse gas (GHG) emissions and product carbon footprints by 2050 [1], alongside intermediate goals for 2030 [2]. These carbon neutrality goals involve implementing measures to reduce both absolute and specific GHG emissions within a defined time frame, spanning from a baseline year to a target year. The most common approaches to achieving both long-term and intermediate carbon neutrality targets include pursuing various decarbonization strategies, such as climate action projects.

This is an open access article under the CC BY 4.0 license

Since the term "climate action project" can have multiple interpretations and is associated with different criteria, this study adopts a broader definition, namely that of a decarbonization project. Such a project is defined as one or more activities designed to reduce or prevent GHG emissions and/or increase carbon capture within the operational boundaries of an oil and gas company. Given the diversity of decarbonization pathways [3-5], a key challenge for oil and gas companies committed to low-carbon development is determining the most optimal decarbonization projects. Companies often set additional global goals and face constraints when striving for carbon neutrality, such as ensuring positive net present value for decarbonization projects, maximizing carbon credits upon project completion, and leveraging green financing to support sustainable development initiatives[1]. This means that they need to assess not only the emissions reduction potential of decarbonization projects but also their broader environmental, economic, and social effects.

Previous studies addressing project assessments in the oil and gas sector incorporate elements of multi-factor assessment models considering environmental, social, and economic aspects in the implementation of investment projects [6]. Some studies have also proposed synchronizing these models with the project life cycle in the course of their practical application [7, 8]. Additionally, environmental and economic assessments of corporate operations and projects have been proposed, using indicator groups related to production, environmental protection, and environmental economic activities [9]. In other studies, terms such as "strategic environmental assessment" are used to refer to evaluating the potential environmental and socio-environmental impacts of strategic decisions, such as regional or sectoral development plans [10]. Similarly, "environmental and economic assessment" is intended to support technical and economic decision-making by incorporating environmental considerations alongside technological and economic factors [11, 12]. However, comprehensive environmental and economic assessments specific to decarbonization projects have received limited attention in the academic literature.

The purpose of this study is to develop a methodology for the environmental and economic assessment of decarbonization projects within oil and gas companies. The main objectives are to address the following research questions: What indicators should shape the foundation of the assessment system for decarbonization projects in the oil and gas sector? How should these projects be ranked to identify those with the highest priority?

Methods.

An algorithm has been developed for assessing decarbonization projects in the oil and gas sector, accounting for both internal and external factors. The algorithm follows a deductive approach, where the conditions for implementing the decarbonization project are progressively clarified, and additional parameters with indirect impacts are evaluated as the process unfolds. The comparative assessment of these projects, used for ranking, takes into consideration their environmental, social, and economic benefits not only for the company itself but also for the region and national economy.

The concept of climate efficiency is introduced to measure the effectiveness of actions aimed at reducing and/or preventing greenhouse gas emissions or increasing their capture, expressed in specific quantitative terms. This concept is enhanced by incorporating sustainable development factors, including economic efficiency and the minimization of negative environmental impacts.

The research acknowledges the role of feasibility studies as key tools for investment decision-making. Since their results have a major influence on the ranking of decarbonization projects, they are considered along with the project's contribution to achieving carbon neutrality targets.

[1] Resolution of the Government of the Russian Federation of September 21, 2021, N 1587 "On Approval of the Criteria for Sustainable (Including Green) Development Projects and the Verification System Requirements for Sustainable Development Projects in the Russian Federation".

This is an open access article under the CC BY 4.0 license

The approach to the quantitative assessment of the economic efficiency of decarbonization projects is based on net present value and its components. However, it is refined by accounting for the specific aspects of decarbonization project implementation. These include the use of green taxonomy incentives and carbon trading mechanisms [13-16], as well as penalties for exceeding GHG emissions quotas [17]. Additional environmental impacts and other factors affecting the project's cash flow, both positive and negative, are also considered.

The development of the algorithm and indicators is based on the following assumptions:

• The decision-making process for selecting a decarbonization project follows the principle of maximizing emission reduction while ensuring that negative social, environmental, and economic impacts remain within acceptable limits. A decarbonization project could potentially lead to environmental degradation and/or an increase in negative effects, which should be considered during project selection.

• To prevent the deterioration of environmental indicators beyond the scope of the project, additional sustainable development criteria are introduced to safeguard against the decline in indirect parameters.

• Since the social impact is challenging to quantify, this study uses financial indicators such as contributions to insurance and pension funds, healthcare costs, and employee wages associated with project implementation. The analysis of the social significance of a project focuses solely on parameters that can be measured through financial data. Consequently, indicators such as the Human Development Index, changes in quality of life, and health-related impacts (e.g., morbidity), which can also be affected by decarbonization projects, are excluded due to the difficulty in applying a universal and objective comparative assessment. However, these factors are expressed in monetary terms to reflect the project's contribution to social development.

• The quantitative absolute indicators used for assessing decarbonization projects are based on traditional approaches to conducting feasibility studies aimed at analyzing investment projects, with the added consideration of environmental and economic aspects.

• The methodology does not impose restrictions on investment volumes or project timelines.

This study proposes a five-stage process for the selection, assessment, and ranking of potential decarbonization projects:

Stage 1 involves the preliminary selection of decarbonization projects. This includes eliminating those that cannot be implemented due to non-compliance with strategic planning documents or conflicts with stated objectives. At this stage, the feasibility of the decarbonization project is assessed.

Stage 2 assesses the remaining projects for economic, environmental, and climate efficiency. In this study, environmental efficiency encompasses aspects of the natural environment, such as air, water, and soil pollution, while climate-related issues are treated as a separate category. At this stage, the project's contribution to GHG emissions reduction is evaluated, ensuring alignment with sustainable development criteria.

Stage 3 deals with a qualitative assessment of the project's contribution to decarbonization and sustainable development goals. The project is evaluated based on its adherence to priority criteria, with the accumulated total used for comparison.

Stage 4 involves a quantitative assessment of the project's environmental, climate, and investment efficiency for the company implementing the project. Additionally, the socio-economic impact of the project on national and regional economies is considered.

This is an open access article under the CC BY 4.0 license

Stage 5 is dedicated to the comparative analysis of the priority project's specific indicators against those of other decarbonization projects, including projects undertaken by other companies.

The primary research methods employed in this study are decomposition, classification, and strategic analysis, drawing on current practical materials related to the topic.

Discussion.

Decarbonization efforts encompass a broad array of methods and tools [3-5, 15]. The climate efficiency of each decarbonization strategy can be evaluated within the context of a specific industrial process, company, or segment of the oil and gas industry. For instance, targeted measures such as reducing methane leaks or curbing the flaring of associated petroleum gas can be implemented, alongside broader strategies that include improving energy efficiency, increasing the share of renewable energy in energy consumption, or carbon sequestration [18, 19].

However, the outcomes of a decarbonization project can vary significantly depending on factors such as production scale, regional, geographical, and climatic conditions, and the characteristics of the oil and gas segment in which it is applied. The same project may yield different results depending on the internal and external environments of the company. The external environment includes factors beyond the company's control, while internal factors consist of those within the company's direct management and control. Identifying and qualitatively assessing these factors helps categorize decarbonization strategies suitable for a company (Fig.1).

External factors can set the direction for decarbonization, while internal factors serve as the mechanisms through which it is implemented. For example, in response to rising demand for low-carbon raw materials, a company might increase the share of low-carbon components in its products to meet consumer needs and expectations. By managing internal factors, a company can reduce emissions across different scopes[2]. To lower the carbon footprint of products, a company might select materials, services, equipment, and suppliers that produce fewer GHG emissions, thereby reducing scope 3 emissions[3] [20]. To cut indirect energy emissions in scope 2, the company might explore local climatic advantages for using low-carbon, renewable energy sources[4]. Reducing other indirect emissions in Scope 3 could involve optimizing supply chain logistics to favor local consumers and minimize transportation emissions. By combining various internal and external factors, a company can develop a tailored decarbonization strategy and prioritize its projects accordingly.

Ranking decarbonization projects and determining their priority in the oil and gas industry is a complex problem, which is solved based on economic efficiency assessments [21]. Decarbonization projects, which focus on reducing, preventing, or capturing GHG emissions, can have varying degrees of impact on the natural environment, social well-being, and the economy [22]. Thus, a comprehensive assessment of these projects is essential [23, 24]. The ranking process is further complicated by the fact that it extends beyond mere compliance with legal regulations and does not solely focus on technical and economic indicators such as projected carbon pricing. Strategic decision-making must consider a broad range of factors, including principles of sustainable development that integrate environmental, financial, climatic, and social aspects [25-28].

[2] A Corporate Accounting and Reporting Standard. URL: https://ghgprotocol.org/sites/default/files/standards/ghg-protocol-revised.pdf (accessed 15.11.2023).

[3] Technical Guidance for Calculating Scope 3 Emissions (version 1.0). Supplement to the Corporate Value Chain (Scope 3) Accounting & Reporting Standard. URL: https://ghgprotocol.org/sites/default/files/standards/Scope3_Calculation_Guidance_0.pdf (accessed 15.11.2023).

[4] Order of the Ministry of Natural Resources and Environment of the Russian Federation of June 29, 2017, N 330 "On Approval of Methodological Guidelines for the Quantitative Determination of the Volume of Indirect Energy-Related Emissions of Greenhouse Gases".

This is an open access article under the CC BY 4.0 license

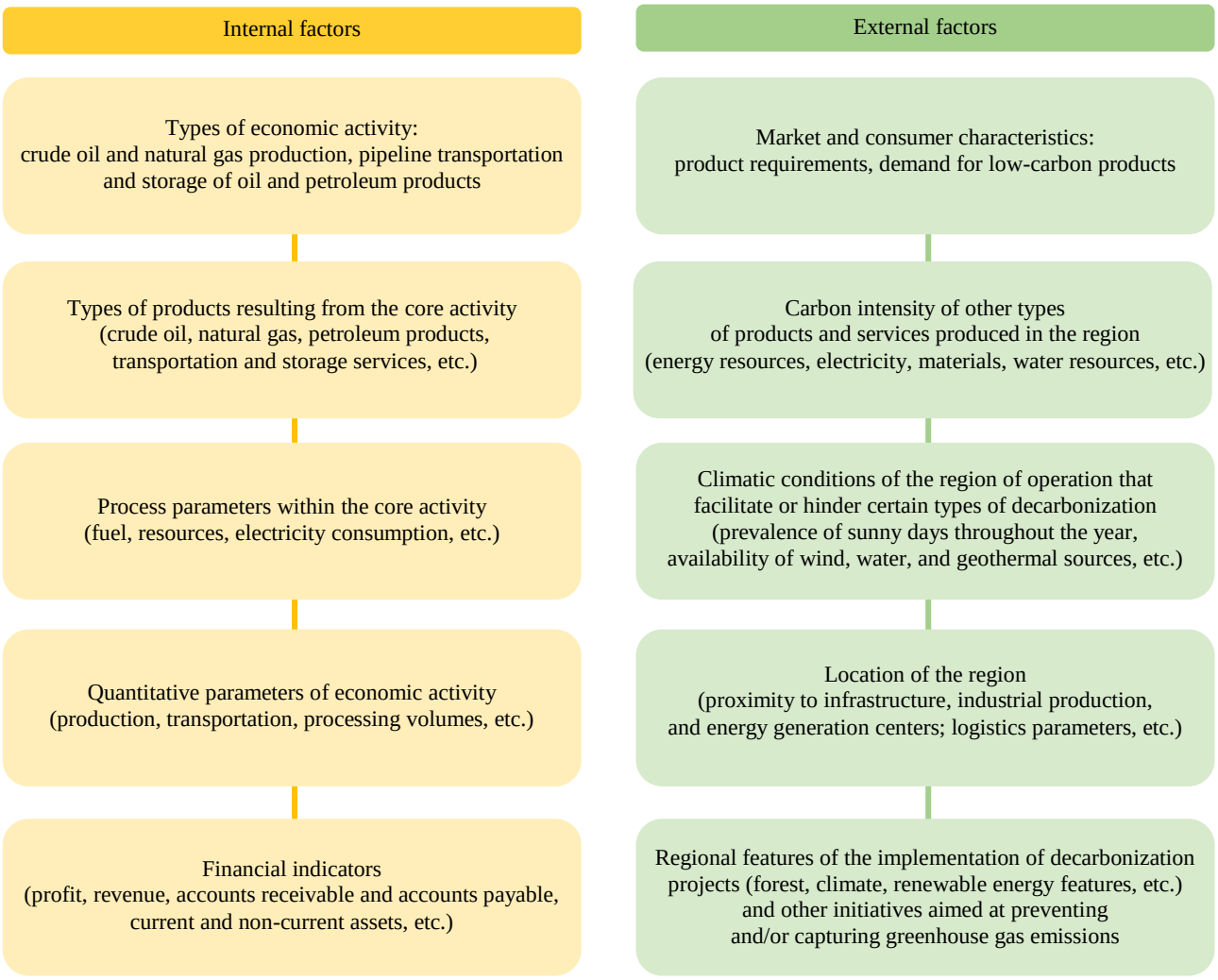

Fig.1. Factors influencing the choice of a decarbonization path
RES – renewable energy sources

In line with the concept of sustainable development, which evaluates projects not only in terms of achieving the UN's Sustainable Development Goal N 13 (Climate Action) but also with respect to other goals such as resource efficiency, air and water quality preservation, employment, and innovation[5], it is essential to conduct a step-by-step, multi-criteria assessment of decarbonization projects. This approach helps identify projects that meet the maximum number of sustainable development goals while remaining economically viable for the oil and gas company [29].

The key indicator for determining high-priority projects is the simultaneous fulfillment of the conditions outlined in Fig.2. Projects that meet only one or two conditions are considered lower priority.

From a sustainable development perspective, the fundamental criteria for ranking decarbonization projects include the reduction and/or prevention of greenhouse gas emissions and/or an increase in carbon capture, the minimization of negative environmental impacts [30], and the maximization of resource, heat, material, and energy savings. Additionally, projects that reduce operational costs and maximize positive net present value hold higher priority [31].

[5] Sustainable Development Goals. URL: https://www.un.org/sustainabledevelopment/ru/sustainable-development-goals/ (accessed 15.11.2023).

This is an open access article under the CC BY 4.0 license

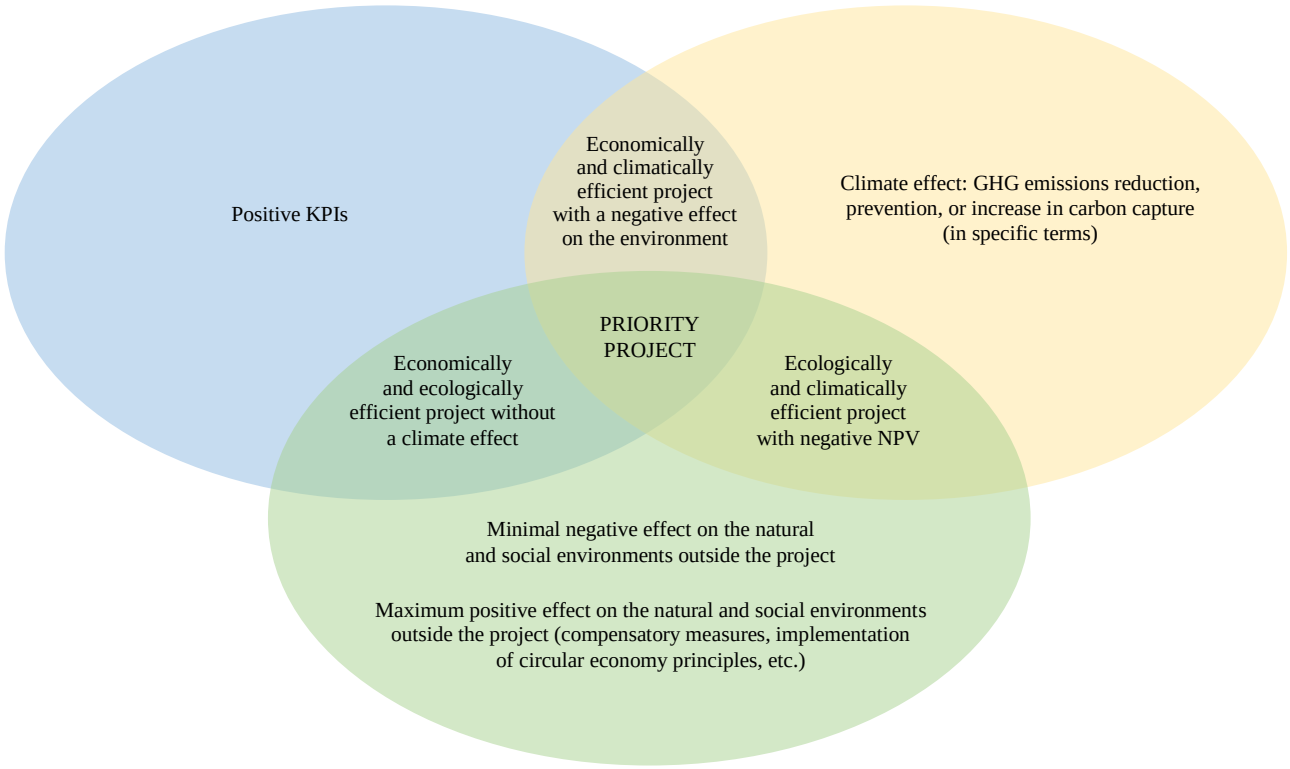

Fig.2. Conditions for prioritizing a decarbonization project

NPV – net present value

Oil and gas companies' strategic planning documents may include various targets that limit the feasibility of certain decarbonization methods:

• increasing hydrocarbon production or introducing high-carbon products (e.g., bitumen);

• expanding operations in regions or countries where low-carbon development principles have not been integrated into local production activities.

Due to this, stage 1 of the decarbonization project assessment process involves comparing the project's decarbonization approach with the company's general policy, goals, and strategy. This step also checks the project's potential effectiveness (Fig.3).

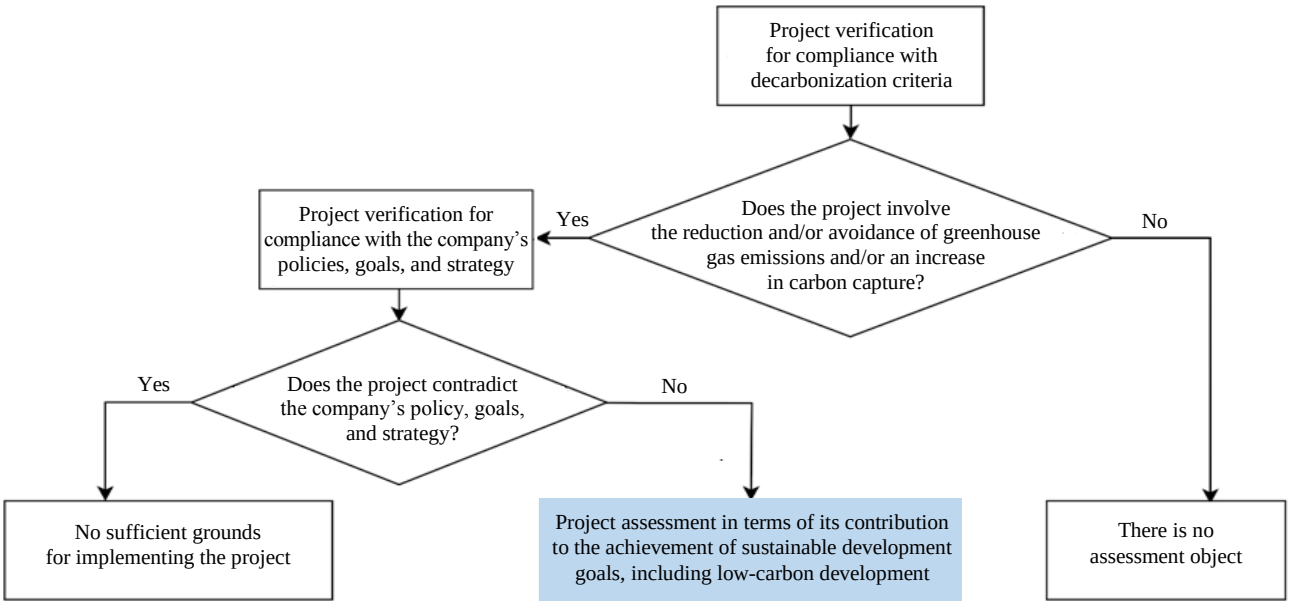

Fig.3. Stage 1 – Preliminary selection of decarbonization projects, feasibility assessment

This is an open access article under the CC BY 4.0 license

Journal of Mining Institute. 2024. Vol. 270. P. 1038-1055
© Nadezhda A. Sheveleva, 2024

Guided by stage 1 of the process of selecting, assessing, and ranking decarbonization projects (Fig.3), after excluding projects that fail to reduce greenhouse gas emissions, either in absolute or specific terms, and that conflict with the company's strategic planning documents, the process moves to stage 2, which includes a qualitative assessment of the project's alignment with environmental, social, climate, and economic efficiency criteria [32, 33], as well as its adherence to the principles of sustainable development (Fig.4).

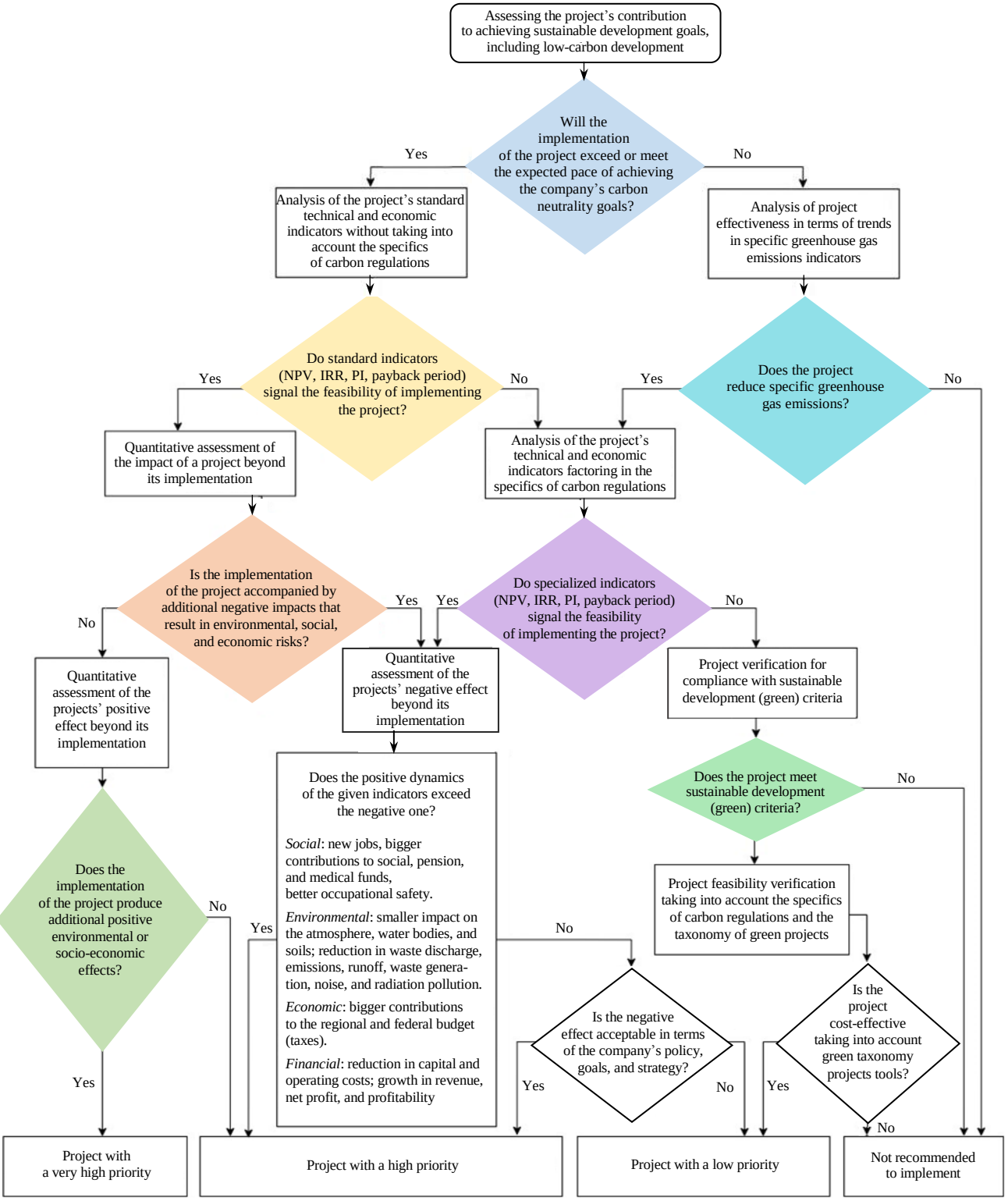

Fig.4. Stage 2 – Project assessment based on the criteria of economic, environmental, and social efficiency, and sustainable development principles

IRR – internal rate of return; PI – profitability index

This is an open access article under the CC BY 4.0 license

At stage 2, several projects may pass the criteria, making it necessary to rank and compare them. Stage 3 involves a quantitative assessment of how well each project meets these criteria. Figure 5 illustrates the principle of incrementally adding value to projects based on how well they align with the priority criteria. Each subsequent criterion, ranked higher than the previous one, is evaluated on the condition that the lower criterion has been met. The priority of a project increases with the difficulty of meeting these criteria: point 1 represents the most challenging but highest-priority condition, while point 8 is the easiest to fulfill, though it does not guarantee high priority.

It is important to distinguish between points 2 and 6 of the quantitative assessment (Fig.5). This study proposes two approaches to conducting a feasibility study: the standard approach (point 2) and a specialized approach (point 6). The standard approach follows traditional methods of financial analysis, using tools such as NPV, PI, IRR, and payback period. In this case, the project's cash flow is calculated without factoring in low-carbon regulation mechanisms, answering the question of whether the decarbonization project is economically viable on its own.

Projects with positive results from the standard assessment – without considering carbon regulation tools – are generally more attractive (point 2) than those relying on specialized tools (point 6). This is because these projects reduce operational costs, increase production efficiency with the same or lower GHG emissions, and thus show a lower carbon footprint. Examples include energy efficiency improvements [34], higher durability of equipment, better utilization of raw materials, reduction in hydrocarbon leaks, and prevention of emergencies resulting in major damage and hydrocarbon losses. However, decarbonization projects often do not exhibit high economic efficiency by traditional measures, which is why carbon management tools (e.g., carbon credits or penalties for exceeding GHG quotas) were introduced to boost their attractiveness.

The order of criteria for assessing decarbonization projects is as follows. Since reducing production volumes does not qualify as either a climate project or a decarbonization project, the first criterion focuses on reducing specific rather than absolute emissions [35]. The second criterion assesses absolute emissions, but instead of comparing emissions before and after project implementation, which would limit the increase in the scale of production activities, the comparison is based on "without the project" versus "with the project" scenarios [36], aligning with climate standards such as ISO 14064-2, Gold Standard, Global Carbon Council, and Verra, etc.

Next, a specialized economic assessment is conducted to encourage companies to undertake decarbonization projects. If the project shows positive economic indicators, compliance with national sustainable development regulations is added as a broader criterion. At this stage, the project is evaluated against the best available technologies (BAT) to ensure that it does not exceed legal limits, though these are less strict than the subsequent criterion, namely minimal negative impact on other social and environmental spheres (water bodies, soil, air, biodiversity) or the absence of such impact.

A more complex condition follows: the project must positively impact operational indicators, such as reducing operating costs. Finally, technical and economic indicators are considered without the use of support measures for GHG reduction. If the project is economically viable without such incentives, it is highly prioritized (point 2). If a project fulfills all of these criteria and significantly reduces emissions, it achieves the highest priority (point 1). The threshold for significance is determined by the company and may be based on meeting or exceeding average annual GHG reduction targets, or achieving/exceeding the expected target by a specific year.

This is an open access article under the CC BY 4.0 license

This is an open access article under the CC BY 4.0 license

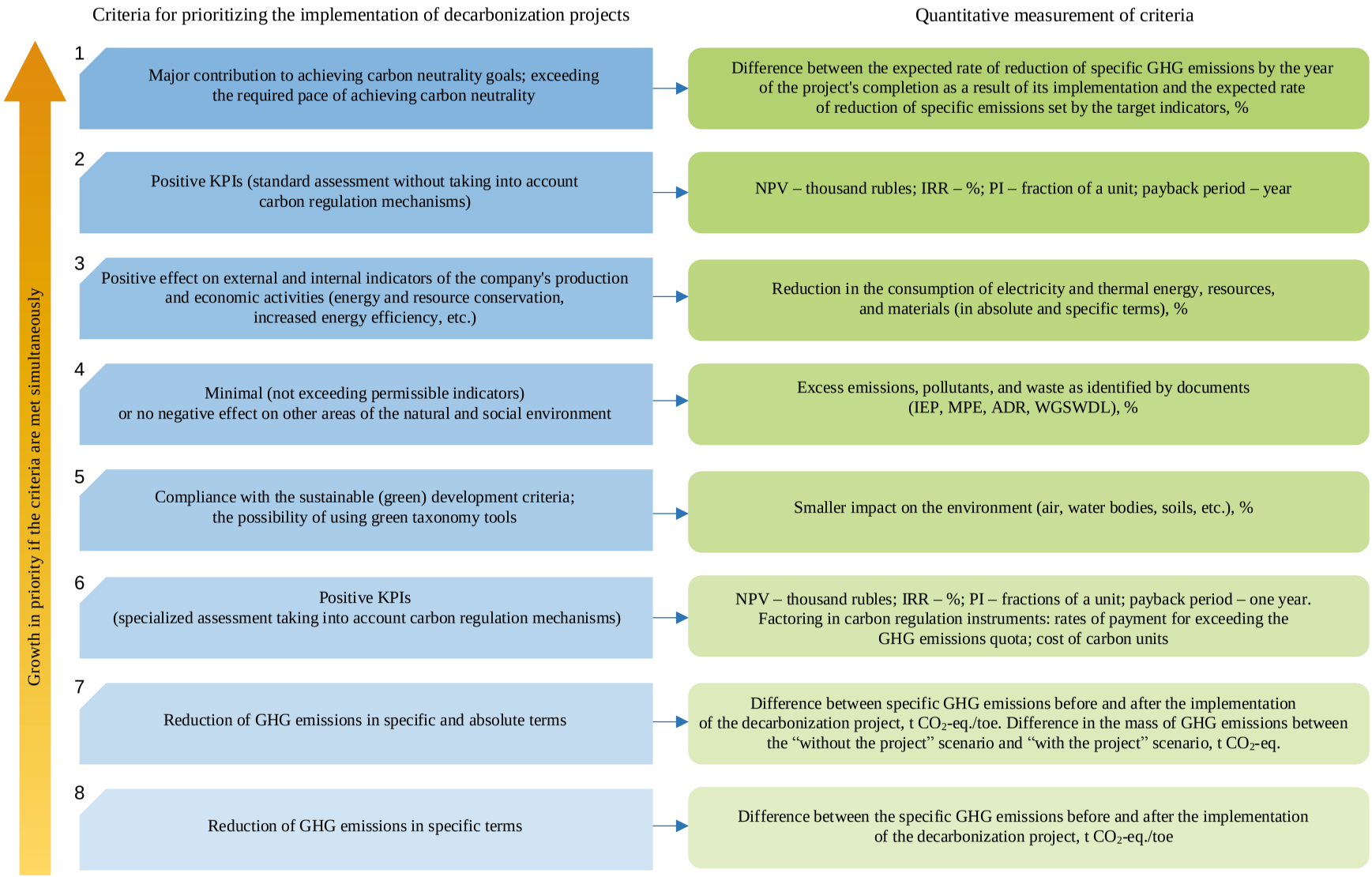

Fig.5. Stage 3 – Quantitative assessment of the project's compliance with the criteria using the principle of incremental priority

IEP – integrated environmental permit; MPE – maximum permissible emissions; ADR – allowable discharge rates; WGSWDL – waste generation standards and waste disposal limits

For instance, if a project reduces both absolute and specific emissions but fails to show positive results in the economic assessment, even with carbon regulation mechanisms, it would be assigned priority level 7. Alternatively, if the project aligns with sustainable development criteria (point 5) but fails to minimize negative environmental impacts (e.g., due to generating a large volume of new waste during equipment maintenance), it would not qualify for priority level 4.

The possibility of advancing through priority levels is determined by the measurability of assessment results based on the indicators outlined in the diagram section covering the quantitative measurement of criteria. At this stage, it becomes clear to what extent the decarbonization project will help the company meet or exceed its carbon neutrality targets, or whether only a marginal reduction in specific GHG emissions can be expected. If a project focuses solely on reducing absolute GHG emissions, it is assigned a lower priority because its effectiveness is dependent on production volumes and asset sales. This approach, according to national legislation, does not qualify as a climate project or a valid emissions reduction method.

In conducting the environmental, economic, and climate assessments, a comprehensive system of indicators is proposed. These indicators reflect the project's impact on various environmental elements (such as pollutant emissions, wastewater discharge, and water resource usage), the social environment (including changes in staff numbers, pension contributions, medical and insurance payments), and contributions to regional and federal tax revenues.

There are numerous approaches to defining the stages of investment projects. Depending on the research objectives, stages can be categorized as pre-investment, investment, operational, or decommissioning. For the purposes of this study, the first two stages are combined due to the absence of a detailed investment analysis. The decarbonization projects are assessed through three stages:

• pre-operational (design, equipment procurement and installation, construction, dismantling, reconstruction, and upgrading);

• operational (the use of equipment and technologies aimed at reducing GHG emissions);

• post-operational (equipment dismantling and land reclamation if necessary due to the end of the lifecycle).

This study focuses exclusively on the operational stage, as it directly relates to the project's impact on scope 1 and scope 2 emissions. The pre-operational and post-operational stages, which are associated with scope 3 emissions, are not included in the analysis because no national-level methodological guidelines are available for these stages. However, for net present value calculations, the capital expenditures of the pre-operational stage are included, as they are necessary for such assessments. The absolute indicators related to the operational stage of decarbonization projects are presented in Table 1.

Decision-making regarding the implementation of investment projects primarily relies on their technical and economic indicators [37, 38]. Consequently, this assessment is conducted at the next stage.

At stage 4 of the selection, assessment, and ranking of decarbonization projects, it is proposed to identify absolute indicators that reflect the impact of the decarbonization project both within the company and at the national level. These indicators are expressed in physical and monetary terms (see Table 1). Lines 1-7 present indicators related to the impact of the decarbonization project on the company, with Lines 1-5 focusing on the project's cost aspects and Lines 6-7 addressing revenue aspects. Lines 8-9 reflect the project's influence on the national economy and the social sphere.

This is an open access article under the CC BY 4.0 license

Journal of Mining Institute. 2024. Vol. 270. P. 1038-1055
© Nadezhda A. Sheveleva, 2024

Table 1

Stage 4 – A system for quantitative climate, environmental, and economic assessment of decarbonization projects using absolute indicators

N	Decarbonization project parameter	Physical aspect	Value, thousand rubles
1	Energy consumption, MWh, Gcal	Volume of electricity and thermal energy consumption	Electricity and thermal energy costs
2	Resource consumption, m^3, t	Volume of resource consumption within the main activity (water, sand, steam, proppant, cement, foam insulation, chemical reagents, additives, metal structures, fuel, other materials)	Resource costs
3	Impact on other components of the environment, t	Volume of waste generation, incineration, and disposal*; volume/mass of pollutant discharges into water bodies; volume/mass of pollutant emissions into the atmosphere	Payment for negative environmental impact
4	Climate damage caused by failure to comply with legal requirements, thousand tons of CO_2-eq.	Amount of greenhouse gas emissions exceeding the established quota (if applicable)	Payment for exceeding the established GHG emissions quotas
5	Capital expenditures of the decarbonization project, including those aimed at the production of new products (if applicable), units	The number of units of purchased equipment and materials categorized as capital expenditures; services rendered by third-party organizations (design, research and development, etc.); work performed by third-party organizations (construction, installation, etc.)	Equipment, work, and services costs
6	Climate efficiency, thousand tons of CO_2-eq.	Change scope 1, 2, and 3 emissions; change in capturing GHG emissions; change in the prevention of GHG emissions	Value of carbon units (emission reduction units)
7	Additional financial effect, toe; TJ, MW	Production of standard products; production of new products	Revenue from sales of additional volumes of standard products and/or new products produced as a result of the decarbonization project (if applicable)
8	State of the economy (budget) of the region or country, thousand rubles	Taxes (value-added tax (VAT), income tax, property tax)	Tax contributions to regional and federal budgets as a result of the implementation of the decarbonization project and related projects, including taxes covering social, insurance, pension, and medical needs
9	Social efficiency, number of people	The difference between the number of new jobs created by the project and the number of previously existing jobs (taking into account the suspension of other projects or works, if applicable)	

* Condition: If the waste was previously buried but is subjected to incineration within the framework of the decarbonization project, the positive effect is not taken into account.

Given the potential for divergent trends among these parameters, it is recommended to identify quantitative indicators of potential changes. This requires determining absolute indicators that can estimate the project's revenue, operating costs, and the economic effects beyond the project itself. Utilizing absolute indicators allows for a comparative assessment of decarbonization projects, making it possible to analyze one project in isolation or to compare multiple projects against each other. This approach helps identify the feasibility of implementing a specific project in relation to others executed by the same company.

This is an open access article under the CC BY 4.0 license

Based on the information in Table 1, a method can be developed for quantitatively assessing the decarbonization project in absolute monetary terms (over the entire implementation period) by comparing cash inflows and outflows:

• for the company, the internal impact of a decarbonization project can be expressed as

$$D_{int} = \sum_{t=0}^{T} \frac{\left(ER_i \times P_{CU} - CAPEX \times r_{greenium} + \Delta OPEX + Prod_{NEW} \times P_{Prod_{NEW}} \right)_t}{\left(1+r\right)^t}, \quad (1)$$

where ER_i is the total amount of emission reduction resulting from the implementation of decarbonization project i (thousand t CO_2-eq); P_{CU} is the cost of one unit of GHG emission reduction (carbon unit) (thousand rub./thousand t CO_2-eq); $CAPEX$ is capital expenditures for the decarbonization project (thousand rub.); $r_{greenium}$ is the correction coefficient accounting for preferential financing terms (if applicable), assuming the decarbonization project qualifies as a sustainable project, including green projects; $Prod_{NEW}$ is the number of new products resulting from the decarbonization project (units); $P_{Prod_{NEW}}$ is costs per unit of new products (thousand rub./unit); t is the year; r is the discount rate, %; $\Delta OPEX$ is the change in operating costs due to the implementation of the decarbonization project, assuming there are GHG emission quotas which may be exceeded,

$$\begin{cases} \Delta OPEX = -\left(C_{energy_i} + C_{materials_i} + C_{impact_i}\right) + \\ + CR_{energy_D} + CR_{materials_D} + CR_{impact_D} - \left(\left(E - ER_i\right) - E_q\right)T_e; \\ \left(E - ER_i\right) > E_q; \end{cases}$$

C_{energy_i} is energy consumption costs to implement the decarbonization project (thousand rub.); CR_{energy_D} is reduction in energy consumption costs from the decarbonization project (thousand rub.); $C_{materials_i}$ is resource and material consumption costs for the decarbonization project (thousand rub.); $CR_{materials_D}$ is reduction in resource and material consumption costs due to the project (thousand rub.); C_{impact_i} is payment for the negative environmental impact of the decarbonization project (thousand rub.); CR_{impact_D} is reduction in the payment for negative environmental impact as a result of the project (thousand rub.); E is baseline corporate GHG emissions without the decarbonization project (thousand tons of CO_2-eq); E_q is the quota for GHG emissions (if any) (thousand t of CO_2-eq).; T_e is payment for exceeding the established emission quota (thousand rub.).

If no quotas are set or there is no excess, the formula simplifies accordingly:

$$\begin{cases} \Delta OPEX = -\left(C_{energy_i} + C_{materials_i} + C_{impact_i}\right) + \\ + CR_{energy_D} + CR_{materials_D} + CR_{impact_D}; \\ \left(E - ER_i\right) \le E_q; \end{cases}$$

• for the national economy, the external economic efficiency of the decarbonization project can be represented as:

$$D_{ext} = \Delta Tax + \Delta Payments, \quad (2)$$

This is an open access article under the CC BY 4.0 license

where ΔTax is change in tax payments, factoring in possible reductions from core activities and increases resulting from project implementation (thousand rub.); $\Delta Payments$ is change in social security contributions, accounting for potential reductions from core activities and increases resulting from the decarbonization project (e.g., the net increase in the number of employees) (thousand rub.).

By employing these absolute indicators, we can derive specific indicators that enable further comparison of decarbonization projects based on a unified parameter, both in physical and monetary terms (Table 2).

Table 2

Stage 5 – A system for quantitative climate, environmental, and economic assessment of decarbonization projects using specific indicators

Indicator	Description	Units of measurement
Climate impact	Change in the carbon footprint of products sold throughout the supply chain	t CO_2-eq./toe; thousand t CO_2-eq./TJ
Energy consumption	Change in electricity consumption per product unit produced or sold	MWh/toe; MWh/boe; MWh/thousand rub.
Resource consumption	Consumption of individual types of resources and materials used within the framework of core activities (water, sand, proppant, cement, foam insulation, chemical reagents, additives, fuel, other materials) per unit of manufactured output	t/toe; m^3/toe; t/TJ; m^3/TJ
Environmental impact	Mass of waste produced, incinerated, or disposed of; mass of pollutant discharges into water bodies; mass of pollutant emissions into the atmosphere per unit of output	t of waste by hazard class/toe, t of pollutants by type/toe, t of waste by hazard class/TJ, t of pollutants by type/TJ
Costs	Capital and operating costs per mass of GHG emissions reduced	thousand rub./t CO_2-eq.
Economy/climate ratio	Capital and operating costs per revenue from GHG emission reduction units, carbon unit price	thousand rub./thousand rubles
Tax/climate ratio	Taxes resulting from project implementation (VAT, property tax, income tax) per mass of GHG emissions reduction	thousand rub./t CO_2-eq.
Society/climate ratio	Insurance, pension, and medical taxes paid for the staff involved in project implementation for the mass of GHG emissions reduction; salaries	thousand rub./t CO_2-eq.

In assessing specific indicators, some analyses use the volume of manufactured products, while others rely on the volume of sold products. This distinction arises because sold products account for the processes of transportation and delivery to the end consumer, aligning more closely with comprehensive approaches that evaluate all stages along the product's value chain. In this context, the volume of products is adjusted to account for technological losses and inventory that remains unsold due to economic or logistical reasons. Considering the volume of manufactured products is useful for analyzing and optimizing production processes and operational activities.

Specific indicators are employed to gauge the effectiveness of project implementation by comparing the specific indicators from the base year with those from the reporting year if the project is ongoing, or with the completion year if the project has been completed. These specific indicators for the reporting year can also help identify the highest priority project among several possibilities, focusing on the most significant key specific indicator for the company.

This is an open access article under the CC BY 4.0 license

An example of a project that demonstrates the results of Stage 5 in the proposed algorithm – utilizing a quantitative climate, environmental, and economic assessment system for a decarbonization project – is the initiative to increase the utilization of associated petroleum gas (APG) at the A field in the Khanty-Mansi Autonomous Okrug – Yugra, which has been underway since 2018. Over the 15-year period under consideration, the volume of APG production has reached 1,424.85 million m^3. The decarbonization project aims to reduce greenhouse gas emissions from APG flaring by generating electricity with the help of a natural gas-fired reciprocating engine (RE). This initiative increases the level of APG utilization from 95 to 99 % while ensuring compliance with existing legislative requirements[6]. In this case, the reduction in emissions is not a result of external factors, nor does it stem from a decrease in economic activity or cause an increase in emissions outside the project. Thus, it can be concluded that the project meets the established criteria[7]. The initial data for the project, detailed in Table 3, include parameters that are considered in the context of either the decarbonization project (items 4, 6, 9, 10, and 11) or the entire company (items 5, 7, 8, 12, and 13). This approach assesses the impact of the decarbonization project on the main production activities of the company. The revenue from the sale of carbon units (item 11) is calculated by multiplying the number of verified emission reduction units by the selling price of the carbon units.

Table 3

Case study: Initial data without and with the decarbonization project

N	Parameter	No project	With project
1	APG production, million m^3	1424.85	1424.85
2	APG utilization, % of production	95	99
3	APG utilization, million m^3	1353.61	1410.60
4	APG flaring, million m^3	71.24	14.25
5	Capital investments (project), thousand rub.	0.00	102900.00
6	Operating expenses, thousand rub.	561000.00	400943.60
7	Waste generated, t	582.00	593.64
8	Pollutant emissions generated, t	1781.06	413.21
9	Greenhouse gas emissions generated, including	249448.49	1172.93
	flaring, t CO_2-eq.	249448.49	1164.15
	natural gas-fired reciprocating engine, t CO_2-eq.	0.00	8.79
10	Electricity generated, MWh	0.00	30.90
11	Revenue from carbon units, thousand rub.	0.00	496568.68
12	Payment for waste generation, thousand rub.	552.90	563.96
13	Payment for pollutant emissions, thousand rub.	534.32	123.96

Note. The table is based on decarbonization project data.

Additional positive outcomes of the project include a major reduction in pollutant emissions released into the atmosphere, as well as a decrease in operating costs for the energy supply of the field infrastructure. This reduction is primarily due to the generated electricity being utilized on-site rather than being sold as a new product. However, there are also some negative consequences associated with the project. These include a 2 % increase in waste generated as a result of RE servicing,

[6] Resolution of the Government of the Russian Federation of November 8, 2012, N 1148 "On Calculating Fees for Negative Environmental Impact from Emissions into the Atmosphere Caused by APG Flaring and (or) Dispersion". URL: https://base.garant.ru/70257422/ (accessed 15.11.2023).

[7] Order of the Ministry of Economic Development of Russia of May 11, 2022, N 248 "On Approval of the Criteria and Procedure for Attributing Projects Implemented by Legal Entities, Individual Entrepreneurs or Individuals to Climate Projects, Form and Procedure for Submitting a Climate Project Implementation Report".

This is an open access article under the CC BY 4.0 license

as well as a 54 % rise in the payments for pollutant emissions (nitrogen dioxide, nitrogen oxide, etc.) associated with RE operation[8]. Despite these challenges, revenue generated from the sale of carbon units offsets the costs associated with waste generation and pollutant emissions, as well as the capital costs of the project. The net discounted cash flow for the decarbonization project is estimated at 53,624.00 thousand rub., calculated using a discount rate of 15 %. The resulting specific indicators are presented in Table 4.

Table 4

Quantitative assessment of the decarbonization project: Results

The system of quantitative assessment indicators for decarbonization projects	No project	With project
Climate impact, t CO_2-eq./toe	16.41	0.08
Environmental impact (t/toe), including	0.79	0.59
waste	0.05	0.05
pollutant emissions	1.52	1.13
Costs, thousand rub./t CO_2-eq.	n/a	0.46
Economy/climate ratio, thousand rub./thousand rub.	n/a	0.23
Tax/climate ratio, thousand rub./t CO_2-eq.	n/a	0.42
Society/climate ratio, thousand rub./t CO_2-eq.	n/a	0.05

Note. Oil production for the period under review amounted to 10,626.90 thousand t. To convert it to toe, a coefficient of 1.43 was used.

The project's impact on the climate is assessed within the defined boundaries of variable industrial processes, specifically comparing the handling of associated petroleum gas (APG) within the "without the project" and "with the project" scenarios. This approach excludes other greenhouse gas emissions to eliminate the influence of external variable factors. As a result of the project implementation, the economic and climatic coefficient (Table 4), which is evaluated within the context of the APG utilization decarbonization project, has decreased. To achieve a reduction of one ton of CO_2-equivalent emissions, the project incurred total costs of 460 rub. per ton of CO_2-equivalent, as indicated by the project cost metrics. The economic and climatic coefficient, which is less than 1, stands at 0.23, indicating that revenue from the sale of carbon units exceeds the capital and operating costs of the project. Furthermore, for each ton of GHG emissions reduced, there are additional fiscal implications: 420 rub. in taxes and 50 rub. in social security contributions, which are reflected in the fiscal and socio-climatic coefficients.

Discussion.

Oil and gas companies that have established targets for reducing GHG emissions face the challenge of selecting priority decarbonization projects or groups of projects [2, 31]. These initiatives are not only aimed at achieving the specified goals but also at acquiring additional benefits, such as maximizing NPV and minimizing negative impacts on the surrounding social and natural environments, as well as the climate, both within and outside the projects [11]. Furthermore, these projects must comply with the criteria set by climate project standards and regulatory requirements. The wide array of decarbonization opportunities [3, 5] allows companies to identify several viable projects, considering their geographical, infrastructural, and technological parameters [7]. Typically, companies evaluate the potential economic efficiency of design solutions.

However, each project will exhibit different emission reduction metrics, capital and operating costs, environmental impact indicators, and associated payments for negative impacts. Consequently, this variability necessitates the involvement of different managers and workers for each project. All differences can be assessed in monetary terms using formula (1), which provides a universal financial

[8] Resolution of the Government of the Russian Federation of September 13, 2016, N 913 "On Negative Environmental Impact Payment Rates and Additional Coefficients".

This is an open access article under the CC BY 4.0 license

representation of each project. Standard feasibility study tools often lack a detailed evaluation of environmental impact payments and fail to incorporate carbon regulation instruments or preferential financing terms aligned with green taxonomy. As a result, such assessments tend to be less accurate. By refining existing tools, it becomes possible to account for the nuances of climate regulation and quantitatively assess the environmental impacts of these projects.

For instance, a company can evaluate the potential revenue from selling carbon units over the entire project lifecycle, compare the result with capital and operating costs, assess the reduction in tax payments, and analyze how environmental impact payments will change due to the decarbonization project.

Moreover, for a comprehensive analysis and decomposition of quantitative assessment components, it is crucial not to overlook the qualitative stage of evaluation. This stage identifies whether the project affects the surrounding social and natural environments and whether new types of products emerge from its implementation, facilitating better synchronization of the decarbonization project with other aspects of corporate economic activities.

Another important aspect involves assessing specific parameters – such as energy consumption and coefficients of economic and climate efficiency (see Table 2) which will support informed decision-making when comparing indicators obtained in previous assessment stages under otherwise equal conditions. Future research could focus on adapting budgeting tools for both decarbonization projects and broader applications.

Conclusion.

In developing a methodology for the environmental and economic assessment of decarbonization projects in the oil and gas sector, we identified internal and external factors influencing project selection, determined the economic, climatic, and environmental conditions necessary for ranking these projects, and proposed a five-stage process for selecting, assessing, and ranking potential decarbonization initiatives. This process includes evaluating project feasibility and compliance with established criteria, which are structured according to increasing priority. Additionally, we introduced tools for quantitative assessment and comparative analysis of decarbonization projects using both absolute and specific indicators.

The selection of optimal decarbonization projects for an oil and gas company can be achieved through qualitative and quantitative analyses, encompassing a multi-criteria assessment of projects based on climatic, environmental, economic, and social factors. The diverse nature of decarbonization projects necessitates a universal mechanism for comparative analysis, as proposed in this study. Clarifying priorities and establishing additional criteria set by companies will improve management decision-making methods aimed at achieving GHG emission reduction goals and facilitate the automation of greenhouse gas emission management processes.

REFERENCES

1. Zhoujie Wang, Songyan Li, Zhijun Jin et al. Oil and gas pathway to net-zero: Review and outlook. *Energy Strategy Reviews*. 2023. Vol. 45. N 101048. DOI: 10.1016/j.esr.2022.101048

2. Cherepovitsyna A., Sheveleva N., Riadinskaia A., Danilin K. Decarbonization Measures: A Real Effect or Just a Declaration? An Assessment of Oil and Gas Companies' Progress towards Carbon Neutrality. *Energies*. 2023. Vol. 16. Iss. 8. N 3575. DOI: 10.3390/en16083575

3. Grushevenko E., Kapitonov S., Melnikov Yu. et al. Decarbonization of the oil and gas industry: International experience and Russia's priorities. Moscow: Moskovskaya shkola upravleniya SKOLKOVO, 2021, p. 158 (in Russian).

4. Romasheva N., Cherepovitsyna A. Renewable Energy Sources in Decarbonization: The Case of Foreign and Russian Oil and Gas Companies. *Sustainability*. 2023. Vol. 15. Iss. 9. N 7416. DOI: 10.3390/su15097416

5. Sheveleva N.A. Decarbonization strategies and methods for oil and gas sector. *Environmental protection in oil and gas complex*. 2023. N 2 (311), p. 25-31 (in Russian). DOI: 10.33285/2411-7013-2023-2(311)-25-31

This is an open access article under the CC BY 4.0 license

6. Cherepovitsyn A.E., Tsvetkov P.S., Evseeva O.O. Critical analysis of methodological approaches to assessing sustainability of arctic oil and gas projects. *Journal of Mining Institute.* 2021. Vol. 249, p. 463-478. DOI: 10.31897/PMI.2021.3.15

7. Kirillov I.S. An assessment of investment projects in the Russian oil and gas industry: Economic, social, and environmental aspects: Avtoref. dis. … kand. ekon. nauk. Moscow: Finansovyi universitet pri Pravitelstve Rossiiskoi Federatsii, 2013, p. 24 (in Russian).

8. Vurdova N.G., Lishchuk A.N. The impact of environmental-economic risks on the effectiveness of the investment-construction project for the reconstruction of wastewater treatment facilities of oil refineries. *Environmental protection in oil and gas complex.* 2023. N 3 (312), p. 23-31 (in Russian). DOI: 10.33285/2411-7013-2023-3(312)-23-31

9. Yarygin G.A., Vilchek G.E. Utilizing strategic environmental assessment to optimize offshore oil and gas projects. *Neftegaz*.RU. 2013. N 11-12, p. 42-45 (in Russian).

10. Dyakov M.Yu., Mikhailova E.G., Sharakhmatova V.N. Strategic environmental assessment in regional planning. *Problems of Territory's Development.* 2019. N 2 (100), p. 80-94 (in Russian). DOI: 10.15838/ptd.2019.2.100.5

11. Krainova E.A., Mushba B.V. Ecological and economic balance of decision-making during the energy transition to decarbonization of the oil and gas industry. *Equipment and technologies for oil and gas complex*. 2022. N 5 (209), p. 37-44 (in Russian). DOI: 10.33285/1999-6942-2022-5(209)-37-44

12. Pinaev V.E. Modeling of assessment system for oil and gas projects industry case study YaNAO. *Naukovedenie*. 2016. Vol. 8. N 4, p. 13 (in Russian).

13. Novoselova I.Yu., Novoselov A.L. Environmental multiplier of federal and regional budgets' participation in mining companies' projects. *Economics, taxes & law*. 2022. Vol. 15. N 3, p. 99-109 (in Russian). DOI: 10.26794/1999-849X-2022-15-3-99-109

14. Novoselova I.Yu., Novoselov A.L. Modeling of regional trade in environmental pollution quotas. *Economics, taxes & law*. 2022. Vol. 15. N 4, p. 96-106 (in Russian). DOI: 10.26794/1999-849X-2022-15-4-96-106

15. Vetrova M.A., Bogdanova A.A., Yarullina I.E. Decarbonization of oil industry in the context of circular development of economy. *Problems of Modern Economics*. 2021. N 3 (79), p. 196-199 (in Russian).

16. Rekord S.I., Kulikov D.V. International aspects in formation of technological model of decarbonization of natural gas. *Problems of Modern Economics*. 2019. N 3 (71), p. 176-180 (in Russian).

17. Kozenyasheva M.M., Savinova A.A. Decarbonization in the field of international shipping. *Equipment and technologies for oil and gas complex*. 2023. N 1 (217), p. 60-65 (in Russian). DOI: 10.33285/1999-6942-2023-1(217)-60-65

18. Zaedinov A.V. Modernization of the business-model of climate projects in the context of formation of the Russian sequestration industry. *Problems of Modern Economics*. 2023. N 2 (86), p. 202-206 (in Russian).

19. Jenvey N. Technology Focus: Decarbonization. *Journal of Petroleum Technology*. 2021. Vol. 73. Iss. 7, p. 64. DOI: 10.2118/0721-0064-JPT

20. Danilin K.P., Cherepovitsyna A.A., Beloshitskiy A.V. Oil and gas companies' greenhouse gases emissions reporting: Scope 3. *Oil Industry Journal*. 2023. N 5, p. 139-144 (in Russian). DOI: 10.24887/0028-2448-2023-5-139-144

21. Kurka T. Application of the analytic hierarchy process to evaluate the regional sustainability of bioenergy developments. *Energy*. 2013. Vol. 62, p. 393-402. DOI: 10.1016/j.energy.2013.09.053

22. Ilinova A.A., Romasheva N.V., Stroykov G.A. Prospects and social effects of carbon dioxide sequestration and utilization projects. *Journal of Mining Institute.* 2020. Vol. 244, p. 493-502. DOI: 10.31897/PMI.2020.4.12

23. Singh H., Chengxi Li, Peng Cheng et al. Real-Time Optimization and Decarbonization of Oil and Gas Production Value Chain Enabled by Industry 4.0 Technologies: A Critical Review. *SPE Production & Operation*. 2023. Vol. 38. Iss. 3, p. 433-451. DOI: 10.2118/214301-PA

24. Ponkratov V.V., Kuznetsov A.S., Muda I. et al. Investigating the Index of Sustainable Development and Reduction in Greenhouse Gases of Renewable Energies. *Sustainability*. 2022. Vol. 14. Iss. 22. № 14829. DOI: 10.3390/su142214829

25. Agbaji A.L., Morrison R., Lakshmanan S. ESG, Sustainability and Decarbonization: An Analysis of Strategies and Solutions for the Energy Industry. SPE EuropEC – Europe Energy Conference featured at the 84th EAGE Annual Conference & Exhibition, 5-8 June 2023, Vienna, Austria. OnePetro, 2023. N SPE-214346-MS. DOI: 10.2118/214346-MS

26. Cortez M.C., Andrade N., Silva F. The environmental and financial performance of green energy investments: European evidence. *Ecological Economics*. 2022. Vol. 197. N 107427. DOI: 10.1016/j.ecolecon.2022.107427

27. Boguslavsky D.V., Sharov K.S., Sharova N.P. Using Alternative Sources of Energy for Decarbonization: A Piece of Cake, but How to Cook This Cake? *Environmental Research and Public Health*. 2022. Vol. 19. Iss. 23. N 16286. DOI: 10.3390/ijerph192316286

28. Tsai W.-H. Carbon Emission Reduction – Carbon Tax, Carbon Trading, and Carbon Offset. *Energies*. 2020. Vol. 13. Iss. 22. N 6128. DOI: 10.3390/en13226128

29. Al Kindi O.M., Al Hinai S., Ghefeili H. et al. Decarbonization Will Not Come for Free: Asset-M Marginal Abatement Cost Curve. SPE EuropEC – Europe Energy Conference featured at the 84th EAGE Annual Conference & Exhibition, 5-8 June 2023, Vienna, Austria. OnePetro, 2023. N SPE-214414-MS. DOI: 10.2118/214414-MS

30. Yasemi S., Khalili Y., Sanati A., Bagheri M. Carbon Capture and Storage: Application in the Oil and Gas Industry. *Sustainability*. 2023. Vol. 15. Iss. 19. N 14486. DOI: 10.3390/su151914486

31. Telegina E.A., Chapaikin D.A. Directions of the Energy Transition in the Policy of Global Oil and Gas Companies. *Studies on Russian Economic Development.* 2022. Vol. 33. N 5, p. 555-560. DOI: 10.1134/S1075700722050148

This is an open access article under the CC BY 4.0 license

32. Gorbacheva N.V. Comparative analysis of decarbonising economy in Siberia and Scandinavia megaregions: Price, value and values of energy. *Voprosy Ekonomiki.* 2023. N 10, p. 124-148 (in Russian). DOI: 10.32609/0042-8736-2023-10-124-148

33. Porfiriev B.N., Shirov A.A., Kolpakov A.Y., Edinak E.A. Opportunities and risks of the climate policy in Russia. *Voprosy Ekonomiki.* 2022. N 1, p. 72-89 (in Russian). DOI: 10.32609/0042-8736-2022-1-72-89

34. Kolpakov A.Yu. Energy Efficiency: Its Role in Inhibiting Carbon Dioxide Emissions and Defining Factors. *Studies on Russian Economic Development.* Vol. 31. N 6, p. 691-699. DOI: 10.1134/S1075700720060076

35. Yuh-Ming Tsai, Cherng-Yuan Lin. Effects of the Carbon Intensity Index Rating System on the Development of the Northeast Passage. *Journal of Marine Science and Engineering*. 2023. Vol. 11. Iss. 7. N 1341. DOI: 10.3390/jmse11071341

36. Glebov L.S., Glebova E.V. CO_2 emission in the production and use of diesel fuel and biodiesel. *Environmental protection in oil and gas complex.* 2021. N 2 (299), p. 23-27 (in Russian). DOI: 10.33285/2411-7013-2021-2(299)-23-27

37. Karaeva A., Magaril E., Al-Kayiem H. et al. Approaches to the assessment of ecological and economic efficiency of investment projects: Brief review and recommendations for improvements. *WIT Transactions on Ecology and the Environment*. 2021. Vol. 253, p. 515-525. DOI: 10.2495/SC210421

38. Makepa D.C., Chihobo H.C., Musademba D. Techno-economic analysis and environmental impact assessment of biodiesel production from bio-oil derived from microwave-assisted pyrolysis of pine sawdust. *Heliyon.* 2023. Vol. 9. Iss. 11. N e22261. DOI: 10.1016/j.heliyon.2023.e22261

Author **Nadezhda A. Sheveleva,** *Candidate of Economics, Researcher, Associate Professor, sheveleva.n@gubkin.ru, https://orcid.org/0009-0000-7243-3196* (*Luzin Institute for Economic Studies of the Kola Science Centre of the RAS, Apatity, Russia*; *Gubkin Russian State University of Oil and Gas, Moscow, Russia*)

The author declares no conflicts of interests.

This is an open access article under the CC BY 4.0 license

ISSN 2411-3336; e-ISSN 2541-9404

JOURNAL OF MINING INSTITUTE

Zapiski Gornogo instituta

Journal homepage: pmi.spmi.ru

Erratum

Correction to “Determination of the grid impedance in power consumption modes with harmonics”

Skamyin A.N., Dobush V.S., Jopri M.H.

On page 443 of article is missing “Acknowledgment” section indicating funding for the research.

It should be read:

Acknowledgment. The study was funded by the Russian Science Foundation grant N 21-79-10027.

These errors do not affect the conclusions of the article. The correction has been to the html and pdf versions of the article.

Skamyin A.N., Dobush V.S., Jopri M.H. Determination of the grid impedance in power consumption modes with harmonics // Journal of Mining Institute. 2023. Vol. 261. p. 443-454. DOI: 10.31897/PMI.2023.25 URL: https://pmi.spmi.ru/pmi/article/view/16031

Published online: 20.12.2024

Published in open access under the CC BY 4.0 license